ISOLATION AND CHARACTERISATION OF ANTIPLASMODIAL COMPOUNDS FROM *XEROPHYTA* SPECIES AND THE BIOAVAILABILITY, METABOLIC AND EFFICACY EVALUATION OF 9-O-ACETYLHYDNOCARPIN IN A MOUSE MODEL

Lubbe Wiesner

Thesis presented for the degree of
Doctor of Philosophy in Pharmacology
Faculty of Health Sciences
University of Cape Town

February 2008

Supervisors: Prof. PJ Smith and Dr. WE Campbell

DECLARATION

It is herewith declared that the work represented in this thesis is the independent work of the undersigned (except where acknowledgements indicate otherwise) and has not been submitted at any other University for a degree. In addition, copyright of this thesis is hereby ceded in favour of the University of Cape Town.

_____

JL Wiesner

_____

Date

PREFACE

The experimental work presented in this thesis was performed at the Pharmacology Division at the Department of Medicine at the Faculty of Health Sciences, of the University of Cape Town, South Africa. Plant material from *X. villosa* and *X. retinervis* were collected and dried. Plant products were extracted from the leave bases using different organic solvents. These extracts were tested for antiplasmodial activity and the most promising ones were further purified to obtain single compounds. These compounds were tested for antiplasmodial activity and cytotoxicity and structural information was obtained to determine their structures. The bioavailability, metabolism and *in vivo* efficacy of the most active antiplasmodial compound were investigated in a mouse model.

This thesis has been divided into twelve chapters. Chapter 1 presents an introduction to malaria, traditional medicine and traditional healing, medicinal plants, natural products and malaria medicine, drug discovery and development, antiplasmodial development of plant derived products, as well as the scope of the study. Chapters 2 to 6 present *in vitro* work and Chapter's 7 to 10 present *in vivo* animal testing. The research summary, final thoughts and research prospects, as well as presentations and manuscripts (in preparation) are presented in Chapter 11. Methodology details of all experimental work are presented in Chapter 12. A comprehensive and descriptive section about the method development process of the novel methodologies, which have been developed for the bioavailability and metabolism studies, is also presented in Chapter 12. Plant collection and extract preparation are presented in Chapter 2. Antiplasmodial activity and cytotoxicity screening of *X. villosa* and *X. retinervis* extracts are presented in Chapter 3. Isolation of pure compounds is presented in Chapter 4. Antiplasmodial activity and cytotoxicity screening of isolated compounds are presented in Chapter 5. Structural elucidation of antiplasmodial compounds that were isolated from *Xerophyta* species is presented in Chapter 6. Antimalarial assessment of the most active antiplasmodial compound (9-O-acetylhydnocarpin) in a mouse model (using a polar formulation) is presented in Chapter 7. Bioavailability investigation of 9-O-acetylhydnocarpin in mice is presented in Chapter 8. A metabolite study of 9-O-acetylhydnocarpin in mice is presented in Chapter 9. Chapter 10 provides an optimised assessment of the antimalarial activity of 9-O-acetylhydnocarpin in mice, using an improved dosing strategy. HPLC, UV, MS and NMR spectra are presented in Appendix 1. Body weight and %parasitaemia data of

antimalarial experiments are presented in Appendix 2. Bioavailability data is presented in Appendix 3. Metabolite spectral data is presented in Appendix 4.

ACKNOWLEDGEMENTS

I would also like to thank and acknowledge the following persons and institutions:

Elmarie and family, for your love and support.

Prof. Peter Smith, for making this project possible and for teaching me so much more than science.

Dr. Bill Cambell, for supervising this project and for teaching me NMR interpretation.

Dr. PC Zietsman, for collecting the plant material.

Carmen Lategan and Sumya Salie, for facilitating and screening my extracts and compounds.

Dr. Jean McKenzie, for NMR analysis.

Pamisha Pillay, for optical rotation analysis of compound 5.

Noor Salie, for teaching and assisting me with the animal work, and for all the positive energy and friendship.

Trevor Finch, for teaching and assisting me with the animal work, and for taking care of the animals.

A special thanks to the postgraduate students in the traditional medicine group at Pharmacology, Tracy, Faith, Carmen, Mamello and Paula for all the interesting discussions and assistance.

Thanks to the Pharmacology department and the NRF for the financial assistance.

Thank you, God, for giving me the opportunity to discover a small part of your wonderful creation.

ABSTRACT

Malaria is one of the most serious infectious diseases of the tropics, and has a significant impact on health and economic systems worldwide. The malaria situation is deteriorating faster at present than at any time in the past, due to drug and insecticide resistance and environmental and social changes. Malaria control relies strongly on drug treatment, but many of the first-line treatments are failing due to the parasites ability to develop resistance against drug action over time. There is an urgent need to discover new classes of antimalarial compounds, which use different mechanisms of action against the *Plasmodium* parasites, and to develop some of these compounds into antimalarial drugs. Most of the existing antimalarial drugs originated from higher plants as novel compounds or chemically modified derivatives. South Africa is rich in plant diversity with about 3 000 species that are used as medicines, yet very little is known about their antimalarial activity. One of these species as well as a related species from the same genus were targeted as a potential source for novel antimalarial compounds.

X. villosa and *X. retinervis* were targeted as a potential source of new antiplasmodial compounds. The compounds were grouped according to their polarity using sequential solvent extraction. Ethyl acetate sub-fractions of the methanol extracts of both species were screened against chloroquine sensitive (D10) and resistant (K1) *P. falciparum* strains and showed excellent antiplasmodial activity.

Six pure compounds were successfully isolated from *X. villosa* and two from *X. retinervis* using two reverse phase HPLC gradient systems. These isolated compounds were screened against a chloroquine sensitive (D10) *P. falciparum* strain. Two of these compounds showed good antiplasmodial activity, three showed mild activity, and one showed no activity. The two most active compounds were also screened against a chloroquine resistant (K1) *P. falciparum* strain and showed similar antiplasmodial activity (compared to the D10 strain), which indicates that these compounds probably use a different mechanism of action against the parasites (compared to chloroquine). Cytotoxicity testing of the extracts and isolated compounds was done to determine their toxic properties against living cells, and all tested extracts and compounds showed little toxicity. The two most active compounds showed good selective antiplasmodial activity.

The chemical structures of the three most active antiplasmodial compounds were determined using mass spectrometry and nuclear magnetic resonance spectroscopy (1D and 2D). The most active compound was identified as 9-O-acetylhydnocarpin. This is the first study that has shown the presence of 9-O-acetylhydnocarpin in *X. villosa*. The second best compound was identified as hydnocarpin. Again this is the first report of the presence of hydnocarpin in *X. villosa* and *X. retinervis*. The third best compound was identified as the flavonoid luteolin and showed mild antiplasmodial activity.

Bioavailability and metabolite studies of 9-O-acetylhydnocarpin were conducted in a mouse model, and the information that was generated during these experiments was used to design an improved treatment strategy for *in vivo* antimalarial testing on *P. berghei* infected mice. The antiplasmodial compound, 9-O-acetylhydnocarpin showed a reasonable level of protection for the mice against the malaria parasites, but could not cure the animals under the tested experimental conditions.

TABLE OF CONTENTS

LIST OF FIGURES

LIST OF TABLES

ABBREVIATIONS

% Nom	Percentage of Nominal Concentration
^{13}C	Carbon 13
^{1}H	Proton
2D	Two Dimensional
APAD	3-acetylpyridine adenine dinucleotide
API	Atmospheric Pressure Ionisation
BLQ	Below Limit of Quantification
CHO	Chinese Hamster Ovarian cells
C_{max}	Maximum Expected Concentration
COSY	Correlation Spectroscopy
CV%	Coefficient of Variation
DM	Dichloromethane
DMSO	Dimethyl sulfoxide
EA	Ethyl acetate
ELISA	Enzyme Linked Immunosorbent Assay
ESI	Electrospray Ionisation
HEPES	N-[2-Hydroxyethyl]-piperazine-N'-[2-Ethansulphonic acid]
HMQC	Heteronuclear Multiple Quantum Correlation
HPLC	High Performance Liquid Chromatography
HSQC	Heteronuclear Single Quantum Correlation
IC_{50}	50% of cell growth inhibited
ISTD	Internal Standard
IV	Intravenous Injection
LC	Liquid Chromatography
LC-MS	Liquid Chromatography Mass Spectrometry
LC-MS/MS	Liquid Chromatography Mass Spectrometry/Mass Spectrometry
LDH	Lactate Dehydrogenase assay
LLOQ	Lower Limit of Quantification
MeOH	Methanol
MRM	Multi Reaction Monitoring
MS	Mass Spectrometer
MS/MS	Mass Spectrometry/Mass Spectrometry
MTT	3-[4,5-Dimethylthiazol-2-yl]-2,5-diphenyltetrazolium bromide
PBS	Phosphate Buffered Saline
PE	Petroleum ether
pLDH	Parasite Lactate Dehydrogenase assay
Q1	Quadrupole 1
Q3	Quadrupole 3
Q-TOF	Time of Flight mass spectrometer
RBC	Red Blood Cells
SMEDDS	Self Microemulsifying Drug Delivery System
STD	Calibration Standard
STDEV	Standard deviation
TFA	Trifluoroacetic acid
TIC	Total Ion Chromatogram
WHO	World Health Organisation

CHAPTER 1

Literature review

1 Literature review

1.1 Malaria

1.1.1 History

Malaria has troubled humanity since ancient times. Evidence of malaria was found in Chinese and Egyptian documents, which are more than 6000 years old. The ancient Greeks noted that people who were exposed to swamp lands usually develop fevers. The Italians later on called this disease mal'aria, due to the awful smell near swamps. Historical documents by the Vedic civilization in India, which date back 1600 B.C., also show evidence of malaria. The first clinical symptoms and complications of malaria were described by Hippocrates during the fifth century B.C. Many years later, during the 1880s, the first single-celled *Plasmodium* parasites were observed in blood by French Scientist Alphonse Laveran. The mosquito vector, which is responsible for transmitting the disease, was only discovered approximately twenty years later, by scientists from India and Italy. The major features of the parasitic life cycle were described by Sir Ronald Ross in 1902. He received the Nobel Prize for this work. Much progress has been made during the 20th century towards the understanding of the disease [WHO, 1986; NIAID, 2007; Johns Hopkins Bloomberg School of Public Health].

1.1.2 International malaria perspective

Malaria is a major threat to the human race and results in more than a million deaths per year. It is found in the tropical and sub-tropical regions of the world where more than half of the world's population lives. The environmental conditions in these regions are ideal for parasite and vector development. The global distribution of malaria is presented in figure 1.

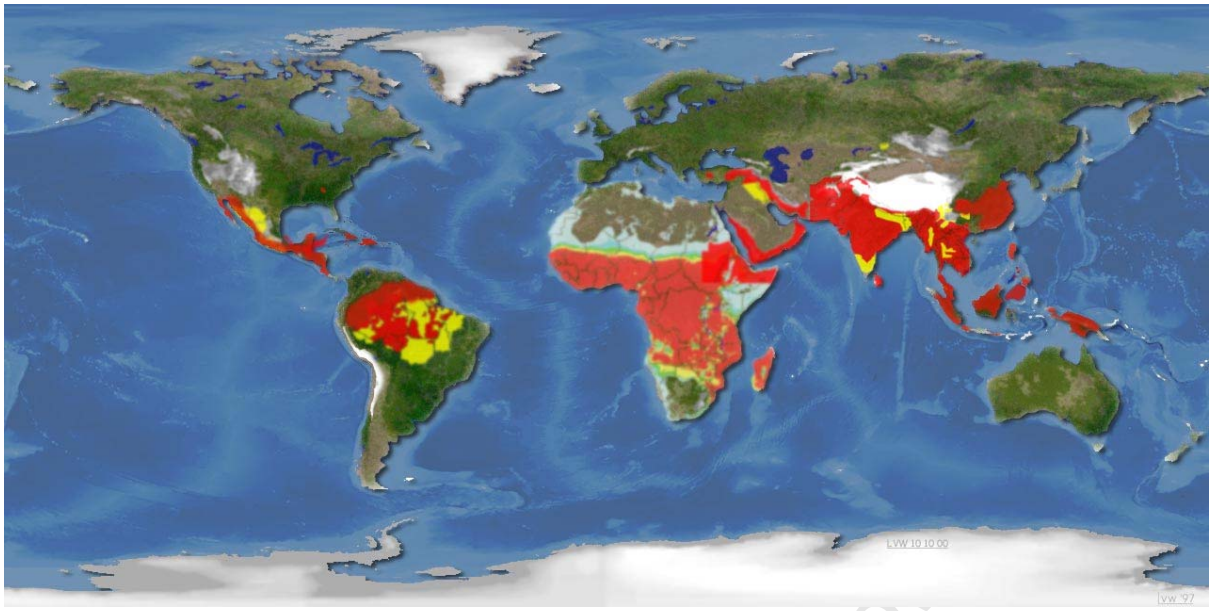

Figure 1 Global distribution of malaria transmission risk [World Malaria Map]

The worldwide malaria situation is deteriorating faster at present than at any time in the past. We are facing a rapidly increasing disease burden because of more people moving into malaria regions, deforestation, building of dams and irrigation systems in agriculture, climate changes and global warming. The number of new malaria infections has increased dramatically during the last decade. More than 2 billion people (40% of the human population) are at risk of being infected, mostly in the tropics and subtropics, and about 50% of these live in sub-Saharan Africa. The disease is currently endemic in 107 countries. In 1990, 80% of malaria cases were reported in Africa, and the rest found in countries such as India, Brazil, Afghanistan, Sri-Lanka, Thailand, Indonesia, Vietnam, Cambodia, China, and others. About 300 to 500 million malaria infections occur per year, and 90% of these are also concentrated in sub-Saharan Africa. Children are particularly susceptible, and according to the WHO, more children die from malaria than any other single disease. Pregnant women are the second highest risk group for malaria infection [World Health Report, 1999, 2005; Bremen, 2001; Johns Hopkins Bloomberg School of Public Health].

1.1.3 Malaria situation in South Africa

KwaZulu-Natal, Mpumalanga and Limpopo are malaria endemic areas, and the Northern Cape and North West provinces occasionally experience malaria infections. The malaria season is usually experienced between October and May. A relatively high occurrence of malaria cases were experienced between 1996 and 2000, especially in KwaZulu-Natal. The treatment strategy was altered in 1998, and chloroquine was replaced with sulfadoxine-pyrimethamine as first-line treatment, due to parasite resistance that has developed against chloroquine. Unfortunately, sulfadoxine-pyrimethamine has lost its efficacy relatively fast and was replaced with artemisinin-based combinatorial treatment during 2001, which resulted in more than a 75% reduction in malaria deaths within one year. The Lubombo Spatial Development Initiative programme was established in 1999, which included South Africa, Swaziland and Mozambique. This project aimed to manage and reduce malaria in these regions, which would contribute towards economic development. The first-line treatment was replaced with co-artemether in some areas, and DDT was reintroduced as insecticide in spraying programmes. This project was very successful: a 90% reduction in KwaZulu-Natal, a 75% reduction in Mpumalanga, a 90% reduction in Swaziland and an 88% reduction in Mozambique, were observed. The South African Health Department also received an award by the World Health Organization for the best malaria control management programme in Africa, due to the sharp decrease in malaria morbidity and mortality [Department of Health, South Africa; Medical Research Council, South Africa; World Health Organization; Roper *et al*., 2003].

1.1.4 Economic burden

The current spending on malaria prevention and treatment is less than $100 million per year, but the actual needs are more than an order of magnitude greater. The World Health Organisation estimates that $2,5 billion per year is required for effective prevention and treatment programmes as from 2007. The world's poorest countries and their people cannot afford western medicine for malaria treatment and rely on local flora to prevent and treat malaria. People have used plants for many centuries to treat malaria and it seems that they will continue to do so for many years to come [Sachs and Malaney, 2002].

1.1.5 Malaria the disease

Malaria is described as an infectious disease which is characterized by extreme exhaustion, fever, chills, and anaemia. The malaria symptoms usually begin 10 days to 4 weeks after infection. Symptoms are: high fever, shaking chills, sweating, headache, muscle aches, tiredness, and sometimes nausea, vomiting and diarrhoea. Malaria is often described as a flu-like illness due to its related symptoms. The malaria parasite modifies human red blood cells, causing them to attach to the surface of blood vessels, which lead to blockage of capillaries to the brain and other organs. The clinical response after infection with protozoan parasites varies, due to genetic makeup, age, parasite species and duration of infection. The diagnosis of malaria is difficult because symptoms are unspecific and mimic other diseases. A definite diagnosis is only possible if blood is tested for parasite presence and should be tested at different time intervals because parasites may disappear from peripheral blood during the schizogonic phase of the parasites life cycle. Severe malaria is caused when more than 5% of the red blood cells are infected with parasites (hyperparasitaemia). Severe anaemia is caused by the destruction of red blood cells and cerebral malaria is caused by the obstruction of small brain vessels.

Malaria is caused by *Plasmodium* protozoan parasites and is transmitted to humans by female *Anopheles* mosquitos. There are four species of the *Plasmodium* protozoan parasite that infect humans; *Plasmodium falciparum*, *Plasmodium vivax*, *Plasmodium ovale* and *Plasmodium malariae*. *P. falciparum* is the most common and deadliest species, which causes 90% of malaria deaths worldwide. If the disease is not promptly treated, severe infection with *P. falciparum* may lead to coma, severe anaemia, cerebral malaria, hypoglycaemia, renal failure, acidosis, repeated convulsions and finally death. *P. vivax* accounts for approximately 70-80 million malaria cases annually. *P. vivax* is not as lethal as *P. falciparum*, but can have major negative effects on general health, growth and development. Young red blood cells (reticulocytes) are infected by this species. *P. vivax* is found in Asia, the Western Pacific and the Americas. *P. vivax* infections do not occur in West Africa, because of the absence of Duffy blood group antigens in West Africans. These antigens are required for red blood cell invasion. This species have dormant liver stage parasites, hypnozoites, which can cause relapses if left untreated. *P. malariae* has a relatively low occurrence, but is still found in Africa. It causes typical malaria-like symptoms, but can also persist in the blood for years without ever producing symptoms. *P. ovale* is the rarest of the four human malaria parasites, and is found in Tropical Africa

and some Western Pacific islands. *P. ovale* infections rarely cause clinical symptoms, because of the low occurrence of parasitaemia [Miller *et al*., 1976; Oaks *et al*., 1991; Cogswell, 1992; Faye *et al*., 1998; Mendis *et al*., 2001; NIAID, 2007].

1.1.6 Life cycle of *P. falciparum*

The life cycle of the malaria parasite (figure 2) is complex and requires two hosts to complete its life cycle. The parasites alternate between female *Anopheles* mosquitos and human hosts. The human host is infected during blood feeding of infected mosquitos. Sporozoites are inoculated during this process, and migrate rapidly through the bloodstream to the liver where hepatocytes are invaded. The parasites undergo a series of asexual replications during the liver stage infection. The liver stage infection is asymptomatic, regardless of the many parasites that are generated during this phase. After some time the infected hepatocytes rupture and merozoites are released into the bloodstream. These "free" merozoites invade erythrocytes, and undergo a series of asexual replication within the host erythrocyte. After some time the infected erythrocytes rupture and merozoites are released, which infect other erythrocytes every 48 hours. The parasites feed on the globin part of haemoglobin, which is the source of amino acids. Haem, which is toxic to the parasites, is released during the feeding process. The parasites however, have developed mechanisms to detoxify haem. This by-product is polymerised by the parasites to form haemozoin, which is stored as a non-toxic complex in the parasites food vacuole. Some of the merozoites develop into either male or female gametocytes and are ingested by another mosquito vector during a blood meal. The gametocytes fuse inside the mosquito's mid-gut and form zygotes. A series of sexual replications occur inside the mosquito and sporozoites are formed, which migrate to the salivary glands of the mosquito and are released into another human host during the next blood meal [Oaks *et al*., 1991; NIAID, 2007].

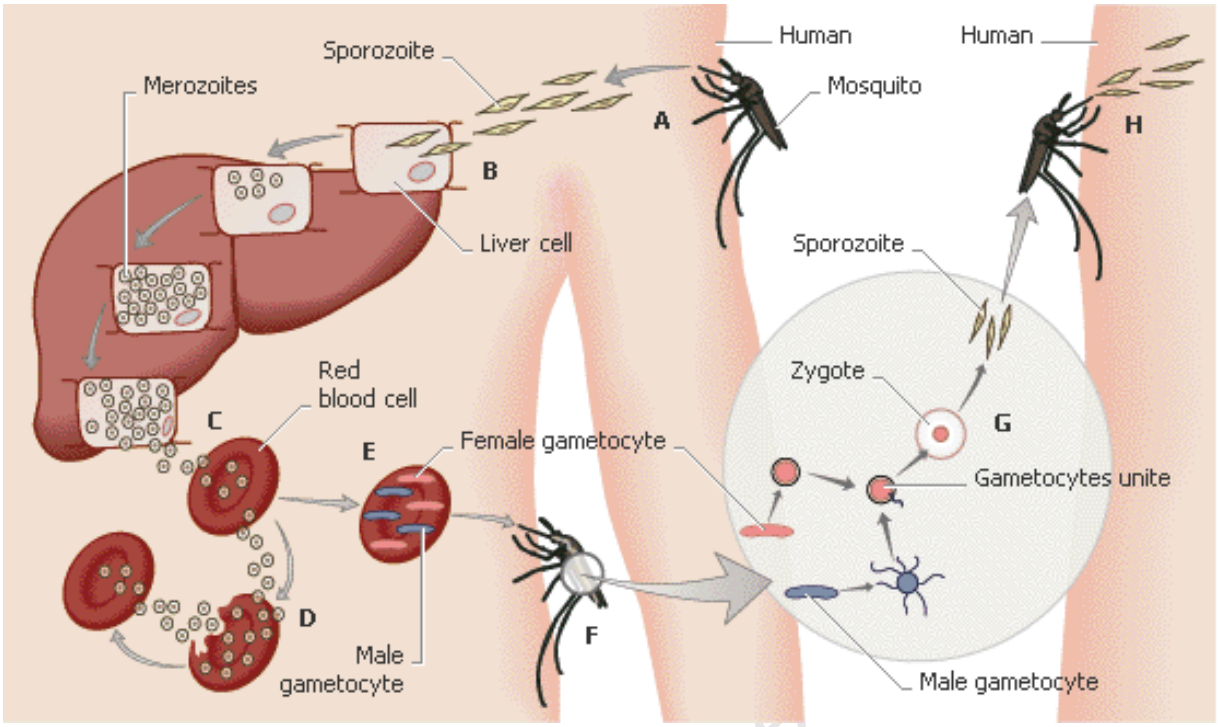

Figure 2 Life cycle of *P. falciparum* parasites [Life cycle of the malaria parasite]

1.1.7 Malaria control

People have used natural products for many centuries to control malaria, but since the development of modern science alternative methodologies and strategies have been developed to control the disease. Many different strategies are used to control the disease, including traditional medicines, antiplasmodial drugs, insecticides and bed nets. Paraffin has also been used to coat marshes to prevent the development of mosquito larvae, and many attempts have been made to drain stagnant water to keep mosquitos from breeding. Insecticides such as the chlorinated hydrocarbons (DDT and dieldrin), organophosphate compounds (malathion, fenitrothion), carbamates (propoxure), pyrethrins and pyrethroids are used to target the mosquito hosts. Mosquitos become resistant to insecticides over time, therefore insecticides are used alternately in spraying programmes. Insecticides are normally applied to the interior of houses and are very effective against some species, but are ineffective against species that stay primarily outside buildings. Outdoor spraying is the option of choice in malaria epidemic areas where mosquitos stay outside buildings, but may have an impact on environmental conditions and should be monitored closely when this control method is used [Oaks *et al*., 1991; NIAID, 2007].

1.1.8 Antimalarial drugs

A number of antimalarial drugs have been developed during modern times, which specifically target either the liver or blood stage parasites. Examples of liver stage drugs are doxycycline, proguanil and pyrimethamine. Examples of blood stage drugs are quinine, chloroquine and artemisinin. Most antimalarial drugs target the intra-erythrocytic growth stage of the parasites, thus preventing the development of the parasites [Oaks *et al*., 1991].

Antimalarial drugs can be classified into three main groups. The first group consists of the quinoline based antimalarials (figure 3), which are also the most frequently used drugs. These drugs include: quinine and its derivatives (chloroquine, amodiaquine and mefloquine). The second group includes the antifolate drugs (figure 4), which are dihydrofolate reductase inhibitors. These drugs are: pyrimethamine, proguanil, sulfonamides and sulfones. The third group (figure 5) consists of artemisinin and its derivatives: artesunate and artemether.

quinine

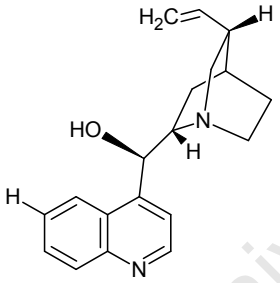

chloroquine

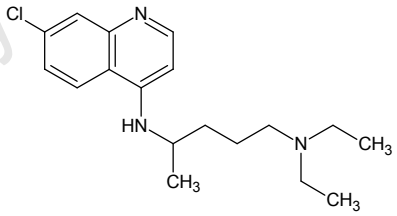

amodiaquine

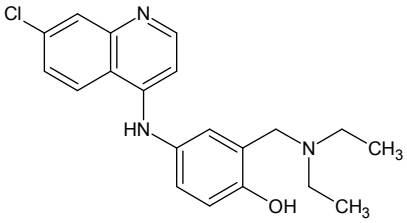

mefloquine

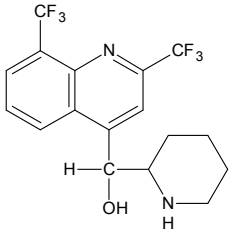

Figure 3 Chemical structures of the quinoline based antimalarials

pyrimethamine

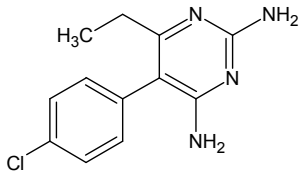

sulfadoxine

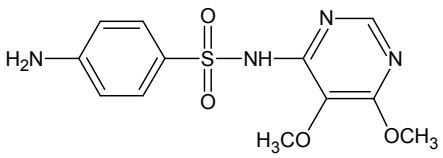

proguanil

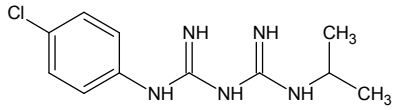

dapsone

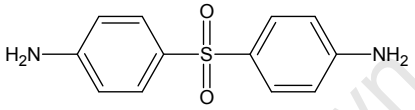

Figure 4 Chemical structures of the antifolate drugs

artemisinin

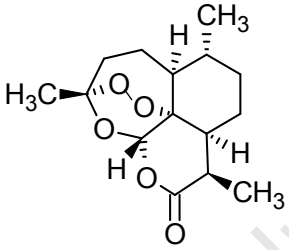

artesunate

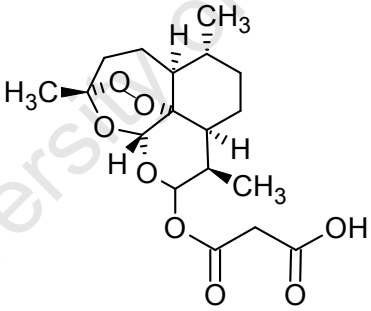

artemether

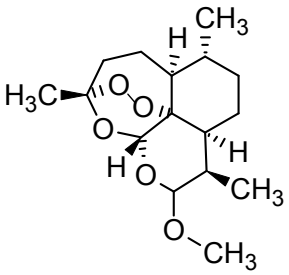

Figure 5 Chemical structures of artemisinin and its derivatives

1.1.8.1 Quinoline based antimalarials

One of the first effective treatments in modern malaria medicine was quinine, an antimalarial compound that was first isolated from the bark of the *Cinchona* tree. At present, quinine is still used as an option for second-line treatment. Chloroquine was synthesised in the 1930s as a less toxic analogue of quinine and has been used extensively as the mainstay antimalarial drug for many decades. Chloroquine is safe, cost effective and suitable for oral administration. Unfortunately, resistance of *P. falciparum* to chloroquine appeared in Thailand in 1957 and in Colombia and Venezuela in 1960.

Chloroquine resistance has now spread to most countries. It was at first restricted to the Indochinese peninsula (Asia), but spread westwards and towards the neighbouring islands in the south and east during the 1970s. Chloroquine resistance in Africa happened much later, and it took a decade to spread across the continent. Chloroquine resistance in Africa was not linked to a new mutation, but appeared due to a gradual spread from South-East Asia. Chloroquine resistant *P. falciparum* malaria has not been observed in countries of Central America and the island of Hispaniola. Chloroquine accumulates in the parasite's food vacuole, and interferes with the polymerization of toxic haem that is produced during haemoglobin digestion. This leads to parasite death due to haem poisoning. The chloroquine resistant strains (mutations of the pfct gene) accumulate less drug and are therefore better protected against haem poisoning. These strains become dominant over time under constant chloroquine pressure. The precise mode of action still remains to be understood [Mehlotra *et al*., 2001; Wellems and Plowe, 2001; World Health Organization, 2005].

Chloroquine resistance has led to the development of the synthetic analogues amodiaquine and mefloquine. Amodiaquine is more effective than chloroquine against chloroquine resistant *P. falciparum* parasites, but could lose its efficacy fast if used intensively in choroquine resistance areas. Amodiaquine was first studied as a single-drug therapy at a dose of 25-30 mg/kg, and later on as a combination treatment strategy with sulfadoxine-pyrimethamine or artesunate. Mefloquine was also introduced to many countries, but resistance occurred soon thereafter [Boudreau *et al*., 1982; Lobel *et al*., 1998; Ringwald *et al*., 1998; Rwagacondo *et al*., 2003; World Health Organization, 2005].

1.1.8.2 Antifolate drugs

Chloroquine was replaced by a combination formulation of sulfadoxine and pyrimethamine in most countries at the beginning of the 1980s. This combination treatment became ineffective in Thailand and bordering countries, because of parasite resistance. Parasite resistance against sulfadoxine-pyrimethamine treatment spread fast in South America. Malawi was the first country in East Africa to replace chloroquine with sulfadoxine-pyrimethamine as first-line treatment during the early 1990s, and other African countries followed during the late 1990s. Parasite resistance against sulfadoxine-pyrimethamine also spread relatively fast in East Africa, because of extensive use. Antifolate resistance has emerged rapidly. It takes about 2 years for the parasites to develop resistance against

antifolate drugs when used intensively at national level. Sulfadoxine-pyrimethamine kills the malaria parasite through inhibition of two successive enzymes in the biosynthesis of folic acid. Mutations in the *dhfr* and *dhps* genes are responsible for parasite resistance against sulfadoxine-pyrimethamine [Doumbo *et al*., 2000; Nsimba *et al*., 2004; World Health Organization, 2005].

1.1.8.3 Artemisinin and its derivatives

Artemisinin was first isolated from the Chinese medicinal plant *qing hao* (*Artemisia annua*) in 1971. Artemisinin contains an endoperoxide group that may be responsible for the antimalarial activity. It belongs to the sesquiterpene lactone family of compounds (figure 5). Artemisinin is poorly water and oil soluble, hence the low bioavailability after oral administration. Structural modifications were made to improve these properties and resulted in artesunate (figure 5) which is water soluble and artemether (figure 5) which is oil soluble. Artesunate can be administered intravenously and artemether intramuscularly. Artemisinin and its related analogues are effective against multi-drug resistant strains of *P. falciparum* parasites and are used to treat uncomplicated and severe forms of malaria.

The mechanism of action of artemisinin and its derivatives is not fully understood, but it seems to involve two steps. The endoperoxide bridge is initially cleaved to produce artemisinin-derived free radicals, which are strong alkylating agents. The second step involves covalent bond formation with various parasite proteins. The initial activation step appears to be catalysed by ferrous haem and free iron (Fe II), and is thought to be responsible for the selective toxicity to malaria parasites. Artemisinin and its derivatives are very potent antimalarial agents. Patients on these treatment regimens are normally clinically cured within 3 days. Low levels of resistance have been reported, and some decrease of *in vitro* sensitivity has also been reported [Zhang *et al.,* 1992; Hien and White, 1993; Meshnick, 1994; Kamchonwongpaisan and Meshnick, 1996; Krishna *et al*., 2004; World Health Organization, 2005].

1.1.9 Need for new strategies

The genetic diversity of the malaria parasite is responsible for its ability to escape adverse conditions imposed by drug therapy. Genotypes that are not affected by the drug therapy escape undamaged and pass along their resistance to its progeny. The drug sensitive genotypes die and the more drug resistant genotypes survive, as a result parasites

become resistant against drug efficacy over time. For this reason most antimalarial therapies that are used extensively have lost their efficacy over time.

Additional control measures such as vaccines and new anti-malarial compounds are urgently needed. Vaccines have proven to control other infectious diseases most cost-effectively. It has also been shown that malaria can be preventable by vaccination, both in experimental animals and humans. A significant progress has been made in the understanding of the immune mechanisms involved in malaria protection and in identifying vaccine candidate antigens and their genes during the last decade. Several new vaccines have entered Phase I/II clinical trials. Malaria vaccines are probably the best option for gaining control of malaria, but it will probably take many more years to develop [Nussenzweig and Nussenzweig, 1989; Engers and Godal, 1998; Stoute *et al*., 1998; Herrera *et al*., 2002].

New antimalarial compounds that use different mechanisms of action against the malaria parasites (compared to drugs that are currently used) are urgently needed to control the disease effectively during the next few decades. Malaria management programmes are still relying greatly on antimalarial drugs, and because of the phenomenon of drug resistance, it is essential to develop new antimalarial compounds. Traditional medicinal plants and natural products are believed to be an excellent source for new antimalarial compounds.

1.2 Traditional medicine and Traditional healing

Traditional medicine has been used to treat health problems around the world for centuries, but has not always been appreciated by modern medicine. Traditional medicines are generally prepared by traditional healers from different ethnic groups and are mainly natural medicinal plant products. A renewed interest in this field, especially from the Western world, was observed during the previous few decades, because of more people seeking alternative or complementary remedies to treat health problems. Examples of traditional remedies are: herbal medicine from many different cultures, Oriental therapies, Ayuverdic medicine, acupuncture, homeopathy and aromatherapy. These remedies have become more available, which resulted in an increasing number of traditional medicines being used globally. Western medicine has been introduced to most parts of the world for a long time, but most people, especially those from rural areas of Africa, Asia and South America still prefer to use traditional medicine for their health problems. The reason for this preference is because traditional medicine is more affordable and easily available than modern medicine. Traditional medicine has also been part of people's tradition and culture.

The preferred use of traditional medicine in developing countries could also be ascribed to traditional medicine having less adverse effects than Western medicine. Another reason may be the fact that no resistance to whole-plant extracts has been recorded. It is estimated by the WHO that 80% of the world's population still relies exclusively on traditional medicine for their physical and psychological health needs. It has also been observed that people that are living in urban areas in developing countries still consult traditional healers. Some people consult medical doctors first, but if their health condition is not resolved, traditional healers are consulted. Others do just the opposite: they consult traditional healers first, and if their health condition is not resolved, medical doctors are consulted. There are also those people that only consult traditional healers. Most of the traditional medicine knowledge is transferred verbally from one generation to the next through traditional healers [Baker *et al*., 1995; World Health Organization, 1998, 2002; Willcox and Bodeker, 2000].

There are approximately 200 000 practising traditional healers in South Africa, which is eight times more than medical doctors. Traditional healers are still consulted by about

80% of the black South African population, because of the high cost of modern medicine, as well as the unavailability of medical infrastructure in rural areas. It also has much to do with cultural background and believe. It is also believed by many South Africans that disease is caused by a supernatural phenomenon, which involves ancestral spirits, social relations or the environment. The traditional healers can relate to peoples cultural and believe backgrounds and treat them accordingly. They are also highly appreciated in their communities and are often seen as leaders. In the South African context, which is rich in cultural diversity, traditional healers are described as people who are practising indigenous medicine.

There are three main groups of traditional healers within the Zulu, Xhosa and Sotho communities. The first group refers to the herbalists (90% male) who have an extensive knowledge about medicinal herbs and plant derived medicines (Zulu: inyanga, Xhosa: ixwele, Sotho: nqaka). The second group refers to diviners (90% female) who integrate ancestral spirits and supernatural forces into their healing rituals (Zulu: isangoma, Xhosa: amagquira, Sotho: dingaka). The third group refers to faith healers in the Zulu community of a Christian denomination and heal through religious intervention and prayer. They are known as umthandazi. There are also traditional healers within the Khoi-San communities of the Kalahari and descendants of the Dutch settlers [Edwards, 1986; Kale, 1995; De Wet, 1998; Cocks and Moller, 2002].

1.3 Medicinal plants

1.3.1 Global perspective

Higher plants form the basis of traditional medicine, and were once the major source of medicines in the world. A few examples of medicinal plants that were used during ancient times are: *Papaver somniferum* (poppy juice), *Commiphora* species (myrrh), *Glycyrrhiza glabra* (liquorice), *Cupressus sempevrens* (cypress) and *Cedrus* species (cedar). These plants are still used today to treat a range of health conditions. It is estimates that about 20 000 species of higher plants are currently being used globally to treat health conditions [Akerele, 1993; Phillipson, 1994; Baker *et al*., 1995; Cragg and Newman, 2001].

1.3.2 Local perspective

Medicinal plants are part of the daily lives of many South Africans and are an important part of its indigenous knowledge. Extracts from these plants have been used to treat infectious diseases and other health problems for many centuries. The medicinal plant knowledge is transferred verbally from one generation to the next, which increases the risk of losing this knowledge. Nowadays, much of this knowledge gets lost because of the fast tempo of urbanization and acculturation.

South Africa is rich in species diversity with more than 30 000 species of higher plants recorded, which is about 10% of the earth's plant diversity. The Cape Floral Kingdom alone has more than 9 000 species. South Africans use about 3 000 species as medicines, and about 350 of these are the most commonly used. The most frequently used medicinal plants of South Africa are described in Medicinal Plants of South Africa and Zulu Medicinal Plants, and it is also noted that relatively little scientific work has been done on the medicinal plants of South Africa. The market value of the informal and commercial trade in medicinal plants was estimated in 1998 at about 60 million American dollars per year, which is significant in the broader South African economic context. Conservation measurements had to be implemented due to the unsustainable and uncontrolled harvesting activities of many of the popular medicinal plants. Some of these species are being cultivated to reduce the stress on natural populations. South Africa's medicinal plants are extremely important potential sources of new therapeutic agents or starting materials for drug synthesis. South Africa's natural product contribution to world medicines are: buchu (*Agathosma betulina*), Cape aloes (*Aloe ferox*) and devil's claw

(*Harpagophytum procumbens)* [Mander *et al*., 1995; Mander 1998; Coetzee *et al*., 1999; Van Wyk *et al*., 2002; Hutchings *et al*].

1.3.3 Plant-derived drugs

Medicinal plant extracts that are used in traditional medicine contain many components that are thought to contribute to the overall healing effect. In modern medicine the illness is mostly targeted by a single specific active ingredient. The foundation for the isolation of pharmacologically active compounds from medicinal plants was laid in 1804 when morphine was isolated from *Papaver somniferum* L. (Opium) [Farnsworth, 1984].

Traditional herbal medicine is thought to be a good source for potential pharmacological active compounds, because of extensive screening that took place over many years. Scientific evidence also indicated a favourable correlation between biological activity and traditional use. Bioactive natural products and their chemically modified derivatives are still presenting more than 50% of all clinically used drugs, worldwide. The higher plants contribution is about 25%. Some well known examples of plant-derived drugs are: Digoxin (atrial fibrillation), isolated from *Digitalis purpurea*; Morphine (analgesic), isolated from *Papaver somnifernum;* Ephedrine (bronchodilator), isolated from *Ephedra sinica;* Quinine (antimalarial), extracted from the bark of *Cinchona* species; Vincristine (anticancer), obtained from *Catharanthus roseus;* Atropine (anticholinergic), obtained from *Atropa belladonna;* Reserpine (antihypertensive), isolated from *Rauwolfia serpentine;* Salicylic acid, isolated from the bark of the *Salix* species; Taxol (anticancer), isolated from the *Taxus* species; and Artemisinin (antimalarial), extracted from *Artemisia annua* [Farnsworth, 1990; Akerele, 1993; De Smet, 1997; Newman *et al*., 2003; Newman and Cragg, 2007].

1.4 Natural products and malaria medicine

Humanity has used local natural products for the treatment and prevention of malaria for many centuries. More than 1200 plant species are currently used throughout the world to treat malaria. These medications are available where modern drugs are not. At present up to 75% of patients choose to use traditional medicines to treat malaria. Traditional antimalarial medicines present a good and reliable source for the discovery of novel antimalarial compounds that could be developed into new drugs. Several antimalarial drugs have been discovered from natural products, and some of these have been chemically modified to improve drug efficacy. The two most important discoveries from plants were quinine from *Cinchona* species and artemisinin (qinghaosu) from *Artemisia annua*. The discovery of these two compounds has been a milestone in the history of modern medicine for malaria [Willcox and Bodeker, 2004].

1.4.1 *Cinchona*

Cinchona bark has been used to treat malaria for many centuries. It is safe, effective and affordable and will probably be in use for many years to come. *Cinchona* belongs to the Rubiaceae family and comprises of 23 species. *Cinchona* is indigenous to South America, but is cultivated in many tropical countries today. The most important *Cinchona* species are: *Cinchona ledgeriana*, *Cinchona officinalis* and *Cinchona succirubra*. Many claims were made about the discovery of *Cinchona* bark for the treatment of malaria but it is not clear who made the original discovery. Alkaloids were discovered in the bark of *Cinchona* plants at the beginning of the 19th century. French chemists, Pierre Pelletier and Joseph Caventou discovered the first two alkaloids and named the first cinchonine and the second quinine. Today, about thirty alkaloids have been isolated from *Cinchona* species and some of these have good antiplasmodial activity [Andersson, 1998; Karle and Bhattacharjee, 1999]. Examples of the most well-known *Cinchona* alkaloids are presented in figure 6.

Quinine and quinidine have excellent pharmacokinetic properties with low toxicity and are regularly used to treat malaria patients. Scientific evidence also confirms that extracts from *Cinchona* bark are as effective as quinine for the treatment against *P. falciparum* and *P. vivax* parasites. A period of synthetic organic chemistry followed after the discovery of quinine and its related antiplasmodial alkaloids. The molecular scaffold of quinine was

used as a template for synthesizing quinine derivatives. A number of useful aminoquinoline-based antimalarials were developed into synthetic antimalarial drugs. Examples of these drugs are: pamaquine, chloroquine, amodiaquine, pentaquine, primaquine, and mefloquine [Kofoed *et al*., 1999; Kofoed *et al*., 2002; Willcox *et al*., 2004].

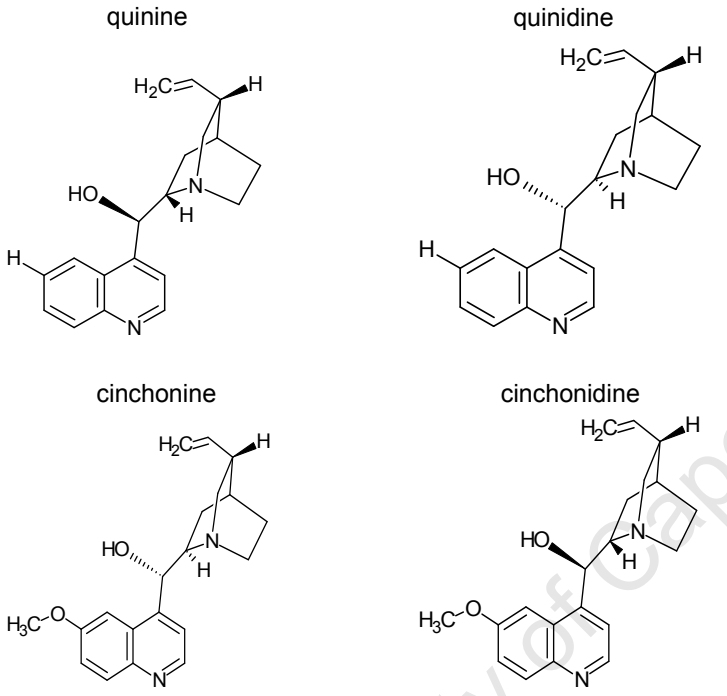

Figure 6 Examples of the most well-known *Cinchona* alkaloids

1.4.2 *Artemisia annua*

Artemisia belongs to the Asteraceae family and comprises over 400 species. Artemisinin was originally isolated from *Artemisia annua* in China (1971), and was also found in two other species: *Artemisia lancea* and *Artemisia apiacea*. It is not clear where the genus name *Artemisia* originated from. Ferreira believes the genus is named after the Greek goddess Artemis which means "she who heals sickness". Bruce-Chwatt believes that the genus *Artemisia* was named after Queen Artemisia of Caria (Turkey). *A. annua* is the only member of the *Artemisia* genus with an annual cycle, therefore the species name *annua*. *A. annua* has been used as a medicinal plant for many years, the earliest record dating back to 168 BC. Li Shizhen has described the use of *A. annua* for malarial fever treatment in 1596 [Bruce-Chwatt, 1982; Ferreira *et al*., 1997; Tan *et al*., 1998; Willcox *et al*., 2004].

1.5 Drug discovery and development

1.5.1 Introduction

Many of the drugs used today have been isolated from natural products, and some have been chemically modified. Natural products have been used by many cultures around the world to treat disease for a very long time, even before written history was recorded. Early scientists found that the bioactivity from crude plant extracts could be reproduced by isolating constituents from the same extract. This discovery laid the foundation of the modern scientific presentation of orthodox pharmaceuticals. During most of the twentieth century the pharmaceutical industry shifted their focus to synthetic molecules, and has not taken plant extracts and the potential of the natural world to provide new biological active compounds seriously. There was an unexpected shift back to traditional medicine during the last 20 to 25 years, because of worldwide interest in herbal medicine. Plant derived extracts are now recognised by modern science as a potential source for new active chemical entities [Houghton and Raman, 1998].

1.5.2 General approach in drug discovery and development

A general methodology approach in drug discovery and development is presented in figure 7, which contains four major research areas namely *in vitro* studies, animal testing, clinical testing and marketing. Drug discovery and development is a complex and expensive process. The cost to develop a new drug ranges between 150 - 800 million US dollars and takes on average twenty years to reach the market. The initial step is the discovery of new compounds, either from biological products or from organic synthesis, and to screen these compounds against *in vitro* models. The active compounds are then taken further in animal testing (toxicity, safety, efficacy, selectivity, mechanism, metabolism and pharmacokinetics). The pre-clinical compounds then enter clinical testing in phase I, II and III studies. The final step is marketing of the new product where post marketing surveillance takes place. Generic products become available twenty years after the original filing of application occurred [Katzung, 2004].

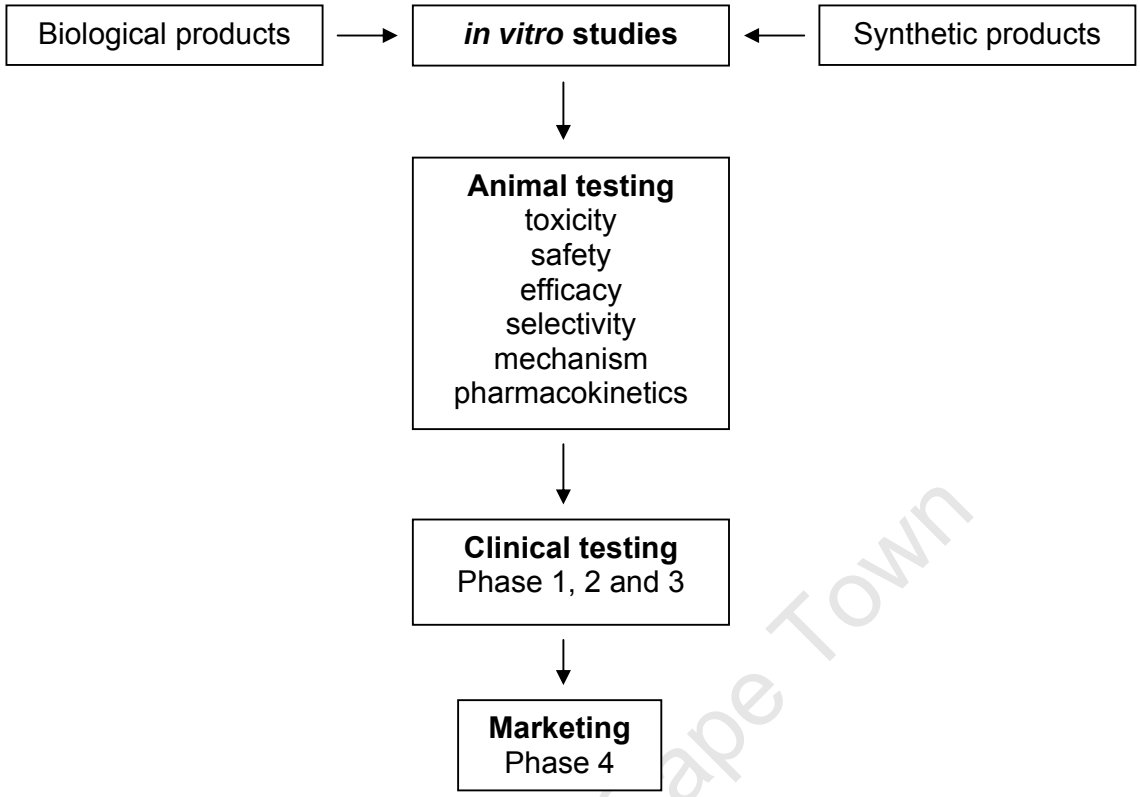

Figure 7 Flow-diagram of the general drug discovery and development process

1.5.3 Stages in drug discovery

Drug discovery and development requires different stages (figure 8). This process begins with screening compounds against biological targets or whole organisms. Compounds that show *in vitro* bioactivity are defined as hits. These hits can be considered for further testing in animal models of the disease. During this early development stage the compound's pharmacokinetic properties are also investigated in the same animal model. Compounds that are active in the animal model with good quality pharmacokinetic properties are defined as leads. The lead compounds then undergo a series of optimization and efficacy studies to prove good pharmaceutical properties. Once the lead reaches a stage where it can be considered for testing in humans it is defined as a drug candidate. The drug candidate then enters preclinical testing and finally clinical testing in proper drug development platforms [Nwaka and Ridley, 2003].

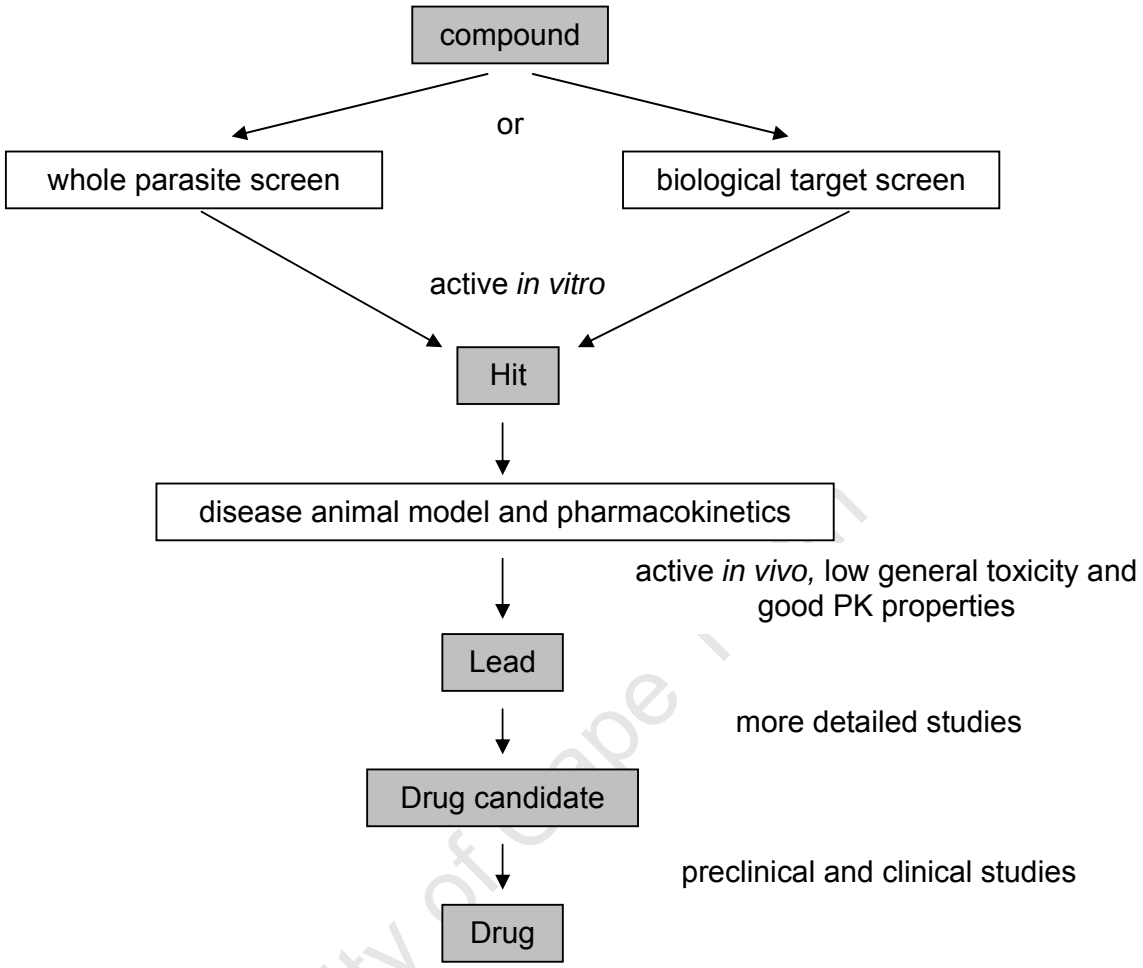

Figure 8 Flow-diagram of the different stages in drug discovery

1.5.4 Approaches in drug discovery

Fundamental approaches in drug discovery can be classified as short to medium term and long term processes. The short to medium term approach is the exploitation of known compounds or compound classes. For example: combinations of existing drugs, which offer possibilities of reduced toxicity; shorter treatment regimens; slower development of resistance and synergy; and new indications for existing drugs, which offer major savings. This approach has been shown to be very successful in the antiparasitic drug development platform and has delivered many drugs that are currently in use. The long term approach requires the discovery of new compounds or compound classes. For example: improvement to known drugs and compound classes, by making use of chemical modification and organic synthesis, and focused sample collection, where large libraries of

compounds are screened against whole organisms to discover new active compounds that are unrelated to known compounds. The search for novel active compounds in natural products, especially medicinal plants, is considered attractive because of their structural diversity [Mpia and Pepin, 2002; Rosenthal, 2003; TDR, 2003; Kremsner and Krishna 2004].

1.5.5 Challenges in antiparasitic drug discovery

Many of the drugs that are used to treat antiparasitic diseases have been introduced decades ago and are far from ideal. The markets have been unsuccessful in facilitating the discovery and development of new antiparasitic drugs during recent years. During 1975 and 1999, 1300 new drugs were introduced for all indications, but only 13 were for antiparasitic diseases. The discovery and development of antiparasitic drugs is not more expensive or technically difficult than for other diseases. The estimated cost of bringing a new antimalarial to the market is estimated at 300 million US dollars. The average cost of each new drug for other diseases is about 500 million US dollars. The discovery and development of antiparasitic drugs is not commercially driven. Many of the drugs used to treat these tropical infectious diseases have previously been used for other indications. Today the picture is more optimistic, as many new partnerships have been established between the public and private sectors. New funds were introduced for antiparasitic drug discovery by generous organisations, like the Bill and Melinda Gates foundation. Examples of public-private partnerships are: Medicines for Malaria Venture, Drugs for Neglected Diseases and the Institute for One World Health [Trouiller, 2002; Medicines for malaria venture; Nwaka and Ridley, 2003; Kettler and Marjanovic, 2004; Ridley 2004].

1.6 Antiplasmodial evaluation of plant derived products

1.6.1 Introduction

The clinical efficacy of herbal antimalarials is often questioned and debated by the scientific community. There are probably two complementary approaches that can be followed to validate the clinical effectiveness of herbal antimalarials: firstly, by conducting clinical trials and secondly, by performing biological *in vitro* and *in vivo* testing. Unfortunately, inconsistencies are often experienced when laboratory findings are compared with field studies. The complexity of the *Plasmodium* life cycle makes it difficult to select appropriate laboratory models; however four stages of the parasites life cycle could be targeted and are described in 1.6.3.1.

1.6.2 Traditional medicine as sources of antiplasmodial compounds

Plant derived traditional medicine has developed over many years and is in general accepted as a good source for potential pharmacological active compounds. More than 1200 plant species are used to treat malaria and can be categorized in three groups: Firstly, plants which directly inhibit parasite development at either the erythrocytic stage or the hepatic stage. The second group consists of plants that affect host-parasite relationships for example immunostimulants and antipyretics. The third group has no clear effect on malaria, but may probably have a psychosomatic effect (ethnomedical beliefs). Much progress have been made during the last few years in our understanding of the biology and biochemistry of the malaria parasite and it has also been shown that the erythrocytic stage of the *Plasmodium* parasite is the most important target in malaria chemotherapy. It is therefore suggested that traditional medicine be evaluated for its ability to inhibit parasites in the blood stage, as well as in the hepatic stage of parasite development [Olliaro and Goldberg, 1995; Rasoanaivo, 2002].

1.6.2.1 Plant material

The biological identity of the plant material must be verified by a professional taxonomist and voucher specimens of the plants must also be kept at the organization where the work is performed or should be kept at an officially recognized herbarium. The details of the plant harvesting conditions must be recorded, such as the time of collection, season, and stage of the plant development. The plant parts that are collected must be the same as the material that is used in the traditional preparations. The plant material is generally air-

dried at room temperature and is also protected from direct sunlight. The dried material is then macerated to a fine powder using a blender and kept at -20 °C in the laboratory until extraction. In some cases the material is processed fresh to prevent enzymatic degradation or hydrolysis. It is also important to make sure that the plant material is not contaminated with other plant material that grows nearby. The plant material should also be inspected for viral, bacterial or fungal infections. Such infections may alter the metabolism of the plant and unexpected products could be formed [Houghton and Raman, 1998].

1.6.2.2 Ethnopreparation-based extraction

Leaman and co-workers showed that the degree of local consensus about a given remedy is a good indicator of its potential biological efficacy. They conducted a study on malaria remedies derived from natural sources of the Kenyah civilization, which live in the highland forests of Kalimantan (Indonesian Borneo) and Sarawak (Malaysian Borneo). These people have developed 17 local plant-derived remedies to treat malaria. The results from Leaman's study confirmed the rational selection and use of traditional remedies for malaria by the Kenyah people [Leaman *et al*., 1995].

It is observed in the scientific literature that the traditional healer's recipes, for preparing these tradition medicines, are often ignored in medicinal plant evaluation programmes. The ethno-based extraction methodology approach is strongly recommended for the evaluation of traditional medicines in antimalarial drug discovery and development programmes. The plant extracts should be prepared in exactly the same way as described by the healers, and it is therefore important to consult the healers before extraction is performed.

1.6.2.3 Solvent extraction

The recipes for preparing traditional antimalarial remedies are not always available, or described in the medicinal plant literature. Therefore, scientists have to rely on other extraction methods to evaluate such plant products for their efficacy and safety. There are many different solvent extraction approaches described in the literature. The conventional approach is to separate compounds according to their polarity into groups. Non-polar solvents, such as petroleum ether, cyclohexane, heptane or hexane are firstly used to "defat" the plant material. The non-polar plant constituents are extracted with these non-

polar solvents. Hexane is usually avoided because of its toxicity and flammability. The remaining plant material is then extracted with organic solvents of increasing polarities, such as dichloromethane and ethyl acetate. Thereafter, the residue is extracted with methanol or ethanol and finally with water. This approach is based on the Roman principle of solubility: *similia similibus solvuntur* (the similar dissolves the similar) [Gessler *et al*., 1994; Houghton and Raman, 1998].

Another approach is to use mixtures of ethanol and water to selectively target the more polar compounds [Munoz *et al*., 2000]. Simonsen and co-workers also showed that ethanol can be used to successfully extract more polar compounds from plant material [Simonsen *et al*., 2001]. Alcohol extraction with a Soxhlet apparatus has been used for various parts of antimalarial plants. [Sharma and Sharma, 1999] This methodology approach is avoided by many groups because of the risk of alternating labile constituents.

Alternative extraction methods are: percolation, infusions with hot solvents, reflux extraction, steam distillation, supercritical fluid extraction and many more industrial processes. The extraction process is usually followed by clean-up techniques to separate compounds of interest from unwanted substances. Examples of these techniques are: filtration, precipitation, size exclusion chromatography, solvent partitioning, normal phase chromatography and reverse phase chromatography [Houghton and Raman, 1998].

1.6.2.4 Bioassay-Guided fractionation

The number of plants with confirmed antiplasmodial activity could be significantly increased if the plants are subjected to fractionation before screening. It has also been suggested that plants with moderate antiplasmodial activity should be allocated for bioassay-guided fractionation. There are a few fractionation methods described in the literature, i.e. solvent partitioning, countercurrent distribution, solid-liquid column chromatography and preparative HPLC. Continuous screening for antimalarial activity is performed with all the fractions, and the active fractions are taken further in the fractionation and purification process. [Statz and Coon, 1976; Samuelson *et al*., 1985; Samuelson 1987; Galeffi *et al*., 1997; Houghton and Raman, 1998; Rasoanaivo, 2002; Willcox *et al*., 2004].

1.6.3 Antimalarial bioassays

The worldwide antimalarial drug discovery and development community have developed a number of *in vitro* and *in vivo* screening models for the evaluation of plant extracts and compounds for their antimalarial efficacy and safety, during the last few decades. The focus of these programmes has been on the erythrocytic stage of the parasites development; however, three more targets have been added to these *in vitro* screens.

1.6.3.1 *In vitro* antiplasmodial assays

The first target is the asexual erythrocytic stage, which is mostly targeted by scientists because of the availability of this screening model in many laboratories. The asexual stage *P. falciparum* parasites is maintained in continuous culture and a parasite lactate dehydrogenase assay is used to determine parasite viability [Trager and Jensen, 1976; Makler *et al*., 1993].

Numerous *in vitro* antiplasmodial activity studies, which target the asexual erythrocytic stage, have been carried out on plant extracts and compounds. These screening systems have been used very successfully in evaluating plant extracts and compounds for bioactivity against the erythrocytic stage of the parasites. Two examples of such studies are presented below.

Fischer and co-workers have studied the *in vitro* antiplasmodial activity of nine Brazilian plant species. Six species were selected from the Annonaceae family, two from Menispermaceae and one from Siparunaceae. Ethanol and "alkaloid" extracts were prepared and screened against chloroquine-sensitive and chloroquine-resistant strains of *P. falciparum*. Most of the "alkaloid" extracts were more active than the ethanol extracts. The IC_{50} values, for both strains were between 0.3 - 8.2 µg/ml. The alkaloid extract of *Guatteria australis* was the most active against K1, with an IC_{50} value of 0.3 µg/ml. The screening of these nine plants resulted in 6 potential lead extracts that should be considered for further antiplasmodial bioassay-guided fractionation [Fischer *et al*., 2004]

Chukwujekwu and co-workers have isolated an active antiplasmodial compound from a petroleum ether extract of the leaves of *Hyptis suaveolens*, with an IC_{50} value of 0.1 µg/ml (tested against a chloroquine sensitive D10 strain). Bioassay-guided fractionation resulted

in the isolation of the active, abietane-type diterpenoid endoperoxide, 13α-epi-dioxiabiet-8(14)-en-18-ol [Chukwujekwu *et al*., 2005]

The second target is the hepatic stage of the *Plasmodium* parasites. The hepatic stage *Plasmodium* parasites can also be maintained in culture. This, relatively new methodology has opened up many new strategies in antimalarial research programs. Presently, only tafenoquine and primaquine are used as antirelapse and prophylactic agents. These drugs have shown haematological toxicity and are therefore not ideal drugs. Atovaquone is also used as a hepatic stage inhibitor, but is not an effective antirelapse agent. It is essential to develop new, more effective anti-hepatic stage drugs, because of the following reasons: Firstly, prophylactic drugs prevent parasites from reaching the blood. Secondly, it is commonly accepted that only a few sporozoites are injected into human hosts by Anopheles mosquitos during infection. The probability for mutant hepatic phase parasites emerging under drug pressure is much less compared to the blood stage parasites. It is therefore unlikely that resistance will develop against hepatic stage drugs. This stage of the *Plasmodium* parasites development is an important and attractive target and will play a major role in future antimalarial drug development programmes. Thirdly, more effective antirelapse compounds could prevent recrudescence of *P. vivax*, which causes about 80 million clinical cases annually [Mazier *et al*., 1984, 1985; Marussig *et al*., 1993; Shanks *et al*., 1998; Basco *et al*., 1999; Mendis *et al*., 2001].

The third target is an antidisease screening approach for cerebral malaria. *P. falciparum* infected red blood cells that stick to the endothelium of micro vessels are responsible for cerebral malaria. The adhesion of infected erythrocytes to the endothelium leads to an overexpression of different mediators such as cytokines, which add to the pathology. Compounds that would interfere with adhesion of infected erythrocytes to endothelial cells might be of interest. Two enzyme linked immunosorbent assays (ELISA) have been developed to screen compounds for potential anti-cerebral malaria activity [Muanza *et al*., 1996; Salgame *et al*., 1997; Pino *et al*., 2003].

The fourth target is the sexual erythrocytic stage, which is asymptomatic (similar to the hepatic stage). However, prevention of gametocyte formation would prevent parasite transmission to mosquitos. This target is especially important in parasite genomes which carry drug resistant alleles. Rodent models and *in vitro P. falciparum* screening models

have been established to target this stage of parasite development [Ramakaran and Peters, 1970; Hogh *et al*., 1998].

1.6.3.2 Cytotoxicity assays

The next phase is to investigate the general cytotoxicity of extracts or compounds that have shown good antiplasmodial activity. These tests are performed to determine the potential of an extract or compound to selectively inhibit parasite growth without damaging host cells.

The selectivity index was introduced to evaluate an extract or a compound's specificity to parasite cells, and is defined as the ratio of the IC_{50} cytotoxicity to the IC_{50} antiplasmodial activity. These selectivity index values are used as a guide in selecting plant extracts or compound for further examination (the higher the value, the better the selectivity to the malaria parasites). There are several methods available for performing cytotoxicity tests and are described by Husoy and co-authors [Husoy *et al*., 1993].

A few examples of studies that incorporate cytotoxicity testing for extract or compound evaluation are presented below.

Kanokmedhakul and co-workers have isolated a novel, 1,3-dihydroxy-2-methyl-5,6-dimethoxyanthraquinone and six other known anthraquinones, a β-sitosterol, and two known triterpenoids from the roots and stems of *Prismatomeris fragrans*. These compounds have been evaluated for their antiplasmodial, antituberculosis, antifungal and anticancer cell properties. The antiplasmodial assay showed that only β-acetylolean-12-en-28-olic acid exhibited moderate antimalarial activity (IC_{50} value of 5.9 µg/ml against K1, which is a multidrug resistant *Plasmodium falciparum* strain). This compound also showed moderate cytotoxicity to a NCI-H187 cell line (IC_{50} value of 9.4 µg/ml) [Kanokmedhakul *et al*., 2005].

Otshudi and co-authors studied the antimicrobial, antiplasmodial and cytotoxic properties of four bisbenzylisoquinoline alkaloids, i.e., cycleanine, cycleanine-N-oxide, isochondodendrine and cocsoline. These alkaloids were isolated from roots of *Epinetrum villosum* (Exell) Troupin, which belongs to the Menispermaceae family. Isochondodendrine was the most active compound against FcB1, a chloroquine resistant,

P. falciparum strain, with an IC_{50} value of 0.2 µM (which correlated well with quinine's IC_{50} value, which was 0.21 µM). This compound also showed a favourable selectivity index value of 175. Cocsoline was the second most active compound, with an IC_{50} value of 0.54 µM. The selectivity index value of this compound was 9.3, which indicates some degree of toxicity [Otshudi *et al*., 2005].

Zirihi and co-workers have studied the antiplasmodial activity and cytotoxic affect of four steroidal alkaloids (holarrhetine, conessine, holarrhesine and isoconessimine) that were isolated from an ethanol extract of the stem bark of *Funtumia elastica*. Bioassay-guided fractionation of the ethanol extract was performed to obtain the antiplasmodial compounds. The compounds were screened against an FcB1, which is a chloroquine-resistant, *P. falciparum* strain, and showed IC_{50} values ranging from 0.97 to 3.39 µM. These compounds were also screened against a rat L-6 cell line to determine their general toxicity, and showed weak cytotoxicity, ranging from 5.13 to 36.55 µM [Zirihi *et al*., 2005].

De Mesquita and co-workers have studied the antiplasmodial activity of 27 species of native Brazilian Cerrado plants, which are commonly used by traditional healers to treat malaria and other diseases. Hexane and ethanol extracts from various parts of the plants were prepared and screened against an FcB1, a chloroquine resistant, *P. falciparum* strain. Sixteen of these extracts showed good antiplasmodial activity against FcB1, with IC_{50} values below 10 µg/ml. Some of these extracts were also tested for general toxicity against L-6 cell lines of rats and MRC-5 cell lines of humans. Four of these extracts showed selectivity index values above 10, which could be considered for further antiplasmodial evaluation [de Mesquita *et al*., 2007].

Pillay and co-workers have studied the antiplasmodial activity of *Oncosiphon piluliferum*, which belongs to the Asteraceae family. They have isolated sesquiterpene lactones of the germacranolide and eudesmanolide type through conventional chromatographic techniques and bioassay-guided fractionation. They have also studied the antiplasmodial and cytotoxicity activities of these compounds. Five of these compounds showed good antiplasmodial activity against the D10, chloroquine sensitive, *Plasmodium falciparum* strain, with IC_{50} values between 0.4 and 4.4 µg/ml. These compounds were also screened against Chinese Hamster Ovarian cells and showed to be toxic to these cells at similar concentrations. [Pillay *et al*., 2007].

These above mentioned studies illustrate the value of performing cytotoxicity testing on extracts or compounds with good antiplasmodial properties. These screens are used to select active, as well as selective antiplasmodial extracts or compounds in antimalaria drug discovery and development programmes.

1.6.3.3 *In vivo* antiplasmodial assays

The most active and selective extracts or compounds are normally selected for *in vivo* antiplasmodial evaluation during the early stages of drug development, however studies on this subject are limited, especially for plant derived pure compounds. The reference test for blood schizontocidal activity of plant extracts or compounds is the Peters 4-day suppressive test on mice infected with *Plasmodium berghei* Anka parasites, and a few variations on this method have developed during the years. The plant extract or compound is administered to *P. berghei* infected mice as described by Peters and co-workers, and is evaluated according to the reduction in parasitaemia [Peters *et al*., 1975].

A few examples of studies that have included *in vivo* antimalarial testing for extract or compound evaluation are presented below.

Muthaura and co-workers have studied the antiplasmodial activity and cytotoxicity of methanolic and water extracts of five medicinal plant species that are used for malaria treatment by the Kwale people in Kenya. They have also studied the *in vivo* activity of these extracts in a *P. berghei* mouse model. Four of the plants showed good, selective activity against the D6, chloroquine sensitive, strain, with IC_{50} values below 10 µg/ml. The water extract of *Maytenus undata* showed to be the most promising extract, with an IC_{50} value of 0.95 µg/ml against D6, and 1.90 µg/ml against W2 (chloroquine resistant strain). The selectivity index value of this extract was also favourable, which indicates selective inhibition of the malaria parasites. At least one of the extracts of all the plant species showed good *in vivo* activity in a murine model of *P. berghei* infected mice. This study shows the value of *in vitro* (antiplasmodial and cytotoxicity) and *in vivo* examination of plant extracts to evaluate their potential as sources of antimalarial compounds [Muthaura *et al*., 2007].

Ojo-Amaize and co-workers have isolated hypoestoxide (a diterpene) from *Hypoestes rosea*, which is an indigenous Nigerian plant. This species belongs to the Acanthaceae

family. They have studied the *in vitro* and *in vivo* antiplasmodial activity of this compound. The *in vitro* activity of hypoestoxide against *P. falciparum* parasites was relatively weak, with an IC_{50} of 10 µM (IC_{50} of chloroquine was 0.11 µM). They also showed that the dose required to reduce parasitaemia by 90% in *P. berghei*-infected mice, is much lower than standard antimalaria drugs (SD_{90} = 250 µg/kg versus 5 mg/kg for chloroquine) [Ojo-Amaize *et al*., 2007].

This compound showed relatively poor *in vitro* activity, and excellent *in vivo* activity. These rather unexpected *in vivo* results should be explored further.

Portet and co-workers have isolated four monoterpene or prenyl-substituted dihydrochalcones, and the following known compounds: 2',6'-dihydroxy-4'-methoxydihydrochalcone, linderatone, strobopinin, adunctin E and (-)-methyllinderatin from the leaves of *Piper hostmannianum* var. *berbicense*. The compounds were screened against F32, which is a chloroquine sensitive *P. falciparum* strain, and FcB1, which is a chloroquine resistant *Plasmodium falciparum* strain. (-)-Methyllinderatin was the most active antiplasmodial compound against both strains. These compounds were also tested for cytotoxicity against a human cell line, MCF7. The selectivity index values of (-)-methyllinderatin, against F32 and FcB1, were 12.2 and 13.0, respectively, which indicate relatively good selectivity for the malaria parasites. The *in vivo* activity of (-)-methyllinderatin was also studied in a *Plasmodium oinckei petteri* mice model, and an 80% reduction of parasitaemia at a dose of 20 mg/kg/day was observed [Portet *et al*., 2007].

These above mentioned studies are the first step in animal testing of good, selective *in vitro* antiplasmodial compounds or extracts, and are used to evaluate the efficacy *in vivo*.

Milligram quantities of test material are needed for these *in vivo* efficacy tests, which poses a great challenge for phytochemists. The isolation of antiplasmodial pure compounds from plant extracts is a time consuming and expensive task, especially if the compound of interest is only present in low amounts. Many of the antimalarial drug discovery and early drug development programmes are carried out at academic and governmental institutions, with limited resources, which may be the explanation for the relatively few publications in this field. It is often observed that *in vivo* efficacy testing is only performed in polar chemical environments, which is not always the best method of testing compounds in

animal models. Compounds should be evaluated for efficacy in animal models in an optimised chemical environment, which leads to the subject of formulation. The test compound should be available at the target site at high enough levels to have a chance to inhibit parasite growth.

The intention of the *in vivo* phase of this project is to illustrate the importance of conducting bioavailability and metabolic testing, in the same animal model that will be used for efficacy testing, before *in vivo* efficacy testing is performed. This approach should give the investigator a better understanding about the chemical properties of the test compound in a complex animal model. This approach will also require less starting material for initial bioavailability and metabolic studies. It should also assist with the decision making process regarding which compounds should be taken further in the early drug development process, which will require relatively high amounts of the test compound.

Bioavailability and metabolic evaluation of active *in vitro* compounds is one of the most important secondary screening procedures in drug development and should also be included on a larger scale in preliminary antimalarial screening programmes. Literature on this subject is limited; however, a few examples of pharmacokinetic studies in mice are presented next (other research fields):

Bryant and co-workers have shown that pharmacokinetic screening for the selection of new drug discovery candidates could be greatly enhanced through the use of liquid chromatography-atmospheric pressure ionization tandem mass spectrometry. They have compared the time required to develop a conventional GC-NPD method with a new LC-MS/MS method, and have reported that it takes about 3 weeks to develop a GC-NPD method, and 1 week to develop an LC-MS/MS method. LC-MS/MS methods could be developed in less time compared to conventional methods, and are also more selective and sensitive analytical detection systems [Bryant *et al*., 1997].

Feng and co-workers have developed and validated a highly sensitive Electrospray LC-MS/MS assay for the analysis of a bradykinin antagonist polypeptide B201 (NSC 710295) in mouse plasma. They have used a Finnigan LCQ ion trap mass spectrometer as a detection system, which was set in the selected reaction monitoring mode. The transitions of the ions were: *m/z* 938.9^{3+} to 816.0^{2+} for B201, and m/z 674.3^{2+} to 665.7^{2+} for the

internal standard. A C_{18} solid phase extraction method was developed to extract B201 and the internal standard from plasma, 200 µl of sample was used (plasma from four animals per time point was pooled). Chromatography was performed on a reverse phase C_8 column, using a gradient mobile phase which consisted of TFA in water and acetonitrile. They have used the assay method to study the pharmacokinetics of B201 in mice. A preliminary two-compartment model was constructed. Bioavailability was poor, only 1%. This study shows that LC-MS/MS assays can be used to quantify "test compounds", in the low nanogram per ml concentrations, in mouse blood. This study shows the ability to develop very sensitive and selective analytical methods that can be used for pharmacokinetic studies of "test compounds" in mice [Feng *et al*., 2002].

Jia and co-authors have developed a high-throughput LC-MS/MS system, which was used for pharmacokinetic screening of three anti-tubercular ethambutol analogs in human, dog, rat and mouse plasma. They developed a protein precipitation method (using acetonitrile) to extract the compounds of interest from the plasma samples (200 µl). Chromatography was performed on a gradient reversed phase C_{18} column, and the mobile phase consisted of methanol, 5 mM ammonium acetate and 0.1% TFA. They used a PE Sciex API 3000 triple quadrupole mass spectrometer as a detection system, which was set in the multi reaction monitoring mode, and was also set in the positive Electrospray mode. The transitions of the ions were: *m/z* 377 to 224 for SQ37, *m/z* 307 to 154 for SQ59 and *m/z* 331 to 178 for SQ109. The oral bioavailability of SQ59, SQ37 and SQ109, was 5.1%, 20.1% and 7.8%, respectively. They also reported that the use of LC-MS/MS has greatly enhanced their ability to profile many drug candidates simultaneously in a single sample [Jia *et al*., 2005].

Singh and Vingkar have used a reverse phase HPLC system to study the oral bioavailability of primaquine (incorporated into lipid nanoemulsion) in mouse blood. The animals were sacrificed at every time point and average animal data was used to construct drug-concentration time profiles. Primaquine is an antirelapsing drug, and is very important in *P. vivax* and *P. ovale* relapse treatment strategies. This drug acts specifically on the relapse causing pre-erythrocytic schizonts, which are found mainly in the liver. Unfortunately, treatment is limited due to severe tissue toxicity caused when primaquine is administered at relatively high doses. Lipid nanoemulsion has been used successfully in improving bioavailability for many other drugs. Singh and Vingkar have studied the

bioavailability of primaquine when incorporated into oral lipid nanoemulsion having particle size in the range of 10-200 nm. Effective antimalarial activity has been reported, against *P. berghei* infection in mice, at a 25% lower dose as compared to conventional oral dose. The HPLC analytical system was successfully used to analyse the mouse samples, however many animals have been used to evaluate the lipid nanoemulsion drug delivery system. Quadrupole mass spectrometers are much more sensitive and selective detection systems compared to conventional HPLC detectors, which poses the possibility to develop methods that only use very small sample volumes. Such methods would make it possible to collect samples from all the sampling points from one mouse. These animals could also be re-used after a recovery period of about 3 weeks [Singh and Vingkar, 2008].

From an ethical perspective it is also important to work towards a more focused *in vivo* screening system. Bioavailability and metabolic studies should reduce the number of compounds that are normally tested for *in vivo* efficacy, which will lessen the animal numbers significantly.

The first objective for the more focused *in vivo* testing was to develop methodology that could study a test compounds bioavailability properties in mice. The intention was to use one animal for all the sampling points and to use three animals per experimental group. The animals will also be reused after a recovery period of about 2 weeks. The second objective was to develop methodology that could study the metabolics of the test compound in mouse blood, urine and faeces. The intention was to use only one animal for this experiment. The new methodology would also require no killing of animals during the bioavailability and metabolic experiments.

An understanding of the absorption, distribution, metabolism and excretion of a test compound is essential in order to be able to design effective treatment regimens. The *P. berghei* mouse model is the most frequently used animal model for efficacy testing, but is rather a challenging model for pharmacokinetic and metabolic studies, because of the animal's small blood volume. However, triple quadrupole mass spectrometry has been successfully applied to detect trace amounts of compounds from biological matrixes in similar applications.

1.7 Scope of Study

It is the intention of this study to identify and characterise antiplasmodial compounds within the *Xerophyta* genus, and to evaluate the most promising compound in a mouse model.

The first objective of this project was to isolate and characterise new antiplasmodial compounds from the Xerophyta genus. This objective was subdivided into the following categories:

- *in vitro* antiplasmodial screening and cytotoxicity testing of *X. villosa* and *X. retinervis* extracts
- isolation of potential antiplasmodial compounds
- *in vitro* antiplasmodial screening and cytotoxicity testing of potential antiplasmodial compounds
- structural elucidation of the most promising compounds

A second objective was to study the bioavailability and metabolism of the most promising compound in a mouse model and to use this information to design a treatment strategy to investigate the antimalarial activity of this compound in a mouse model. This objective was subdivided into the following categories:

- bioavailability study of the most promising compound in a mouse model
- metabolism investigation
- *in vivo* antimalarial study of the most promising compound in a mouse model

CHAPTER 2

X. villosa and *X. retinervis*

2 *X. VILLOSA* AND *X. RETINERVIS*

2.1 Introduction

The Medicinal Plants of South Africa and a M. Sc thesis by Dianne Chen were used to select plants for this project [Van Wyk *et al*., 2002; Chen, 1997]. The following two species of the *Xerophyta* genus (figure 9) were selected as a potential source of antimalarial compounds: *Xerophyta villosa* (Bak.) and *Xerophyta retinervis* Bak. FP. [Arnold and De Wet, 1993].

X. retinervis has antimicrobial, anti-ulcer, central nervous system and anti-inflammatory activity. Extracts from *X. retinervis* are also used as traditional remedies for health problems like nose bleeding, asthma and general aches. *Xerophyta* species belong to the family Velloziaceae and is usually found in rocky areas in the northern grassland areas of South Africa. These plants have thick erect stems which are covered with leaf bases. The secondary metabolites from these plants are poorly known, but some biflavonoids have been isolated from *X. retinervis* with the main compound amentoflavone. Differences in flavonoid patterns between genera within the Velloziaceae have also been reported previously. [Williams *et al*., 1994; Chen, 1997; Van Wyk *et al*., 2002].

X. villosa was collected at the Blyde River Canyon Nature Reserve (Mpumalanga, South Africa) and *X. retinervis* was collected on a farm at Hoedspruit (Mpumalanga, South Africa).

Plant collection information is presented in Chapter 12 (12.1).

X. villosa

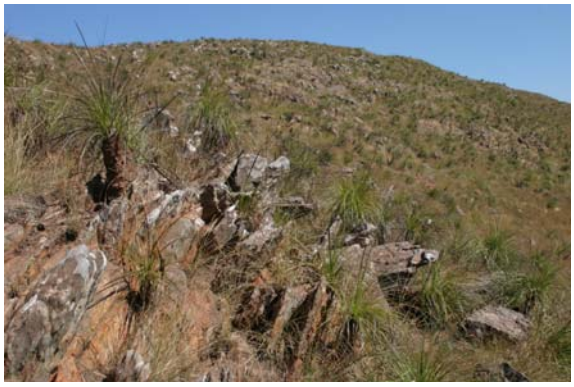

X. retinervis

X. villosa

X. retinervis

Dried plant material of *X. villosa*

Leave bases of *X. villosa*

Figure 9 Photograph gallery of *X. villosa* and *X. retinervis*

The ethno-based extraction methodology approached (as suggested in 1.6.2.2) could not be followed for this project, because of the non specific use of *Xerophyta* as traditional medicine by traditional healers. It was decided to follow the "*similia similibus solvuntur"* extraction approach, as discussed in 1.6.2.3, to group the plant constituents according to its polarity in different groups. Different extraction procedures were used for the two *Xerophyta* species and are described in Chapter 12 (12.2).

A flow-diagram, which summarises the extraction procedure, is presented in figure 10.

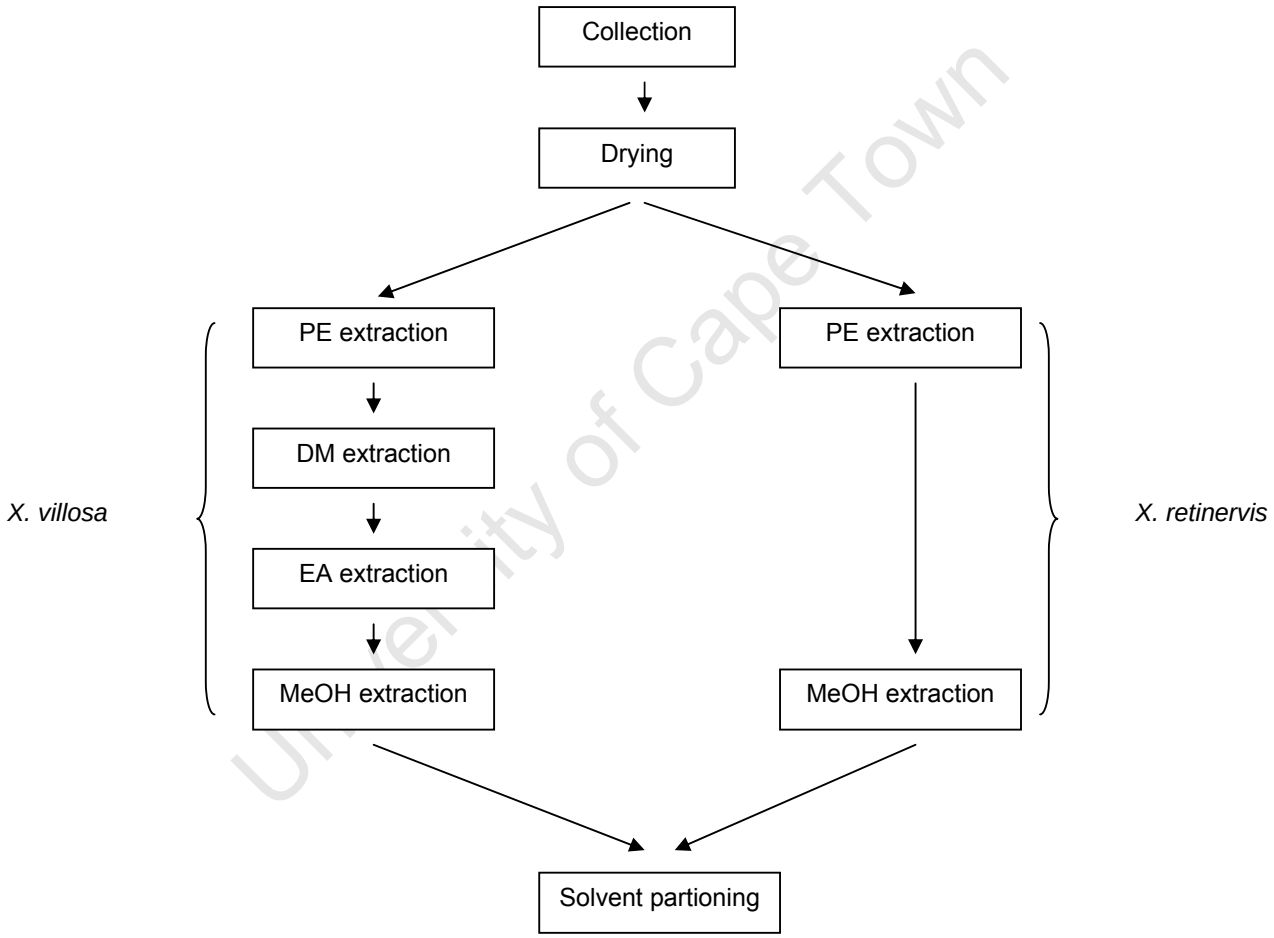

Figure 10 Flow-diagram of the *X. villosa* and *X. retinervis* extraction model

2.2 Results

The recovery yields of the *X. villosa* and *X. retinervis* extracts are presented in tables 1 and 2, respectively.

Table 1 Extraction yields of *X. villosa* extracts

Extract	Mass (g)	% yield
Petroleum ether	0.76	1.9
Dichloromethane	0.08	0.2
Ethyl acetate	0.13	0.3
Methanol	1.50	3.8

The methanol extract was further separated into two fractions as described in Chapter 12 (12.2). Liquid-liquid extraction was performed on the methanol extract to separate the less polar compounds from the more polar compounds. The yields of the aqueous and organic layers were 0.3 g and 1.1 g, respectively (0.1 g loss).

Table 2 Extraction yields of *X. retinervis* extracts

Extract	Mass (g)	% yield
Petroleum ether	0.5	1.0
Methanol	0.5	1.0

The methanol extract was also separated into two groups using liquid-liquid extraction and is also described in Chapter 12 (12.2). The yields of the aqueous and organic layers were 0.1 g and 0.3 g, respectively (0.1 g loss).

2.3 Discussion

The plant material was collected during the cold winter period in Mpumalanga, South Africa. During this period the plants are in a dormant state as can be seen in the photographs presented in figure 9.

X. villosa plant material was extracted sequentially with organic solvents of increasing polarities: petroleum ether, dichloromethane, ethyl acetate and methanol. The highest yield was observed in the methanol extract (3.8%). *X. retinervis* plant material was extracted initially with petroleum ether, followed by methanol. The extraction yields for both extracts were 1%.

Previous work by Dianne Chen reported the presence of a novel flavonolignan (which showed moderate antiplasmodial activity during preliminary screening) in a methanol extract from *X. retinervis*. It was reported that the compound precipitated out of solution after the methanol extract was dried and redissolved in ethyl acetate. At this stage of the project it was decided to commence the search for antiplasmodial compounds in a similar chemical environment as was reported earlier [Chen, 1997]. The methanol extracts were therefore further subdivided into semi-polar and polar groups by liquid-liquid extraction. The organic fractions from the methanol extracts were considered potential sources for related antiplasmodial compounds. These organic fractions of *X. villosa* and *X. retinervis* yielded 1.1 and 0.3 g material, respectively.

CHAPTER 3

Antiplasmodial activity and cytotoxicity screening of *X. villosa* and *X. retinervis* extracts

3 Antiplasmodial activity and cytotoxicity screening of *X. villosa* and *X. retinervis* extracts

3.1 Introduction

Antiplasmodial activity screening of plant extracts is used to determine the potential of extracts as sources of antiplasmodial compounds [Clarkson *et al*., 2003; Clarkson *et al*., 2004; Fischer *et al*., 2004; Chukwujekwu *et al*., 2005; De Monbrison *et al*., 2006; Pillay *et al*., 2007]. Antiplasmodial activity of crude extracts with IC_{50} values less than 10 µg/ml are considered to be potential sources of antiplasmodial compounds [Rasoanaivo, 2002; Willcox *et al*., 2004]. A good source of antiplasmodial compounds should also inhibit parasites selectively and cause no harm to other cells. Cytotoxicity experiments are used to determine general toxic properties of plant extracts against living cells. Antiplasmodial activity and cytotoxicity information are used to determine selectivity indexes, which are used as a guide to determine the potential of an extract for further investigation. Evaluation criteria on this subject varies, but according to a review article by Richard Pink and co-authors, an active antiplasmodial compound should be at least tenfold more active against the targeted organism than against mammalian cells to be considered for further testing. It was decided to use this selectivity evaluation method as a guideline for extract evaluation [Pink *et al*., 2005].

An antiplasmodial whole parasite screening system was used to test the antiplasmodial activity of these plant extracts. The malaria parasites were cultured according to the method described by Trager and Jensen (with minor modifications) [Trager and Jensen, 1976]. The parasite lactate dehydrogenase assay (pLDH) as described by Makler and co-workers was used to determine parasite viability (with minor modifications) [Makler *et al*., 1993]. Cytotoxicity was tested against Chinese hamster ovarian (CHO) cells. The cells were cultured according to a standard operating procedure prepared by the Pharmacology Department at the University of Cape Town, South Africa. The MTT assay as described by Mosmann (with minor modifications) was used to determine cell viability [Mosmann, 1983]. These assay procedures are described in Chapter 12 (12.3 and 12.4).

The organic fractions, from the methanol extracts, from *X. villosa* and *X. retinervis* were targeted as potential natural sources of new antiplasmodial compounds. These extracts

were screened against a chloroquine sensitive *P. falciparum* strain (D10), and a chloroquine resistant *P. falciparum* strain (K1). Cytotoxicity screening of these extracts were also performed.

3.2 Results

3.2.1 Antiplasmodial activity screening

3.2.1.1 Antiplasmodial screening of the plant extracts against the D10 strain

The antiplasmodial activities of the organic fractions, from the methanol extracts, from *X. villosa* and *X. retinervis* were determined against the chloroquine sensitive D10 strain. These experiments were done in duplicate and repeated two times on separate days. Chloroquine was used as an internal standard to monitor the experimental conditions and showed IC_{50} values within the acceptable range (6 - 20 ng/ml). The IC_{50} values for the *X. villosa* and *X. retinervis* extracts were 6.0, and 1.4 µg/ml on average, respectively. The parasite survival curves are presented in figures 11 and 12.

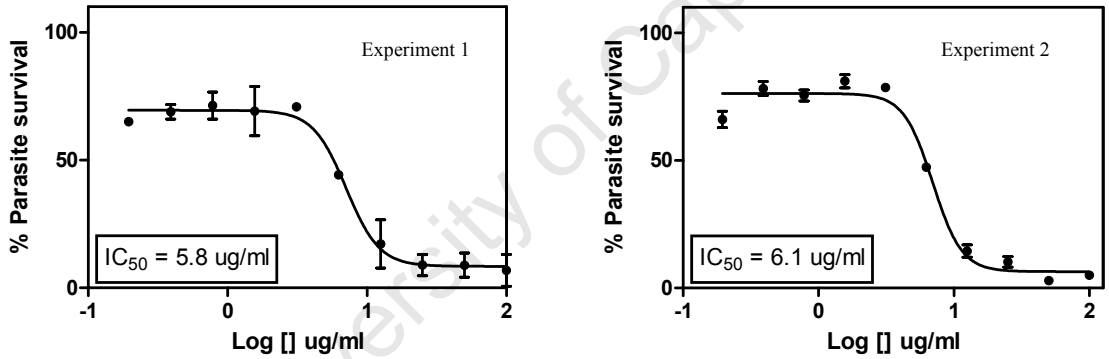

Figure 11 Dose response curves of the *X. villosa* extract on *P. falciparum* D10 parasites

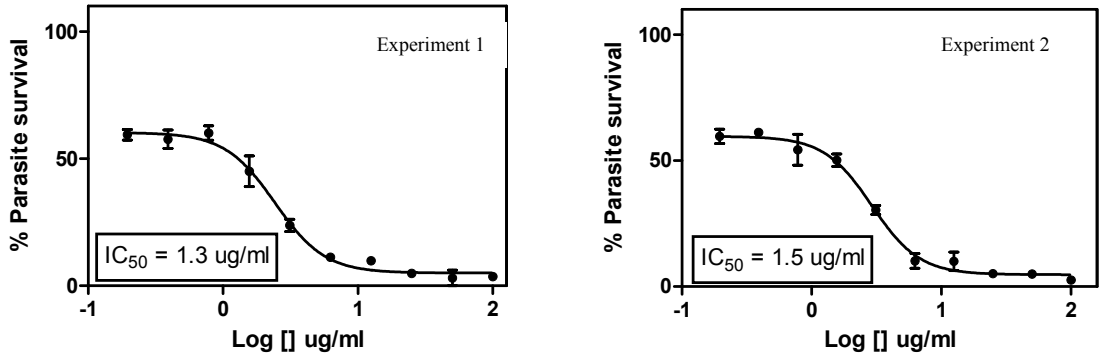

Figure 12 Dose response curves of the *X. retinervis* extract on *P. falciparum* D10 parasites

3.2.1.2 Antiplasmodial activity of the plant extracts against the K1 strain

The antiplasmodial activities of the organic fractions from the methanol extracts from *X. villosa* and *X. retinervis* were determined in duplicate against the chloroquine resistant K1 strain. Chloroquine was used as an internal standard to monitor the experimental conditions and showed IC_{50} values within the acceptable range (150 - 250 ng/ml). The IC_{50} values for the *X. villosa* and *X. retinervis* extracts were 5.4, and 2.2 µg/ml, respectively. The parasite survival curves are presented in figures 13 and 14.

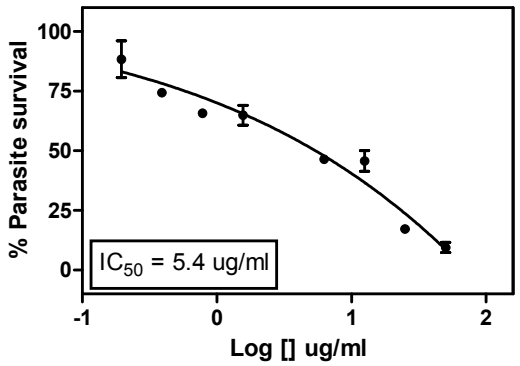

Figure 13 Dose response curve of the *X. villosa* extract on *P. falciparum* K1 parasites

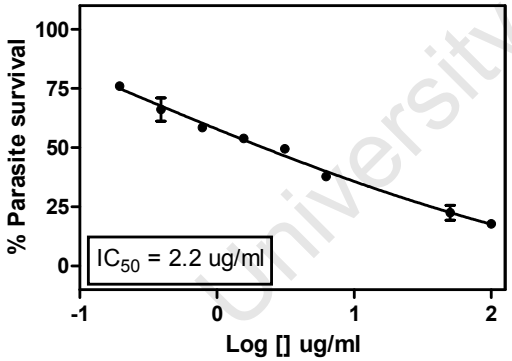

Figure 14 Dose response curve of the *X. retinervis* extract on *P. falciparum* K1 parasites

3.2.2 Cytotoxicity assessment of the plant extracts

Cytotoxicity of the organic fractions from the methanol extracts from *X. villosa* and *X. retinervis* were determined against CHO cells. These experiments were done in triplicate and repeated two times on separate days. Emetine was used as a quality control standard to monitor the experimental conditions and showed IC_{50} values within the acceptable range (40 – 60 ng/ml). The cell viability curves of the organic fractions from the methanol extracts from *X. villosa* and *X. retinervis* are presented in figures 15 and 16 and show IC_{50} values of 90.5 and 80.9 µg/ml on average, respectively.

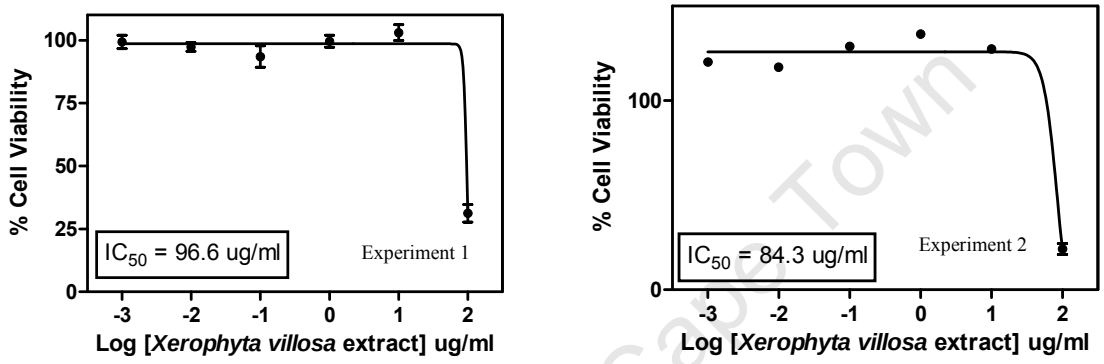

Figure 15 Dose response curves of the *X. villosa* extract on CHO cells

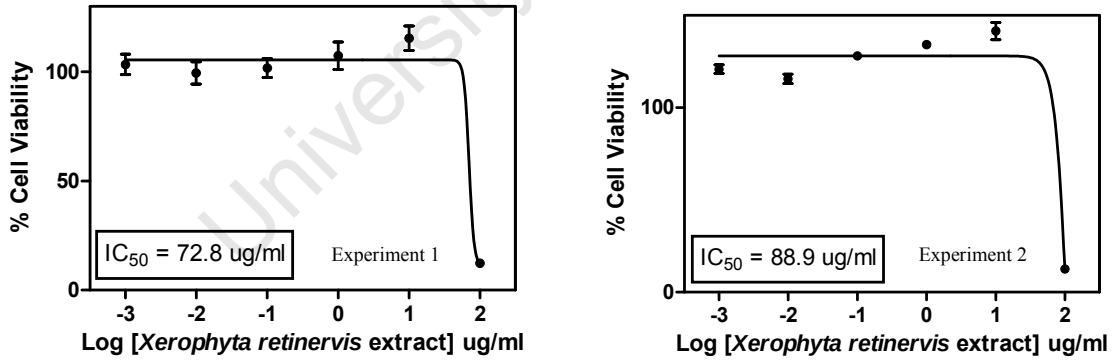

Figure 16 Dose response curves of the *X. retinervis* extract on CHO cells

3.2.3 Selectivity Index

In order to determine the specificity of an extract against the *Plasmodium* parasite the antiplasmodial activity and cytotoxicity are used to calculate a selectivity index value. The cytotoxicity IC_{50} value of the extract is divided by the antiplasmodial IC_{50} value to obtain the selectivity index value. These values are presented in table 3 (calculated for D10 strain).

Table 3 Selectivity index values of the *X. villosa* and *X. retinervis* extracts

Extract	Antiplasmodial activity D10 (IC_{50}, µg/ml)	Cytotoxicity (IC_{50}, µg/ml)	Selectivity Index [a]
X. villosa	6.0	90.5	15.1
X. retinervis	1.4	80.9	57.8

[a] Selectivity Index = cytotoxicity IC_{50}/antiplasmodial D10 IC_{50}

3.3 Discussion

The antiplasmodial activities of the extracts from both species were below 10 µg/ml, which according to Rasoanaivo, Willcox and co-authors are considered to be good potential sources of antiplasmodial compounds [Rasoanaivo, 2002; Willcox *et al*., 2004]. The selectivity index values for both extracts also indicated that the constituents from these extracts selectively inhibit parasite growth. Both extracts are therefore considered to be good quality sources for potential antiplasmodial compounds. The *X. retinervis* extract was superior to the *X. villosa* extract, regarding their antiplasmodial activity; however both extracts were considered good sources of potential antiplasmodial compounds and were taken further in the drug discovery process.

CHAPTER 4

Isolation of pure compounds

4 Isolation of pure compounds

4.1 Introduction

The flavonoid family, from the bioactive *Xerophyta* extracts as described in Chapters 2 and 3, was targeted as a potential source of antimalarial compounds. Flavonoids are one of the most numerous groups of natural products, and are important to humans because many are physiologically active [Harborne *et al.*, 1975]. Flavonoids exist in plants as secondary metabolites as aglycones or glycosides. The aglycones are usually absorbed from the gut by passive diffusion [Pong *et al*., 2005]. A general molecular structure of a flavonoid molecule is presented in figure 17. It consists of 3 major rings (A, C and B) as indicated in the structure. The double bonds in the flavonoid skeleton cause them to absorb visible light, and as a result, give them colour.

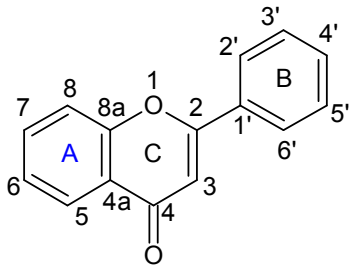

Figure 17 General molecular structure of flavonoids

Hydroxyl groups are almost always present in the flavonoids and are usually attached to the B ring at positions 3' and 4' and to the 5 and 7 positions of the A ring [Harborne *et al.*, 1975].

Flavonoids consist of many different subgroups of which: flavones, isoflavones, flavanones, isoflavanones, flavonols and dihydroflavonols were targeted as potential antimalarial compounds during this project. The general molecular structures of these subgroups are presented in figure 18.

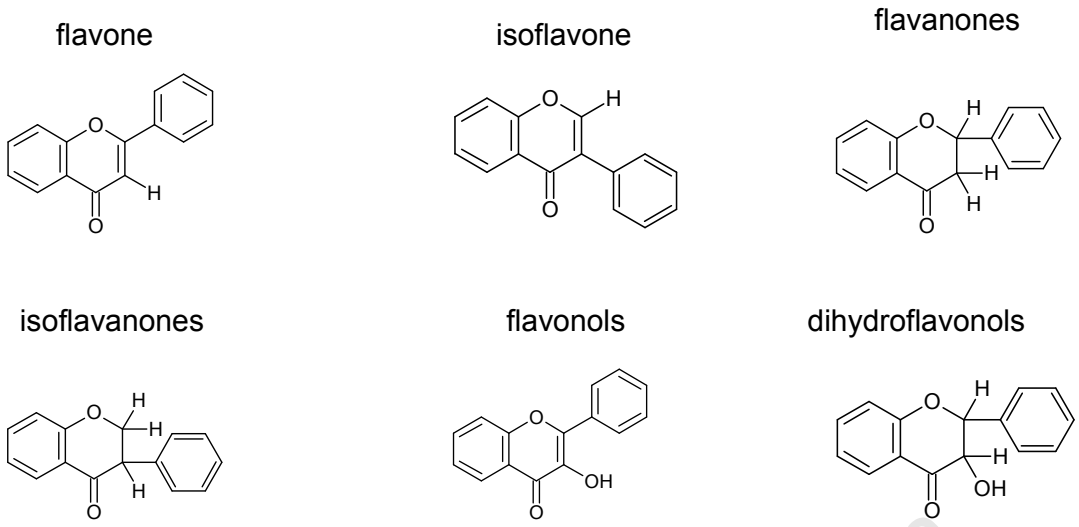

Figure 18 General molecular structures of flavonoid subgroups

Many different analytical techniques are described in the literature for the isolation of pure compounds from complex plant material. The laboratory handbook for the fractionation of natural extracts was used as a guide to design a specific model to isolate compounds for this project [Houghton and Raman, 1998].

An automated, semi-preparative HPLC fraction collection system was used to analyse and fractionate the extracts [Preparative HPLC; Brandt and Kueppers, 2002; Miliauskas *et al*., 2006]. The HPLC system produced milligram quantities of pure compounds in a relatively short period. The methodology of this process is described in Chapter 12 (12.5).

The bioactive methanol extract (organic phase) of *X. villosa* was analysed on HPLC to get a better understanding of the complexity of the extract. The HPLC profile of this extract was also compared to the other two intermediate polar extracts (ethyl acetate and dichloromethane) to examine the similarities and differences in their profiles. This extract was fractionated to obtain six semi-pure compounds. Each of these fractions was further purified on HPLC to obtain pure compounds. The methodology of this process is summarised in figure 19 and described in Chapter 12 (12.5).

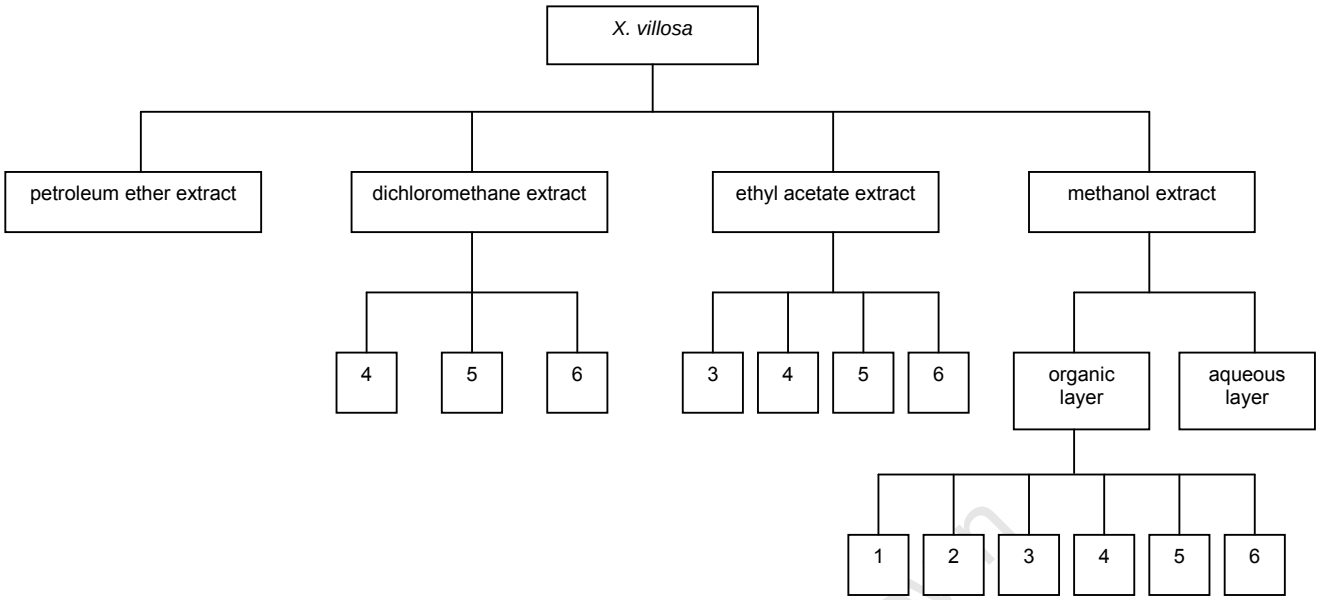

Figure 19 Flow-diagram of *X. villosa* fractionation methodology

The bioactive methanol extract (organic phase) of *X. retinervis* was also analysed on HPLC. This extract was fractionated to obtain two semi-pure compounds. Each of these fractions was further purified on HPLC to obtain single pure compounds. The methodology is summarised in figure 20 and described in Chapter 12 (12.5).

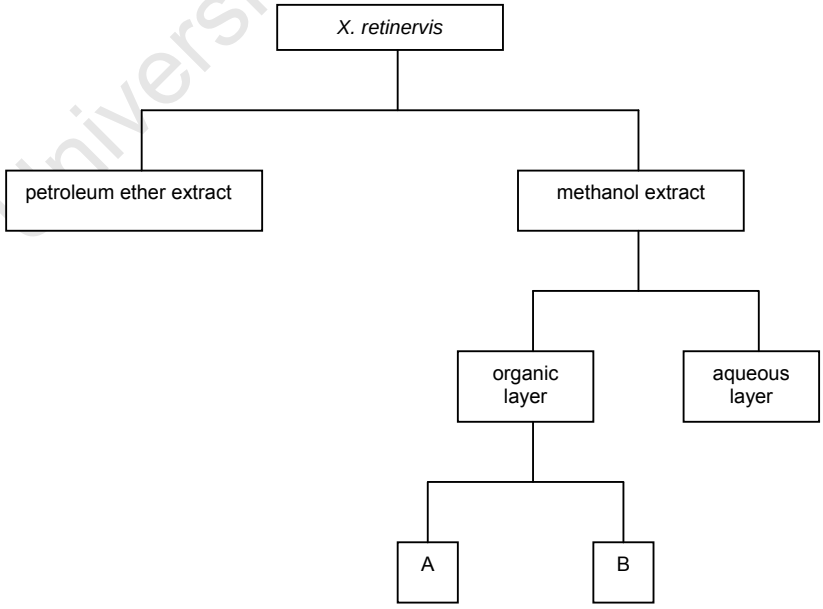

Figure 20 Flow-diagram of *X. retinervis* fractionation methodology

4.2 Results

4.2.1 *X. villosa*

4.2.1.1 Methanol extract (organic phase)

The HPLC chromatogram of this extract is presented in figure 21. Six major peaks were observed at 7.1, 9.7, 12.3, 14.5, 18.2 and 20.0 minutes.

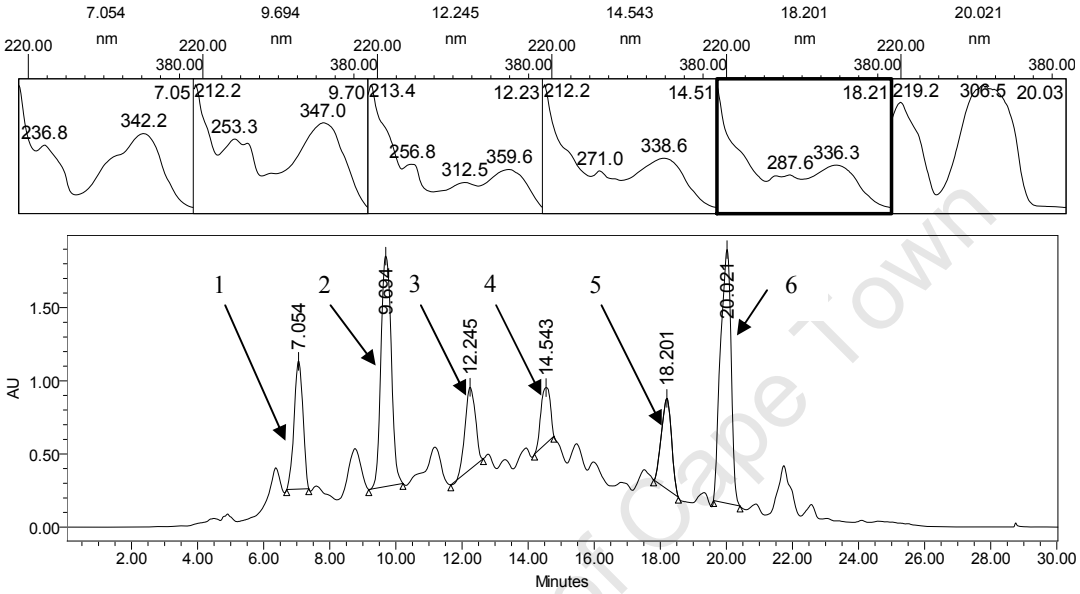

Figure 21 HPLC chromatogram of the *X. villosa* organic layer from the methanol extract

4.2.1.2 Ethyl acetate extract

The HPLC chromatogram of this extract is represented in figure 22. The same major peaks (compared to the methanol extract, organic phase) were also observed for this extract at 7.1, 9.7, 12.2, 14.5, 18.1 and 19.9 minutes.

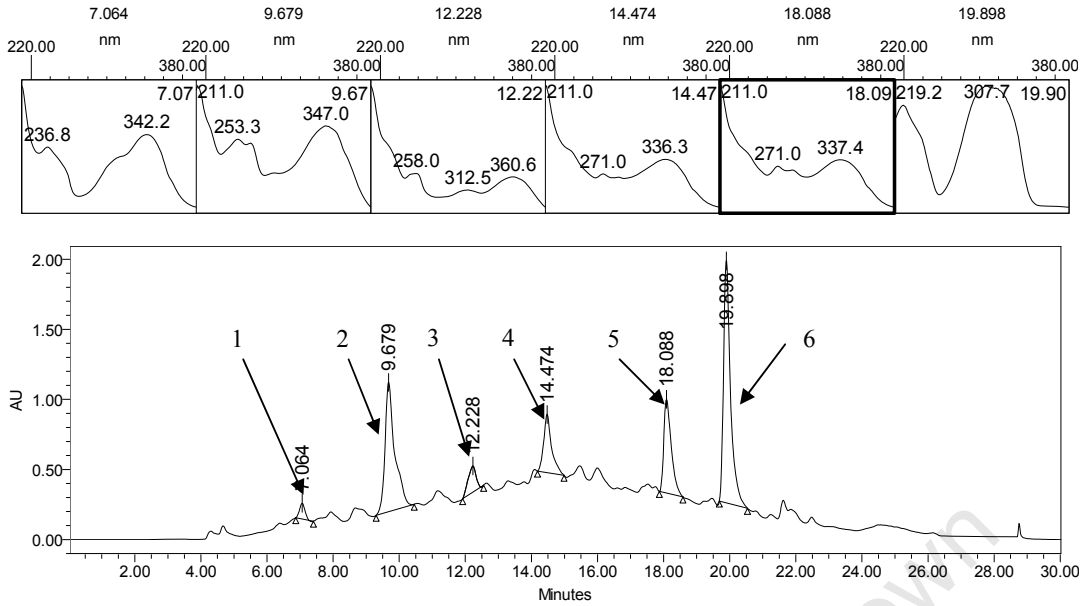

Figure 22 HPLC chromatogram of the *X. villosa* ethyl acetate extract

4.2.1.3 Dichloromethane extract

The HPLC chromatogram of this extract is represented in figure 23. Peaks 4, 5 and 6 (compared to the methanol extract, organic phase) were observed for this extract at 14.6, 18.2 and 20.0 minutes.

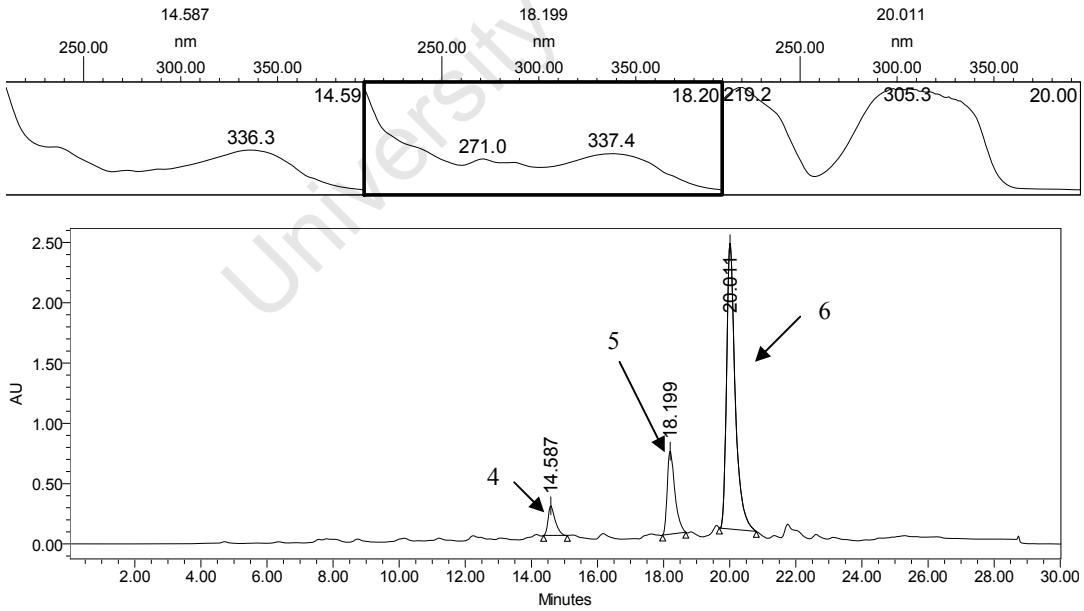

Figure 23 HPLC chromatogram of the *X. villosa* dichloromethane extract

Peaks 4, 5 and 6 from the dichloromethane extract have the same retention time and UV spectra when compared to peaks 4, 5 and 6 from the ethyl acetate extract. Peaks 1, 2, 3, 4, 5 and 6 from the ethyl acetate extract have identical retention times and UV spectra when compared to peaks 1, 2, 3, 4, 5 and 6 from the organic fraction of the methanol extract. It was therefore decided to use the organic fraction of the methanol extract as a source for further fractionation.

4.2.1.4 Fractionation of the 6 major peaks

The HPLC system was optimised for the methanol extract (organic phase). The HPLC chromatogram of the extract that was used for fractionation is presented in figure 24. The methodology used to fractionate this extract is presented in Chapter 12 (12.5).

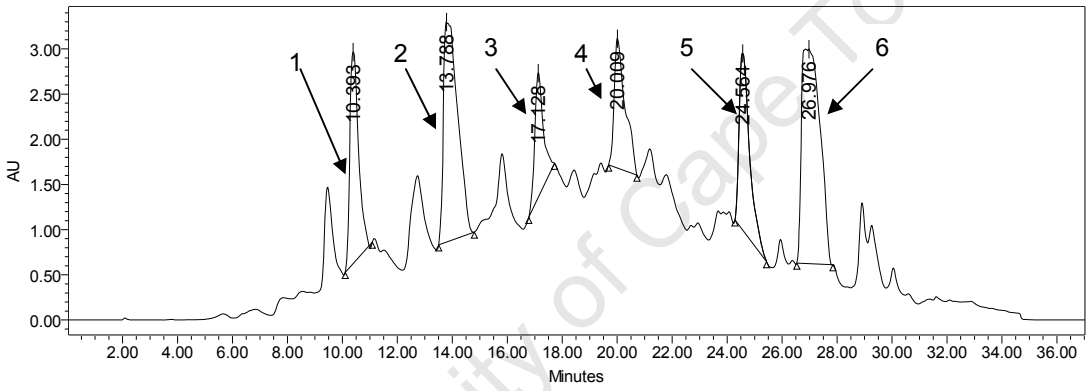

Figure 24 HPLC chromatogram of the *X. villosa* organic layer from the methanol extract

The six major peaks (1, 2, 3, 4, 5 and 6) were collected into separate solvent bottles using an automated HPLC and fraction collector. These fractions were further purified using specific HPLC methods for every fraction. The methodology used to purify these fractions is presented in Chapter 12 (12.5).

4.2.1.4.1 Fraction 1

The HPLC chromatogram of this fraction is presented in figure 25. The peak of interest eluted from the column at 7.1 minutes and was collected into a clean solvent bottle. The isolated material was dried and stored at -20 °C.

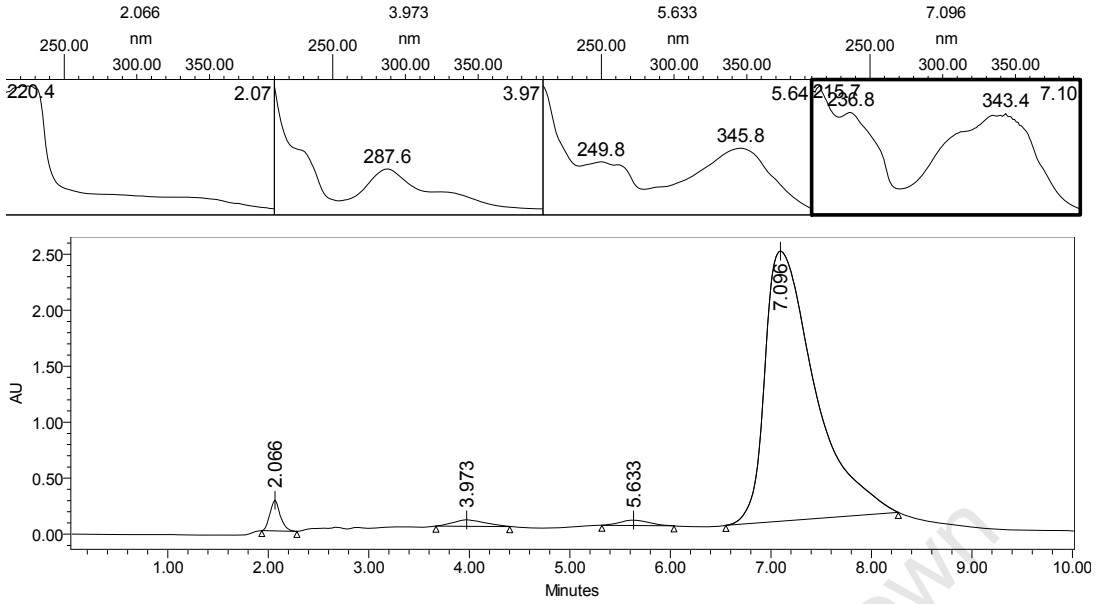

Figure 25 HPLC chromatogram of fraction 1

A small sample was analysed using the same HPLC conditions to test the purity of compound 1. The HPLC chromatogram is presented in figure 26 and the purity according to HPLC was greater than 99%.

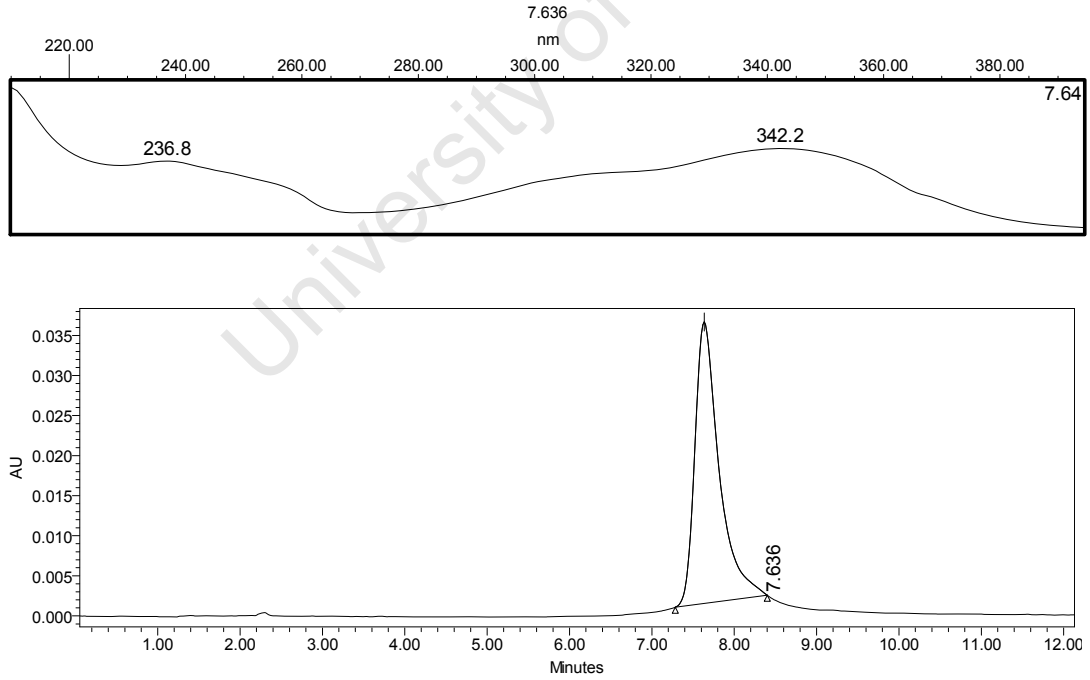

Figure 26 HPLC chromatogram of compound 1

4.2.1.4.2 Fraction 2

The HPLC chromatogram of this fraction is presented in figure 27. The peak of interest eluted from the column at 9.7 minutes and was collected into a clean solvent bottle. The isolated material was dried and stored at -20 °C.

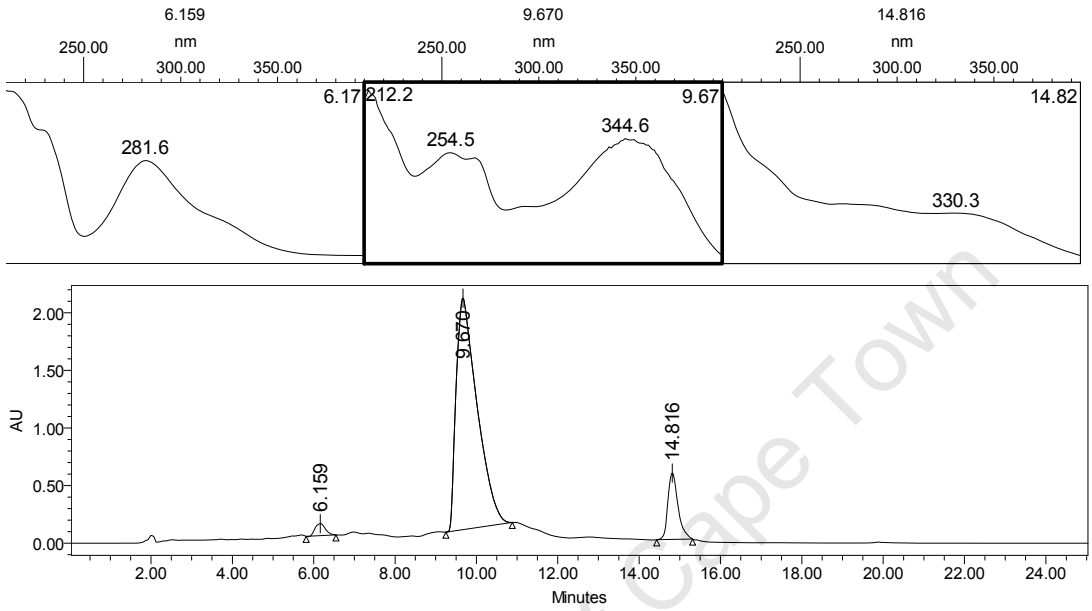

Figure 27 HPLC chromatogram of fraction 2

A small sample was analysed using the same HPLC conditions to test the purity of compound 2. The HPLC chromatogram is presented in figure 28 and the purity according to HPLC was greater than 99%. The small peak at 15 minutes was also present in the blank chromatogram (figure 29), which was injected before this sample. This peak is therefore not related to the test sample.

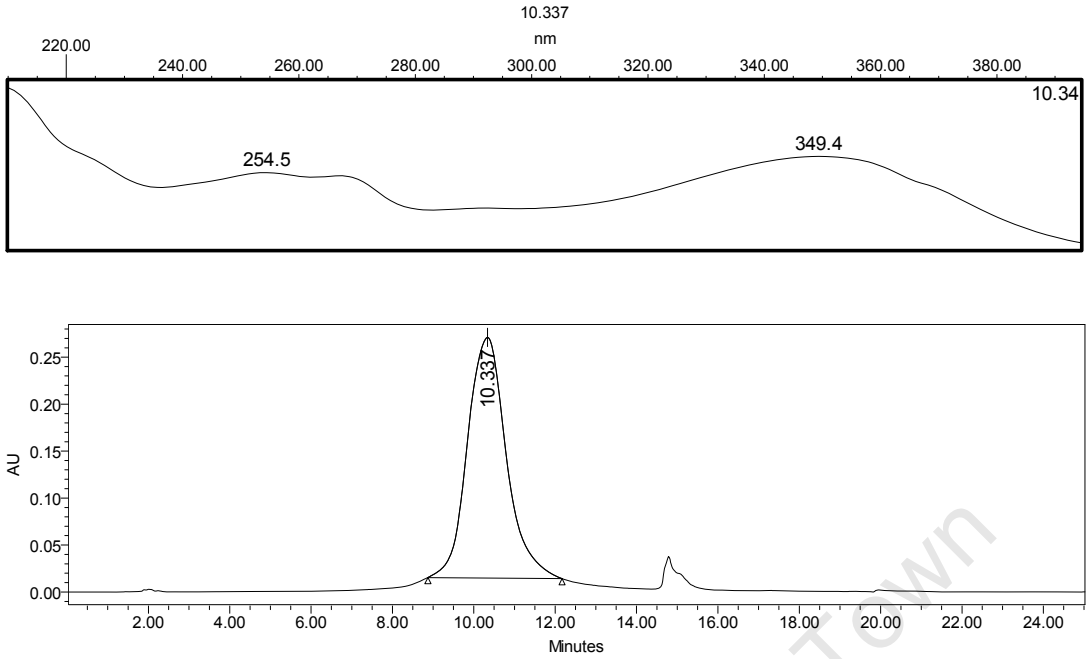

Figure 28 HPLC chromatogram of compound 2

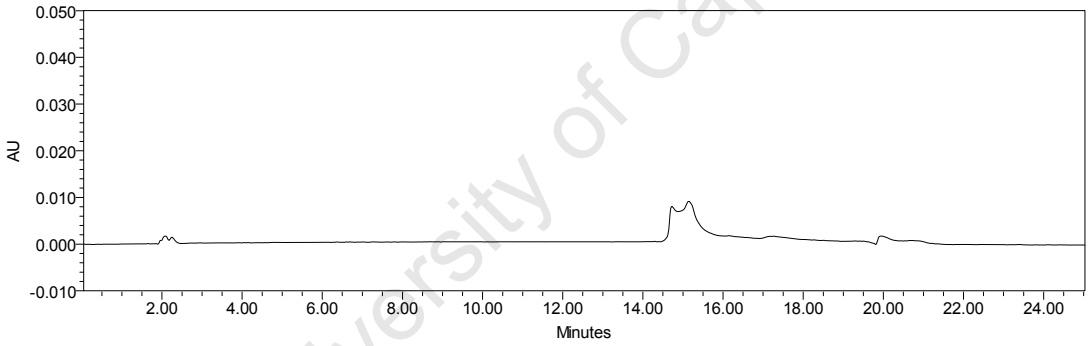

Figure 29 HPLC chromatogram of blank (acetonitrile)

4.2.1.4.3 Fraction 3

The HPLC chromatogram of this fraction is presented in figure 30. The peak of interest eluted from the column at 17.5 minutes and was collected into a clean solvent bottle. The isolated material was dried and stored at -20 °C.

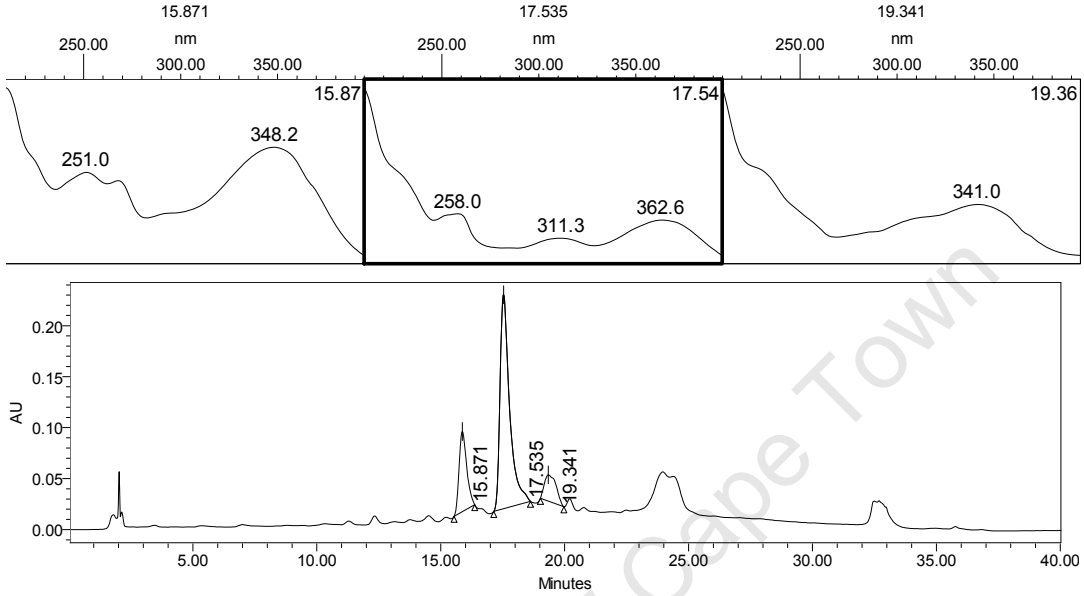

Figure 30 HPLC chromatogram of fraction 3

A small sample was analysed using the same HPLC conditions to test the purity of compound 3. The HPLC chromatogram is presented in figure 31 and the purity according to HPLC was greater than 99%.

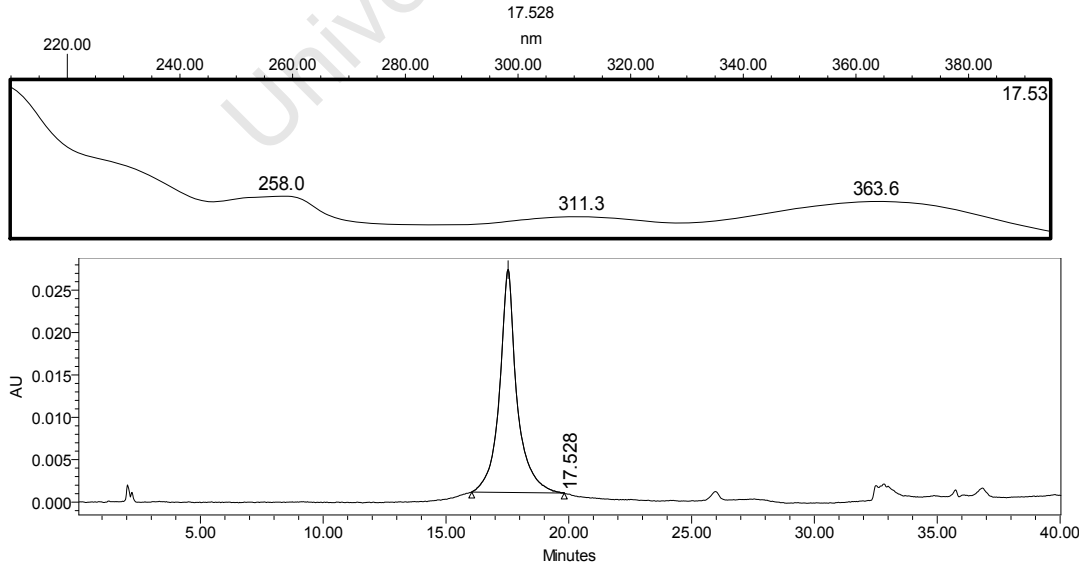

Figure 31 HPLC chromatogram of compound 3

4.2.1.4.4 Fraction 4

The HPLC chromatogram of this fraction is presented in figure 32. The peak of interest eluted from the column at 21.3 minutes and was collected into a clean solvent bottle. The isolated material was dried and stored at -20 °C.

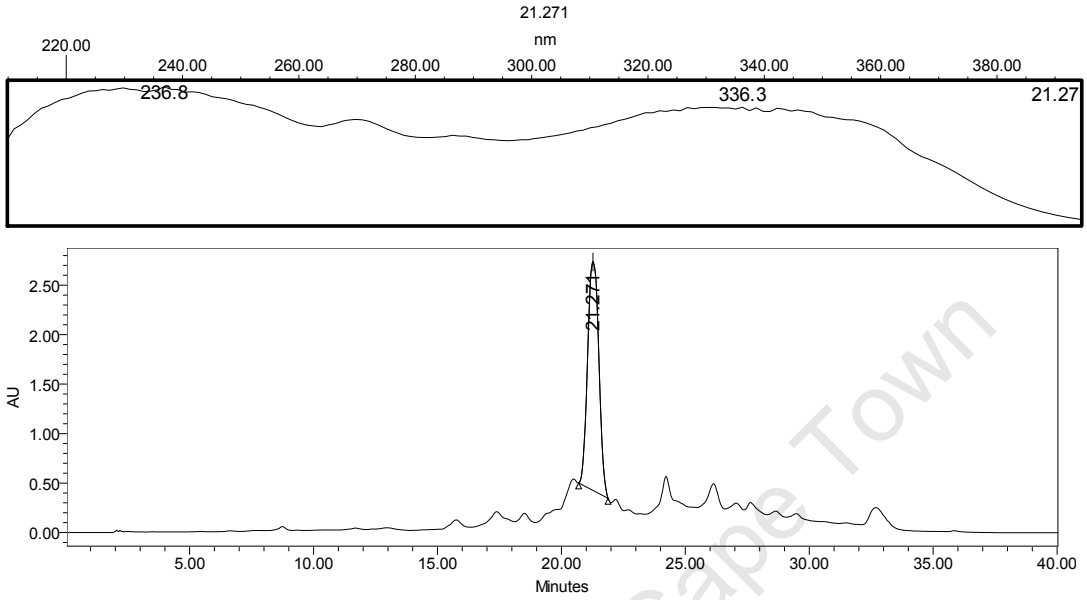

Figure 32 HPLC chromatogram of fraction 4

A small sample was analysed using the same HPLC conditions to test the purity of compound 4. The HPLC chromatogram is presented in figure 33 and the purity according to HPLC was greater than 99%. The small peak at 33 minutes was also present in the blank chromatogram (figure 34), which was injected before this sample. This peak is therefore not related to the test sample.

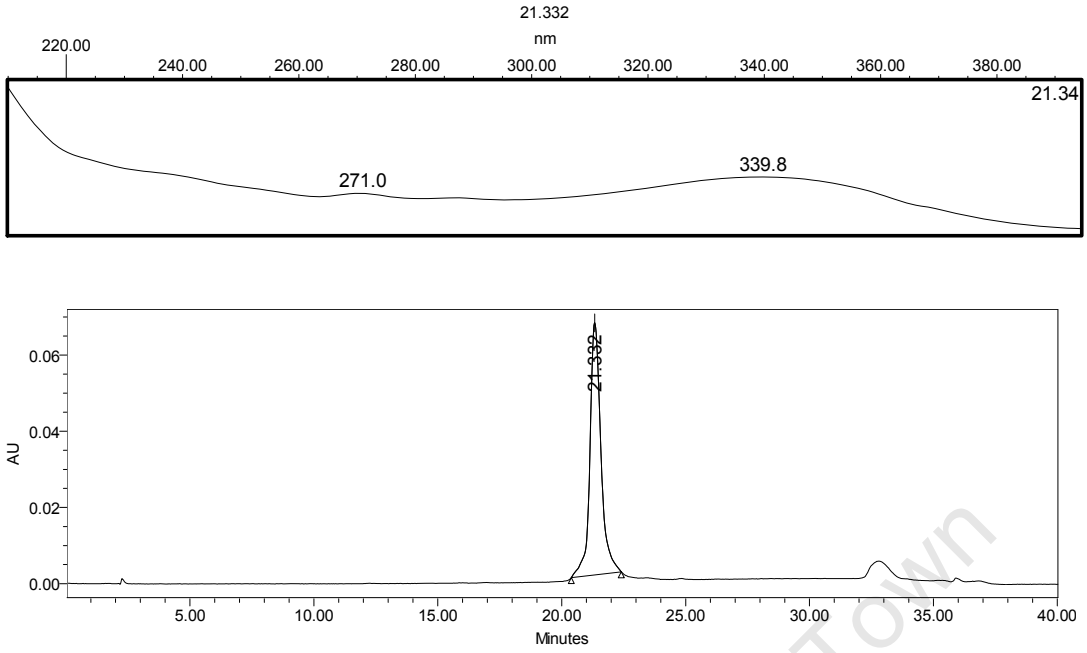

Figure 33 HPLC chromatogram of compound 4

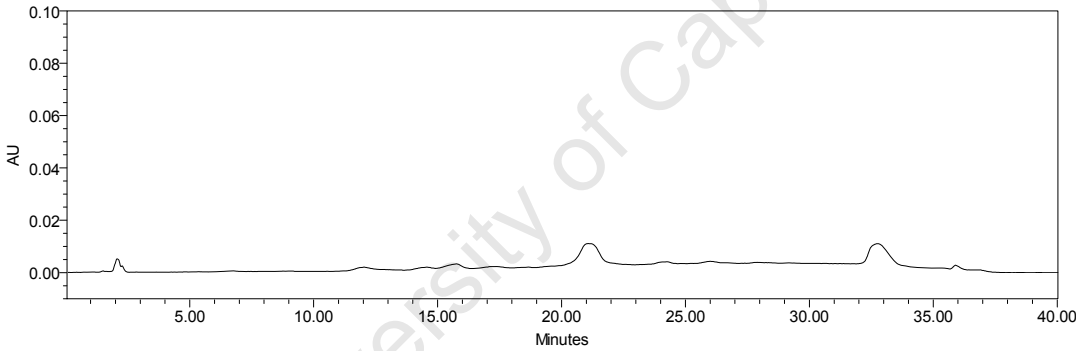

Figure 34 HPLC chromatogram of blank (acetonitrile)

4.2.1.4.5 Fraction 5

The HPLC chromatogram of this fraction is presented in figure 35. The peak of interest eluted from the column at 16.3 minutes and was collected into a clean solvent bottle. The isolated material was dried and stored at -20 °C.

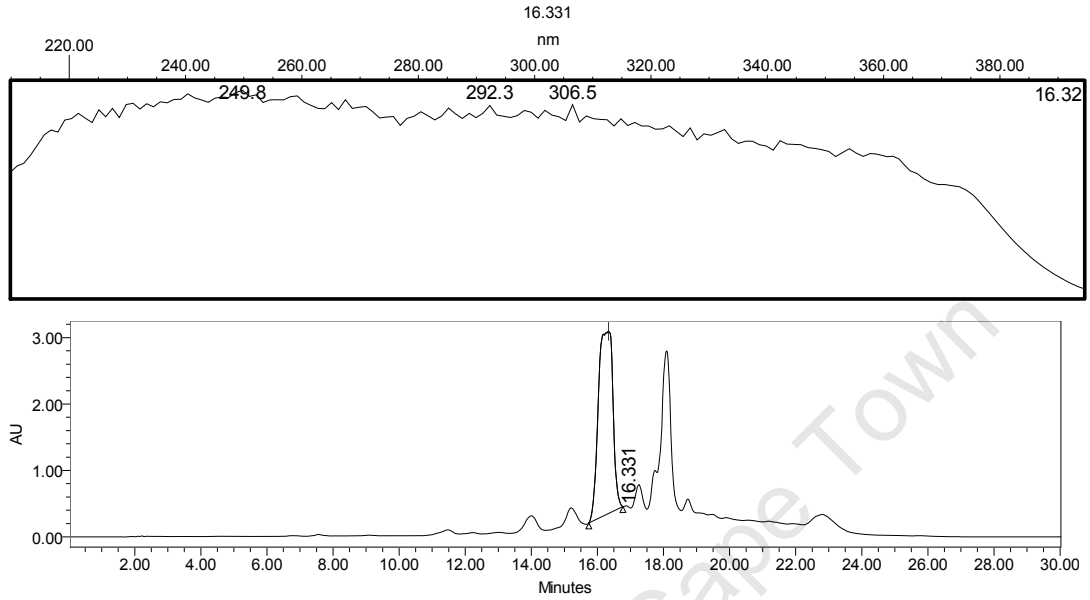

Figure 35 HPLC chromatogram of fraction 5

A small sample was analysed using the same HPLC conditions to test the purity of compound 5. The HPLC chromatogram is presented in figure 36 and the purity according to HPLC was greater than 99%.

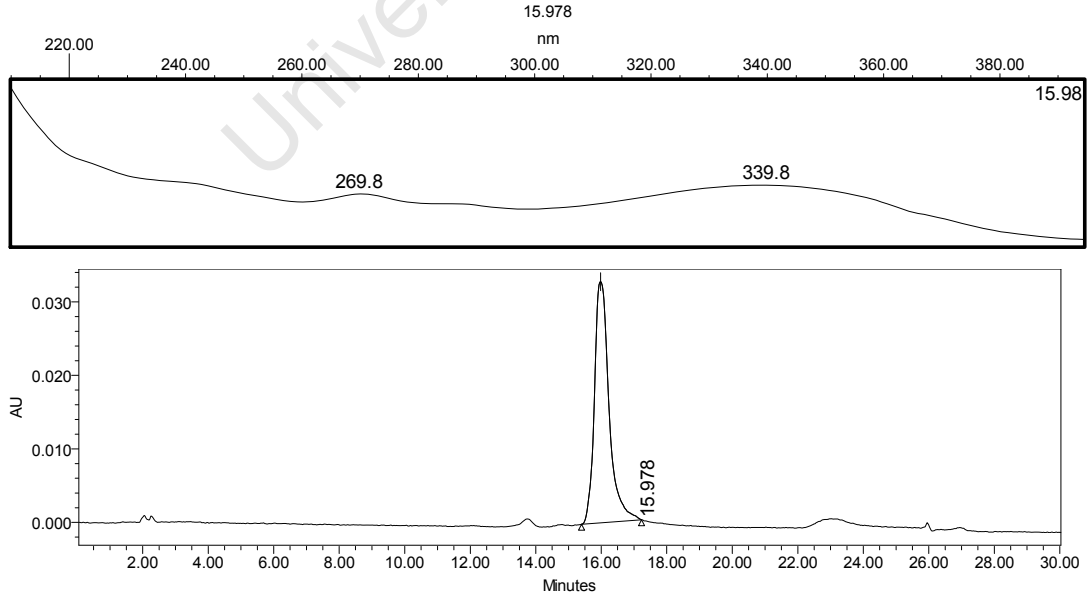

Figure 36 HPLC chromatogram of compound 5

4.2.1.4.6 Fraction 6

The HPLC chromatogram of this fraction is presented in figure 37. The peak of interest eluted from the column at 17.0 minutes and was collected into a clean solvent bottle. The isolated material was dried and stored at -20 °C.

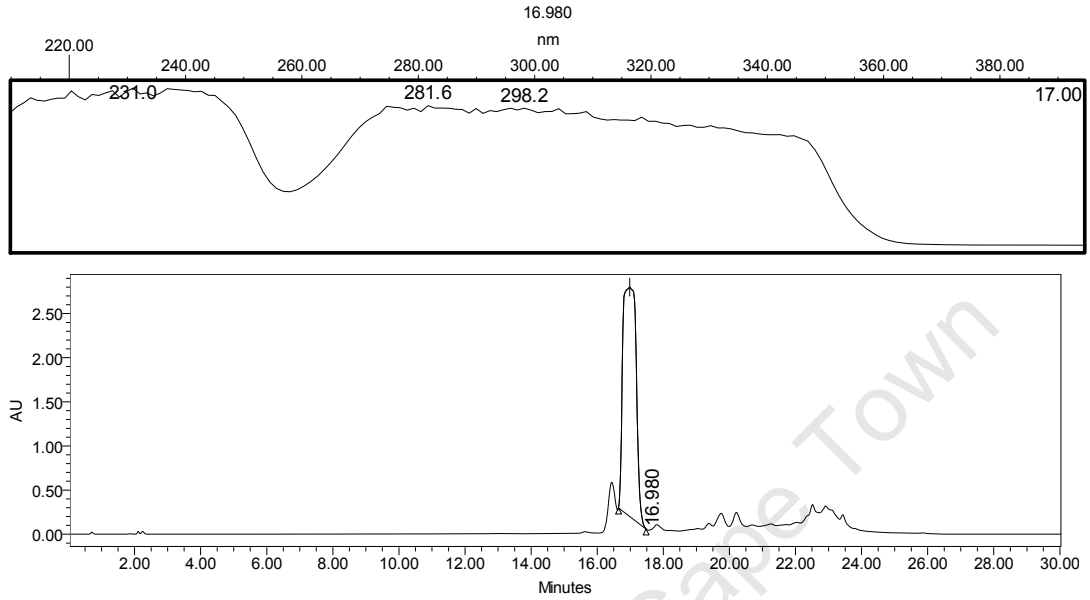

Figure 37 HPLC chromatogram of fraction 6

A small sample was analysed using the same HPLC conditions to test the purity of compound 6. The HPLC chromatogram is presented in figure 38 and the purity according to HPLC was greater than 99%.

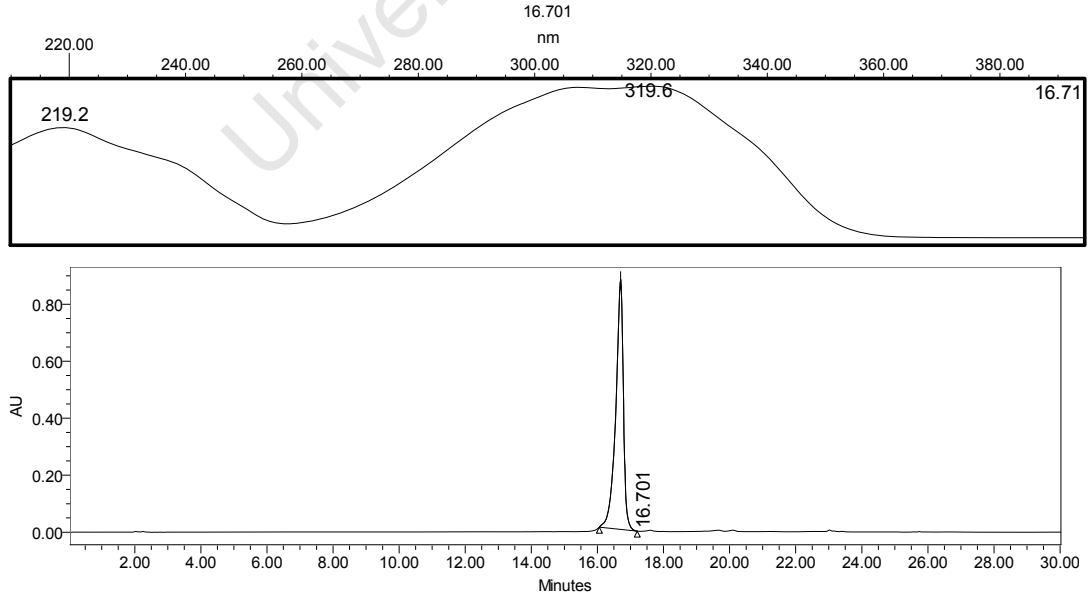

Figure 38 HPLC chromatogram of compound 6

4.2.2 *X. retinervis*

4.2.2.1 Methanol extract (organic phase)

The HPLC chromatogram of this extract is presented in figure 39. Two major peaks were observed at 20.1 and 24.6 minutes. The methodology used to fractionate this extract is presented in Chapter 12 (12.5).

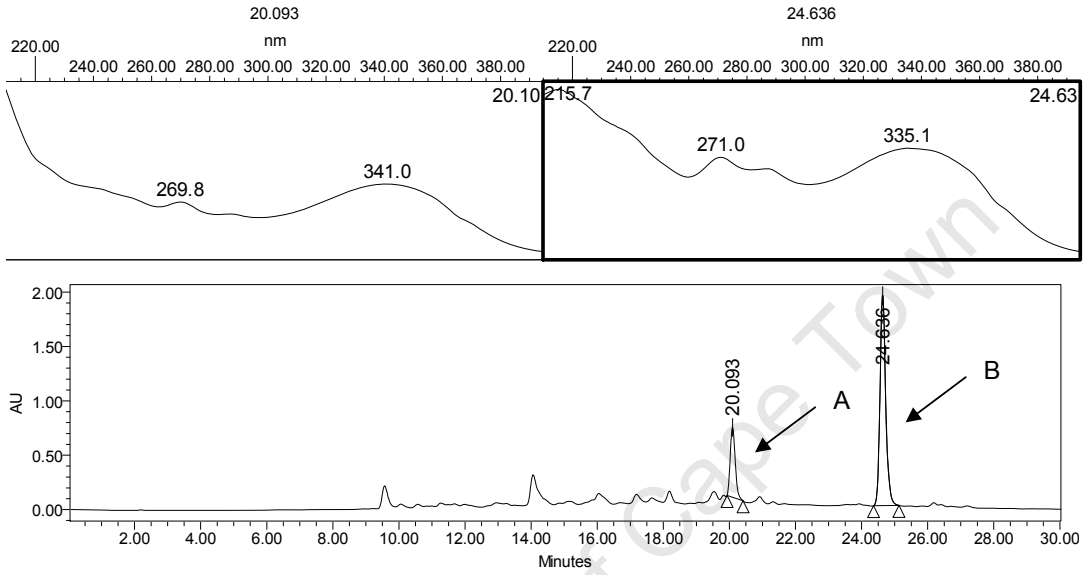

Figure 39 HPLC chromatogram of the *X. retinervis* organic layer from the methanol extract

4.2.2.2 Fractionation of the 2 major peaks

The two major peaks (A and B) were collected into separate solvent bottles using an automated HPLC and fraction collector. The isolated material was dried and stored at -20 °C, until further analysis. Small samples were analysed using a slightly modified HPLC system to test the purity of compounds A and B. HPLC chromatograms are presented in figures 40 and 41. The methodology used to purify these fractions is presented in Chapter 12 (12.5).

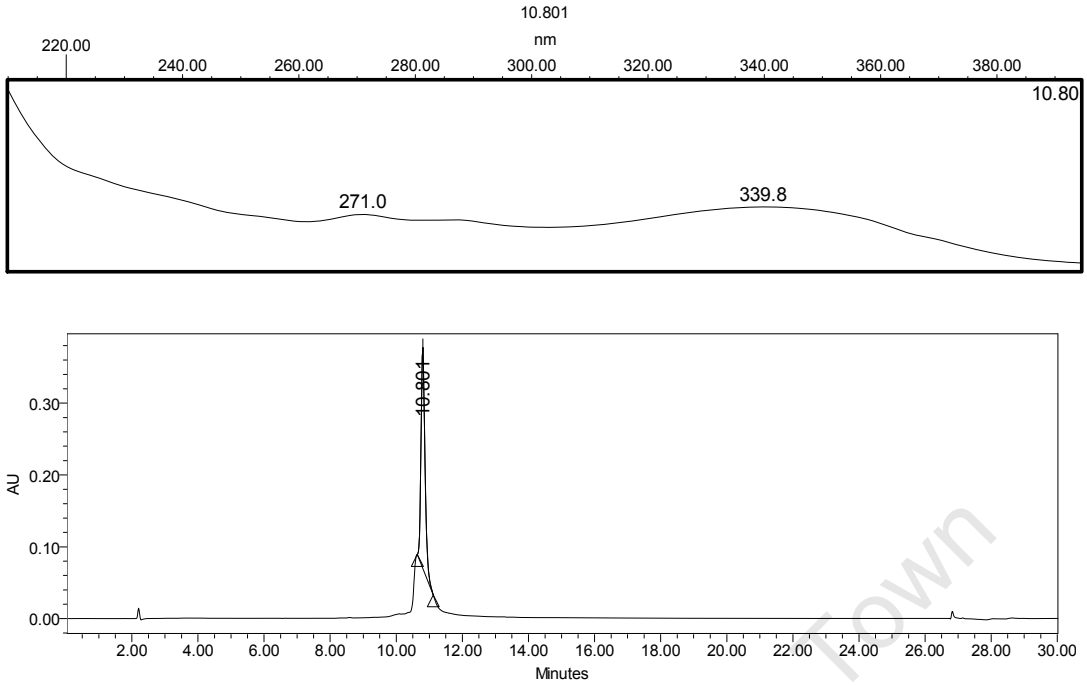

Figure 40 HPLC chromatogram of peak A

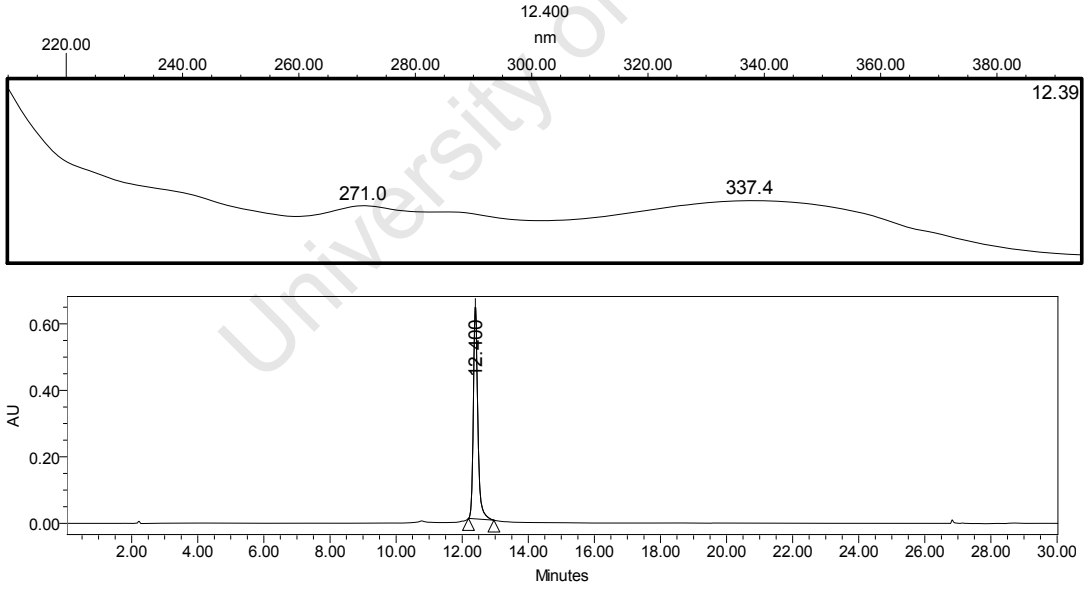

Figure 41 HPLC chromatogram of peak B

4.3 Discussion

The compounds of interest belong to the flavonoid family of natural products and are probably flavones or flavonols. The UV spectra of these compounds show 2 maximum absorbance bands, typical for flavonoids. Many members of the flavonoid family are physiologically active, which would make these compounds a good source to search for antimalarial active compounds [Harborne *et al*., 1975]. These compounds form part of the plants defence system against insect herbivores and pathogens, and are stored in the central vacuoles of cells in relatively high amounts [Salisbury and Ross, 1992].

Xerophyta species "hibernate" during winter, but still need protection against pathogens. It is therefore hypothesised that the compounds of interest would have been present at relatively high concentrations during the time of collection. The leave bases of the *Xerophyta* species are probably used to protect the inner stems against insect herbivores and pathogens, therefore the decision to start off with the leave bases. The extraction methodology, as described in Chapter 12 (12.2), was used to target compounds with intermediate polarities.

The two most abundant compounds isolated from *X. retinervis* were also present in the *X. villosa* extract, therefore the decision to fractionate the crude extract from *X. villosa*. The methanol (organic phase) extract of *X. villosa* as described in 4.2.1.4 was targeted for antimalarial compounds. An automated, semi-preparative reverse phase (C_{18}) HPLC system was used to separate and collect the compounds of interest. A sample of the crude extract at a concentration of 20 mg/ml in DMSO was originally used during fractionation, but yielded low amounts of semi-pure compounds per analytical run. The concentration of the extract was increased to 200 mg/ml, which increased productivity tenfold. With this "upscale approach", about 1 gram crude extract could be fractionated per week to produce 6 semi-pure compounds (20 - 30 mg). The extraction procedure (Chapter 2) was also repeated a few times to obtain enough material for the *in vitro* and *in vivo* animal experiments. These semi-pure fractions were further purified using a second automated, analytical reverse phase HPLC system with different column technology (C_{16} - amide). The chromatography was optimised for each compound by using different mobile phase gradients. Baseline separation between compound of interest and the "impurities" was reached for all applications.

This project not only deals with the isolation and structural elucidation of new antiplasmodial compounds, but also with bioavailability, metabolic and efficacy evaluation of antiplasmodial compounds in an animal model. Animal testing requires relatively high amounts of pure material, so it was decided for practical reasons to focus the fractionation process on the compounds that were present at relatively high amounts. The automated fractionation system as described in Chapter 12 (12.5) was run for a few weeks to obtain enough material for further testing: *in vitro* antiplasmodial and cytotoxicity screening (Chapter 5), structural elucidation (Chapter 6), bioavailability evaluation (Chapter 8), metabolic investigation (Chapter 9) and *in vivo* antimalarial experiments (Chapters 7 and 10). Six compounds were isolated from the leave bases of *X. villosa* with purities above 99% (according to HPLC). Compounds 1 and 2 are light brown, compounds 3, 4 and 5 are light yellow and compound 6 has a light orange colour.

CHAPTER 5

Antiplasmodial activity and cytotoxicity screening of pure compounds isolated from *X. villosa* and *X. retinervis*

5 Antiplasmodial activity and cytotoxicity screening of pure compounds isolated from *X. villosa* and *X. retinervis*

5.1 Introduction

The six isolated compounds from *X. villosa* were targeted as potential selective antiplasmodial compounds.

The same screening assay was used (as was used for screening the extracts) for testing the antiplasmodial activity of the six isolated compounds. Cytotoxicity screening of the six pure compounds was also used to determine their general toxicity. The methodology is described in Chapter 12 (12.3 and 12.4).

5.2 Results

5.2.1 Antiplasmodial activity screening

5.2.1.1 Antiplasmodial screening of 6 pure compounds against the D10 strain

The antiplasmodial activity of the six isolated compounds was determined for the chloroquine sensitive D10 strain. These experiments were done in duplicate and repeated two times on separate days. Chloroquine was used as an internal standard to monitor the experimental conditions and showed IC_{50} values within the acceptable range (6 - 20 ng/ml). The IC_{50} values were 11.1, 9.1, 22.5, 5.5, 2.5 and above 100 µg/ml on average, respectively (compounds 1, 2, 3, 4, 5 and 6). The parasite survival curves are presented in figures 42 - 47.

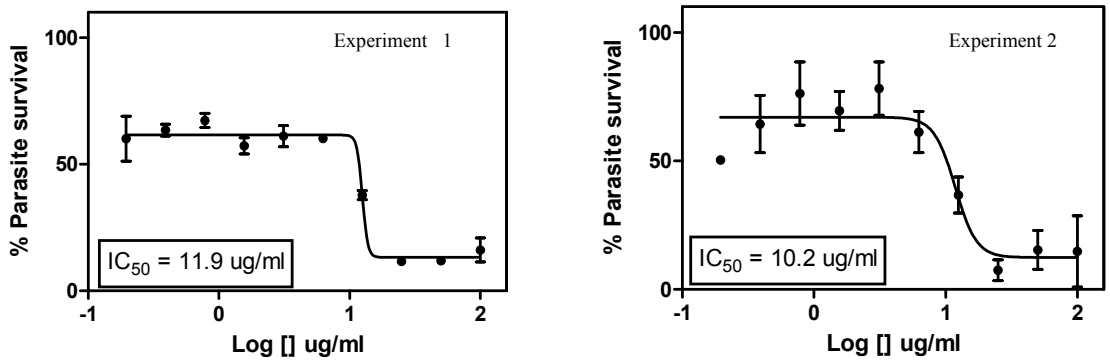

Figure 42 Dose response curves of compound 1 on *P. falciparum* D10 parasites

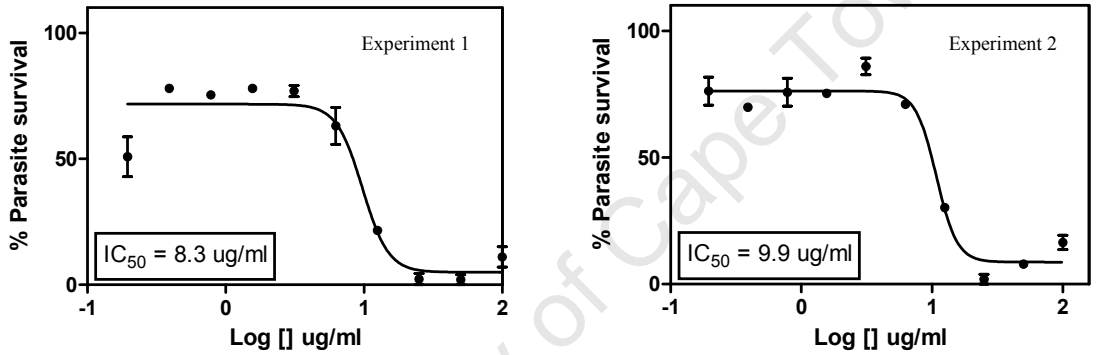

Figure 43 Dose response curves of compound 2 on *P. falciparum* D10 parasites

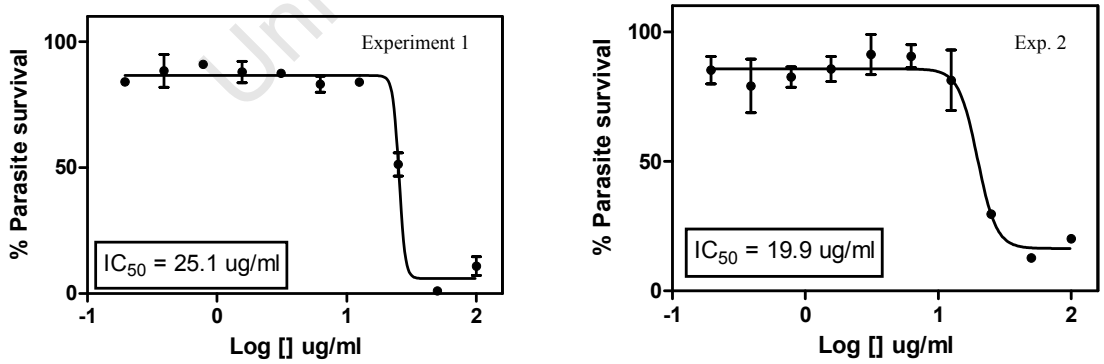

Figure 44 Dose response curves of compound 3 on *P. falciparum* D10 parasites

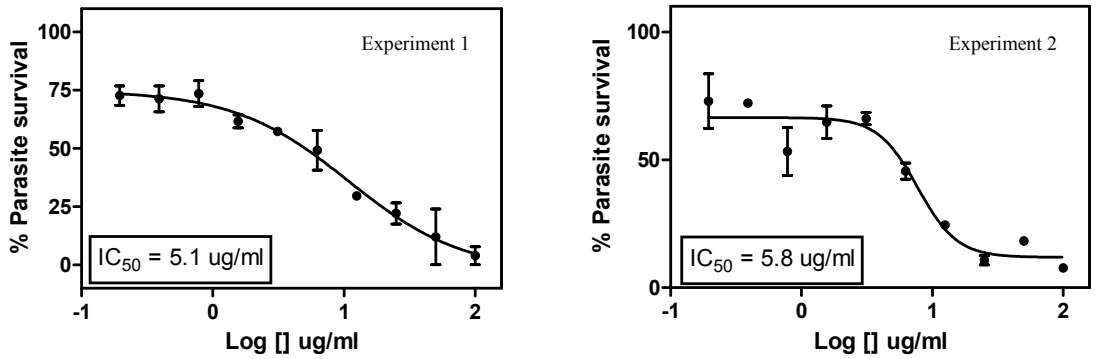

Figure 45 Dose response curves of compound 4 on *P. falciparum* D10 parasites

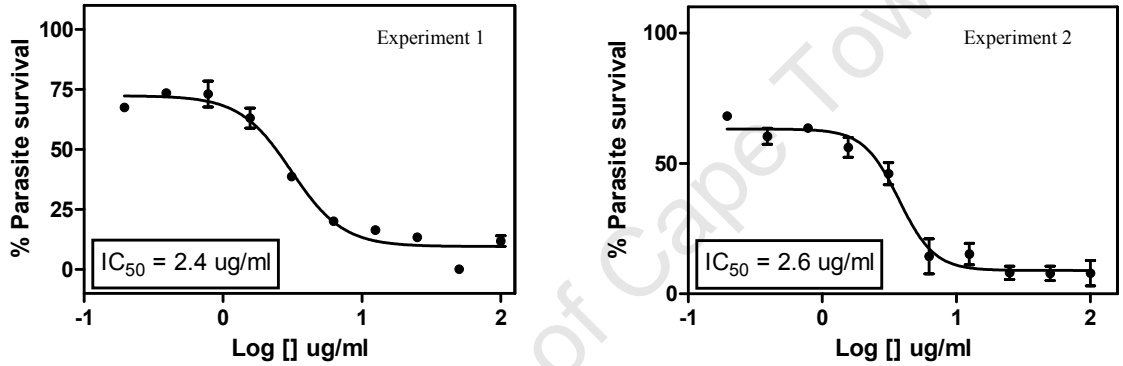

Figure 46 Dose response curves of compound 5 on *P. falciparum* D10 parasites

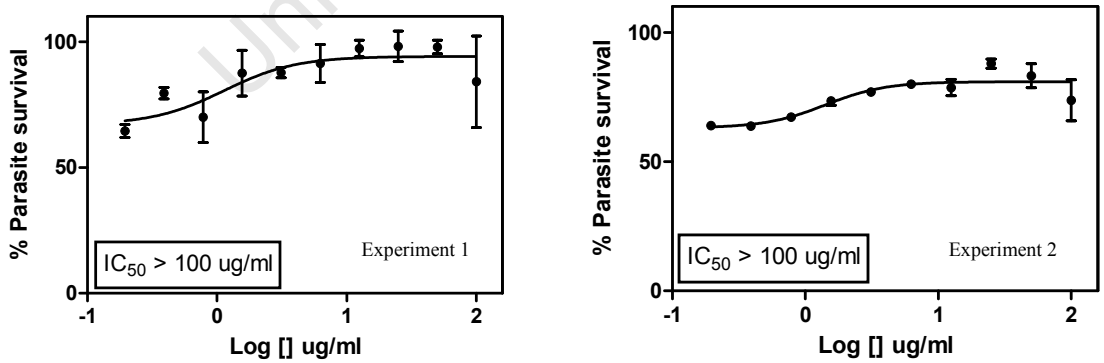

Figure 47 Dose response curves of compound 6 on *P. falciparum* D10 parasites

5.2.1.2 Antiplasmodial screening of compounds 4 and 5 against the K1 strain

Compounds 4 and 5 showed the best antiplasmodial activity when tested against the chloroquine sensitive (D10) strain; consequently it was decided to further investigate their activity against the chloroquine resistant K1 strain. These experiments were done in duplicate. Chloroquine was used as an internal standard to monitor the experimental conditions and showed IC_{50} values within the acceptable range (150 - 250 ng/ml). The IC_{50} values were 4.1 and 1.8 µg/ml, respectively. The parasite survival curves are presented in figures 48 and 49.

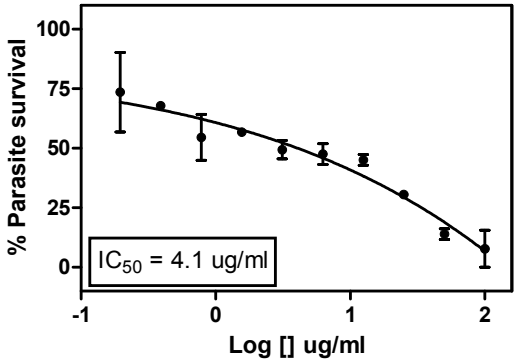

Figure 48 Dose response curve of compound 4 on *P. falciparum* K1 parasites

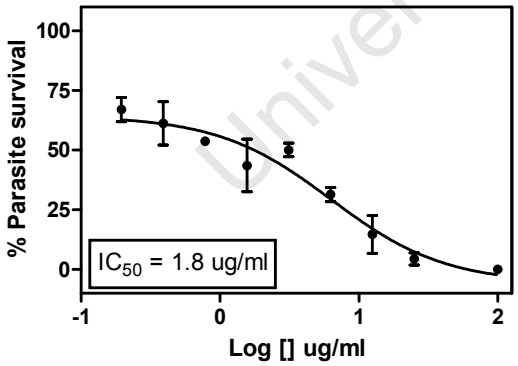

Figure 49 Dose response curve of compound 5 on *P. falciparum* K1 parasites

5.2.2 Cytotoxicity assessment of the 6 isolated compounds

Cytotoxicity assessment was performed on all 6 isolated compounds. These experiments were done in triplicate and repeated two times on separate days. Emetine was used as a quality control standard to monitor the experimental conditions and showed IC_{50} values within the acceptable range (40 – 60 ng/ml). The IC_{50} values were >100, 18.5, >100, 88.3, 95.4 and >100 µg/ml on average, respectively (compounds 1, 2, 3, 4, 5 and 6). The cell viability curves are presented in figures 50 - 55.

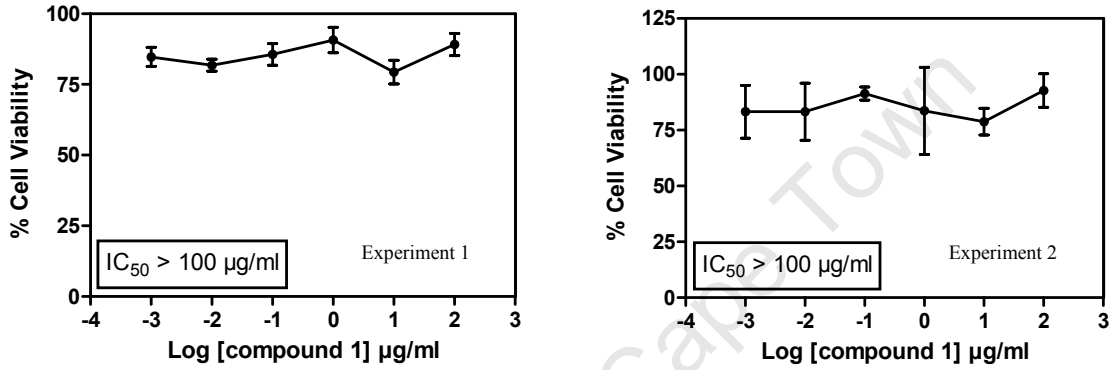

Figure 50 Dose response curves of compound 1 on CHO cells

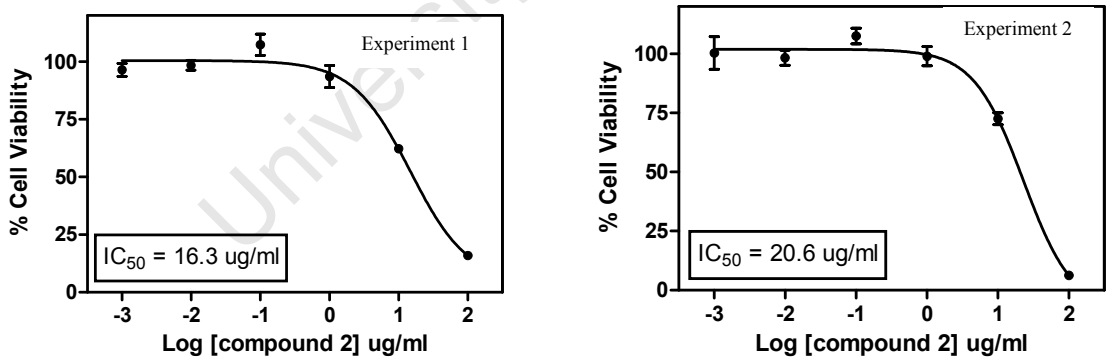

Figure 51 Dose response curves of compound 2 on CHO cells

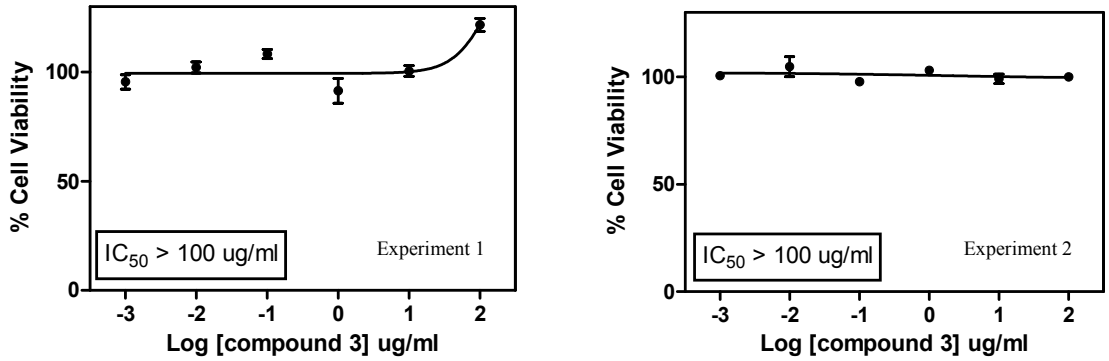

Figure 52 Dose response curves of compound 3 on CHO cells

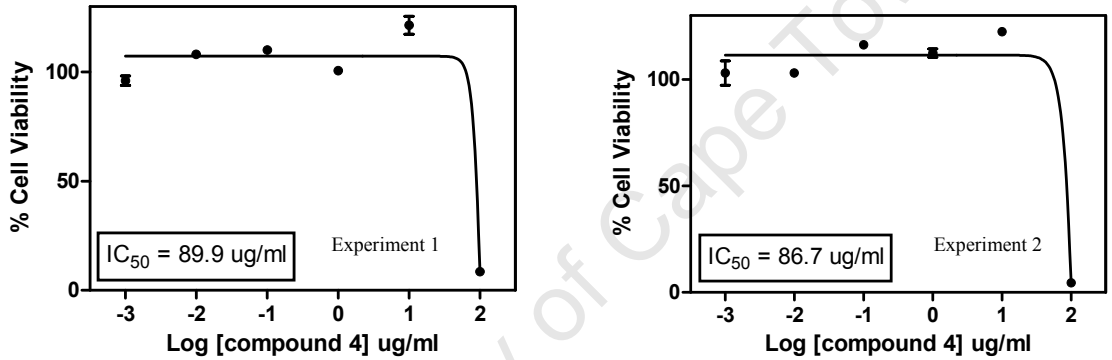

Figure 53 Dose response curves of compound 4 on CHO cells

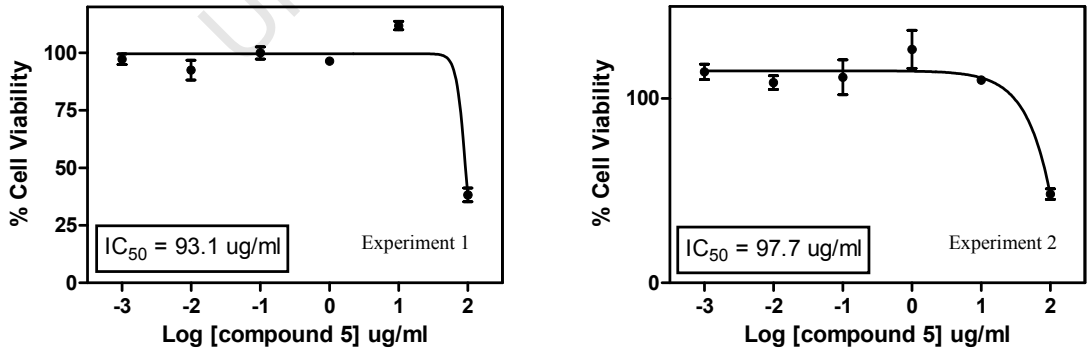

Figure 54 Dose response curves of compound 5 on CHO cells

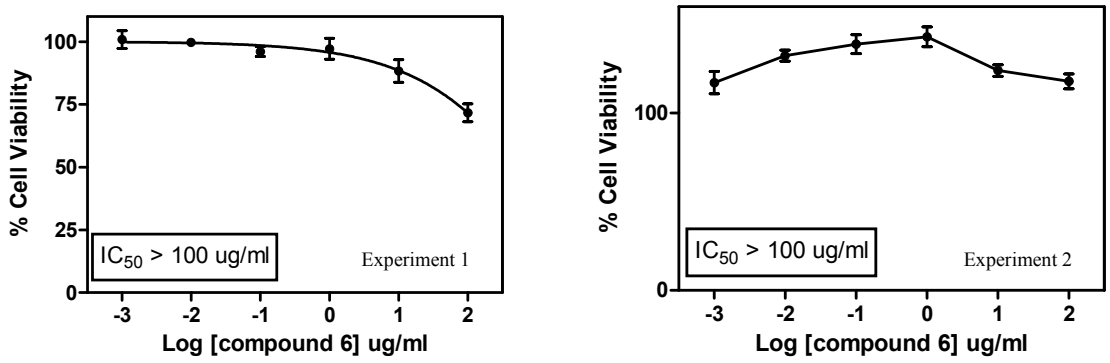

Figure 55 Dose response curves of compound 6 on CHO cells

5.2.3 Selectivity Index

The antiplasmodial activity and cytotoxicity results are summarised in table 4. The selectivity index values were determined for each compound, using the D10 strain (explained in 3.2.3).

Table 4 *in vitro* antiplasmodial activity, cytotoxicity and selectivity index values

Compound	Antiplasmodial activity D10 (IC_{50}, µg/ml)	Antiplasmodial activity K1 (IC_{50}, µg/ml)	Cytotoxicity (IC_{50}, µg/ml)	Selectivity Index [a]
1	11.1	-	>100	> 9.0
2	9.1	-	18.5	2.0
3	22.5	-	>100	> 4.4
4	5.5	4.1	88.3	16.1
5	2.5	1.8	95.4	38.2
6	> 100	-	>100	n/a

[a] Selectivity Index = cytotoxicity IC_{50}/antiplasmodial D10 IC_{50}

5.3 Discussion

The pure compounds were screened against the chloroquine sensitive (D10) *P. falciparum* strain. Two of these compounds showed relatively good antiplasmodial activity, three showed mild activity, and one showed no activity. The two most active compounds were further screened against a chloroquine resistant (K1) strain and showed similar activity compared to the sensitive strain. This information indicates that these compounds are probably using a different parasite inhibitory mechanism than chloroquine.

The pure compounds were also screened against mammalian cells to investigate their specificity to the malaria parasite. The most active compound (5) showed relatively low cytotoxicity and the selectivity index value indicates that this compound selectively inhibits parasites compared to mammalian cells at the same concentration. This compound fits well within the selectivity criteria set by Pink and co-authors and is therefore considered a good candidate for further animal testing [Pink *et al*., 2005].

CHAPTER 6

Structural elucidation of antiplasmodial compounds extracted from *Xerophyta* species

6 Structural elucidation of antiplasmodial compounds extracted from *Xerophyta* species

6.1 Introduction

Ultraviolet spectroscopy was used to identify the class of compound. UV spectra of flavonoids consist of two major absorption maxima bands at 240 – 285 nm and 300 – 400 nm [Harborne *et al*., 1975]. High resolution mass spectrometry is used to determine the mass and atomic composition of a molecule [Clayden *et al*., 2004]. Unit resolution mass spectrometry is used complementary to high resolution mass spectrometry to determine molecular ions. Nuclear magnetic resonance spectroscopy (1D and 2D) is used to identify all the proton and carbon atoms of a molecule [Clayden *et al*., 2004]. Numerous articles have been written about structural elucidation of flavones using NMR spectroscopy. Some of these have been studied to get more insight on typical proton and carbon chemical shifts of this class of natural products [Sahin *et al*., 2004; Moon *et al*., 2005; Park *et al*., 2006].

Antiplasmodial screening and cytotoxicity testing of the 6 isolated compounds revealed that compound 5 would make the best candidate for further *in vivo* experimentation due to its relatively good and selective antiplasmodial activity. At this stage of the project it was decided to do a feasibility study of compound 5 *in vivo* to determine the bioavailability of this compound in mice (Chapter 8). Results from these initial experiments showed that compound 5 gets metabolised to form a product that is identical to compound 4. This compound (4) was the second best candidate, and it was decided to include this compound during this phase of the project. Compounds 1, 2 and 3 showed mild antiplasmodial activities and compound 6 was inactive against the parasites. An internal standard was required for bioavailability experiments (Chapter 8). Compound 2 was tested during initial bioavailability experiments as an internal standard for the assay method, and showed promising results. Compound 2 was also the third most active compound against the malaria parasites. For these reasons the inclusion here.

UV spectroscopy, mass spectrometry and nuclear magnetic resonance spectroscopy (1D and 2D) techniques were used to resolve the structures. The methodology is presented in Chapter 12 (12.6).

6.2 Structural elucidation of compound 2

The proposed chemical structure of compound 2 (figure 56) resulted from ultraviolet spectroscopy, unit resolution mass spectrometry, high resolution mass spectrometry and nuclear magnetic resonance spectroscopy (1D and 2D).

6.2.1 Chemical structure

The proposed chemical structure of compound 2 (figure 56) consists of a 3 ring system with hydroxyl groups at position 5, 7, 3′ and 4′.

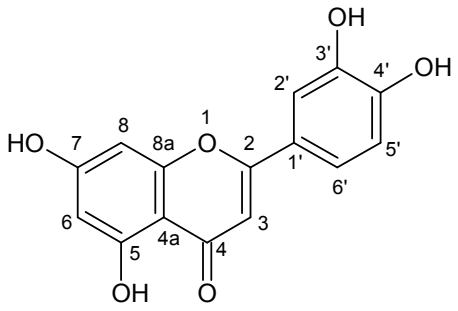

Figure 56 Proposed chemical structure of compound 2

6.2.2 Results

6.2.2.1 Ultraviolet spectroscopy

The UV spectrum of compound 2 is presented in appendix 1 (figure 127).

6.2.2.2 Mass spectrometry

6.2.2.2.1 Unit resolution mass spectrometry

The unit resolution mass spectrum of compound 2 is presented in appendix 1 (figure 128) showing the molecular ion $[M+H]^+$ at m/z 287.6.

6.2.2.2.2 High resolution mass spectrometry

The accurate mass spectrum of compound 2 is presented in appendix 1 (figure 129) showing the molecular ion $[M+H]^+$ at m/z 287.0550, which corresponded to the molecular formula $C_{15}H_{10}O_6$ of compound 2 (calculated mass 287.0556).

6.2.2.3 Nuclear magnetic resonance spectroscopy

6.2.2.3.1 ^{1}H NMR spectrum

The ^{1}H NMR spectrum of compound 2 is presented in appendix 1 (figure 130). Peak assignments according to 2D experiments are presented in figure131.

6.2.2.3.2 ^{13}C NMR spectrum

The ^{13}C NMR spectrum of compound 2 is presented in appendix 1 (figure 132). Peak assignments according to 2D experiments are presented in figure 133.

6.2.2.3.3 COSY spectrum of compound 2

Results from the proton correlation spectroscopy experiment are presented in appendix 1 (figure 134), with detailed spectral information presented in figure 135.

6.2.2.3.4 HSQC spectrum of compound 2

Results from the heteronuclear single quantum proton correlation spectroscopy experiment are presented in appendix 1 (figure 136).

6.2.2.3.5 HMQC spectrum of compound 2

Results from the heteronuclear multiple bond quantum coherence experiment are presented in appendix 1 (figure 137). Detailed spectral information is presented in figure 138.

6.2.2.3.6 Summary of NMR spectral data

Results from the NMR experiments are presented in table 5.

Table 5 NMR data of compound 2

Position	δ ^{1}H	δ ^{13}C	COSY	HMQC
2	-	163.77	-	-
3	6.67 s	102.74	-	C-1′, C-2, C-4, C-4a
4	-	181.53	-	-
4a	-	103.57	-	-
5-OH	12.97 s	157.17	-	C-5
6	6.19 d	93.72	-	C-4a, C-5, C-7, C-8
7	-	164.03	-	-
8	6.44 d	98.71	-	C-4a, C-6, C-7, C-8a
8a	-	161.36	-	-
1′	-	121.36	-	-
2′	7.39 d (1.75 Hz)	113.24	-	C-2, C-3′, C-6′
3′	-	149.61	-	-
4′	-	145.62	-	-
5′	6.89 d (8.30 Hz)	115.89	H-6′	C-1′, C-4′
6′	7.41 dd (8.33Hz, 2.09 Hz)	118.87	H-2′ H-5′	C-2, C-2′

6.2.3 Discussion

Two maximum absorbance bands were observed at 255 and 349 nm, which is typical for flavonoids.

The high resolution mass spectrum of compound 2 suggested 15 carbons, 10 hydrogens and 6 oxygen atoms, which correlate well with the proposed chemical structure of compound 2 (figure 56).

Spectral analysis of the ^{1}H, ^{13}C, COSY, HSQC and HMQC NMR spectra revealed the following structural information about compound 2:

The ^{1}H NMR spectrum showed two aromatic spin systems in the downfield region typical for aromatic signals (δ 6.0 – 8.0 ppm). These coupling patterns suggested the presence of the following sub-structures:

Substructure 1

The proton at position 6 is meta-coupled to the proton at position 8. The proton at position 8 is also meta-coupled to the proton at position 6. Substructure 1 is presented in figure 57.

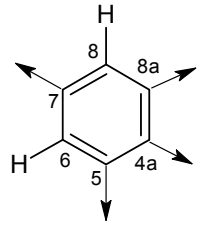

Figure 57 H-6 and H-8 from substructure 1

Substructure 2

The proton at position 2′ is meta-coupled (1.75 Hz) to the proton at position 6′. The proton at position 5′ is ortho-coupled (8.30 Hz) to the proton at position 6′. The proton at position 6′ is ortho-coupled (8.33 Hz) to the proton at position 5′ and meta-coupled (2.09 Hz) to the proton at position 2′. Substructure 2 is presented in figure 58.

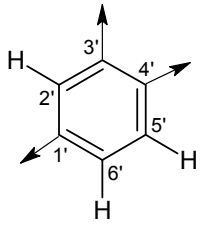

Figure 58 H-2′, H-5′ and H-6′ from substructure 2

The proton spectrum also indicated two singlets, an olefinic proton (figure 59) at δ 6.67 which is typical for an α,β-unsaturated carbonyl system and a acidic phenolic proton (figure 60) which is in a close proximity to a carbonyl group at δ 12.97 ppm.

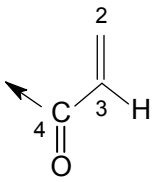

Figure 59 Substructure 3: α,β-unsaturated carbonyl system

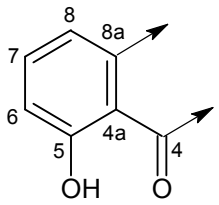

Figure 60 Substructure 4: acidic phenolic proton

The ^{13}C NMR spectrum confirmed the presence of 15 carbon atoms which matches up with the suggested chemical formula that was revealed from the high resolution mass spectrum. The COSY spectrum showed connectivities between the protons at positions 5′ and 6′. Analysis of the HSQC spectrum revealed information about proton-carbon connectivities as can be seen in table 5. The HMBC spectrum was used to assign the remaining carbons and the correlation information was used to connect the different substructures as follows:

Connection of substructures 1, 2, 3 and 4

H-6′ showed connectivity to C-2, H-3 showed connectivities to C-2, C-4, C-4a, and both H-6 and H-8 showed connectivities to C-4a, and H-8 also showed connectivity to C-8a. The following substructure is suggested:

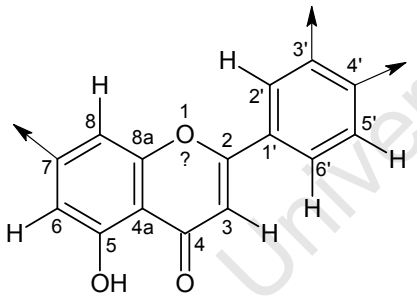

Figure 61 Substructure X (connection of substructures 1, 2, 3 and 4)

The chemical shifts of C-7, C-3′ and C-4′ (δ 164.03, 149.61 and 145.62, respectively) suggested the presence of three –OH groups. The unknown atom at position 1 of substructure X was assigned an oxygen atom as suggested by chemical shifts of C-8a and C-2 (δ 161.36 and 163.77 ppm, respectively). The proposed chemical structure is presented in figure 56.

6.3 Structural elucidation of compound 4

The proposed chemical structure of compound 4 (figure 62) resulted from ultraviolet spectroscopy, unit resolution mass spectrometry, high resolution mass spectrometry and nuclear magnetic resonance spectroscopy (1D and 2D).

6.3.1 Chemical structure

The proposed chemical structure of compound 4 is presented in figure 62.

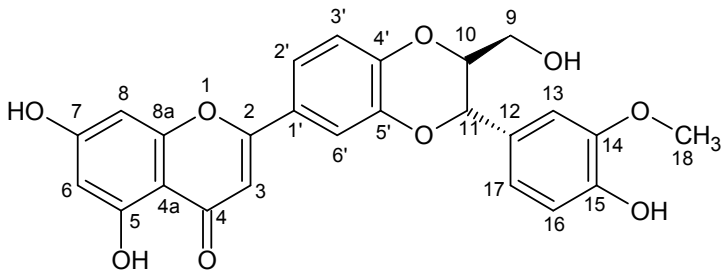

Figure 62 Proposed chemical structure of compound 4

6.3.2 Results

6.3.2.1 Ultraviolet spectroscopy

The UV spectrum of compound 4 is presented in appendix 1 (figure 139).

6.3.2.2 Mass spectrometry

6.3.2.2.1 Unit resolution mass spectrometry

The mass spectrum of compound 4 is presented in appendix 1 (figure 140) showing the molecular ion $[M+H]^+$ at m/z 465.8.

6.3.2.2.2 High resolution mass spectrometry

The accurate mass spectrum of compound 4 is presented in appendix 1 (figure 141) showing the molecular ion $[M+H]^+$ at m/z 465.1193, which corresponded to the molecular formula $C_{25}H_{20}O_9$ of compound 4 (calculated mass 465.1186).

6.3.2.3 Nuclear magnetic resonance spectroscopy

6.3.2.3.1 ^{1}H NMR spectrum

The ^{1}H NMR spectrum of compound 4 is presented in appendix 1 (figure 142). Peak assignments according to 2D experiments are presented in figure 143.

6.3.2.3.2 ^{13}C NMR spectrum

The ^{13}C NMR spectrum of compound 4 is presented in appendix 1 (figure 144). Peak assignments according to 2D experiments are presented in figure 145.

6.3.2.3.3 COSY spectrum of compound 4

Results from the proton correlation spectroscopy experiment are presented in appendix 1 (figure 146). Detailed spectral information is presented in figure 147.

6.3.2.3.4 HSQC spectrum of compound 4

Results from the heteronuclear single quantum proton correlation spectroscopy experiment are presented in appendix 1 (figure 148). Detailed spectral information is presented in figure 149.

6.3.2.3.5 HMQC spectrum of compound 4

Results from the heteronuclear multiple bond quantum coherence experiment are presented in appendix 1 (figure 150). Detailed spectral information is presented in figure 151.

6.3.2.3.6 Summary of NMR spectral data

Results from the NMR experiments are presented in table 6.

Table 6 NMR data of compound 4

Position	δ ^{1}H	δ ^{13}C	COSY	HMQC
2	-	162.81	-	-
3	6.89 s	103.83	-	C-2, C-4, C-4a, C-1′
4	-	181.67	-	-
4a	-	103.67	-	-
5	12.91 s	161.32	-	-
6	6.20 d (2.02 Hz)	98.82	-	C-5, C-8, C-4a
7	-	164.22	-	-
8	6.53 d (2.01 Hz)	94.00	-	C-6, C-7, C-8a C-4a
8a	-	157.24	-	-
9α, 9β	4.12 m	59.96	H-9, H-10	-
10	4.28 m	76.26	H-9, H-11	-
11	5.03 d (7.85 Hz)	77.89	H-10	C-11, C-12, C-13, C-17
12	-	126.84	-	-
13	7.04 d (1.88 Hz)	111.68	-	C-10, C-14, C-17
14	-	147.05	-	-
15	-	147.54	-	-
16	6.81 d (8.00 Hz)	115.23	H-17	C-12, C-14
17	6.85 m	120.50	H-16	C-12, C-14, C-15
18 (OMe)	3.78 s	55.61	-	C-14
1′	-	123.60	-	-
2′	7.61 dd (8.20 Hz, 2.10 Hz)	119.80	H-3′	-
3′	7.09 d (8.53 Hz)	117.42	H-2′	C-1′, C-5′, C-4′
4′	-	146.99	-	-
5′	-	143.56	-	-
6′	7.68 d (2.24 Hz)	114.73	-	C-2, C-5′, C-4′, C-2′

6.3.3 Discussion

Two maximum absorbance bands were observed at 271 and 340 nm, which is typical of flavonoids.

The high resolution mass spectrum of compound 4 suggested 25 carbons, 20 hydrogens and 9 oxygen atoms, which correlate well with the proposed chemical structure of compound 4 (figure 62).

Spectral analysis of the ^{1}H, ^{13}C, COSY, HSQC and HMQC NMR spectra revealed the following structural information about compound 4:

The ^{1}H NMR spectrum showed three aromatic spin systems in the downfield region typical for aromatic signals (δ 6.0 – 8.0 ppm). These coupling patterns suggested the presence of the following sub-structures:

Substructure 1

The proton at position 6 is meta-coupled (2.02 Hz) to the proton at position 8. The proton at position 8 is also meta-coupled (2.01 Hz) to the proton at position 6. Substructure 1 is presented in figure 63.

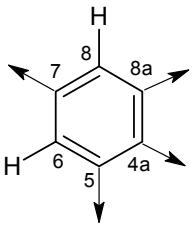

Figure 63 H-6 and H-8 from substructure 1

Substructure 2

The proton at position 2′ is ortho-coupled (8.20 Hz) to the proton at position 3′ and meta-coupled (2.10 Hz) to the proton at position 6′. The proton at position 3′ is ortho-coupled (8.53 Hz) to the proton at position 2′. The proton at position 6′ is meta-coupled (2.24 Hz) to the proton at position 2′. Substructure 2 is presented in figure 64.

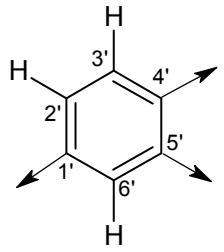

Figure 64 H-2′, H-3′ and H-6′ from substructure 2

Substructure 3

The proton at position 13 is meta-coupled (1.88 Hz) to the proton at position 17. The proton at position 16 is ortho-coupled (8.00 Hz) to the proton at position 17. A multiplet signal at 6.85 ppm suggested the presence of a proton at position 17, which shows connectivities to the protons at positions 11, 13 and 16. Substructure 3 is presented in figure 65.

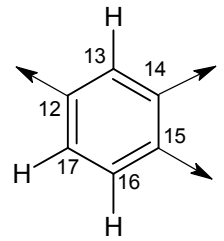

Figure 65 H-13, H-16 and H-17 from substructure 3

The proton spectrum also revealed a fourth spin system of protons attached to oxygenated aliphatic carbons. Two multiplet signals at 4.12 and 4.28 ppm, and a doublet signal at 5.03 ppm which is ortho-coupled (7.85 Hz) to the proton at position 10 suggested substructure 4 (figure 66).

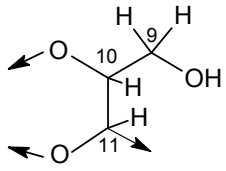

Figure 66 H-9's, H-10 and H-11 from substructure 4

The proton spectrum also indicated three singlets. A methoxyl group (figure 67) at δ 3.78, an olefinic proton (figure 68) at δ 6.89 which is typical for an α,β-unsaturated carbonyl system and an acidic phenolic proton (figure 69) which is in a close proximity to a carbonyl group at δ 12.91 ppm.

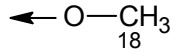

Figure 67 Substructure 5: methoxyl group

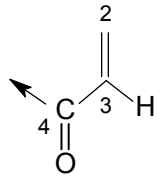

Figure 68 Substructure 6: α,β-unsaturated carbonyl system

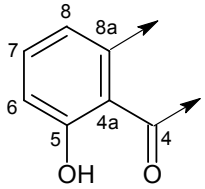

Figure 69 Substructure 7: acidic phenolic proton

The ^{13}C NMR spectrum confirmed the presence of 25 carbon atoms which matches up with the suggested chemical formula that was revealed from the high resolution mass spectrum. The COSY spectrum showed connectivities between the protons at positions 2′ and 3′; 16 and 17; 9, 10 and 11 which confirm the presence of substructures 1, 2, 3 and 4. Analysis of the HSQC spectrum revealed information about proton-carbon connectivities as can be seen in table 6. The HMBC spectrum was used to assign the remaining carbons and the correlation information was used to connect the different substructures as follows:

Connection of substructures 1, 2, 6 and 7

H-6′ showed connectivity to C-2, H-3 showed connectivities to C-2, C-4, C-4a and C-1, and both H-6 and H-8 showed connectivities to C-4a, and H-8 also showed connectivity to C-8a. The following substructure is suggested:

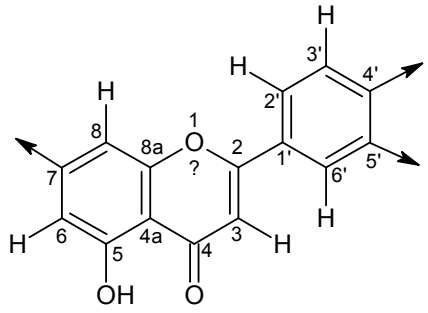

Figure 70 Substructure X (connection of substructures 1, 2, 6 and 7)

Connection of substructures 3 and 4

H-13 and H-17 were long ranged coupled to C-11; H-11 showed connectivities to C-10, C-12, C-13 and C-17. The following substructure is suggested:

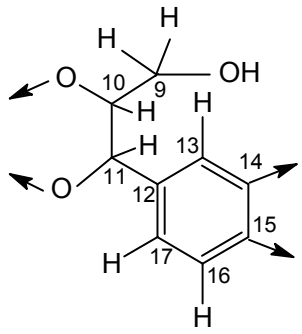

Figure 71 Substructure Y (connection of substructures 3 and 4)

Connection of substructures X and Y

Substructure X was connected at C-4′ and C-5′ to substructure Y's two oxygen atoms as suggested by its chemical shifts of δ 146.99 and δ 143.56 ppm respectively. The chemical shifts of C-5, C-7 and C-15 (δ 161.32, 164.22 and 147.54, respectively) suggested the presence of three –OH groups. C-14's chemical shift (δ 147.05) also indicated an oxygen bond; in this case C-14 was bound to a methoxy-group. The methyl protons were observed as a strong singlet at δ 3.78 which is typical of methoxyl protons. The unknown atom at position 1 of substructure X was assigned to an oxygen atom as suggested by chemical shifts of C-8a and C-2 (δ 157.24 and 162.81 ppm, respectively). The proposed structure for compound 4 is presented in figure 62.

6.4 Structural elucidation of compound 5

The proposed chemical structure of compound 5 (figure 72) resulted from ultraviolet spectroscopy, unit resolution mass spectrometry, high resolution mass spectrometry and nuclear magnetic resonance spectroscopy (1D and 2D).

The chemical structure of this compound has not been published previously, therefore the inclusion of the optical rotation (6.4.2.1) and melting point (6.4.2.2) data. The methodology is presented in Chapter 12 (12.6).

6.4.1 Chemical structure

The proposed chemical structure of compound 5 is presented in figure 72.

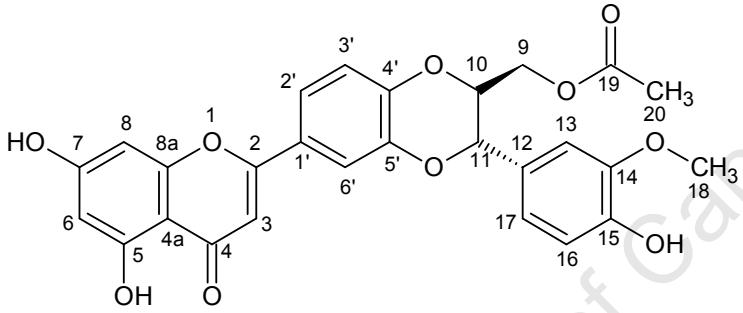

Figure 72 Proposed chemical structure of compound 5

6.4.2 Results

6.4.2.1 Optical rotation

Optical rotation: +0.201

6.4.2.2 Melting point

Melting point: 255.5 – 256.0 °C

6.4.2.3 Ultraviolet spectroscopy

The UV spectrum of compound 5 is presented in appendix 1 (figure 152).

6.4.2.4 Mass spectrometry

6.4.2.4.1 Unit resolution mass spectrometry

The mass spectrum of compound 5 is presented in appendix 1 (figure 153) showing the molecular ion $[M+H]^+$ at m/z 507.7.

6.4.2.4.2 High resolution mass spectrometry

The accurate mass spectrum of compound 5 is presented in appendix 1 (figure 154) showing the molecular ion $[M+H]^+$ at m/z 507.1298, which corresponded to the molecular formula $C_{27}H_{22}O_{10}$ of compound 5 (calculated mass 507.1291).

6.4.2.5 Nuclear magnetic resonance spectroscopy

6.4.2.5.1 ^{1}H NMR spectrum

The ^{1}H NMR spectrum of compound 5 is presented in appendix 1 (figure 155). Peak assignments according to 2D experiments are presented in figure 156.

6.4.2.5.2 ^{13}C NMR spectrum

The ^{13}C NMR spectrum of compound 5 is presented in appendix 1 (figure 157). Peak assignments according to 2D experiments are presented in figure 158.

6.4.2.5.3 COSY spectrum of compound 5

Results from the proton correlation spectroscopy experiment are presented in appendix 1 (figure 159). Detailed spectral information is presented in figure 160.

6.4.2.5.4 HSQC spectrum of compound 5

Results from the heteronuclear single quantum proton correlation spectroscopy experiment are presented in appendix 1 (figure 161). Detailed spectral information is presented in figure 162.

6.4.2.5.5 HMQC spectrum of compound 5

Results from the heteronuclear multiple bond quantum coherence experiment are presented in appendix 1 (figure 163). Detailed spectral information is presented in figure 164.

6.4.2.5.6 Summary of NMR spectral data

Results from the NMR experiments are presented in table 7.

Table 7 NMR data of compound 5

Position	δ ^{1}H	δ ^{1}H**	δ ^{13}C	δ ^{13}C**	COSY	HMQC
2	-	-	162.64	162.66	-	-
3	6.91 s	6.82 s	103.96	103.99	-	C-2, C-4, C-4a, C-1′
4	-	-	181.67	181.69	-	-
4a	-	-	103.67	103.73	-	-
5	12.90 s	12.90 s	161.30	161.35	-	-
6	6.20 d (2.02 Hz)	6.20 d (2.08 Hz)	98.84	98.87	-	C-5, C-7, C-8, C-4a
7	-	-	164.26	164.25	-	-
8	6.54 d (2.02 Hz)	6.53 d (1.98 Hz)	94.05	94.07	-	C-6, C-7, C-8a, C-4a
8a	-	-	157.25	157.28	-	-
9α, 9β	4.11 m, 3.97 m	4.03 m	62.37	62.41	H-9, H-10	C-10, C-11, C-19
10	4.6 m	4.6 m	74.82	74.89	H-9, H-11	-
11	5.06 d (7.99 Hz)	5.05 d (8.12 Hz)	76.19	76.25	H-10	C-10, C-12, C-13, C-17
12	-	-	125.96	126.01	-	-
13	7.06 d (1.91 Hz)	7.03 d (1.92 Hz)	111.65	111.72	-	C-11, C-13, C-17
14	-	-	147.33*	147.38*	-	-
15	-	-	147.66*	147.71*	-	-
16	6.82 d (8.02 Hz)	6.81 d (8.12 Hz)	115.36	115.42	H-17	C-12, C-14, C-15
17	6.89 m	6.87 d (8.12 Hz)	120.59	120.63	H-16	C-11, C-13, C-14
18 (OMe)	3.78 s	3.78 s	55.59	55.65	-	-
19 (OCO)	-	-	169.92	169.98	-	-
20 (OMe)	2.05 s	2.04 s	20.36	20.38	-	-
1′	-	-	123.87	123.89	-	-
2′	7.64 dd (8.53 Hz, 2.16 Hz)	7.58 dd (8.55 Hz, 2.35 Hz)	120.12	120.13	H-3′	C-4′
3′	7.13 d (8.56 Hz)	7.07 d (8.54 Hz)	117.59	117.59	H-2′	C-1′, C-5′, C-4′
4′	-	-	146.87	146.89	-	-
5′	-	-	143.00	143.02	-	-
6′	7.74 d (2.22 Hz)	7.65 d (2.35 Hz)	114.91	114.91	-	C-2, C-5′, C-4′, C-2′

δ ^{1}H** and δ ^{13}C** [Chen, 1997]

* indicates assignments interchangeable

6.4.3 Discussion

Two maximum absorbance bands were observed at 270 and 340 nm, which is typical of flavonoids.

The high resolution mass spectrum of compound 5 suggested 27 carbons, 22 hydrogens and 10 oxygen atoms, which correlate well with the proposed chemical structure of compound 5 (figure 72).

Spectral analysis of the ^{1}H, ^{13}C, COSY, HSQC and HMQC NMR spectra revealed the following structural information about compound 5.

The ^{1}H NMR spectrum showed three aromatic spin systems in the downfield region typical for aromatic signals (δ 6.0 – 8.0 ppm). These coupling patterns suggested the presence of the following substructures:

Substructure 1

The proton at position 6 is meta-coupled (2.02 Hz) to the proton at position 8. The proton at position 8 is also meta-coupled (2.02 Hz) to the proton at position 6. Substructure 1 is presented in figure 73.

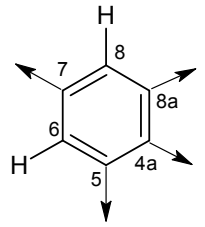

Figure 73 H-6 and H-8 from substructure 1

Substructure 2

The proton at position 2′ is ortho-coupled (8.53 Hz) to the proton at position 3′ and meta-coupled (2.16 Hz) to the proton at position 6′. The proton at position 3′ is ortho-coupled (8.56 Hz) to the proton at position 2′. The proton at position 6′ is meta-coupled (2.22 Hz) to the proton at position 2′. Substructure 2 is presented in figure 74.

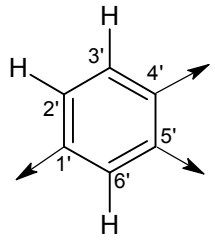

Figure 74 H-2′, H-3′ and H-6′ from substructure 2

Substructure 3

The proton at position 13 is meta-coupled (1.91 Hz) to the proton at position 17. The proton at position 16 is ortho-coupled (8.02 Hz) to the proton at position 17. A multiplet signal at 6.89 ppm suggested the presence of a proton at position 17, which shows connectivities to the protons at positions 11, 13 and 16. Substructure 3 is presented in figure 75.

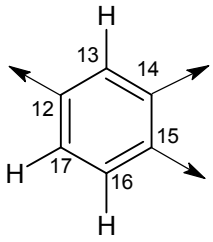

Figure 75 H-13, H-16 and H-17 from substructure 3

The proton spectrum also revealed a fourth spin system of protons attached to oxygenated aliphatic carbons. Three multiplet signals at 3.97, 4.11 and 4.6 ppm, and a doublet signal at 5.06 ppm which is ortho-coupled (7.99 Hz) to the proton at position 10 suggested substructure 4 (figure 76).

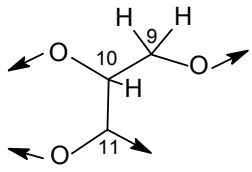

Figure 76 H-9's, H-10 and H-11 from substructure 4

The proton spectrum also indicated four singlets. An o-acetyl group at δ 2.05 (figure 77), a methoxyl group (figure 78) at δ 3.78, an olefinic proton (figure 79) at δ 6.91 which is typical

for an α,β-unsaturated carbonyl system and an acidic phenolic proton (figure 80) which is in a close proximity to a carbonyl group at δ 12.90 ppm.

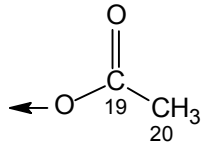

Figure 77 Substructure 5: O-acetyl group

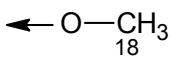

Figure 78 Substructure 6: methoxyl group

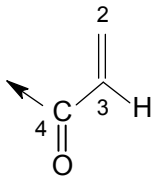

Figure 79 Substructure 7: α,β-unsaturated carbonyl system

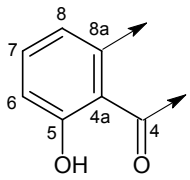

Figure 80 Substructure 8: acidic phenolic proton

The ^{13}C NMR spectrum confirmed the presence of 27 carbon atoms which matches up with the suggested chemical formula that was revealed from the high resolution mass spectrum. The COSY spectrum showed connectivities between the protons at positions 2′ and 3′; 16 and 17; 9, 10 and 11 which confirm the presence of substructures 1, 2, 3 and 4. Analysis of the HSQC spectrum revealed information about proton-carbon connectivities as can be seen in table 7. The HMBC spectrum was used to assign the remaining carbons and the correlation information was used to connect the different substructures as follows:

Connection of substructures 1, 2, 7 and 8

H-6′ showed connectivity to C-2, H-3 showed connectivities to C-2, C-4, C-4a and C-1, and both H-6 and H-8 showed connectivities to C-4a, and H-8 also showed connectivity to C-8a. The following substructure is suggested:

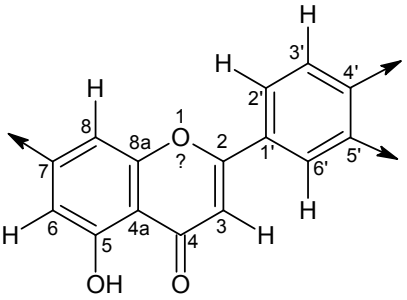

Figure 81 Substructure X (connection of substructures 1, 2, 7 and 8)

Connection of substructures 3, 4 and 5

H-13 and H-17 were long ranged coupled to C-11; H-11 showed connectivities to C-10, C-12, C-13 and C-17; the two H-9 protons showed connectivities to C-10 and C-11; and the protons in the OCOMe group showed connectivities to C-9, The following substructure is suggested:

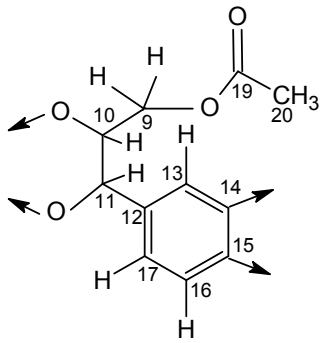

Figure 82 Substructure Y (connection of substructures 3, 4 and 5)

Connection of substructures X and Y

Substructure X was connected at C-4′ and C-5′ to substructure Y's two oxygen atoms as suggested by its chemical shifts of δ 146.87 and δ 145.00 ppm respectively. The chemical shifts of C-5, C-7 and C-15 (δ 161.30, 164.26 and 147.66, respectively) suggested the presence of three –OH groups. C-14's chemical shift also indicated an oxygen bond; in this case C-14 was bound to a methoxy-group. The methyl protons were observed as a strong singlet at δ 2.05 which is typical of methoxyl protons. The unknown atom at position 1 of substructure X was assigned to an oxygen atom as suggested by chemical shifts of C-8a and C-2 (δ 157.25 and 162.64 ppm, respectively). The proposed structure for compound 5 is presented in figure 72.

6.5 Conclusion

Structural elucidation of compounds 2, 4 and 5 revealed the following information about their structures:

Compound 2 is a known flavonoid, luteolin [Boersma *et al*., 2002]. Mild antiplasmodial activity was observed for this compound (Chapter 5). This compound was only used as an internal standard during initial bioavailability experiments (Chapter 8).

Compound 4 is a known flavonolignan, hydnocarpin [Antus *et al*., 1982; Sharma and Hall, 1991; Stermitz *et al*., 2000; Stermitz *et al*., 2001]. This compound showed relatively good and selective antiplasmodial activity (Chapter 5). This is however the first study that shows the presence of hydnocarpin in *X. villosa* and *X. retinervis*. The bioavailability of this compound was also studied in a mouse model (Chapter 8).

Spectral data of compound 5 were identical to a flavonolignan isolated by Chen [Chen, 1997]. This compound showed relatively good and selective antiplasmodial activity and further *in vivo* experiments were conducted on this compound (Chapters 7, 8, 9 and 10). This is the first study that shows the presence of 9-O-acetylhydnocarpin in *X. villosa*.

Structural analysis of compounds 1, 3 and 6 were not discussed during this phase of the project, however analysis was performed on compounds 1 and 3 and revealed the following information:

The accurate mass spectrum of compound 1 is showing the molecular ion $[M+H]^+$ at m/z 271.0613. The proposed chemical formula of compound 1 is: $C_{15}H_{10}O_5$. Spectral analysis of the ^1H, ^{13}C, COSY, HSQC and HMQC spectra revealed the following structural information about compound 1: compound 1 is a small flavone with hydroxyl groups at position 7, 2′ and 3′.

The accurate mass spectrum of compound 3 is showing the molecular ion $[M+H]^+$ at m/z 525.1560. The proposed chemical formula of compound 3 is: $C_{31}H_{24}O_8$. Spectral analysis of the ^1H, ^{13}C, COSY, HSQC and HMQC spectra could not reveal the structure of the compound at this stage of the project, and it was decided not to continue with the structural elucidation of this compound, because of its mild activity.

Compound 6 was inactive against the malaria parasites, therefore the decision to not perform spectral analysis on this compound.

Compounds 1 and 2 are small flavones with similar antiplasmodial activity (11.1 µg/ml and 9.1 µg/ml, respectively, D10 strain). Compounds 4 and 5 are related flavonolignans, compound 4 was about two times more active compared to the two small flavones, and compound 5 was about four times more active compared to the two small flavones.

It appears that the lignan component of the flavonolignans is responsible for a 2 fold improvement in the antiplasmodial activity when compared to the small flavones. The acetyl group at position 9 (figure 72) improved activity twofold.

CHAPTER 7

Antimalarial assessment of 9-O-acetylhydnocarpin in mice

7 Antimalarial assessment of 9-O-acetylhydnocarpin in mice

7.1 Introduction

The next phase of this project was to evaluate the activity of the most promising antiplasmodial compound in an animal model. There are different animal models available for antimalarial drug testing, i.e. the *P. berghei* parasite mouse model and the *P. falciparum* or *P. vivax* parasite Aotus monkey model. The mouse model is usually used for the initial *in vivo* screening of antiplasmodial compounds, and those that perform well during these early tests could be further tested in the primate model. There are many different dosing strategies discussed in the literature, and the most frequently used technique is the 4 day suppressive treatment strategy. Mice are infected with *P. berghei* parasites and treatment starts after 24 hours, once a day for 4 days [Peters *et al*., 1975, 1993; Herrera *et al*., 2002; Gumede *et al*., 2003; Waako *et al*., 2005; Muthaura *et al*., 2007; Ojo-Amaize *et al*., 2007; Portet *et al*., 2007].

The *P. berghei* mouse model was selected for the initial efficacy study of 9-O-acetylhydnocarpin. According to a review article by Richard Pink and co-authors, potential lead antimalarial compounds should show parasite inhibition when administered at concentrations below 100 mg/kg to test animals, consequently it was decided to begin treatment at a concentration of 100 mg/kg (DMSO : water, 1:9 v/v) [Pink *et al*., 2005].

Isolating pure compounds from natural products is a laborious and expensive process. An amount of 2.91 mg pure compound per mouse per treatment is required for dosing at a concentration of 100 mg/kg (average weight of mouse = 29.1 g). The amount of pure material was limited, hence the decision to include three mice per group. The animals were infected with *P. berghei* parasites as described in Chapter 12 (12.9). The 4 day suppressive treatment strategy, with minor modifications, was followed to evaluate the antimalarial activity of 9-O-acetylhydnocarpin in mice. The positive control group was infected with *P. berghei* parasites and treated with chloroquine at a concentration of 10 mg/kg. The negative control group was also infected with *P. berghei* parasites, and was treated with placebo samples which consisted of a solution of DMSO and water (1:9, v/v), without the test compound. The test compound group was also infected with *P. berghei* parasites, and was treated with 9-O-acetylhydnocarpin at a concentration of 100 mg/kg in a solution of DMSO and water (1:9, v/v), once a day on days 2, 3, 4 and 5.

The use of animals in research is a controversial and complicated subject in modern times; consequently it was essential to obtain ethical approval for this part of the project by the ethics committee of the University of Cape Town. A manuscript prepared by the South African Medical Research Council about guidelines on ethics for medical research and the use of animals in research was used as a reference source when compiling the application [Austin *et al*., 2004]. Ethical approval was granted by the Animal Research Ethics Committee, Faculty of Health Sciences, University of Cape Town (Project number: 006/034) for studying the antimalarial activity of 9-O-acetylhydnocarpin in a mouse model.

Figure 83 summarises the allocation of the experimental groups, treatment schedule, sampling and the endpoint of the experiment.

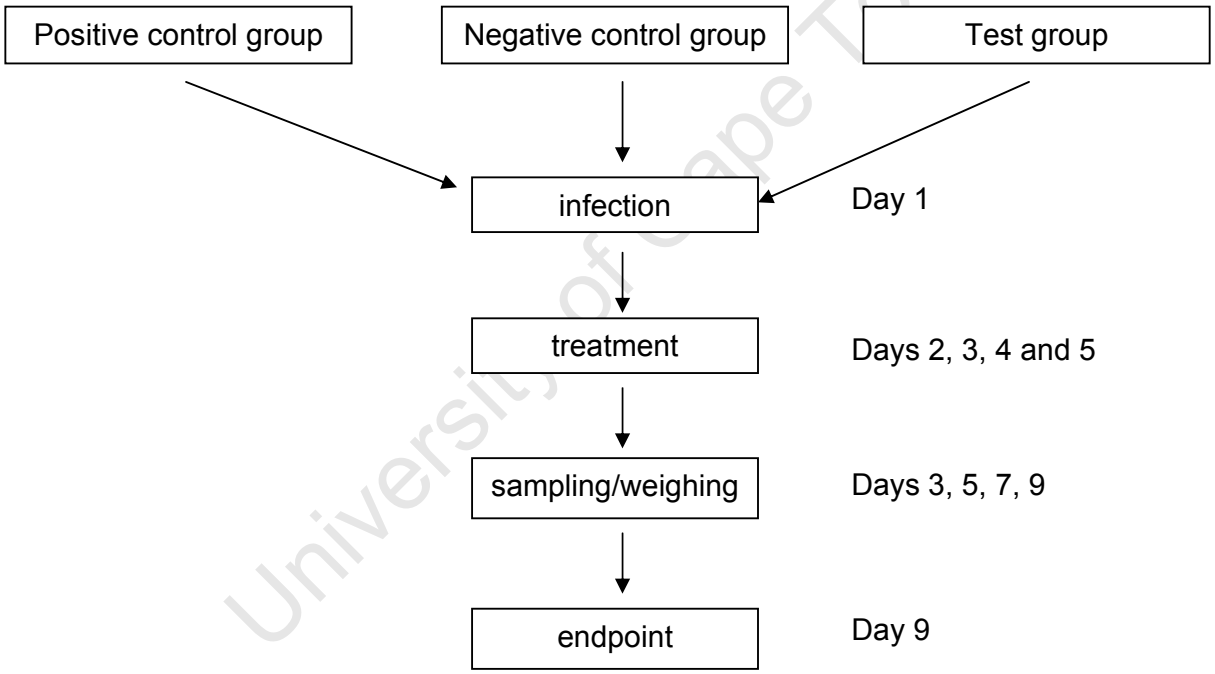

Figure 83 Flow-diagram of the antimalarial assessment animal model, which included the experimental groups, treatment schedule, sampling and the endpoint of the experiment

7.2 Results

The following parameters were evaluated: Body weight, %Parasitaemia and %Chemo suppression. The body weight and percentage parasitaemia data of the mice is presented in appendix 2 (tables 50 and 51) and is summarised in figures 84 and 85. The mean %Parasitaemia and %Chemo suppression data is presented in table 8. The %Chemo suppression of the test compound in a polar formulation (water : DMSO, 90:10, v/v) was determined on day 7 using the following formula:

%Chemo suppression = ((A-B)/A) x 100

A was the mean parasitaemia in the negative control and B was the parasitaemia in the test group. Compound activity was determined by the %reduction of parasitaemia in the treated group compared to untreated group [Tona *et al*., 2001].

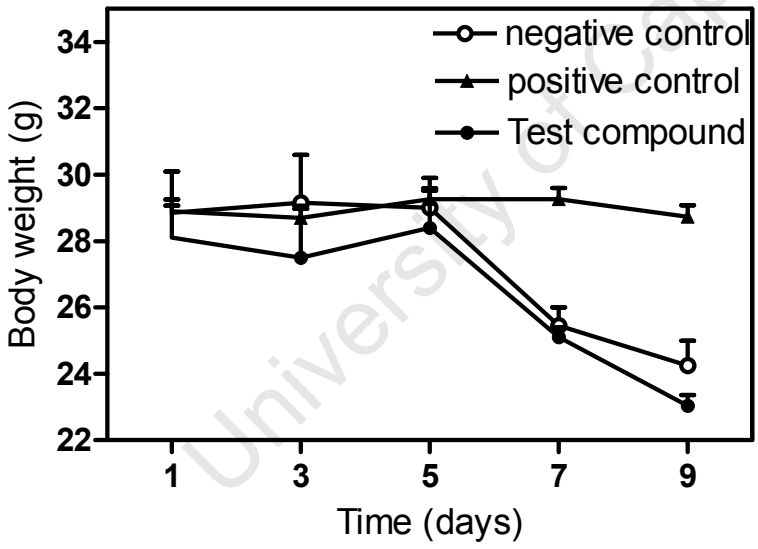

Figure 84 Body weight vs. Time graph of mice treated with a polar 100 mg/kg 9-O-acetylhydnocarpin formulation using the 4 day suppressive treatment strategy (control groups included)

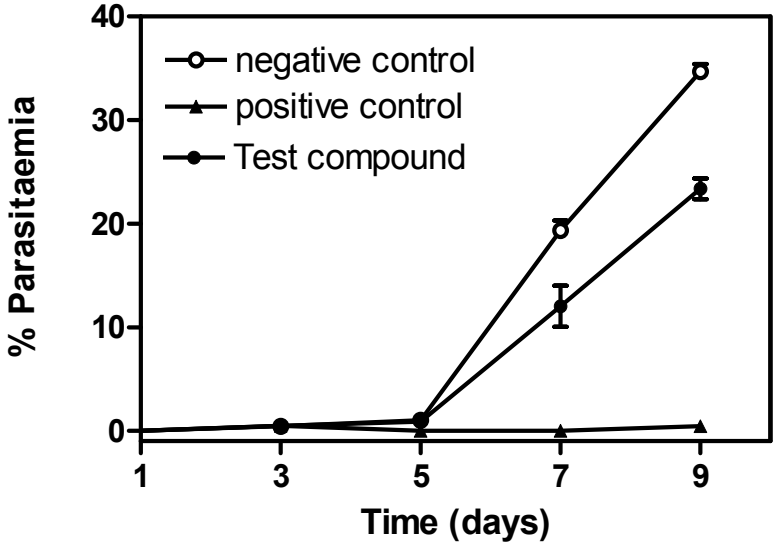

Figure 85 % Parasitaemia vs. Time graph of mice treated with a polar 100 mg/kg 9-O-acetylhydnocarpin formulation using the 4 day suppressive treatment strategy (control groups included)

Table 8 Mean %Parasitaemia and %Chemo suppression data

Treatment	%Parasitaemia	%Chemo suppression
Test group (polar)	12.0 ± 3.4	38.1
Negative control	19.4 ± 1.3	0
Positive control	0.0 ± 0	100

7.3 Discussion

A 38.1% reduction of parasitaemia was observed on day 7 in the group that was treated with the test compound compared to the placebo group, and the weight loss of the test group was comparable with the placebo group. The test compound showed a reasonable degree of parasite inhibition, but could not provide complete protection. Chemo suppression is normally measured around day 5, but because of relatively low parasitaemia levels (in both the test and placebo groups), it was decided to measure the reduction of parasitaemia on day 7.

The test compound was not doing that well in the animal model, and it was hypothesised that it may be a bioavailability problem due to inadequate formulation, or that the test compound was metabolised extensively to inactive metabolites by CYP450 enzymes.

Pink and co-workers have shown the importance of conducting bioavailability and metabolism investigation during early development. These studies aim to improve treatment formulations and are also vital when compounds are selected for *in vivo* activity testing [Pink *et al*., 2005].

The next objective of this project was to evaluate the test compounds absorption, distribution, metabolism and excretion properties in the same mouse model as was used during the efficacy study.

CHAPTER 8

Bioavailability investigation of 9-O-acetylhydnocarpin in mice

8 Bioavailability evaluation of 9-O-acetylhydnocarpin in mice

8.1 Introduction

Bioavailability evaluation of active *in vitro* compounds in animals is one of the most important secondary screening procedures in drug development and should also be included on a larger scale in preliminary antimalarial screening. Drug formulation plays an important part during this phase of the development process. Drug formulation is a comprehensive field and numerous articles have been written on this subject. A few relevant examples are presented below [Rieckmann *et al*., 1996; Shearer *et al*., 2005; Guidance for Industry, 2007].

Morazzoni and co-workers have studied the pharmacokinetics of structurally related compounds (to 9-O-acetylhydnocarpin) in rats. The structurally related compound, silybin, was formulated with a phosphatidylcholine complex and was administered orally to rats. Silybin was also administered in a control formulation, using the natural silymarin extract. An HPLC method was used to analyse the samples. Pharmacokinetic profiles were constructed and the two formulations compared. The silybin-phosphatidylcholine complex showed a 10-fold increase in relative bioavailability compared to the control formulation [Morazzoni *et al*., 1993].

Hitte and co-authors have described general formulation strategies for oral delivery of poorly soluble drugs. Oral administration is the preferred method of administration for antimalarial drugs, but is unfortunately restricted to compounds that could cross the gastric mucosa. Compounds that have the potential to cross these membranes should be at least moderately water-soluble. Many of the compounds that are discovered during *in vitro* screening programmes are poorly water-soluble, thus limiting their use as potential drug candidates. There are many methods that could improve solubility, thereby improving bioavailability. Accelerating agents, such as surfactants, wetting agents and dispersants are used to facilitate dissolution or dispersion. Polyethylene glycol (PEG) is an example of a dispersion-enhancing agent that is also used as a precipitation prevention solvent of poorly aqueous soluble compounds. Polar materials, such as gelatine and lecithin are used to improve the “wetability” of hydrophobic compounds through polar interaction. Polar materials are also used as emulsifying agents. Controlled-release matrix technologies have also been developed for these poorly soluble compounds. The use of

alkalising agents in electrolyte-based systems is also well established in the pharmaceutical field [Hite *et al*., 2003].

Kuentz and co-workers have showed the relevance of using “in silico” pharmacokinetic tools for preclinical formulation development. These new technologies could improve the formulation development process [Kuentz *et al*., 2006].

Monodiglycerides and their derivatives are widely used in the food industry as emulsifiers. These molecules form a range of various liquid crystalline structures when present in an aqueous environment. The structures could potentially dissolve active ingredients and act as drug delivery vehicles. Some of these structures have also been shown to protect compounds against degradation [Sagalowicz *et al*., 2006].

The development of sustained delivery systems for herbal medicines is challenging because of its complexity in composition. Lu and co-workers have developed a synchronized and sustained release glyceryl monostearate matrix system for the silymarin compounds (taxifolin, silychristin, silydianin, isosilybin and silybin) [Lu *et al*., 2007].

A multi-unit floating gel bead delivery system was synthesized with calcium alginate, sunflower oil and the drug of interest through an emulsification process. Tang and co-workers have tested both hydrophobic and hydrophilic drugs and have observed a sustained release of the drugs for more than 12 hours [Tang *et al*., 2007].

Various analytical techniques are described in the literature for analysing samples from pharmacokinetic studies. These techniques can be summarized in two main groups: firstly, HPLC coupled with fluorescence, UV, electrochemical, MS or MS/MS detectors; and secondly, GC coupled with NPD, ECD, FID, MS or MS/MS detectors. The physical and chemical properties of the test compound as well as the biological model are used to decide which analytical system will be appropriate. [Chu *et al*., 2006; Mackie *et al*., 2005; Jia *et al*., 2005; Somers *et al*., 2003; Choi *et al*., 2004; Anupongsanugool *et al*., 2005; DuPont *et al*., 2004; Zhang and Brodbelt, 2004; Schmidt, 2004; Ward *et al*., 2001].

The *P. berghei* mouse model was selected for efficacy testing; therefore the same animal model was required for bioavailability testing. The limited blood volume makes it rather

challenging to study the bioavailability of antiplasmodial compounds in mice. Literature on this subject is limited, so it was clear that new methodology had to be developed to study the bioavailability of antiplasmodial compounds in mouse blood. The aim was to use one animal for all the sampling points. This would require a sensitive and selective analytical method that could measure trace amounts of the test compound in only 10 µl of blood. A highly sensitive and selective analytical system was required, so it was decided to use triple quadrupole mass spectrometry coupled with HPLC. New, specific and sensitive LC-MS/MS methodology was developed to analyse mouse blood samples, which were generated during bioavailability studies. The method development phase of this part of the project is described and presented in Chapter 12 (12.7).

One of the main focus areas of this project is to show the importance of conducting bioavailability studies (using different administration routes and formulations) during early drug development. Information that results from such studies should give the investigator more insight about the biological availability of the test compound at the target site, and should also be used to design an optimised formulation and dosing strategy during further efficacy studies.

A comprehensive bioavailability study of the most active antiplasmodial compound (9-O-acetylhydnocarpin) was conducted in a mouse model, using different administration routes and formulations.

Ethical approval was granted by the Animal Research Ethics Committee, Faculty of Health Sciences, University of Cape Town (Project number: 006/034) for this project.

8.2 Initial bioavailability study of 9-O-acetylhydnocarpin in mice

8.2.1 Introduction

A preliminary investigation of the bioavailability of 9-O-acetylhydnocarpin in mice was performed using LC-MS/MS analysis. A highly selective, sensitive and consistent bioanalytical method for analysing animal samples was developed. The methodology is described and presented in Chapter 12 (12.7.1 and 12.7.2).

9-O-Acetylhydnocarpin was administered orally at a concentration of 200 mg/kg in a solution which consisted of water and DMSO (9:1, v/v) to healthy mice. Blood samples were collected at 0, 1, 2, 3 and 5 hours after administration. One animal per sampling point was used at this stage of the project.

8.2.2 Results

The study samples and calibration standards were analysed according to the method described in Chapter 12 (12.7.2). The calibration curve and the back-calculated results of the standards are presented in appendix 3 (figure 165 and table 56). A quadratic regression weighted 1/x was used for the statistical analyses. Representative chromatograms are presented in appendix 3 (figure 166). The back-calculated results of study samples are presented in table 9.

Table 9 Back-calculated concentrations of 9-O-acetylhydnocarpin

Sample (hours)	Peak Area	Calculated conc. (ng/ml)
0	0	No Peak
1	0	No Peak
2	0	No Peak
3	2400	29.8
5	0	No Peak

8.2.3 Discussion

The analytical method performed well and 9-O-acetylhydnocarpin could be detected at very low amounts. In most of the samples 9-O-acetylhydnocarpin was below the limit of quantification, except for the sample that was collected at 3 hours after administration, but was only present at very low levels. 9-O-Acetylhydnocarpin was administered at relatively high concentrations (200 mg/kg) and one expected to observe high levels in the samples, but this was not the case. 9-O-Acetylhydnocarpin has an acetyl group at carbon 9, which is probably hydrolysed under low pH conditions or hydrolysed by esterase enzymes in the blood. It seems that 9-O-acetylhydnocarpin is metabolised rapidly, but may form metabolites that are still active.

The next phase of this project was to search for these metabolites by making use of precursor ion experiments [Applied Biosystems MDS Sciex].

8.3 Metabolite investigation

8.3.1 Introduction

LC-MS technology is the analytical option of choice in the search for metabolites. Some of these experiments include LC-MS scans, precursor ion experiments and neutral loss scans. At this stage of the project it was thought that the acetyl group of 9-O-acetylhydnocarpin was hydrolysed under low pH conditions in the stomach or by esterase enzymes in the blood to form a hydrolysed product which would have the identical structure of hydnocarpin (Chapter 6). This hydrolysed product would have the same carbon backbone as the parent compound. The product ion mass spectra of 9-O-acetylhydnocarpin and hydnocarpin should have similar product ions. An Applied Biosystems API 2000 mass spectrometer was used to search for this hydrolysed product. The monoisotopic masses of 9-O-acetylhydnocarpin and hydnocarpin are 506.1213 and 464.1107, respectively. The experiments were carried out in the positive ion mode, and $[M+H]^+$ ions were expected (507 for the 9-O-acetylhydnocarpin ion and 465 for the hydrolysed product, hydnocarpin). The precursor ion scan methodology is described and presented in Chapter 12 (12.7.3).

8.3.2 Results

The total ion chromatogram is presented in appendix 3 (figure 167). Mass spectra of the peaks at 0.8, 2.4 and 3.5 minutes are also presented in appendix 3 (figures 168 to 170).

8.3.3 Discussion

The peak at 0.8 minutes resulted in stable precursor ions with masses of 499.5 and 540.0 which may be metabolites. The peak at 2.4 minutes resulted in a stable precursor ion with a mass of 465, which matches up with the proposed molecular ion of the hydrolysed product. The peak at 3.5 minutes resulted in a few stable precursor ions, including 507, which is the molecular ion of 9-O-acetylhydnocarpin. These peaks represent trace amounts of the parent compound. The hydrolysis reaction probably occurs in the stomach of the mice where pH conditions are relatively low or in the blood by esterase enzymes. The mass spectrum of the hydrolysed compound is identical to the mass spectrum of compound 4 (Chapter 6). Their MS/MS spectra are also identical. This compound was the second most active antiplasmodial compound (Chapter 5), therefore the inclusion of the hydrolysed product during the following bioavailability experiments.

8.4 Bioavailability study of 9-O-acetylhydnocarpin and its hydrolysed product in mice using different formulations and administration routes

8.4.1 Introduction

The precursor ion experiments showed that the hydrolysed product of 9-O-acetylhydnocarpin is present in the study samples. The LC-MS/MS method was modified to also detect the hydrolysed product of 9-O-acetylhydnocarpin and was used to study the bioavailability of this product in a mouse model. The bioavailability of 9-O-acetylhydnocarpin and its hydrolysed product was relatively low when administered in a polar chemical environment as was reported previously. The test compound is poorly water soluble which may be the reason for the low blood levels that were measured. A drug delivery system was required that could carry the test drug across membranes. Formulation plays an important role in delivering drugs to the target site and is an important part of early drug development.

At this stage of the project it was decided to study the effect of different administration routes and formulations to get a better understanding about the bioavailability properties of the test compound under the different experimental conditions.
An oral vs. subcutaneous comparison study was conducted using a polar and non polar formulation to examine the bioavailability of these compounds under different chemical and administration environments.

A further objective was to develop an assay method that was more sensitive and used less sample, so that one animal was used for all sampling periods. The mice would not be sacrificed at every time point, and could be reused after a recovery period of about two weeks. The intent was to develop methodology that uses 10 µl of blood per sampling point with six sampling times per animal. Less than 10% of an animal's blood is removed by this methodology, which should not affect the animal's health in any negative way. It should also not have a significant impact on bioavailability results.

The low levels of 9-O-acetylhydnocarpin and the hydrolysed product that were observed during the previous animal experiments may be due to low absorption from the gastrointestinal tract, which may be a matter of formulation [Yanyu *et al*., 2006 Yanyu *et al*., 2006].

A second possibility may be that 9-O-acetylhydnocarpin is absorbed, but undergoes extensive metabolism by the CYP450 enzymes that occur predominantly in the liver [Katzung, 2004].

Surfactants, e.g. PEG and Tween® 80 are often used in formulations to improve bioavailability by enhancing the solubility of test compounds [Hite *et al*., 2003].

Tween® 80 was chosen as a possible delivery vehicle for the test compound. It consists of fatty acid esters of sorbitan polyethoxylates [Tween® 80 by LC-MS].

Experiments used here are intended to give more insight into the matters raised above. Two experiments were designed, the first should have answers to the first topic and the second should answer the metabolism topic.

For the first experiment, Tween® 80 was used as a delivery vehicle and was orally administered to mice. A control group of mice was included, with the test compound was administered in the standard polar format (water : DMSO; 90:10, v/v).

For the second experiment, Tween® 80 was also used as a delivery vehicle but was subcutaneously administered to mice. A control group of mice was included, with the test compound was administered in the standard polar format (water : DMSO; 90:10, v/v).
The experimental design is presented in Chapter 12 (12.7.4).

8.4.2 Results

The calibration standards were extracted and analysed in duplicate. The calibration curves are presented in appendix 3 (9-O-acetylhydnocarpin: figure 171, hydrolysed product: figure 172). The back-calculated results are presented in appendix 3 (9-O-acetylhydnocarpin: table 57, hydrolysed product: table 58). A quadratic regression weighted 1/x was used for the statistical analyses. Representative chromatograms of calibration standards at the LLOQ and C_{max} are presented in appendix 3 (figures 173 and 174). Representative chromatograms of a study sample are presented in appendix 3 (figure 175). Results of the animal samples are presented in sections 8.4.2.1 and 8.4.2.2. The results of the oral dose experiments are summarised in tables 10, 11, 12 and 13. The results of the subcutaneous dose experiments are summarised in tables 14, 15, 16 and

17. Concentration vs. Time graphs of 9-O-acetylhydnocarpin and the hydrolysed product as obtained after a single subcutaneous dose of 9-O-acetylhydnocarpin in the test formulation (100 mg/kg) are presented in figures 86 and 87.

8.4.2.1 Oral dose experiment

8.4.2.1.1 Test formulation

Table 10 Whole blood concentrations of 9-O-acetylhydnocarpin

Time (hours)	Mouse 1 (µg/ml)	Mouse 2 (µg/ml)	Mouse 3 (µg/ml)
0	0	0	0
1	BLQ	BLQ	BLQ
2	BLQ	BLQ	BLQ
3	BLQ	BLQ	BLQ
5	BLQ	0.346	0.318
7	BLQ	BLQ	BLQ

BLQ = below limit of quantification

Table 11 Whole blood concentrations of the hydrolysed product

Time (hours)	Mouse 1 (µg/ml)	Mouse 2 (µg/ml)	Mouse 3 (µg/ml)
0	0	0	0
1	0.317	BLQ	BLQ
2	BLQ	BLQ	BLQ
3	BLQ	BLQ	BLQ
5	BLQ	BLQ	BLQ
7	BLQ	BLQ	BLQ

8.4.2.1.2 Control formulation

Table 12 Whole blood concentrations of 9-O-acetylhydnocarpin

Time (hours)	Mouse 1 (µg/ml)	Mouse 2 (µg/ml)	Mouse 3 (µg/ml)
0	0	0	0
1	BLQ	BLQ	BLQ
2	BLQ	BLQ	BLQ
3	BLQ	BLQ	BLQ
5	BLQ	BLQ	BLQ
7	BLQ	BLQ	BLQ

Table 13 Whole blood concentrations of the hydrolysed product

Time (hours)	Mouse 1 (µg/ml)	Mouse 2 (µg/ml)	Mouse 3 (µg/ml)
0	0	0	0
1	BLQ	BLQ	BLQ
2	BLQ	BLQ	BLQ
3	BLQ	BLQ	BLQ
5	BLQ	BLQ	BLQ
7	BLQ	BLQ	BLQ

8.4.2.2 Subcutaneous dose experiment

8.4.2.2.1 Test formulation

Table 14 Whole blood concentrations of 9-O-acetylhydnocarpin

Time (hours)	Mouse 1 (µg/ml)	Mouse 2 (µg/ml)	Mouse 3 (µg/ml)
0	0	0	0
1	0.632	1.03	0.351
2	0.430	0.512	BLQ
3	0.333	0.731	0.835
5	BLQ	1.18	BLQ
7	BLQ	BLQ	0.0812

Table 15 Whole blood concentrations of the hydrolysed product

Time (hours)	Mouse 1 (µg/ml)	Mouse 2 (µg/ml)	Mouse 3 (µg/ml)
0	0	0	0
1	0.937	0.855	1.18
2	0.598	0.757	0.778
3	0.491	0.801	0.740
5	0.397	1.32	BLQ
7	0.368	BLQ	BLQ

8.4.2.2.2 Control formulation

Table 16 Whole blood concentrations of 9-O-acetylhydnocarpin

Time (hours)	Mouse 1 (µg/ml)	Mouse 2 (µg/ml)	Mouse 3 (µg/ml)
0	0	0	0
1	BLQ	BLQ	BLQ
2	BLQ	BLQ	BLQ
3	BLQ	BLQ	BLQ
5	BLQ	BLQ	BLQ
7	BLQ	BLQ	BLQ

Table 17 Whole blood concentrations of the hydrolysed product

Time (hours)	Mouse 1 (µg/ml)	Mouse 2 (µg/ml)	Mouse 3 (µg/ml)
0	0	0	0
1	BLQ	BLQ	BLQ
2	BLQ	BLQ	BLQ
3	BLQ	BLQ	BLQ
5	BLQ	BLQ	BLQ
7	BLQ	BLQ	BLQ

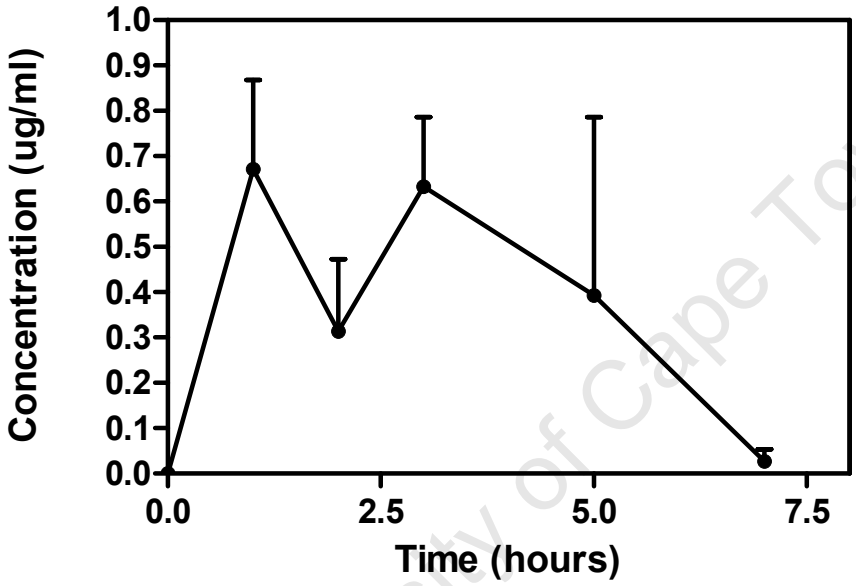

Figure 86 Concentration vs. Time graph of 9-O-acetylhydnocarpin as obtained after a single subcutaneous dose of 9-O-acetylhydnocarpin in the test formulation (100 mg/kg)

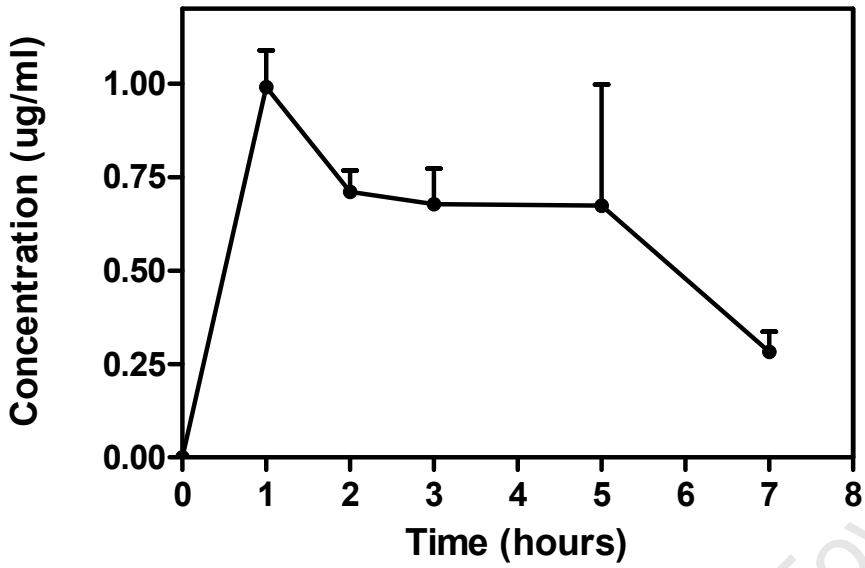

Figure 87 Concentration vs. Time graph of the hydrolysed product as obtained after a single subcutaneous dose of 9-O-acetylhydnocarpin in the test formulation (100 mg/kg)

8.4.3 Discussion

An improved LC-MS/MS method for the determination of 9-O-acetylhydnocarpin and its hydrolysed product in mice whole blood was developed, by making use of a more sensitive mass spectrometer. A micro liquid-liquid filter paper extraction method was developed to extract the compounds of interest from the whole blood samples and was followed by C_{18} reversed phase HPLC and tandem mass spectrometry. The calibration range for both compounds was between 0.313 and 5.0 µg/ml. This assay method was used to quantify 9-O-acetylhydnocarpin and its hydrolysed product in mice whole blood.

Blood levels for 9-O-acetylhydnocarpin and its hydrolysed product obtained during the oral dose experiment were lower than the LLOQ for both the test and control formulations. These results indicate that 9-O-acetylhydnocarpin is poorly absorbed from the gastrointestinal tract or probably metabolised extensively by CYP450 enzymes.

Blood levels for 9-O-acetylhydnocarpin and its hydrolysed product obtained during the subcutaneous dose experiment were relatively high for the Tween® 80 formulation. Blood levels above the LLOQ could be determined for both compounds up to 7 hours after dose. Blood levels in the control group were below the LLOQ for both compounds. These results

show that 9-O-acetylhydnocarpin is bioavailable after subcutaneous dose in the Tween® 80 formulation, and is probably protected against first pass metabolism to some degree. The compounds in the control group should be available after subcutaneous administration, but no levels for both compounds were detected, which is an indication that the compounds were extensively metabolised by probably the CYP450 enzymes.

Results from these experiments show that the test compound is most likely absorbed from the gastrointestinal tract but is extensively metabolised by the liver enzymes.

8.5 Method development and validation of an improved assay method

8.5.1 Introduction

The analytical method that was used during the previous section had a relatively high LLOQ. At this stage of the project a more sensitive method was required to be able to answer some of the questions that were raised previously. A more sensitive analytical model for quantifying the compounds of interest was developed by including an internal standard and improving the extraction method. Compound 2 was selected as an internal standard (6.2). The method development methodology of the new improve analytical model is presented in Chapter 12 (12.7.5).

8.5.2 Validation results

Van Zoonen and co-workers described the importance of method validation in the analytical laboratory [Van Zoonen *et al*., 1999].

This is the final test to demonstrate that the bioassay method is fit to be used as a "tool" to quantify study samples. Shah and co-workers have described the fundamental parameters that are required for validation [Shah *et al*., 2000]. The validation process is also performed to objectively demonstrate the specificity, reliability, sensitivity and suitability of the assay method for the purposes of assaying study samples. A comprehensive method validation is required for analytical methods that are used for analysing samples that are generated during clinical and preclinical studies. This project is about the discovery of selective antiplasmodial compounds, as well as the evaluation of the most active compound in an animal model, keeping this in context, it was decided to develop an accurate and precise analytical method and also show the validity of the method.

8.5.2.1 Analysis of calibration standards

The calibration standards were analysed according to the method described in Chapter 12 (12.7.5). The calibration curves are presented in appendix 3 (9-O-acetylhydnocarpin: figure 176, hydrolysed product: figure 177). The back-calculated results are presented in appendix 3 (9-O-acetylhydnocarpin: table 59, hydrolysed product: table 60). A quadratic regression weighted 1/x was used for the statistical analyses.

8.5.2.2 Stability

Stability information is assessed to ensure that all necessary precautions are taken to ensure that the compound concentration is not affected by internal and external conditions such as matrix-interactions, chemical properties, storage conditions of the drug and the container system. These stability procedures should evaluate the stability of the compound during sample collection and handling, after long-term (frozen at the intended storage temperature) and short-term storage, and after going through freeze and thaw cycles and the analytical process. These experiments should reflect situations likely to be encountered during actual sample handling and analysis [Van Zoonen *et al*., 1999; Shah *et al*., 2000].

8.5.2.2.1 Long term matrix stability

Long term stability should be determined by storing at least three aliquots of each of the low and high concentrations under the same conditions as the study samples. The time that the samples are stored should exceed the time between the date of first sample collection and the date of last sample analysis. The samples that were used to test long term matrix stability were prepared on the sixteenth of March 2007. The standards that were used to construct the calibration curve were prepared on the third of May 2007.

These samples were analysed and peak areas and means as well as the calculated differences between the two sets of aliquots are summarised in appendix 3 (tables 61 and 62). Both compounds were found to be stable for at least 48 days when stored at – 20 °C.

8.5.2.2.2 On bench and Freeze-thaw stability

The FDA Guidance suggested that three freeze and thaw cycles should be determined to ensure compound stability for analytical methods used for clinical sample analysis. They also indicated that at least three aliquots at each of the low and high concentrations should be stored at the intended storage temperature for 24 hours and thawed unassisted at room temperature. After the samples have been thawed completely, they should be refrozen for 12 to 24 hours at the same conditions. This cycle should be repeated two more times, and analysed after the third cycle. If it is found that an analyte is unstable at the intended temperature, these stability samples should be frozen at –70 °C and tested again as described above [Guidance for Industry, 2001].

Spiked solutions of 9-O-acetylhydnocarpin and the hydrolysed product in whole blood at two different concentrations (10 and 0.625 µg/ml) were frozen at -20°C and put through three freeze and thaw cycles. The samples were also left on ice for 2 hours after being thawed. These samples were analysed and peak areas and means as well as the calculated differences between the two sets of aliquots are summarised in appendix 3 (tables 63 and 64).

9-O-Acetylhydnocarpin was found to be stable at high and low concentrations as indicated in table 63. The hydrolysed product was also found to be stable when tested at high concentrations and a slight decrease in measured concentration was observed when tested at low concentrations as indicated in table 64.
The animal samples and calibration standards were only thawed once on ice to prevent degradation.

8.5.2.3 Specificity

Specificity of a method is the ability to differentiate and quantify the compound of interest in the presence of other components in the sample. There are potential interfering substances in a biological matrix that include endogenous matrix components, metabolites, decomposition products and other xenobiotics [Van Zoonen *et al*., 1999; Shah *et al*., 2000].

The very high specificity of the LC-MS/MS assay procedure precludes the detection of any compounds that do not possess the capability to produce the specific molecular ion followed by formation of the specific product ion produced and monitored in the mass spectrometer.

Blank sample extracts were positioned in the injection sequence immediately after the highest calibration standard in order to assess possible carry-over effects. The autosampler needle was rinsed with acetonitrile after every injection for 5 seconds. No significant carry-over was observed. An example of a chromatogram of a blank whole blood extract injected after the highest standard is presented in appendix 3 (figure 178).

8.5.2.4 Limit of quantification

The lower limit of quantification (LLOQ) of a method should have a signal/noise value greater than 5 [Van Zoonen *et al*., 1999; Shah *et al*., 2000]. The LLOQ of this method was set at 0.078 µg/ml (concentration of lowest STD) for both compounds. The signal/noise values for both compounds were much higher than 5. The LLOQ chromatograms are presented in appendix 3 (figure 179).

8.5.2.5 Recovery

The recovery of a compound is the detector response obtained from an amount of compound added to and extracted from the biological matrix, compared to the detector response obtained for the true concentration of the pure authentic standard. The recovery should be consistent, precise and reproducible, and need not be 100% [Van Zoonen *et al*., 1999; Shah *et al*., 2000].

Recovery is the measure of the compounds losses incurred during sample processing, and is defined as: Recovery (%) = (peak area of standard/peak area of sample spiked in mobile phase) x 100

Peak areas of a standard and theoretical peak areas obtained from the samples spiked in mobile phase are used in calculating the recovery of the compounds according to the above mentioned formula.

The concentration of the standard was 10 µg/ml for 9-O-acetylhydnocarpin and the hydrolysed product spiked in whole blood. The concentration of the sample spiked in mobile phase was 1 µg/ml for 9-O-acetylhydnocarpin and the hydrolysed product. The extracted samples were diluted ten times during the extraction process (10 µl sample, 100 µl extract) to give an effective concentration of 1 µg/ml in the final extracted sample, therefore no dilution factor needs to be taken into account.

The concentration of the internal standard in the organic solvent used during the extraction of the standard was 1 µg/ml. The internal standard gets concentrated 2.5 times during the extraction (250 µl organic solvent gets concentrated to 100 µl in the mobile phase). The concentration of the sample spiked in mobile phase was 1 µg/ml for the internal standard. A 2.5 x concentrating factor was included for calculating the internal standards recovery.

Recovery (9-O-acetylhydnocarpin) = (196000/234500) * 100
= 84%

Recovery (hydrolysed product) = (87100 / 78950) x 100
= 110%

Recovery (internal standard) = ((25600 x 2.5) / 76450) x 100
= 84%

8.5.3 Discussion

A reliable, accurate and more sensitive analytical method was developed for determining 9-O-acetylhydnocarpin and its hydrolysed product in mice whole blood. This method was used as a quantification "tool" during the next section of this project.

8.6 Bioavailability study of 9-O-acetylhydnocarpin and its hydrolysed product in mice using a self-microemulsifying drug delivery system

8.6.1 Introduction

A lipid based self-microemulsifying drug delivery system (SMEDDS) improved the bioavailability of silymarin compounds significantly in a study conducted by Wu and co-workers [Wu *et al*., 2006]. These compounds are structurally related to 9-O-acetylhydnocarpin; consequently it was decided to investigate this drug delivery system as a possible vehicle to improve the bioavailability of the compounds investigated in this study. This formulation consists of silymarin, Tween® 80, ethyl linoleate and ethanol. The authors tested different compositions and found the optimal formulation as follows: silymarin (8.5%), ethanol (9.2%), Tween® 80 (54.9%) and ethyl linoleate (27.4%). The bioavailability of silymarin was studied in rabbits by making use of the optimal SMEDDS formulation. It was found that the bioavailability of the silymarin compounds was improved 49 fold when compared to the usual suspension.

The test compound was formulated using the SMEDDS formulation Chapter 12 (12.7.6). The SMEDDS formulation was tested orally and subcutaneously as follow:

Oral dose experiment

9-O-Acetylhydnocarpin was administered orally at a concentration of 200 mg/kg (SMEDDS formulation) to three healthy mice (male, C57BL6). Blood samples (10 µl) were collected just before, and at 0.5, 1, 2, 5 and 7 hours after administration.

Subcutaneous dose experiment

9-O-Acetylhydnocarpin was administered subcutaneously at a concentration of 200 mg/kg (SMEDDS formulation) to three healthy mice (male, C57BL6). Blood samples (10 µl) were collected just before, and at 0.5, 1, 2, 5 and 7 hours after administration.

8.6.2 Results

The study samples and calibration standards were analysed according to the method described in Chapter 12 (12.7.5). Two additional standards were included at the lower end of the calibration curve, and 10 µl was injected onto the column.

Although the internal standard technique is widely used in chromatography, this does not inevitably improve the precision of an assay method; in fact it may even impair the precision of the assay, as was observed during this phase of the project [Haefelfinger, 1981]. The internal standard was found to be unstable in the organic solvent when it was left on the bench for 24 hours, therefore the decision to exclude the internal standard.

Calibration curves (analysed in duplicate) are presented in appendix 3 (9-O-acetylhydnocarpin: figure 180, hydrolysed product: figure 181). The back-calculated results are presented in appendix 3 (9-O-acetylhydnocarpin: table 65, hydrolysed product: table 66). A quadratic regression weighted 1/x was used for the statistical analyses. Representative chromatograms of calibration standards at the LLOQ and Cmax are presented in appendix 3 (figures 182 and 183, respectively). Representative chromatograms of a study sample are also presented in appendix 3 (figure 184).

The results of the oral dose experiments are summarised in tables 18 and 19. Concentration vs. Time graphs of 9-O-acetylhydnocarpin and the hydrolysed product as obtained after a single oral dose of 9-O-acetylhydnocarpin in the SMEDDS formulation (200 mg/kg) are presented in figures 88 and 89.

The results of the subcutaneous dose experiments are summarised in tables 20 and 21. Concentration vs. Time graphs of 9-O-acetylhydnocarpin and the hydrolysed product as obtained after a single subcutaneous dose of 9-O-acetylhydnocarpin in the SMEDDS formulation (200 mg/kg) are presented in figures 90 and 91.

8.6.2.1 Oral dose experiment

Table 18 Whole blood concentrations of 9-O-acetylhydnocarpin

Time (hours)	Mouse 1 (µg/ml)	Mouse 2 (µg/ml)	Mouse 3 (µg/ml)
0	0	0	0
0.5	0.243	0.469	0.388
1	BLQ	0.526	BLQ
2	BLQ	BLQ	BLQ
5	BLQ	BLQ	0.396
7	-	0.537	-

BLQ = below limit of quantification

Table 19 Whole blood concentrations of the hydrolysed product

Time (hours)	Mouse 1 (µg/ml)	Mouse 2 (µg/ml)	Mouse 3 (µg/ml)
0	0	0	0
0.5	0	0	0
1	0	0	0
2	0	0	0
5	0	0	0
7	0	0	0

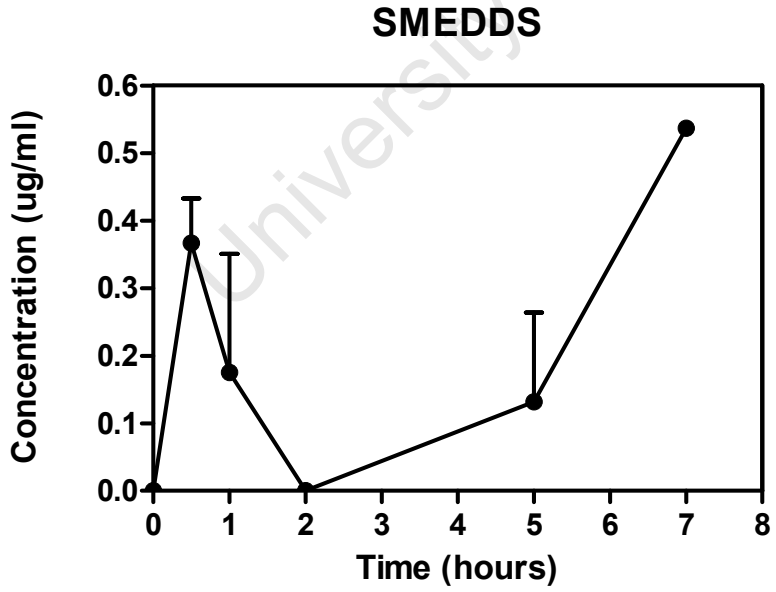

Figure 88 Concentration vs. Time graph of 9-O-acetylhydnocarpin as obtained after a single oral dose of 9-O-acetylhydnocarpin in the SMEDDS formulation (200 mg/kg)

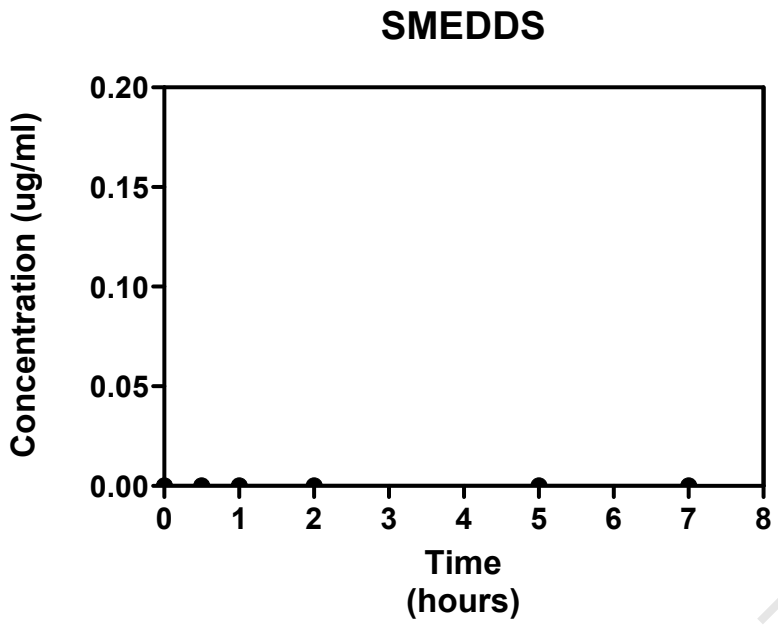

Figure 89 Concentration vs. Time graph of the hydrolysed product as obtained after a single oral dose of 9-O-acetylhydnocarpin in the SMEDDS formulation (200 mg/kg)

8.6.2.2 Subcutaneous dose experiment

Table 20 Whole blood concentrations of 9-O-acetylhydnocarpin

Time (hours)	Mouse 1 (µg/ml)	Mouse 2 (µg/ml)	Mouse 3 (µg/ml)
0	0	0	0
0.5	0.262	0.451	0.433
1	0.149	0	0.303
2	0.0961	0	0.363
5	0.415	0	0.108
7	0.152	0.374	0

Table 21 Whole blood concentrations of the hydrolysed product

Time (hours)	Mouse 1 (µg/ml)	Mouse 2 (µg/ml)	Mouse 3 (µg/ml)
0	0	0	0
0.5	0.119	0.109	0.104
1	0.149	0.108	0.122
2	0.135	0.102	0.126
5	0.194	0.127	0.153
7	0.0869	0.127	0.0867

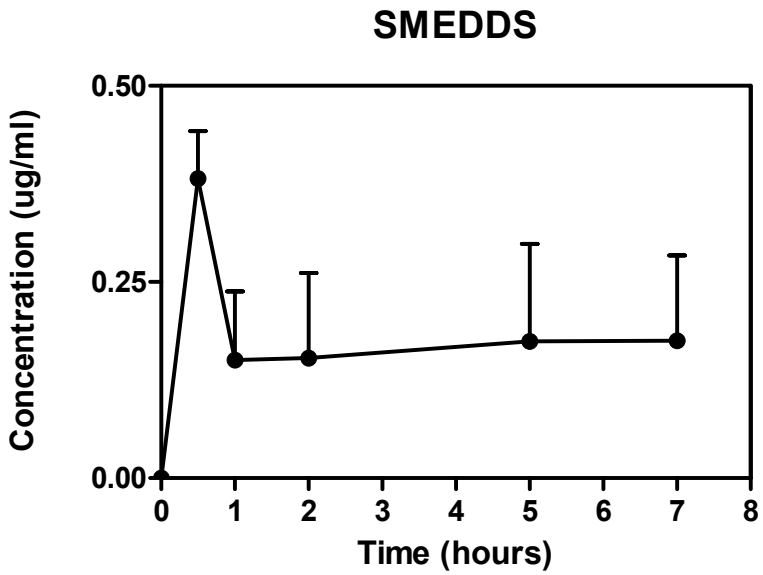

Figure 90 Concentration vs. Time graph of 9-O-acetylhydnocarpin as obtained after a single subcutaneous dose of 9-O-acetylhydnocarpin in the SMEDDS formulation (200 mg/kg)

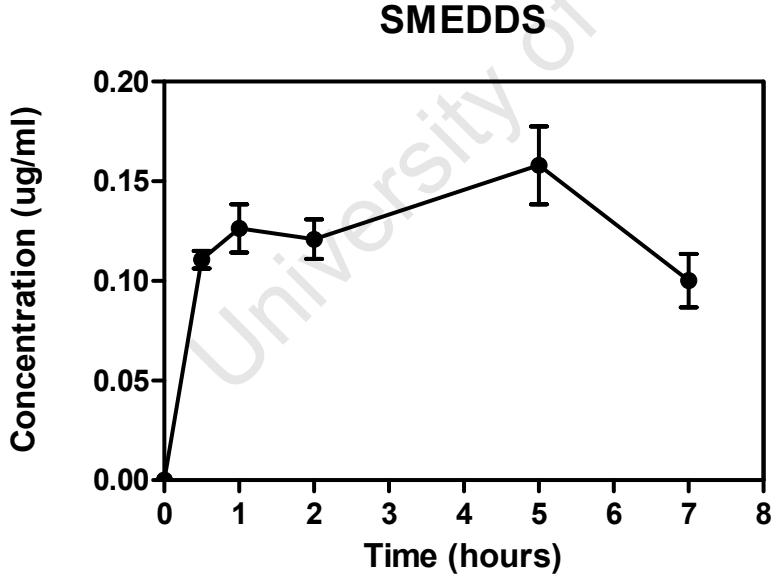

Figure 91 Concentration vs. Time graph of the hydrolysed product as obtained after a single subcutaneous dose of 9-O-acetylhydnocarpin in the SMEDDS formulation (200 mg/kg)

8.6.3 Discussion

The same LC-MS/MS method was used as described in 8.5. The calibration range for both compounds was between 0.0781 and 10.0 µg/ml. This assay method was used to quantify 9-O-acetylhydnocarpin and its hydrolysed product in mice whole blood, using the SMEDDS drug delivery system.

Relatively high levels for 9-O-acetylhydnocarpin could be determined for up to 7 hours, using the SMEDDS oral dose formulation. An enterohepatic circulation effect was observed for the test compound. These results indicate that 9-O-acetylhydnocarpin is absorbed from the gastrointestinal tract, but is rapidly metabolised by the CYP450 enzymes in the liver to probably glucuronidated metabolites. These conjugated metabolites are reintroduced back into the blood system as free molecules as observed by the enterohepatic circulation effect. No levels were detected for the hydrolysed product, which indicates that this formulation protects the test compound against the hydrolysis reaction.

The concentration of the test compound was relatively high after 30 minutes, using the SMEDDS subcutaneous dose formulation, but reached almost steady state after an hour, and lasted for up to seven hours. The hydrolysed product was also observed after 30 minutes but at lower concentrations, and could also be followed for up to seven hours. The SMEDDS formulation also protects the compound against hydrolysis, but to a lesser extent than was observed for the oral dose experiment. The SMEDDS formulation, administered subcutaneously delivered the test compounds at almost steady state.

The SMEDDS formulation improved bioavailability drastically for the oral dose experiment, however higher blood levels of the test compound were expected, if the relatively high dose of 200 mg/kg is brought in context. This indicates that the test compound and its hydrolysed product are extensively metabolised by the CYP450 liver enzymes to probably glucuronidated metabolites.

8.7 Bioavailability study of 9-O-acetylhydnocarpin and its hydrolysed product in mice using Pheroid technology as a drug delivery system after oral administration

8.7.1 Introduction

Pheroid technology is a novel universal drug delivery and carrier system that enhances bioavailability and efficacy. It has also been suggested that the system most likely protects compounds from Phase I and II metabolism. The intellectual property of the Pheroid technology was purchased by the North-West University of South Africa from MeyerZall (Pty) Ltd in 2003. It was tested for a broad range of drugs and showed promising results. The department of Pharmaceutics at the North-West University has granted permission (in writing by Anne Grobler) for testing the Pheroid drug delivery system in this project. The Pheroid system is a colloidal system of modified essential fatty acids with stable lipid-based vesicular structures, known as Pheroids, with size ranging from 200 to 440 nm. These vesicles are distributed uniformly in a dispersion medium which may be modified depending on the application. The Pheroids consist mainly of ethylated and pegylated polyunsaturated fatty acids. Omega-3 and omega-6 are included but arachidonic acid is excluded. The fatty acids are in the cis-conformation and therefore compatible with the orientation of human fatty acids [Grobler *et al*.].

It was decided to investigate this drug delivery system as a possible vehicle to improve bioavailability of the test compound under investigation. 9-O-Acetylhydnocarpin was formulated using the pheroid system, at a concentration of 10 mg/ml. This 9-O-acetylhydnocarpin pheroid formulation was administered orally to three healthy mice (male, C57BL6), at 2 mg per mouse (200 µl of a 10 mg/ml formulation). Blood samples (10 µl) were collected just before, and at 0.5, 1, 2, 5 and 7 hours after administration.

8.7.2 Results

The study samples and calibration standards were analysed according to the method described in Chapter 12 (12.7.5). A new set of calibration standards was prepared, with the LLOQ set at 0.0780 µg/ml, and the highest standard set at 2.5 µg/ml, for 9-O-acetylhydnocarpin and its hydrolysed product. Representative chromatograms of calibration standards at the LLOQ and C_{max} are presented in appendix 3 (figures 185 and 186, respectively). Representative chromatograms of a study sample are presented in appendix 3 (figure 187).

The calibration curves of 9-O-acetylhydnocarpin and its hydrolysed product are presented in appendix 3 (figures 188 and 189, respectively). The back-calculated results and calibration curve statistics are presented in appendix 3 (tables 67 and 68 for 9-O-acetylhydnocarpin and the hydrolysed product, respectively). A quadratic regression weighted 1/x was used for the statistical analyses.

The results of the oral dose experiments are summarised in tables 22 and 23. A Concentration vs. Time graph of 9-O-acetylhydnocarpin obtained after a single oral dose of 9-O-acetylhydnocarpin in the Pheroid formulation (2 mg/mouse) is presented in figure 92.

Table 22 Whole blood concentrations of 9-O-acetylhydnocarpin

Time (hours)	Mouse 1 (µg/ml)	Mouse 2 (µg/ml)	Average (µg/ml)
0	0	0	0
0.5	BLQ	0.0862	BLQ
1	BLQ	BLQ	BLQ
2	BLQ	BLQ	BLQ
5	0.337	BLQ	0.1685
7	0.909	0.533	0.721

BLQ = below limit of quantification

Table 23 Whole blood concentrations of the hydrolysed product

Time (hours)	Mouse 1 (µg/ml)	Mouse 2 (µg/ml)	Mouse 3 (µg/ml)
0	0	0	0
0.5	BLQ	BLQ	BLQ
1	BLQ	BLQ	BLQ
2	BLQ	BLQ	BLQ
5	BLQ	BLQ	BLQ
7	BLQ	BLQ	BLQ

BLQ = below limit of quantification

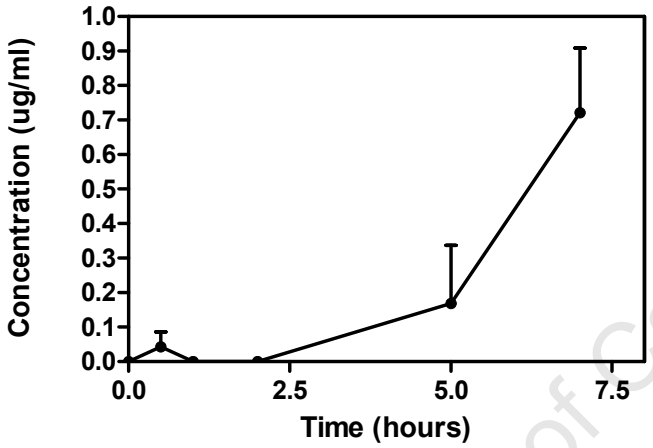

Figure 92 Concentration vs. Time graph of 9-O-acetylhydnocarpin obtained after a single oral dose of 9-O-acetylhydnocarpin in the Pheroid formulation (2 mg/mouse)

8.7.3 Discussion

The same LC-MS/MS method was used as described in 8.5. The calibration range for both compounds was between 0.0781 and 2.5 µg/ml. This assay method was used to quantify 9-O-acetylhydnocarpin and its hydrolysed product in mice whole blood, using the Pheroid drug delivery system.

Relatively high levels for 9-O-acetylhydnocarpin could be determined at 5 and 7 hours, using the Pheroid formulation. A relatively long absorption delay was observed for the test compound.

These results indicate that 9-O-acetylhydnocarpin is absorbed from the gastrointestinal tract, when administered in the Pheroid formulation, but at a much later stage than was

previously observed for the SMEDDS formulation. A glimpse of the enterohepatic effect was observed for one animal, but is considered insignificant, because of the low level that was reached at 0.5 hours after dose.

No levels were detected for the hydrolysed product, which indicates that the Pheroid formulation protects the test compound against hydrolysis.

The Pheroid formulation delayed the absorption of the test compound considerably, and it was probably absorbed from the latter part of the gastrointestinal tract. Bioavailability was improved significantly if compared to the SMEDDS formulation. Less of the test compound was administered and higher levels were reached at 7 hours (2 mg for Pheroid and 5 mg for SMEDDS). The Pheroid drug carrier and delivery system thus proved to be superior to the others that were tested.

8.8 Bioavailability study of 9-O-acetylhydnocarpin and its hydrolysed product in mice after intravenous administration

8.8.1 Introduction

Results of the preceding experiments indicated that the test compound undergoes extensive metabolism soon after absorption from the gastrointestinal tract. It was decided to study the test compound's clearance rate after intravenous injection (IV) to prove this theory. Results from this experiment should give more insight about the compounds metabolism.

The Pheroid delivery system was the most promising formulation tested; consequently it was decided to use this formulation as the injection vehicle for the IV experiments. A control group was also included which consisted of the test compound in a polar environment.

Test formulation

9-O-Acetylhydnocarpin was administered intravenously (200 µl) at a concentration of 100 µg/ml in a pheroid-saline solution to 3 healthy mice (male, C57BL6). The mice were anesthetised for this procedure. Blood samples (10 µl) were collected just before, and at 2, 10, 30, 60, 120 and 240 minutes after administration.

Control formulation

9-O-Acetylhydnocarpin was administered intravenously (200 µl) at a concentration of 100 µg/ml in a saline solution to 3 healthy mice (male, C57BL6). The mice were also anesthetised for this procedure. Blood samples (10 µl) were collected just before, and at 2, 10, 30, 60, 120 and 240 minutes after administration.

8.8.2 Results

The study samples and calibration standards were analysed according to the method described in 8.5. A new set of calibration standards was prepared, with the LLOQ set at 0.0195 µg/ml, and the highest standard set at 1.25 µg/ml, for 9-O-acetylhydnocarpin and its hydrolysed product. The standards were analysed in four-fold.

Representative chromatograms of calibration standards at the LLOQ and C_{max} are presented in appendix 3 (figures 190 and 191, respectively). Representative chromatograms of a study sample are presented in appendix 3 (figure 192). The calibration curves of 9-O-acetylhydnocarpin and its hydrolysed product are presented in appendix 3 (figures 193 and 194, respectively). The back-calculated results and calibration curve statistics are presented in appendix 3 (tables 69, 70, 71 and 72 for 9-O-acetylhydnocarpin and the hydrolysed product, respectively). A linear regression weighted 1/x was used for the statistical analyses.

The results of the IV dose experiments of the Pheroid formulation are summarised in tables 24 and 25. Concentration vs. Time graphs of 9-O-acetylhydnocarpin and the hydrolysed product obtained after single IV injections of 9-O-acetylhydnocarpin in the Pheroid formulation (20 µg/mouse) are presented in figure 93 and 94, respectively.

The results of the IV dose experiments of the control formulation are summarised in tables 26 and 27. Concentration vs. Time graphs of 9-O-acetylhydnocarpin and the hydrolysed product obtained after single IV injections of 9-O-acetylhydnocarpin in the control formulation (20 µg/mouse) are presented in figure 95 and 96, respectively.

8.8.2.1.1 Test formulation

Table 24 Whole blood concentrations of 9-O-acetylhydnocarpin

Time (min)	Mouse 1 (µg/ml)	Mouse 2 (µg/ml)	Mouse 3 (µg/ml)
0	0	0	0
2	0.432	0.272	0.653
10	0.0501	0.0275	0.0699
30	0.0329	0.0558	0.0499
60	0.0407	BLQ	0.0320
120	BLQ	BLQ	0.0314
240	BLQ	0.0219	0.0414

BLQ = below limit of quantification

Table 25 Whole blood concentrations of the hydrolysed product

Time (min)	Mouse 1 (µg/ml)	Mouse 2 (µg/ml)	Mouse 3 (µg/ml)
0	0	0	0
2	0.214	0.130	0.304
10	0.0226	0.0248	0.0348
30	BLQ	0.0288	BLQ
60	BLQ	BLQ	BLQ
120	BLQ	BLQ	BLQ
240	BLQ	BLQ	BLQ

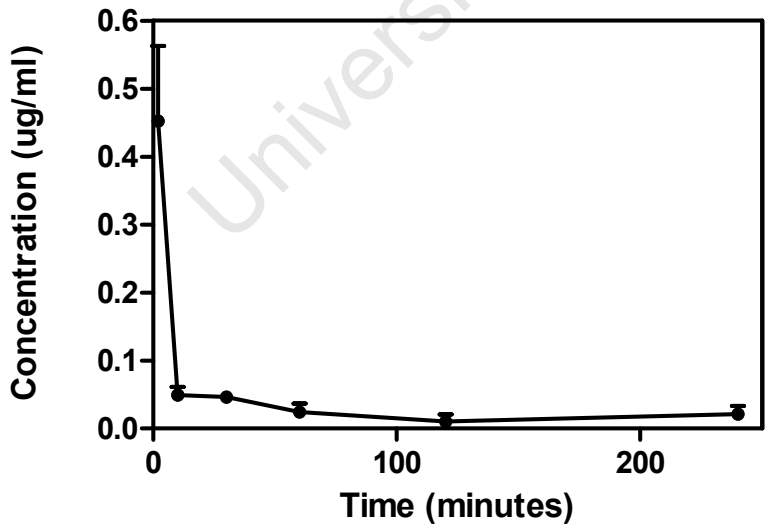

Figure 93 Concentration vs. Time graph of 9-O-acetylhydnocarpin as obtained after single intravenous injections of 9-O-acetylhydnocarpin in the Pheroid formulation (20 µg/mouse)

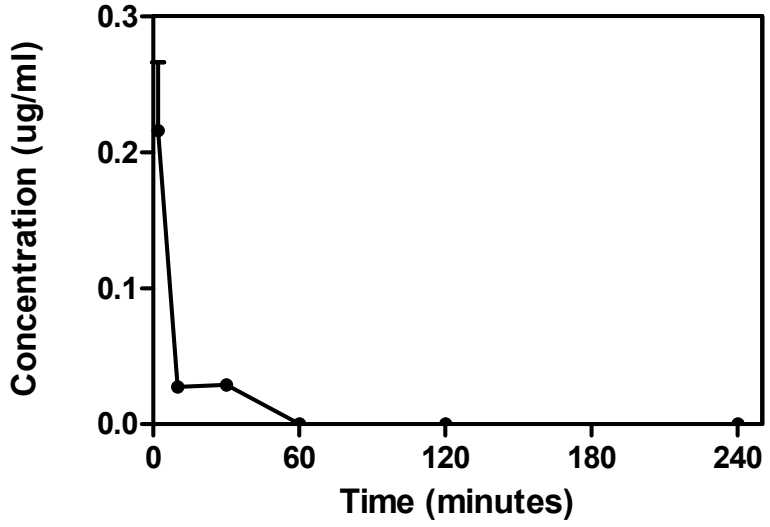

Figure 94 Concentration vs. Time graph of the hydrolysed product obtained after single intravenous injections of 9-O-acetylhydnocarpin in the Pheroid formulation (20 µg/mouse)

8.8.2.1.2 Control formulation

Table 26 Whole blood concentrations of 9-O-acetylhydnocarpin

Time (min)	Mouse 1 (µg/ml)	Mouse 2 (µg/ml)	Mouse 3 (µg/ml)
0	0	0	0
2	0.161	0.113	0.134
10	0.0382	0.0416	0.0307
30	BLQ	BLQ	0.0231
60	0.0196	BLQ	BLQ
120	BLQ	BLQ	BLQ
240	BLQ	BLQ	BLQ

Table 27 Whole blood concentrations of the hydrolysed product

Time (min)	Mouse 1 (µg/ml)	Mouse 2 (µg/ml)	Mouse 3 (µg/ml)
0	0	0	0
2	0.418	0.316	0.381
10	0.0621	0.0626	0.0434
30	BLQ	0.0295	0.0215
60	BLQ	BLQ	BLQ
120	BLQ	BLQ	BLQ
240	BLQ	BLQ	BLQ

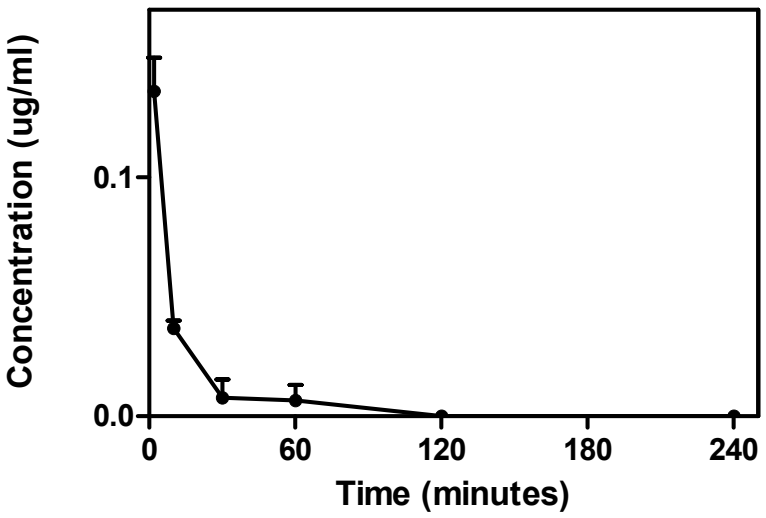

Figure 95 Concentration vs. Time graph of 9-O-acetylhydnocarpin as obtained after single intravenous injections of 9-O-acetylhydnocarpin in the control formulation (20 µg/mouse)

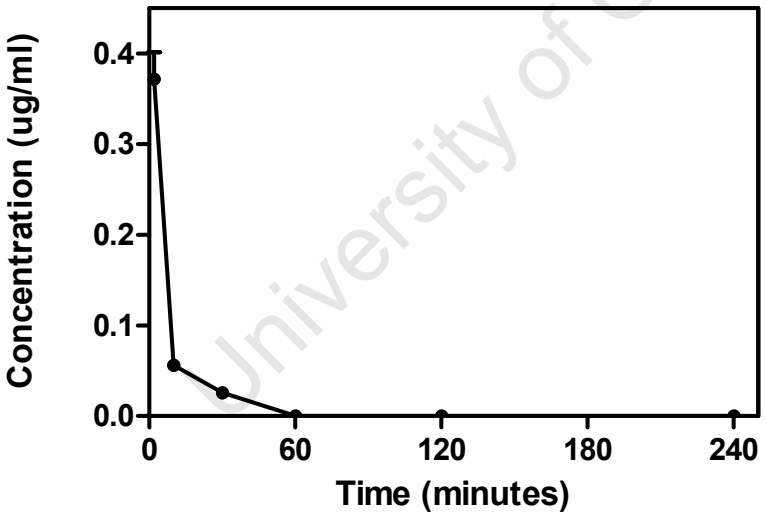

Figure 96 Concentration vs. Time graph of the hydrolysed product obtained after single intravenous injections of 9-O-acetylhydnocarpin in the control formulation (20 µg/mouse)

8.8.3 Discussion

The intravenous experimental results showed fast clearance of the test compound, as about 90% of the compound is metabolised within 10 minutes. These results prove that extensive metabolism occurs after absorption by probably the CYP450 liver enzymes.

The initial level of the test compound in the Pheroid group was about three times higher than for the control group, which indicates some level of protection against the CYP450 liver enzymes by the Pheroid formulation. The initial level of the hydrolysed product in the Pheroid group was lower than for the control group, which indicates some level of protection against the esterase enzymes by the Pheroid formulation.

8.9 Conclusion

A comprehensive bioavailability study of 9-O-acetylhydnocarpin and its hydrolysed product was conducted in mice using LC-MS/MS analysis.

A new micro extraction technique that uses only 10 µl of sample was developed. The test compound and hydrolysed product were selectively extracted from mice blood with consistent recoveries above 80%. This technique made it possible to study bioavailability in one animal over a period of six sampling points. It also reduced the number of animals that are usually required for these kinds of experiments.

A highly sensitive, selective and accurate LC-MS/MS method was developed and validated, and was used as a quantitative tool for sample analysis. The final method could accurately detect levels as low as 20 ng/ml for both compounds in 10 µl samples.

Results from these experiments showed that the test compound is absorbed from the gastrointestinal tract if administered in the right formulation. Relatively high blood levels were observed for the SMEDDS and Pheroid oral formulations.

The Pheroid and SMEDDS oral formulations improved bioavailability significantly, but because of rapid metabolism, levels were lower than expected.

A comparison of the test compounds blood levels and *in vitro* IC_{50} values indicate that the test compound will probably not reach high enough blood levels for curing infected animals, although parasite inhibition may still be observed at these levels. One should also keep in mind that different *Plasmodium* species were used for *in vitro* and *in vivo* testing and would probably have different IC_{50} values. Metabolites may also be active and present at high enough levels to inhibit parasite growth *in vivo*.

Bioavailability (biological availability) can be described as the extent to which a compound is utilized pharmacologically. Pharmacokinetics on the other hand is the science of the mathematical assessment of drug distribution in terms of model systems, of rate constants of transfer, of rate constants of metabolism and excretion, and of apparent volumes of distribution compartments. It was intended to study the test compounds biological

availability in a mouse model, and to use this information to construct concentration vs. time graphs, and ultimately to construct a pharmacokinetic model for the test compound that was evaluated. The outcome of the bioavailability studies, which were performed by using different formulations and administration routes, unfortunately resulted in relatively poor bioavailability profiles. Therefore it was decided not to construct a pharmakocinetic model for the test compound [Curry, 1977].

The outcome of these findings led to the following logical step in the early development process, which is the search for metabolites *in vivo* as well as investigating the metabolism of structurally related compounds.

CHAPTER 9

Metabolite study of 9-O-acetylhydnocarpin

9 Metabolite study of 9-O-acetylhydnocarpin

9.1 Introduction

Metabolite studies are vital in the drug discovery process, but are expensive and time consuming. The pharmaceutical industry has shown the importance of conducting metabolite studies before drug candidates are selected during the drug development process. Results from these studies should give more insight on drug candidate selection.

During the last few years mass spectrometry has emerged as the analytical instrument of choice used for the identification of metabolites. Tandem mass spectrometers have become the keystone of metabolite identification. Tandem quadrupole mass spectrometers generally consist of an isolation stage and fragmentation stage within the same instrument. There are numerous different tandem MS experiments that can be used to identify metabolites, even though the same basic series of events are followed. The ion of interest is first isolated on the basis of its mass/charge ratio and is then passed into the collision cell, which is filled with an inert gas such as helium or argon, and a potential difference is applied. The energized ions collide with the gas molecules resulting in fragment ions, which moves out of the cell and hit the detector. The product ions correspond to part of the unknown molecule. The product ion mass spectrum contains the "puzzle pieces" of the unknown molecule. Interpretation of this spectrum is supported by infusing the parent compound and performing the same fragmentation experiment as was used for the unknown metabolite. Comparing the product ion mass spectrum of the unknown metabolite with the product ion mass spectrum of the known parent compound an experienced operator can identify the overall structure and would be able to indicate the changes in the molecule.

Metabolite identification using LC-MS instruments is a systematic approach. The first step in metabolite identification is LC-MS experiments, the second step is precursor ion experiments, the third step is neutral loss scans, the fourth step is LC-MS/MS experiments and the fifth step is MRM experiments. The last step is accurate mass measurement, which should result in the empirical formula of the unknown metabolite [Applied Biosystems MDS Sciex; Clarke *et al*., 2001; Willoughby *et al*., 2002; Gangl *et al*., 2002].

The metabolism of structurally related compounds was studied to get a better understanding about general metabolic routes of this group of compounds. The pharmacology of silybin, which is structurally related to 9-O-acetylhydnocarpin, is described in the literature [Pharmacology of Silymarin]. Silybin is isolated from the seeds of the milk thistle *Silybin marianum*. Silybin, which is a flavonolignan, is the main compound in the silymarin extract. Silybin is an important hepatoprotective drug (Flavobiom™, Legalon™) used to treat liver damage and is also used as a liver-protecting drug [Morazzoni and Bombardelli, 1995; Kren *et al*., 1997; Flora *et al*., 1998; Alikaridis *et al*., 2000; Dvorak *et al*., 2003; Kvasnicka *et al*., 2003; Davis-Searles *et al*., 2005; Kren and Walterova, 2005].

The chemical structures of 9-O-acetylhydnocarpin, hydnocarpin (hydrolysed product) and silybin are presented in figure 97. These compounds are structurally related and would probably have similar pharmacokinetic properties. These compounds are known as flavonolignans, with 9-O-acetylhydnocarpin and hydnocarpin belonging to the flavone subgroup and silybin to the flavonol subgroup. General chemical structures of these compounds are presented and discussed in Chapter 4 (4.1).

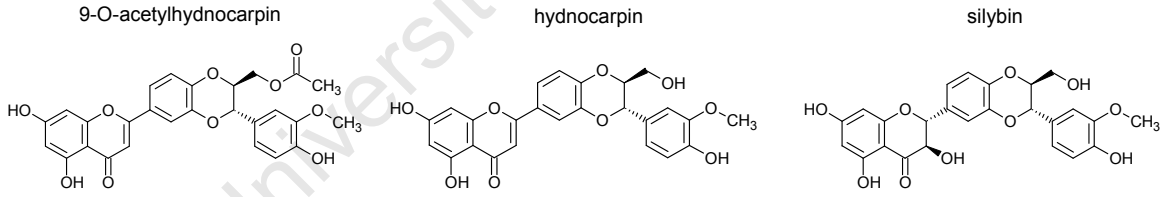

Figure 97 Chemical structures of 9-O-acetylhydnocarpin, hydnocarpin and silybin

Silybin is poorly water soluble and is generally administered as a plant extract. Bioavailability of silybin is relatively low after oral administration, with highest plasma concentrations reached between 4 and 6 hours in humans. Silybin and related compounds of the silymarin extract are quickly conjugated with glucuronic acid and sulphate in the liver. These conjugated metabolites are extracted from the blood into the bile, and are found in levels corresponding to 80% of the total dose that was administered. A small fraction is extracted in the urine [Pharmacology of Silymarin]. Kren and co-authors

showed that the main silybin conjugate in humans is its 20β-D-glucuronate [Kren *et al*., 2000].

The following enterohepatic circulation of the silymarin compounds is suggested after oral administration of silymarin: intestinal absorption, conjugation in the liver, excretion in the bile, hydrolysis by the intestinal flora, and reuptake in the intestine.

Cytochrome P450 enzymes play an important role in the metabolism of the silymarin compounds. 9-O-Acetylhydnocarpin is structurally related to these compounds and has the same functional groups which points towards a similar metabolic pathway. The study of the metabolic pathway of drugs is a comprehensive field and advanced analytical instrumentation is required to study these metabolites qualitatively and quantitatively [Glue and Clement, 1999; Kumar and Clark, 2006; Petushkova *et al*., 2006; Yao *et al*., 2007]. Bioavailability of flavonoids has been found to be lower than expected from its favourable lipophilicity, because of its extensive metabolic effect in the small intestine. The major metabolic pathway for flavonoids is Phase II metabolism such as glucuronidation and sulphatation [Pong *et al*., 2005; Han *et al*., 2005].

LC-MS/MS technology was used to search for metabolites of 9-O-acetylhydnocarpin in a mouse model. The methodology is presented in Chapter 12 (12.8).

9.2 Metabolite study of 9-O-acetylhydnocarpin in mice

The target site for activity testing of the test compound was the animal's blood system, and for that reason it was decided to target this matrix for metabolite discovery. Metabolites end up in the urine and faeces eventually, therefore the addition of these two matrixes in the metabolite search. An Applied Biosystems 3200 Q-Trap mass spectrometer was used for the metabolite search. It was decided to focus on the discovery of potential metabolites for this project. The identification of metabolites is a much more involved process and would fall outside the scope of this project. Different tests were conducted in the search for these potential metabolites, which include LC-MS, precursor ion, neutral loss and LC-MS/MS experiments.

9.2.1 LC-MS analysis

An oral dose (200 µl) of 9-O-acetylhydnocarpin (200 mg/kg), using the SMEDDS formulation, was administered to a mouse. Blood, urine and faeces samples were collected and prepared for LC-MS analysis as described in Chapter 12 (12.8.1). The LC-MS analysis methodology is also described in Chapter 12 (12.8.2).

9.2.1.1 Results

9.2.1.1.1 Blood samples

The total ion chromatograms of the control (red) and test (blue) blood samples are presented in figure 98. The retention times of the test compound and its hydrolysed product could not be identified with the relatively unspecific LC-MS scan experiment, therefore a more sensitive and selective MRM experiment was conducted to illustrate the retention times of these compounds using the HPLC gradient as described in Chapter 12 (12.8.2). The test compound and its hydrolysed product eluted at 11.8 and 10.7 minutes, respectively (figure 99).

The mass spectrum of each of the peaks was subtracted from the background. TIC chromatograms, showing background (green selection) subtraction, as well as mass spectra (blue selection) of each of the peaks are presented in appendix 4 (figures 195 to 208).

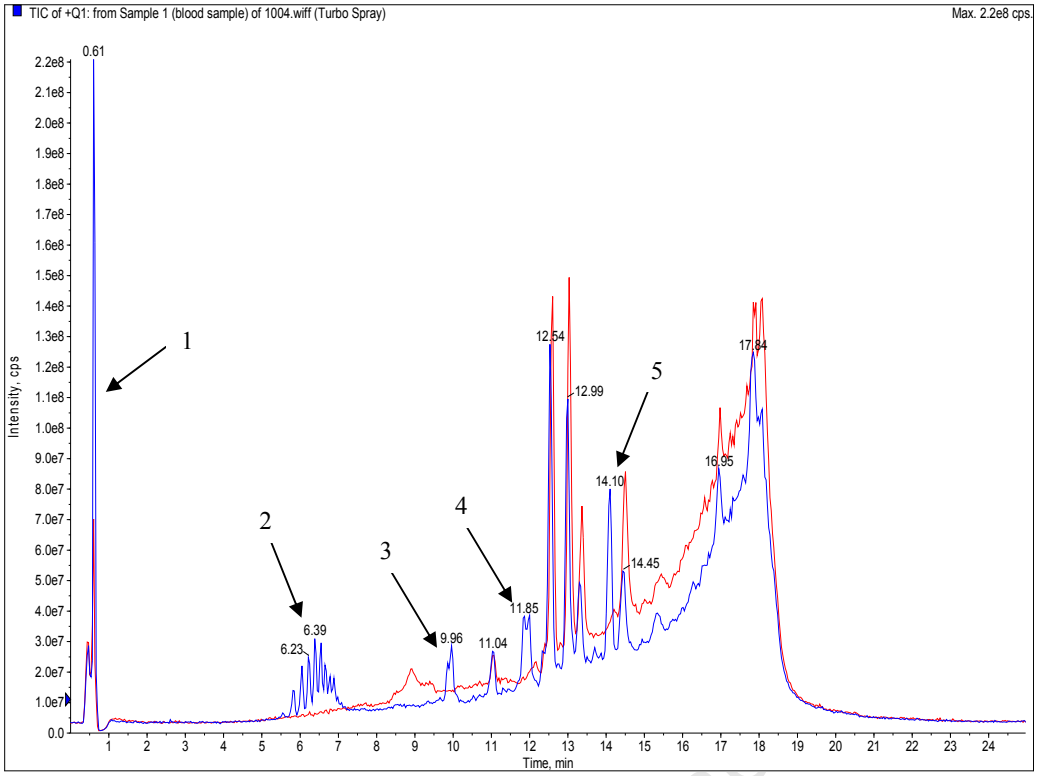

Figure 98 Total ion chromatograms of the control and test blood samples

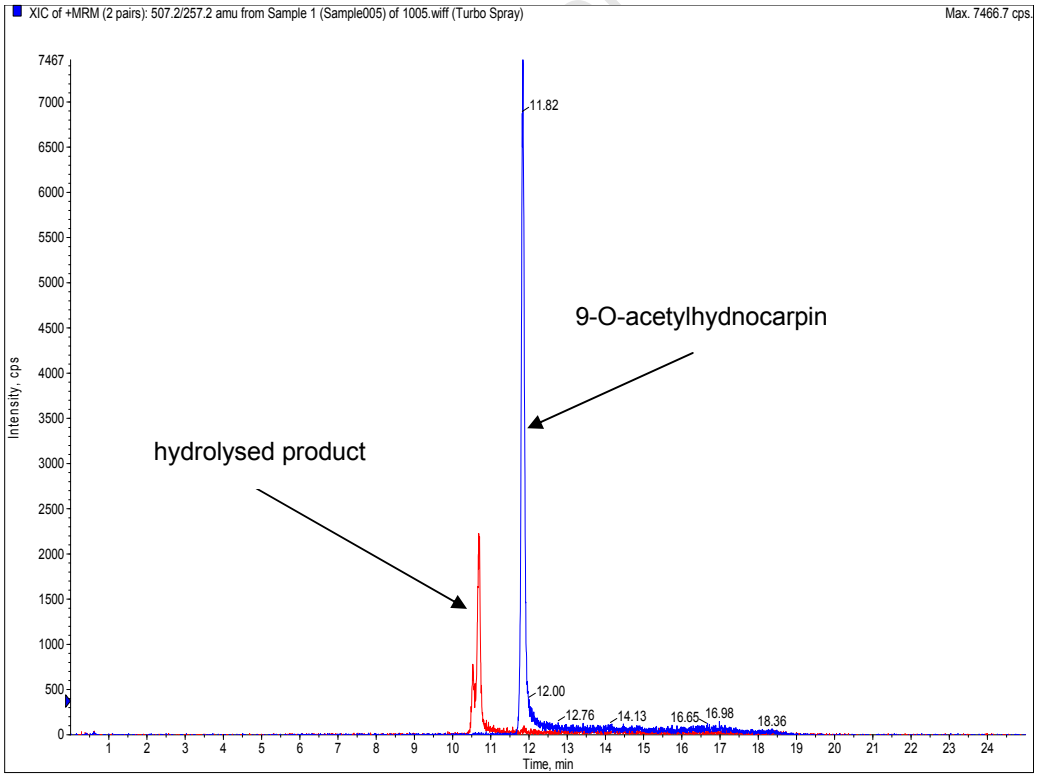

Figure 99 MRM chromatogram of 9-O-acetylhydnocarpin and its hydrolysed product

9.2.1.1.2 Urine samples

The total ion chromatograms of the control (red) and test (blue) urine samples are presented in figure 100. Mass spectra of peak groups 1 and 2 are also presented in appendix 4 (figures 209 and 210, background subtraction was performed).

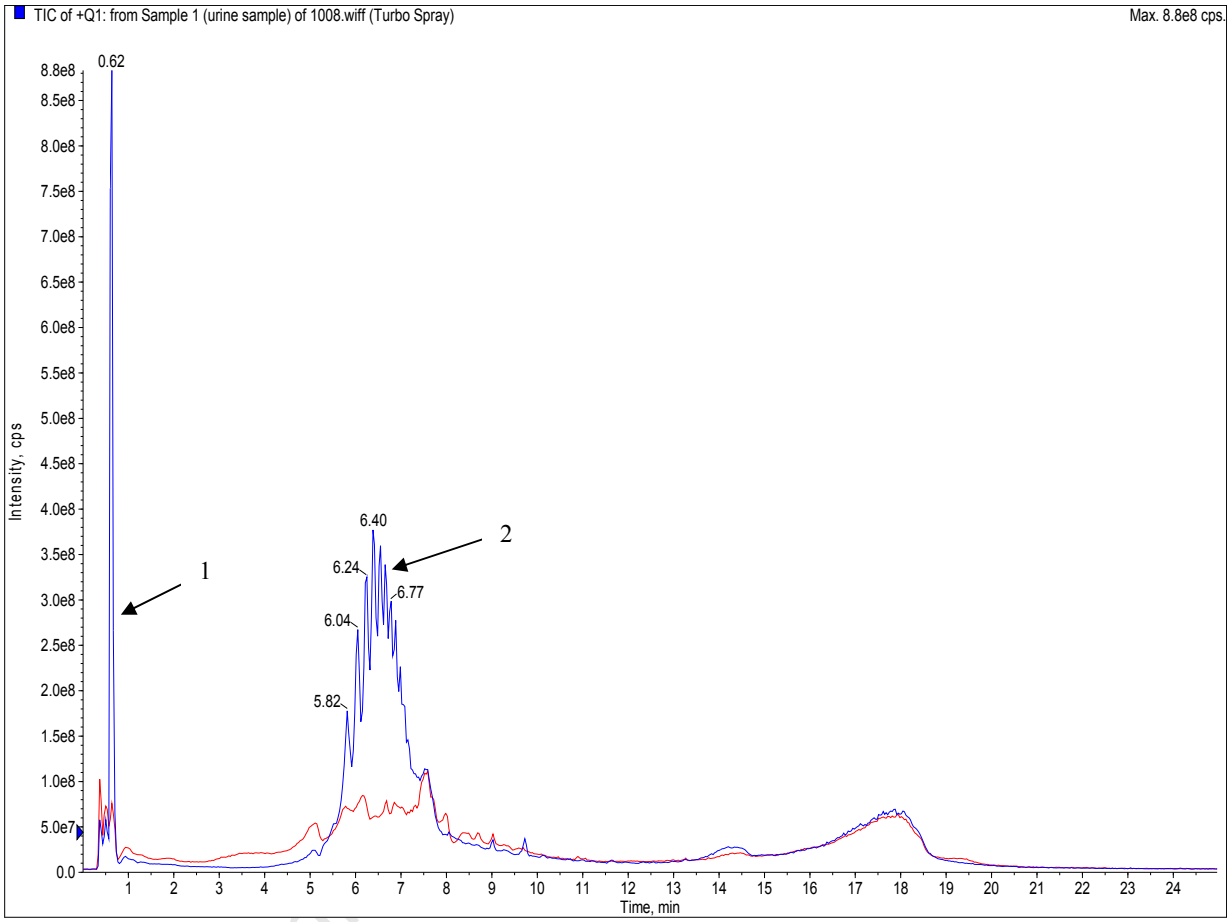

Figure 100 Total ion chromatograms of the control and test urine samples

9.2.1.1.3 Faeces samples

The total ion chromatograms of the control (red) and test (blue) faeces samples are presented in figure 101. Mass spectra of the most prominent peak groups 1, 2, 3 and 4 are presented in appendix 4 (figures 211 to 214, background subtraction was performed).

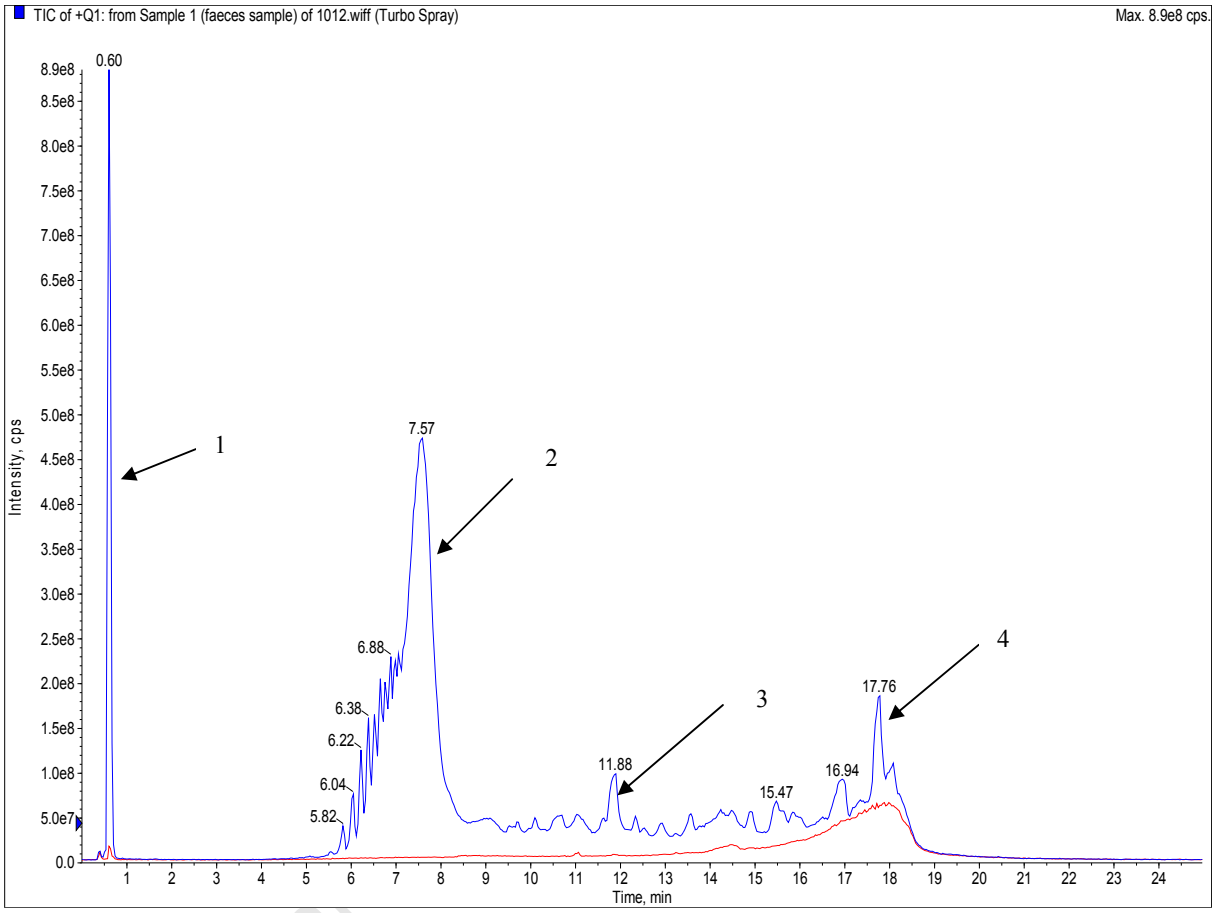

Figure 101 Total ion chromatograms of the control and test faeces samples

9.2.1.2 Discussion

9.2.1.2.1 Blood sample

The retention times of 9-O-acetylhydnocarpin and its hydrolysed product were 11.8 and 10.7 minutes, respectively (figure 99). 9-O-Acetylhydnocarpin and its hydrolysed product were present in the blood, but at relatively low concentrations compared to the potential metabolites. These two compounds could not be identified in LC-MS scan mode, therefore the inclusion of the more sensitive and specific MRM chromatogram. This chromatogram is included to illustrate the retention times of 9-O-acetylhydnocarpin and its hydrolysed product, using the HPLC gradient system as described in Chapter 12 (12.8.2).

The total ion chromatogram of the test sample showed additional peaks compared to the control sample (figure 98). These peaks are considered potential metabolite peaks, because of their absence in the control sample. Five of these peak groups were observed in the chromatogram. The first group eluted at the front of the chromatogram at 0.6 minutes. The second group eluted between 5.5 and 7.0 minutes. A third group was observed at about 9.9 minutes, a fourth group at 11.8 minutes, and a fifth peak at 14.1 minutes.

The mass spectrum of the frontal peak (figure 195) contained quite a few ion peaks, which suggested the presence of more than one metabolite. These potential metabolites are extremely polar and are difficult to separate under reverse phase HPLC conditions.

The second group consisted of 8 well separated peaks. The mass spectra of these peaks (figures 196 to 203) contained less ion peaks, which suggested the possibility of single metabolites.

The third group consisted of 2 partially separated peaks. The mass spectra of these peaks (figures 204 and 205) also suggested the possibility of single metabolites.

The fourth group also consisted of 2 partially separated peaks. The mass spectra of these peaks (figures 206 and 207) also suggested the possibility of single metabolites.

The fifth group contained a single peak and the mass spectrum (figure 208) also suggested the possibility of a single metabolite.

The outcome of this experiment suggested the presence of quite a few metabolites in blood, which are present at relatively high concentrations.

9.2.1.2.2 Urine sample

The total ion chromatogram of the test sample showed two additional peak groups compared to the control sample (figure 100). A relatively large frontal peak was observed at 0.6 minutes, similar to the blood sample. A second, very large and broad peak group eluted between 5.5 and 8.0 minutes, similar to the blood sample.

The mass spectra (figure 209 and 210) of both peak groups consisted of many peak ions, which suggested the presence of many metabolites in the urine.

These results suggested that both polar and intermediate polar metabolites are effectively extracted from the blood into the urine at relatively high concentrations.

9.2.1.2.3 Faeces sample

The total ion chromatogram of the test sample showed a number of additional peak groups compared to the control sample (figure 101). A relatively large frontal peak was observed at 0.6 minutes, similar to the blood sample. A second, very large and broad peak group eluted between 5.5 and 8.5 minutes, similar to the blood sample. A third peak eluted at 11.9 minutes. A fourth peak eluted at 17.8 minutes. A series of minor peaks eluted between 9 and 19 minutes.

The mass spectra (figure 211 and 212) of peak groups 1 and 2 consisted of many peak ions, which is similar to the blood and urine sample. The mass spectrum (figure 213) of peak 3 showed the molecular ion of the test compound, which therefore suggested the presence of the test compound in the faeces at relatively high concentrations. The mass spectrum (figure 214) of peak 4 suggested the possibility of a single metabolite. These results suggested that the unchanged test compound, polar, intermediate polar and non polar metabolites are effectively removed from the gastrointestinal and blood systems and end up in the faeces at relatively high concentrations.

9.2.2 Precursor ion scan analysis

The same samples that were used for LC-MS analysis were also used for precursor experiments. The methodology is described in Chapter 12 (12.8.3).

9.2.2.1 Results

9.2.2.1.1 Blood samples

The precursor ion chromatograms of the control (red) and test (blue) blood samples are presented in figure 102. A precursor ion chromatogram, showing background (green selection) subtraction, as well as the mass spectrum (blue selection) of peak 1 is presented in appendix 4 (figure 215).

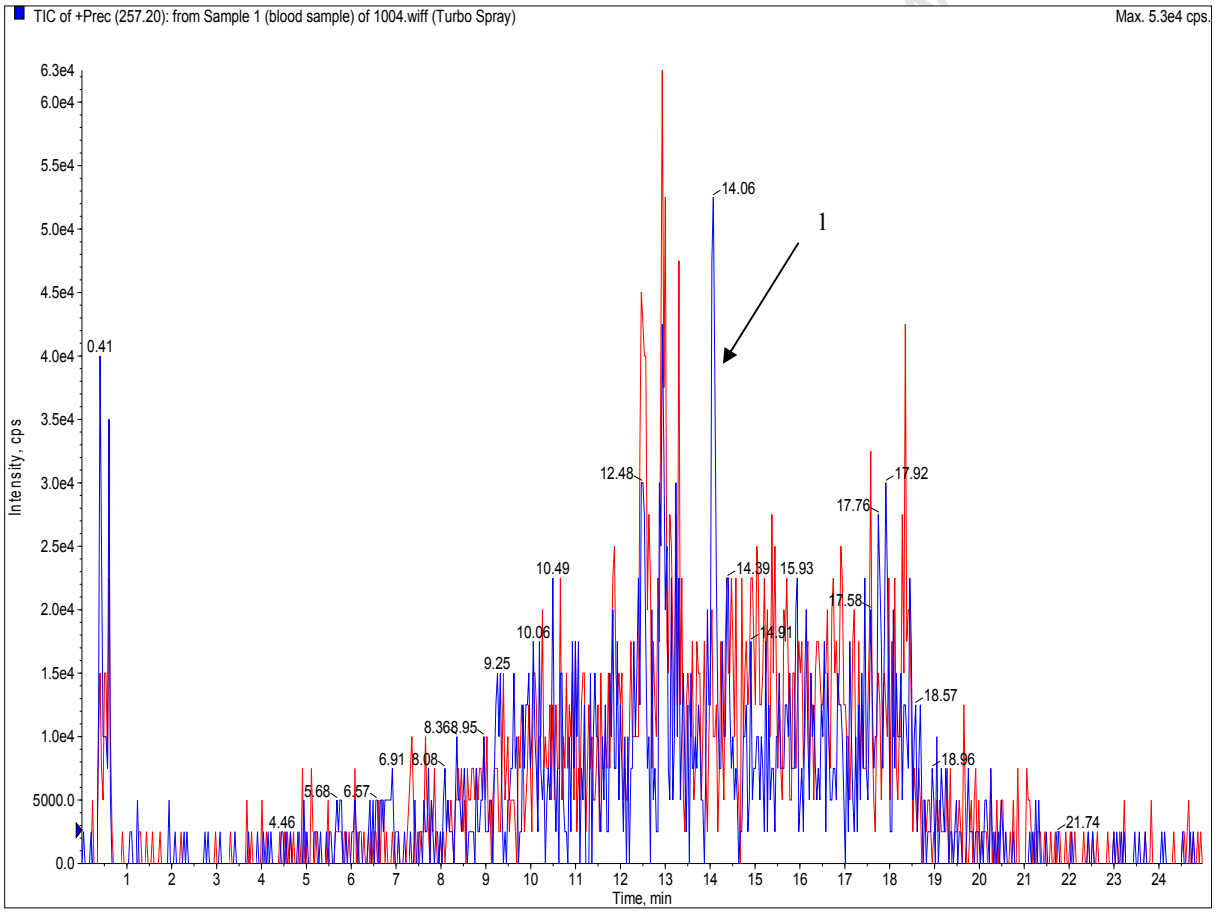

Figure 102 Precursor ion chromatograms of the control and test blood samples

9.2.2.1.2 Urine samples

The precursor ion chromatograms of the control (red) and test (blue) urine samples are presented in figure 103. Precursor ion chromatograms, showing background (green selection) subtraction, as well as mass spectra (blue selection) of peaks 1 and 2 are presented in appendix 4 (figures 216 and 217).

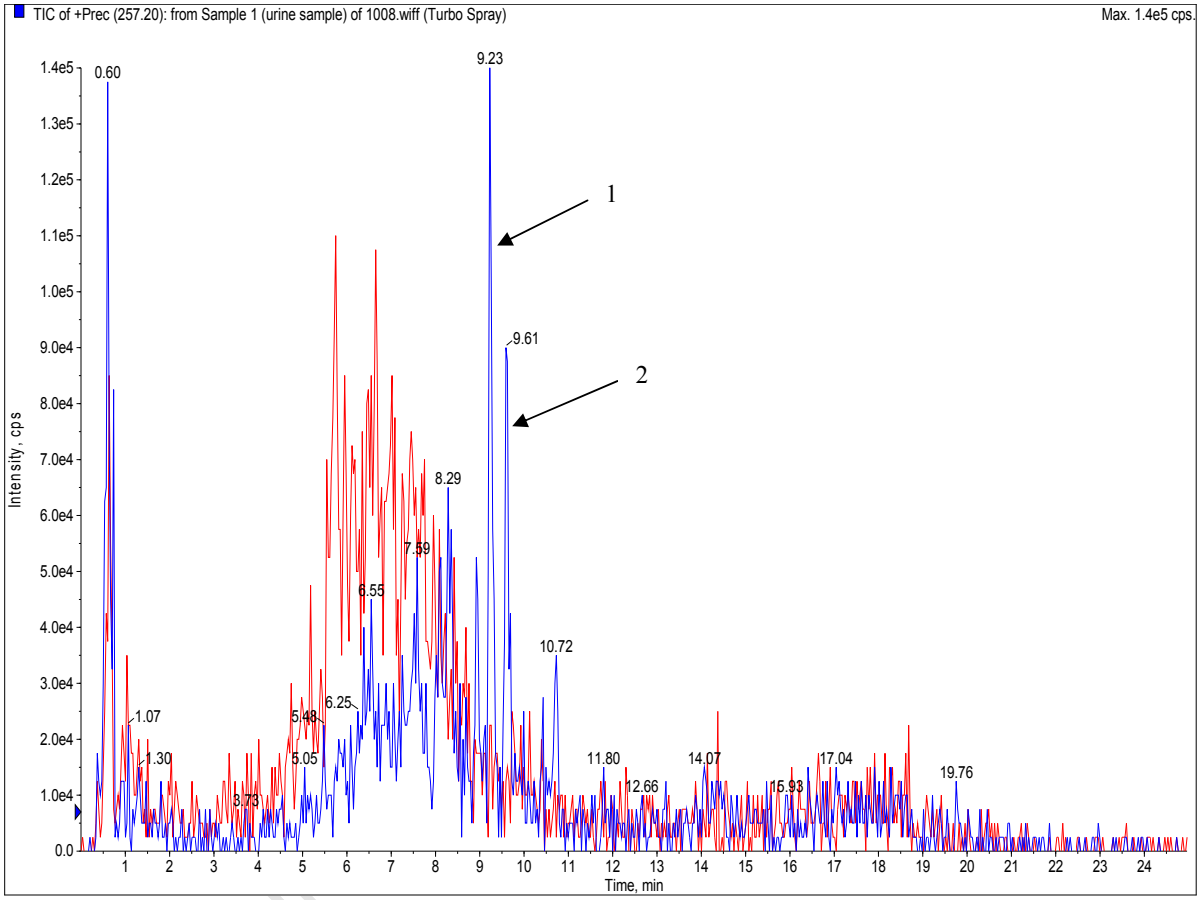

Figure 103 Precursor ion chromatograms of the control and test urine samples

9.2.2.1.3 Faeces samples

The precursor ion chromatograms of the control (red) and test (blue) faeces samples are presented in figure 104. Precursor ion chromatograms, showing background (green selection) subtraction, as well as mass spectra (blue selection) of peaks 1, 2 and 3 are presented in appendix 4 (figure 218, 219 and 220).

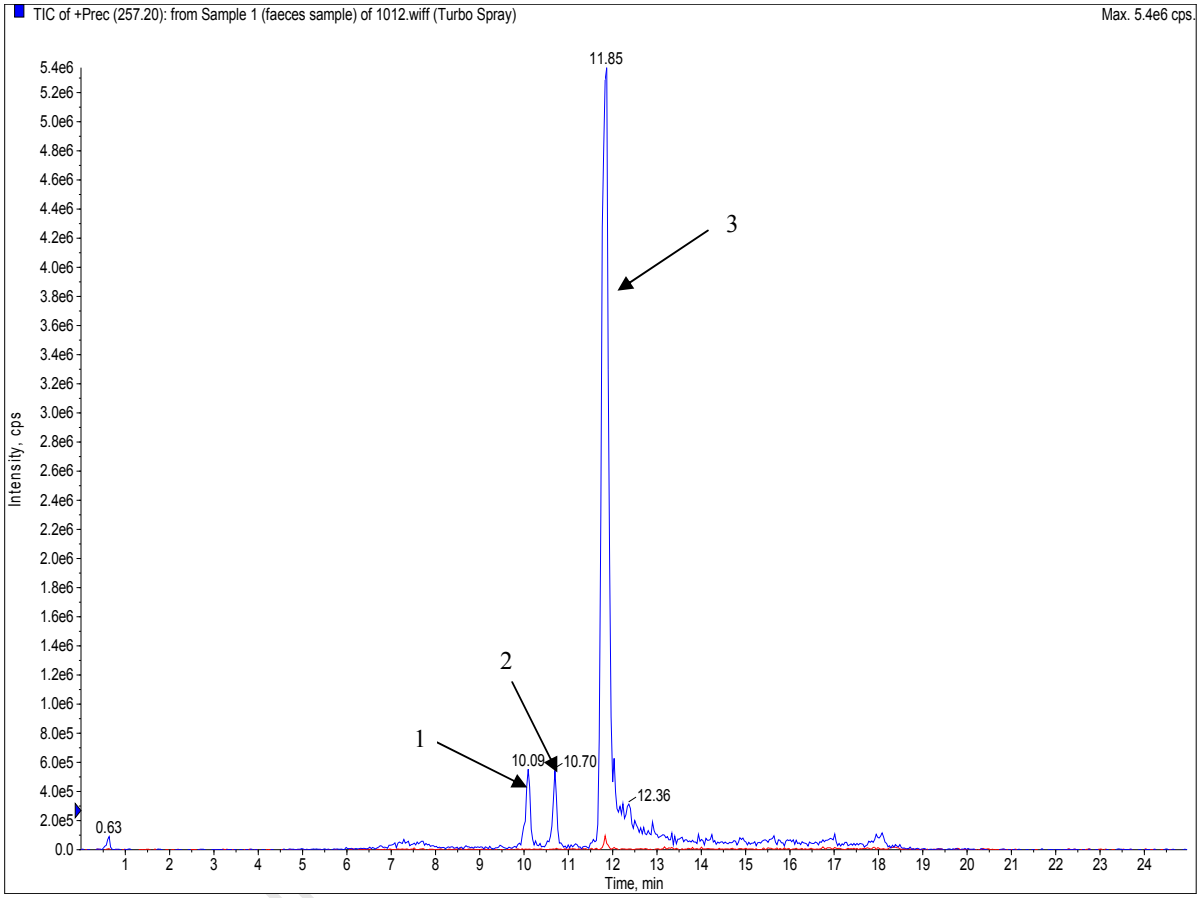

Figure 104 Precursor ion chromatograms of the control and test faeces samples

9.2.2.2 Discussion

9.2.2.2.1 Blood sample

The precursor ion chromatogram of the test sample showed one additional peak (14.06 minutes) compared to the control sample (figure 102). The mass spectrum (figure 215) of this peak showed two major ion peaks at 567.2 Da and 589.1 Da. The ion peak at 589 Da is probably the sodium adduct of 567, which suggest the presence of a single metabolite.

9.2.2.2.2 Urine sample

The precursor ion chromatogram of the test sample showed two additional peaks (9.2 and 9.6 minutes) compared to the control sample (figure 103). The mass spectrum (figure 216) of the peak at 9.2 minutes showed two major ion peaks at 464.9 and 641.3. A mass shift of 176 Da is observed, which suggest the presence of a glucuronidated metabolite. The mass spectrum (figure 217) of the peak at 9.6 minutes also showed two major ion peaks at 465.3 Da and 640.6 Da. A mass shift of about 176 Da is also observed, which suggests the presence of another glucuronidated metabolite, probably an isomer.

9.2.2.2.3 Faeces sample

The precursor ion chromatogram of the test sample showed three additional peaks (10.1, 10.7 and 11.9 minutes) compared to the control sample (figure 104).

The mass spectrum (figure 218) of the first peak at 10.1 minutes showed a major peak at 451.5 Da. A mass difference of about 14 Da from the hydrolysed product is observed, which is probably an O-dealkylation (R-O-CH_3 => R-OH) metabolite of the hydrolysed product. The methoxyl group at position 14 (figure 72) is probably metabolised to a hydroxyl group.

The mass spectrum (figure 219) of the second peak at 10.7 minutes showed a major peak at 465.3 Da. This ion peak matches up well with the molecular ion of the hydrolysed product of 9-O-acetylhydnocarpin. This information suggests the presence of the hydrolysed product of 9-O-acetylhydnocarpin in the faeces at relatively high concentrations.

The mass spectrum (figure 220) of the third peak at 11.9 minutes showed a major peak at 507.4 Da. This ion peak matches up well with the molecular ion of 9-O-acetylhydnocarpin.

This information suggests the presence of the test compound in the faeces at relatively high concentrations.

9.2.3 Neutral loss scan analysis

The same samples that were used for LC-MS and precursor ion scan analysis were also used for neutral loss experiments. The methodology is described in Chapter 12 (12.8.4).

9.2.3.1 Results

9.2.3.1.1 Blood samples

The neutral loss chromatograms of the control (red) and test (blue) blood samples are presented in figure 105. A neutral loss chromatogram, showing background (green selection) subtraction, as well as the mass spectrum (blue selection) of peak 1 (potential metabolite) is presented in appendix 4 (figure 221).

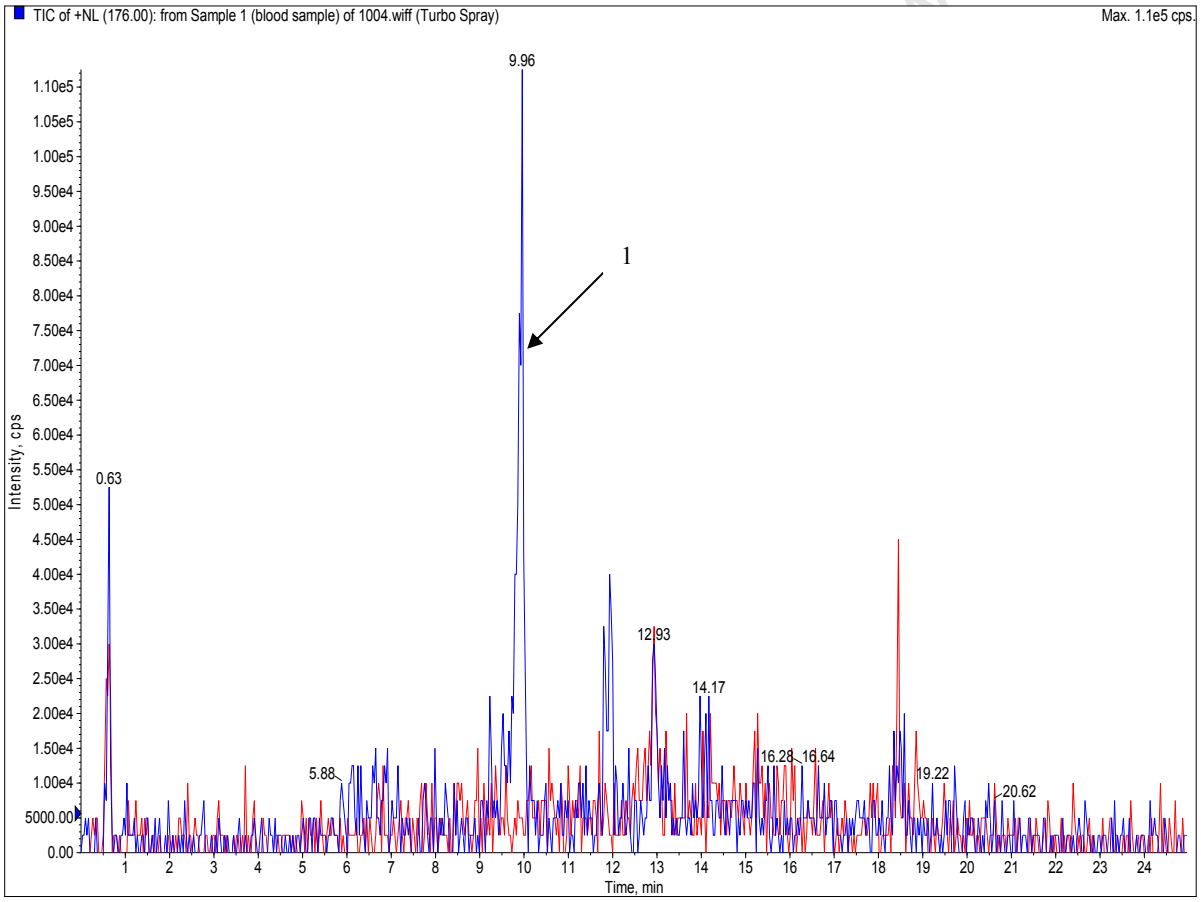

Figure 105 Neutral loss chromatograms of the control and test blood samples

9.2.3.1.2 Urine samples

Neutral loss chromatograms of the control (red) and test (blue) urine samples are presented in figure 106. Neutral loss chromatograms, showing background (green selection) subtraction, as well as their mass spectra (blue selection) of peaks 1 to 5 (possible metabolites) are presented in appendix 4 (figures 222 to 226).

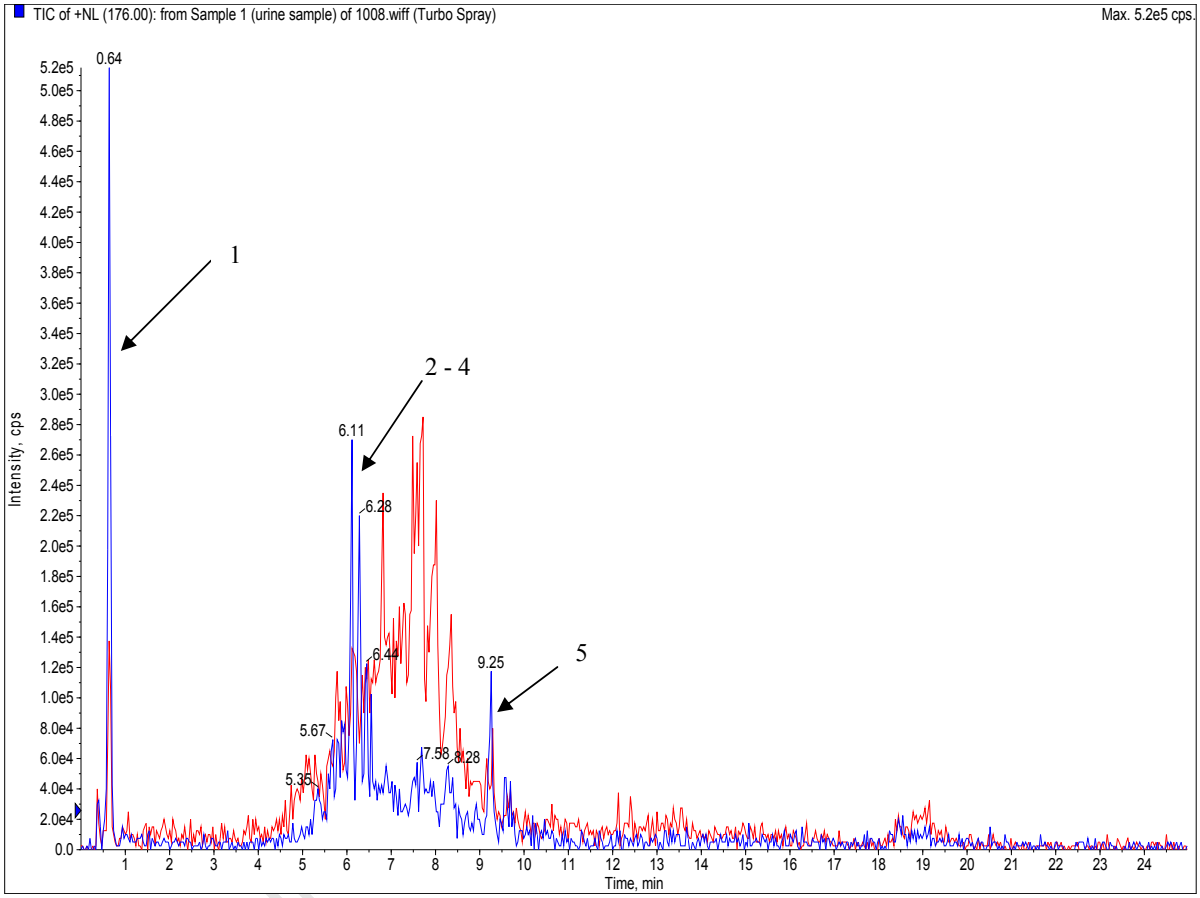

Figure 106 Neutral loss chromatograms of the control and test urine samples

9.2.3.1.3 Faeces samples

Neutral loss chromatograms of the control (red) and test (blue) faeces samples are presented in figure 107. Neutral loss chromatograms, showing background (green selection) subtraction, as well as their mass spectra (blue selection) of peak groups 1, 2 and 3 (possible metabolites) are presented in appendix 4 (figures 227 to 229).

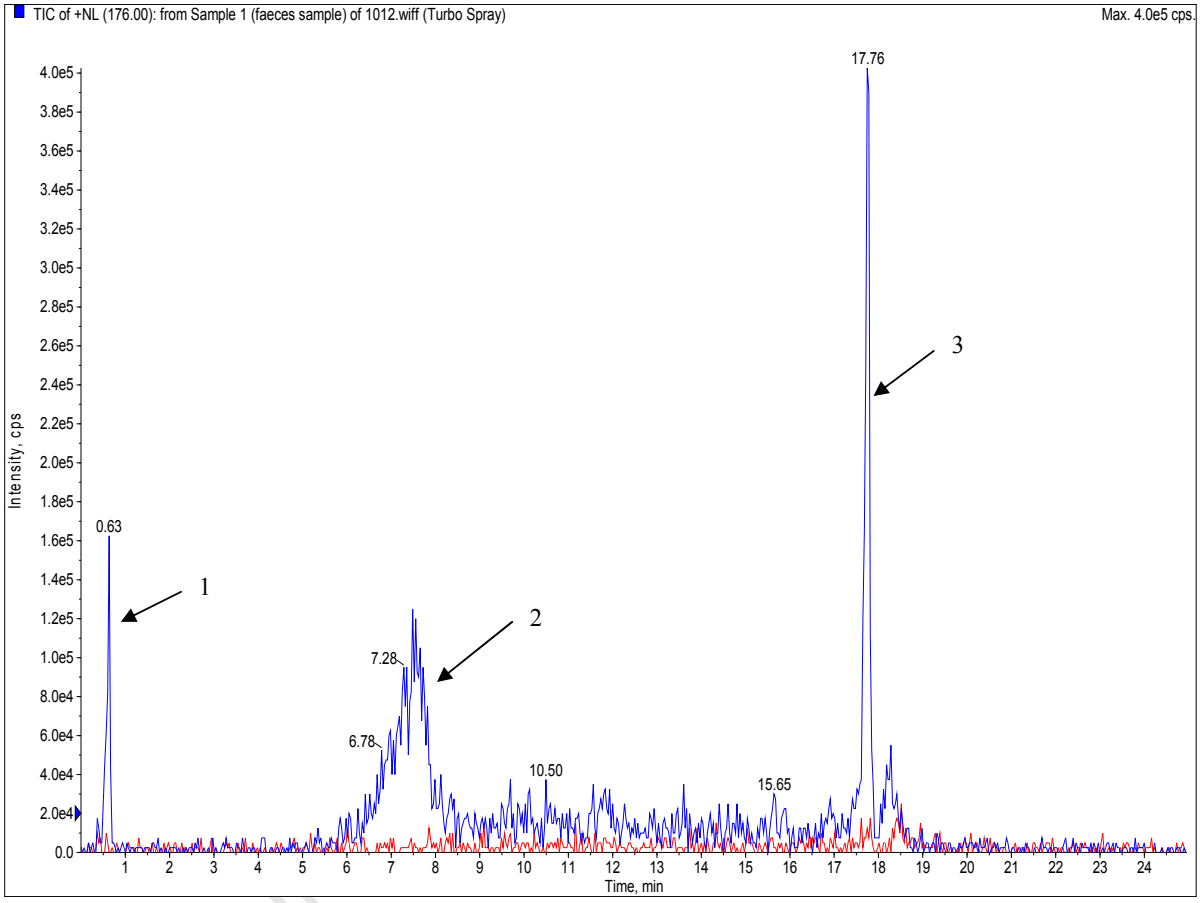

Figure 107 Neutral loss chromatograms of the control and test faeces samples

9.2.3.2 Discussion

9.2.3.2.1 Blood

The neutral loss chromatogram of the test sample showed one additional peak at 10.0 minutes, compared to the control sample (figure 105).

The mass spectrum (figure 221) of this peak showed three major peak ions, 425.2, 441.2 and 458.2 Da. The masses of these peak ions are relatively low, which makes the suggestion of a potential glucuronidated metabolite inconclusive.

9.2.3.2.2 Urine

The neutral loss chromatogram of the test sample showed five additional peaks at 0.6, 6.1, 6.3, 6.4 and 9.3 minutes, compared to the control sample (figure 106).

The mass spectrum (figure 222) of the first peak at 0.6 minutes showed a number of peak ions, with relatively high masses, which suggested the presence of probably a few glucuronidated polar metabolites.

The mass spectrum (figure 223) of the second peak at 6.1 minutes showed a major peak ion of 657.3 Da, which suggested the presence of a glucuronidated metabolite.

The mass spectrum (figure 224) of the third peak at 6.3 minutes showed a major peak ion of 701.4 Da, which suggested the presence of another glucuronidated metabolite.

The mass spectrum (figure 225) of the fourth peak at 6.4 minutes showed a major peak ion of 745.5 Da, which suggested the presence of another glucuronidated metabolite.

The mass spectrum (figure 226) of the fifth peak at 9.3 minutes showed a major peak ion of 641.3 Da, which suggested the presence of a glucuronidated metabolite of the hydrolysed product (465 + 176).

9.2.3.2.3 Faeces

The neutral loss chromatogram of the test sample showed three additional peak groups at 0.6, 5.5 - 8.5 and 17.8 minutes, compared to the control sample (figure 107).

The mass spectrum (figure 227) of the first peak at 0.6 minutes showed a number of peak ions, with relatively high masses, which suggested the presence of probably a few glucuronidated polar metabolites.

The mass spectrum (figure 228) of the second peak group at 5.5 – 8.5 minutes showed a number of peak ions, with relatively high masses, which suggested the presence of probably a few glucuronidated polar metabolites.

The mass spectrum (figure 229) of the third peak at 17.8 minutes showed a major peak ion of 593.2 Da, which suggested the presence of another glucuronidated metabolite.

9.2.4 LC-MS/MS analysis

The same samples that were used for LC-MS, precursor ion scan and neutral loss scan analysis were also used for LC-MS/MS analysis. The methodology is described in Chapter 12 (12.8.5).

9.2.4.1 Results and discussion

The quality of the product ion mass spectra was not sufficient to identify the metabolites; therefore it was decided not to include the spectra. The amount of metabolite ions was not adequate to obtain good quality MS/MS spectra. Much more material would be required and more specific extraction methods needed to obtain higher concentrations of the metabolites. This would fall outside the scope of this project and it was decided not to pursue this subject any further.

9.3 Conclusion

LC-MS, precursor ion scan and neutral loss scan experiments were conducted in mouse blood, which resulted in the discovery of several polar and semi-polar metabolites.

The results of the urine sample showed the presence of these and other metabolites, which include the following glucuronidated species: isomers of 641 Da (glucuronidated metabolites of the hydrolysed product; 465 + 176), 657.3 Da, 701.4 Da, and 745.5 Da.

The faeces sample spectra also indicated the presence of many of the above mentioned metabolites, as well as an O-dealkylated metabolite of 451.5 Da. The test compound and hydrolysed product were also present at relatively high concentrations.

9-O-Acetylhydnocarpin is metabolised extensively by the liver enzymes and is removed from the blood system, via the liver and kidneys.

The test compound and its hydrolysed product could not be detected with these methods in the blood. A more sensitive MRM method was required to detect these compounds in the blood. The metabolites are present at higher concentrations in the blood compared to the test and hydrolysed compounds. These metabolites are present at the target site and may also be active against the *P. berghei* parasites.

CHAPTER 10

Antimalarial assessment of 9-O-acetylhydnocarpin in mice using SMEDDS and Pheroid formulations

10 Antimalarial assessment of 9-O-acetylhydnocarpin in mice using SMEDDS and Pheroid formulations

10.1 Introduction

The antimalarial assessment of 9-O-acetylhydnocarpin (polar formulation, presented in Chapter 7) indicated limited protection for the mice against the parasites. One of the significant outcomes of the bioavailability studies, presented in Chapter 8, is the introduction of improved drug delivery systems. The SMEDDS and Pheroid formulations were used as delivery and carrier systems for the antimalarial assessment of 9-O-acetylhydnocarpin. The 4 day suppressive treatment strategy, with minor modifications, was followed as described in Chapter 7 [Peters *et al*., 1975].

Ethical approval was granted by the Animal Research Ethics Committee, Faculty of Health Sciences, University of Cape Town (Project number: 006/034) for studying the antimalarial activity of 9-O-acetylhydnocarpin in mice. The same experimental procedure was followed as was presented in Chapters 7 and 12 (12.9).

The test compound was tested using the SMEDDS and Pheroid formulations at a concentration of 100 mg/kg. The animals were treated once a day on days 2, 3, 4, 5 and 6. The negative control groups received placebo treatment (formulation without test drug). The positive control group received chloroquine at 10 mg/kg for 5 days (once per day on days: D2, D3, D4, D5 and D6).

Figure 108 summarises the allocation of the experimental groups, treatment schedule, sampling and the endpoint of the experiment.

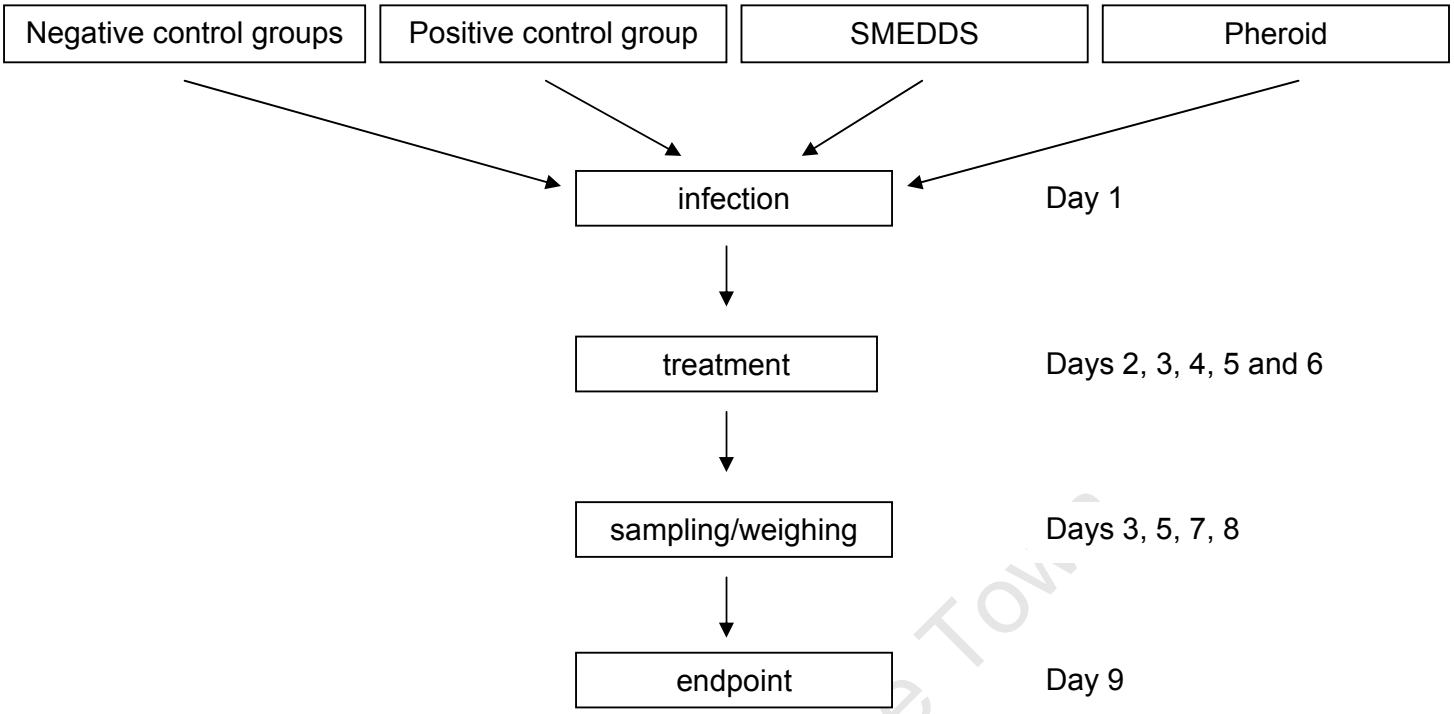

Figure 108 Flow-diagram of the antimalarial assessment animal model using the SMEDDS and Pheroid formulations, which included the experimental groups, treatment schedule, sampling and the endpoint of the experiment

10.2 Results

The following parameters were evaluated: Body weight, %Parasitaemia and %Chemo suppression. The body weight and percentage parasitaemia data of the mice is presented in appendix 2 (tables 52 - 55) and is summarised in figures 109 - 112. The %Chemo suppression of the test compound in the SMEDDS and Pheroid formulations are presented in tables 28 and 29, respectively. The %Chemo suppression determination was done on day 7, as described in Chapter 7.

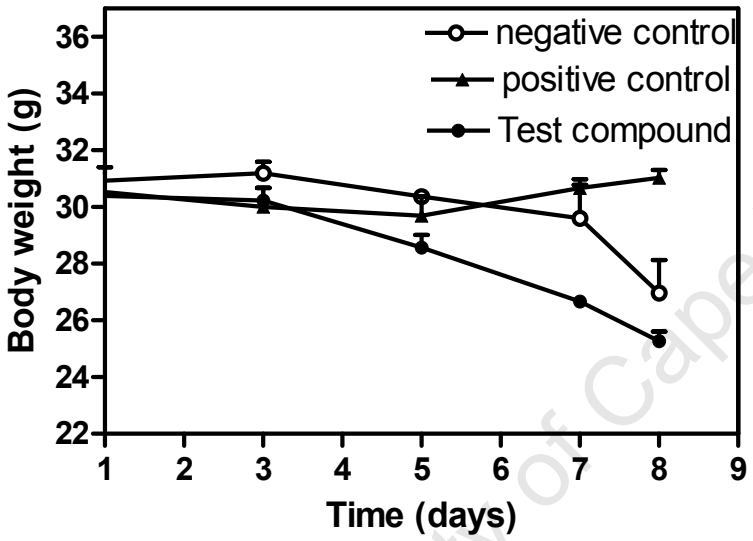

Figure 109 Body weight vs. Time graph of mice treated with a 100 mg/kg 9-O-acetylhydnocarpin SMEDDS formulation using a 5 day suppressive treatment strategy (control groups included)

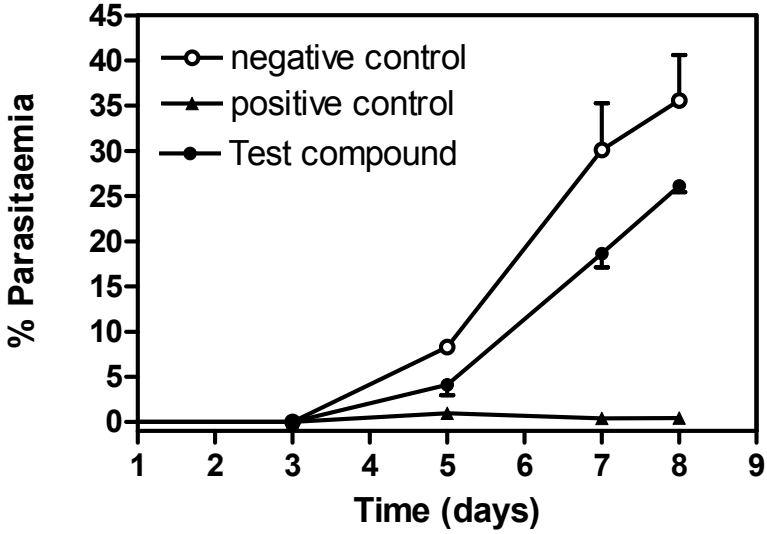

Figure 110 % Parasitaemia vs. Time graph of mice treated with a 100 mg/kg 9-O-acetylhydnocarpin SMEDDS formulation using a 5 day suppressive treatment strategy (control groups included)

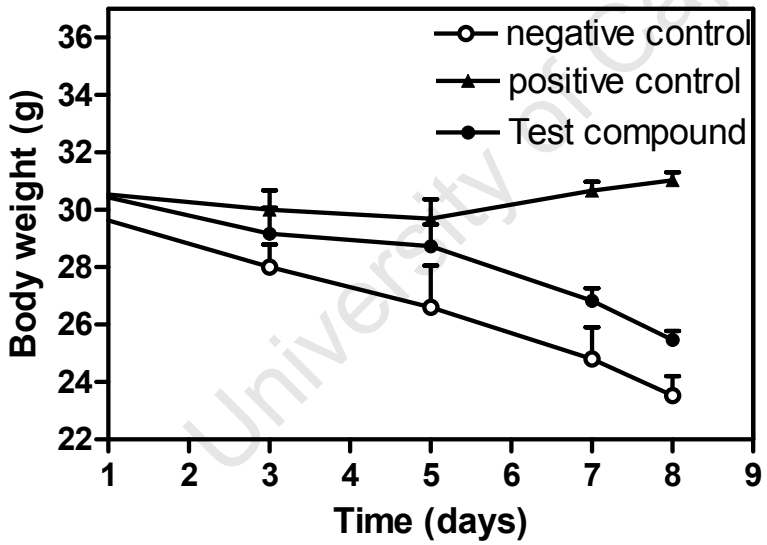

Figure 111 Body weight vs. Time graph of mice treated with a 100 mg/kg 9-O-acetylhydnocarpin Pheroid formulation using a 5 day suppressive treatment strategy (control groups included)

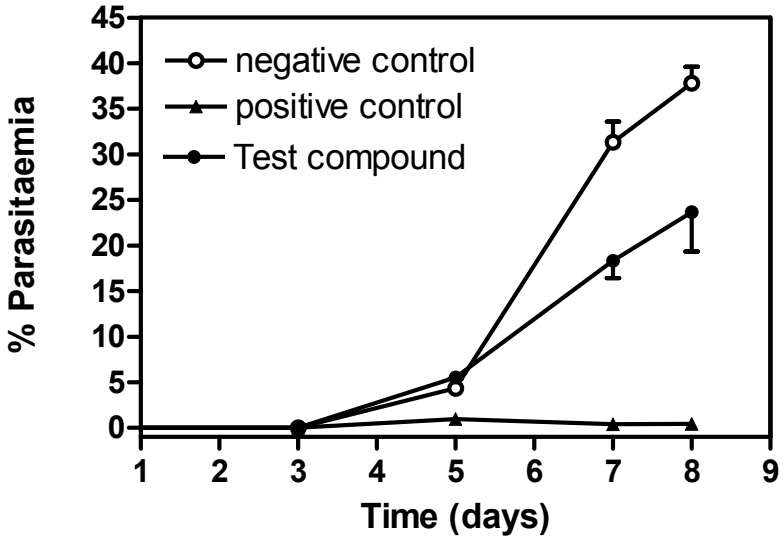

Figure 112 % Parasitaemia vs. Time graph of mice treated with a 100 mg/kg 9-O-acetylhydnocarpin Pheroid formulation using a 5 day suppressive treatment strategy (control groups included)

Table 28 Mean %Parasitaemia and %Chemo suppression data

Treatment	%Parasitaemia	%Chemo suppression
Test group (SMEDDS)	18.6 ± 2.6	38.2
Negative control	30.1 ± 7.4	0
Positive control	0.4 ± 0.3	98.7

Table 29 Mean %Parasitaemia and %Chemo suppression data

Treatment	%Parasitaemia	%Chemo suppression
Test group (Pheroid)	18.3 ± 3.3	41.7
Negative control	31.4 ± 3.2	0
Positive control	0.4 ± 0.3	98.7

10.3 Discussion

Chemo suppression is normally measured around day 5, but because of relatively low parasitaemia levels on day 5 (in both the test and placebo groups), it was decided to measure the reduction of parasitaemia on day 7.

10.3.1 SMEDDS formulation

The *P. berghei* infected mice were treated with 9-O-acetylhydnocarpin at a concentration of 100 mg/kg formulated with SMEDDS. The body weight of the group that received the test compound decreased over time in a similar way as the placebo group. It appears that the animals discontinue feeding when parasitaemia gets to about 5%. The test compound formulated with SMEDDS at the tested concentration showed parasite reduction of 38.2%, but could not provide complete protection against the parasites.

10.3.2 Pheroid formulation

The *P. berghei* infected mice were treated with 9-O-acetylhydnocarpin at a concentration of 100 mg/kg formulated with Pheroid as described in Chapter 12 (12.9). The body weight of the group that received the test compound also decreased over time in a similar way as the placebo group. The test compound formulated with Pheroid at the tested concentration also showed a similar degree of parasite inhibition compared to the SMEDDS formulation.

The outcome of these experiments showed similar parasite reduction compared to the polar formulation (Chapter 7). The improved drug delivery systems were not effective enough to deliver 9-O-acetylhydnocarpin to its target site at high enough levels. The poor bioavailability properties (Chapter 8) and extensive metabolism (Chapter 9) of 9-O-acetylhydnocarpin in mice are probably the major reasons for its limited protection ability against the malaria parasites (*in vivo*).

CHAPTER 11

Research summary, final thoughts and research prospects, presentations and manuscripts

11 Research summary, final thoughts and research prospects, presentations and manuscripts

11.1 Research summary

A new class of antiplasmodial compounds was discovered from the *Xerophyta* genus. These compounds fit into the flavonoid natural class of compounds, and are known as flavones. The most promising compound (9-O-acetylhydnocarpin) isolated from this group, selectively killed *P. falciparum* parasites of both chloroquine sensitive (D10) and resistant (K1) strains at fairly low concentrations. This compound was considered to be a selective antiplasmodial compound because of its favourable antiplasmodial activity and cytotoxicity properties.

The activity of 9-O-acetylhydnocarpin was tested in a polar formulation using the *P. berghei* mouse model. The test compound showed some protection for the mice against the parasites, but could not inhibit all parasites. At this stage of the projects many questions came to mind about why the compound did not perform as well as was seen during the *in vitro* experiments. For this reason it was decided to conduct a bioavailability investigation in a similar mouse model to find answers to some of the questions raised. Results from these experiments showed that 9-O-acetylhydnocarpin is poorly absorbed from the gastrointestinal tract in a polar formulation. Many different formulations and administration routes were tested. The outcome of these investigations showed that if the correct formulation is used relatively high blood levels could be reached. The concentration of the test compound was still lower than expected. Milligram quantities were administered and low microgram maximum levels were reached in the blood. Literature indicated high microgram levels for drugs that are absorbed well and which are not metabolised rapidly [Curry, 1977; Creasey, 1979]. The results of these bioavailability experiments indicated that the compound may be metabolised quite rapidly.

The test compound was injected intravenously and the outcome of this experiment showed that 9-O-acetylhydnocarpin is metabolised rapidly. These results led to the metabolite study. Results from these experiments showed that the test compound is quickly metabolised once it enters the bloodstream by the liver enzymes, and is extracted into the urine and faeces. These metabolites are present at higher concentrations at the target

site, compared to 9-O-acetylhydnocarpin. The results of the bioavailability and metabolite studies were used to develop an improved dosing strategy for *in vivo* antimalarial testing on *P. berghei* infected mice. The improved formulations of the test compound did not reach high enough blood levels for curing the infected animals, however a reasonable degree of parasite inhibition was observed.

The work presented in this thesis showed an improved evaluation system for plant derived antimalarial products. It is also proposed that *in vitro* active antiplasmodial compounds be examined for its bioavailability and metabolic properties before or parallel to evaluation of its activity in animal models. Compounds with poor pharmacokinetic properties will not make good candidates for further animal testing and should not be taken further in animal efficacy studies. The usual approach in antimalarial compound evaluation is direct animal efficacy testing after *in vitro* activity and cytotoxicity testing. The new, improved evaluation system introduced a secondary screening test before or at least parallel to *in vivo* efficacy testing in a mouse model. This model should give investigators better insight in selecting compounds for further testing.

11.2 Final thoughts and research prospects

The work presented in this thesis suggested that the sequence in evaluating antiplasmodial compounds in animal testing be altered as follows: Firstly, administer the test compound intravenously to mice and study the compounds clearance rate. This experiment will only require small amounts of pure material and would give the investigator valuable information about the compounds stability in the animal's bloodstream. Secondly, if the outcome of this experiment is favourable, administer the test compound orally in a polar and non-polar formulation to mice and study the compounds blood levels. If the outcome of both the intravenous and oral experiments are favourable, bioavailability can be calculated which would give a good indication of the potential of a compound to be considered for further animal testing (metabolic, efficacy and toxicity studies). The introduction of bioavailability and metabolic studies before, or at least parallel to efficacy studies should give more focus to antimalarial screening programmes, and would assist in selecting better drug candidates for further animal testing.

The proposed antimalarial evaluation model would result in less animal's being sacrificed unnecessarily for compounds that would in any case not make good pharmacological compounds. The initial phases of this screening system would also require small amounts of the test compound, which is often a challenging factor in isolating pure compounds from plants.

The most active compound, 9-O-acetylhydnocarpin, showed moderate *in vitro* activity against *P. falciparum* parasites when compared to chloroquine; however the activity of this compound was fairly specific to the malaria parasites as was indicated during the toxicity tests. 9-O-Acetylhydnocarpin did not dissolve well in the aqueous test solution that was used for the *in vitro* screening assays due to its hydrophobic nature. More water-soluble derivatives could be synthesised that will improve water-solubility, which could improve activity. Kren and co-authors have shown that glycosylation of silybin, which is structurally related to 9-O-acetylhydnocarpin, increased water-solubility up to 30 times. A similar synthetic chemical modification approached could probably be followed for 9-O-acetylhydnocarpin, which would improve water-solubility [Kren *et al*., 1997].

9-O-Acetylhydnocarpin showed an approximate 38% reduction of parasitaemia (Chapters

7 and 10), but could not protect the animals entirely. It has been shown in Chapters 8 and 9 that 9-O-acetylhydnocarpin is metabolised rapidly by the liver enzymes in mice to mainly glucuronidated metabolites, due to the hydroxyl functional groups. These metabolites were removed quite rapidly from the blood. The bioavailability of 9-O-acetylhydnocarpin and its metabolites were not sufficient to protect the animals against the malaria parasites.

9-O-Acetylhydnocarpin is a good candidate for synthetic structural modification, because of its selective activity against *P. falciparum* parasites. The hydroxyl functional groups are recognised by Phase II liver enzymes and should therefore be modified to more stable groups. The 9-O-acetyl group should also be removed by acidic hydrolysis and the resulting hydroxyl group should then be modified to a more stable group. The general antiplasmodial activity of 9-O-acetylhydnocarpin may also be improved if the hydroxyl groups are replaced with relatively small active groups. 9-O-Acetylhydnocarpin is present in relatively high concentrations in the *Xerophyta* genus, which makes it feasible to obtain enough starting material for chemical modification.

The work suggested above falls outside the scope of this project and should be considered for future projects.

11.3 Presentations

Parts of the work presented in this thesis have been presented as oral presentations at the Pharmacology department (University of Cape Town) and at the South African Pharmacology and Toxicology Congress, 2007.

JL Wiesner, WE Campbell and PJ Smith
Bioavailability Study of 9-O-acetylhydnocarpin in mice
UCT Pharmacology, Medical Research Council of South Africa, Traditional Medicine Research Committee, 1 October 2007

JL Wiesner, WE Campbell and PJ Smith
Antimalarial Study of Bioactive Compounds Isolated from *Xerophyta* species
South African Pharmacology and Toxicology Congress, North West Province, South Africa, 2-5 October 2007

11.4 Manuscripts in preparation

The following manuscripts are currently being prepared for submission to journals for publication.

JL Wiesner, WE Campbell and PJ Smith
Antiplasmodial compounds isolated from *X. villosa* and *X. retinervis*

JL Wiesner, WE Campbell and PJ Smith
Antimalarial study of 9-O-acetylhydnocarpin in mice

CHAPTER 12

Materials and methods

12 Materials and methods & methodology development

New methodologies have been developed for the work presented in Chapters 8 and 9, therefore the addition of a comprehensive and descriptive section about the method development process that was required to investigate the biological availability and metabolism of the test compound in a mouse model (12.7 and 12.8).

The methodologies of Chapters 2, 3, 4, 5, 6, 7 and 10 are presented in sections 12.1, 12.2, 12.3, 12.4, 12.5, 12.6 and 12.9.

12.1 Collection and preparation of plant material

Two different *Xerophyta* species were collected by Dr. P.C. Zietsman (collector No. 4350).

X. villosa was collected on the first of June, 2006. A voucher specimen (NMB 22615) was also collected and is kept at the herbarium of the national museum in Bloemfontein, South Africa. The plant material was collected at Claremont, Blyde River Canyon Nature Reserve, Mpumalanga, South Africa (Latitude: 24 degrees, 32 minutes, 56.4 seconds; Longitude: 30 degrees, 45 minutes, 8.6 seconds).

X. retinervis was collected on the tenth of July, 2006. A voucher specimen (NMB 22616) was also collected and is kept in the herbarium of the national museum in Bloemfontein, South Africa. The plant material was collected on a farm at Hoedspruit, Mpumalanga, South Africa (Latitude: 24 degrees, 20 minutes, 6.9 seconds; Longitude: 30 degrees, 51 minutes, 4.9 seconds).

The plant material was dried at room temperature for 3 weeks. The leave bases were removed and macerated to a fine powder using a blender. The powder was stored at -20 °C.

12.2 Solvent extraction

12.2.1 *X. villosa*

The plant powder (40 g) was extracted with petroleum ether (500 ml) on a horizontal shaker for 24 hours. This solvent extraction with petroleum ether was repeated until no further colour change was observed. The petroleum ether extract was filtered using paper filters (3HW, 320 mm, Lasec SA) and the organic solvent was separated from the extract using a Büchi rotavapor R-200/205 (Büchi Labortechnik AG Schweiz). The dried powder that remained after petroleum ether extraction was further extracted using dichloromethane (500 ml), followed by ethyl acetate and finally methanol and the same methodology was performed as was used for the petroleum ether extraction. The methanol extract was further separated into two fractions using solvent partioning. The methanol extract was dried and dissolved in ethyl acetate (300 ml), and water (100 ml, Millipore water) was added to a separation funnel and shaken for 10 minutes. The funnel was left on the bench for 30 minutes for the two layers to separate completely. The aqueous phase was separated from the organic phase. The aqueous phase was dried using a DURA-DRV II freeze-drying instrument (FTS SYSTEMS, NY USA). Ethyl acetate was separated from the extracted material using a rotary evaporation system.

12.2.2 *X. retinervis*

The plant powder (50 g) was extracted with petroleum ether (1 litre) on a horizontal shaker for 24 hours. The solvent extraction with petroleum ether was repeated until no further colour change was observed. The petroleum ether extract was filtered and the organic solvent was separated from the extract using a rotor evaporating system. The dried powder that remained after the petroleum ether extraction was further extracted using methanol (1 litre) until no further colour change was observed and the same methodology was performed as was used for the petroleum ether extraction. The methanol extract was further separated into two groups using liquid-liquid extraction. The methanol extract was dried and dissolved in ethyl acetate (300 ml) and water (100 ml, Millipore water) was added to a separation funnel and shaken for 10 minutes. The funnel was left on the bench for 30 minutes for the two layers to separate completely. The aqueous phase was separated from the organic phase. The aqueous phase was dried using a freeze-drying instrument. The ethyl acetate was separated from the extracted material using a rotary evaporation system.

12.3 Antiplasmodial screening assay

12.3.1 Cultivation of malaria parasites

The chloroquine sensitive D10 strain (derived from Papua New Guinea) [Ekong *et al*., 1993] of *P. falciparum* was cultured according to the method described by Trager and Jensen, with minor modifications [Trager and Jensen, 1976]. A standard operating procedure, prepared by the Pharmacology Department at the University of Cape Town, was followed and is described below.

"The parasites were sustained with RPMI 1640 (Biowhittaker) medium at a 5% haematocrit. Albumax II (lipid rich bovine serum albumin) (GibcoBRL) (25 g/l), hypoxanthine (44 mg/l), HEPES (6 g/l), sodium bicarbonate (2.1 g/l) and gentamycin (50 mg/l) were added as supplement reagents. O^+ RBC (Western Province Blood Transfuse Service, Groote Schuur Hospital, Cape Town, South Africa) was added regularly to the medium to keep the parasitaemia between 5 and 10%. Parasitaemia was determined on a daily basis along with changing the medium. The cultures were kept at 37 °C in an incubator with an atmosphere of 93% N_2, 3% O_2 and 4% CO_2." [Clarkson, 2002]

The parasites were synchronised with D-sorbital [Lambros and Vanderberg, 1979].

12.3.2 Lactate dehydrogenase assay

The parasite lactate dehydrogenase assay (pLDH) as described by Makler and co-workers was used to determine parasite viability, with minor modifications [Makler *et al*., 1993]. A standard operating procedure, prepared by the Pharmacology Department at the University of Cape Town, was followed and is described below.

"This is a specific method that distinguish parasite LDH from host LDH by using 3-acetylpyridine adenine dinucleotide (APAD). The pLDH uses APAD as a coenzyme in the conversion of pyruvate to lactate and reduces it to APADH. The formation of APADH can be calorimetrically measured by the reduction of a yellow nitroblue tetrazolium (NBT) salt to a blue formazan product. The amount of blue formazan product is proportional to the pLDH activity. The pLDH activity can therefore be monitored by using the Malstat reagent which contains: triton (1 ml/l), APAD (0.33 g/l), TRIS buffer (3.3 g/l) and 1.96 mM NBT with 0.24 mM PES (Sigma) solution in Millipore water. The test plates were incubated for

48 hours. The malstat reagent (100 µl) and NBT/PES (25 µl) solution were added to new micro titre plates. The test plates were removed from the incubator and the parasites were re-suspended within the original test plates before transferring 15 µl of the parasites with a multi-channel pipette into the corresponding well of the plates containing the Malstat reagents and NBT/PES solution. The absorbance of the formed formazan salts was then measured at a wavelength of 620 nm using a 7520 microplate reader (Cambridge Technology). The absorbance data were transformed into percentage viability using an excel spreadsheet and a non-linear regression analysis model in GraphPad Prism 4 was used to determine the 50% inhibitory concentration (IC_{50}) of the extracts or compounds against the parasites." [Clarkson, 2002]

A representative example of samples tested in a 96 well plate is presented in figure 113.

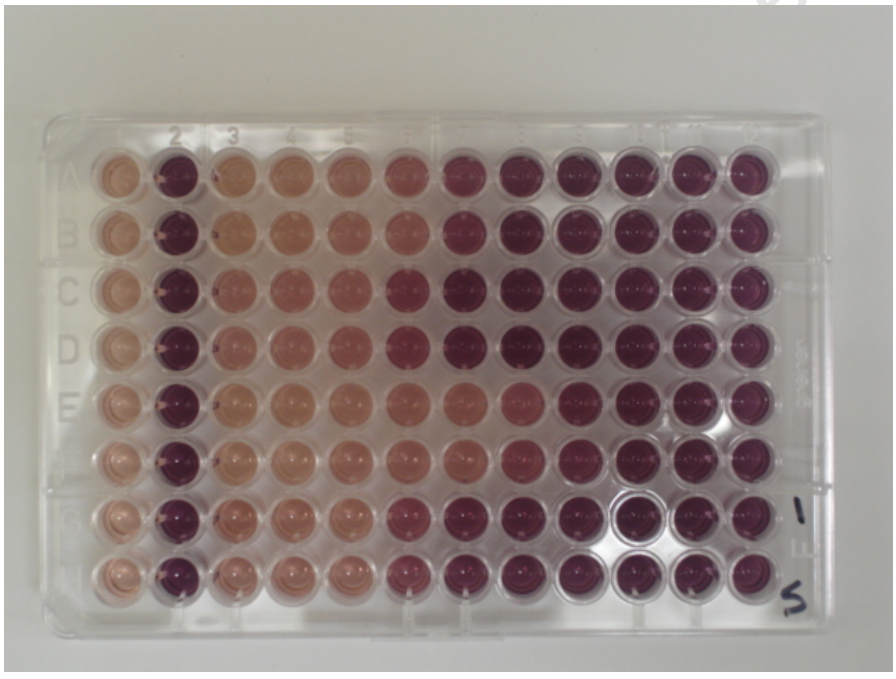

Figure 113 A representative example of a 96 well plate

12.4 Cytotoxicity assay

12.4.1 Cell culture

A standard operating procedure, prepared by the Pharmacology Department at the University of Cape Town, was followed and is described, next. "The cells were routinely maintained as adherent monolayers in 75 cm^3 culture flasks in complete medium consisting of Dulbecos Modified Eagles Medium (Highveld Biologicals, Lyndhurst, South Africa) : Hams F-12 medium (Sigma, St Louis, MO, USA) (1:1), and was supplemented with 10% heat inactivated fetal bovine serum (Highveld Biologicals, Lyndhurst, South Africa). The cells were incubated in a 5% CO_2 – air humidified atmosphere at 37 °C. The culture medium was changed every 3 days and the cells sub-cultured, which involved digestion of the cellular matrix with 1% trypsin solution." [Clarkson, 2002]

12.4.2 MTT cytotoxicity assay

The MTT assay as described by Mosmann, with minor modifications was used to determine cell viability [Mosmann, 1983]. This is a reliable method to measure metabolic activity of cell cultures *in vitro* for the assessment of growth characteristics, IC_{50}-values and cell survival [Sieuwerts *et al*., 1995]. A standard operating procedure, prepared by the Pharmacology Department at UCT, was followed and is described below.

"The assay method distinguishes living cells from dead ones, and the signal generated is dependent on the level of activation of the cells. It can be used to measure cytotoxicity, proliferation or activation. This assay measure the formation of a water insoluble purple formazan product, once yellow water soluble tetrazolium salt is metabolized by living cells. The intensity of the formazan product is measured by a microplate reader and is proportional to the metabolic activity and number of cells in each microplate well. MTT (25 µl) at a concentration of 5 mg/ml in PBS was added to each well after initial incubation. The plates were incubated again for 4 hours at 37 °C. The plates were centrifuged for 10 minutes at 2050 rpm, and the supernatant washed from the wells without disturbing the formazan crystals. DMSO (100 µl) was added to each well and the plate was shaken for 5 minutes to dissolve the crystals. The absorbance of the formazan salt was measured at 540 nm.

The following formula was used to calculate the cell viability:

% Viability = ((Aλ540 test well “cells + drug”) / (Aλ540 cell control well “cells + no drug”)) x 100

Dose response curves were constructed using nonlinear dose response analysis with GraphPad Prism 4 software and Microsoft Excel.”

12.5 HPLC fractionation

12.5.1 *X. villosa*

12.5.1.1 Methanol extract (organic phase)

The extract was dried and reconstituted in a mixture of acetonitrile and DMSO (2:1, v/v) at a concentration of 20 mg/ml and 50 µl was injected onto a semi preparative C_{18} analytical HLPC column (SUPELCO Discovery® C_{18}, 25 cm x 10 mm, 5 µm). The chromatogram was recorded at 330 nm and a gradient (table 30) was used at a flow-rate of 3 ml/min.

Table 30 HPLC gradient of semi-preparative HPLC system

Time	% acetonitrile	% water
0	30	70
20	70	30
21	100	0
24	100	0
25	30	70
30	30	70

12.5.1.2 Ethyl acetate extract

The dried ethyl acetate extract was dissolved in acetonitrile at a concentration of 10 mg/ml, and the same HPLC system, as was used for the methanol (organic phase) extract, was used to analyse this extract.

12.5.1.3 Dichloromethane extract

The dried dichloromethane extract was dissolved in acetonitrile at a concentration of 8 mg/ml, and the same HPLC system, as was used for the methanol (organic phase) extract, was used to analyse this extract.

12.5.1.4 Fractionation of the 6 major peaks

The dried organic phase (liquid-liquid extraction) from the methanol extract was dried and reconstituted in DMSO at a concentration of 200 mg/ml. The mobile phase gradient (table 31) was slightly changed to improve the separation on column.

Table 31 HPLC gradient of semi-preparative HPLC system

Time	% acetonitrile	% water
0	30	70
25	70	30
26	90	10
28	90	10
29	30	70
37	30	70

The six major peaks (1, 2, 3, 4, 5 and 6) were collected in separate solvent bottles using an automated HPLC and fraction collector. These fractions were further purified using specific HPLC methods for every fraction.

12.5.1.4.1 Fraction 1

The dried material from fraction 1 was dissolved in DMSO at a concentration of 5 mg/ml and 50 µl was injected onto a C_{16} amide analytical HLPC column (SUPELCO, Discovery Amide C_{16}, 15 cm x 4.6 mm i.d. x 5 µm). The chromatogram was recorded at 330 nm and an isocratic mobile phase was used at a flow-rate of 1 ml/min, which consisted of acetonitrile and water (25:75, v/v). The column was cleaned after each injection by increasing acetonitrile to 90% for 5 minutes, and equilibrated for 5 minutes using the isocratic mobile phase as described above. The peak of interest eluted from the column at 7.1 minutes and was collected in a clean solvent bottle using an automated HPLC and fraction collector. Acetonitrile was removed using a Büchi rotary evaporator and the water was removed using a freeze-drying instrument. The dried material was stored at -20 °C.

12.5.1.4.2 Fraction 2

The dried material from fraction 2 was dissolved in DMSO at a concentration of 5 mg/ml and 50 µl was injected onto the same C_{16} amide analytical HLPC column as was used for fraction 1. The chromatogram was also recorded at 330 nm and an isocratic mobile phase was used at a flow-rate of 1 ml/min, which consisted of acetonitrile and water (30:70, v/v). The peak of interest eluted from the column at 9.7 minutes and was collected in a clean solvent bottle using an automated HPLC and fraction collector. The column was cleaned and equilibrated as described in table 32. Fraction 2 was dried and stored at -20 °C.

Table 32 HPLC mobile phase

Time	% acetonitrile	% water
0	30	70
12	30	70
13	90	10
17	90	10
18	30	70
25	30	70

12.5.1.4.3 Fraction 3

The dried material from fraction 3 was dissolved in DMSO at a concentration of 1 mg/ml and 20 µl was injected onto the same C_{16} amide analytical HLPC column as was used for fraction 1. The chromatogram was also recorded at 330 nm and a gradient mobile phase was used at a flow-rate of 1 ml/min, which consisted of acetonitrile and water (table 33). The peak of interest eluted from the column at 17.5 minutes and was collected in a clean solvent bottle using an automated HPLC and fraction collector. Fraction 3 was dried and stored at -20 °C.

Table 33 HPLC gradient of analytical HPLC system

Time	% acetonitrile	% water
0	25	75
30	45	55
31	90	10
33	90	10
34	25	75
40	25	75

12.5.1.4.4 Fraction 4

The dried material from fraction 4 was dissolved in DMSO at a concentration of 5 mg/ml and 40 µl was injected onto the same C_{16} amide analytical HLPC column as was used for fraction 1. The chromatogram was recorded at 330 nm and a gradient mobile phase was used at a flow-rate of 1 ml/min, which consisted of acetonitrile and water (table 34). The peak of interest eluted from the column at 21.3 minutes and was collected in a clean solvent bottle using an automated HPLC and fraction collector. Fraction 4 was dried and stored at -20 °C.

Table 34 HPLC gradient of analytical HPLC system

Time	% acetonitrile	% water
0	25	75
30	50	50
31	90	10
33	90	10
34	25	75
40	25	75

12.5.1.4.5 Fraction 5

The dried material from fraction 5 was dissolved in DMSO at a concentration of 5 mg/ml and 50 µl was injected onto the same C_{16} amide analytical HLPC column as was used for fraction 1. The chromatogram was also recorded at 330 nm and a gradient mobile phase was used at a flow-rate of 1 ml/min, which consisted of acetonitrile and water (table 35). The peak of interest eluted from the column at 16.3 minutes and was collected in a clean solvent bottle using an automated HPLC and fraction collector. Fraction 5 was dried and stored at -20 °C.

Table 35 HPLC gradient of analytical HPLC system

Time	% acetonitrile	% water
0	30	70
20	60	40
21	90	10
23	90	10
24	30	70
30	30	70

12.5.1.4.6 Fraction 6

The dried material from fraction 6 was dissolved in DMSO at a concentration of 5 mg/ml and 50 µl was injected onto the same C_{16} amide analytical HLPC column as was used for fraction 1. The chromatogram was recorded at 330 nm and a gradient mobile phase was used at a flow-rate of 1 ml/min, which consisted of acetonitrile and water (table 36). The peak of interest eluted from the column at 17.0 minutes and was collected in a clean solvent bottle using an automated HPLC and fraction collector. Fraction 6 was dried and stored at -20 °C.

Table 36 HPLC gradient of analytical HPLC system

Time	% acetonitrile	% water
0	20	80
20	60	40
21	90	10
23	90	10
24	20	80
30	20	80

12.5.2 *X. retinervis*

12.5.2.1 Methanol extract (organic phase)

The extract was dried and reconstituted in a mixture of acetonitrile and DMSO (2:1, v/v) at a concentration of 20 mg/ml and 50 µl was injected onto a semi preparative C_{18} analytical HLPC column (SUPELCO Discovery® C18, 25 cm x 10 mm, 5 µm). The chromatogram was recorded at 330 nm and a gradient (Table 37) was used at a flow-rate of 2 ml/min.

Table 37 HPLC gradient of semi-preparative HPLC system

Time	% acetonitrile	% water
0	30	70
25	70	30
26	30	70
30	30	70

The two major peaks were collected in separate solvent bottles using an automated HPLC connected to a fraction collector. Fractions A and B were dried and stored at -20 °C. The dried fractions were dissolved in acetonitrile and analysed using a C_{18} analytical column (Phenomenex, C_{18}, 15 cm x 4.6 i.d. x 5 µm) to test the purity of the collected peaks. The chromatograms were recorded at 330 nm and the same gradient (table 37) was used at a flow-rate of 1 ml/min.

12.6 Structural elucidation

12.6.1 Ultraviolet spectroscopy

A Waters 996 photodiode array detector was used to obtain UV spectra of compounds 2, 4 and 5. These spectra are presented in appendix 1.

12.6.2 Mass spectrometry

A unit resolution mass spectrometer was used to search for the molecular ions of interest; once these ions were detected a high resolution mass spectrometer was used to accurately determine the masses of the molecular ions.

12.6.2.1 Unit resolution mass spectrometry

An Applied Biosystems API 3200 linear ion trap mass spectrometer was used to determine the molecular ions of compounds 2, 4 and 5. Small samples of these compounds were dissolved in acetonitrile and 0.1% formic acid (1:1, v/v) at a concentration of 500 ng/ml and infused into the mass spectrometer at 5 µl/min in the positive ion mode. The mass spectra of these compounds are presented in appendix 1, showing the molecular ions.

12.6.2.2 High resolution mass spectrometry

A Waters Q-TOF mass spectrometer was used to determine the accurate mass of compounds 2, 4 and 5. Small samples of these compounds were dissolved in acetonitrile and 0.1% formic acid (1:1, v/v) at a concentration of 500 ng/ml and infused into the mass spectrometer at 5 µl/min in the positive ion mode. The accurate mass spectra of these compounds are presented in appendix 1, showing the molecular ions.

12.6.3 Nuclear magnetic resonance spectroscopy

A Varian Inova 600 mHz NMR instrument was used to analyse compounds 2, 4 and 5. ^{1}H, ^{13}C and 2D experiments (COSY, HSQC and HMQC) were conducted and are presented in appendix 1.

12.6.4 Optical rotation

The optical rotation of compound 5 was measured at 25 °C on a Perkin-Elmer 241 polarimeter at 598 nm (Na D-line) using a 1,001 dm cell. The compound was dissolved in DMSO at a concentration of 5.0 mg/ml.

12.6.5 Melting point

The melting point of compound 5 was measured on a SANYO Gallenkamp variable electrical apparatus (supplied by United Scientific, Cape Town).

12.7 Bioavailability investigation of 9-O-acetylhydnocarpin in mice

12.7.1 Mice

Mice (male, 8 to 12 weeks old, C57BL6) were obtained from the University of Cape Town's Animal Unit and kept at the animal laboratory of the liver research group (Groote Schuur Hospital, Old main building, level K).

12.7.2 Initial bioavailability study of 9-O-acetylhydnocarpin in mice

9-O-Acetylhydnocarpin was administered orally (figure 114) at a concentration of 200 mg/kg in a solution which consisted of water and DMSO (9:1, v/v) to healthy mice. Blood samples were collected at 0, 1, 2, 3 and 5 hours after administration. One animal per sampling point was used at this stage of the project.

Figure 114 Example of a mouse receiving oral treatment

12.7.2.1 Method development of an assay method for the determination of 9-O-acetylhydnocarpin in mice whole blood

An analytical method was needed to quantitatively determine the concentration of 9-O-acetylhydnocarpin in whole blood samples to follow the concentration vs. time profile for 5 hours after a 200 mg/kg single dose was given to healthy mice. Blood samples (100 µl) were taken before administration of the study medication and thereafter at the following time periods: 0, 1, 2, 3, and 5 hours. A relatively high volume of sample was required at this point of the project; therefore one mouse per sample point was used to obtain average initial bioavailability information. The samples were stored at – 20 °C until analysed. An

Applied Biosystems API-2000 mass spectrometer (MS) coupled to a high performance liquid chromatography (HPLC) system was used to analyse the samples.

12.7.2.1.1 Mass Spectrometer optimisation

Infusion experiments of 9-O-acetylhydnocarpin were conducted in acidic, neutral and basic chemical environments in both the positive and negative ESI modes to select the molecular ion of interest. The best result was obtained when infused in an acidic chemical environment (0.1% formic acid : methanol, 1:1, v/v) at a flow rate of 10 µl/min. A protonated molecular ion $[M+H]^+$ was found at m/z 507 (figure 115), which correlates with the high resolution data presented in Chapter 6 and appendix 1.

The molecular ions were selected in the first mass filter and fragmented in the collision cell to form product ions (figure 116). The most abundant product ion (257) was selected and the MS set at the multiple reaction monitoring mode (MRM).

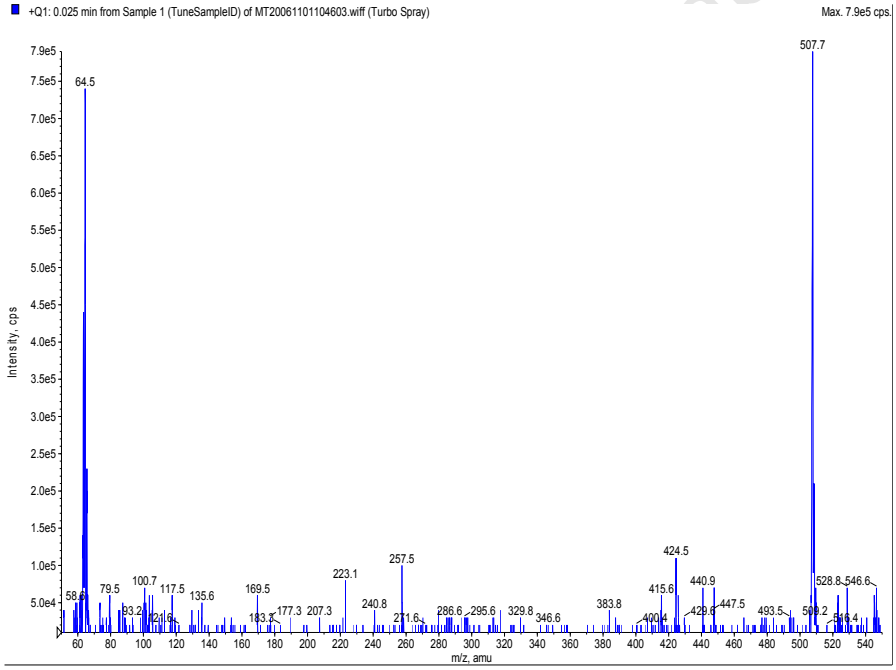

Figure 115 Mass spectrum of 9-O-acetylhydnocarpin showing the $[M+H]^+$ ion

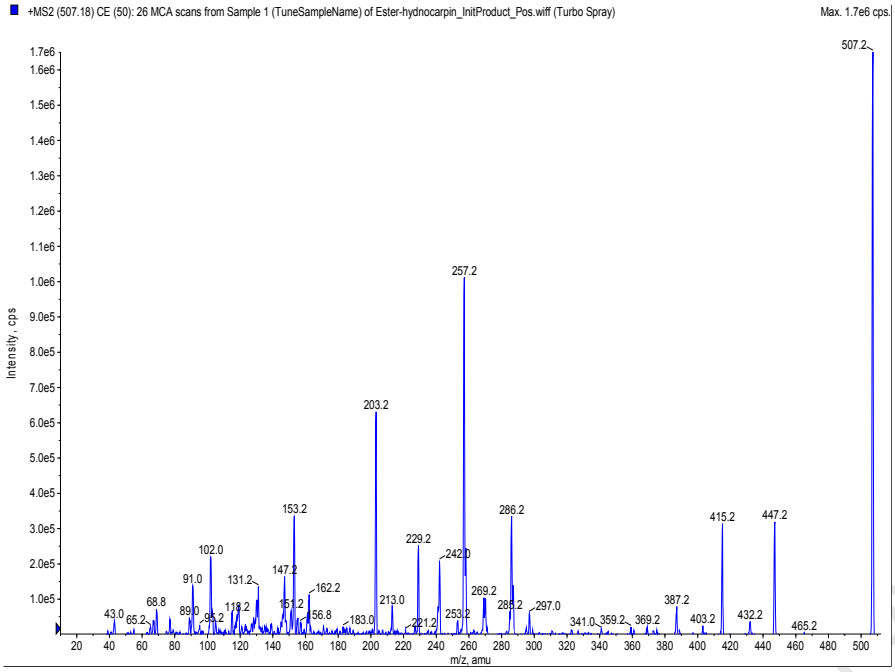

Figure 116 Product ion mass spectrum of the protonated molecular ion and the product ions

The mass spectrometer was set to detect 9-O-acetylhydnocarpin (507 → 257) in the MRM mode. Detection was performed on an API 2000 mass spectrometer (ESI in the positive ion mode, MRM) and the settings on the apparatus are summarised in tables 38 and 39.

Table 38 ESI settings

Nebulizer gas (arbitrary value)	50
Turbo spray (arbitrary value)	50
Curtain gas (arbitrary value)	10
Heated nebulizer (°C)	400
Ionspray voltage (V)	4500
Resolution	unit

Table 39 MS/MS settings

	9-O-acetylhydnocarpin
Average mass	506.4656
Exact mass	506.1213
Protonated molecular ion (m/z)	507.2
Product ion (m/z)	257.2
Dwell time (ms)	150
Declustering potential (V)	71
Entrance potential (V)	11
Collision cell entrance potential (V)	22
Collision energy (eV)	55
Collision cell exit potential (V)	4
Collision activated dissociation gas	medium
Scan type	MRM
Polarity	positive
Pause time	5 ms

12.7.2.1.2 Chromatography development

A primary stock solution of 9-O-acetylhydnocarpin was prepared in acetonitrile at a concentration of 2 mg/ml. A secondary stock solution was prepared by spiking the primary stock solution in acetonitrile : 0.1% formic acid (1:1, v/v) to obtain a concentration of 1 µg/ml. Mobile phase was prepared consisting of acetonitrile and a 0.1% formic acid solution (70:30, v/v). A Phenomenex® C_{18} (15 cm x 4.6 mm, 5 µm) column was set up and equilibrated for 20 minutes by pumping the mobile phase at a constant flow rate of 0.3 ml/min through the column. The injection volume was 10 µl. This mobile phase resulted in very good chromatography. The retention time was 3.2 minutes for 9-O-acetylhydnocarpin (figure 117).

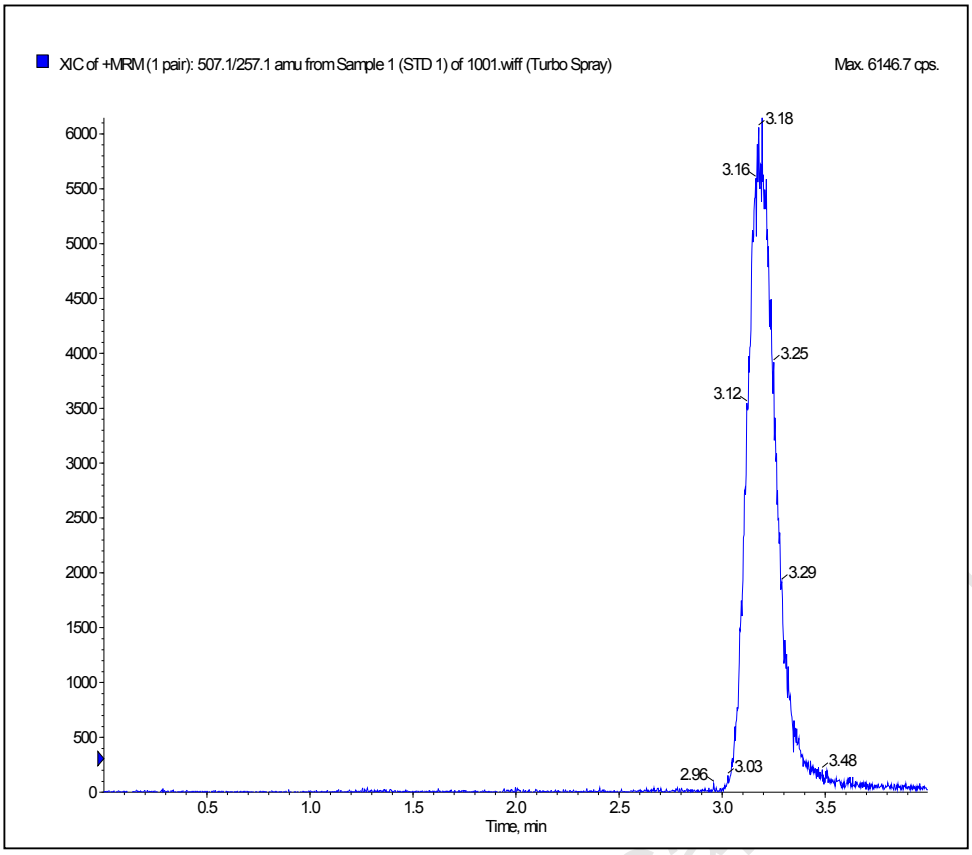

Figure 117 LC-MS/MS chromatogram of 9-O-acetylhydnocarpin

12.7.2.1.3 Extraction

A specific extraction method was needed to extract 9-O-acetylhydnocarpin from blood. Liquid-liquid extraction is often used to extract drugs from samples in clinical testing laboratories, so it was decided to commence the extraction development process with solvent extraction. Different organic solvents and buffers were tested and the best repeatable recovery (70%) was obtained with ethyl acetate and a 0.1 M carbonate buffer at pH 10.2. The blood samples were thawed in a water bath at 37 °C, briefly vortexed and centrifuged for 1 minute at 1300 G. Blood samples (100 µl) were pipetted in glass tubes. The sodium carbonate buffer (200 µl, 0.1 M, pH 10.2) and ethyl acetate (2 ml) organic solvent were added and the samples vortexed for 1 minute and centrifuged at 1300 G for 1 minute. The organic phase was transferred to clean glass tubes. The organic solvent was evaporated under a gentle stream of nitrogen at room temperature. The dried samples were reconstituted with mobile phase and vortexed for 15 seconds. The extracts were transferred to autosampler vials and 5 µl was injected onto the HPLC column.

12.7.2.1.4 Preparation of calibration standards

Whole blood was collected and cooled on ice before spiking with the reference standard to prevent hydrolysis by the esterase enzymes. A stock solution with a concentration of 1 mg/ml 9-O-acetylhydnocarpin was prepared in DMSO. A pool of blank whole blood was spiked with the stock solution to obtain a standard with a concentration of 1 µg/ml. This standard was serially diluted with blank whole blood to attain standards with the following concentrations: 500, 250, 125, 62.5, 31.3, 15.6, 7.8, 3.9 and 1.95 ng/ml. The calibration standards were aliquoted in polypropylene tubes and stored at approximately -20°C.

12.7.3 Metabolite investigation

12.7.3.1 Precursor ion experiment

The mass spectrometer was set in the precursor ion mode and Q3 was set to stabilise the most abundant product ion of 9-O-acetylhydnocarpin and hydnocarpin, which was 257. Q1 was set to scan between 400 and 600 to search for the hydrolysed product. The extracted blood samples that were used during the previous experiment (12.7.2) were combined and analysed here. The same analytical column was used as described in 12.7.2.1.2. A gradient mobile phase was used which consisted of acetonitrile and 0.1% formic acid. The organic phase was increased from 50% to 70% over a period of 4 minutes.

12.7.4 Bioavailability study of 9-O-acetylhydnocarpin and its hydrolysed product in mice using different formulations and administration routes

12.7.4.1 Experimental design

12.7.4.1.1 Oral dose experiment

Test formulation: 9-O-Acetylhydnocarpin was administered orally at a concentration of 100 mg/kg in Tween® 80 (Aldrich, Cat.: 27,436-4) to three healthy mice. Blood (10 µl) was collected just before, and at 1, 2, 3, 5 and 7 hours after administration.

Control formulation: 9-O-Acetylhydnocarpin was administered orally at a concentration of 100 mg/kg in 10% DMSO (water : DMSO; 90:10, v/v) to three healthy mice. Blood (10 µl) was collected just before, and at 1, 2, 3, 5 and 7 hours after administration.

12.7.4.1.2 Subcutaneous dose experiment

Test formulation: 9-O-Acetylhydnocarpin was administered subcutaneously (figure 118) at a concentration of 100 mg/kg in Tween® 80 (Aldrich, Cat.: 27,436-4) to three healthy mice. Blood (10 µl) was collected just before, and at 1, 2, 3, 5 and 7 hours after administration.

Control formulation: 9-O-Acetylhydnocarpin was administered subcutaneously at a concentration of 100 mg/kg in 10% DMSO (water : DMSO; 90:10, v/v) to three healthy mice. Blood (10 µl) was collected just before, and at 1, 2, 3, 5 and 7 hours after administration.

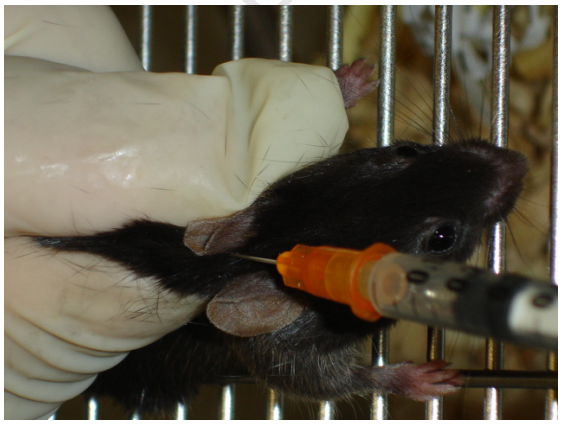

Figure 118 Example of a mouse receiving subcutaneous treatment

12.7.4.2 Method development of a more sensitive assay method

An analytical method was needed to quantitatively determine the concentration of 9-O-acetylhydnocarpin and the hydrolysed product in whole blood samples to follow the concentration vs. time profile for 7 hours after a 100 mg/kg single dose was given to healthy mice. Blood samples (10 µl) were taken before administration of the study medication and thereafter at the following time periods: 0, 1, 2, 3, 5, 7 hours. The samples were spotted onto filter paper (Whatman® 3 filters) and left to dry at room temperature. The filter paper was stored at – 20 °C until analysed. An Applied Biosystems 3200 Q-trap mass spectrometer coupled to a high performance liquid chromatography system was used to analyse the samples.

12.7.4.2.1 Mass Spectrometer optimisation

The previous sample analysis was done on an Applied Biosystems API 2000 instrument. During those experiments, 100 µl of sample was used for analysis and one animal per time point was used. A more sensitive detection method was needed to study the bioavailability of these compounds per animal, only 10 µl blood was collected per time point, and 6 samples were collected per animal. The proposed range for the 10 µl extraction method was 0.313 to 5 µg/ml. An Applied Biosystems 3200 Q-trap mass spectrometer, which is a much more sensitive instrument, was used for analysing these study samples.

12.7.4.2.1.1. 9-O-Acetylhydnocarpin

Infusion experiments of 9-O-acetylhydnocarpin were conducted in acidic, neutral and basic chemical environments (at a concentration of 100 ng/ml) in both the positive and negative ESI modes to select the molecular ion of interest. The best result was obtained when infused in an acidic chemical environment (0.1% formic acid : methanol, 1:1, v/v) at a flow rate of 10 µl/min. A protonated molecular ion $[M+H]^+$ was found at m/z 507 (figure 119).
The molecular ion was selected in the first mass filter and fragmented in the collision cell to form product ions (figure 120). The most abundant product ion (257) was selected and the MS set in the multiple reaction monitoring mode (MRM).

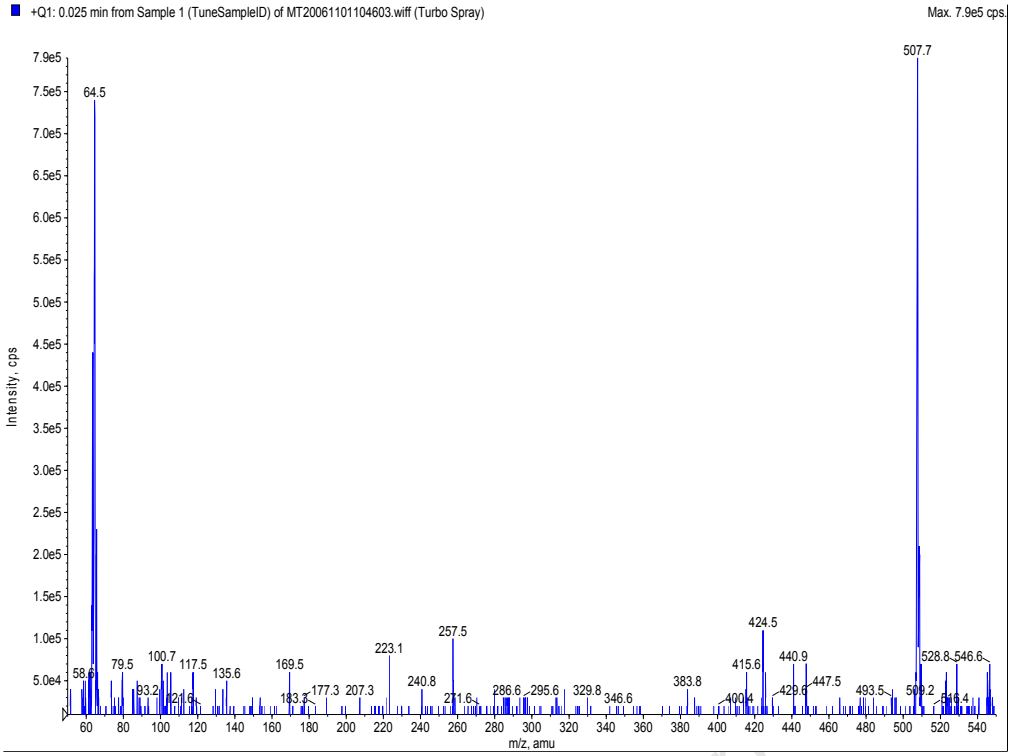

Figure 119 Mass spectrum of 9-O-acetylhydnocarpin showing the $[M+H]^+$ ion

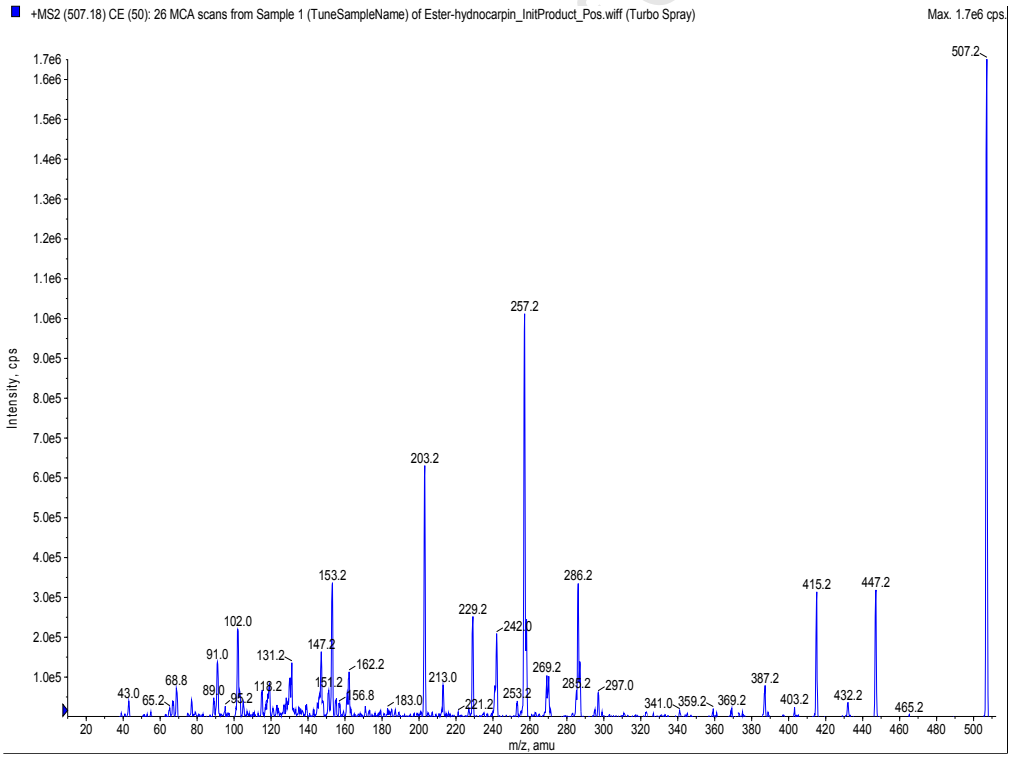

Figure 120 Product ion mass spectrum of the protonated molecular ion and the product ions

12.7.4.2.1.2. Hydrolysed compound

The same methodology was used to optimise the mass spectrometer for the hydrolysed product. The mass spectrum of the hydrolysed product is presented in figure 121 and the product ion mass spectrum in figure 122. The most abundant product ion (257) was selected and the MS set in the multiple reaction monitoring mode (MRM).

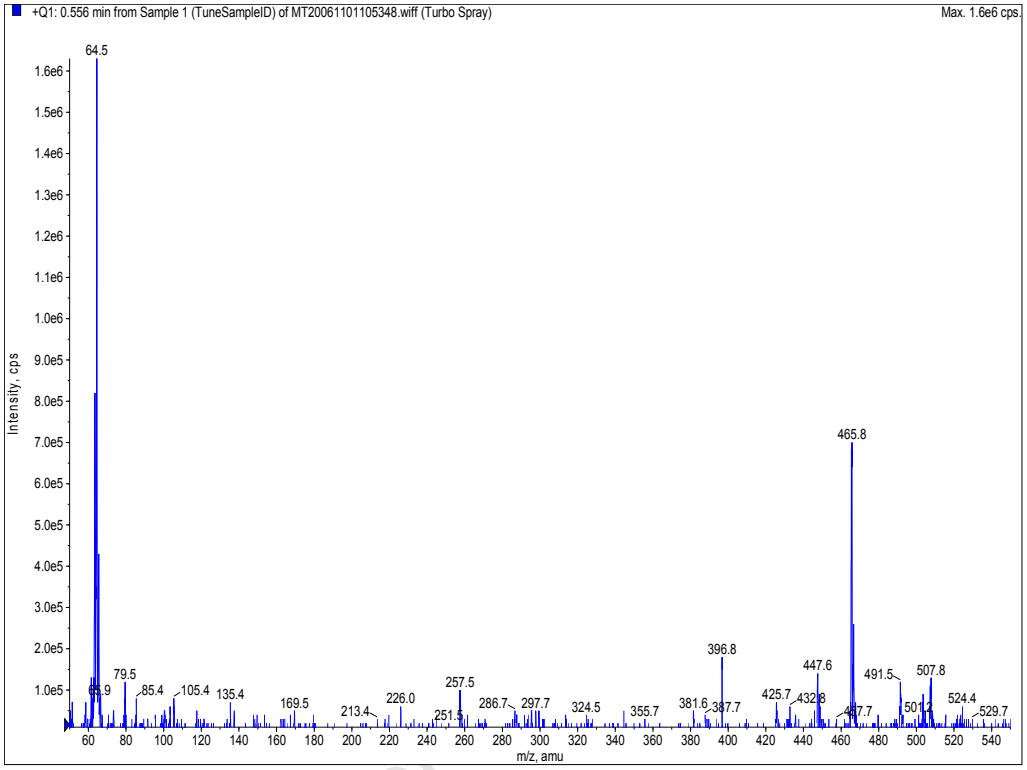

Figure 121 Mass spectrum of the hydrolysed product showing the $[M+H]^+$ ion (m/z 465)

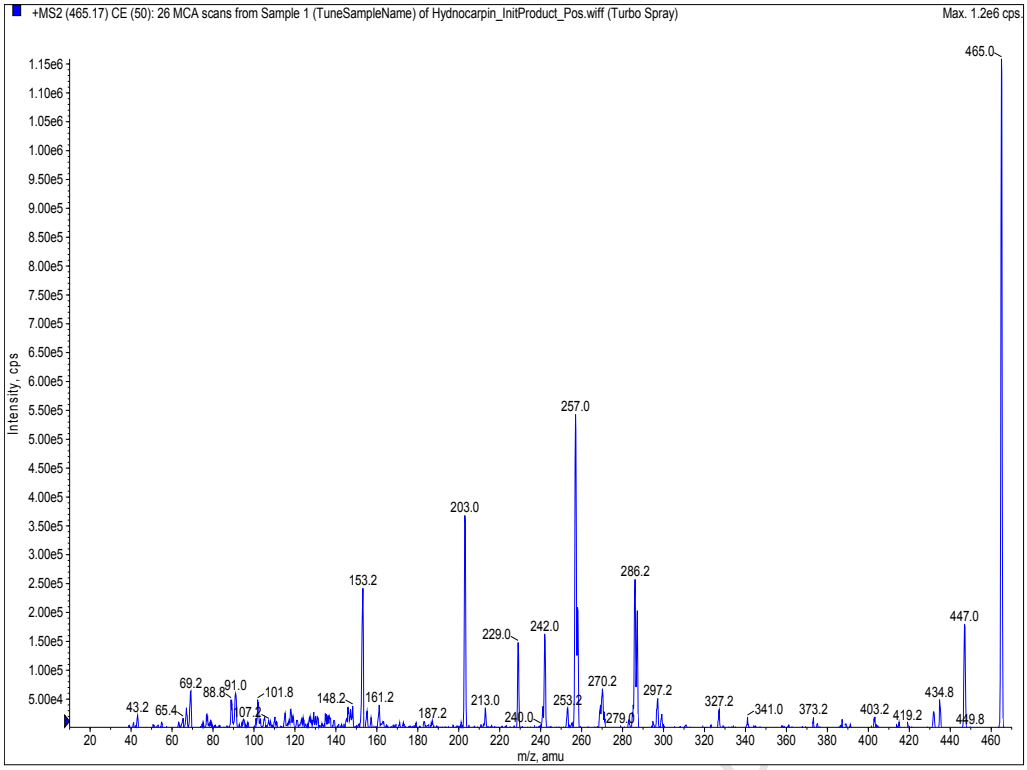

Figure 122 Product ion mass spectrum of the protonated molecular ion and the product ions

The mass spectrometer was set to detect 9-O-acetylhydnocarpin (507 → 257) and its hydrolysed product (465 → 257) in the MRM mode. Detection was performed using an Applied Biosystems 3200 Q-trap mass spectrometer (ESI in the positive ion mode, MRM) and the settings on the apparatus are summarised in tables 40 and 41.

Table 40 ESI settings

Nebulizer gas (arbitrary value)	50
Turbo spray (arbitrary value)	50
Curtain gas (arbitrary value)	10
Heated nebulizer (°C)	400
Ionspray voltage (V)	4500
Resolution	unit

Table 41 MS/MS settings

	9-O-acetylhydnocarpin	Hydrolysed product
Average mass	506.4656	464.4284
Exact mass	506.1213	464.1107
Protonated molecular ion (m/z)	507.2	465.2
Product ion (m/z):	257.2	257.2
Dwell time (ms)	150	150
Declustering potential (V)	71	71
Entrance potential (V)	11	10.5
Collision cell entrance potential (V)	22	26
Collision energy (eV)	55	51
Collision cell exit potential (V)	4	4
Collision activated dissociation gas	medium	medium
Scan type	MRM	MRM
Polarity	positive	positive
Pause time	5 ms	5 ms

12.7.4.2.2 Chromatography development

A primary stock solution of 9-O-acetylhydnocarpin and its hydrolysed product was prepared in acetonitrile at a concentration of 2 mg/ml. A secondary stock solution was prepared by spiking the primary stock solution in acetonitrile : 0.1% formic acid (1:1, v/v) to obtain a concentration of 1 ug/ml of both compounds. Mobile phase was prepared consisting of acetonitrile and a 0.1% formic acid solution (70:30, v/v). A Phenomenex® Gemini™ C_{18} (5 cm x 2 mm, 5 µm) column was set up and equilibrated for 20 minutes by pumping the mobile phase at a constant flow rate of 0.3 ml/min through the column. The injection volume was 10 µl. This mobile phase resulted in very good chromatography. The retention time was 1.05 minutes for 9-O-acetylhydnocarpin and 0.75 minutes for the hydrolysed product (figure 123).

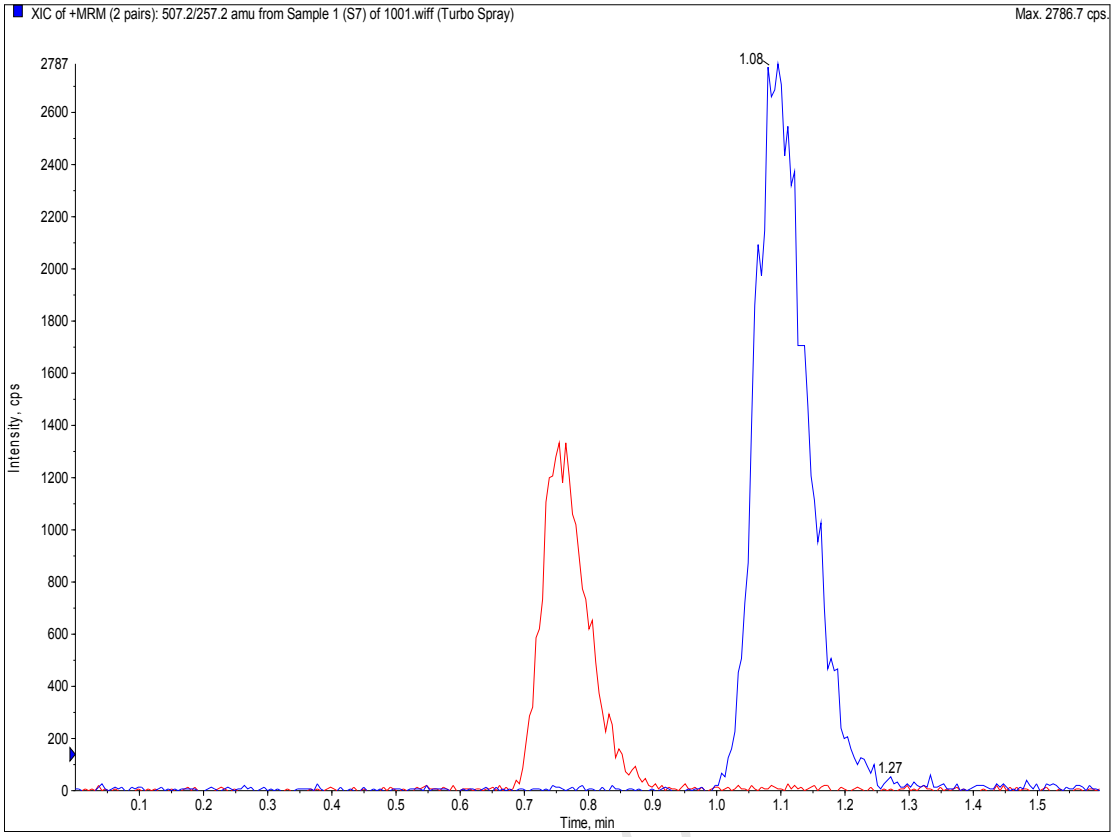

Figure 123 LC-MS/MS chromatogram of 9-O-acetylhydnocarpin and its hydrolysed product

12.7.4.2.3 Extraction

A specific extraction method was needed to extract 9-O-acetylhydnocarpin and the hydrolysed product from small volumes of blood (10 µl). Liquid-liquid extraction is often used to extract compounds from whole blood samples. Different organic solvents and buffers were tested. The best recovery for both compounds was obtained with ethyl acetate and water (pH 7). A liquid-liquid filter paper extraction method was developed. The whole blood samples (10 µl) were spotted onto filter paper and left on the bench for 20 minutes to dry. The dried spots were cut out and transferred to clean test tubes. Water (200 µl) was added and the samples were briefly vortexed. The samples were ultra-sonicated for 5 minutes and left on the bench for another 5 minutes. Ethyl acetate was added (1 ml) and the samples were vortexed for 30 seconds. The organic layers (750 µl) were transferred to clean test tubes after centrifugation (3000 rpm for 1 minute). The samples were dried (30 minutes) in a rotary evaporation system at 30 °C. The dried

samples were reconstituted with mobile phase (100 µl) and 5 µl injected onto the column for analysis.

12.7.4.2.4 Preparation of calibration standards

Whole blood was collected and cooled on ice before spiking with reference standards to prevent hydrolysis by the esterase enzymes. A stock solution with a concentration of 1 mg/ml for both 9-O-acetylhydnocarpin and the hydrolysed product was prepared in DMSO. A pool of blank whole blood was spiked with the stock solution to obtain a standard with a concentration of 10 µg/ml for both compounds. This standard was serially diluted with blank whole blood to attain standards with the following concentrations: 5, 2.5, 1.25, 0.625 and 0.313 µg/ml. The calibration standards were aliquoted in polypropylene tubes and stored at approximately -20°C.

12.7.5 Method development of an improved assay method

12.7.5.1 Mass Spectrometer optimisation

An Applied Biosystems 3200 Q-trap mass spectrometer was used to analyse the study samples.

12.7.5.1.1 9-O-Acetylhydnocarpin

The same mass spectrometer conditions were used as described in 12.7.4.2.1.1.

12.7.5.1.2 Hydrolysed product

The same mass spectrometer conditions were used as described in 12.7.4.2.1.2.

12.7.5.1.3 Internal standard

The same methodology was used to optimise the mass spectrometer for the internal standard. The mass spectrum of the internal standard is presented in figure 124 and the product ion mass spectrum in figure 125. The most abundant product ion (153) was selected and the MS set in the multiple reaction monitoring mode (MRM).

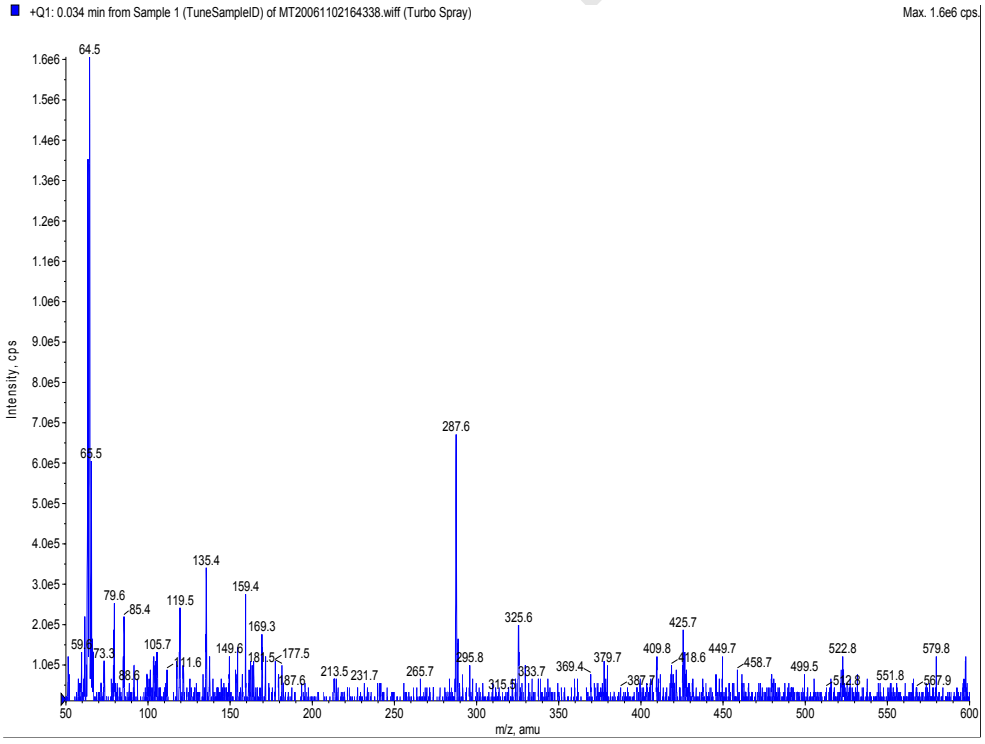

Figure 124 Mass spectrum of the internal standard showing the $[M+H]^+$ ion (m/z 287)

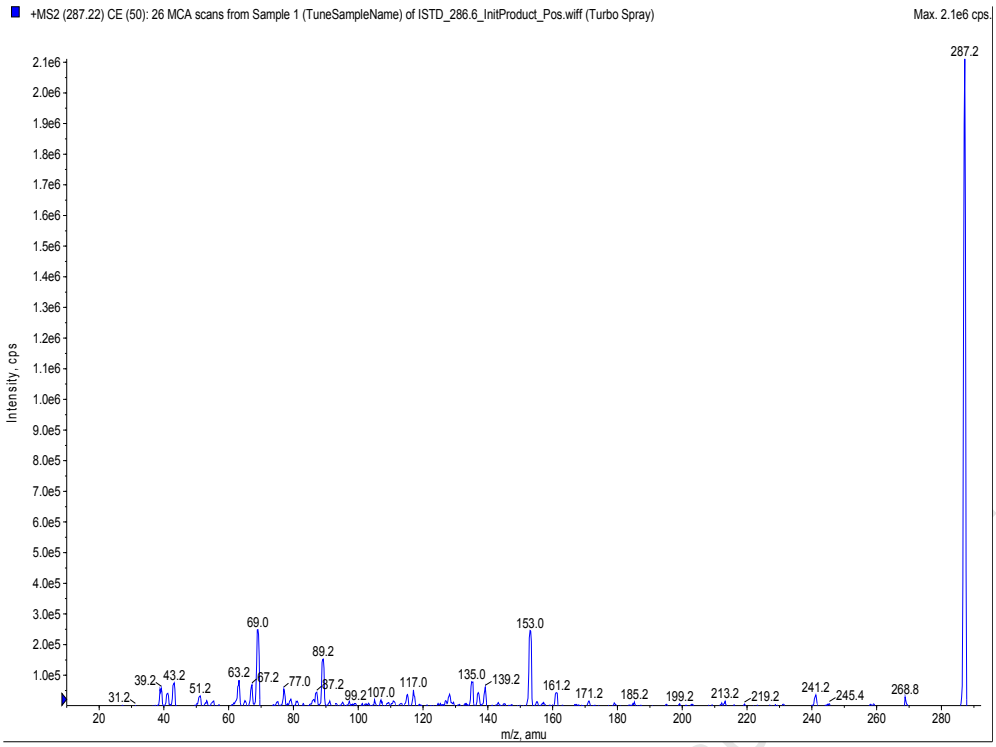

Figure 125 Product ion mass spectrum of the protonated molecular ion and the product ions

Detection was performed on an Applied Biosystems 3200 Q-trap mass spectrometer (ESI in the positive ion mode, MRM) and the settings on the apparatus are summarised in tables 42 and 43.

Table 42 ESI settings

Nebulizer gas (arbitrary value)	50
Turbo spray (arbitrary value)	50
Curtain gas (arbitrary value)	10
Heated nebulizer (°C)	400
Ionspray voltage (V)	4500
Resolution	unit

Table 43 MS/MS settings

	9-O-acetylhydnocarpin	Hydrolysed product	Internal standard
Average mass	506.4656	464.4284	286.2408
Exact mass	506.1213	464.1107	286.0477
Protonated molecular ion (m/z)	507.2	465.2	287.2
Product ion (m/z):	257.2	257.2	153.2
Dwell time (ms)	150	150	150
Declustering potential (V)	71	71	76
Entrance potential (V)	11	10.5	8.5
Collision cell entrance potential (V)	22	26	16
Collision energy (eV)	55	51	45
Collision cell exit potential (V)	4	4	4
Collision activated dissociation gas	medium	medium	medium
Scan type	MRM	MRM	MRM
Polarity	positive	positive	positive
Pause time	5 ms	5 ms	5 ms

12.7.5.2 Chromatography development

A primary stock solution of 9-O-acetylhydnocarpin, the hydrolysed product and the internal standard was prepared in acetonitrile at a concentration of 2 mg/ml. A secondary stock solution was prepared by spiking the primary stock solution in acetonitrile : 0.1% formic acid (1:1, v/v) to obtain a concentration of 1 µg/ml of all compounds. Mobile phase was prepared consisting of acetonitrile and a 0.1% formic acid solution (70:30, v/v). A Phenomenex® Gemini™ C_{18} (5 cm x 2 mm, 5 µm) column was set up and equilibrated for 20 minutes by pumping the mobile phase at a constant flow rate of 0.3 ml/min through the column. The injection volume was 5 µl. This mobile phase resulted in very good chromatography. The retention time was 1.05 minutes for 9-O-acetylhydnocarpin, 0.75 minutes for the hydrolysed product and 0.60 minutes for the internal standard (figure 126).

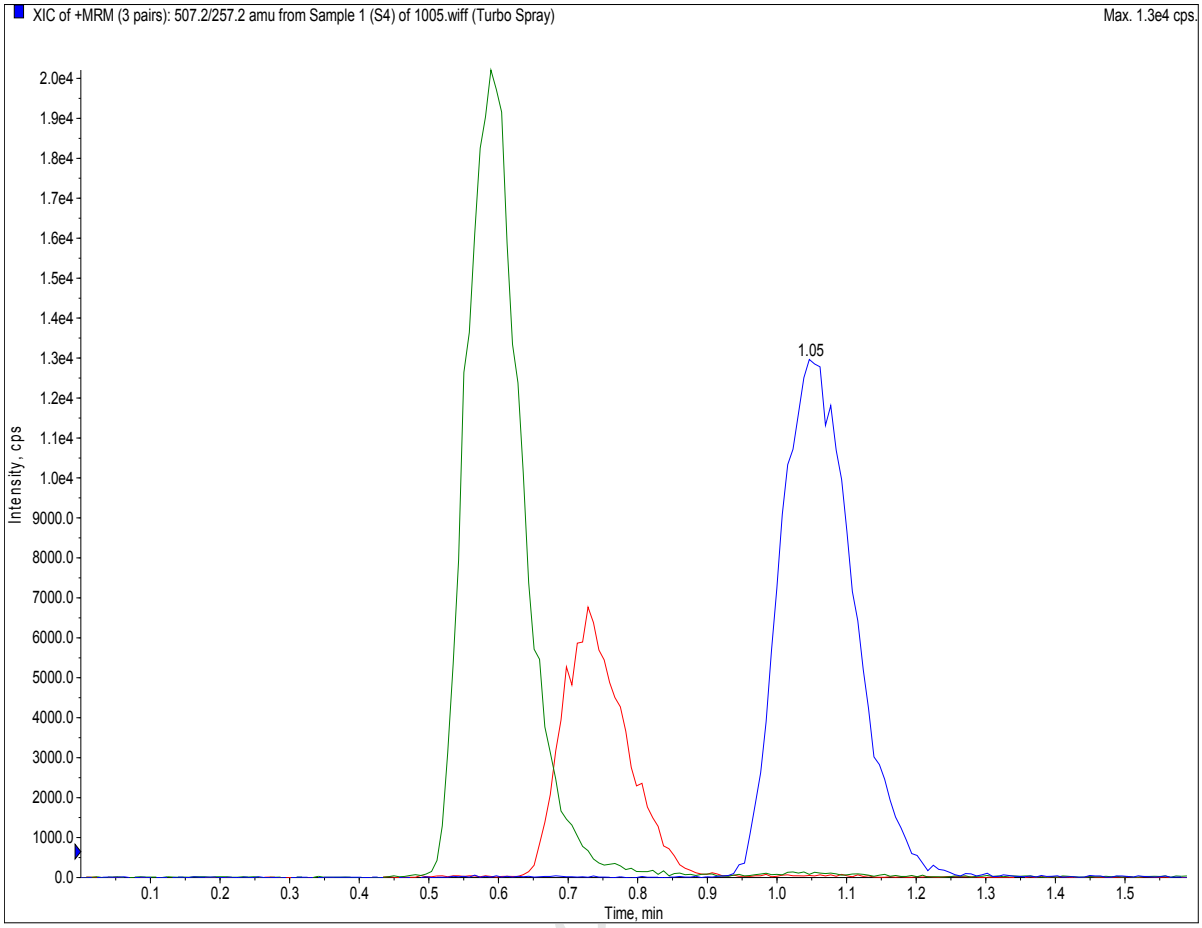

Figure 126 LC-MS/MS chromatogram of 9-O-acetylhydnocarpin, the hydrolysed product and the internal standard

12.7.5.3 Extraction

A more robust liquid-liquid extraction method was developed. Sodium carbonate buffer (50 µl, 0.1 M, pH 10.2) was pipetted into 1.5 ml polypropylene eppendorf tubes and blood samples (10 µl) were added to the buffer (on ice). Ethyl acetate (250 µl) was added and the samples vortexed for 20 seconds and centrifuged at 1300 G for 5 minute. The internal standard was spiked into the organic solvent to obtain a concentration of 1 µg/ml. The organic phase was transferred to clean glass inserts and evaporated by making use of a cold trap under vacuum conditions at 30 °C. The dried samples were reconstituted with mobile phase (100 µl), vortexed for 10 seconds, and 5 µl was injected onto the HPLC column.

12.7.5.4 Preparation of calibration standards

Whole blood was collected and cooled on ice before spiking with reference standards to prevent hydrolysis by the esterase enzymes. A stock solution with a concentration of 1 mg/ml for both 9-O-acetylhydnocarpin and the hydrolysed product was prepared in DMSO. A pool of blank whole blood was spiked with the stock solution to obtain a standard with a concentration of 10 µg/ml for both compounds. This standard was serially diluted with blank whole blood to attain standards with the following concentrations: 5, 2.5, 1.25, 0.625, 0.313, 0.156 and 0.078 µg/ml. The calibration standards were aliquoted into polypropylene tubes and stored at approximately -20°C.

12.7.6 Bioavailability study of 9-O-acetylhydnocarpin and its hydrolysed product in mice using a self-microemulsifying drug delivery system

12.7.6.1 Experimental design

9-O-Acetylhydnocarpin was formulated as described Wu and co-workers [Wu *et al*., 2006]. The compositions of the formulation substances are presented in table 44.

Table 44 SMEDDS formulation

Formulation agents	Composition (%)	Mass (mg)
9-O-acetylhydnocarpin	8.5	50
Ethanol	9.2	53.6
Tween® 80	54.9	321.3
Ethyl linoleate	27.4	161

9-O-Acetylhydnocarpin was purified with HPLC as described in Chapter 4 (HPLC purity above 99%). Ethanol was purchased from Merck® (purity > 99.9%, HPLC grade), Tween® 80 was purchased from Aldrich® (lab grade) and ethyl linoleate was purchased from Sigma® (99% pure).

12.8 Metabolite study of 9-O-acetylhydnocarpin in mice

12.8.1 Sample preparation

12.8.1.1 Blood samples

The parent compound is quickly absorbed from the gastrointestinal tract and blood levels could be detected 30 minutes after dosage (Chapter 8). Metabolites should also be present in the blood soon after the parent compound is present; therefore blood samples (50 µl) were collected at 0.5 h, 1h and 2 hours after administration by cutting the tip of the tail.

The extraction method that was previously used, for extraction of 9-O-acetylhydnocarpin and the hydrolysed product, was designed to selectively extract these two compounds from mice blood. Metabolites are often more polar than their parent compounds and may not extract into the organic phase as was used previously. For that reason it was decided to use a simple protein precipitation method to extract the compounds of interest from the mice blood.

The combined blood sample (100 µl) was pipetted into a 1.5 ml polypropylene eppendorf tube and acetonitrile (300 µl) was added. The sample was vortexed for 1 minute and centrifuged at 1300 G for 5 minutes. The supernatant was transferred to a clean eppendorf tube and 100 µl of a 0.1% formic acid solution was added. The sample was briefly vortexed and stored at – 70 °C until analysed. A control sample (blood sample just before drug was administered) was also prepared using the same extraction method as described above.

12.8.1.2 Urine samples

Urine samples were collected over a period of 6 hours. The combined sample was diluted (50x) with a mixture of acetonitrile and 0.1% formic acid (1:1, v/v). The sample was briefly vortexed and stored at – 70 °C until analysed. A control sample (urine sample just before drug was administered) was also prepared using the same methodology as described above.

12.8.1.3 Faeces samples

Faeces samples were collected over a period of 12 hours. The combined sample was placed in a small glass beaker and 20 ml acetonitrile was added. The mixture was stirred on a magnetic stirrer for 10 minutes. The extract was filtered using paper filters (Whatmann® no. 3) and dried under a gentle stream of nitrogen gas. The sample was stored at – 70 °C until analysed. Before analysis, the extract was dissolved in 10 ml of acetonitrile and diluted 50 times with a mixture of acetonitrile and 0.1% formic acid (1:1, v/v). A control sample (faeces sample just before drug was administered) was also prepared using the same methodology as described above.

12.8.2 LC-MS analysis

The mass spectrometer was set in the LC-MS mode. Q1 was set to scan between 400 and 900. This range would cover the molecular ions of all the potential phase I and II metabolites.

The mass spectrometer was coupled in tandem with an Agilent 1200 series HPLC system. A Phenomenex® C_{18} (15 cm x 4.6 mm, 5 µm) column was used to separate the compounds of interest. The column was kept at 20 °C in a column oven. A gradient system (table 45) at a flow rate of 0.3 ml/min was used to separate the metabolites. The injection volume was 10 µl. The analysis of the study samples was performed in the positive ion mode and the settings on the mass spectrometer are summarised in table 46.

Table 45 HPLC gradient of LC-MS experiment

Time (min)	% acetonitrile	% water
0	5	95
15	95	5
16	5	95
25	5	95

Table 46 Mass spectrometer settings

Ion source gas 1 (arbitrary value)	50
Ion source gas 2 (arbitrary value)	50
Curtain gas (arbitrary value)	20
Source temperature (°C)	400
Ionspray voltage (V)	4500
Resolution	unit
Scan time (sec)	2
Declustering potential (V)	71
Entrance potential (V)	10
Scan type	Q1 MS
Polarity	positive

12.8.3 Precursor ion scan analysis

The mass spectrometer was set in the precursor ion mode and Q3 was set to stabilise the most abundant product ion of 9-O-acetylhydnocarpin, which was 257. Q1 was set to scan between 400 and 900. This range would cover all the potential phase 1 and 2 metabolites. The same HPLC gradient system that was used for LC-MS analysis was also used for precursor ion scan analysis (12.8.2). The injection volume was 10 µl. The analysis of the study samples was performed in the positive ion mode and the settings on the mass spectrometer are summarised in table 47.

Table 47 Mass spectrometer settings

Ion source gas 1 (arbitrary value)	50
Ion source gas 2 (arbitrary value)	50
Curtain gas (arbitrary value)	20
Collision gas (arbitrary value)	5
Source temperature (°C)	400
Ionspray voltage (V)	4500
Resolution	unit
Scan time (sec)	2
Declustering potential (V)	71
Entrance potential (V)	10
Collision cell entrance potential (V)	22
Collision energy (eV)	50
Collision cell exit potential (V)	3
Scan type	precursor
Polarity	positive

12.8.4 Neutral loss scan analysis

The mass spectrometer was set in the neutral loss mode to search for potential glucuronidated metabolites. The mass shift between Q3 and Q1 was set at 176. The same HPLC gradient system that was used for LC-MS analysis was also used for neutral loss analysis (12.8.2). The injection volume was 10 µl. The analysis of the study samples was performed in the positive ion mode and the settings on the mass spectrometer are summarised in table 48.

Table 48 Mass spectrometer settings

Ion source gas 1 (arbitrary value)	50
Ion source gas 2 (arbitrary value)	50
Curtain gas (arbitrary value)	20
Source temperature (°C)	400
Ionspray voltage (V)	4500
Resolution	unit
Scan time (sec)	2
Declustering potential (V)	71
Entrance potential (V)	10
Collision cell entrance potential (V)	22
Collision energy (eV)	50
Collision cell exit potential (V)	3
Collision activated dissociation gas	medium
Scan type	Neutral loss
Polarity	positive

12.8.5 LC-MS/MS analysis

The mass spectrometer was set in the LC-MS/MS mode. Q1 was set to stabilise the molecular ions of the potential metabolites described above. Q3 was set to scan between 50 and the mass of the molecular ion minus about 10 mass units. This range would cover the product ions of the potential phase I and II metabolites.

The same HPLC gradient system that was used for LC-MS analysis was also used for LC-MS/MS analysis (12.8.2). The injection volume was 10 µl. The analysis of the study samples was performed in the positive ion mode and the settings on the mass spectrometer are summarised in table 49.

Table 49 Mass spectrometer settings

Ion source gas 1 (arbitrary value)	50
Ion source gas 2 (arbitrary value)	50
Curtain gas (arbitrary value)	20
Collision gas (arbitrary value)	5
Source temperature (°C)	400
Ionspray voltage (V)	4500
Resolution	unit
Scan time (sec)	2
Declustering potential (V)	71
Entrance potential (V)	10
Collision cell entrance potential (V)	25
Collision energy (eV)	50
Collision cell exit potential (V)	3
Scan type	MS/MS
Polarity	positive

12.9 Antimalarial assessment of 9-O-acetylhydnocarpin in mice

12.9.1 Mice

Mice (male, 12 to 16 weeks old, C57BL6) were obtained from the University of Cape Town's Animal Unit and kept at the animal laboratory of the liver research group (Groote Schuur Hospital, Old main building, level K). A group of 3 mice were used for each experiment.

12.9.2 Animal model

P. berghei Anka (PbA, Swiss Tropical Institute, Basle) malaria parasites, which is a highly chloroquine sensitive strain, were used to infect the study animals. The parasites, kept in liquid nitrogen, were thawed and passaged intra-peritoneally to donor mice [Rudin *et al*., 1997; Gumede *et al*., 2003]. Parasite infected erythrocytes were collected after 5 days into heparinized tubes by tail bleeding. The parasitaemia was determined using Giemsa stained thin blood smears. Parasitised erythrocytes (1×10^6 per 0.2 ml of saline) were injected intra-peritoneally into the test animals [Gumede, 2003].

BIBLIOGRAPHY

Akerele O (1993)
Nature's medicinal bounty: don't throw it away
World health forum, **14(4)**, 390-395

Alikaridis F, Papadakis D, Pantelia K and Kephalas T (2000)
Flavonolignan production from *Silybum marianum* transformed and untransformed root cultures
Fitoterapia, **71**, 379-384

Andersson L (1998)
A revision of the genus *Cinchona* (Rubiaceae-Cinchoneae)
Memoirs of the New York Botanical Garden, **80**, 25-67

Antus S, Seligmann O and Wagner H (1982)
Structural elucidation of the flavonolignans hydnocarpin and silandrin by partial synthesis
Studies in Organic Chemistry, **11**, 147-151

Anupongsanugool E, Teekachunhatean S, Rojanasthien N, Pongsatha S and Sangdee C (2005)
Pharmacokinetics of isoflavones, daidzein and genistein, after ingestion of soy beverage compared with soy extract capsules in postmenopausal Thai women
BMC Clinical Pharmacology, **5(2)**, 1-10

Applied Biosystems MDS Sciex
Identification of phase I and phase II metabolites of Buspirone on the Q TRAP™ LC/MS/MS system
http://www.biocompare.com/technicalarticle/1364/Identification-Of-Phase-I-And-Phase-II-Metabolites-Of-Buspirone-On-The-Q-TRAP(tm)-LC-MSMS-System-from-Applied-Biosystems-47MDS-Sciex.html

Arnold TH and De Wet BC (1993)
Plants of Southern Africa: Names and distribution
Memoirs of the Botanical Survey of South Africa **No. 62**, Pretoria, p 168

Austin JC, du Toit D, Fraser N, Lloyd P, Mansfield D, Macleod A, Odendaal JSJ and Seier J (2004)
Guidelines on Ethics for Medical Research: Use of Animals in Research and Training
South African Medical Research Council

Baker JT, Borris RP, Carté B, Cordell GA, Soejarto DD, Cragg GM, Gupta MP, Iwu MM, Madulid DR and Tyler VE (1995)
Natural product drug discovery and development: new perspectives on international collaboration
Journal of Natural Products, **58(9)**, 1325-57

Basco LK, Ringwald P, Franetich JF and Mazier D (1999)
Assessment of pyronaridine activity *in vivo* and *in vitro* against the hepatic stages of malaria in laboratory mice
Transactions of the Royal Society of Tropical Medicine and Hygiene, **93**, 651-652

Boersma MG, van der Woude H, Bogaards J, Boeren S, Vervoort J, Cnubben NHP, van Iersel MLPS, Bladeren PJ and Rietjens IMCM (2002)
Regioselectivity of phase II metabolism of luteolin and quercetin by UDP-glucuronosyl transferases
Chemical Research in Toxicology, **15(5)**, 662-670

Botha R
Photograph of *X. retinervis* on title page
http://ecoport.org/

Boudreau EF, Webster HK, Pavanand K and Thosingha L (1982)
Type II mefloquine resistance in Thailand
Lancet, **2(8311)**, 1335

Brandt A and Kueppers S (2002)
Practical aspects of preparative HPLC in pharmaceutical and development production
LC-GC, Europe, 2-5

Bremen J (2001)
The ears of the hippopotamus: manifestations, determinants, and estimates of the malaria burden
The American Journal of Tropical Medicine and Hygiene, **64(1,2)**, 1-11

Bruce-Chwatt LJ (1982)
Qinghaosu: a new antimalarial
British Medical Journal, **284**, 767-768

Bryant MS, Korfmacher WA, Wang S, Nardo C, Nomeir AA and Lin CC (1997)
Pharmacokinetic screening for the selection of new drug discovery candidates is greatly enhanced through the use of liquid chromatography-atmospheric pressure ionization tandem mass spectrometry
Journal of Chromatography A, **777**, 61-66

Chen D (1997)
Phytochemical studies on traditional medicinal plants with antimalarial activities
Masters Thesis in Chemistry at the University of Cape Town
97-121

Choi JS, Choi HK and Shin SC (2004)
Enhanced bioavailability of paclitaxel after oral coadministration with flavone in rats
International Journal of Pharmaceutics, **275**, 165-170

Chu D, Liu W, Huang Z, Liu S, Fu X and Liu K (2006)
Pharmacokinetics and Excretion of Hydroxysafflor Yello A, a Potent Neuroprotective Agent from Safflower, in Rats and Dogs
Planta Medica, **72**, 418-423

Chukwujekwu JC, Smith PJ, Coombes PH, Mulholland DA and Van Staden J (2005)
Antiplasmodial diterpenoid from the leaves of *Hyptis suaveolens*
Journal of Ethnopharmacology, **102**, 295-297

Clarke NJ, Rindgen D, Korfmacher WA and Cox KA (2001)
A four step strategy to characterize metabolites by LC/MS techniques early in the pharmaceutical discovery process - systematic LC/MS metabolite identification in drug discovery
Analytical Chemistry, American Chemical Society, 430 A - 439 A
http://www.forumsci.co.il/HPLC/MetaboliteID_LC-MS-MS.pdf

Clarkson C (2002)
Isolation and characterization of two antiplasmodial diterpenes from *Harpagophytum procumbens* (Devil's Claw) and chemical modification of a related analogue
PhD thesis

Clarkson C, Campbell WE and Smith PJ (2003)
In vitro anitplasmodial activity of abietane and totarane diterpenes isolated from Harpagophytum procumbens (Devil's Claw)
Planta Medica, **69**, 720-724

Clarkson C, Maharaj VJ, Crouch NR, Grace OM, Pillay P, Matsabisa MG, Bhagwandin N, Smith PJ and Folb PI (2004)
In vitro anitplasmodial activity of medicinal plants native to or naturalized in South Africa
Journal of Ethnopharmacology, **92**, 177–191

Clayden J, Greeves N, Warren S and Wothers P (2004)
Determining organic structures
Organic chemistry, 47-79

Cocks M and Moller V (2002)
Use of indigenous and indigenised medicines to enhance personal well-being: A South African case study
Social Science and Medicine, **54**, 387-397

Coetzee C, Jefthas E and Reinten E (1999)
Indigenous plant genetic resources of South Africa
Perspectives on new crops and new uses
J. Janick (ed.), ASHS Press, Alexandria, VA
http://www.hort.purdue.edu/newcrop/proceedings1999/v4-160.html#references

Cogswell FB (1992)
The hypnozoite and relapse in primate malaria
Clinical Microbiological Reviews, **5(1)**, 26-35

Cragg G and Newman D (2001)
Nature's bounty
Chemistry in Britain, **37(1)**, 22-26

Creasey WA (1979)
Drug Disposition in Humans – The Basis of Clinical Pharmacology
Oxford University Press, New York

Curry SH (1977)
Drug disposition and pharmacokinetics
Blackwell Scientific Publications, Oxford London Edinburgh Melbourne

Davis-Searles PR, Nakanishi Y, Kim NC, Graf TN, Oberlies NH, Wani MC, Wall ME, Agarwal R and Kroll DJ (2005)
Milk thistle and Prostate Cancer: Differential effects of pure flavonolignans from *Silybum marianum* on antiproliferative end points in human prostate carcinoma cells
Cancer Research, **65**, 4448-4457

De Monbrison F, Maitrejean M, Latour C, Bugnazet F, Peyron F, Barron D and Picot S (2006)
In vitro antimalarial activity of flavonoid derivatives dehydrosilybin and 8-(1,1)-DMA - kaempferide
Acta Tropica, **97**, 102-107

Department of Health, South Africa (2007)
Malaria
http://www.doh.gov.za/search/index.html

de Mesquita ML, Grellier P, Mambu L, de Paula JE and Espindola LS (2007)
In vitro antiplasmodial activity of Brazilian Cerrado plants used as traditional remedies
Journal of Ethnopharmacology, **110**, 165-170

De Smet PA (1997)
The role of plant derived drugs and herbal medicines in healthcare
Drugs, **54(6)**, 801-840

De Wet T (1998)
Muti Wenyoni: commodification of an African folk medicine
South African Journal of Ethnology, **21**, 165-172

Doumbo OK, Kayentao K, Djimde A, Cortese JF, Diourte Y, Konare A, Kublin JG and Plowe CV (2000)
Rapid selection of *Plasmodium falciparum* dihydrofolate reductase mutants by pyrimethamine prophylaxis
Journal of Infectious Diseases, **182(3)**, 993-996

DuPont MS, Day AJ, Bennett RN, Mellon FA and Kroon PA (2004)
Absorption of kaempferol from endive, a source of kaempferol-3-glucuronide, in humans
Nature, **58(6)**, 947-954

Dvorak Z, Kosina P, Walterova D, Simanek V, Bachleda P and Ulrichova J (2003)
Primary cultures of human hepatocytes as a tool in cytotoxicity studies: cell protection against model toxins by flavonolignans obtained from *Silybum marianum*
Toxicology Letters, **137**, 201-212

Edwards SD (1986)
Traditional and modern medicine in South Africa: A research study
Social Science and Medicine, **22(11)**, 1273-1276

Ekong RM, Robson KJH, Baker DA and Warhurst DC (1993)
Transcripts of the multidrug resistance genes in chloroquine-sensitive and chloroquine-resistant *Plasmodium falciparum*
Parasitology, **106**, 107-115

Engers HD and Godal T (1998)
Malaria vaccine development: current status
Parasitology Today, **14(2)**, 56-64

Farnsworth NR (1984)
The role of medicinal plants in *drug development*
Natural products and drug development, Baillière, Tindal and Cox, London, 8-98

Farnsworth NR (1990)
The role of ethnopharmacology in drug development
Ciba Foundation Symposium, 154(Bioact. Compd. Plants), 2-21

Faye FBK, Konaté L, Rogier C and Trape JF (1998)
Plasmodium ovale in a highly malaria endemic area of Senegal
Transactions of the Royal Society of Tropical Medicine and Hygiene, **92**, 522-525

Feng WY, Chan KK and Covey JM (2002)
Electrospray LC-MS/MS quantitation, stability, and preliminary pharmacokinetics of bradykinin antagonist polypeptide B201 (NSC 710295) in the mouse
Journal of Pharmaceutical and Biomedical Analysis, **28**, 601-612

Ferreira JFS, Simon JE and Janick J (1997)
Artemisia annua: botany, horticulture, pharmacology
Horticultural Reviews, **19**, 319-371

Fischer DCH, de Amorim Gualda NC, Bachiega D, Carvalho CS, Lupo FN, Bonotto SV, de Oliveira Alves M, Yogi A, Santi SMD, Avila PE, Kirchgatter K and Moreno PRH (2004)

In vitro screening for antiplasmodial activity of isoquinoline alkaloids from Brazilian plant species

Acta Tropica, **92**, 261-266

Flora K, Hahn M, Rosen H and Benner K (1998)

Milk thistle (*Silybum marianum*) for the therapy of liver disease

American Journal of Gastroenterology, **93(2)**, 139-143

Galeffi C, Rasoanaivo P, Federici E, Pallazino G, Nicoletti M and Rasolondratovo B (1997)

Two prenylated isoflavanones from *Millettia pervilleana*

Phytochemistry, **45**, 189-192

Gangl E, Utkin I, Gerber N and Vouros P (2002)

Structural elucidation of metabolites of ritonavir and indinavir by liquid chromatography-mass spectroscopy

Journal of Chromatography A, **974(1-2)**, 91-101

Gessler MC, Nkunya MH, Mwasumbi LB, Heinrich M and Tanner M (1994)

Screening Tanzanian medicinal plants for antimalarial activity

Acta Tropica, **56(1)**, 65-77

Glue P and Clement RP (1999)

Cytochrome P450 enzymes and drug metabolism – basic concepts and methods of assessment

Cellular and Molecular Neurobiology, **19(3)**, 309-323

Grobler A, Kotze A and du Plessis J
The design of a skin-friendly carrier for cosmetic compounds using pheroid technology
Department of Pharmaceutics, School of Pharmacy, North-West University, Potchefstroom, South Africa
Research manuscript, 1-42

Guidance for Industry (2001)
Bioanalytical method validation
U.S. Department of Health and Human Services
Food and Drug Administration

Guidance for Industry (2007)
Malaria: Developing drug and nonvaccine biological products for treatment and prophylaxis, 1-29
http://www.fda.gov/cder/guidance/index.htm

Gumede B (2003)
A study of the immune response in murine experimental malaria, with special reference to the effects of South African medicinal plants, artesunate and chloroquine
PhD thesis

Gumede B, Folb P and Ryffel B (2003)
Oral artesunate prevents *Plasmodium berghei* Anka infection in mice
Parasitology International, **52**, 53-59

Han M, Sha X, Wu Y and Fang X (2005)
Oral absorption of Ginsenoside Rb_1 using *in vitro* and *in vivo* models
Planta Medica, **71**, 398-404

Harborne JB, Mabry TJ and Mabry H (1975)
The Flavonoids
Chapman and Hall, London

Haefelfinger P (1981)
Limits of the internal standard technique in chromatography
Journal of Chromatography, **218**, 73-81

Hien TT and White NJ (1993)
Qinghaosu
The Lancet, **341(8845)**, 603-608

Herrera S, Perlaza BL, Bonelo A and Arévalo-Herrera M (2002)
Aotus monkeys: their great value for anti-malarial vaccines and drug testing
International Journal for Parasitology, **32**, 1625-1635

Hite M, Turner S and Federici C (2003)
Oral delivery of poorly soluble drugs
Pharmaceutical Manufacturing and Packing Soucer, part 1 & 2

Hogh B, Gamage-Mendis A, Butcher GA, Thompson R, Begtrup K, Mendis C, Enosse SM, Dgedge M, Barreto J, Eling W and Sinden RE (1998)
The differing impact of chloroquine and pyrimethamine/sulfadoxine upon the infectivity of malaria species to the mosquito vector
American Journal of Tropical Medicine and Hygiene, **58(2)**, 176-182

Houghton PJ and Raman A (1998)
Laboratory handbook for the fractionation of natural products
Kluwer Academic Publishers Group

Husoy T, Syversen T and Jenssen J (1993)
Comparison of four *in vitro* cytotoxicity tests: the MTT assay, NR assay, uridine incorporation and protein measurements
Toxicity in Vitro, **7(2)**, 149-154

Hutchings A, Scott AH, Lewis G and Cunningham A
Zulu Medicinal Plants
University of Natal Press, Pietermaritzburg, South Africa

Jia L, Tomaszewski JE, Noker PE, Gorman GS, Glaze E and Protopopova M (2005)
Simultaneous estimation of pharmacokinetic properties in mice of three anti-tubercular ethambutol analogs obtained from combinatorial lead optimization
Journal of Pharmaceutical and Biomedical analysis, **37**, 793-799

Johns Hopkins Bloomberg School of Public Health
Background Information on Malaria
http://www.jhsph.edu/Malaria/Malaria_Background.html#History

Kale R (1995)
Traditional healers in South Africa: a parallel health care system
British Medical Journal, **310**, 1182-1185

Kamchonwongpaisan S and Meshnick SR (1996)
The Mode of Action of the Antimalarial Artemisinin and its Derivatives
General Pharmacology, **27(4)**, 587-592

Kanokmedhakul K, Kanokmedhakul S and Phatchana R (2005)
Biological activity of Anthraquinones and Triterpenoids from *Prismatomeris fragrans*
Journal of Ethnopharmacology, **100,** 284-288

Karle JM and Bhattacharjee AK (1999)
Stereoelectronic features of the cinchona alkaloids determine their differential antimalarial activity
Bioorganic & Medicinal Chemistry, **7**, 1769-1774

Katzung BG (2004)
Basic and Clinical Pharmacology, Ninth Edition
Lange Medical books/McGraw-Hill Medical Publishing Division

Kettler HE and Marjanovic S (2004)
Engaging biotechnology companies in the development of innovative solutions for diseases and poverty
Nature Reviews Drug Discovery, **3**, 171-176

Kofoed PE, Lopes F, Johansson P, Dias F, Sandström A, Aaby P and Rombo L (1999)
Low-dose quinine for treatment of *Plasmodium falciparum* malaria in Guinea-Bissau
Transactions of the Royal Society of Tropical Medicine and Hygiene, **93**, 547-549

Kofoed PE, Có F, Poulsen A, Cabral C, Hedegaard K, Aaby P and Rombo L (2002)
Treatment of *Plasmodium falciparum* malaria with quinine in children in Guinea-Bissau: one daily dose is sufficient
Transactions of the Royal Society of Tropical Medicine and Hygiene, **96**, 185-188

Kremsner PG and Krishna S (2004)
Antimalarial combinations
Lancet, **364**, 285-294

Kren V, Kubisch, J, Sedmera P, Halada, P, Prikrylova V, Jegorov A, Cvak L, Gebhardt R, Ulrichova J and Simanek V (1997)
Glycosylation of silybin
Journal of the Chemical Society, Perkin Transactions 1, **1**, 2467-2474

Kren V, Ulrichova J, Kosina P, Stevenson D, Sedmera P, Prikrylova V, Halada P and Simanek V (2000)
Chemoenzymatic preparation of silybin β-Glucuronides and their biological evaluation
Drug Metabolism and Disposition, **28(12)**, 1513-1517

Kren V and Walterova D (2005)
Silybin and silymarin – new effects and applications
Biomedical Papers, **149(1)**, 29-41

Krishna S, Uhlemann AC and Haynes RK (2004)
Artemisinins: mechanisms of action and potential for resistance
Drug Resistance Updates, **7(4-5)**, 233-244

Kuentz M, Nick S, Parrott N and Röthlisberger D (2006)
A strategy for preclinical formulation development using GastroPlus™ as pharmacokinetic simulation tool and a statistical screening design applied to a dog study
European Journal of Pharmaceutical sciences, **27**, 91-99

Kumar RA and Clark DS (2006)
High-throughput screening of biocatalytic activity: applications in drug discovery
Chemical Biology, **10**, 162-168

Kvasnicka F, Biba B, Sevcik R, Voldrich M and Kratka J (2003)
Analysis of the active components of silymarin
Journal of Chromatography A, **990**, 239-245

Lambros C and Vanderberg JP (1979)
Synchronization of *Plasmodium falciparum* erythrocytic stages in culture
The Journal of Parasitology, **65(3)**, 418-420

Leaman DJ, Arnason JT, Yusuf R, Sangat-Roemantyo H, Soedjito H, Angerhofer CK and Pezzuto JM (1995)
Malaria remedies of the Kenyah of the Apo Kayan, East Kalimantan, Indonesian Borneo: a quantitative assessment of local consensus as an indicator of biological efficacy
Journal of Ethnopharmacology, **49**, 1-16

Life cycle of the malaria parasite
http://encarta.msn.com/media_461541582/Life_Cycle_of_the_Malaria_Parasite.html

Lobel HO, Varma JK, Miani M, Green M, Todd GD, Grady K and Barber AM (1998)
Monitoring for mefloquine-resistant *Plasmodium falciparum* in Africa: implications for travelers' health
The American Journal of Tropical Medicine and Hygiene, **59(1)**, 129-132

Lu C, Lu Y, Chen J, Zhang W and Wu W (2007)
Synchronized and sustained release of multiple components in silymarin from erodible glyceryl monostearate matrix system
European Journal of Pharmaceutics and Biopharmaceutics, **66**, 210-219

Mackie C, Wuyts K, Haseldonckx M, Blokland S, Gysemberg P, Verhoeven I, Timmerman P and Nijsen M (2005)
New model for intravenous drug administration and blood sampling in the awake rat, designed to increase quality and throughput for *in vivo* pharmacokinetic analysis
Journal of Pharmacological and Toxicological methods, **52**, 293-301

Makler MT, Ries JM, Williams JA, Bancroft JE, Piper RC, Gibbins BL and Hinrichs DJ (1993)
Parasite lactate dehydrogenase as an assay for *Plasmodium falciparum* drug sensitivity
American Journal of Tropical Medicine and Hygiene, **48(6)**, 739-741

Mander M, Mander J, Crouch N, Mckean S and Nichols G (1995)
Catchment action: Growing and knowing muthi plants
Share Net Resource, Howick, South Africa

Mander M (1998)
Marketing of indigenous medicinal plants in South Africa: A case study in KwaZulu-Natal
FAO of the UN. Rome

Marussig M, Motard A, Renia L, Baccam D, Lebras J, Charmot *G* and Mazier D (1993)
Activity of doxycycline against preerythrocytic malaria
The Journal of Infectious Diseases, **168**, 1603-1604

Mazier D, Landau I, Druilhe P, Miltgen F, Guguen-Guillouzo C, Baccam D, Baxter J, Chigot JP and Gentilini M (1984)
Cultivation of the liver forms of *Plasmodium vivax* in human hepatocytes
Nature, **307(5949)**, 367-369

Mazier D, Beaudoin RL, Mellouk S, Druilhe P, Texier B, Trosper J, Miltgen F, Landau I, Paul C, Brandicourt O, Guguen-Guillouzo C and Langlois P (1985)
Complete development of hepatic stages of *Plasmodium falciparum in vitro*
Science, **227(4685)**, 440-442

Medical Research Council, South Africa
Malaria Research Programme: Malaria in South Africa
http://www.malaria.org.za

Medicines for malaria venture
Annual report, 2006
http://www.mmv.org/filesupld/53.pdf

Mehlotra RK, Fujioka H, Roepe PD, Janneh O, Ursos LMB, Jacobs-Lorena V, McNamara DT, Bockarie MJ, Kazura JW, Kyle DE, Fidock DA and Zimmerman PA (2001)
Evolution of a unique *Plasmodium falciparum* chloroquine-resistance phenotype in association with pfcrt polymorphism in Papua New Guinea and South America
Proceedings of the National Academy of Sciences of the United States of America, **98(22)**, 12689-12694

Mendis K, Sina BJ, Marchesini P and Carter R (2001)
The neglected burden of *Plasmodium vivax* malaria
American Journal of Tropical Medicine and Hygiene, **64(1-2)**, 97-106

Meshnick SR (1994)
The mode of action of antimalarial endoperoxides
Transactions of the Royal Society of Tropical Medicine and Hygiene, **88(1)**, 31-32

Miliauskas G, van Beek TA, de Waard P, Venskutonis RP and Sudhölter EJR (2006)
Comparison of analytical and semi-preparative columns for high-performance liquid chromatography-solid-phase extraction-nuclear magnetic resonance
Journal of Chromatography A, **1112**, 276-284

Miller LH, Mason SJ, Clyde DF and McGinniss MH (1976)
The resistance factor to *Plasmodium vivax* in blacks. The Duffy-blood-group genotype, FyFy
The New England Journal of Medicine, **295(6)**, 302-304

Moon BH, Lee Y, Shin C and Lim Y (2005)
Complete assignments of the ^{1}H and ^{13}C NMR data of flavone derivatives
Bulletin of the Korean Chemical Society, **26(4)**, 603-608

Morazzoni P, Montalbetti A, Malandrino S and Pifferi G (1993)
Comparative pharmacokinetics of silipide and silymarin in rats
European Journal of Drug Metabolism and Pharmacokinetics, **18(3)**, 289-297

Morazzoni P and Bombardelli E (1995)
Silybum marianum (Carduus marianus)
Fitoterapia, **66(1)**, 3-42

Mosmann T (1983)
Rapid colorimetric assay for cellular growth and survival: application to proliferation and cytotoxicity assays
Journal of Immunological Methods, **65(1-2)**, 55-63

Mpia B and Pépin J (2002)
Combination of eflornithine and melarsoprol for melarsoprol-resistant Gambian trypanosomiasis
Tropical Medicine & International Health, **7(9)**, 775-779

Muanza K, Gay F, Behr C and Scherf A (1996)
Primary culture of human lung microvessel endothelial cells: a useful *in vitro* model for studying *Plasmodium falciparum*-infected erythrocyte cytoadherence
Research in Immunology, **147**, 149-163

Munoz V, Sauvain M, Bourdy G, Callapa J, Bergeron S, Rojas I, Bravo JA, Balderrama L, Ortiz B, Gimenez A and Deharo E (2000)
A search for natural bioactive compounds in Bolivia through a multidisciplinary approach Part I. Evaluation of the antimalarial activity of plants used by the Chacobo Indians
Journal of Ethnopharmacology, **69**, 127-137

Muthaura CN, Rukunga GM, Chhabra CS, Omar SA, Guantai AN, Gathirwa JW, Tolo FM, Mwitari PG, Keter LK, Kirira PG, Kimani CW, Mungai GM and Njagi ENM (2007)
Antimalarial activity of some plants traditionally used in treatment of malaria in Kwale district of Kenya
Journal of Ethnopharmacology, **112**, 545-551

Newman DJ, Cragg GM and Snader KM (2003)
Natural products as sources of new drugs over the period 1981-2002
Journal of Natural Products, **66**, 1022-1037

Newman DJ and Cragg GM (2007)
Natural Products as Sources of New Drugs over the Last 25 Years
Journal of Natural Products, **70(3)**, 461-477

Nsimba B, Malonga DA, Mouata AM, Louya F, Kiori J, Malanda M, Yocka D, Oko-Ossho J, Ebata-Mongo S and Le Bras J (2004)
Efficacy of sulfadoxine/pyrimethamine in the treatment of uncomplicated *Plasmodium falciparum* malaria in Republic of Congo
American Journal of Tropical Medicine and Hygiene, **70(2)**, 133-138

Nwaka S and Ridley RG (2003)
Virtual drug discovery and development for neglected diseases through public-private partnerships
Nature Reviews Drug Discovery, **2**, 919-928

Nussenzweig RS and Nussenzweig V (1989)
Antisporozoite vaccine for malaria: experimental basis and current status
Rev. Infect. Dis., **11(3)**, 579-585

Oaks SC, Mitchell VS, Pearson GW and Carpenter CCJ (1991)
Malaria: obstacles and opportunities
NATIONAL ACADEMY PRESS, Washington, D.C.
http://books.nap.edu/openbook.php?isbn=0309045274

Ojo-Amaize EA, Nchekwube EJ, Cottam HB, Oyemade OA, Adesomoju AA and Okogun JI (2007)
Plasmodium berghei: Antiparasitic effects of orally administered Hypoestoxide in mice
Experimental Parasitology, **117**, 218-221

Olliaro PL and Goldberg DE (1995)
The *Plasmodium* digestive vacuole: metabolic headquarters and choice drug target
Parasitology today, **11(8)**, 294-297

Otshudi AL, Apers S, Pieters L, Claeys M, Pannecouque C, De Clercq E, Van Zeebroeck A, Lauwers S, Frédérich M and Foriers A (2005)
Biologically active bisbenzylisoquinoline alkaloids from the root bark of *Epinetrum villosum*
Journal of Ethnopharmacology, **102**, 89-94

Park Y, Lee YU, Kim H, Lee Y, Yoon YA, Moon B, Chong Y, Ahn JH, Shim YH and Lim Y (2006)
NMR data of flavone derivatives and their anti-oxidative activities
Bulletin of the Korean Chemical Society, **27(10)**, 1537-1541

Peters W, Portus JH and Robinson BL (1975)
The chemotheraphy of rodent malaria, XXII. The value of drug resistant strains of *P. berghei* in screening for blood schizontocidal activity
Ann. Trop. Med. Parasitol., **69**, 155-171

Peters W, Robinson BL, Tovey G, Rossier JC and Jefford CW (1993)
The chemotherapy of rodent malaria. The activities of some synthetic 1,2,4-trioxanes against chloroquine-sensitive and chloroquine-resistant parasites. Part 3: Observations on 'Fenozan-50F', a difluorinated 3,3′-spirocyclopentane 1,2,4-trioxane
Annals of Tropical Medicine and Parasitology, **87(2)**, 111-123

Petushkova NA, Kanaeva IP, Lisitsa AV, Sheremetyeva GF, Zgoda VG, Samenkova NF, Karuzina II and Archakov AI (2006)
Characterization of human liver cytochromes P450 by combining the biochemical and proteomic approaches
Toxicology in Vitro, **20**, 966-974

Pharmacology of Silymarin
Clinical drug investigation
Pharmacokinetics
http://www.medscape.com/viewarticle/422884_3

Phillipson JD (1994)
Natural products as drugs
Transactions of the Royal Society of Tropical Medicine and Hygiene, **88(1)**, 17-19

Pillay P, Vleggaar R, Maharaj VJ, Smith PJ and Lategan CA (2007)
Isolation and identification of antiplasmodial sesquiterpene lactones from *Oncosiphon piluliferum*
Journal of Ethnopharmacology, **112**, 71-76

Pink R, Hudson A, Mouriès MA and Bendig M (2005)
Opportunities and challenges in antiparasitic drug discovery
Nature reviews, **4**, 727-740

Pino P, Vouldoukis I, Kolb JP, Mahmoudi N, Desportes-Livage I, Bricaire F, Danis M, Dugas B and Mazier D (2003)
Plasmodium falciparum-infected erythrocyte adhesion induces caspase activation and apoptosis in human endothelial cells
Journal of Infectious Diseases, **187**, 1283-1290

Pong NG S, Wong KY, Zhang L and Zuo Z (2005)
Evaluation of the first-pass glucuronidation of selected flavones in gut by Caco-2 monolayer model
Journal of Pharmacy & Pharmaceutical Sciences, **8(1)**, 1-9

Portet B, Fabre N, Roumy V, Gornitzka H, Bourdy G, Chevalley S, Sauvain M, Valentin A and Moulis C (2007)
Activity-guided isolation of antiplasmodial dihydrochalcones and flavanones from *Piper hostmannianum* var. *berbicense*
Phytochemistry, **68**, 1312-1320

Preparative HPLC
Column packing and basic principles
http://www.macherey-nagel.com/web%5CMN-WEB-HPLCKatalog.nsf/WebE/DKUL-4

Ramakaran AE and Peters W (1970)
Action of chloroquine on infectivity of gametocytes of rodent malarias
Transactions of the Royal Society of Tropical Medicine and Hygiene, **64**, 8

Rasoanaivo P (2002)
Pre-clinical evaluation of traditional antimalarials: guidelines and recent results
Abstracts of the third MIM Pan-African Malaria Conference, November 17-22, Arusha, Tanzania, p.88

Ridley RG (2004)
Research on infectious diseases requires better coordination
Nature Medicine (New York, NY, United States), **10(12)**, S137-S140
http://www.nature.com/nm/journal/v10/n12s/pdf/nm1153.pdf

Rieckmann KH, Yeo AET and Edstein MD (1996)
Activity of PS-15 and its metabolite, WR99210, against *P. falciparum* in an *in vivo-in vitro* model
Transactions of the Royal Society of Tropical Medicine and Hygiene, **90**, 568-571

Ringwald P, Bickii J and Basco LK (1998)
Amodiaquine as the first-line treatment of malaria in Yaoundé, Cameroon: presumptive evidence from activity *in vitro* and cross-resistance patterns
Transactions of the Royal Society of Tropical Medicine and Hygiene, **92(2)**, 212-213

Roper C, Pearce R, Bredenkamp B and Gumede B (2003)
Antifolate antimalarial resistance in Southeast Africa: a population bases analysis
The Lancet, **361(9364)**, 1174-1181

Rosenthal PJ (2003)
Antimalarial drug discovery: old and new approaches
The Journal of Experimental Biology, **206**, 3735-3744

Rudin W, Eugster HP, Bordmann G, Bonato J, Muller M, Yamage M and Ryffel B (1997)
Resistance to cerebral malaria in tumor necrosis factor-α/β-deficient mice is associated with a reduction of intercellular adhesion molecule-1 up-regulation and T helper type 1 response
American Journal of Pathology, **150(1)**, 257-266

Rwagacondo CE, Niyitegeka F, Sarushi J, Karema C, Mugisha V, Dujardin JC, Van Overmeir C, Van Den Ende J and D'Alessandro U (2003)
Efficacy of amodiaquine alone and combined with sulfadoxine-pyrimethamine and of sulfadoxine pyrimethamine combined with artesunate
American Journal of Tropical Medicine and Hygiene, **68(6)**, 743-747

Sachs J and Malaney P (2002)
The economic and social burden of malaria
Nature, **415**, 680-685

Sagalowicz L, Leser ME, Watzke HJ and Michel M (2006)
Monoglyceride self-assembly structures as delivery vehicles
Trends in Food Science & Technology, **17**, 204-214

Sahin FP, Ezer N and Calis I (2004)
Three acylated flavone glycosides from *Sideritis ozturkii* - Aytac and Aksoy
Phytochemistry, **65**, 2095-2099

Salgame P, Varadhachary AS, Primiano LL, Fincke JE, Muller S and Monestier M (1997)
An ELISA for detection of apoptosis
Nucleic Acids Research, **25(3)**, 680-681

Salisbury FB and Ross CW (1992)
Plant Physiology, fourth edition
Wadsworth Publishing Company, Belmont, California

Samuelson G, Kyerematen G and Farah M (1985)
Preliminary chemical characterisation of pharmacologically active compounds in aqueous plant extracts
Journal of Ethnopharmacology, **14**, 193-201

Samuelson G (1987)
Plants used in traditional medicine as sources of drugs
Bulletin of the Chemical Society of Ethiopia, **1**, 47-54

Schmidt C (2004)
Analysis of 7,4'-Dihydroxyflavone by positive APCI LC-MS/MS
Varian application note 12
http://www.varianinc.com

Shah VP, Midha KK, Findlay JWA, Hill HM, Hulse JD, McGilveray IJ, McKay G, Miller KJ, Patnaik RN, Powell ML, Tonelli A, Viswanathan CT and Yacobi A (2000)
Bioanalytical method validation – A revisit with a decade of progress
Pharmaceutical Research, **17(12)**, 1551-1557

Shanks GD, Gordon DM, Klotz FW, Aleman GM, Oloo AJ, Sadie D and Scott TR (1998)
Efficacy and safety of atovaquone/proguanil as suppressive prophylaxis for *Plasmodium falciparum* malaria
Clinical Infectious Diseases, **27(3)**, 494-499

Sharma DK and Hall IH (1991)

Hypolipidemic, anti-inflammatory and antineoplastic activity and cytotoxicity of flavonolignans isolated from *Hydnocarpus wightiana* seeds

Journal of Natural Products, **54(5)**, 1298-1302

Sharma P and Sharma JD (1999)

Evaluation of *in vitro* schizontocidal activity of plant parts of *Calotropis procera*: an ethnobotanical approach

Journal of Ethnopharmacology, **68**, 83-95

Shearer TW, Smith KS, Diaz D, Asher C and Ramirez J (2005)

The role of *in vitro* ADME assays in antimalarial drug discovery and development

Combinational Chemistry & High Througput Screening, **8**, 89-98

Sieuwerts AM, Klijn JGM, Peters HA and Foekens JA (1995)

The MTT tetrazolium salt assay scrutinized: How to use this assay reliably to measure metabolic activity of cells *in vitro* for the assessment of growth characteristics, IC_{50}-values and cell survival

European Journal of Clinical Chemistry and Clinical Biochemistry, **33(11)**, 813-823

Simonsen HT, Nordskjold JB, Smitt UW, Nyman U, Palpu P, Joshi P and Varughesa G (2001)

In vitro screening of Indian medicinal plants for antiplasmodial activity

Journal of Ethnopharmacology, **74**, 195-204

Singh KK and Vingkar SK (2008)

Pharmaceutical Nanotechnology: Formulation, antimalarial activity and biodistribution of oral lipid nanoemulsion of primaquine

International Journal of Pharmaceutics, **347**, 136-143

Somers D, Basa L, Impey G and Jones E (2003)

Simultaneous qualitative and quantitative LC-MS/MS analysis of opiates in biological matrices

ASMS 2003 conference poster number TH-134

Statz D and Coon FB (1976)
Preparation of plant extracts for antitumor screening
Cancer Treatment Reports, **60**, 999-1005

Stermitz FR, Lorenz P, Tawara JN, Zenewicz LA and Lewis K (2000)
Synergy in a medicinal plant: Antimicrobial action of berberine potentiated by 5'-methoxyhydnocarpin
Proceedings of the National Academy of Sciences of the United States of America, **97(4)**, 1433-1437

Stermitz FR, Beeson TD, Mueller PJ, Hsiang JF and Lewis K (2001)
Staphylococcus aureus MDR efflux pump inhibitors from a *Berberis* and a *Mahonia* (sensu strictu) species
Biochemical Systematics and Ecology, **29**, 793-798

Stoute JA, Kester KE, Krzych U, Wellde BT, Hall T, White K, Glenn G, Ockenhouse CF, Garcon N, Schwenk R, Lanar DE, Sun P, Momin P, Writz RA, Golenda C, Slaoui M, Wortmann G, Holland C, Dowler M, Cohen J and Ballou WR (1998)
Long-term Efficacy and Immune Responses following Immunization with the RTS,S Malaria Vaccine
The Journal of Infectious Diseases, **178**, 1139-1144

Tan RX, Zheng WF and Tang HQ (1998)
Biologically active substances from the genus *Artemisia*
Planta Medica, **64(4)**, 295-302

Tang YD, Venkatraman SS, Boey FYC and Wang LW (2007)
Sustained release of hydrophobic and hydrophilic drugs from a floating dosage form
International Journal of Pharmaceutics, **336**, 159-165

TDR (2003)
Tropical disease research: progress 2001-2002
http://www.who.int/tdr/publications/publications/pr16.htm

Tona L, Mesia K, Ngimbi NP, Chrimwami B, Okond'ahoka, Cimanga K, de Bruyne T, Apers S, Hermans N, Totte J, Pieters L and Vlietinck A J (2001)
In-vivo antimalarial activity of *Cassia occidentalis*, *Morinda morindoides* and *Phyllanthus niruri*.
Annals of Tropical Medicine and Parasitology, **95(1)**, 47-57

Trager W and Jensen JB (1976)
Human malaria parasites in continuous culture
Science, **193(4254)**, 673-675

Tween® 80 by LC-MS
http://www.wcaslab.com/tech/Tween80.htm

Trouiller P (2002)
Drug development for neglected diseases: a deficient market and a public-health policy failure
Lancet, **359**, 2188-2194

United States Department of Health and Human Services, National Institute of Health, National Institute of Allergy and Infectious Diseases (NIAID)
Understanding Malaria – Fighting an Ancient Scourge
http://www.niaid.nih.gov/publications/malaria/pdf/malaria.pdf

Van Wyk BE, Van Oudtshoorn B and Gericke N (2002)
Medicinal plants of South Africa
Briza Publications, Pretoria, South Africa

Van Zoonen P, Hoogerbrugge R, Gort SM, Van de Wiel HJ and Van't Klooster HA (1999)
Some practical examples of method validation in the analytical laboratory
Trends in Analytical Chemistry, **18(9,10)**, 584-593

Waako PJ, Gumede B, Smith PJ and Folb PI (2005)
The *in vitro* and *in vivo* antimalarial activity of *Cardiospermum halicacabum* L. and *Momordica foetida* Schumch. Et Thonn.
Journal of Ethnopharmacology, **99**, 137–143

Ward KW, Proksch JW, Levy MA and Smith BR (2001)
Development of an *in vivo* preclinical screen model to estimate absorption and bioavailability of xenobiotics
Drug Metabolism and Disposition, **29(1)**, 82-88

Wellems TE and Plowe CV (2001)
Chloroquine-Resistant Malaria
The Journal of Infectious Diseases, **184**, 770-776

Willcox ML and Bodeker G (2000)
Plant-based malaria control: Research initiative on traditional antimalarial methods
Parasitology Today, **16(6)**, 220-221

Willcox ML and Bodeker G (2004)
Traditional herbal medicines for malaria
BMJ, **329**, 1156-1159

Willcox ML, Bodeker G and Rasoanaivo P (2004)
Traditional herbal medicines for modern times
Traditional medicinal plants and malaria & An overview of ethnobotanical studies on plants used for the treatment of malaria
1-431

Williams CA, Harborne JB, Greenham J and Eagles J (1994)
Differences in flavonoid patterns between genera within the Velloziaceae
Phytochemistry, **36(4)**, 931-940

Willoughby R, Sheehan E and Mitrovich S (2002)
A global view of LC/MS – how to solve your most challenging analytical problems
457-458

World Health Organization
Malaria
http://www.who.int/topics/malaria/en/

World Health Organization (1986)
Chemotherapy of malaria (Bruce-Chwatt LJ)
WHO, 2ed edition, Geneva, 211-233

World Health Organization (1998)
Regulatory situation of herbal medicine, a worldwide review
http://whqlibdoc.who.int/hq/1998/WHO_TRM_98.1.pdf

World Health Organization (1999)
World health report, 1999
World Health Organization, Geneva

World Health Organization (2002)
Traditional medicine strategy 2002 -2005
World Health Organization, Geneva

World Health Organization (2005)
Report on global malaria monitoring (1996-2004)
Susceptibility of *Plasmodium falciparum* to antimalarial drugs
World Health Organization

World Health Organization (2005)
World malaria report, 2005
http://rbm.who.int/wmr2005/

World Malaria Map
http://k12education.uams.edu/scvlab/malariaMap.htm

Wu W, Wang Y and Que L (2006)
Enhanced bioavailability of silymarin by self-microemulsifying drug delivery system
European Journal of Pharmaceutics and Biopharmaceutics, **63**, 288-294

Yanyu X, Yunmei S, Zhipeng C and Qineng P (2006)
Preparation of silymarin proliposome: A new way to increase oral bioavailability of silymarin in beagle dogs
International Journal of Pharmaceutics, **319(1-2)**, 162-168

Yanyu X, Yunmei S, Zhipeng C and Qineng P (2006)
The preparation of silybin-phospholipid complex and the study on its pharmacokinetics in rats
International Journal of Pharmaceutics, **307**, 77-82

Yao M, Zhu M, Sinz MW, Zhang H, Humphreys WG, Rodrigues AD and Dai R (2007)
Development and full validation of six inhibition assays for five major cytochrome P450 enzymes in human liver microsomes using an automated 96-well microplate incubation format and LC-MS/MS analysis
Journal of Pharmaceutical and Biochemical Analysis, **44**, 211-223

Zhang F, Gosser DK Jr., and Meshnick SR (1992)
Hemin-catalyzed decomposition of artemisinin (qinghaosu)
Biochemical Pharmacology, **43(8)**, 1805-1809

Zhang J and Brodbelt JS (2004)
Screening flavonoid metabolites of naringin and narirutin in urine after human consumption of grapefruit juice by LC-MS and LC-MS/MS
Analyst, **129**, 1227-1233

Zirihi GN, Grellier P, Guédé-Guina F, Bodo B and Mambu L (2005)

Isolation, characterization and antiplasmodial activity of steroidal alkaloids from *Funtumia elastica* (Preuss) Stapf

Bioorganic & Medicinal Chemistry Letters, **15**, 2637-2640

APPENDIX 1

HPLC, UV, MS and NMR spectra

Compound 2

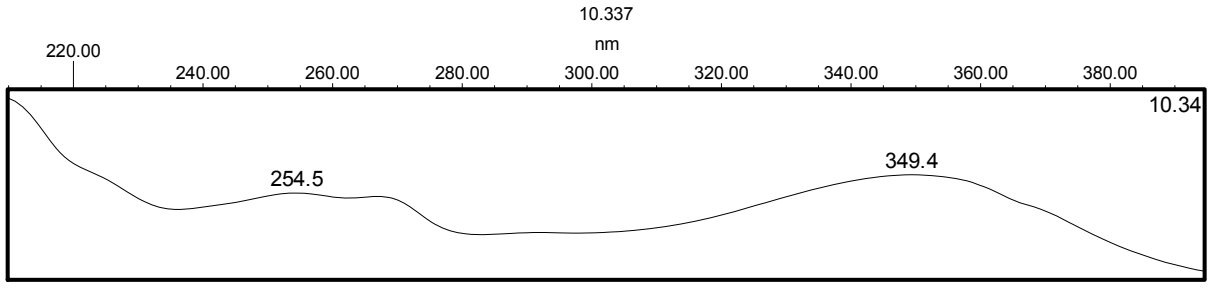

Figure 127 UV spectrum of compound 2

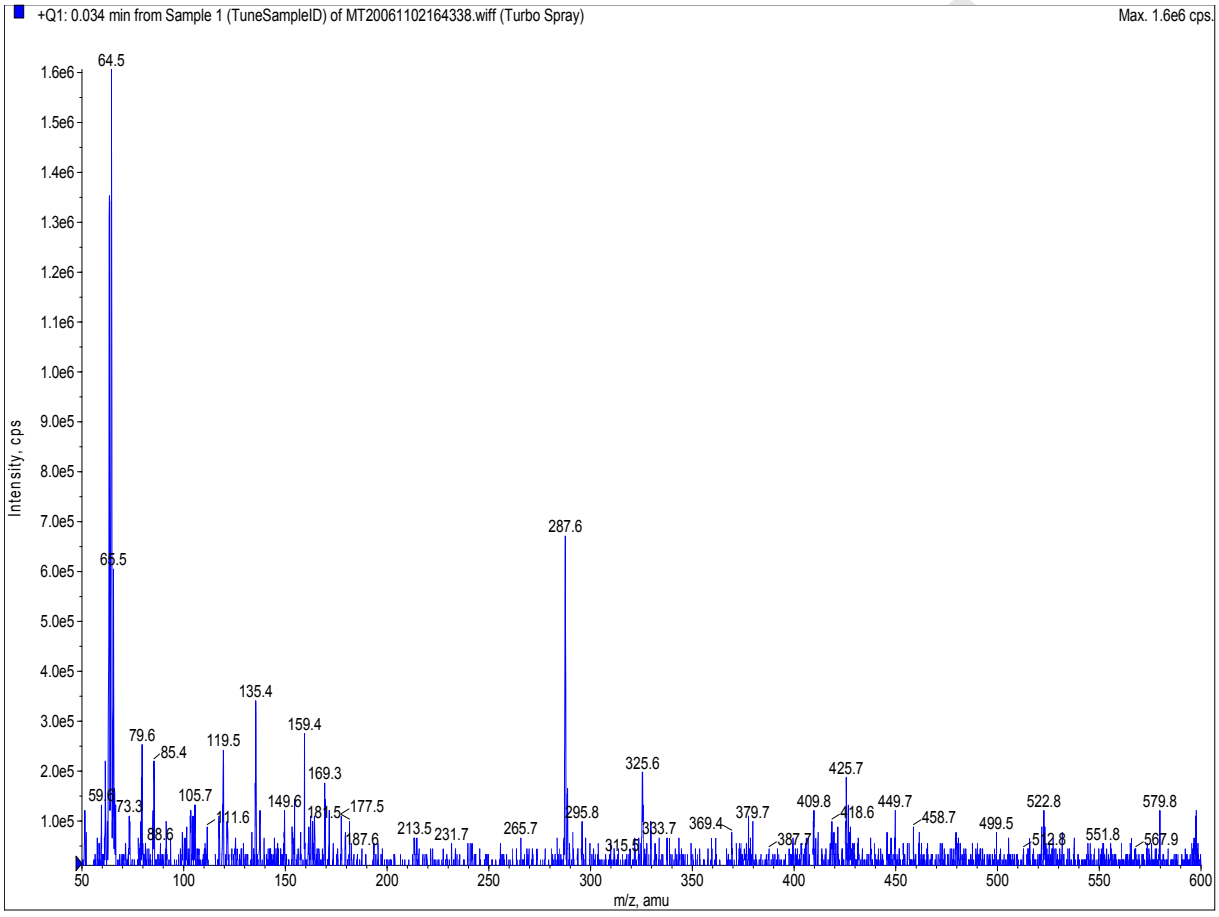

Figure 128 Mass spectrum of compound 2

Mass	Calc. Mass	mDa	PPM	DBE	Formula	Score	C	H	O
287.0550	287.0556	-0.6	-2.0	10.5	C15 H11 O6	1	15	11	6
	287.0403	14.7	51.2	6.5	C11 H11 O9	4	11	11	9
	287.0767	-21.7	-75.6	5.5	C12 H15 O8	3	12	15	8
	287.0919	-36.9	-128.7	9.5	C16 H15 O5	2	16	15	5

LW_UCT_070126_2b 25 (0.272) Cn (Top,4, Ar); Sm (Mn, 2x1.00); Sb (1,40.00); Cm (25:30) TOF MS ES+ 5.87e3

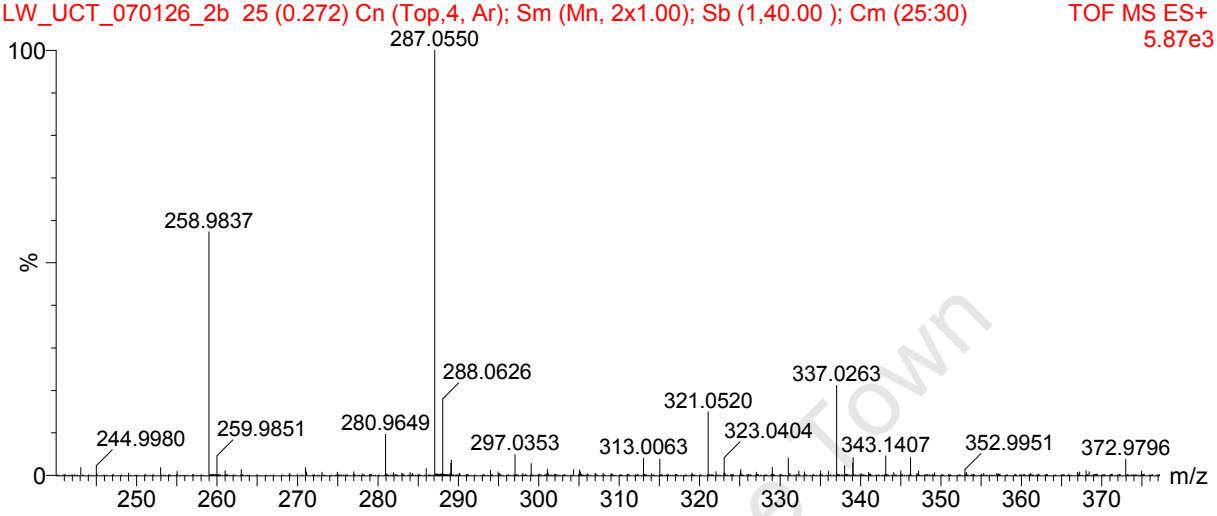

Figure 129 High resolution mass spectrum of compound 2

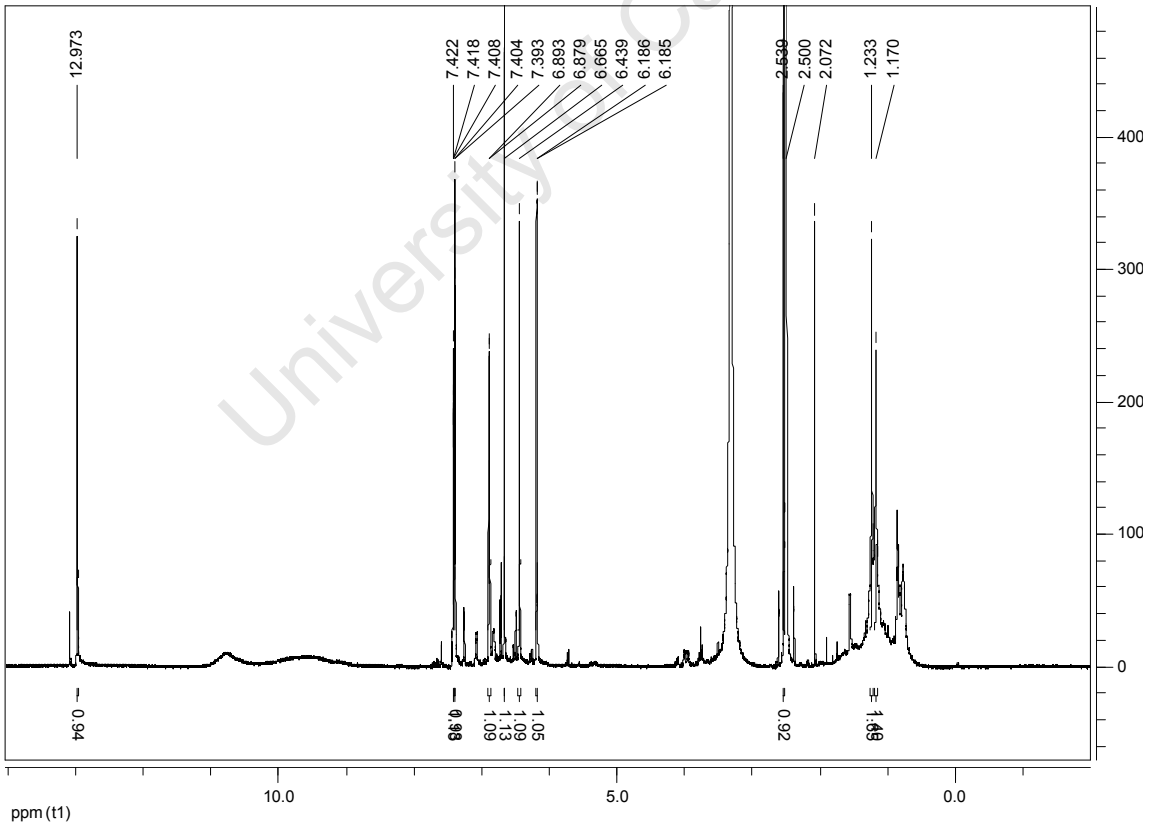

Figure 130 ^{1}H NMR spectrum of compound 2

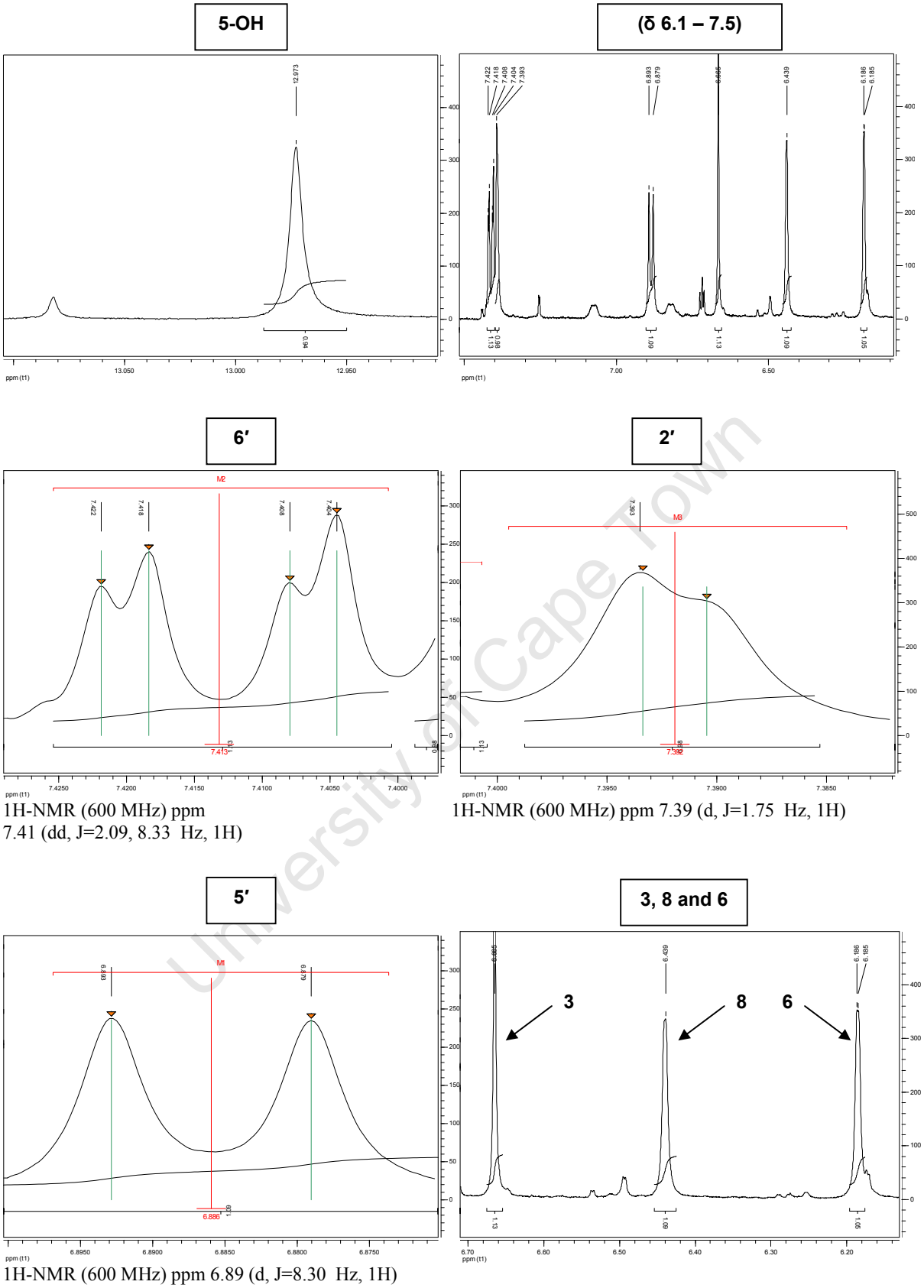

1H-NMR (600 MHz) ppm 7.41 (dd, J=2.09, 8.33 Hz, 1H)

1H-NMR (600 MHz) ppm 7.39 (d, J=1.75 Hz, 1H)

1H-NMR (600 MHz) ppm 6.89 (d, J=8.30 Hz, 1H)

Figure 131 ^{1}H peaks of compound 2

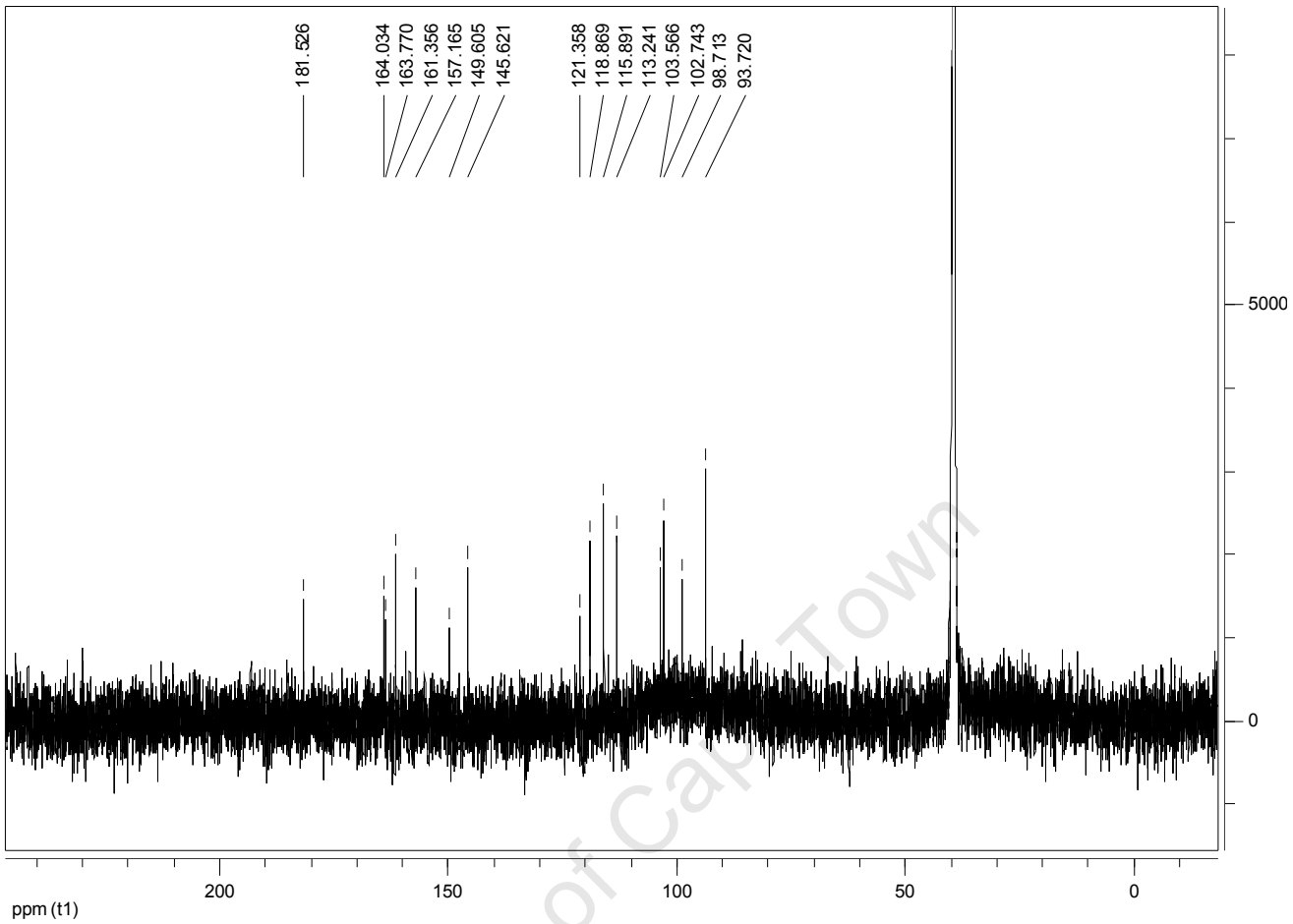

Figure 132 ^{13}C NMR spectrum of compound 2

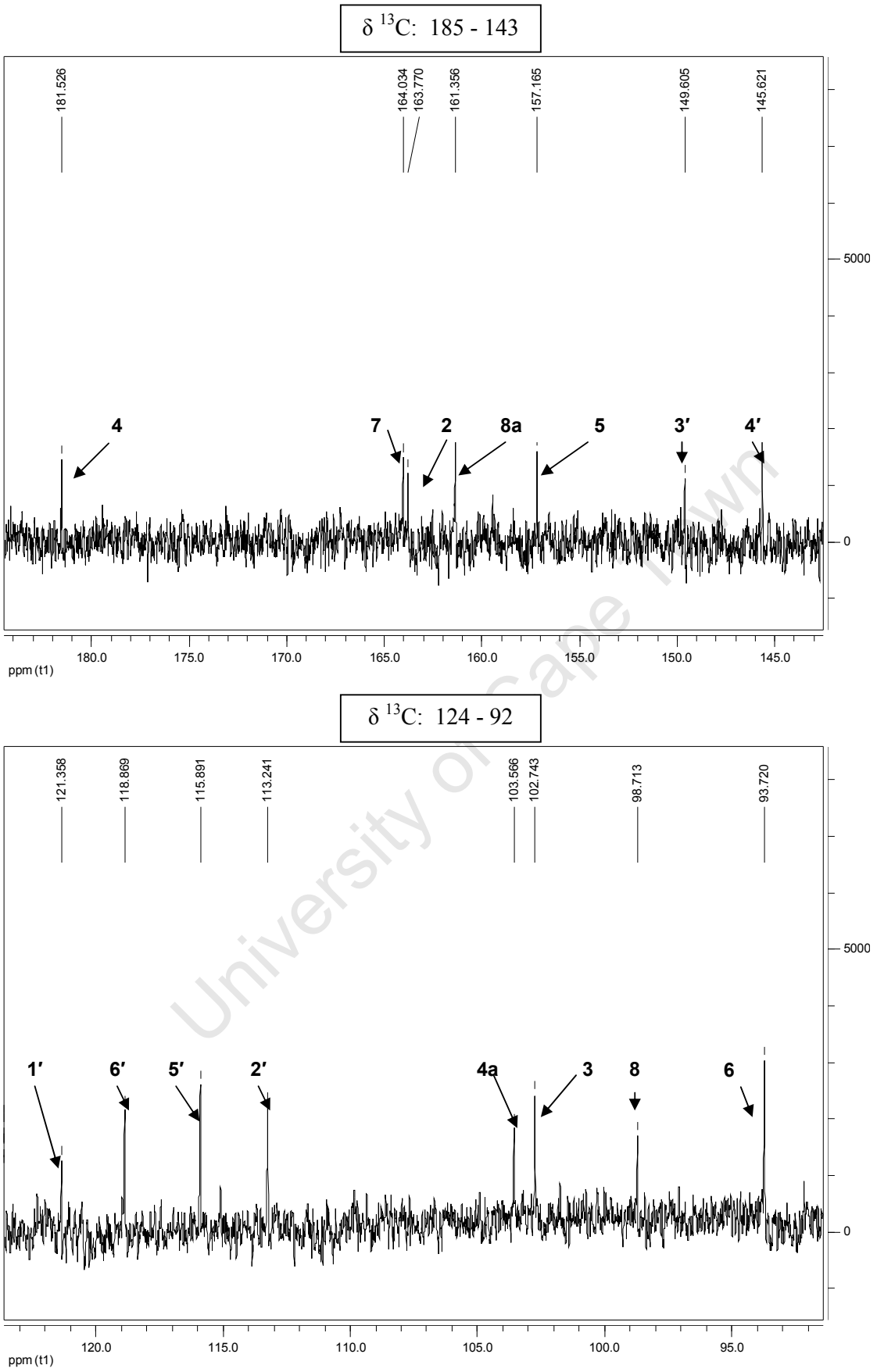

Figure 133 ^{13}C peaks of compound 2

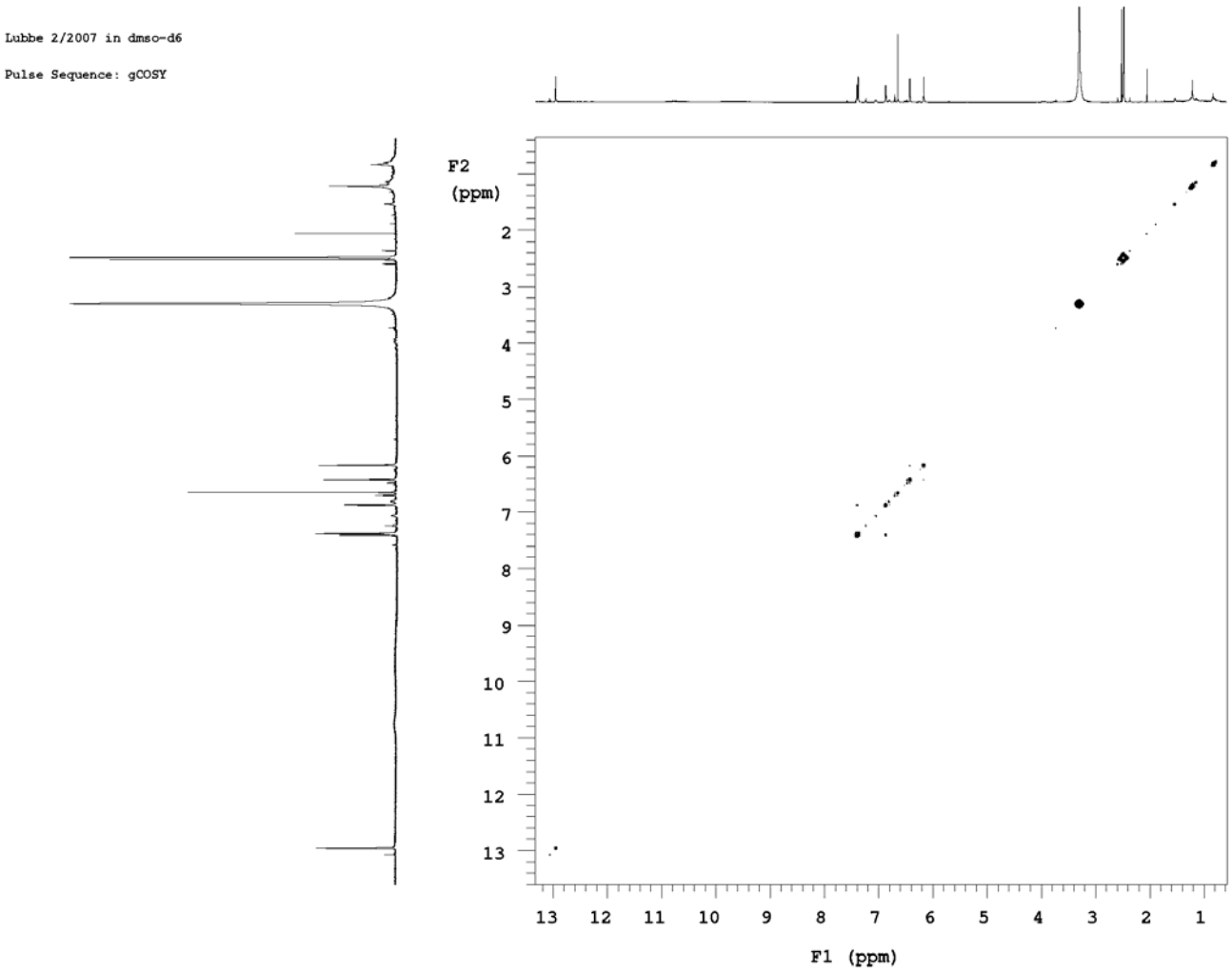

Figure 134 COSY spectrum of compound 2

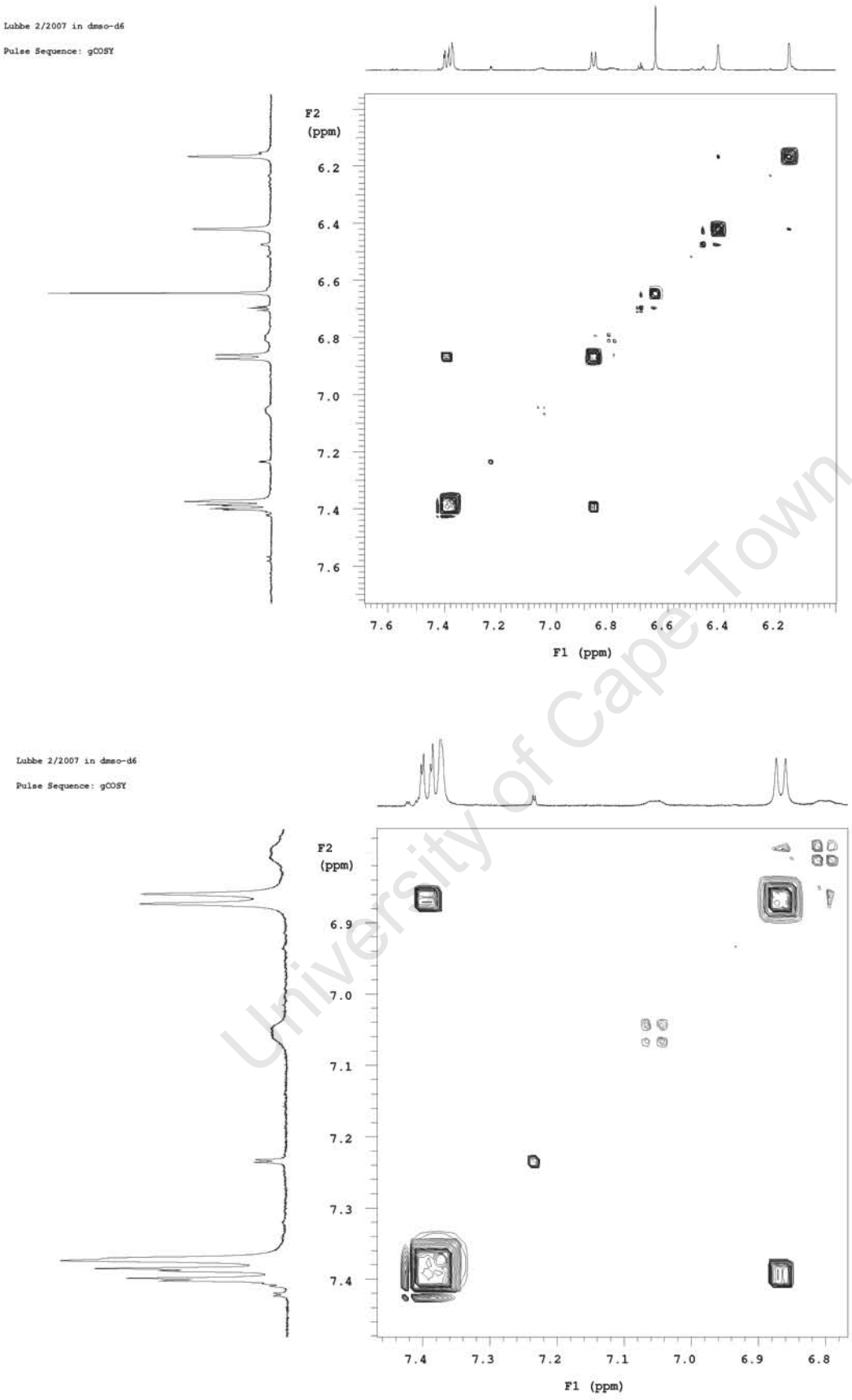

Figure 135 Proton correlations of compound 2

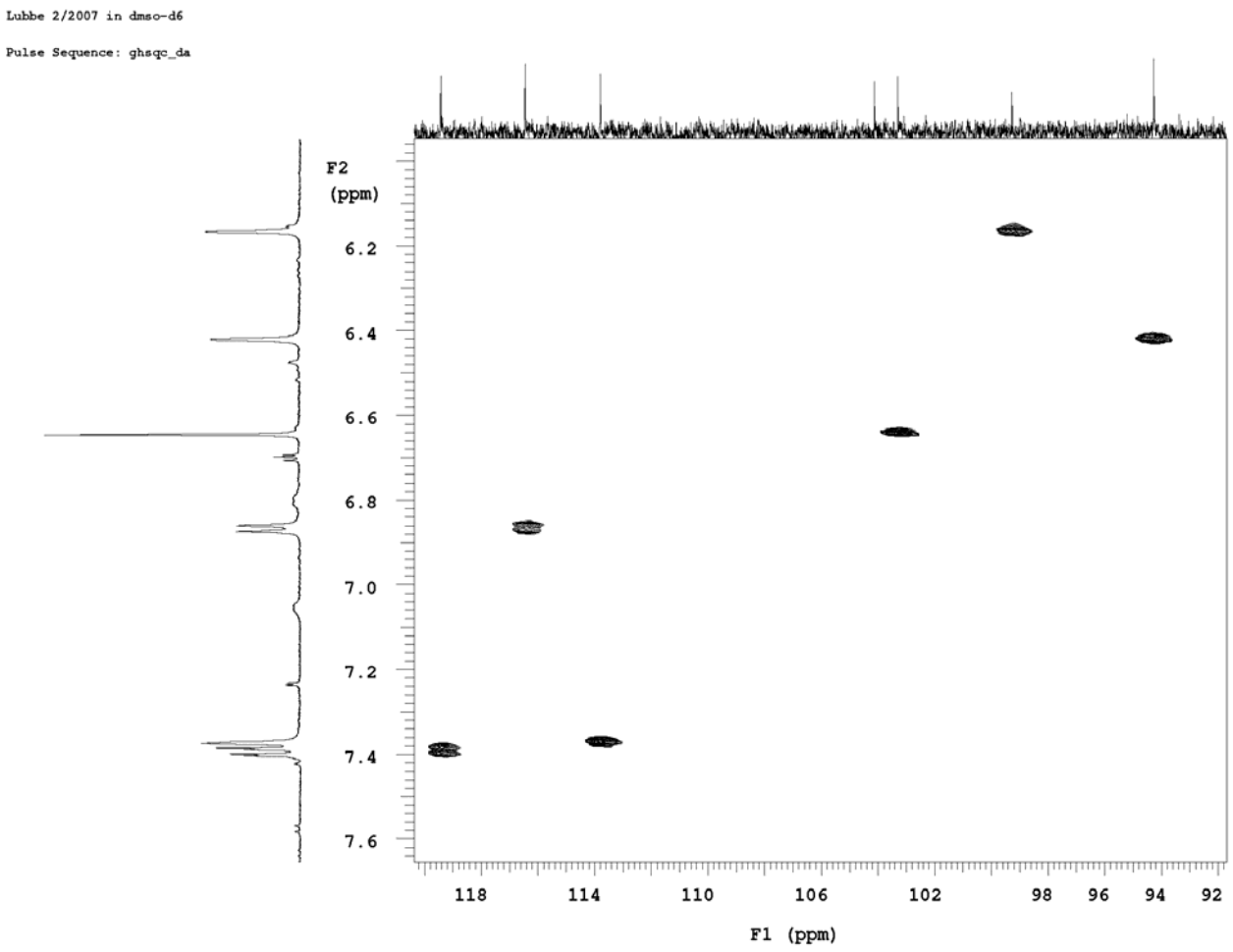

Figure 136 HSQC spectrum of compound 2

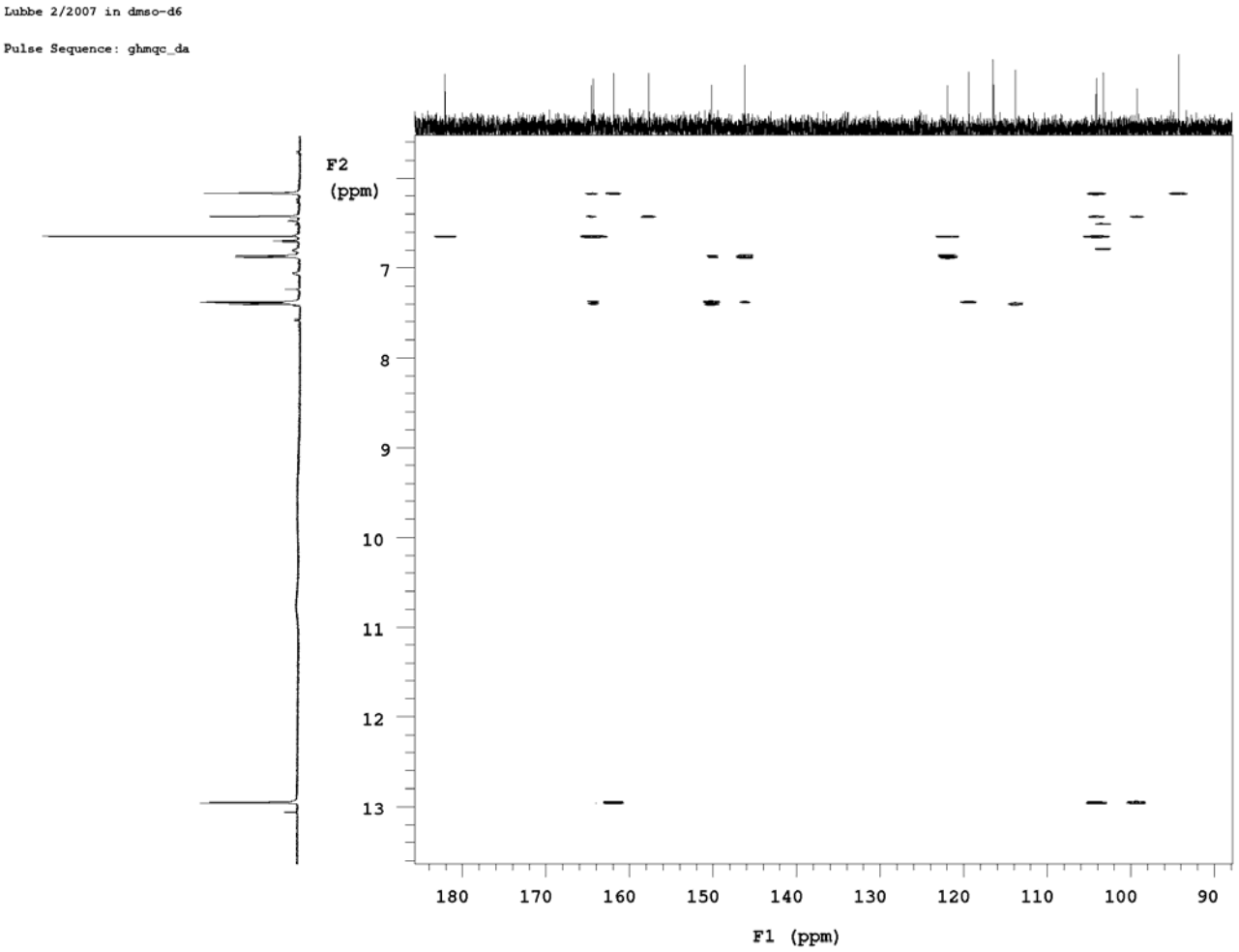

Figure 137 HMQC spectrum of compound 2

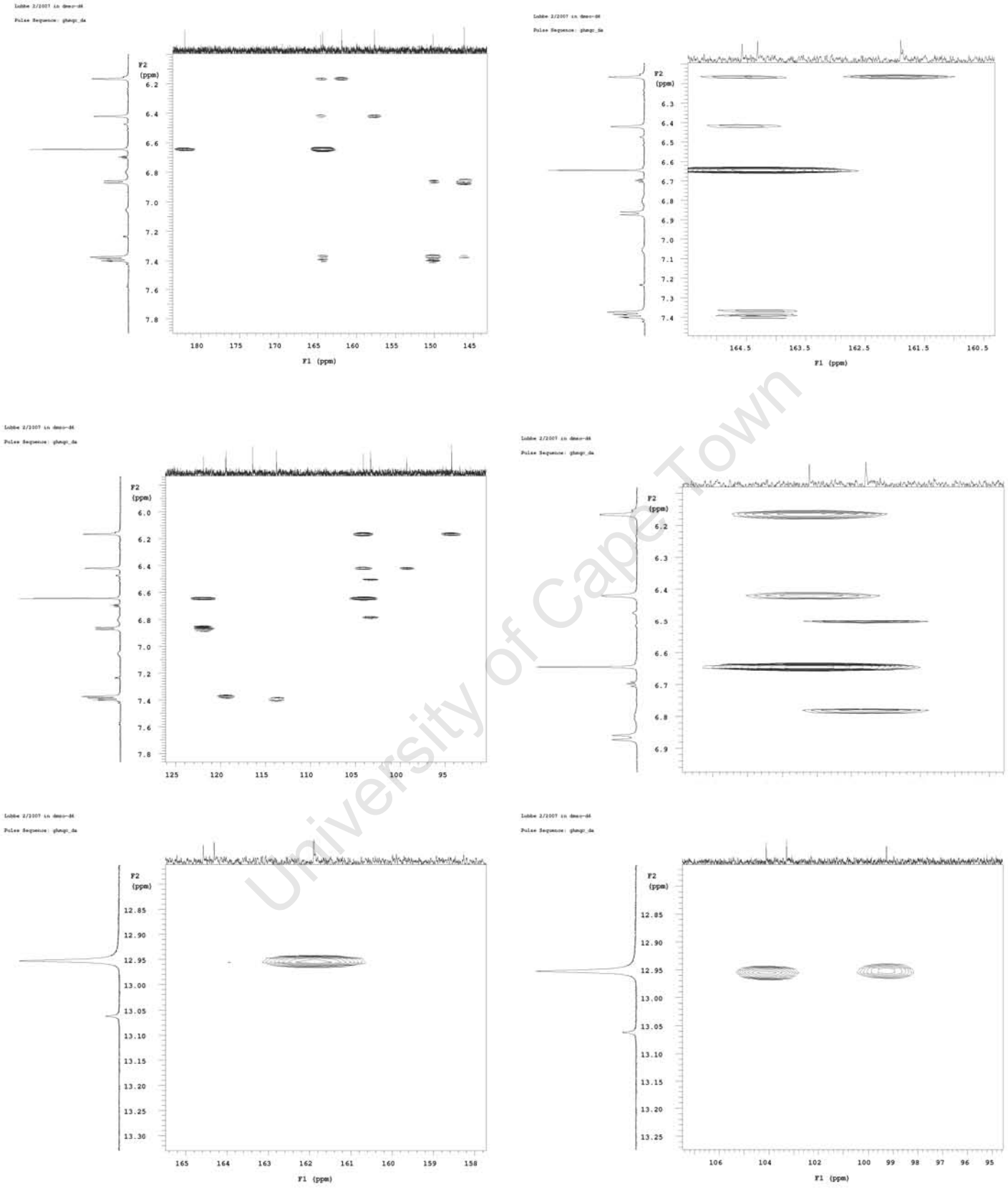

Figure 138 3 bond correlation of compound 2

Compound 4

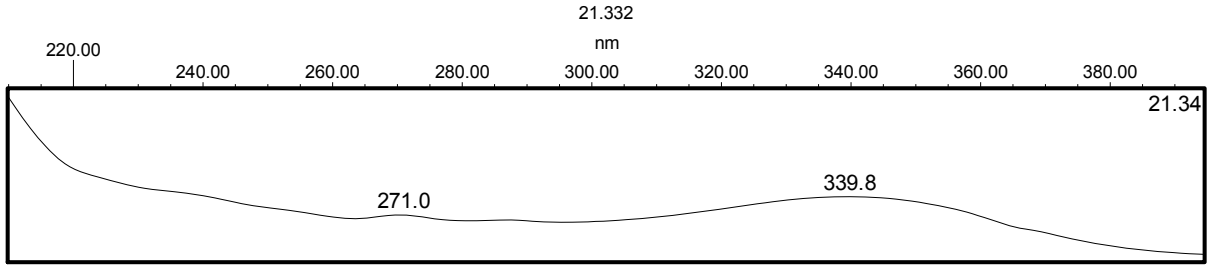

Figure 139 UV spectrum of compound 4

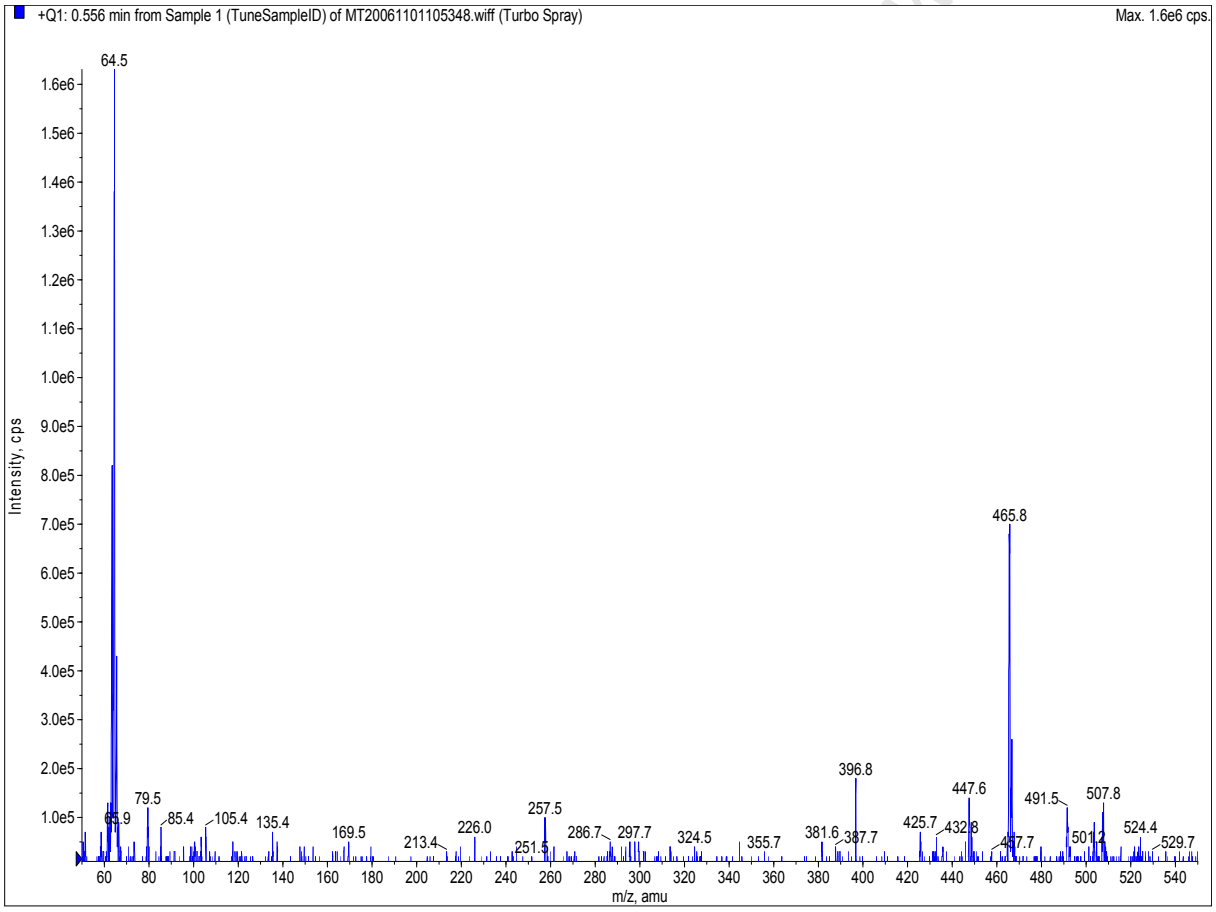

Figure 140 Mass spectrum of compound 4

Mass	Calc. Mass	mDa	PPM	DBE	Formula	Score	C	H	O
465.1193	465.1186	0.7	1.6	15.5	C25 H21 O9	2	25	21	9
	465.1549	-35.6	-76.6	14.5	C26 H25 O8	1	26	25	8

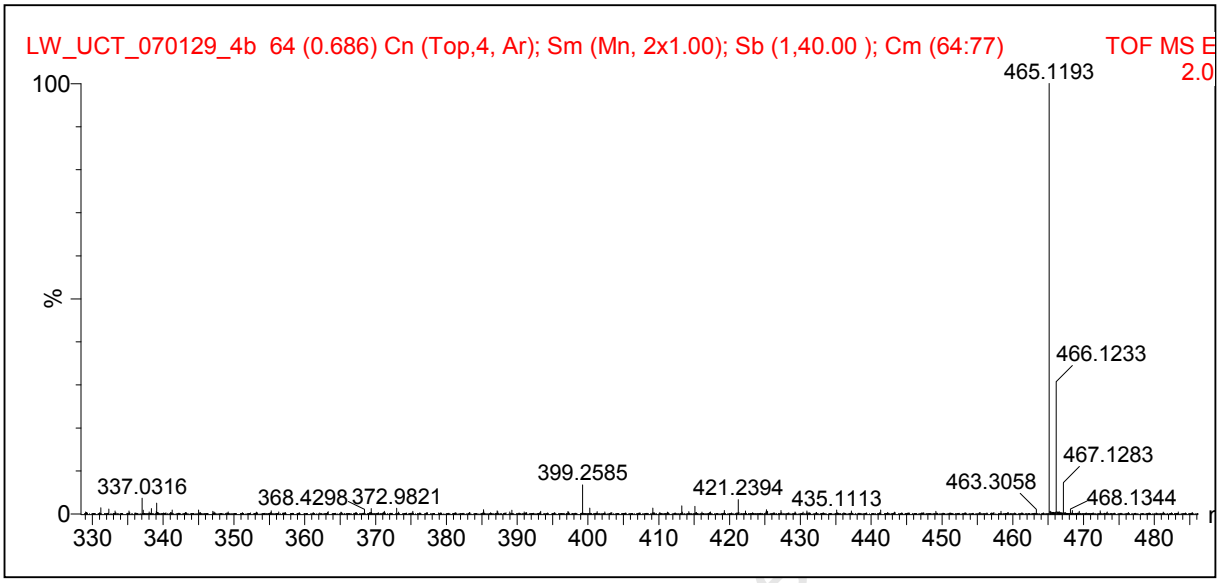

Figure 141 High resolution mass spectrum of compound 4

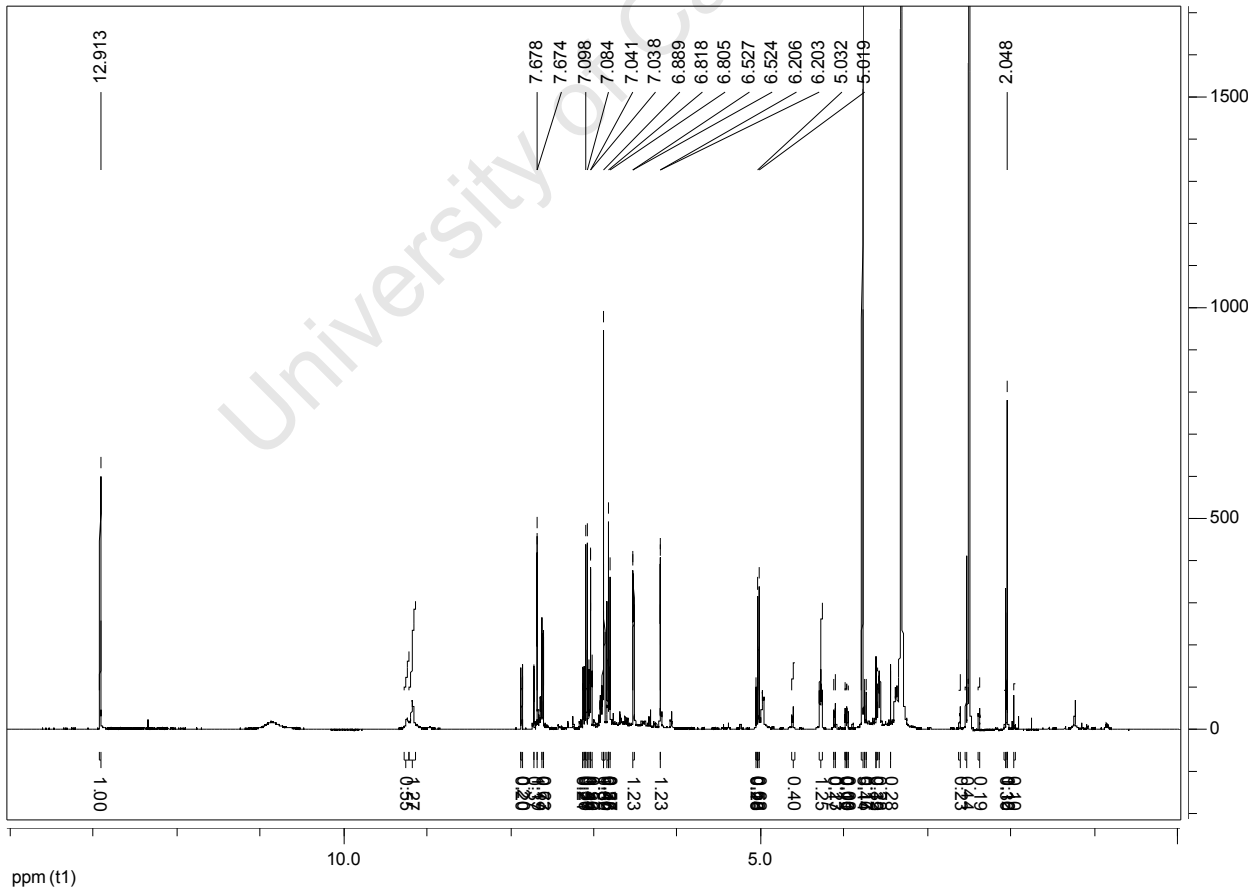

Figure 142 ^{1}H NMR spectrum of compound 4

5

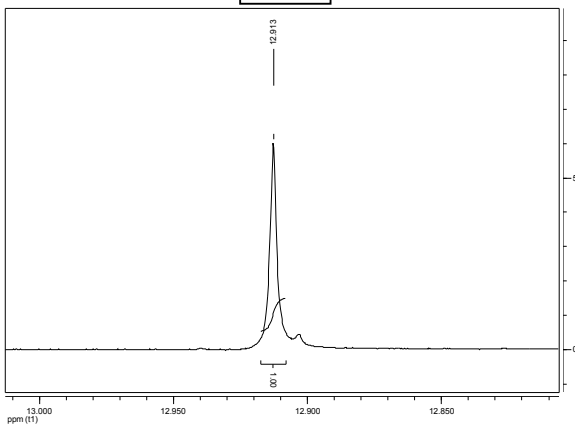

6′

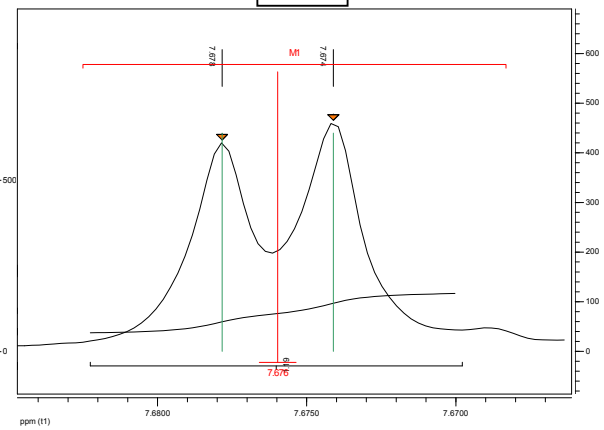

1H-NMR (600 MHz) ppm 7.68 (d, J=2.24 Hz, 1H)

2′

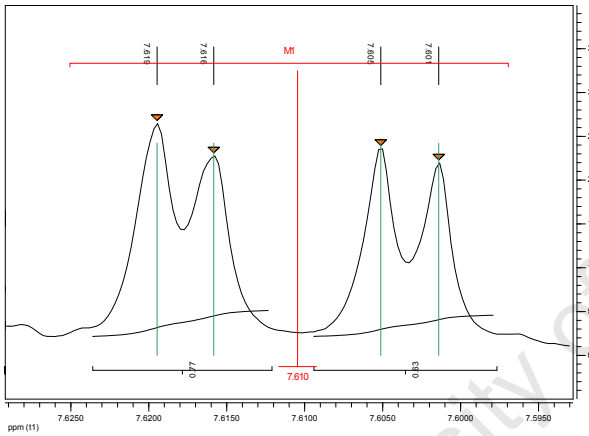

1H-NMR (600 MHz) ppm
7.61 (dd, J=2.21, 8.63 Hz, 1H)

3′

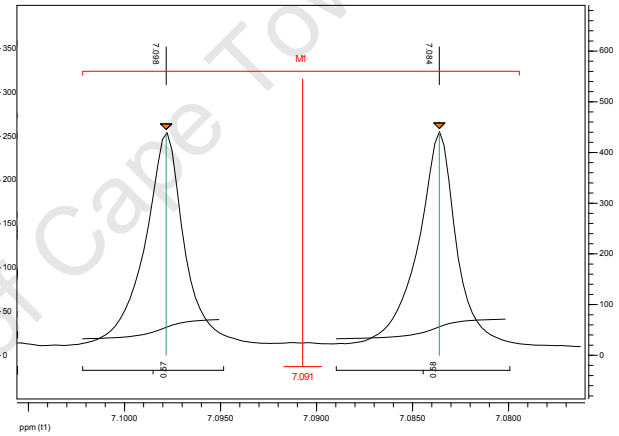

1H-NMR (600 MHz) ppm 7.09 (d, J=8.53 Hz, 1H)

13

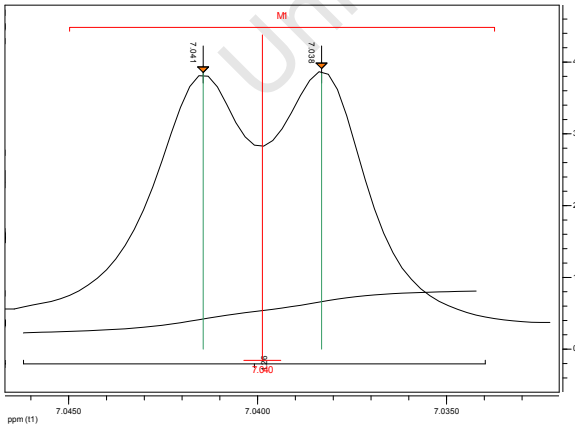

1H-NMR (600 MHz) ppm 7.04 (d, J=1.88 Hz, 1H)

3

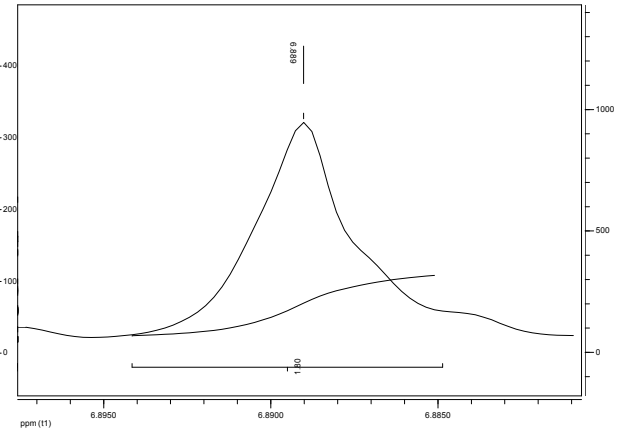

δ 6.88 – 6.80

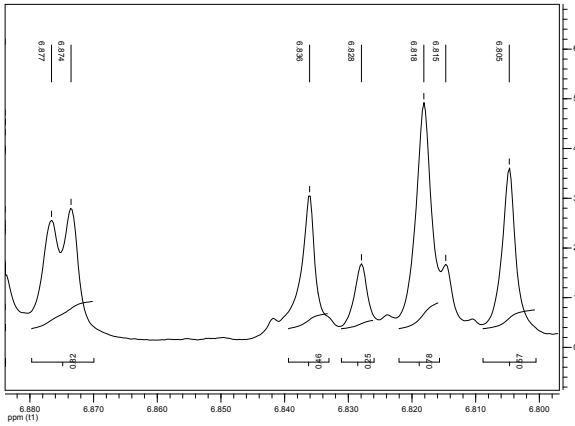

17

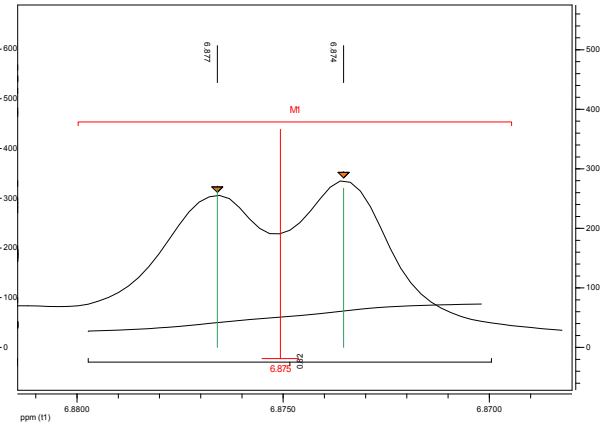

1H-NMR (600 MHz) ppm 6.88 (d, J=1.84 Hz, 1H)

16

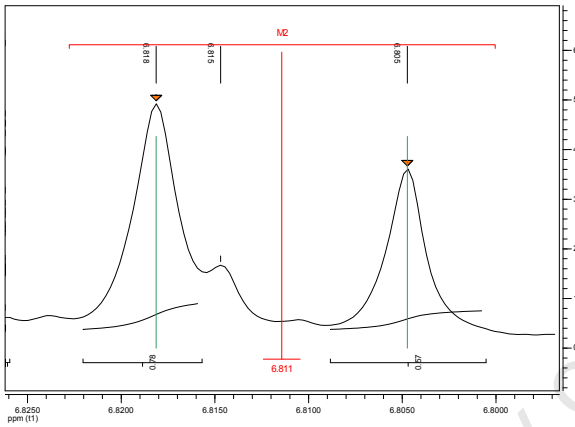

1H-NMR (600 MHz) ppm 6.81 (d, J=8.04 Hz, 1H)

8

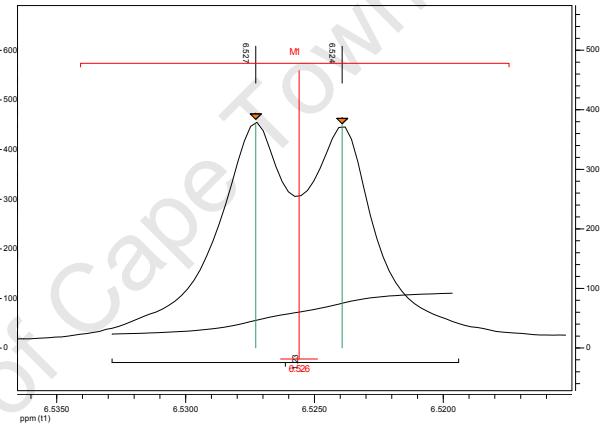

1H-NMR (600 MHz) ppm 6.53 (d, J=2.01 Hz, 1H)

6

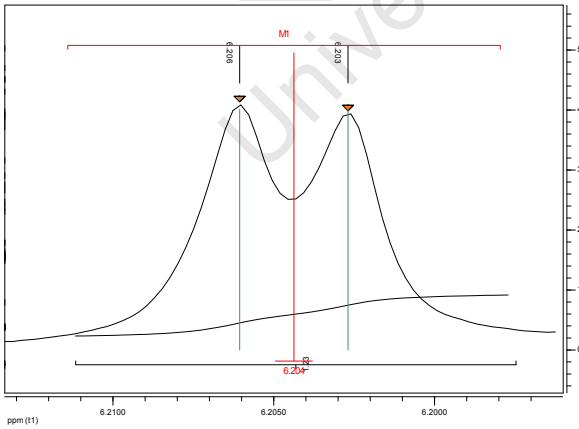

1H-NMR (600 MHz) ppm 6.20 (d, J=2.02 Hz, 1H)

11

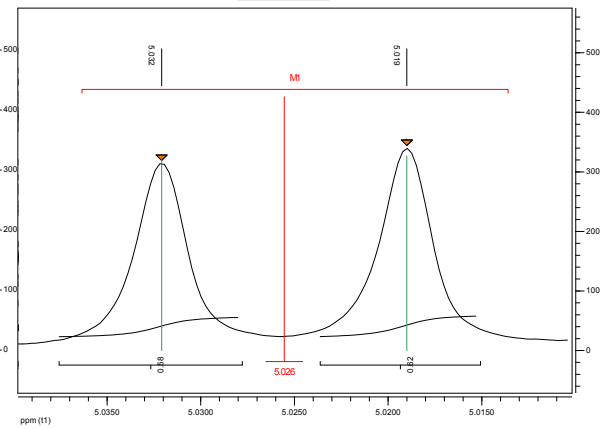

1H-NMR (600 MHz) ppm 5.03 (d, J=7.85 Hz, 1H)

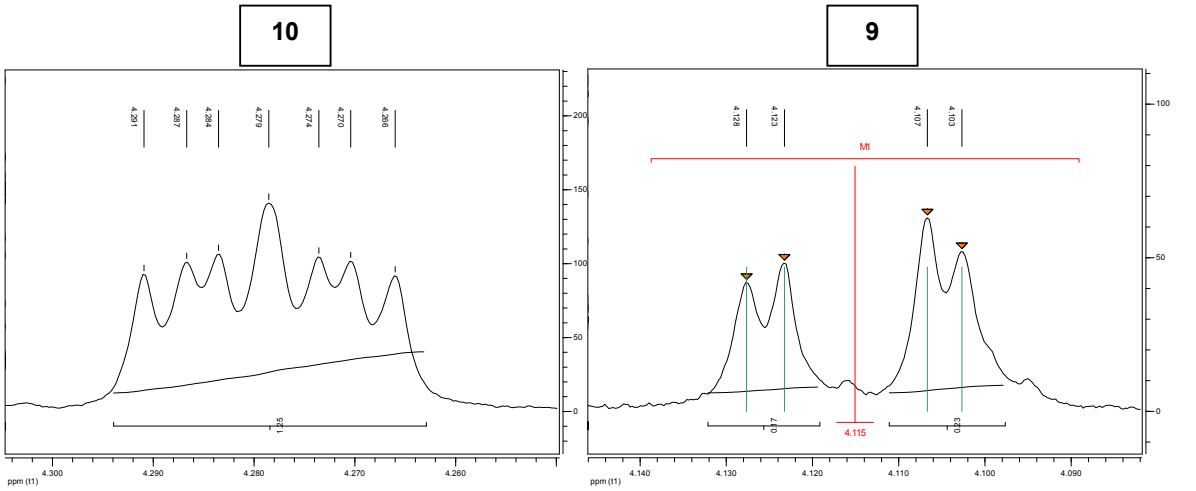

1H-NMR (600 MHz) ppm 4.12 (dd, J=2.51, 12.46 Hz, 1H)

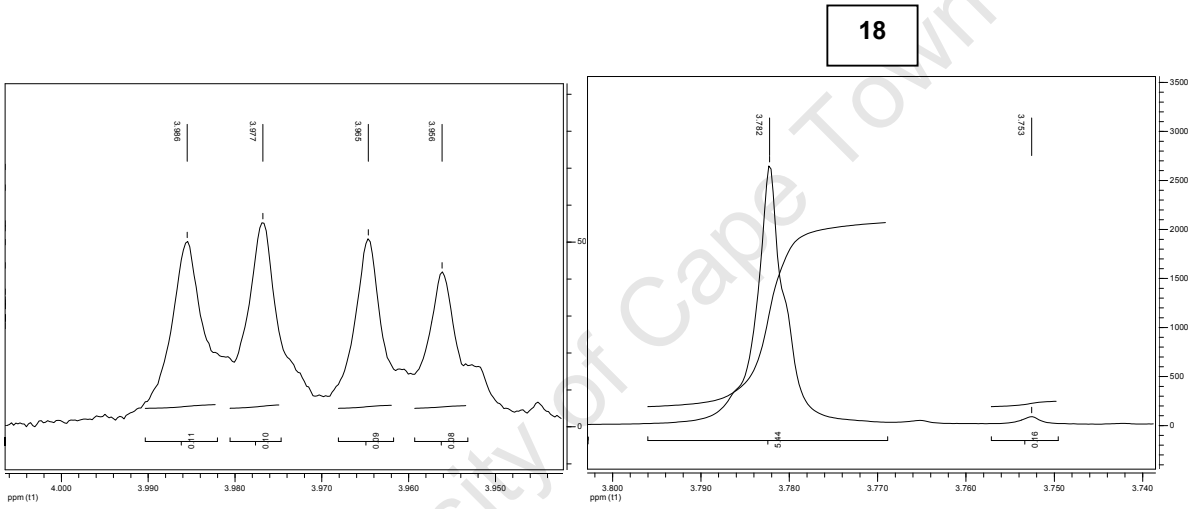

Figure 143 ^{1}H peaks of compound 4

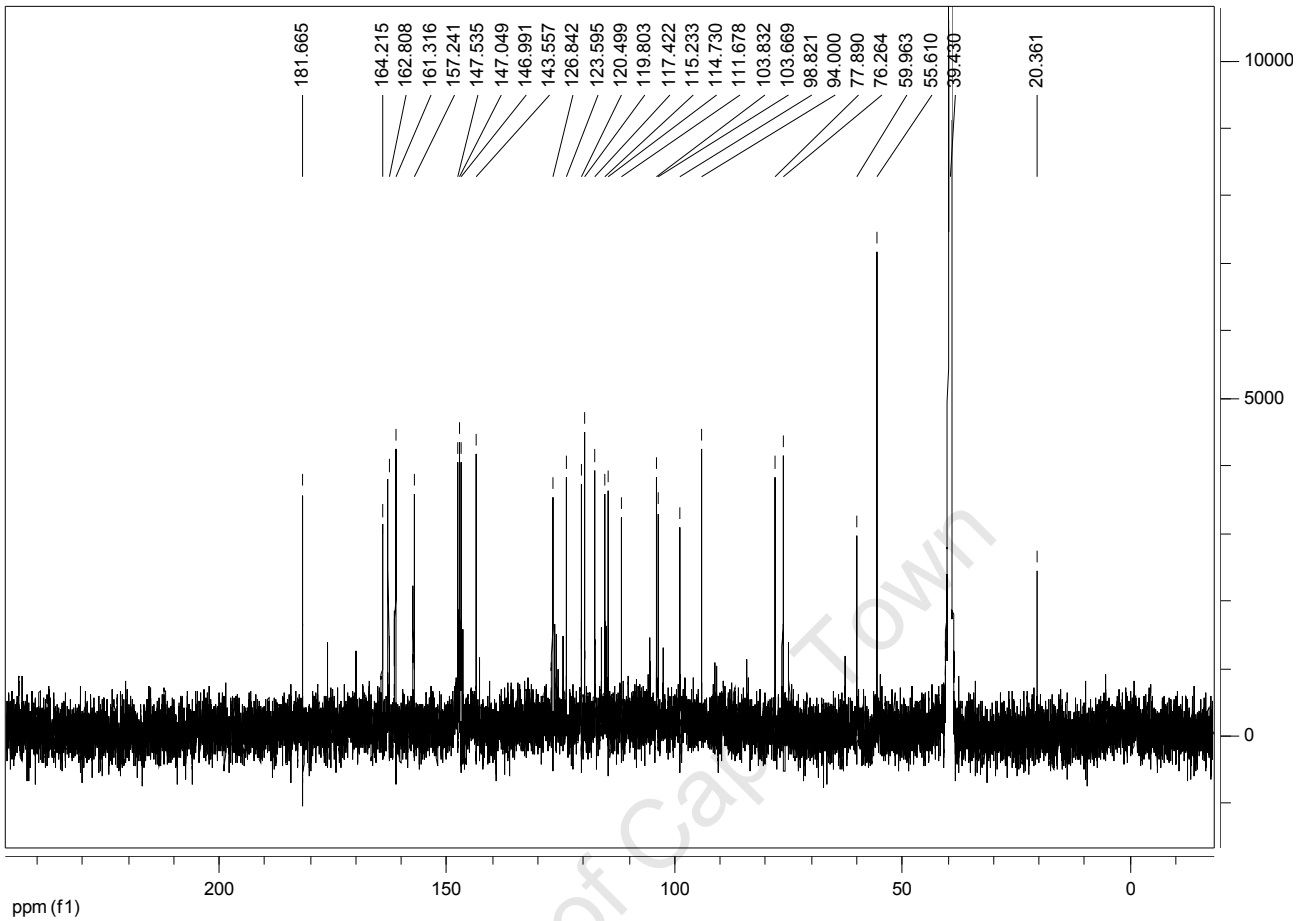

Figure 144 ^{13}C NMR spectrum of compound 4

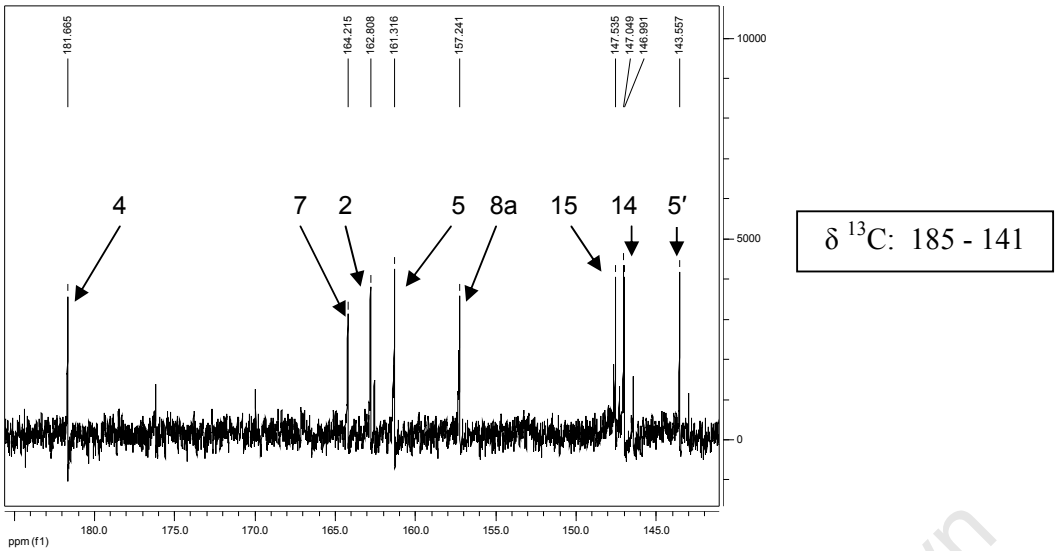

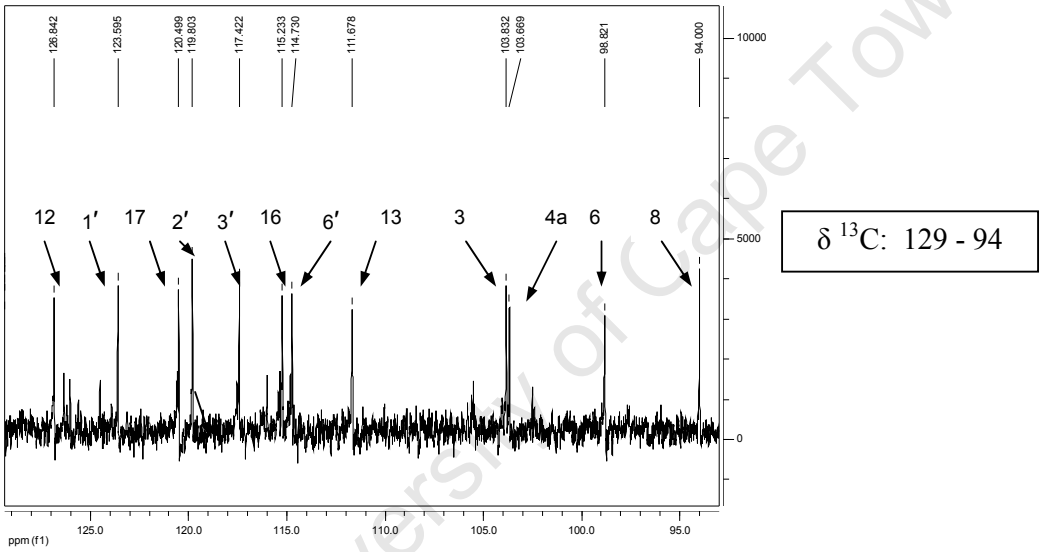

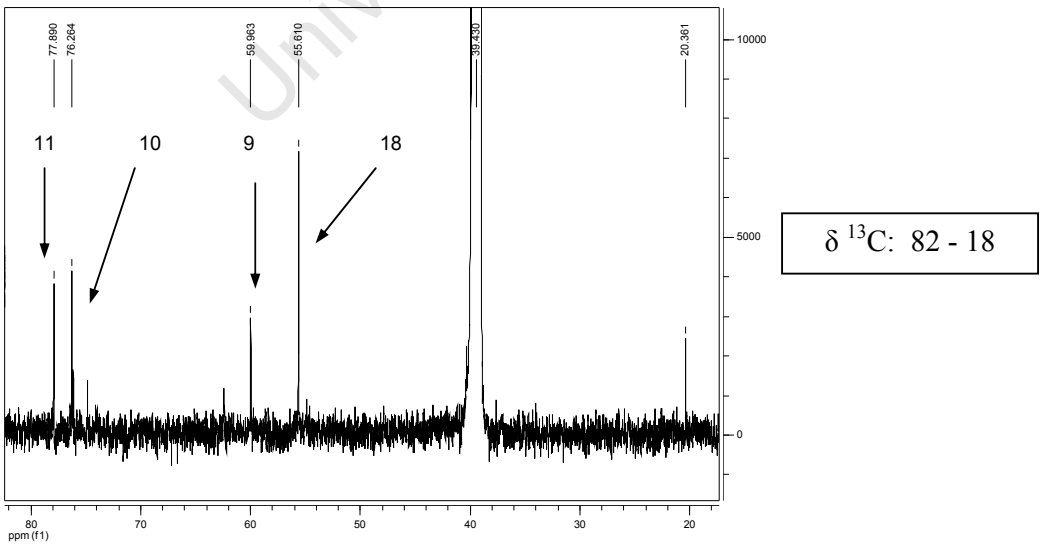

Figure 145 ^{13}C peaks of compound 4

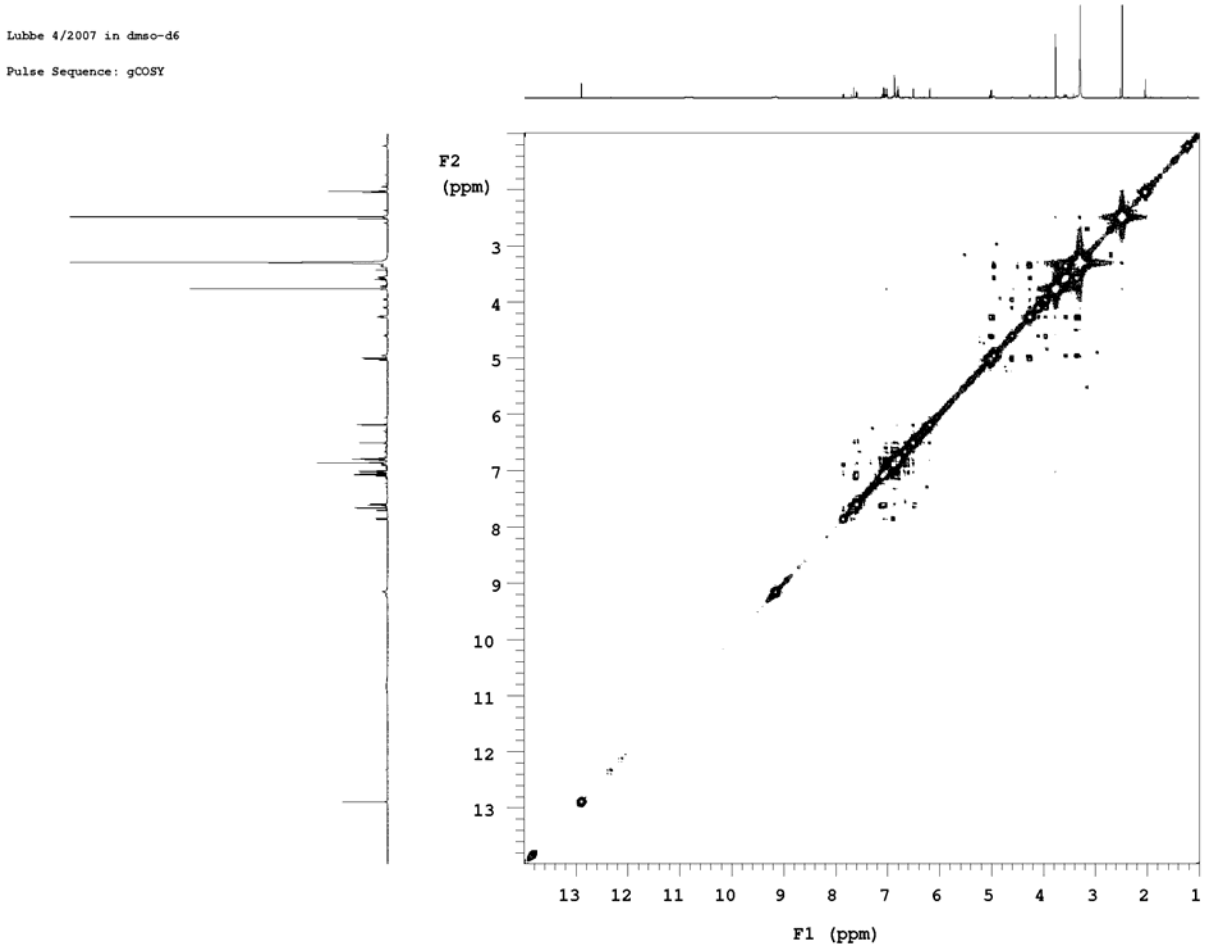

Figure 146 COSY spectrum of compound 4

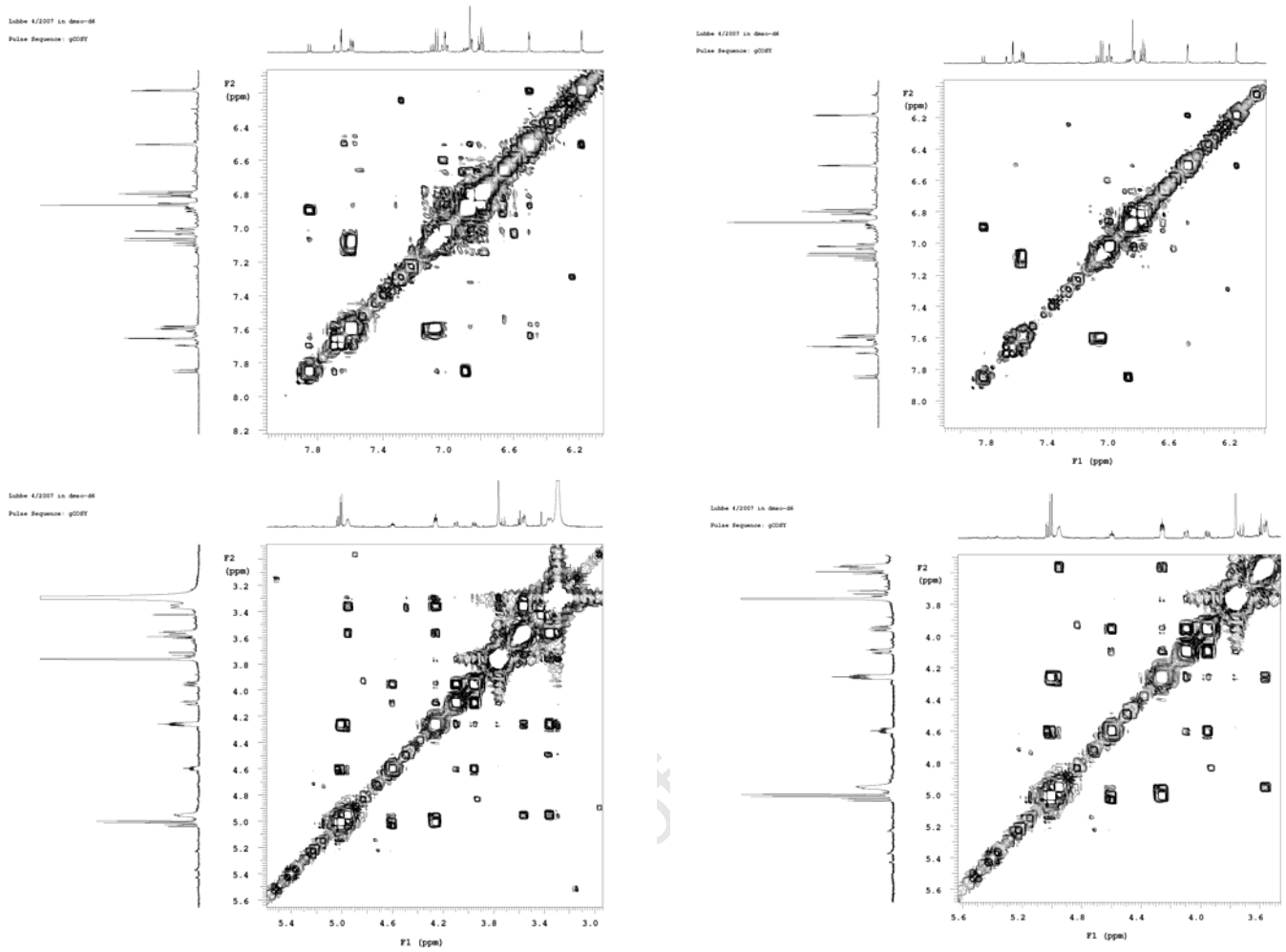

Figure 147 Proton correlations of compound 4

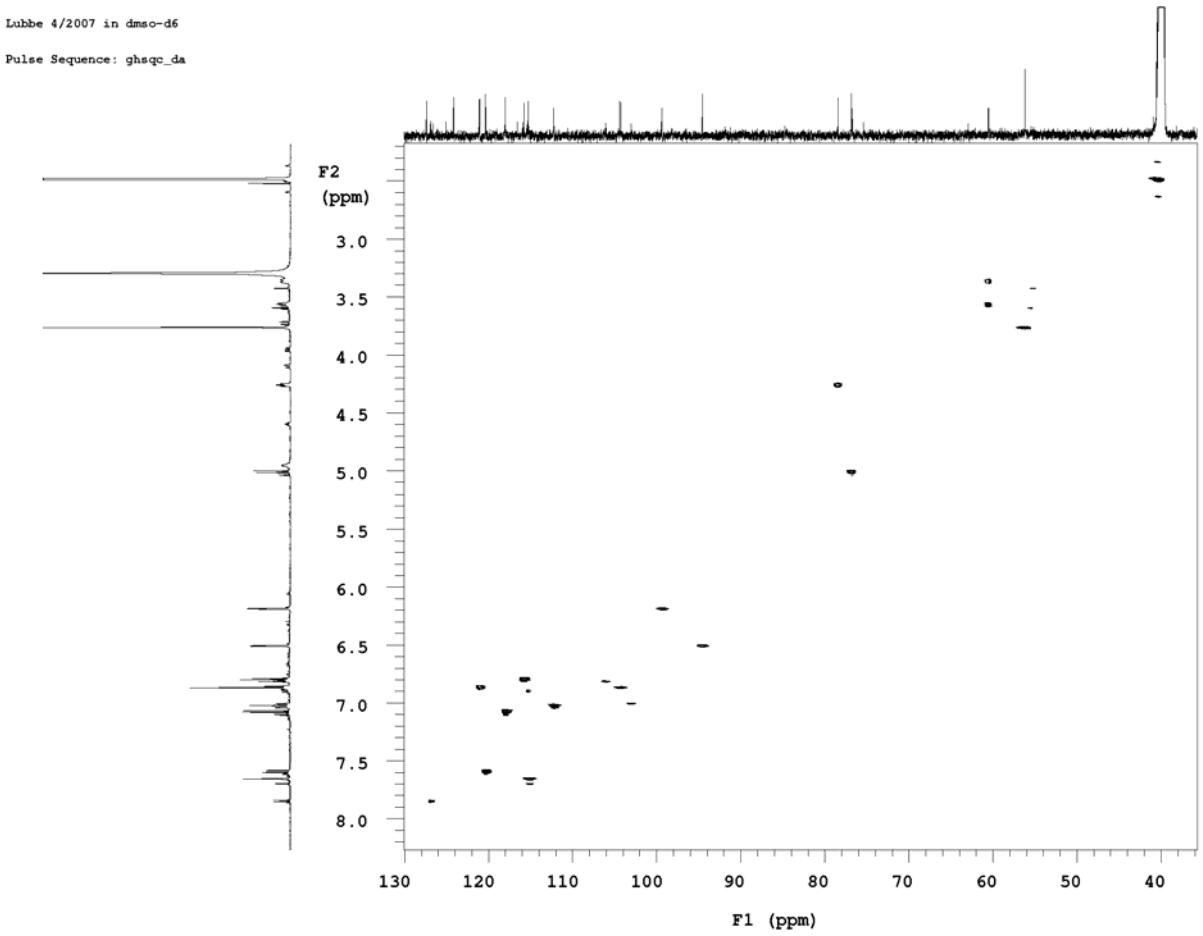

Figure 148 HSQC spectrum of compound 4

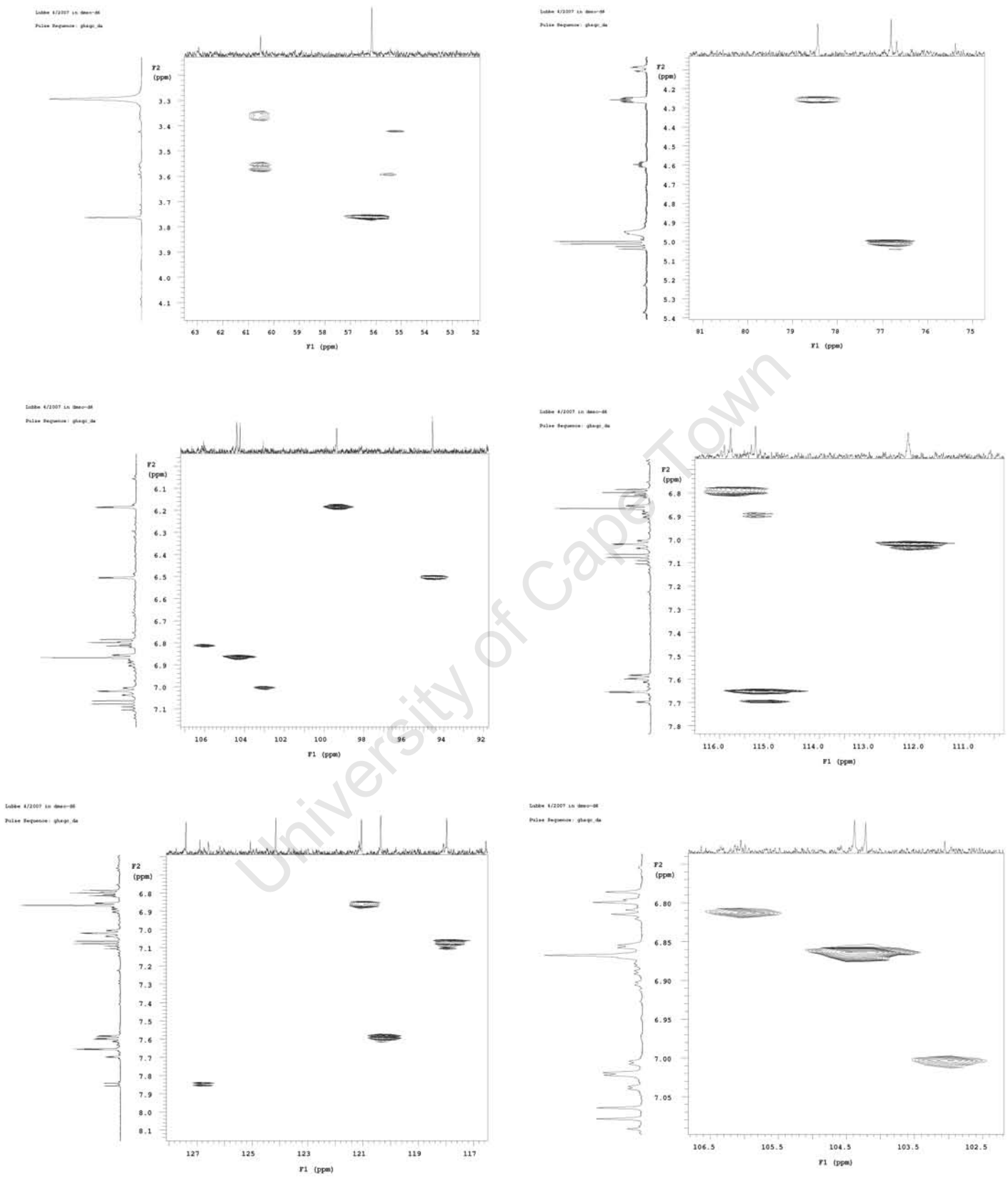

Figure 149 HSQC spectrum of compound 4 (zoom in)

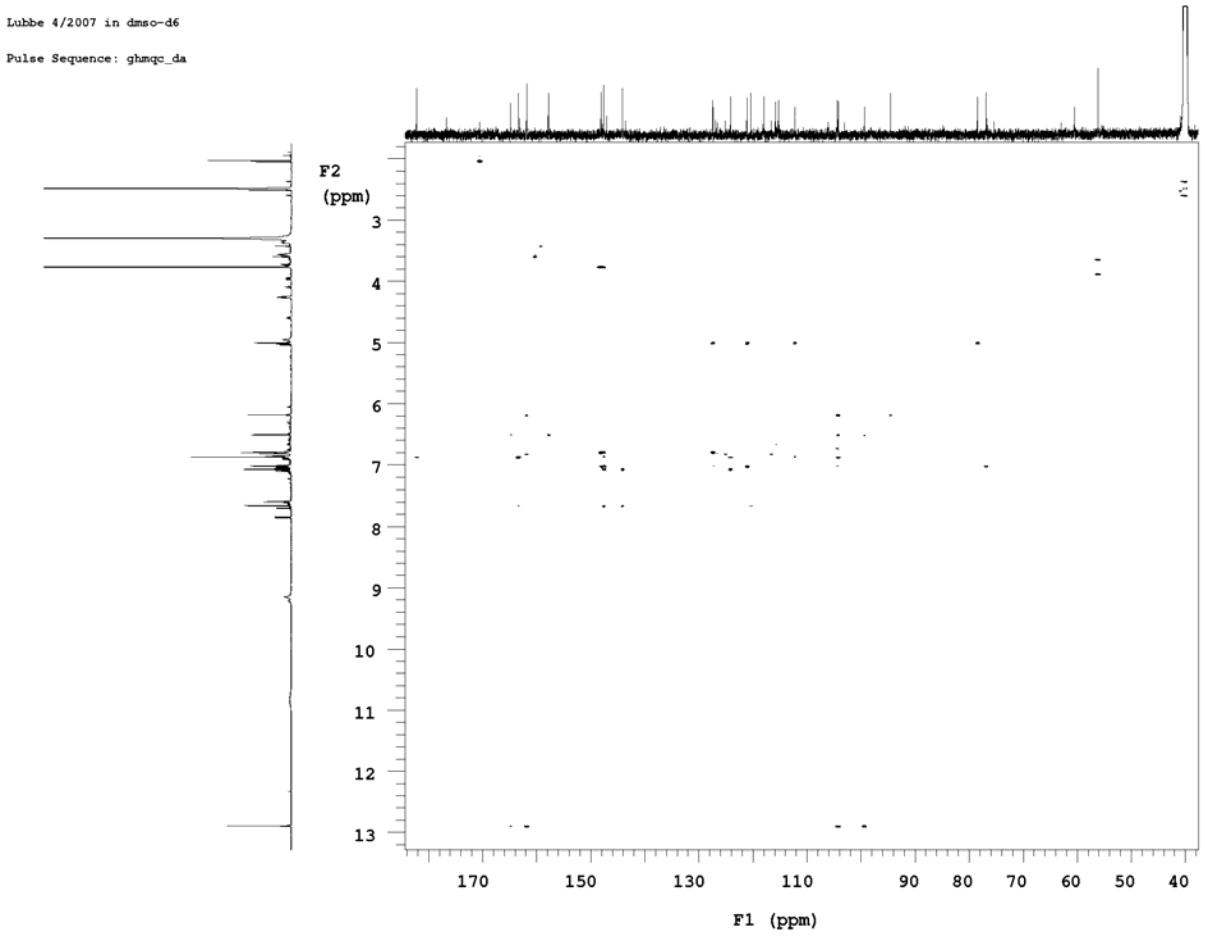

Figure 150 HMQC spectrum of compound 4

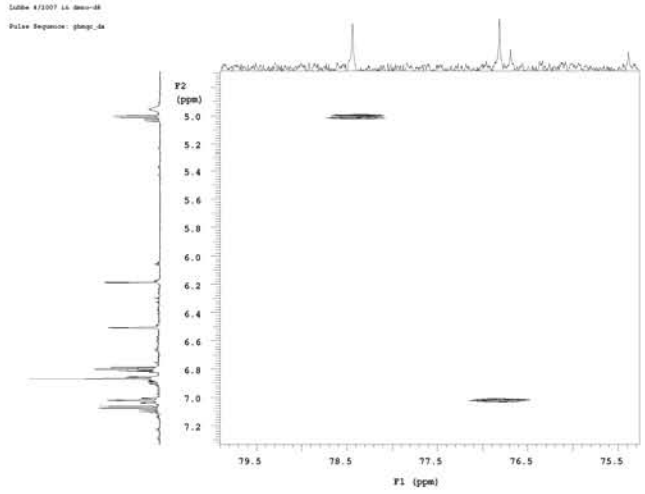

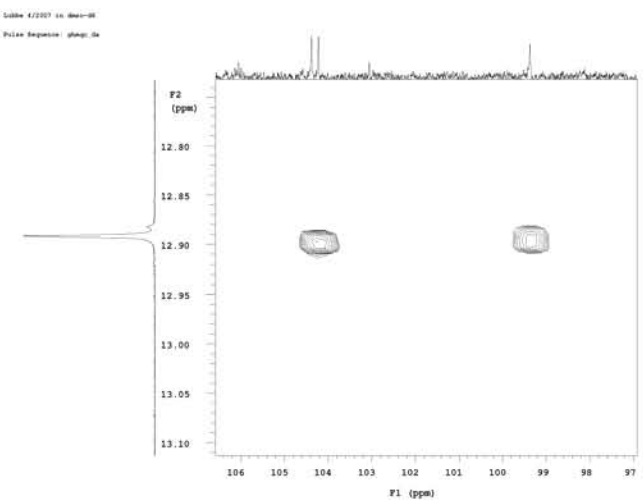

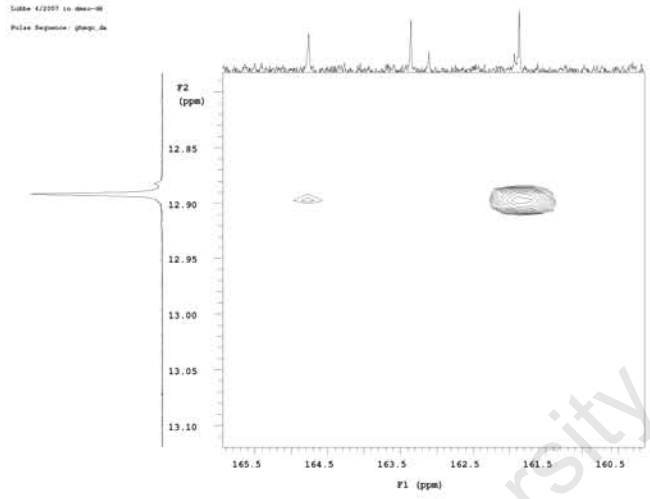

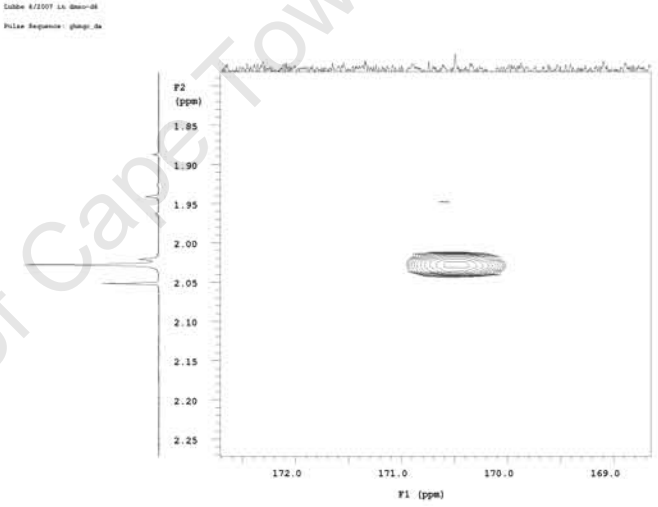

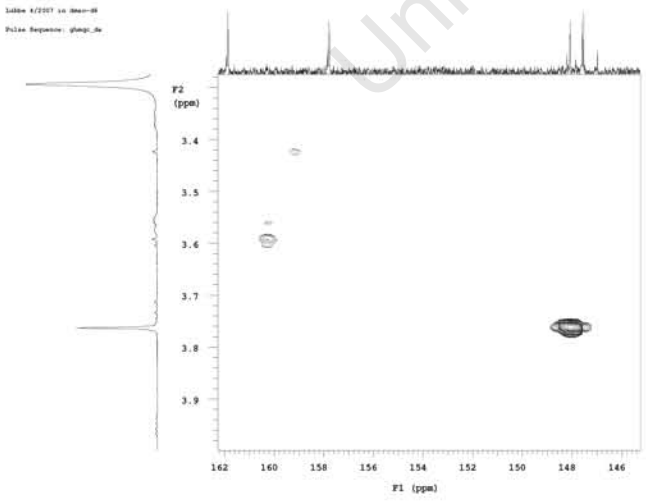

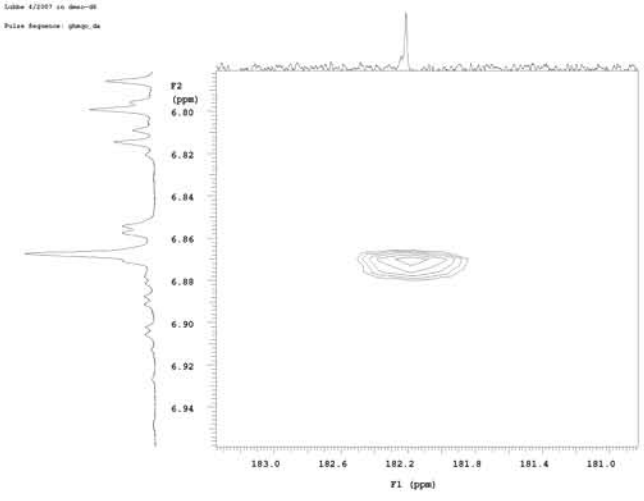

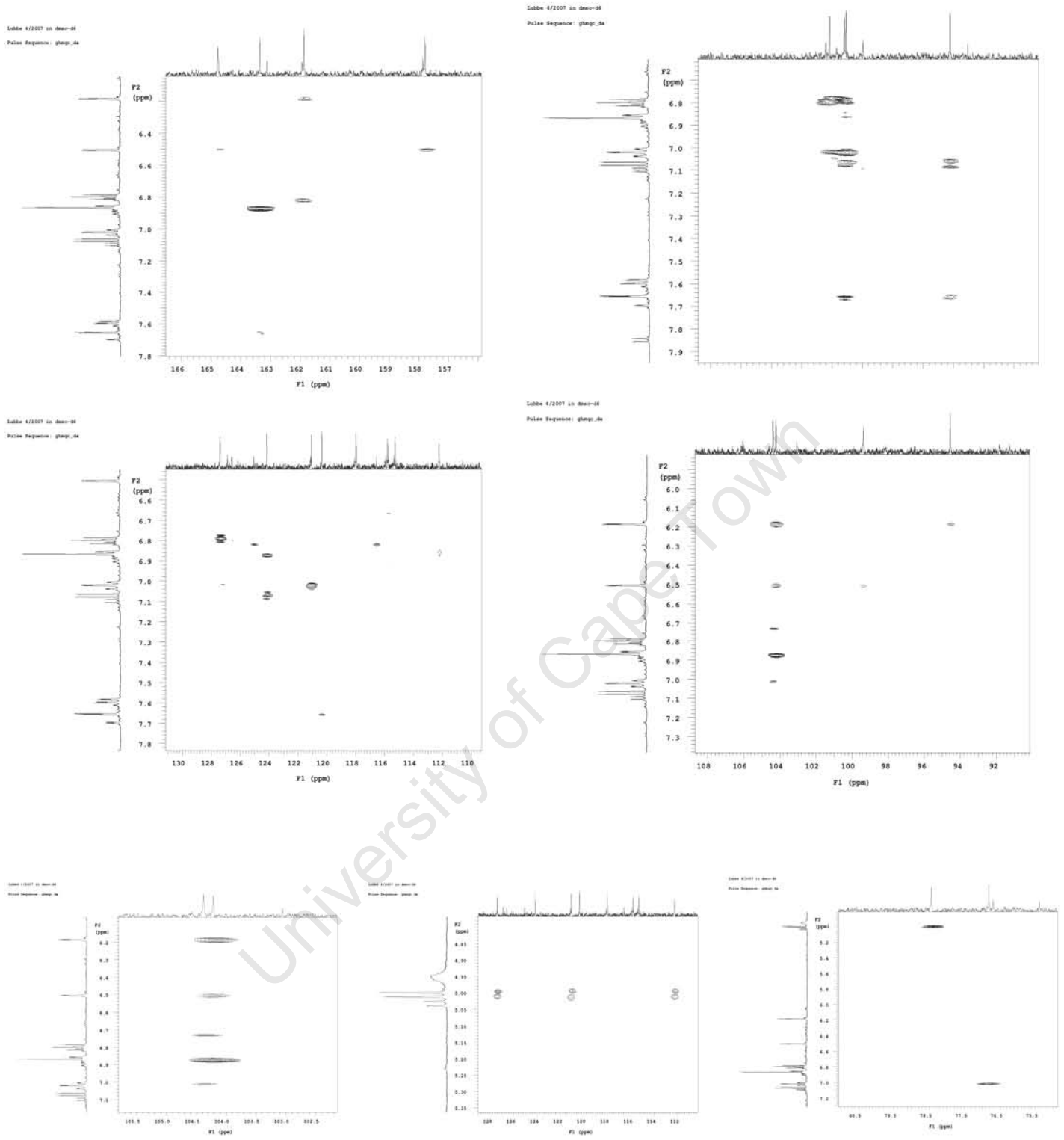

Figure 151 HMQC spectrum of compound 4 (zoom in)

Compound 5

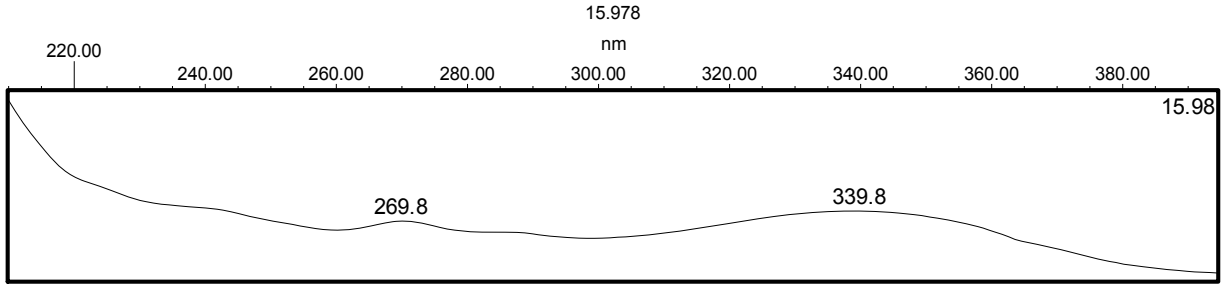

Figure 152 UV spectrum of compound 5

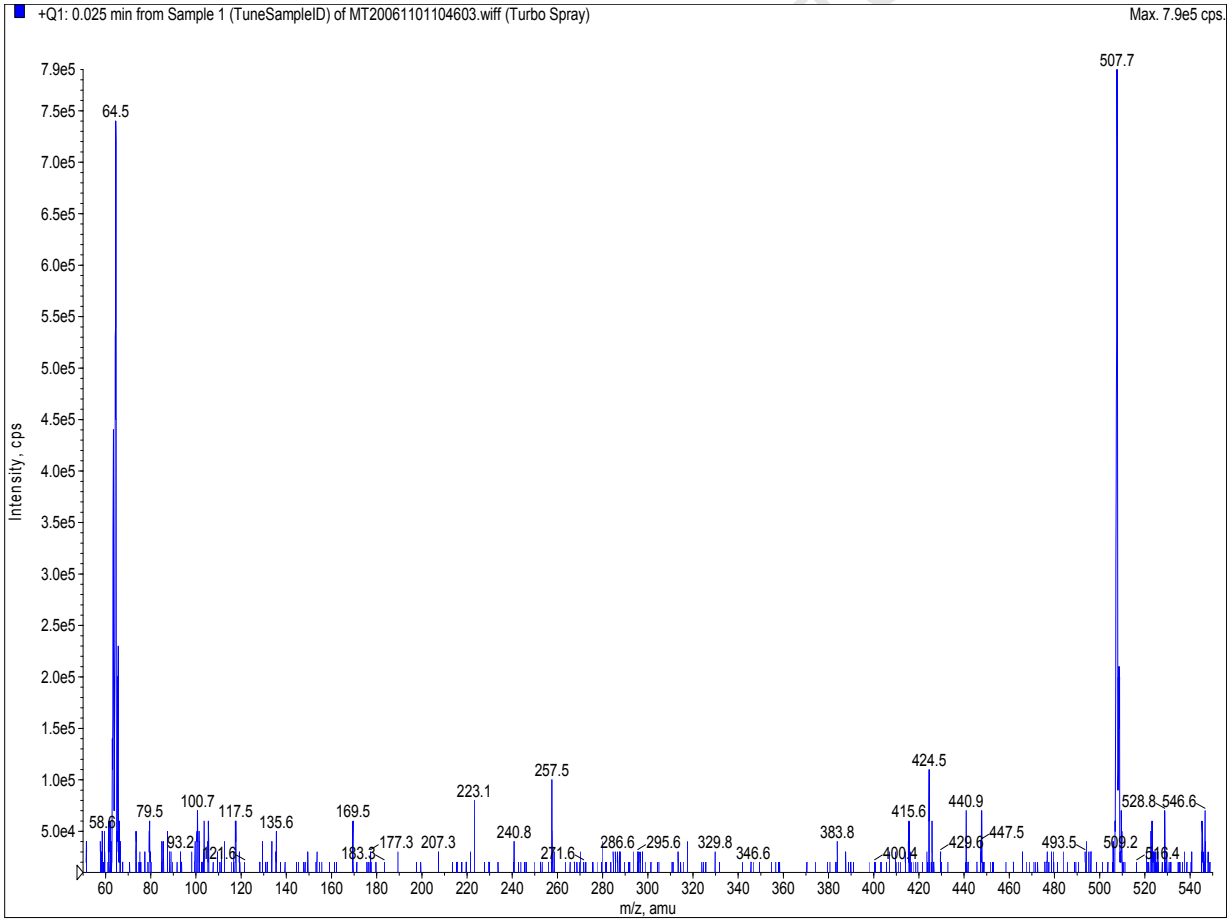

Figure 153 Mass spectrum of compound 5

Mass	Calc. Mass	mDa	PPM	DBE	Formula	Score	C	H	O
507.1298	507.1291	0.7	1.3	16.5	C27 H23 O10	1	27	23	1...
	507.0927	37.1	73.1	17.5	C26 H19 O11	2	26	19	1...

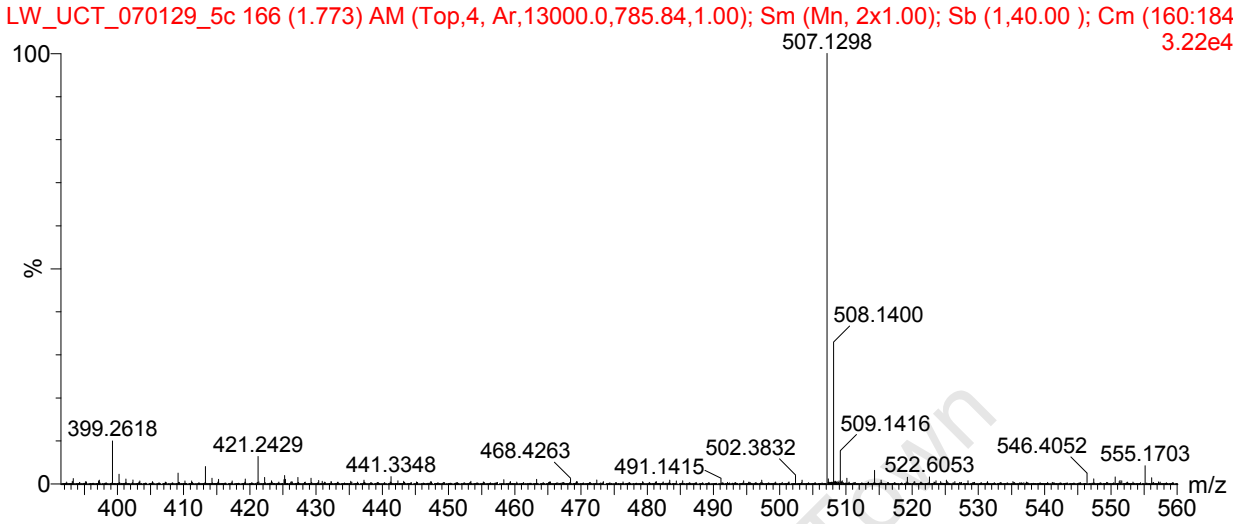

Figure 154 High resolution mass spectrum of compound 5

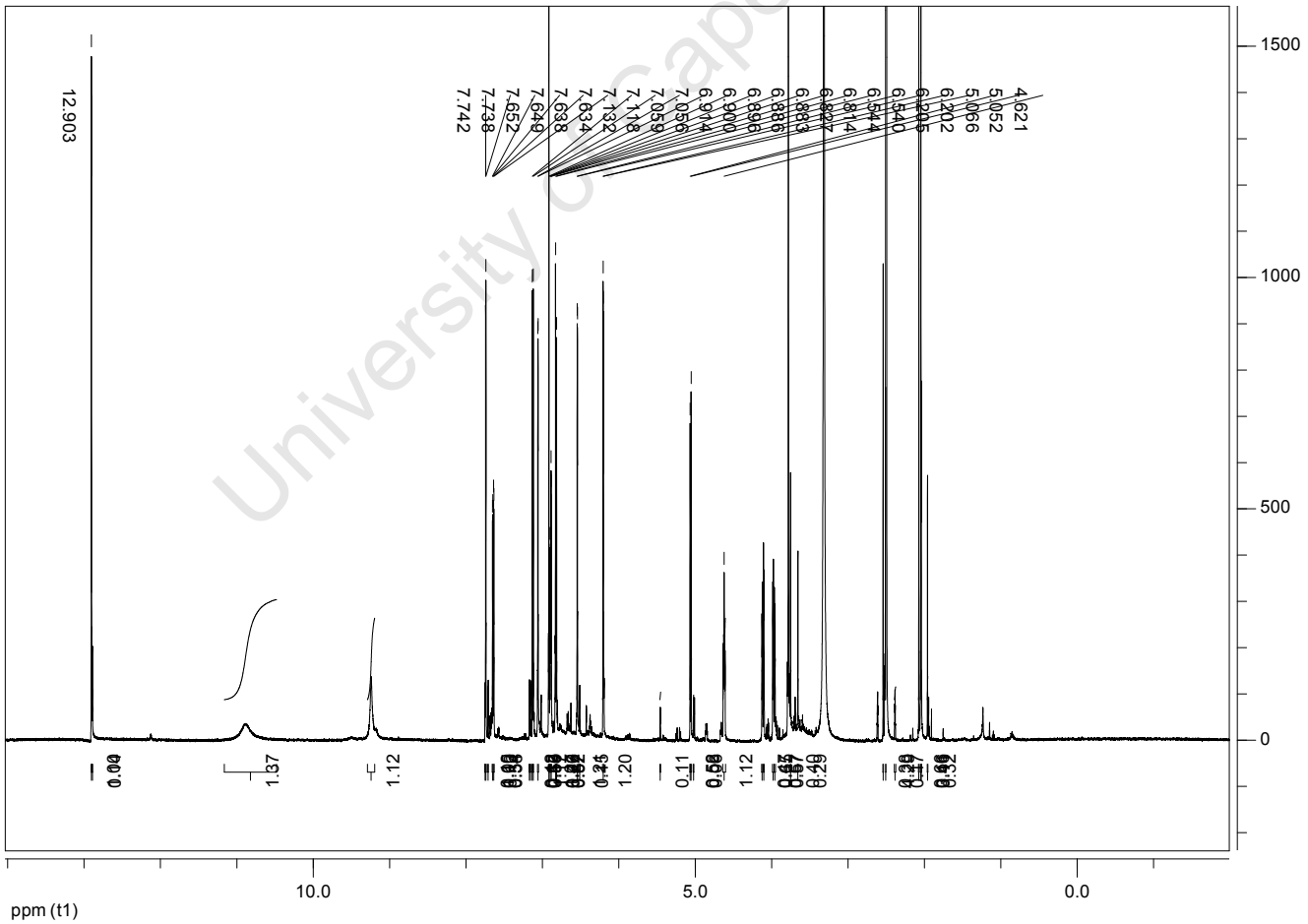

Figure 155 ^{1}H NMR spectrum of compound 5

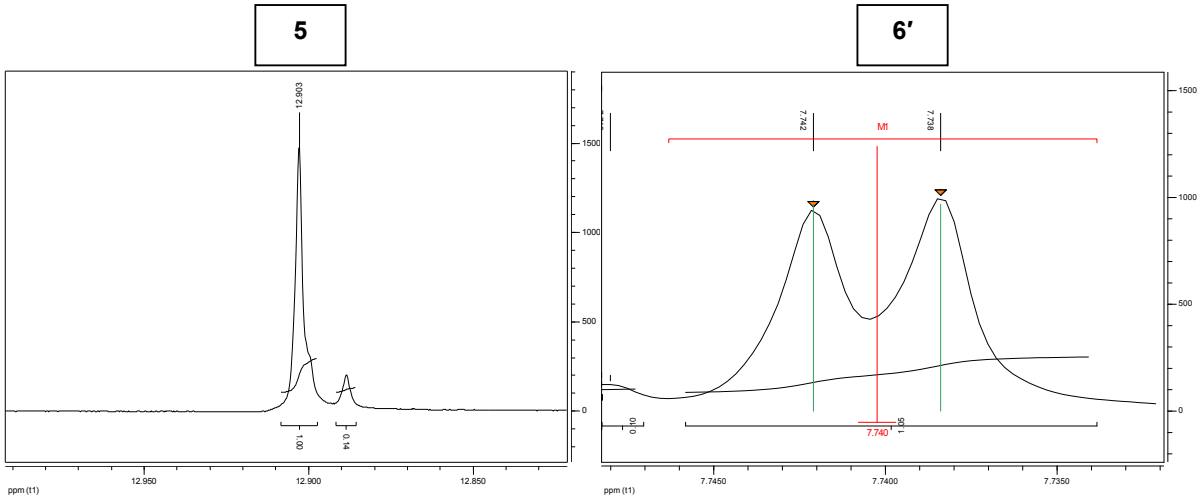

1H-NMR (600 MHz) ppm 7.74 (d, J=2.22 Hz, 1H)

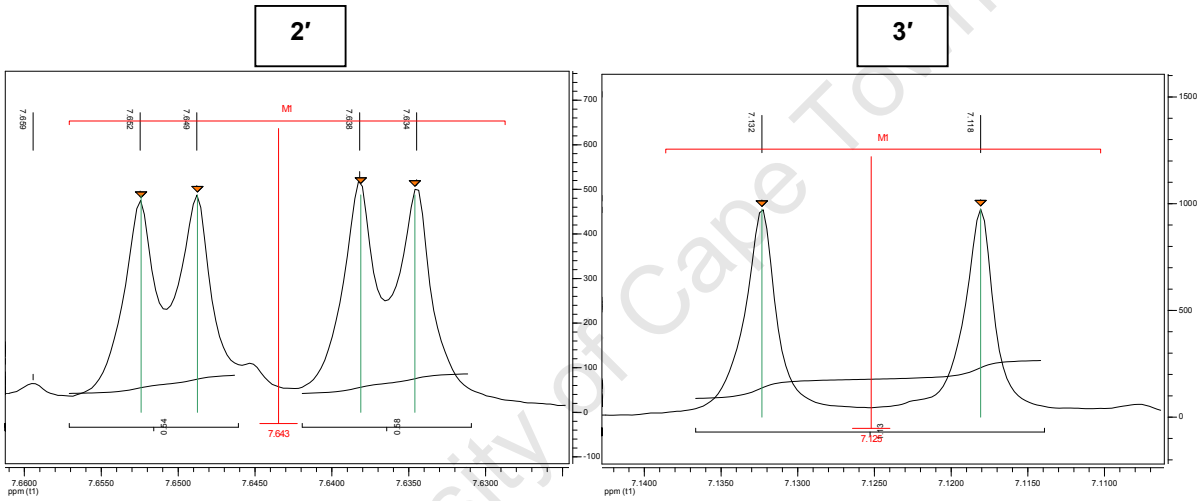

1H-NMR (600 MHz) ppm 7.64 (dd, J=2.16, 8.53 Hz, 1H)

1H-NMR (600 MHz) ppm 7.13 (d, J=8.56 Hz, 1H)

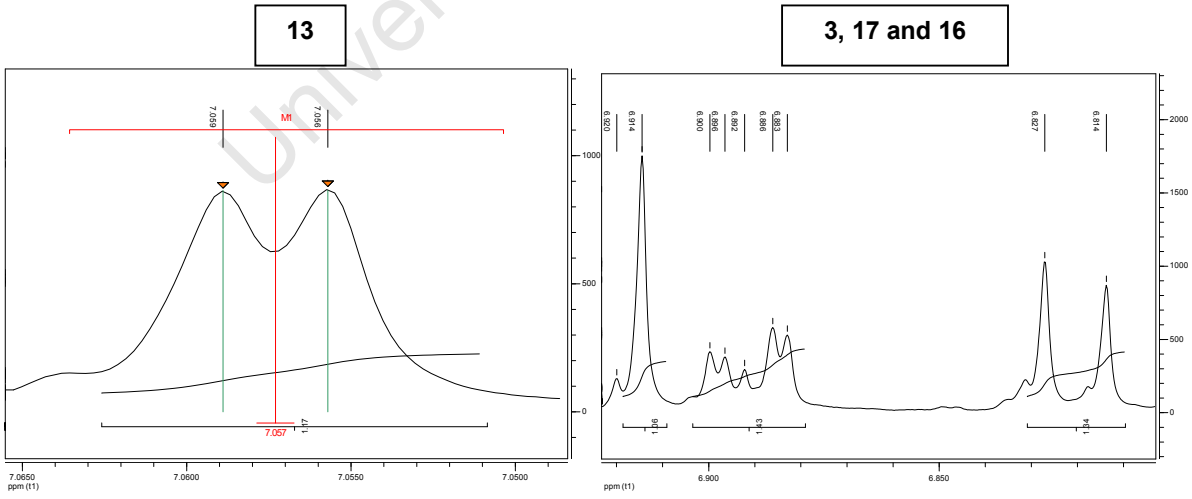

1H-NMR (600 MHz) ppm 7.06 (d, J=1.91 Hz, 1H)

3

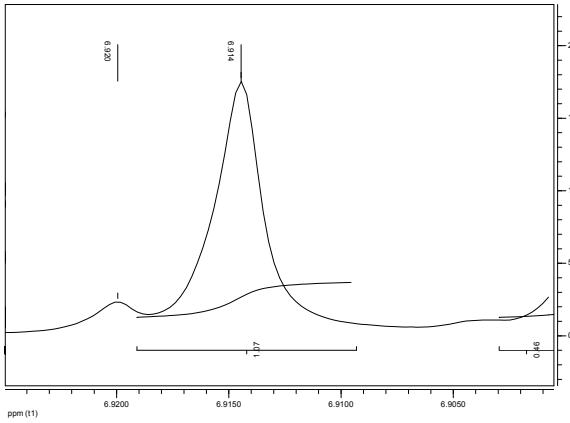

17

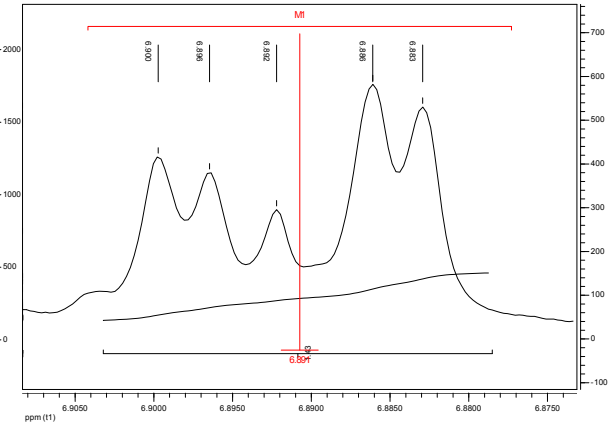

1H-NMR (600 MHz) ppm 6.89 (m)

16

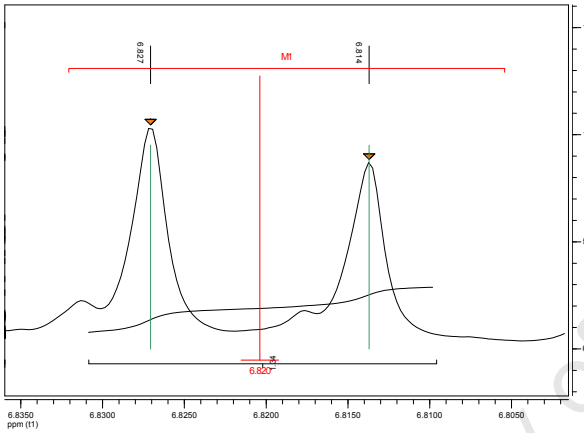

1H-NMR (600 MHz) ppm 6.82 (d, J=8.02 Hz, 1H)

8

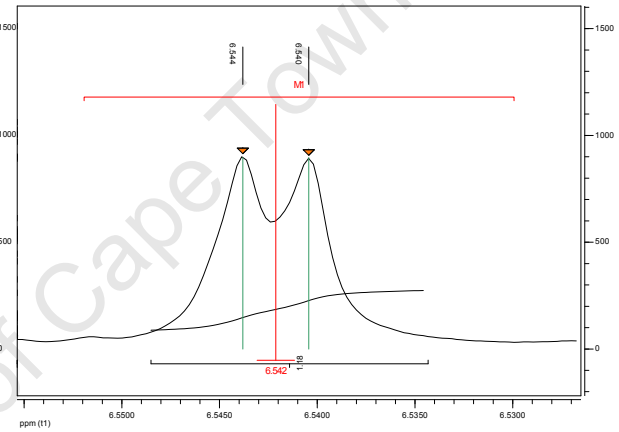

1H-NMR (600 MHz) ppm 6.54 (d, J=2.02 Hz, 1H)

6

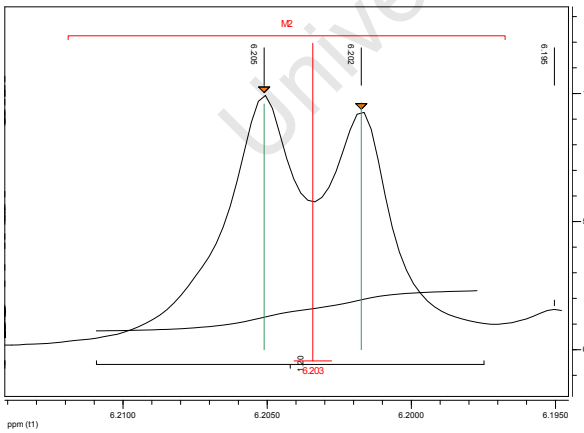

1H-NMR (600 MHz) ppm 6.20 (d, J=2.02 Hz, 1H)

11

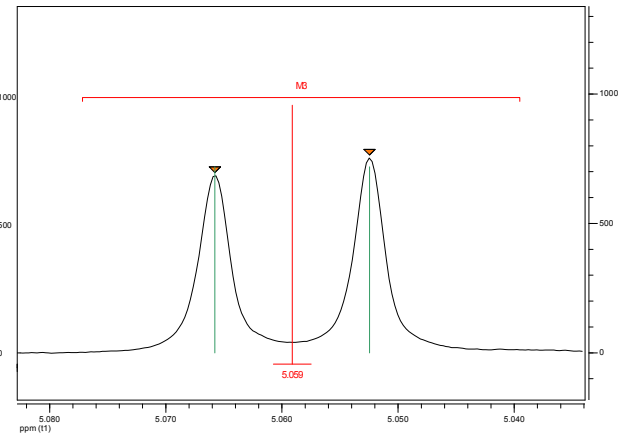

1H-NMR (600 MHz) ppm 5.06 (d, J=7.99 Hz, 1H)

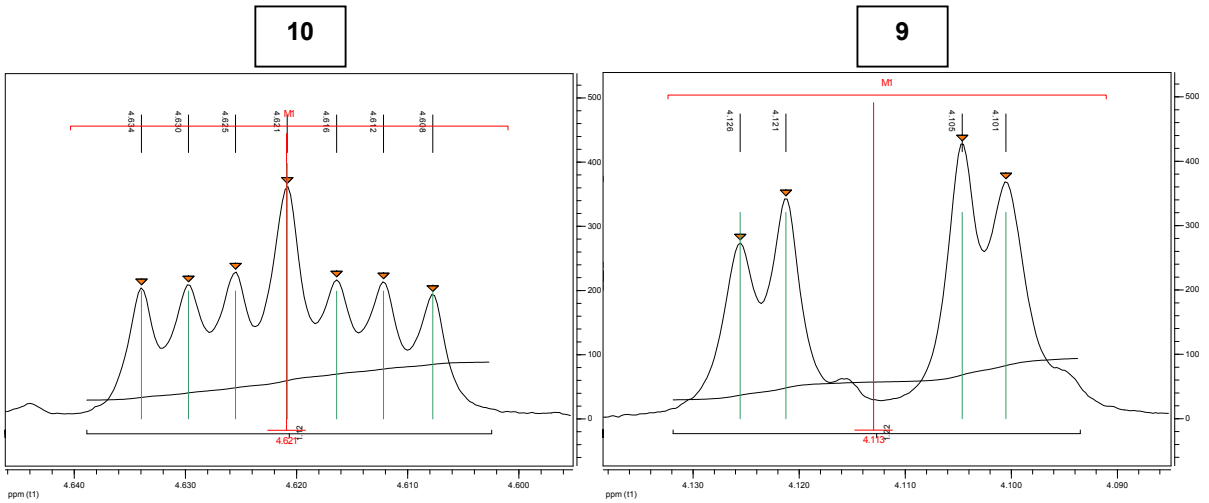

1H-NMR (600 MHz) ppm
4.62 (ddd, J=2.60, 5.13, 7.85 Hz, 1H)

1H-NMR (600 MHz) ppm 4.11 (dd, J=2.53, 12.50 Hz, 1H)

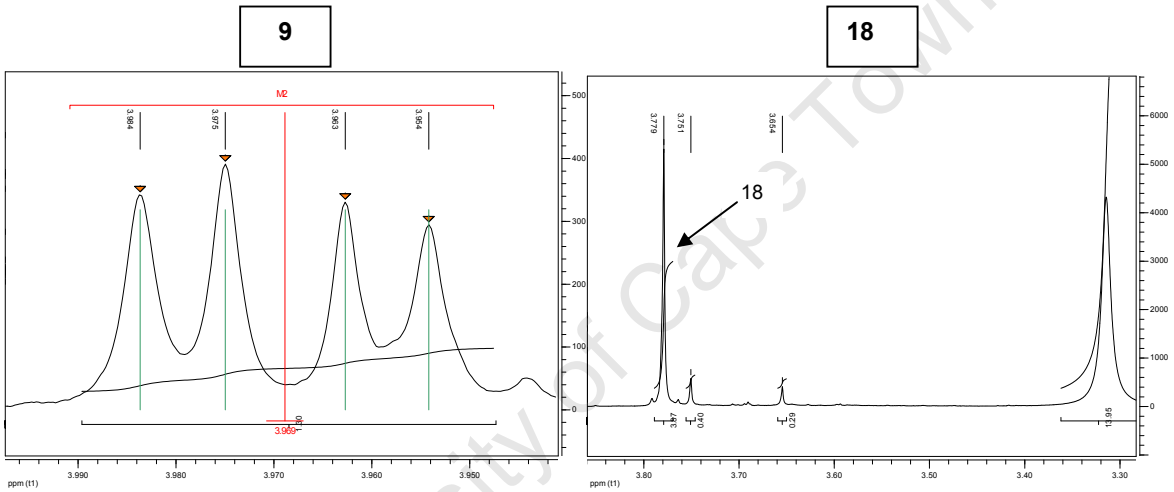

1H-NMR (600 MHz) ppm
3.97 (dd, J=5.17, 12.52 Hz, 1H)

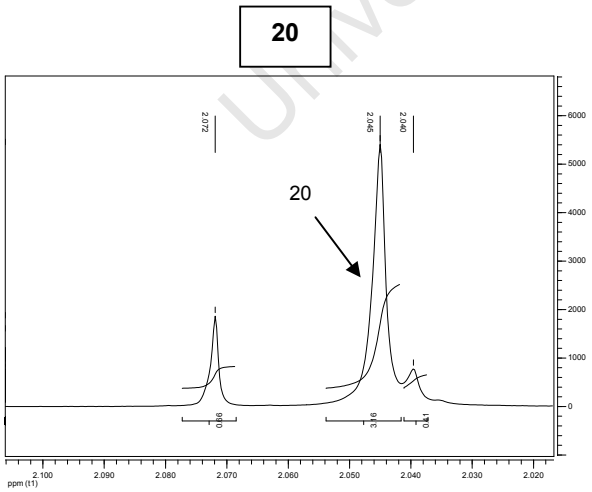

Figure 156 ^{1}H peaks of compound 5

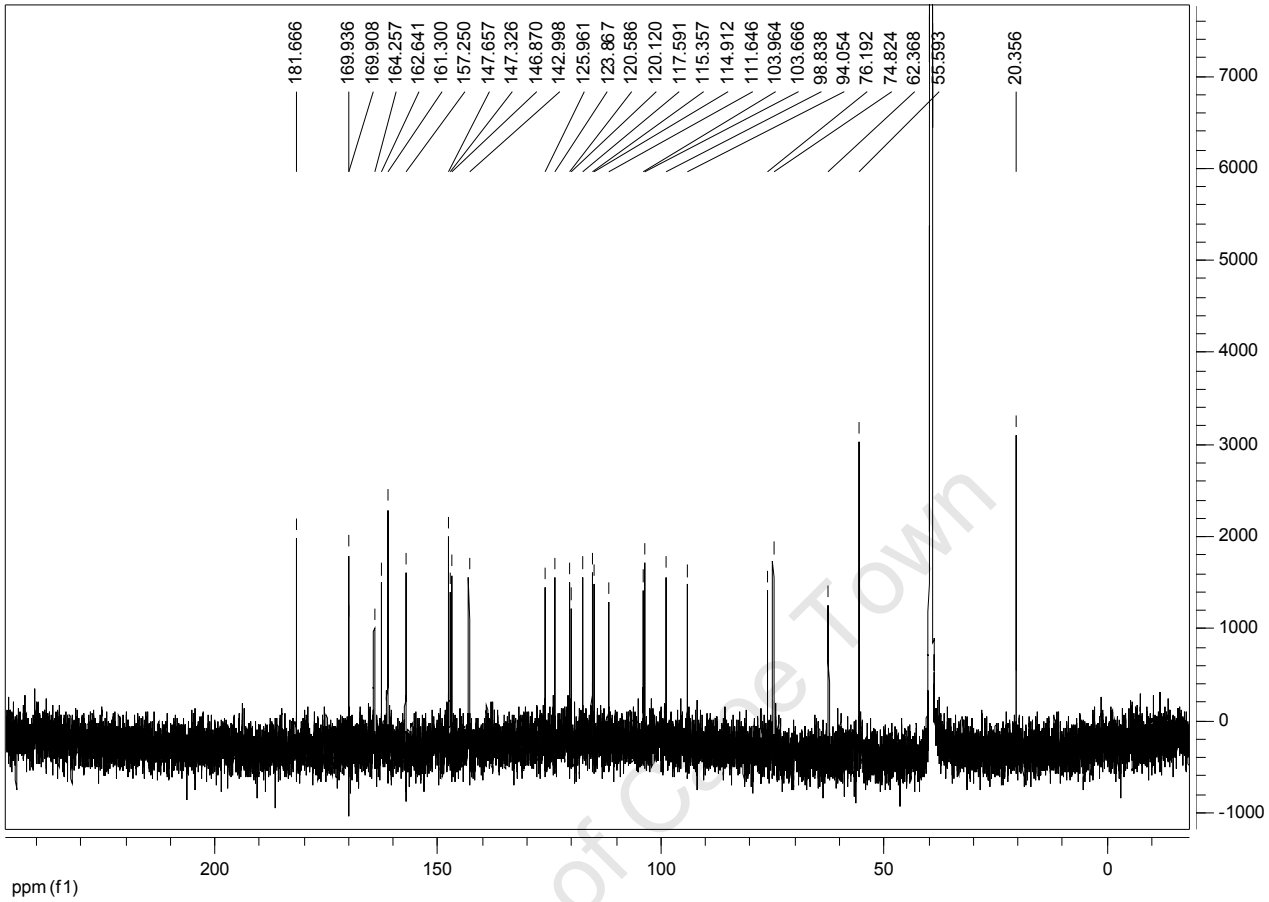

Figure 157 ^{13}C NMR spectrum of compound 5

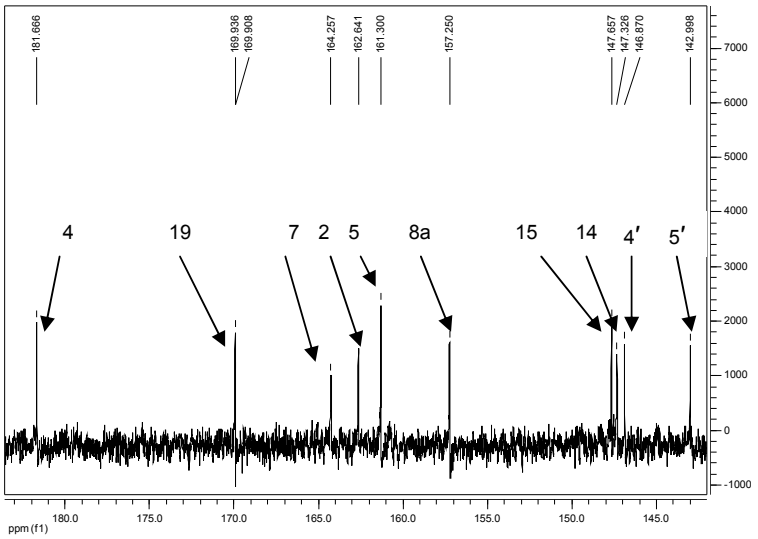

δ ^{13}C: 184 - 142

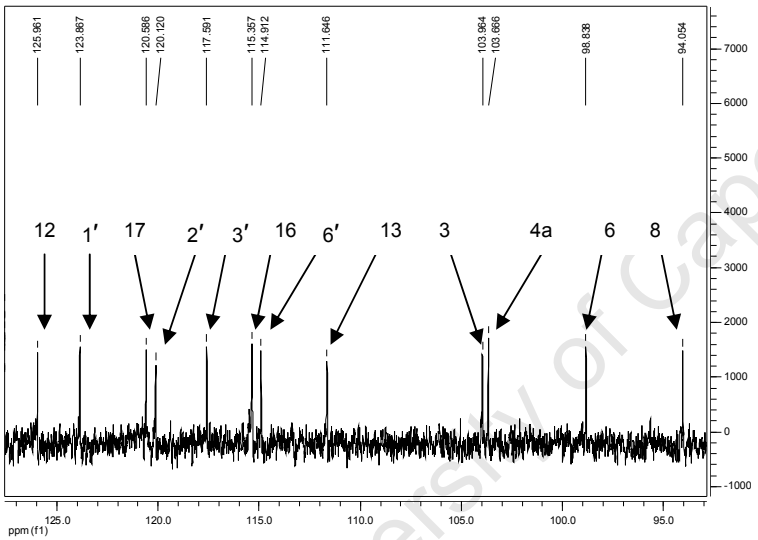

δ ^{13}C: 127 - 93

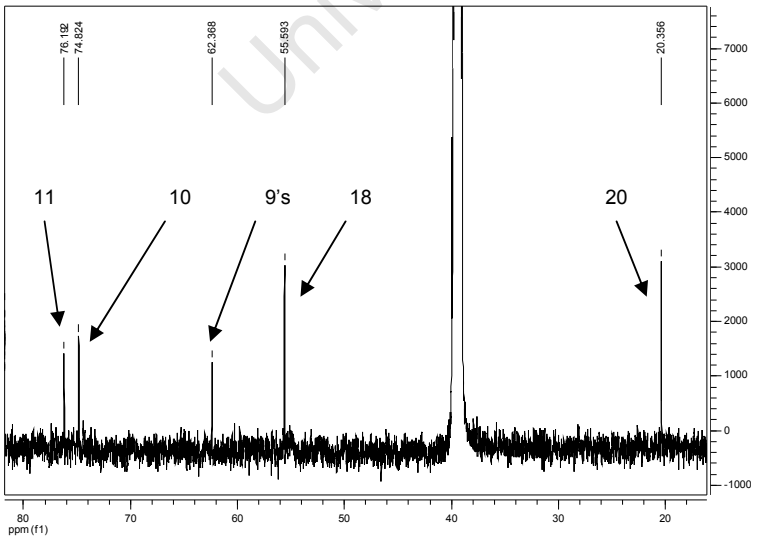

δ ^{13}C: 82 - 16

Figure 158 ^{13}C peaks of compound 5

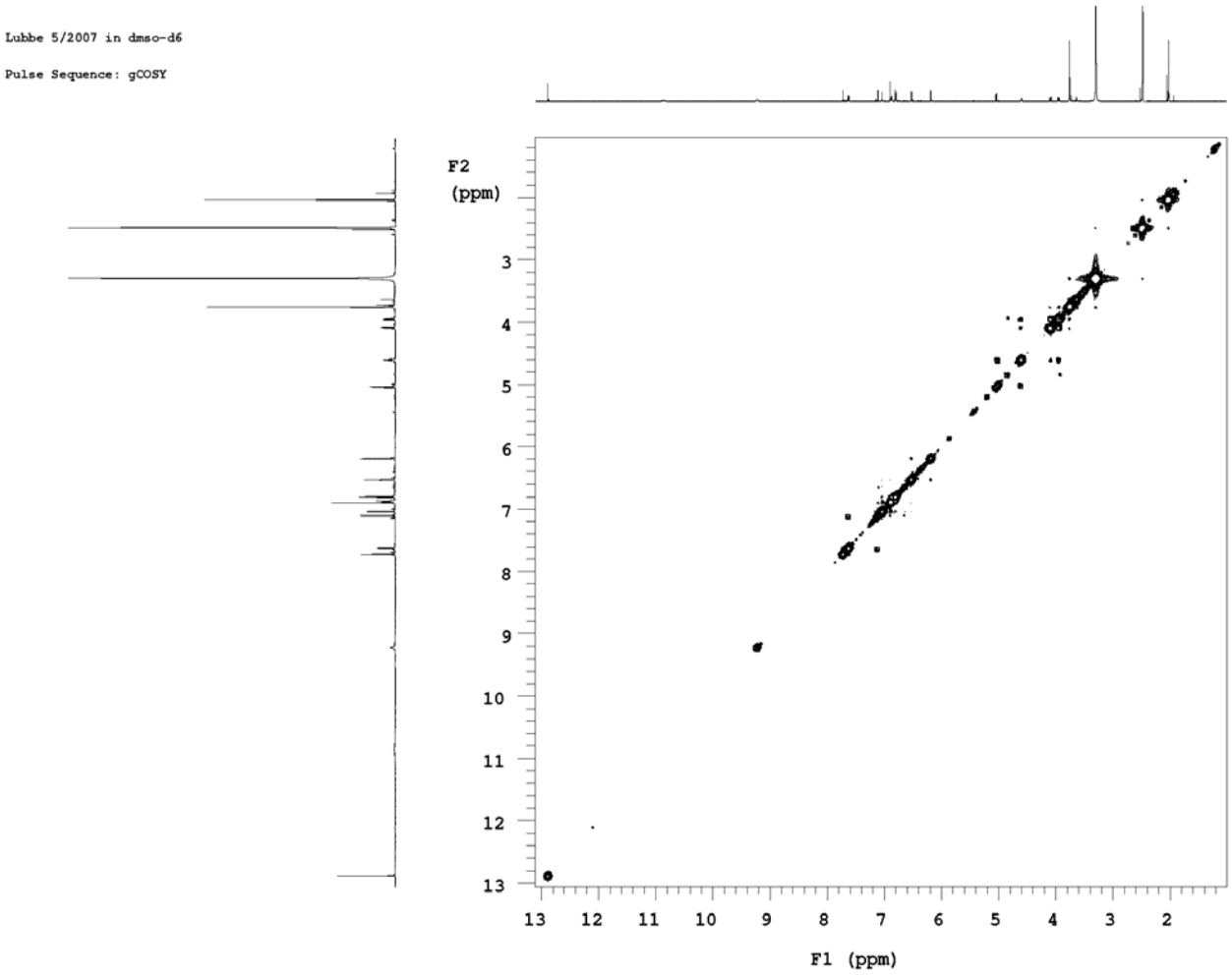

Figure 159 COSY spectrum of compound 5

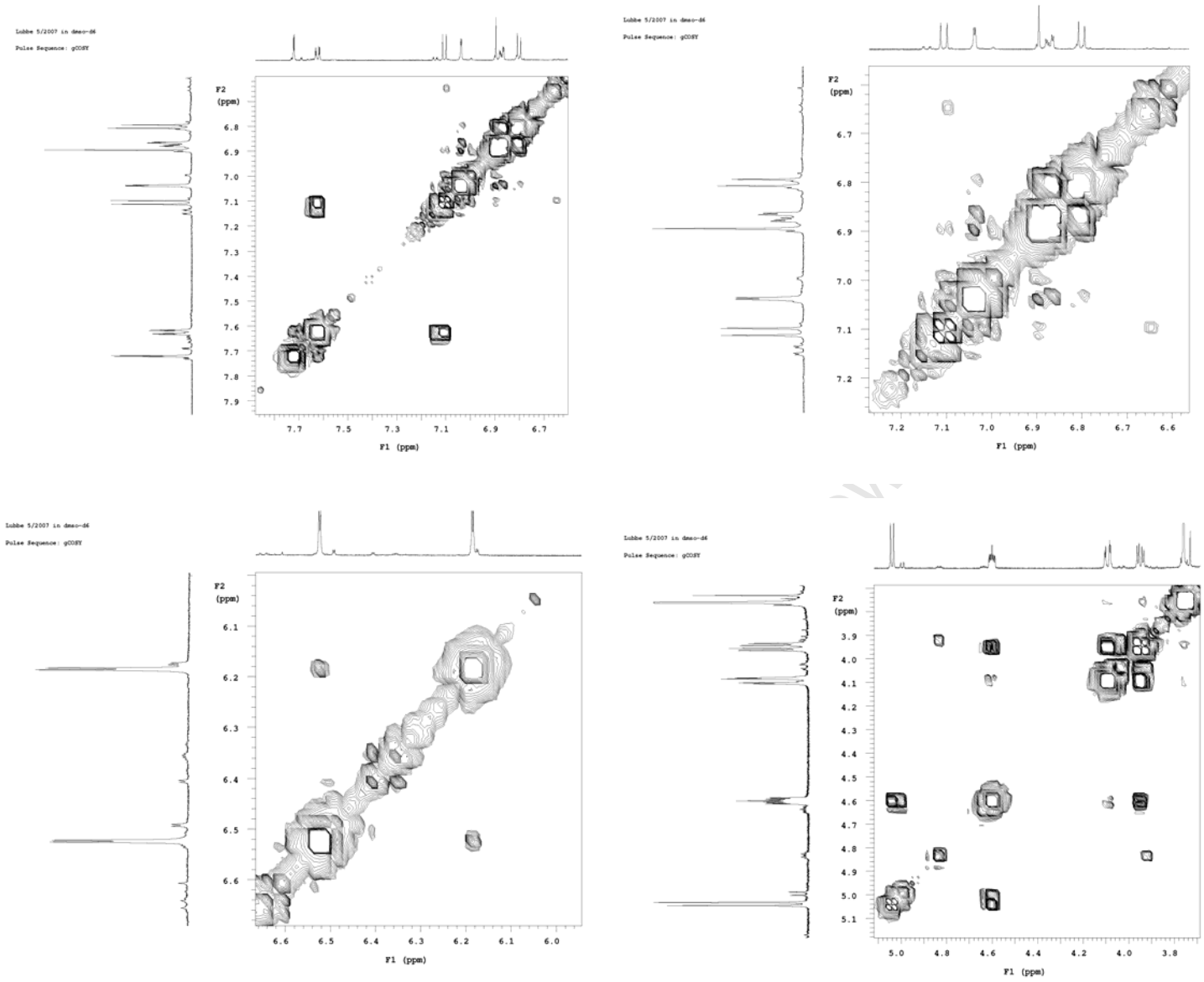

Figure 160 Proton correlations of compound 5 (zoom in)

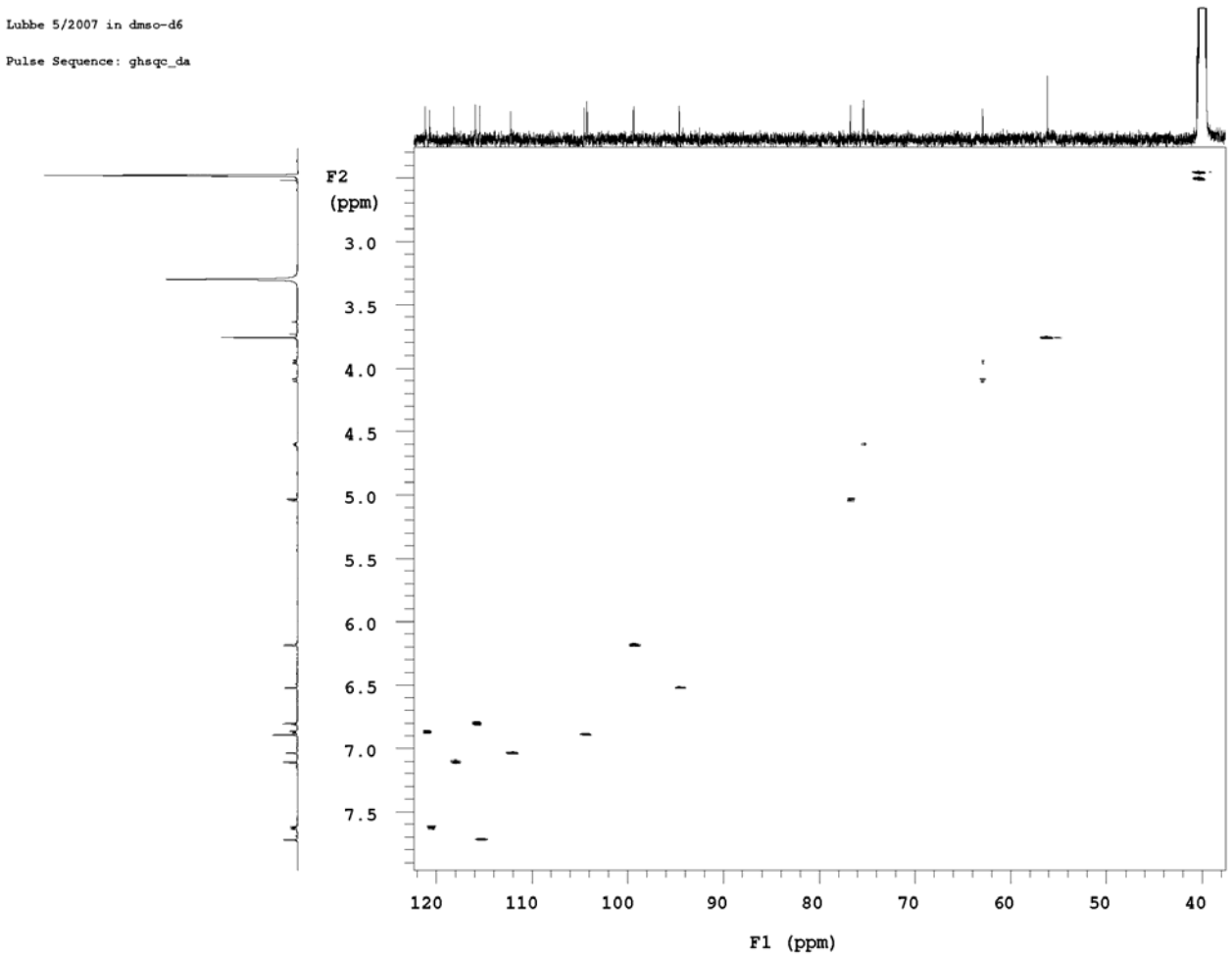

Figure 161 HSQC spectrum of compound 5

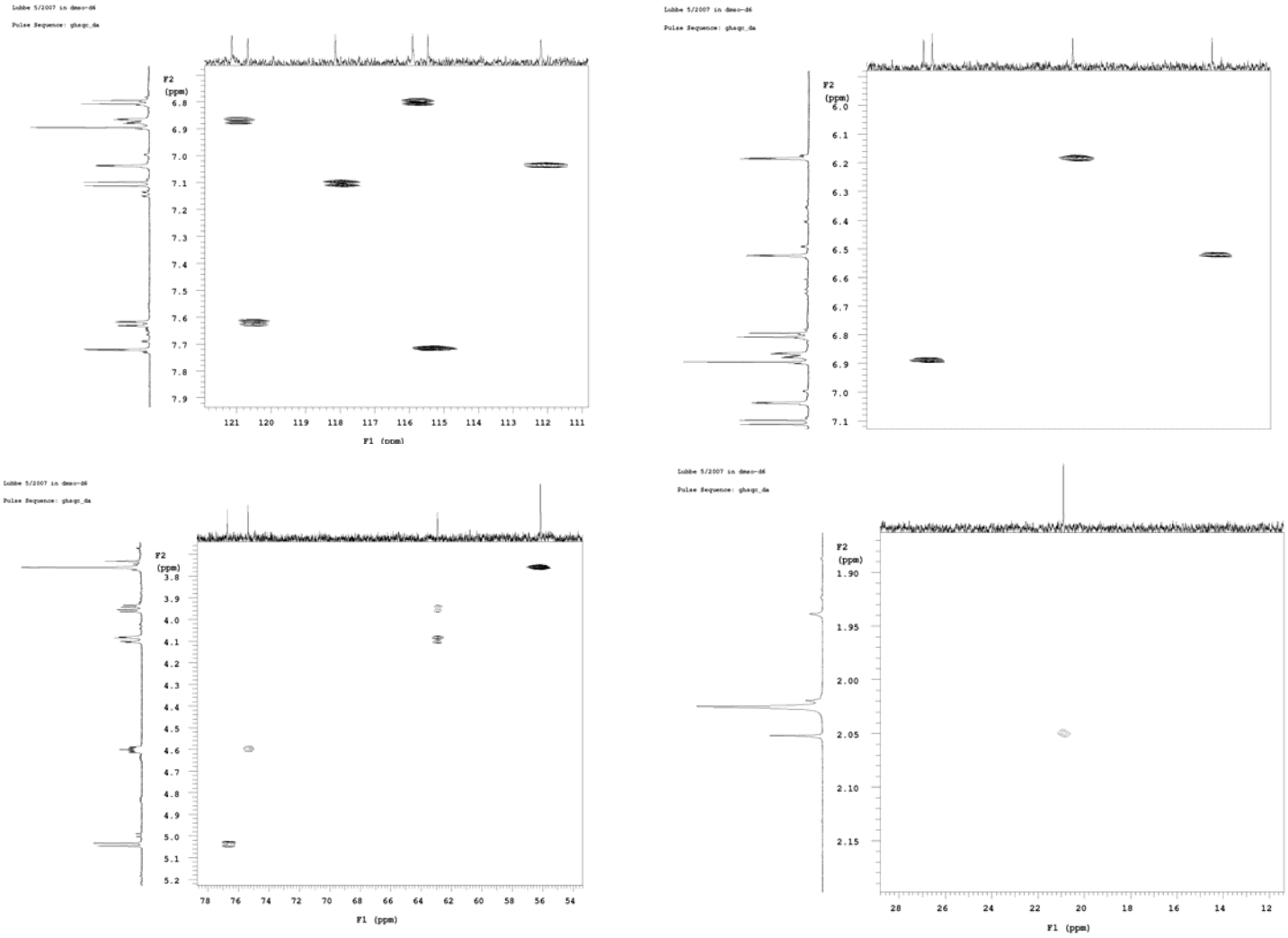

Figure 162 HSQC spectrum of compound 5 (zoom in)

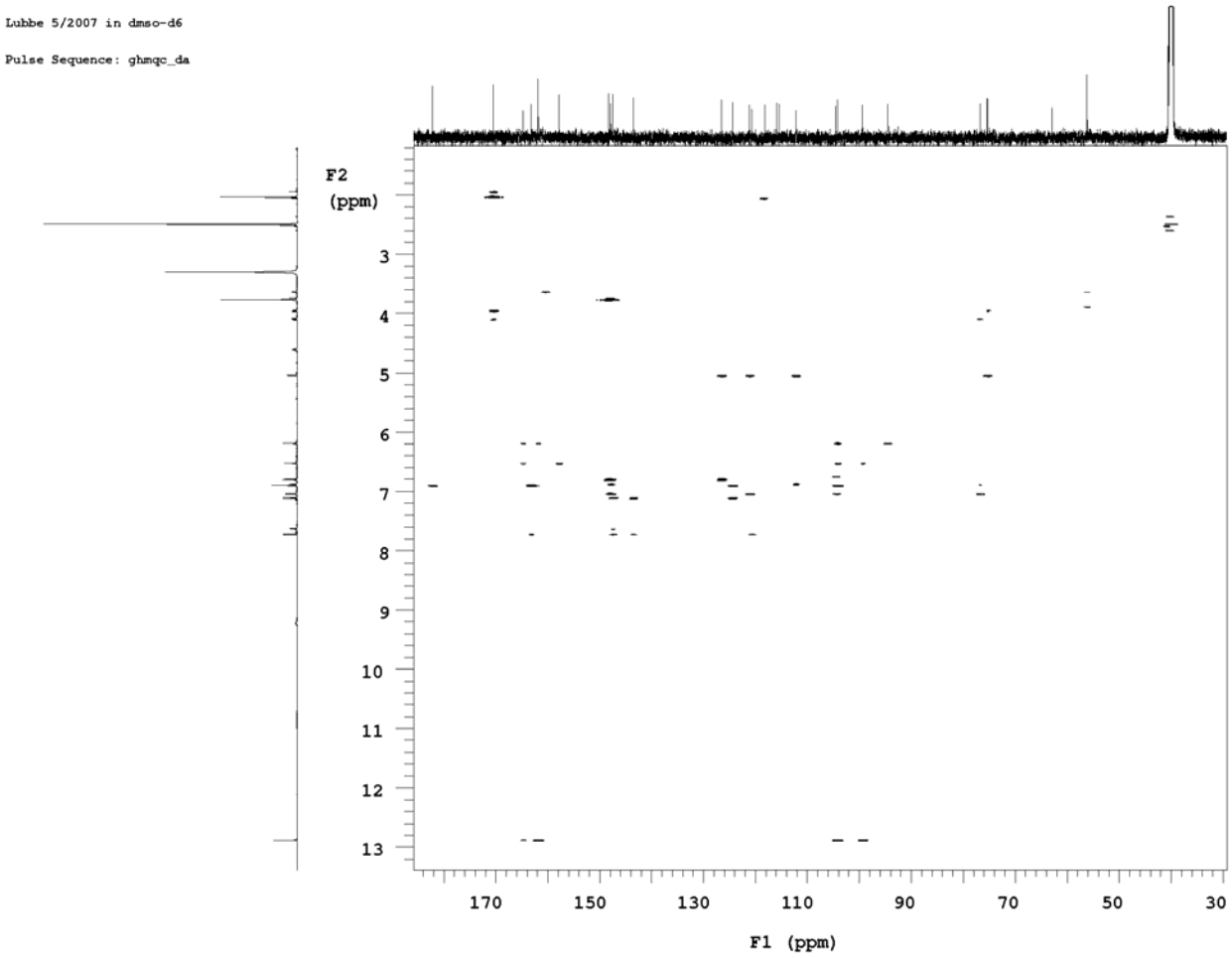

Figure 163 HMQC spectrum of compound 5

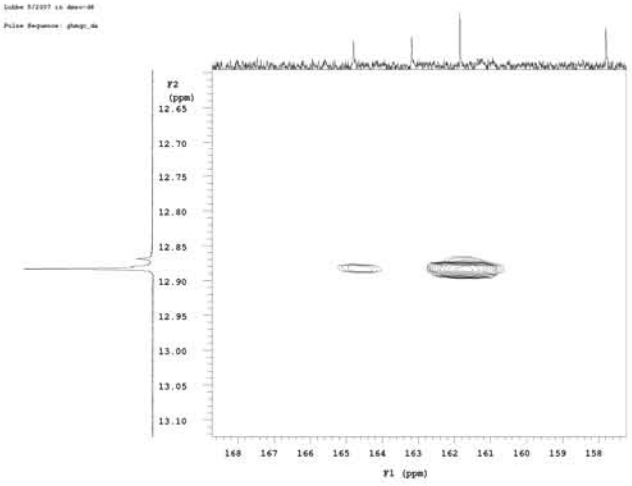

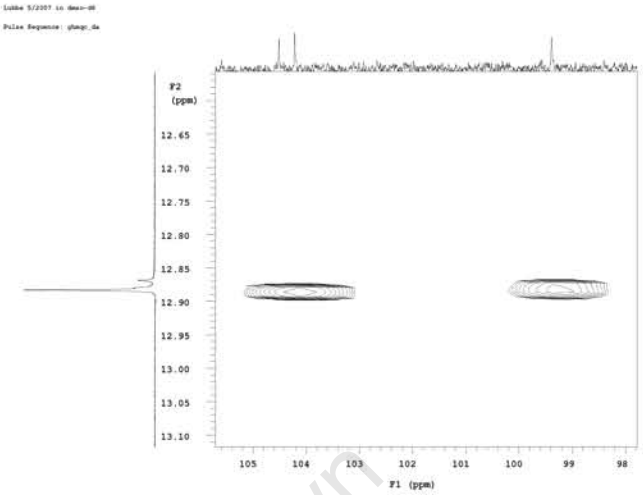

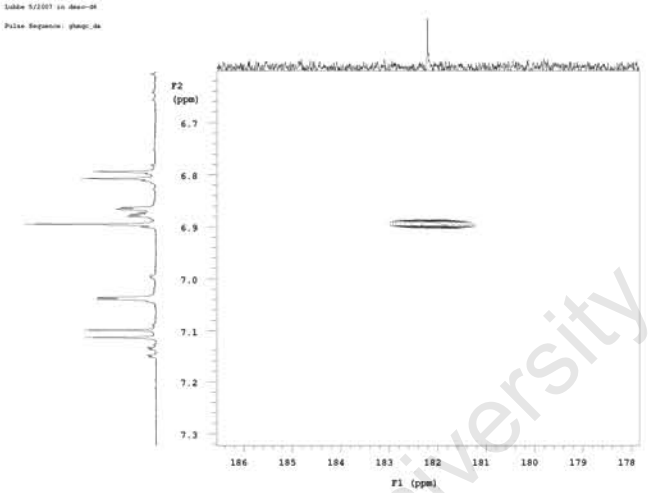

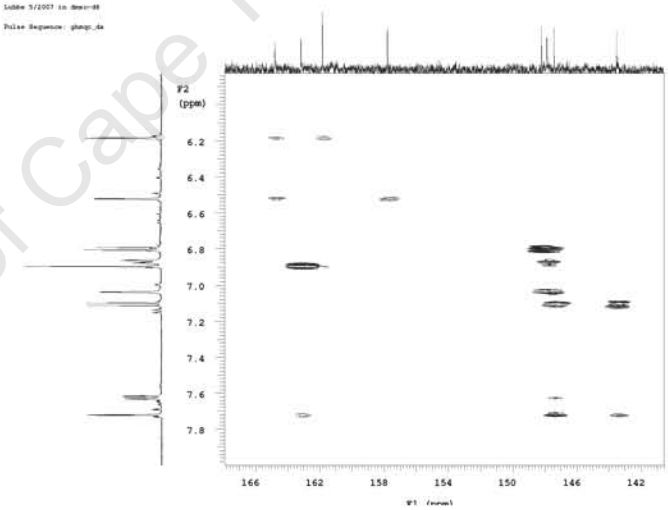

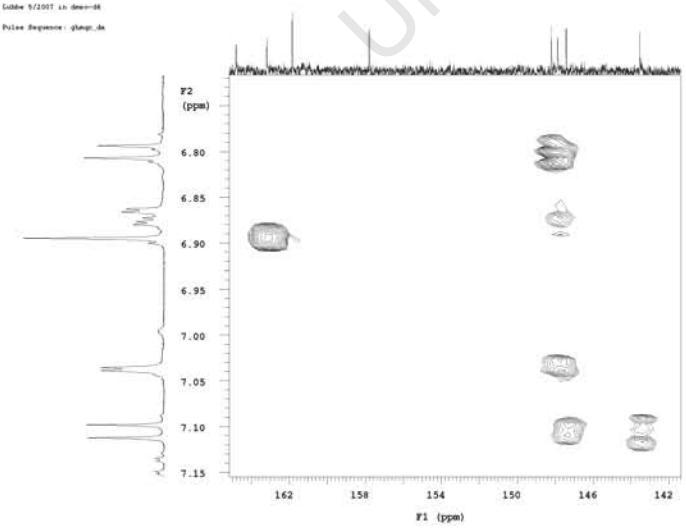

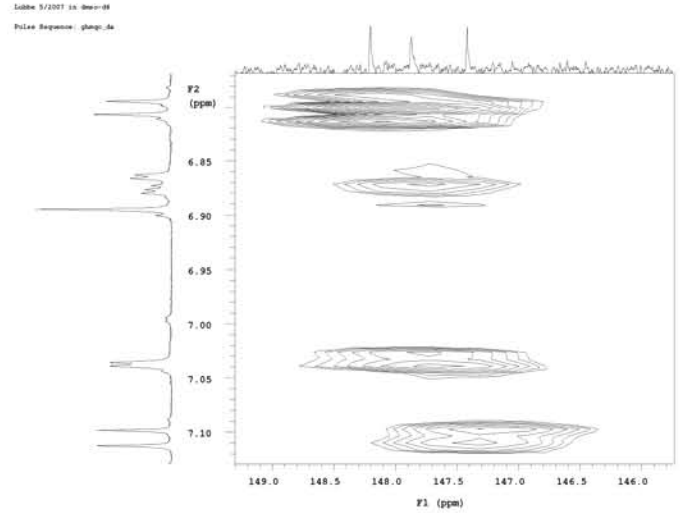

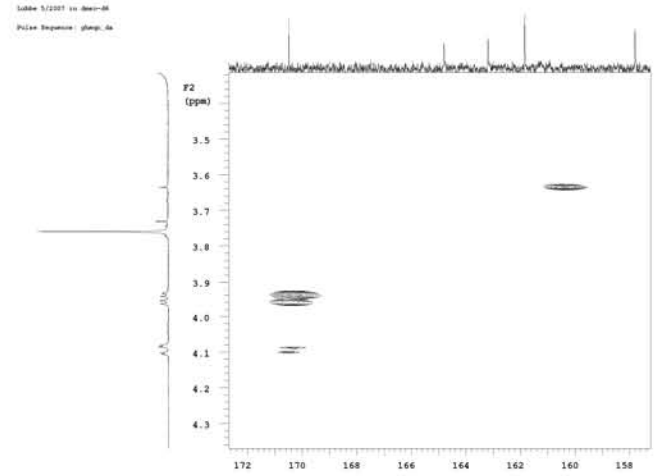

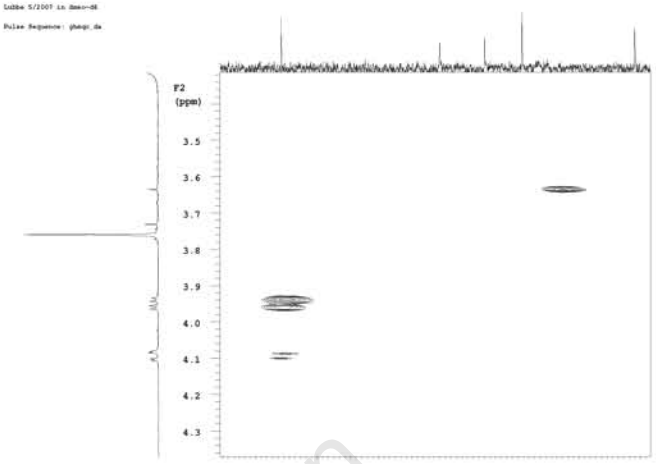

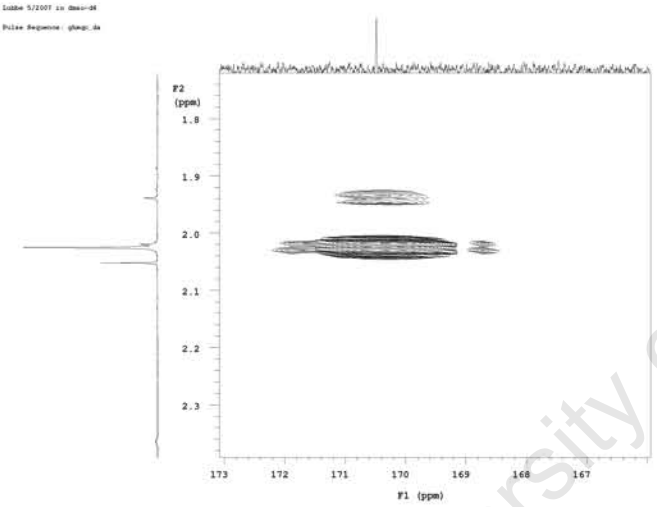

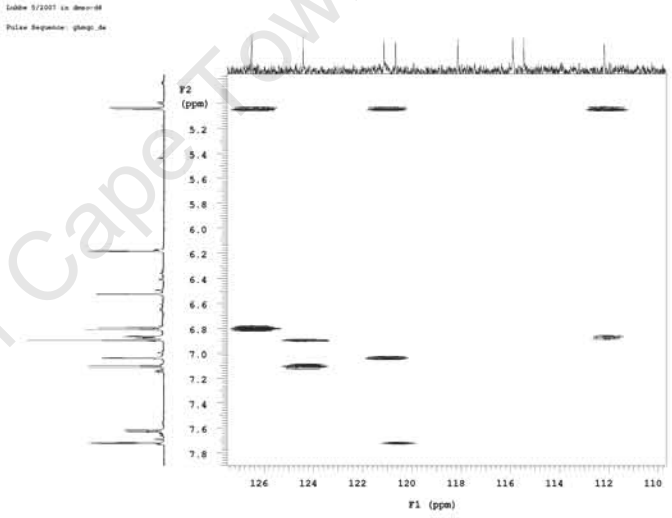

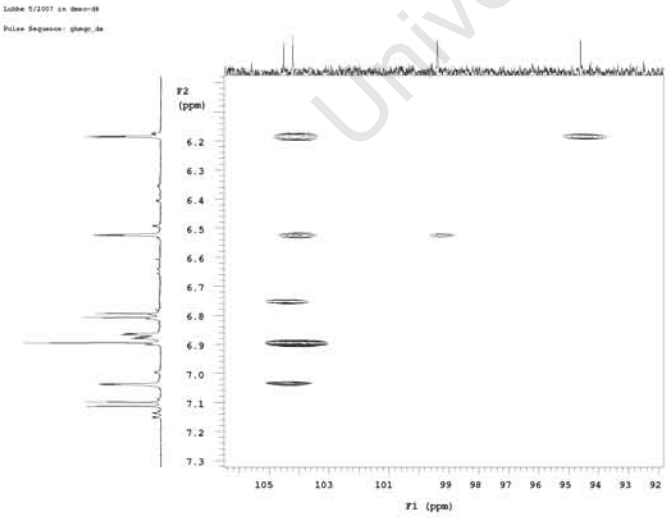

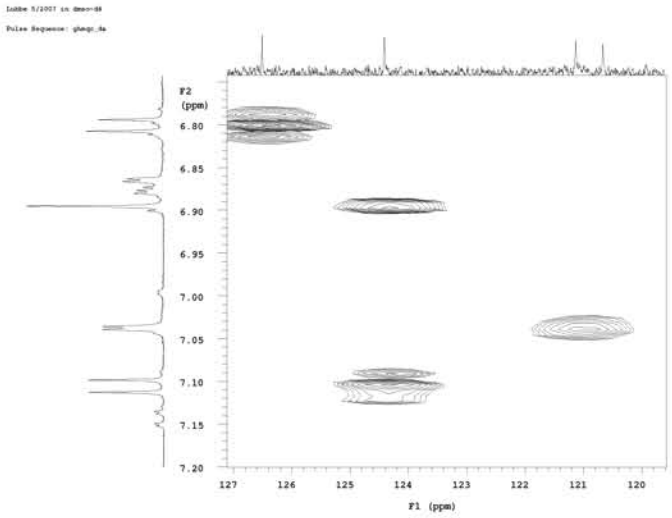

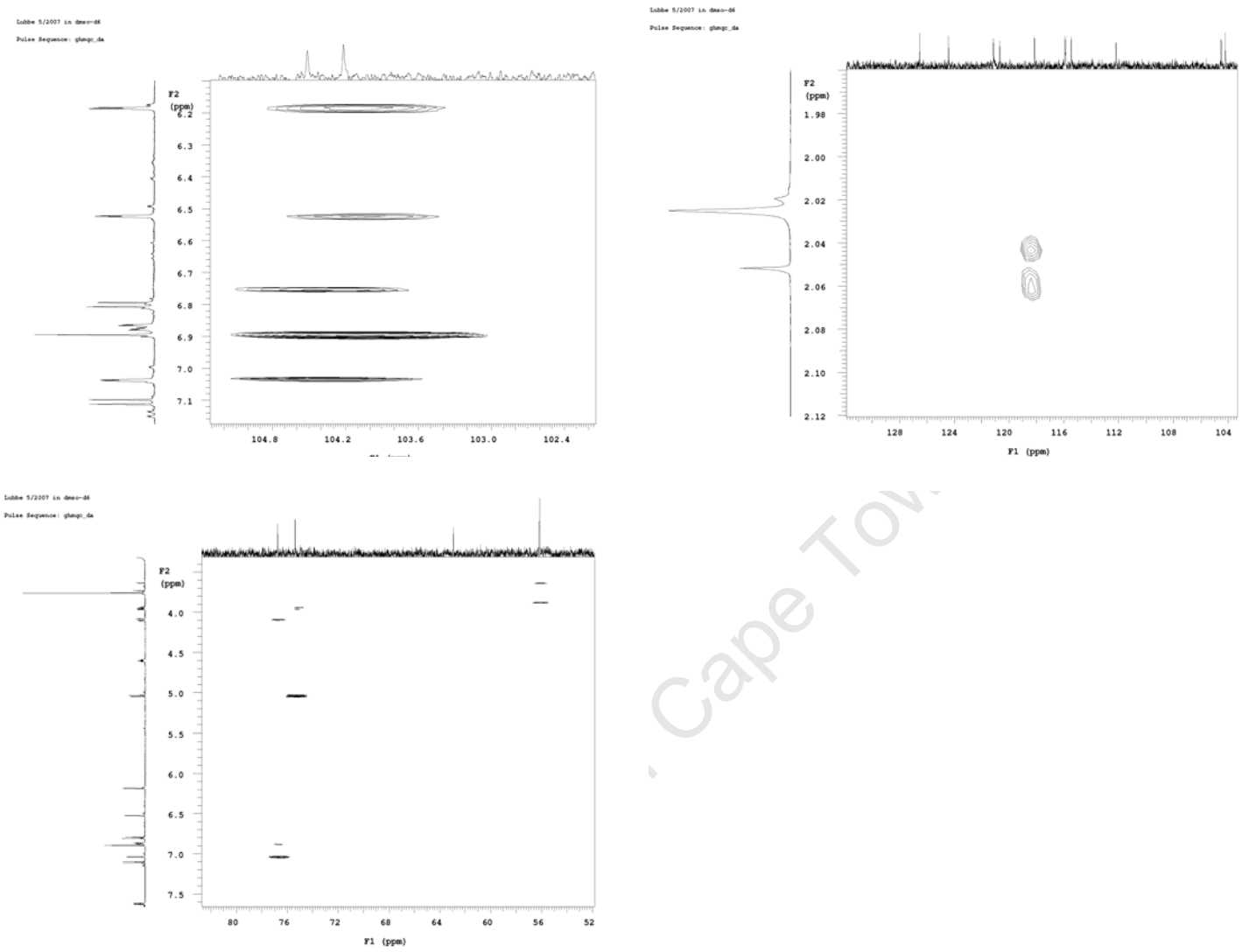

Figure 164 HMQC spectrum of compound 5 (zoom in)

APPENDIX 2

Body weight and % parasitaemia data of mice

Polar formulation

Table 50 Body weight data of mice (g) that were treated with a polar 100 mg/kg 9-O-acetylhydnocarpin formulation using the 4 day suppressive treatment strategy (control groups included)

Treatment	Day 1	Day 3	Day 5	Day 7	Day 9
Chloroquine control, mouse 1	29.6	29.4	29.7	29.9	29.3
Chloroquine control, mouse 2	28.5	28.5	29.3	29.1	28.8
Chloroquine control, mouse 3	28.6	28.2	28.8	28.8	28.1
Placebo control, mouse 1	29.8	29.9	30.4	29.3	24.9
Placebo control, mouse 2	30.1	30.6	29.9	26.0	25.0
Placebo control, mouse 3	27.6	27.7	28.1	24.9	23.5
Test compound, mouse 1	30.0	30.3	30.7	25.4	23.5
Test compound, mouse 2	27.5	26.9	27.8	25.4	23.2
Test compound, mouse 3	26.8	25.3	26.7	24.5	22.4

Table 51 Parasitaemia (%) data of mice that were treated with a polar 100 mg/kg 9-O-acetylhydnocarpin formulation using the 4 day suppressive treatment strategy (control groups included)

Treatment	Day 3	Day 5	Day 7	Day 9
Chloroquine control, mouse 1	0.5	0.0	0.0	0.7
Chloroquine control, mouse 2	0.5	0.0	0.0	0.7
Chloroquine control, mouse 3	0.5	0.0	0.0	0.0
Placebo control, mouse 1	0.5	1.0	3.2*	18.9
Placebo control, mouse 2	0.5	1.1	20.3	34.0
Placebo control, mouse 3	0.4	1.0	18.4	35.4
Test compound, mouse 1	0.5	1.0	16.0	25.4
Test compound, mouse 2	0.5	0.9	9.9	22.4
Test compound, mouse 3	0.5	0.8	10.2	22.3

* Statistical outlier, was not included during %Chemo suppression calculation

SMEDDS formulation

Table 52 Body weight data of mice (g) that were treated with a 100 mg/kg 9-O-acetylhydnocarpin SMEDDS formulation using the 4 day suppressive treatment strategy (control groups included)

Treatment	Day 1	Day 3	Day 5	Day 7	Day 8
Chloroquine control, mouse 1	30.6	31.0	29.3	30.3	31.2
Chloroquine control, mouse 2	30.8	28.7	28.8	30.4	30.5
Chloroquine control, mouse 3	30.2	30.3	31.0	31.3	31.4
Placebo control, mouse 1	30.2	30.8	30.1	29.5	25.7
Placebo control, mouse 2	31.8	32.0	30.5	27.6	25.9
Placebo control, mouse 3	30.8	30.8	30.5	31.7	29.3
Test compound, mouse 1	30.7	31.0	27.7	26.3	24.6
Test compound, mouse 2	30.5	30.2	28.8	26.9	25.7
Test compound, mouse 3	30.0	29.5	29.2	26.8	25.5

Table 53 Parasitaemia (%) data of mice that were treated with a 100 mg/kg 9-O-acetylhydnocarpin SMEDDS formulation using the 4 day suppressive treatment strategy (control groups included)

Treatment	Day 3	Day 5	Day 7	Day 8
Chloroquine control, mouse 1	0	1.0	0.6	1.17
Chloroquine control, mouse 2	0	0.7	0.1	0
Chloroquine control, mouse 3	0	1.2	0.5	0.1
Placebo control, mouse 1	0	8.3	24.9	30.6
Placebo control, mouse 2	0	8.3	35.3	40.6
Placebo control, mouse 3	0	2.2	5.2*	10.4
Test compound, mouse 1	0	6.1	16.7	25.0
Test compound, mouse 2	0	4.0	21.6	28.4
Test compound, mouse 3	0	2.2	17.6	26.0

* Statistical outlier, was not included during %Chemo suppression calculation

Pheroid formulation

Table 54 Body weight data of mice (g) that were treated with a 100 mg/kg 9-O-acetylhydnocarpin pheroid formulation using the 4 day suppressive treatment strategy (control groups included)

Treatment	Day 1	Day 3	Day 5	Day 7	Day 8
Chloroquine control, mouse 1	30.6	31.0	29.3	30.3	31.2
Chloroquine control, mouse 2	30.8	28.7	28.8	30.4	30.5
Chloroquine control, mouse 3	30.2	30.3	31.0	31.3	31.4
Placebo control, mouse 1	29.8	28.8	27.8	25.7	24.0
Placebo control, mouse 2	29.7	26.4	23.7	22.6	22.2
Placebo control, mouse 3	29.4	28.8	28.3	26.1	24.4
Test compound, mouse 1	30.8	30.6	29.9	27.5	26.1
Test compound, mouse 2	30.2	27.5	27.3	27.0	25.1
Test compound, mouse 3	30.3	27.4	29.0	26.0	25.2

Table 55 Parasitaemia (%) data of mice that were treated with a 100 mg/kg 9-O-acetylhydnocarpin pheroid formulation using the 4 day suppressive treatment strategy (control groups included)

Treatment	Day 3	Day 5	Day 7	Day 8
Chloroquine control, mouse 1	0	1.0	0.6	1.17
Chloroquine control, mouse 2	0	0.7	0.1	0
Chloroquine control, mouse 3	0	1.2	0.5	0.1
Placebo control, mouse 1	0	3.3	29.1	36.0
Placebo control, mouse 2	0	2.6	8.0*	9.8
Placebo control, mouse 3	0	5.4	33.6	39.6
Test compound, mouse 1	0	4.7	19.9	28.0
Test compound, mouse 2	0	6.6	14.5	15.0
Test compound, mouse 3	0	5.3	20.6	28.0

* Statistical outlier, was not included during %Chemo suppression calculation

APPENDIX 3

Bioavailability data

Initial bioavailability study of 9-O-acetylhydnocarpin in mice

Calibration curve results & Representative chromatograms

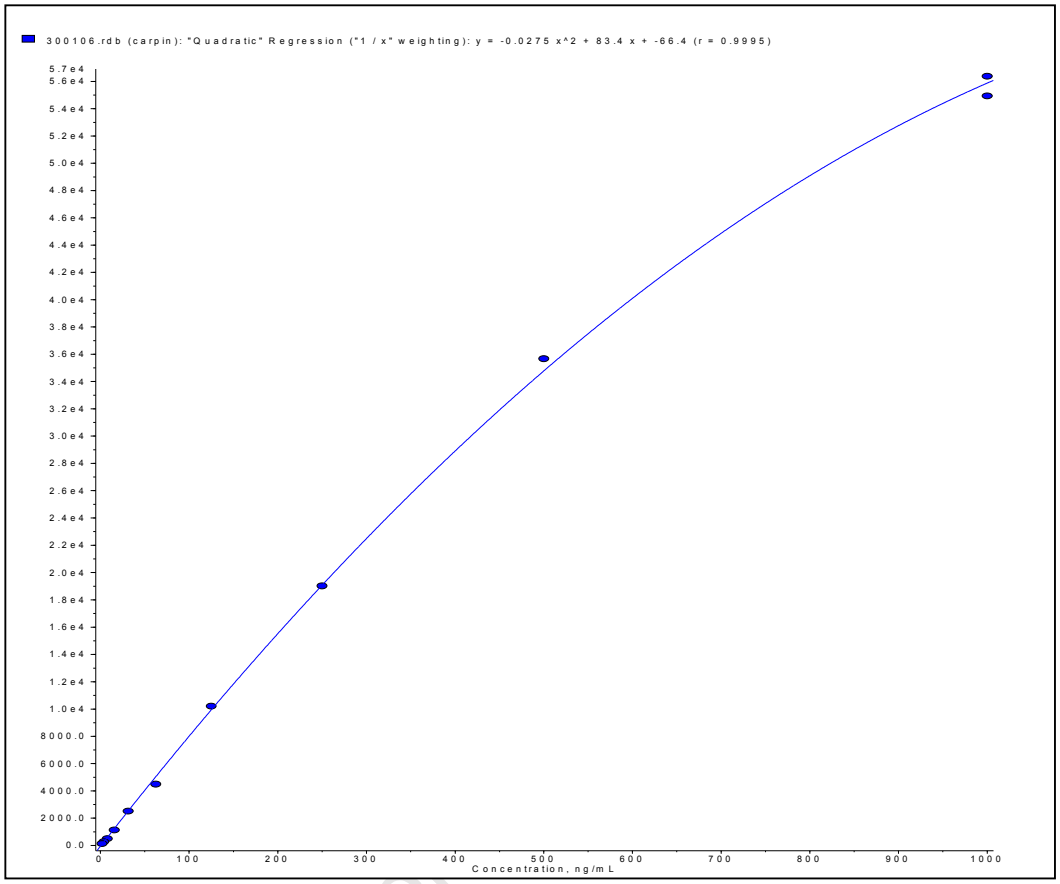

Figure 165 Calibration curve of 9-O-acetylhydnocarpin

Table 56 Back-calculated concentrations of 9-O-acetylhydnocarpin

Sample	Peak Area	Nominal conc. (ng/ml)	Calculated conc. (ng/ml)	Accuracy (%)
STD 1	54900	1000	968	96.8
STD 2	35700	500	516	103
STD 3	19000	250	249	99.7
STD 4	10200	125	129	103
STD 5	4490	62.5	55.6	88.9
STD 6	2520	31.3	31.3	99.9
STD 7	1140	15.6	14.5	92.8
STD 8	501	7.8	6.82	87.4
STD 9	275	3.9	4.09	105
STD 10	131	1.95	2.37	122

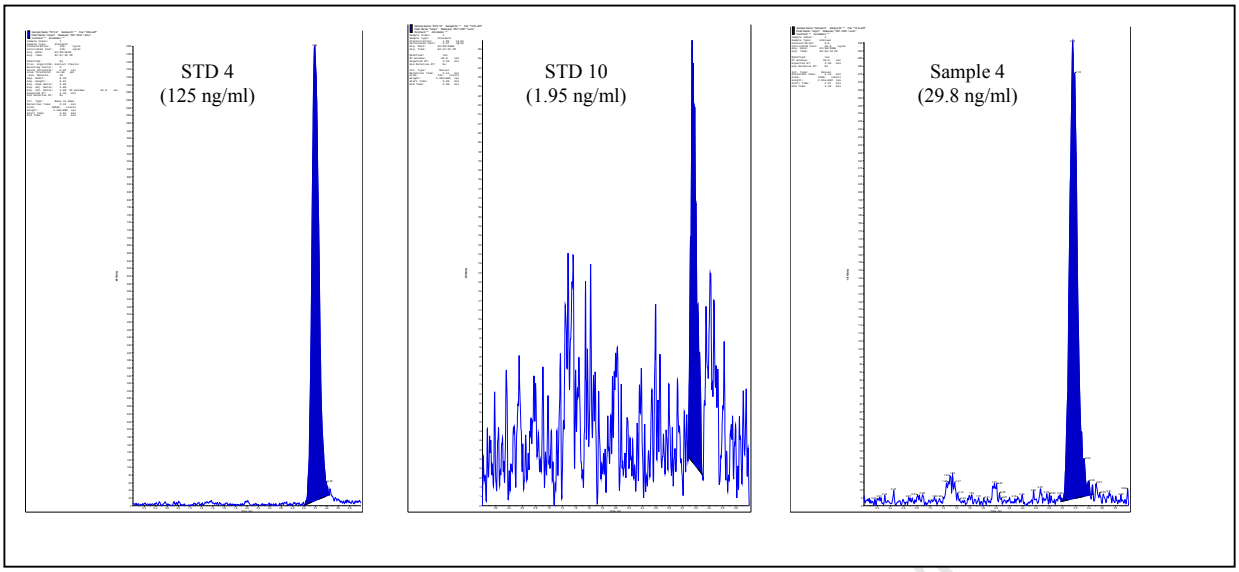

Figure 166 Representative chromatograms: STD 4, STD 10 and sample 4

Metabolite investigation

Total ion chromatogram & Precursor ion mass spectra

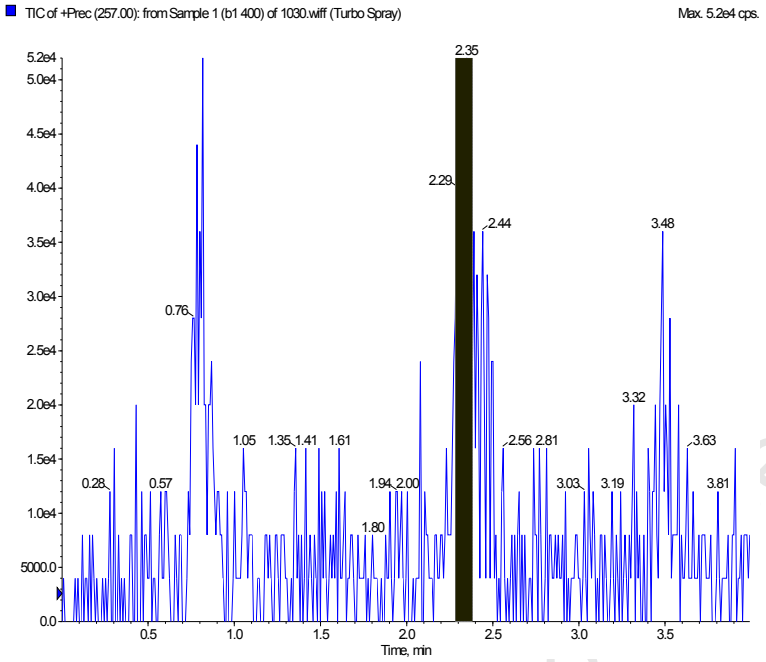

Figure 167 Total ion chromatogram of the 257 precursor ion (combined study sample)

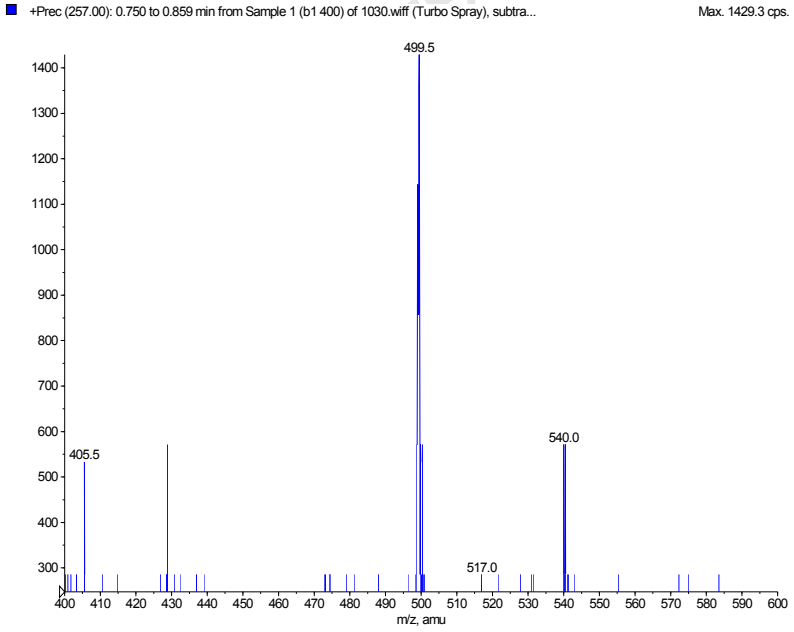

Figure 168 Precursor ion mass spectrum of the peak at 0.8 minutes

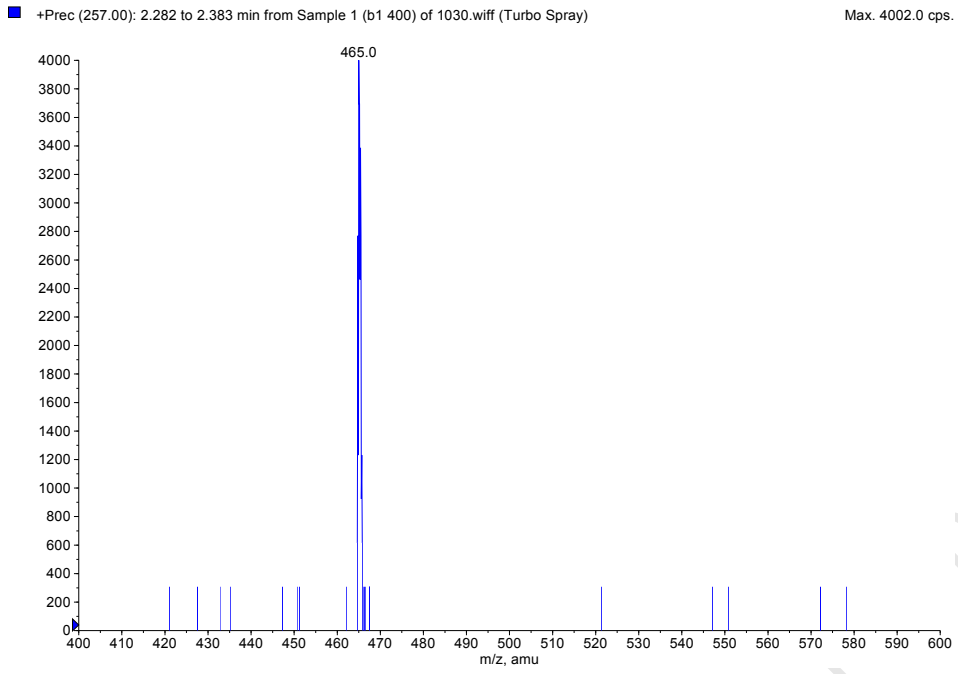

Figure 169 Precursor ion mass spectrum of the peak at 2.4 minutes

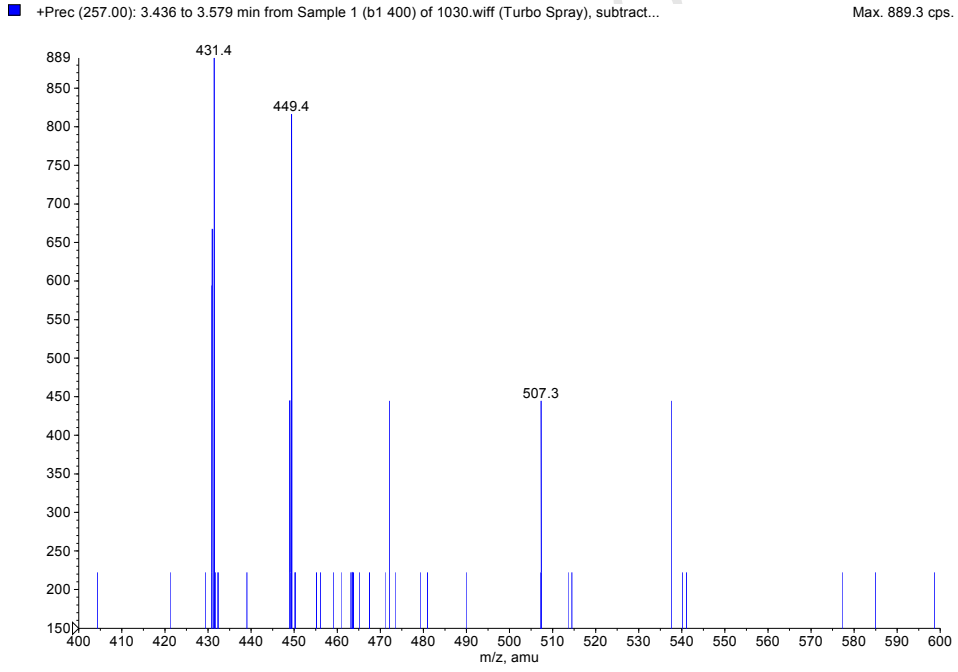

Figure 170 Precursor ion mass spectrum of the peak at 3.5 minutes

Bioavailability study of 9-O-acetylhydnocarpin and its hydrolysed product in mice using different formulations and administration routes

Calibration curve results & Representative chromatograms

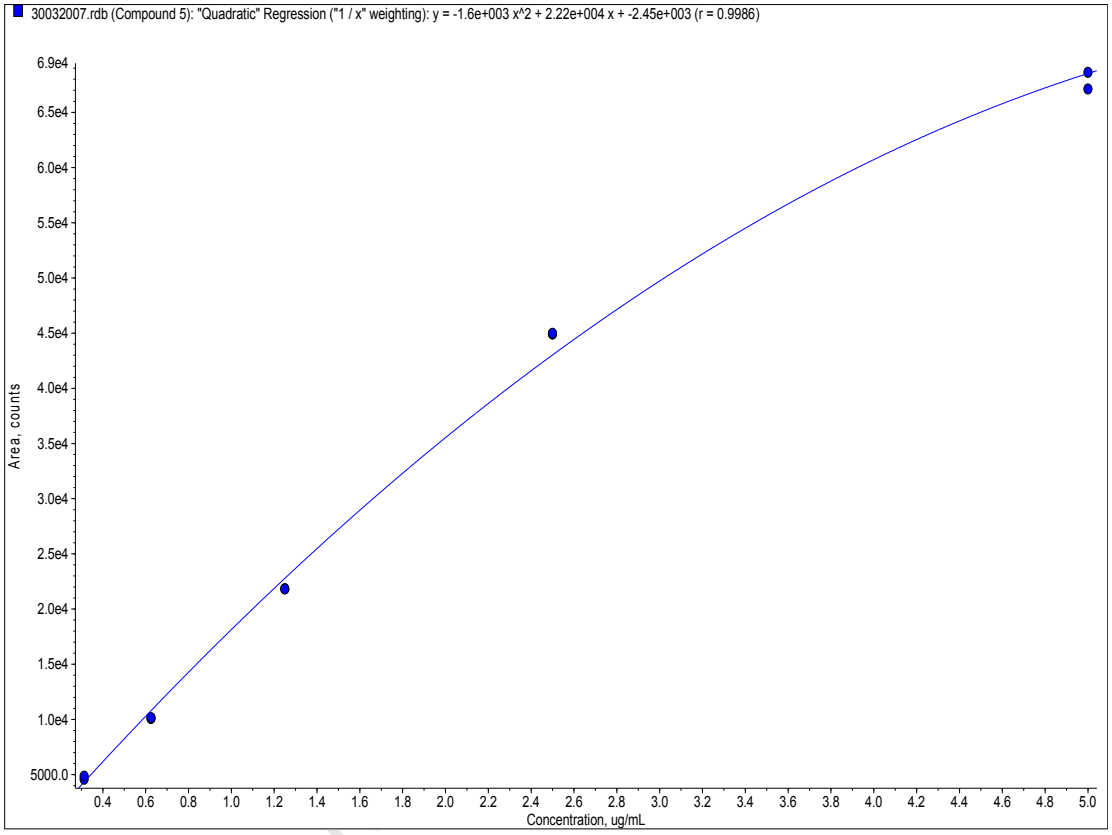

Figure 171 Calibration curve of 9-O-acetylhydnocarpin

Table 57 Back-calculated concentrations of 9-O-acetylhydnocarpin

Sample	Peak Area	Nominal conc. (µg/ml)	Calculated conc. (µg /ml)	Accuracy (%)
STD 1	68600	5	5.02	100
STD 2	44900	2.5	2.63	105
STD 3	21800	1.25	1.20	95.8
STD 4	10100	0.625	0.589	94.3
STD 5	4580	0.313	0.324	104
STD 1	67100	5	4.78	95.7
STD 2	45000	2.5	2.64	106
STD 3	21800	1.25	1.20	95.7
STD 4	10200	0.625	0.594	95.0
STD 5	4860	0.313	0.338	108

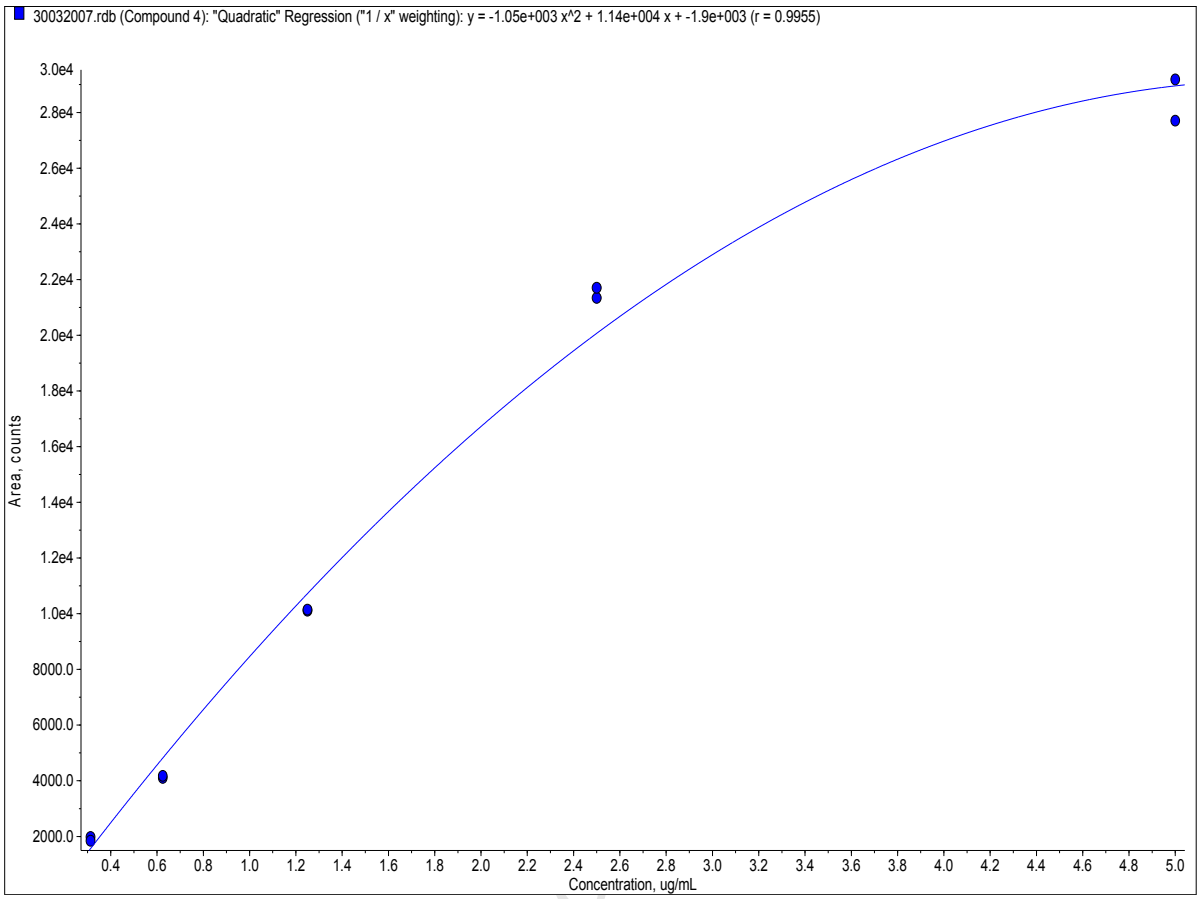

Figure 172 Calibration curve of the hydrolysed product

Table 58 Back-calculated concentrations of the hydrolysed product

Sample	Peak Area	Nominal conc. (µg/ml)	Calculated conc. (µg /ml)	Accuracy (%)
STD 1	29200	5	No Intercept	N/A
STD 2	21300	2.5	2.71	109
STD 3	10100	1.25	1.18	94.4
STD 4	4100	0.625	0.554	88.7
STD 5	1980	0.313	0.351	112
STD 1	27700	5	4.27	85.3
STD 2	21700	2.5	2.78	111
STD 3	10100	1.25	1.18	94.8
STD 4	4170	0.625	0.561	89.8
STD 5	1840	0.313	0.339	108

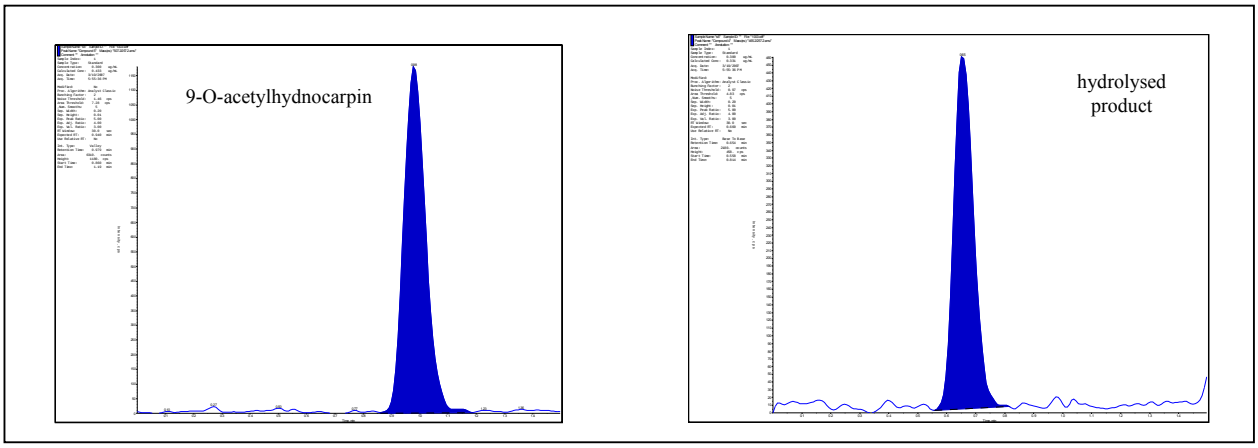

Figure 173 Representative chromatograms at the LLOQ

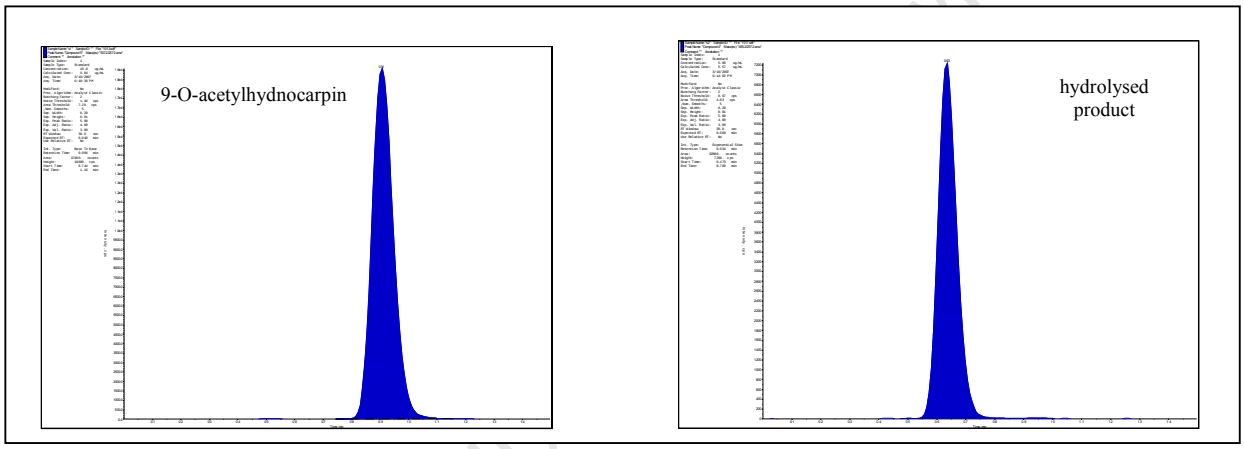

Figure 174 Representative chromatograms at 5 µg/ml

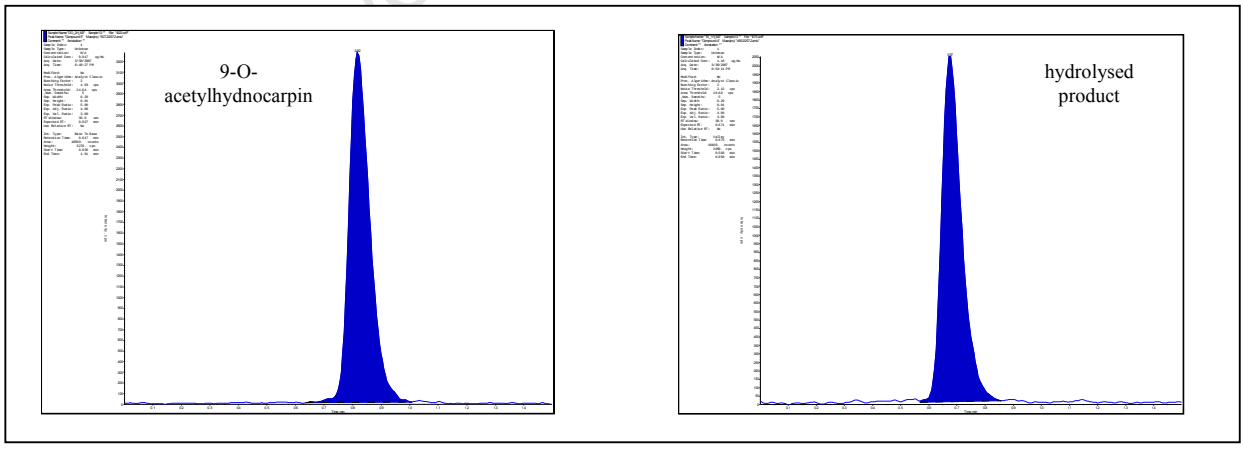

Figure 175 Representative chromatograms of a study sample

Validation data

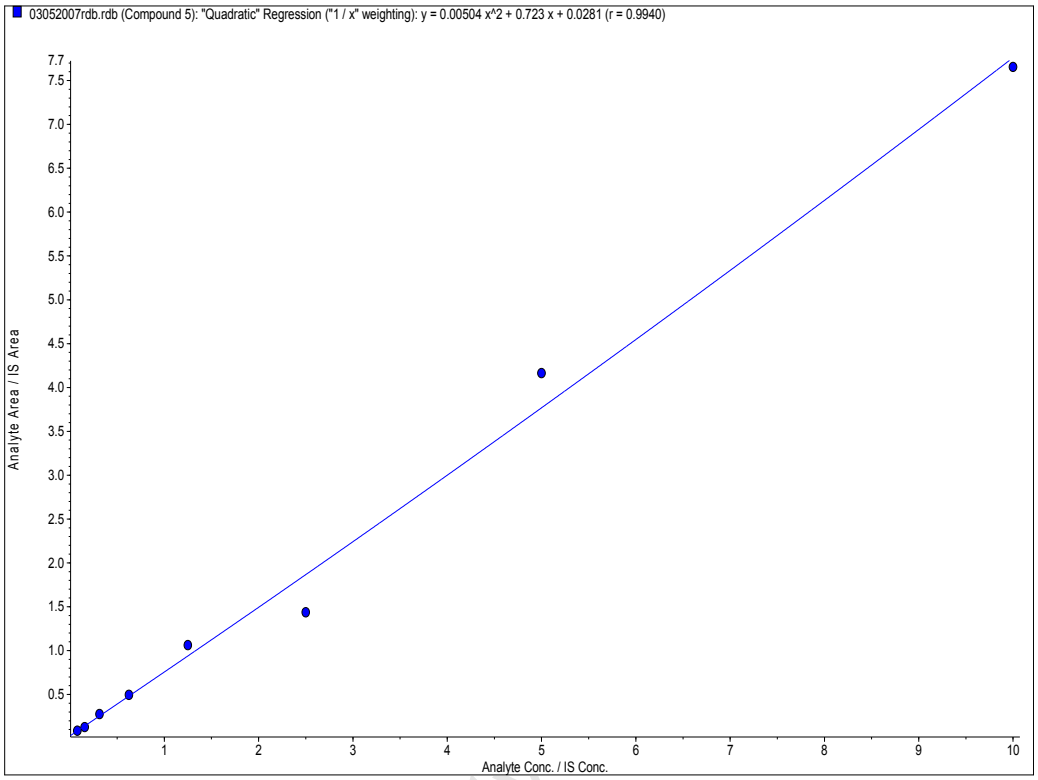

Figure 176 Calibration curve of 9-O-acetylhydnocarpin

Table 59 Back-calculated concentrations of 9-O-acetylhydnocarpin

Sample	Analyte peak area	ISTD peak area	Peak Area Ratio	Nom conc. (µg/ml)	Calc. conc. (µg /ml)	Accuracy (%)
STD 1	196000	25600	7.66	10	9.87	98.7
STD 2	98800	23700	4.17	5	5.51	110
STD 3	48200	33500	1.44	2.5	1.92	76.9
STD 4	22900	21600	1.06	1.25	1.42	113
STD 5	11700	23600	0.496	0.625	0.643	103
STD 6	5980	21700	0.276	0.313	0.341	109
STD 7	3390	26800	0.126	0.156	0.136	87.3
STD 8	2180	25500	0.0855	0.0781	0.0793	102

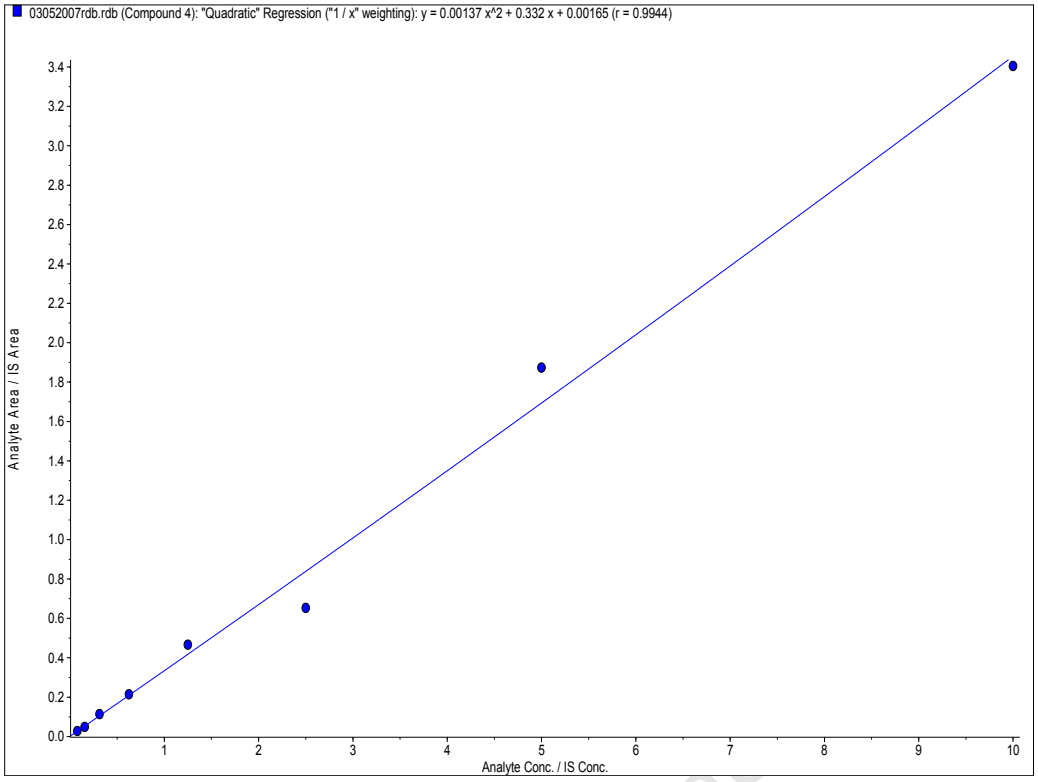

Figure 177 Calibration curve of the hydrolysed product

Table 60 Back-calculated concentrations of the hydrolysed product

Sample	Analyte peak area	ISTD peak area	Peak Area Ratio	Nom conc. (µg/ml)	Calc. conc. (µg /ml)	Accuracy (%)
STD 1	87100	25600	3.40	10	9.86	98.6
STD 2	44400	23700	1.87	5	5.52	110
STD 3	21900	33500	0.654	2.5	1.95	77.9
STD 4	10100	21600	0.468	1.25	1.39	111
STD 5	5060	23600	0.214	0.625	0.64	102
STD 6	2470	21700	0.114	0.313	0.337	108
STD 7	1300	26800	0.0485	0.156	0.141	90.4
STD 8	709	25500	0.0278	0.0781	0.0788	101

Table 61 Long term matrix stability of 9-O-acetylhydnocarpin

Nominal Concentration (µg/ml)	Measured Concentration (µg /ml)	Calculated % of nominal
10	10.9	109.0
10	11.1	111.0
10	10.5	105.0
Mean	10.8	108.3
STDEV	0.31	3.06
CV%	2.8	
% Nom	108	

Nominal Concentration (µg/ml)	Measured Concentration (µg/ml)	Calculated % of nominal
0.625	0.658	105.3
0.625	0.678	108.5
0.625	0.646	103.4
Mean	0.661	105.7
STDEV	0.02	2.59
CV%	2.4	
% Nom	105.7	

Table 62 Long term matrix stability of the hydrolysed product

Nominal Concentration (µg/ml)	Measured Concentration (µg /ml)	Calculated % of nominal
10	10.7	107.0
10	10.7	107.0
10	9.88	98.8
Mean	10.4	104.3
STDEV	0.47	4.73
CV%	4.5	
% Nom	104.3	

Nominal Concentration (µg/ml)	Measured Concentration (µg/ml)	Calculated % of nominal
0.625	0.577	92.3
0.625	0.664	106.2
0.625	0.636	101.8
Mean	0.626	100.1
STDEV	0.04	7.11
CV%	7.1	
% Nom	100.1	

Table 63 On bench and Freeze-thaw stability of 9-O-acetylhydnocarpin

Nominal Concentration (µg/ml)	Measured Concentration (µg /ml)	Calculated % of nominal
10	10.5	105
10	10.1	101
10	9.85	98.5
Mean	10.15	101.5
STDEV	0.33	3.28
CV%	3.2	
% Nom	101.5	

Nominal Concentration (µg/ml)	Measured Concentration (µg/ml)	Calculated % of nominal
0.625	0.568	90.9
0.625	0.659	105
0.625	0.574	91.8
Mean	0.600	96.1
STDEV	0.05	8.14
CV%	8.5	
% Nom	96.1	

Table 64 On bench and Freeze-thaw stability of the hydrolysed product

Nominal Concentration (µg/ml)	Measured Concentration (µg /ml)	Calculated % of nominal
10	10.5	105
10	10.1	101
10	9.85	98.5
Mean	10.15	101.5
STDEV	0.33	3.28
CV%	3.2	
% Nom	101.5	

Nominal Concentration (µg/ml)	Measured Concentration (µg/ml)	Calculated % of nominal
0.625	0.504	80.6
0.625	0.584	93.4
0.625	0.555	88.8
Mean	0.548	87.6
STDEV	0.04	6.48
CV%	7.4	
% Nom	87.6	

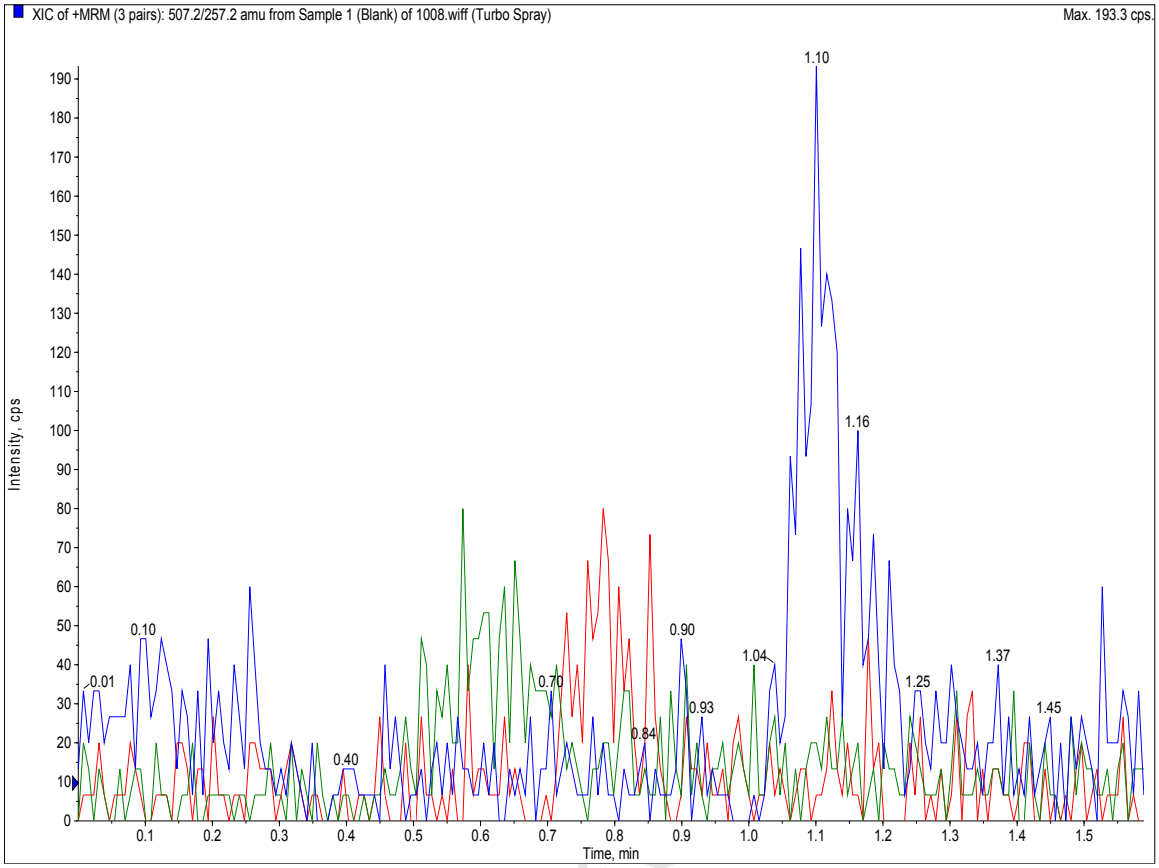

Figure 178 Chromatogram of a blank whole blood extract

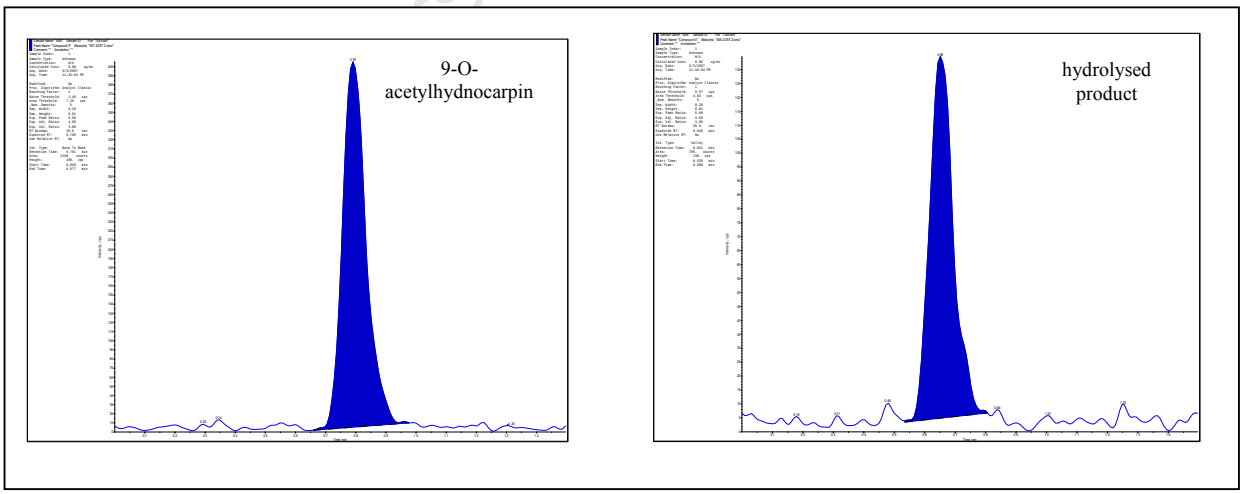

Figure 179 LLOQ chromatograms of 9-O-acetylhydnocarpin and the hydrolysed product

Bioavailability study of 9-O-acetylhydnocarpin and its hydrolysed product in mice using a self-microemulsifying drug delivery system

Calibration curve results & Representative chromatograms

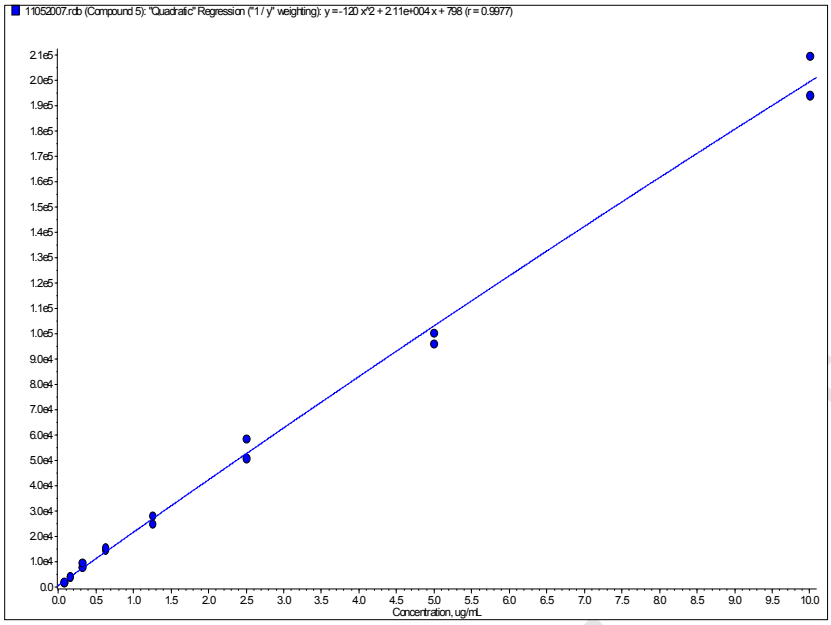

Figure 180 Calibration curve of 9-O-acetylhydnocarpin

Table 65 Back-calculated concentrations of 9-O-acetylhydnocarpin

Sample	Analyte peak area	Nom conc. (µg/ml)	Calc. conc. (µg /ml)	Accuracy (%)
STD 1	194000	10	9.71	97.1
STD 2	96100	5	4.64	92.9
STD 3	58700	2.5	2.79	112
STD 4	28300	1.25	1.31	105
STD 5	14900	0.625	0.672	108
STD 6	7830	0.313	0.334	107
STD 7	4190	0.156	0.161	103
STD 8	1930	0.0781	0.0535	68.6
STD 1	210000	10	10.5	105
STD 2	100000	5	4.86	97.1
STD 3	51000	2.5	2.41	96.5
STD 4	25100	1.25	1.16	92.8
STD 5	15600	0.625	0.704	113
STD 6	9680	0.313	0.422	135
STD 7	4170	0.156	0.160	103
STD 8	2030	0.0781	0.0585	74.9

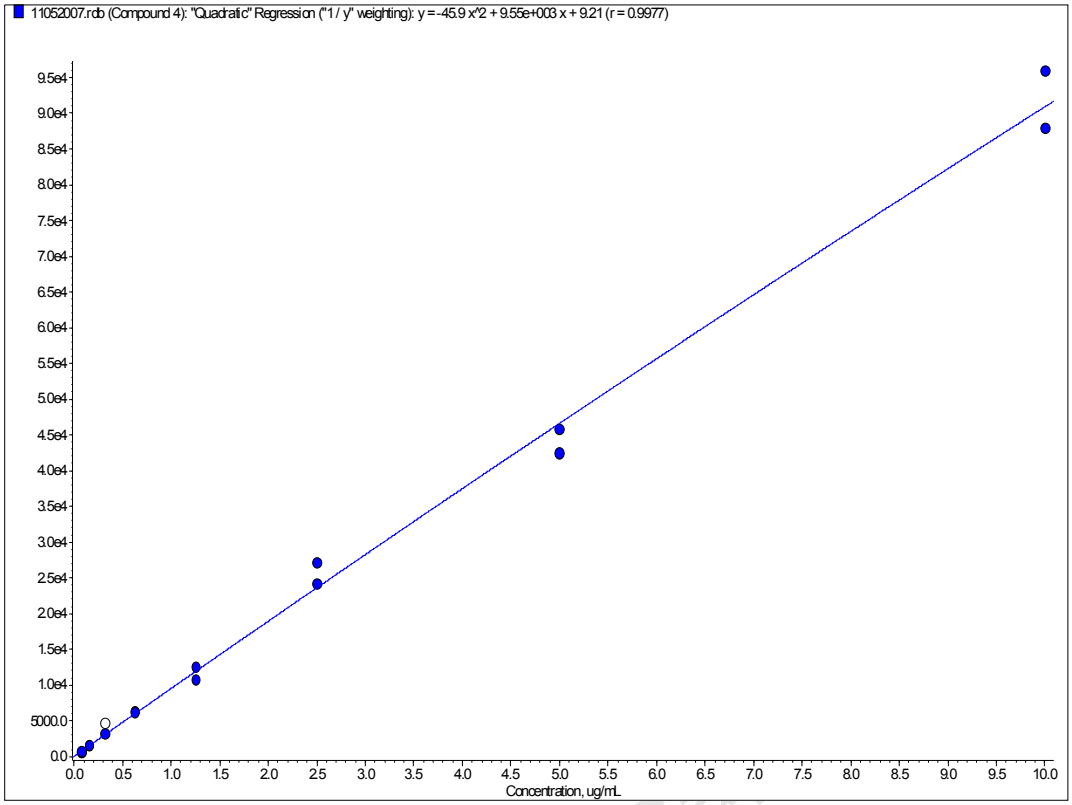

Figure 181 Calibration curve of the hydrolysed product

Table 66 Back-calculated concentrations of the hydrolysed product

Sample	Analyte peak area	Nom conc. (µg/ml)	Calc. conc. (µg /ml)	Accuracy (%)
STD 1	88000	10	9.66	96.6
STD 2	42500	5	4.54	90.9
STD 3	27100	2.5	2.88	115
STD 4	12500	1.25	1.32	105
STD 5	6350	0.625	0.666	107
STD 6	3150	0.313	0.329	105
STD 7	1510	0.156	0.158	101
STD 8	619	0.0781	0.0639	81.9
STD 1	96000	10	10.6	106
STD 2	45800	5	4.91	98.2
STD 3	24200	2.5	2.56	103
STD 4	10800	1.25	1.13	90.7
STD 5	6100	0.625	0.640	102
STD 6	4630	0.313	0.485	155
STD 7	1520	0.156	0.158	101
STD 8	793	0.0781	0.0822	105

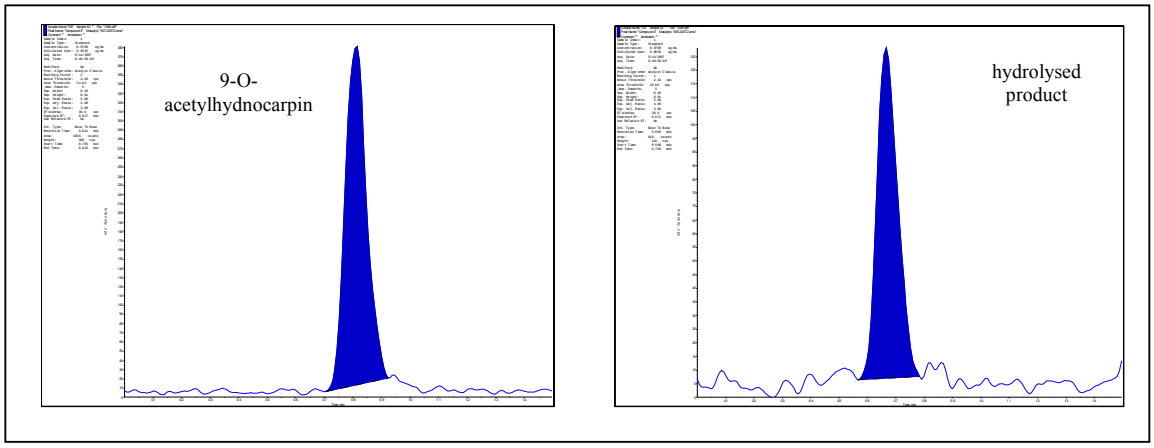

Figure 182 Representative chromatograms at the LLOQ

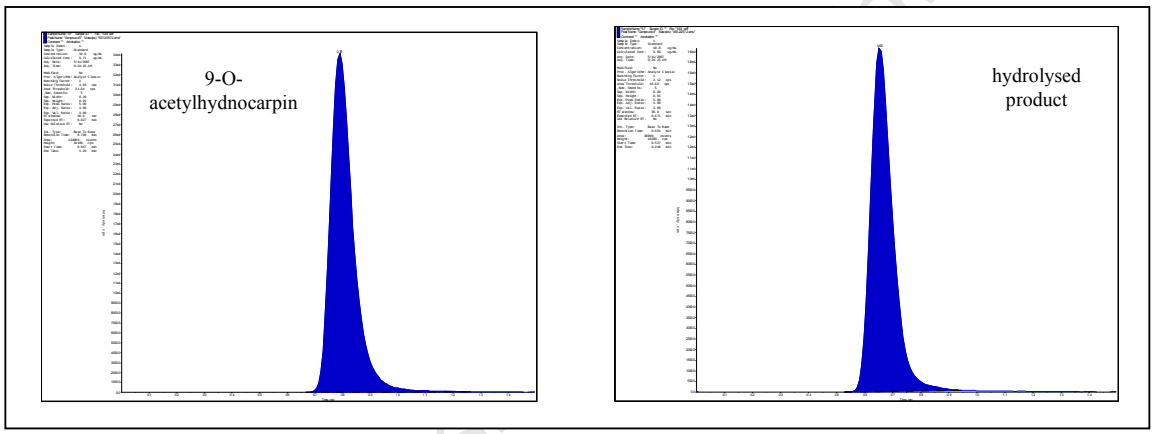

Figure 183 Representative chromatograms at 10 µg/ml

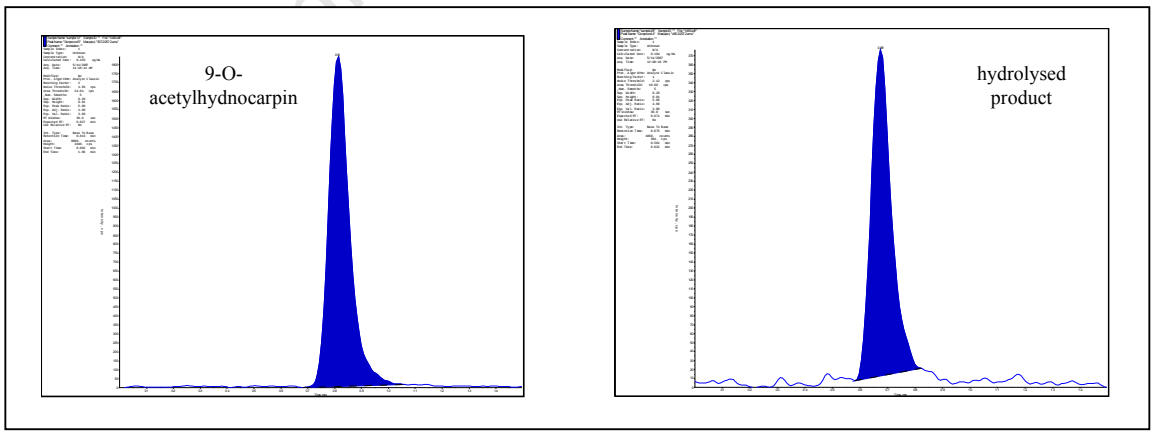

Figure 184 Representative chromatograms of a study sample

Bioavailability study of 9-O-acetylhydnocarpin and its hydrolysed product in mice using Pheroid technology as a drug delivery system after oral administration

Representative chromatograms & Calibration curve results

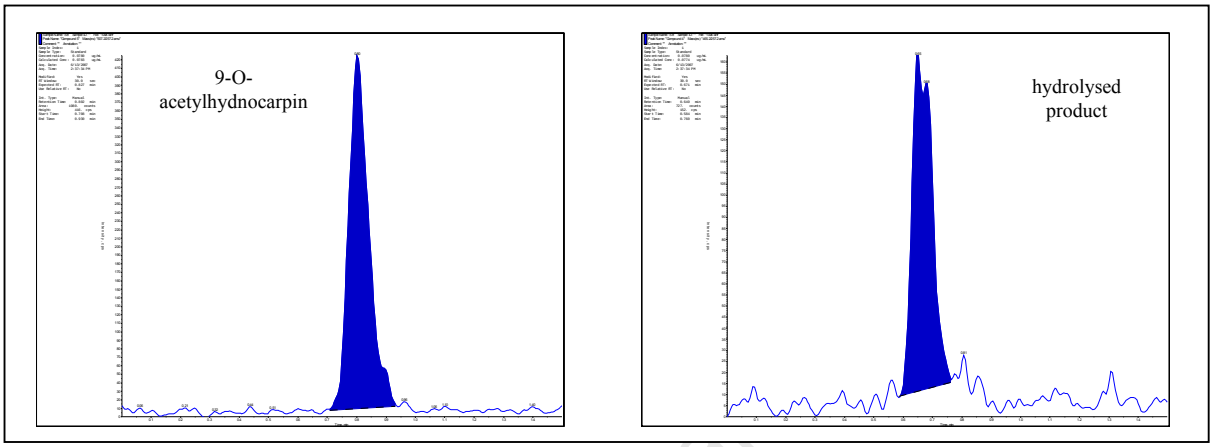

Figure 185 Representative chromatograms at the LLOQ

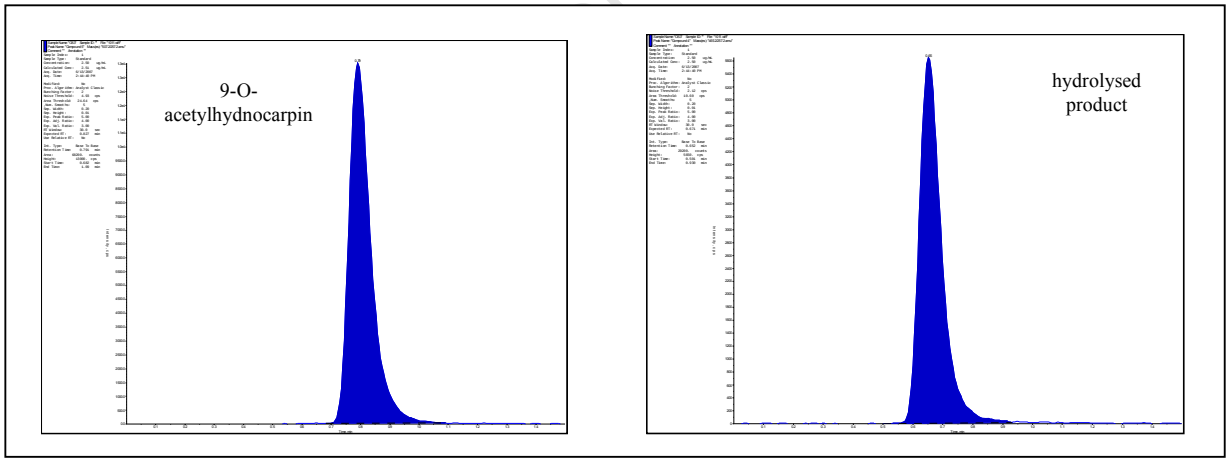

Figure 186 Representative chromatograms at 2.5 µg/ml

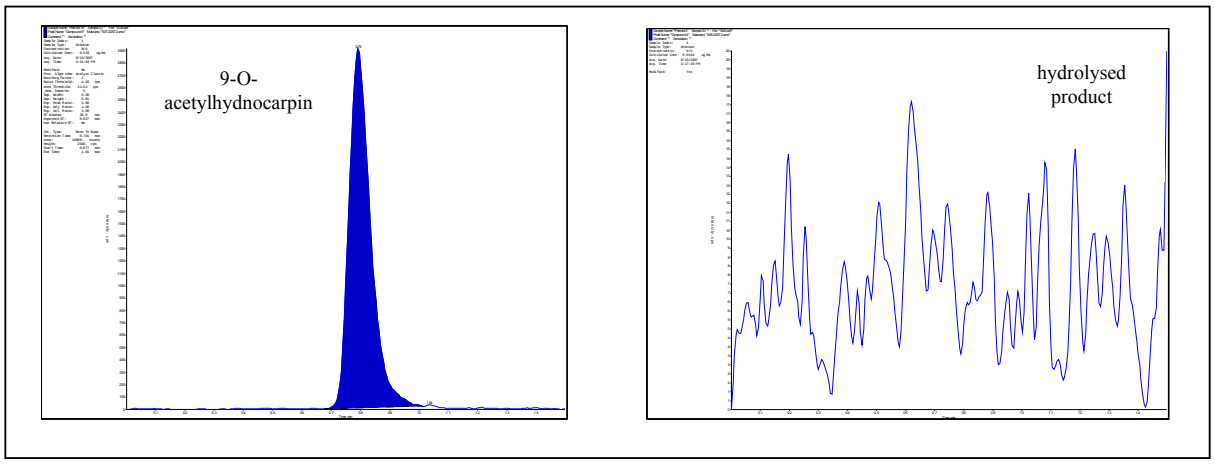

Figure 187 Representative chromatograms of a study sample

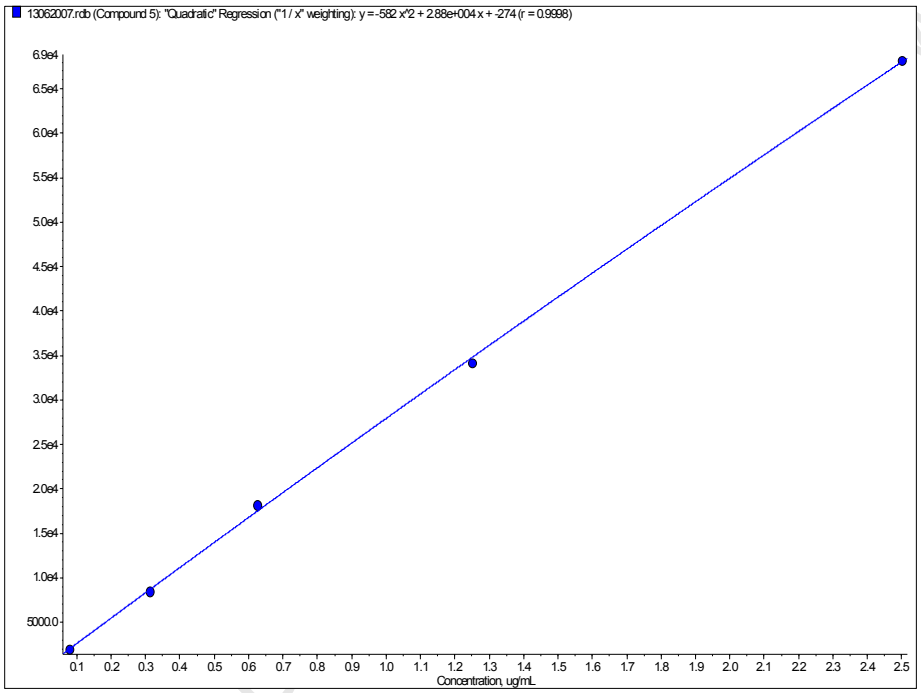

Figure 188 Calibration curve of 9-O-acetylhydnocarpin

Table 67 Back-calculated concentrations of 9-O-acetylhydnocarpin

Standard	Peak area	Nom conc. (µg/ml)	Calc. conc. (µg/ml)	Accuracy (%)
1	1980	0.0780	0.0783	100.4
2	8430	0.313	0.304	97.2
3	18200	0.625	0.650	103.9
4	34200	1.25	1.23	98.2
5	68200	2.50	2.51	100.3

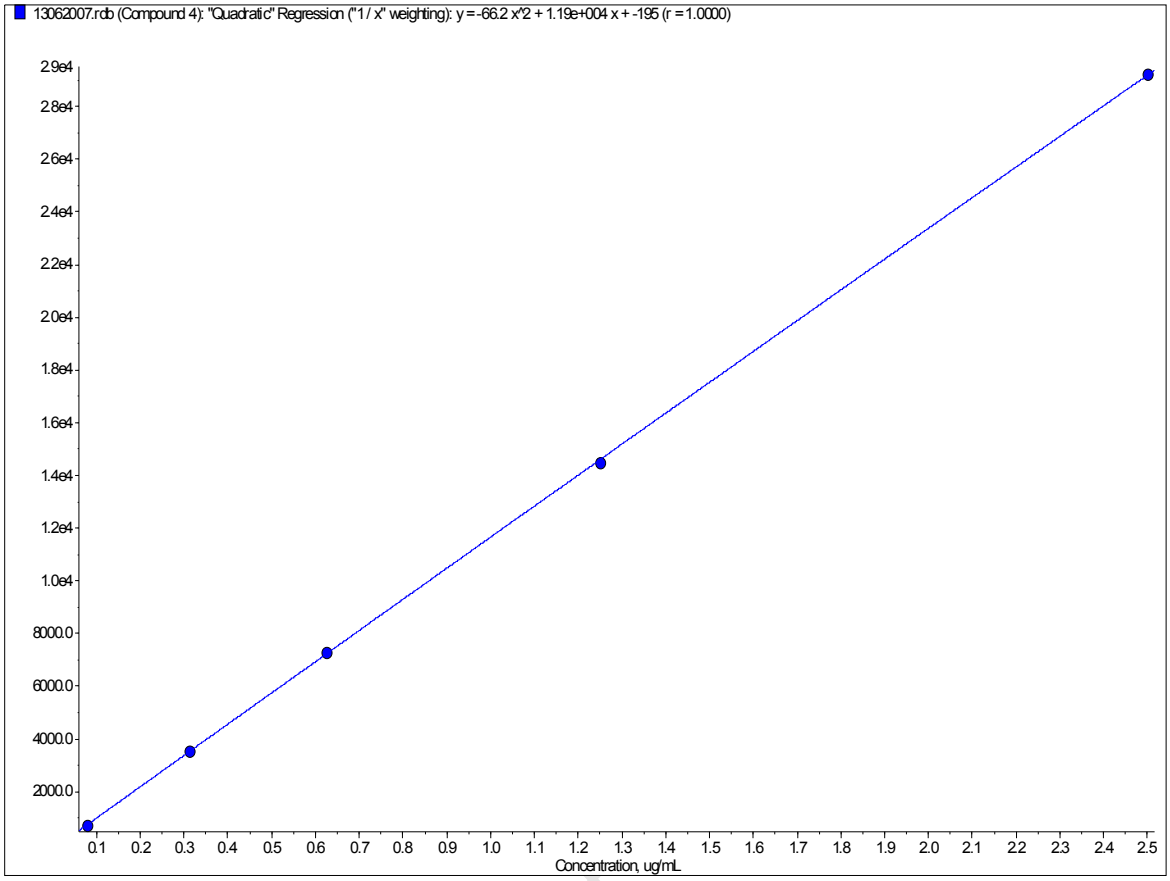

Figure 189 Calibration curve of the hydrolysed product

Table 68 Back-calculated concentrations of the hydrolysed product

Standard	Peak area	Nom conc. (µg/ml)	Calc. conc. (µg/ml)	Accuracy (%)
1	727	0.0780	0.0774	99.2
2	3550	0.313	0.315	100.6
3	7290	0.625	0.631	100.9
4	14500	1.25	1.24	99.2
5	29200	2.50	2.50	100.1

Bioavailability study of 9-O-acetylhydnocarpin and its hydrolysed product in mice after intravenous administration

Representative chromatograms & Calibration curve results

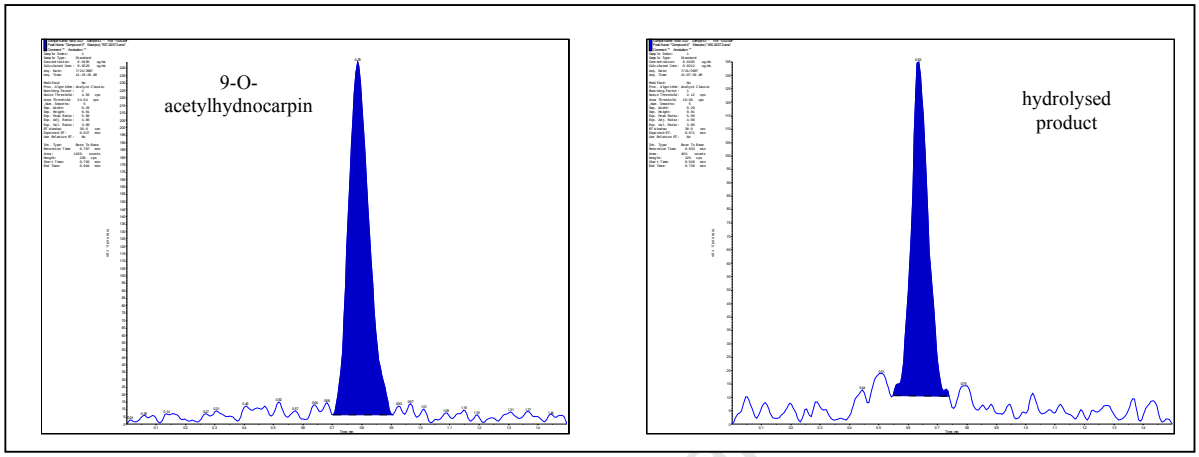

Figure 190 Representative chromatograms at the LLOQ

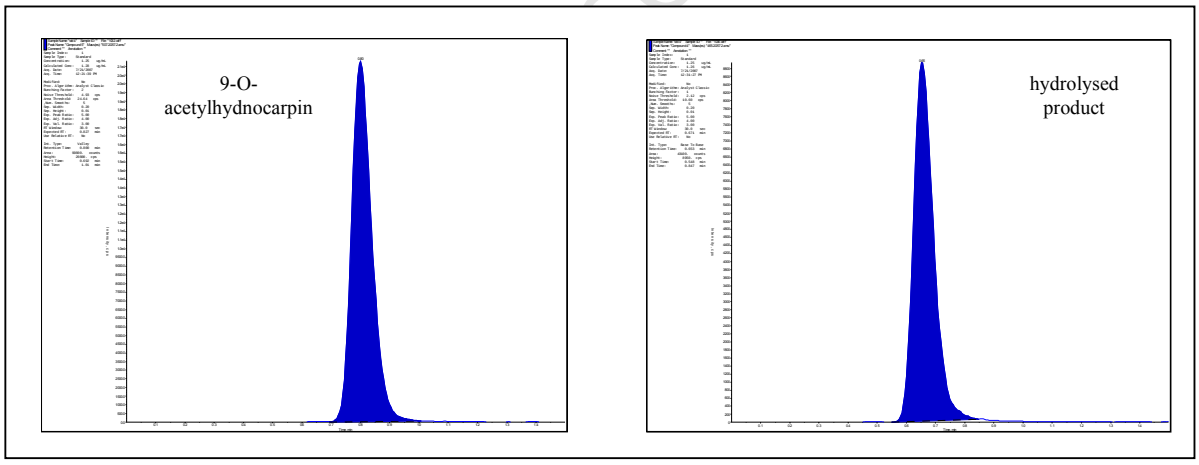

Figure 191 Representative chromatograms at 1.25 μg/ml

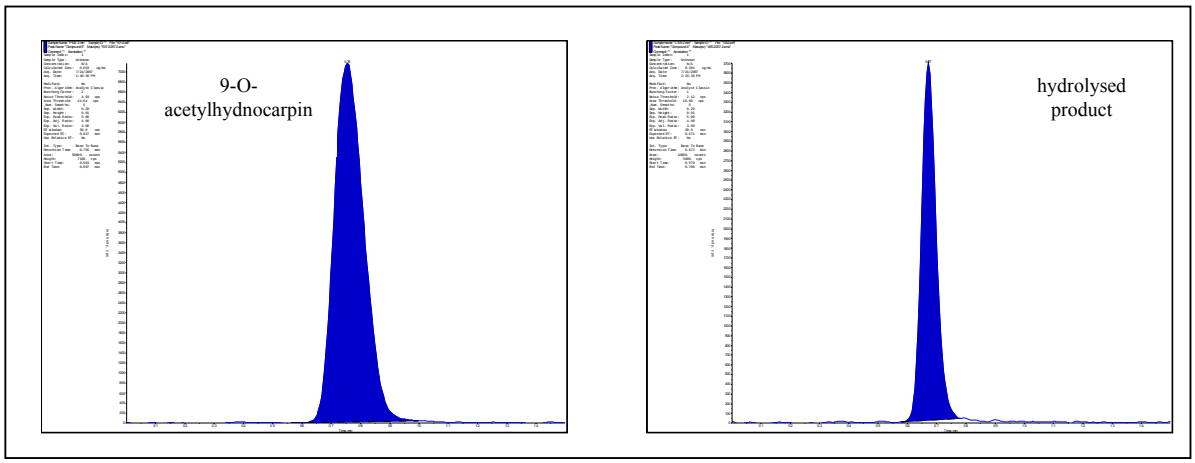

Figure 192 Representative chromatograms of a study sample

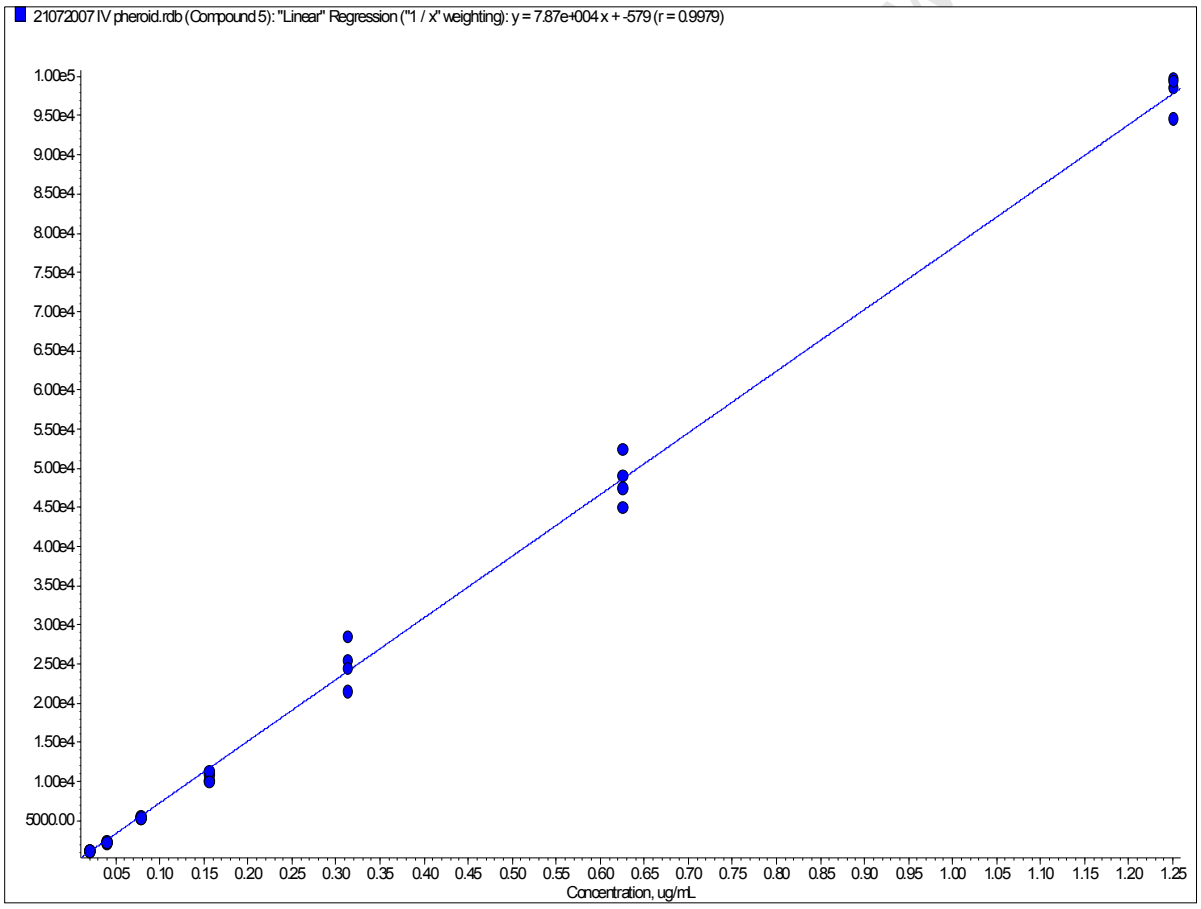

Figure 193 Calibration curve of 9-O-acetylhydnocarpin

Table 69 Back-calculated concentrations of 9-O-acetylhydnocarpin

Standard	Peak area	Nom conc. (µg/ml)	Calc. conc. (µg/ml)	Accuracy (%)
1	1120	0.0195	0.0216	111.0
1	1230	0.0195	0.0230	118.0
1	1170	0.0195	0.0222	114.0
1	1150	0.0195	0.0220	113.0
2	2170	0.0390	0.0350	89.6
2	2370	0.0390	0.0375	96.0
2	2220	0.0390	0.0355	91.1
2	2280	0.0390	0.0363	93.0
3	5340	0.0780	0.0752	96.5
3	5470	0.0780	0.0769	98.5
3	5670	0.0780	0.0794	102.0
3	5350	0.0780	0.0753	96.6
4	10200	0.156	0.137	87.8
4	10900	0.156	0.146	93.7
4	11400	0.156	0.152	97.4
4	9980	0.156	0.134	86.1
5	25500	0.313	0.331	106.0
5	28600	0.313	0.370	118.0
5	24500	0.313	0.319	102.0
5	21500	0.313	0.281	89.8
6	45000	0.625	0.579	92.7
6	47500	0.625	0.611	97.7
6	49100	0.625	0.631	101.0
6	52500	0.625	0.674	108.0
7	99800	1.25	1.28	102.0
7	98600	1.25	1.26	101.0
7	94600	1.25	1.21	96.8
7	99400	1.25	1.27	102.0

Table 70 Summary of calibration curve statistics of 9-O-acetylhydnocarpin

Standard	Nom conc. (µg/ml)	Number Of Values Used	Mean	Standard Deviation	% CV	Accuracy
1	0.0195	4	0.0222	0.000590	2.7	113.9
2	0.0391	4	0.0361	0.001078	3.0	92.4
3	0.0781	4	0.0767	0.001960	2.6	98.4
4	0.156	4	0.142	0.008217	5.8	91.2
5	0.313	4	0.325	0.036781	11.3	103.9
6	0.625	4	0.624	0.039711	6.4	99.8
7	1.25	4	1.25	0.030272	2.4	100.3

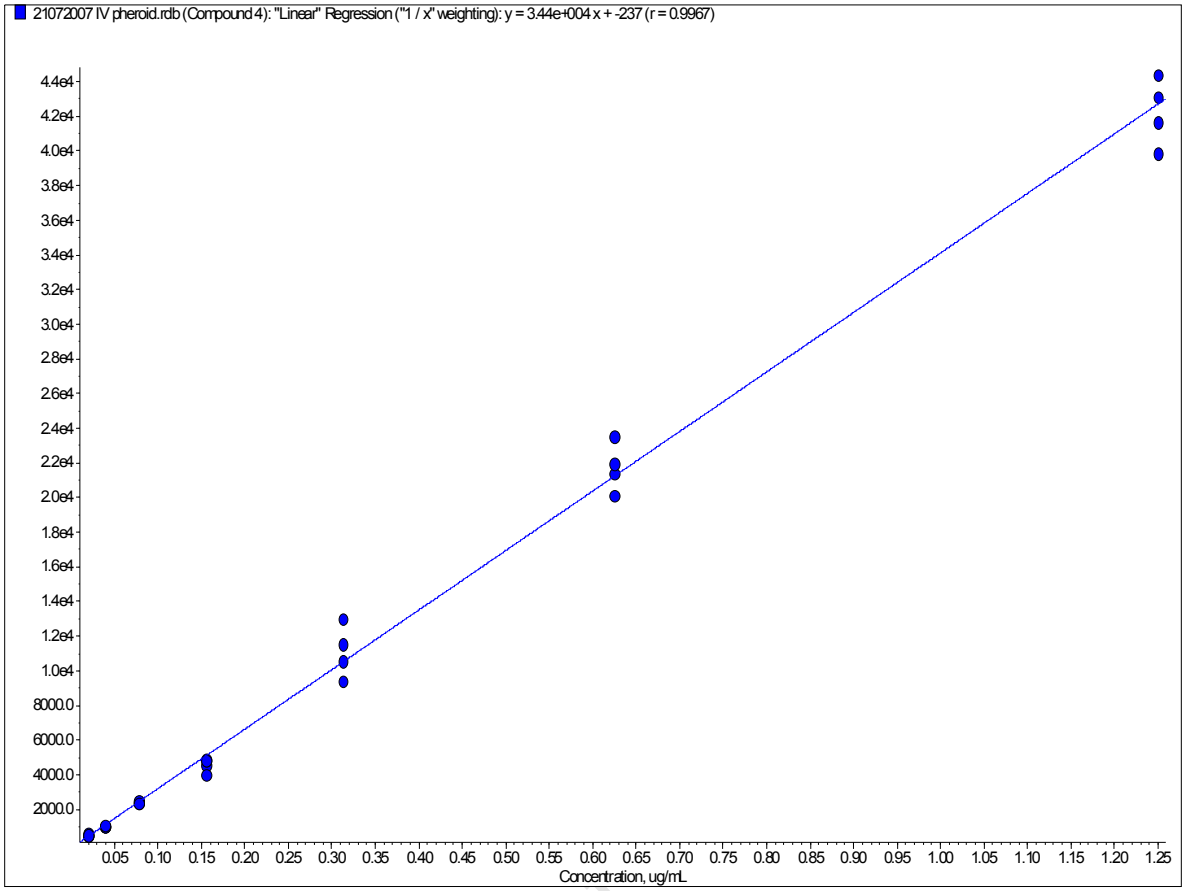

Figure 194 Calibration curve of the hydrolysed product

Table 71 Back-calculated concentrations of the hydrolysed product

Standard	Peak area	Nom conc. (µg/ml)	Calc. conc. (µg/ml)	Accuracy (%)
1	493	0.0195	0.0212	109.0
1	488	0.0195	0.0211	108.0
1	569	0.0195	0.0235	120.0
1	506	0.0195	0.0216	111.0
2	1010	0.0390	0.0364	93.3
2	982	0.0390	0.0355	91.0
2	997	0.0390	0.0359	92.1
2	1070	0.0390	0.0380	97.4
3	2320	0.0780	0.0745	95.5
3	2440	0.0780	0.0778	99.8
3	2510	0.0780	0.0799	102.0
3	2350	0.0780	0.0754	96.6
4	4550	0.156	0.139	89.3
4	4850	0.156	0.148	95.0
4	4810	0.156	0.147	94.2
4	3970	0.156	0.122	78.5
5	11500	0.313	0.342	109.0
5	13000	0.313	0.385	123.0
5	10500	0.313	0.314	100.0
5	9360	0.313	0.279	89.2
6	20100	0.625	0.592	94.7
6	21400	0.625	0.629	101.0
6	21900	0.625	0.646	103.0
6	23500	0.625	0.691	111.0
7	44400	1.25	1.30	104.0
7	41600	1.25	1.22	97.5
7	39800	1.25	1.17	93.3
7	43100	1.25	1.26	101.0

Table 72 Summary of calibration curve statistics of the hydrolysed product

Standard	Nom conc. (µg/ml)	Number Of Values Used	Mean	Standard Deviation	% CV	Accuracy
1	0.0195	4	0.0219	0.00109	5.0	112.1
2	0.0391	4	0.0364	0.00109	3.0	93.4
3	0.0781	4	0.0769	0.00245	3.2	98.6
4	0.156	4	0.139	0.01182	8.5	89.3
5	0.313	4	0.330	0.04467	13.5	105.4
6	0.625	4	0.640	0.04122	6.4	102.3
7	1.25	4	1.24	0.05699	4.6	98.9

APPENDIX 4

Metabolite spectral data

LC-MS analysis: Blood sample
Chromatograms and mass spectra of peak groups 1 - 5

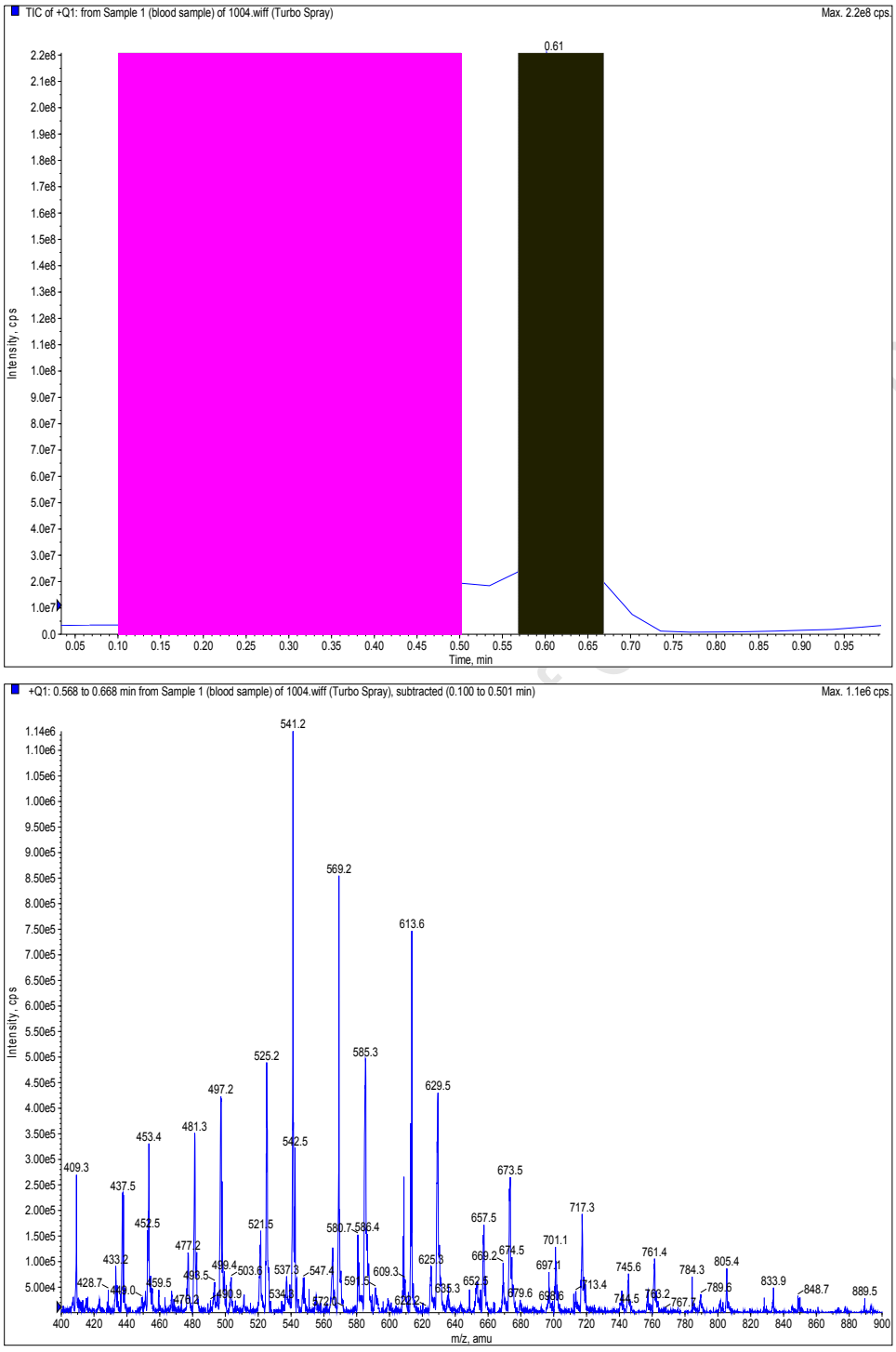

Figure 195 Chromatogram and mass spectrum of peak 1

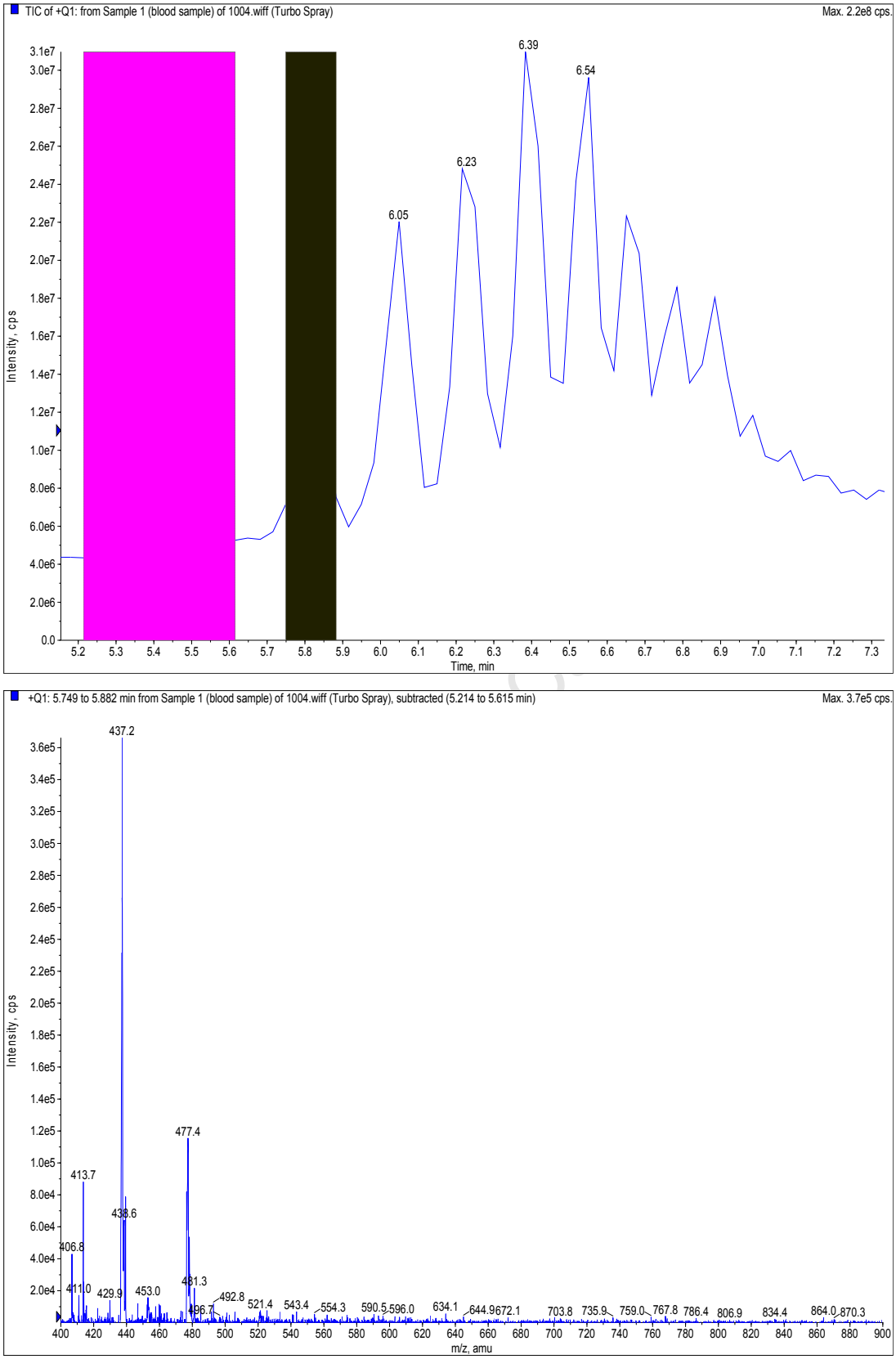

Figure 196 Chromatogram and mass spectrum of peak 2a

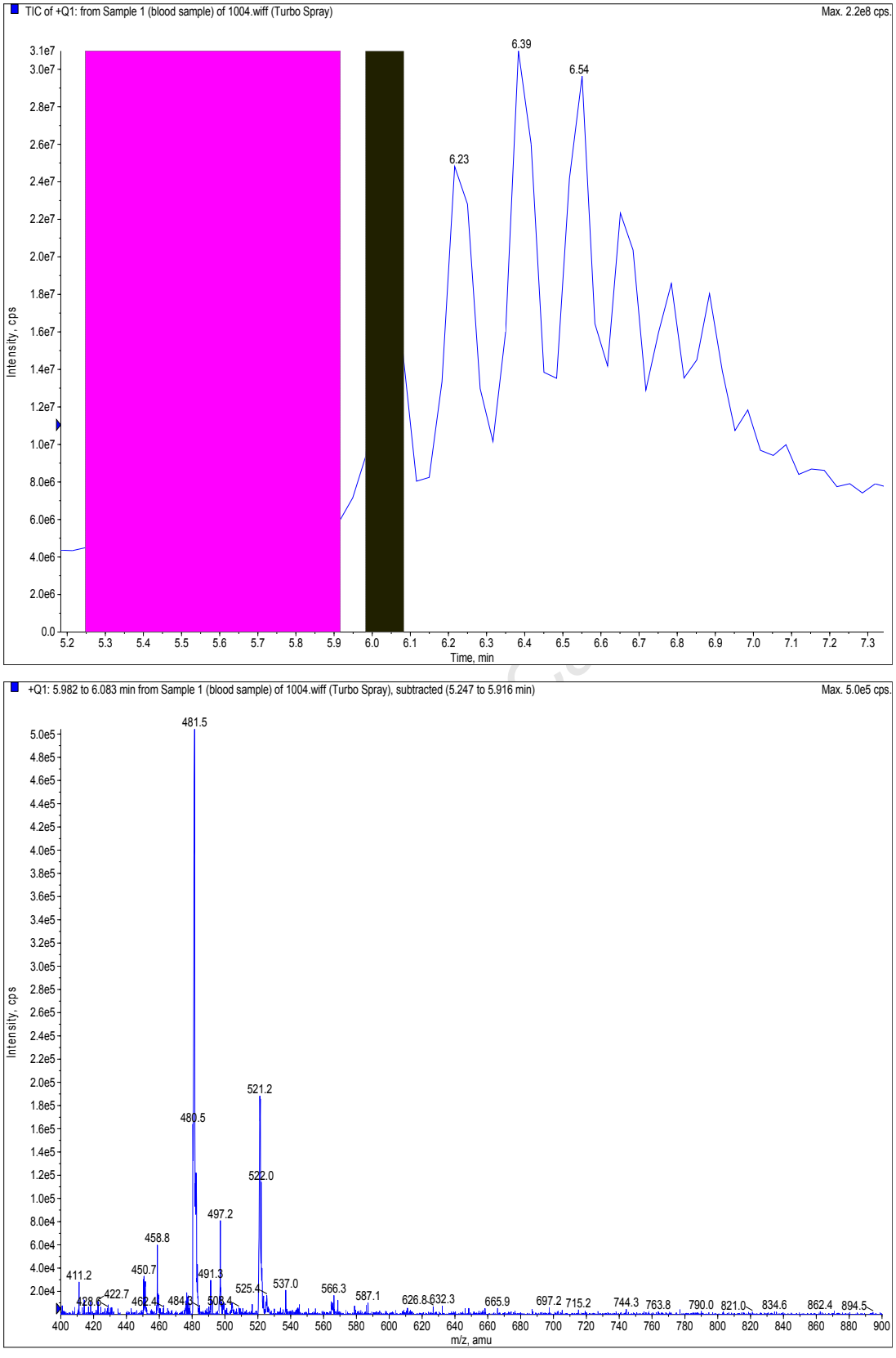

Figure 197 Chromatogram and mass spectrum of peak 2b

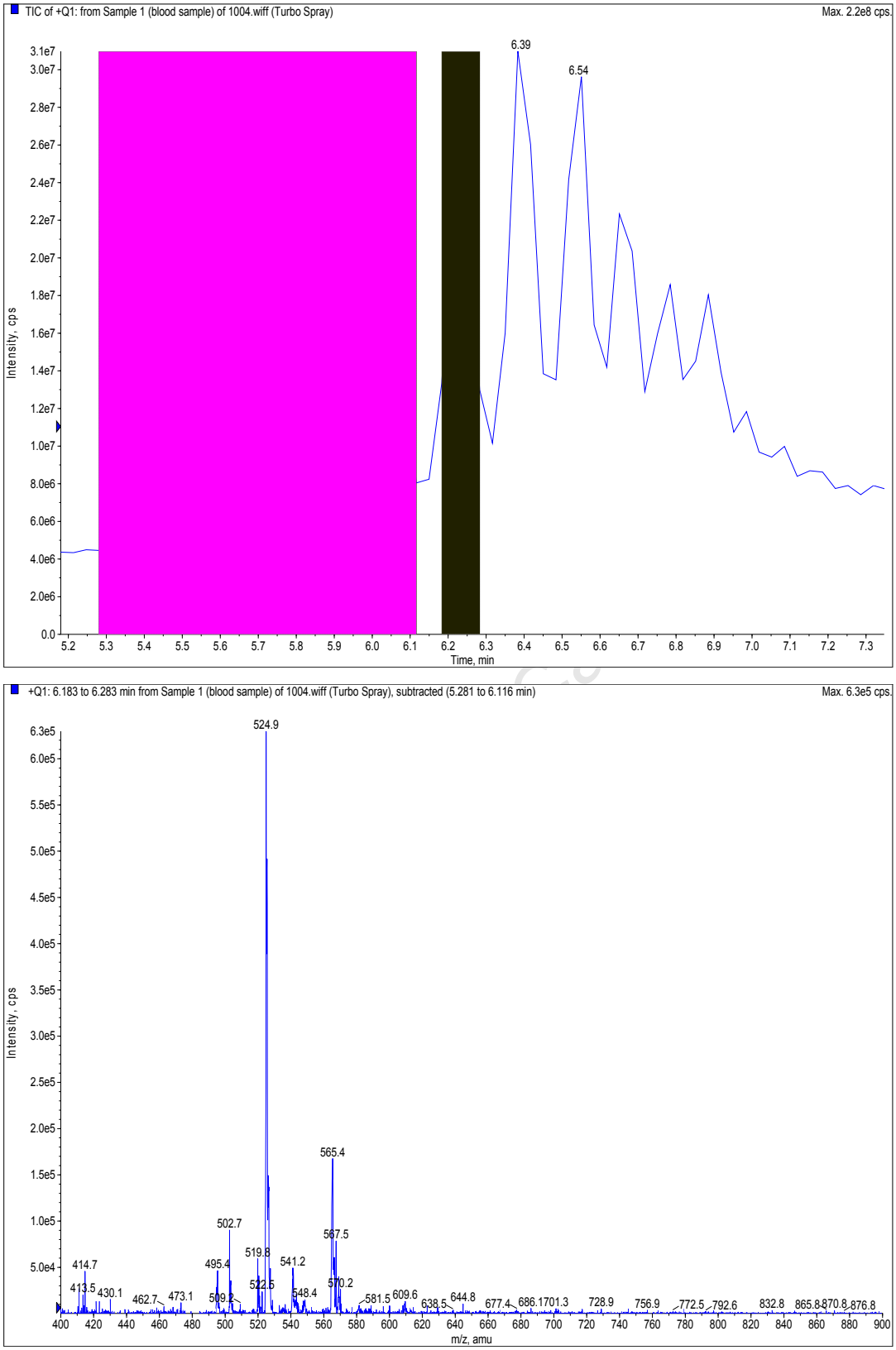

Figure 198 Chromatogram and mass spectrum of peak 2c

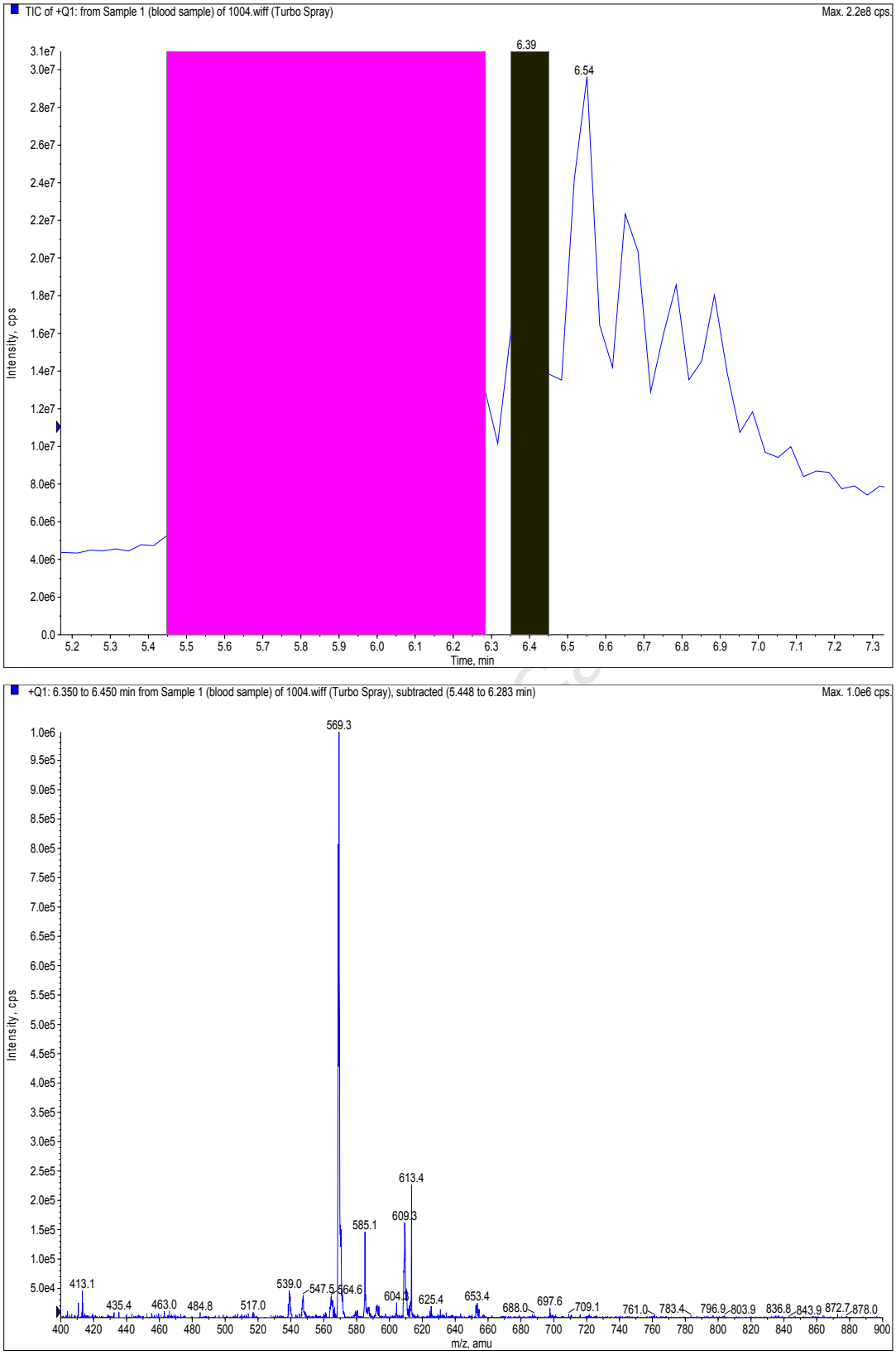

Figure 199 Chromatogram and mass spectrum of peak 2d

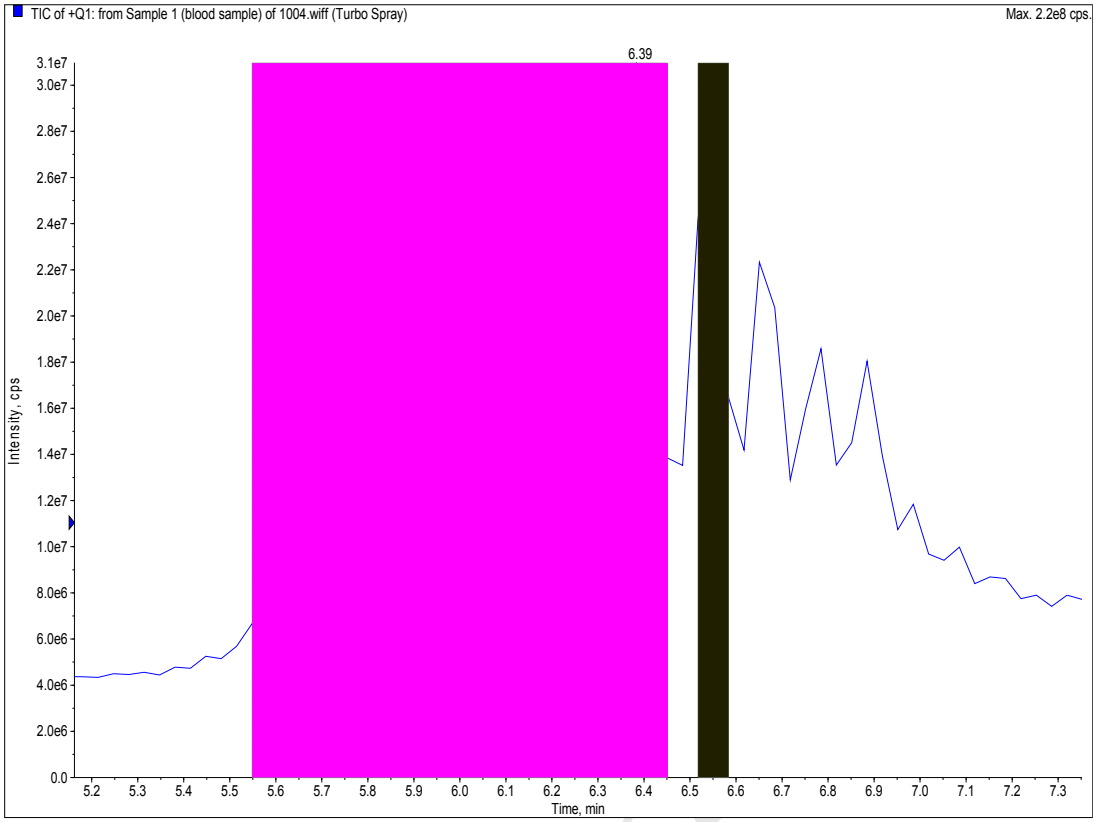

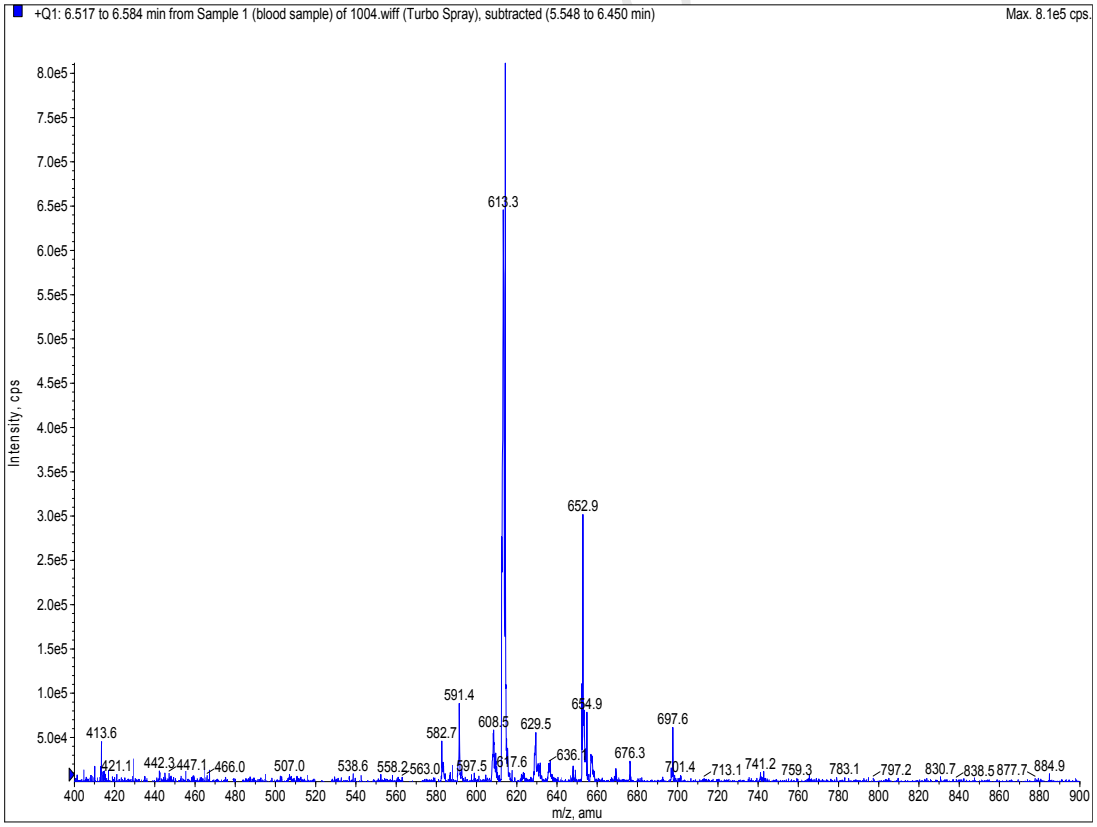

Figure 200 Chromatogram and mass spectrum of peak 2e

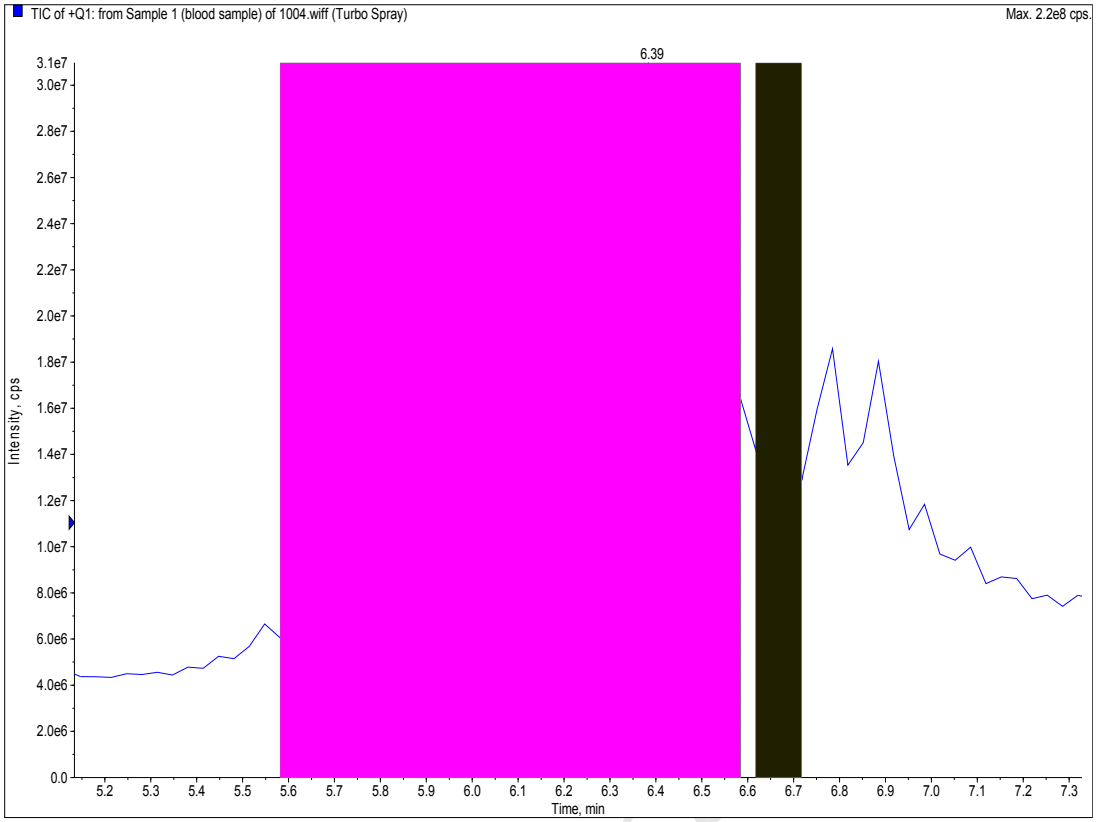

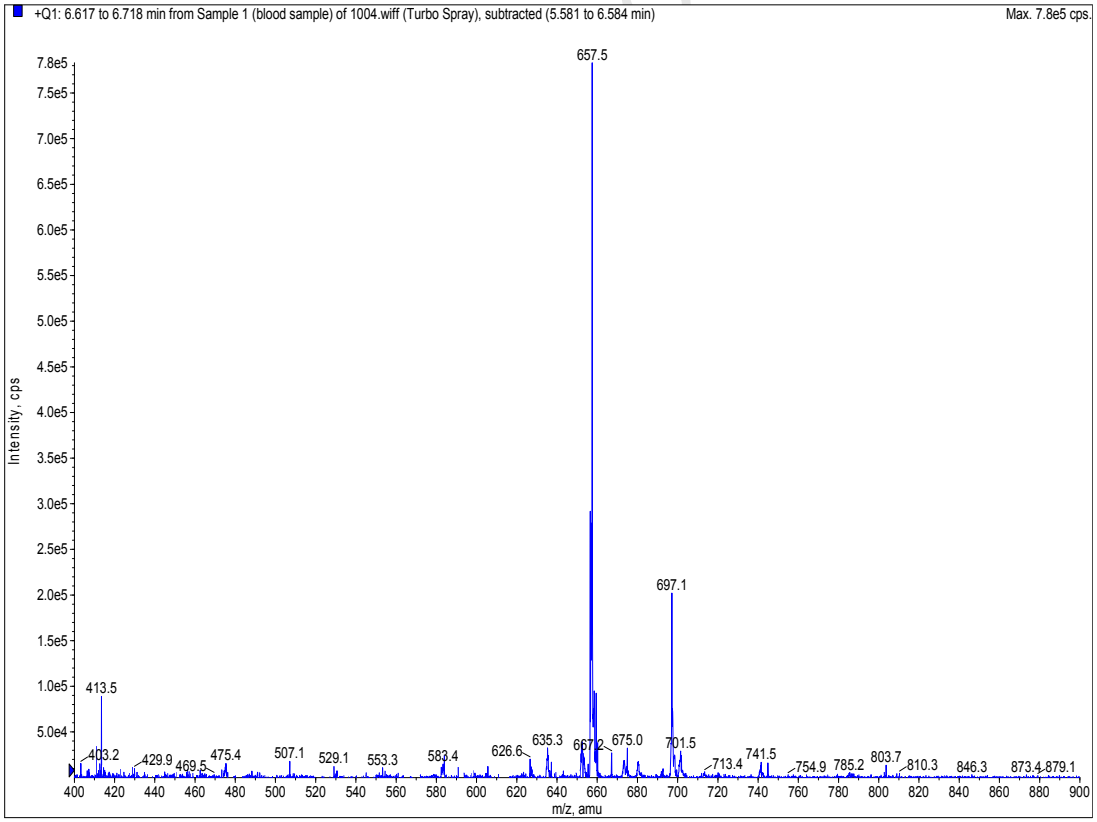

Figure 201 Chromatogram and mass spectrum of peak 2f

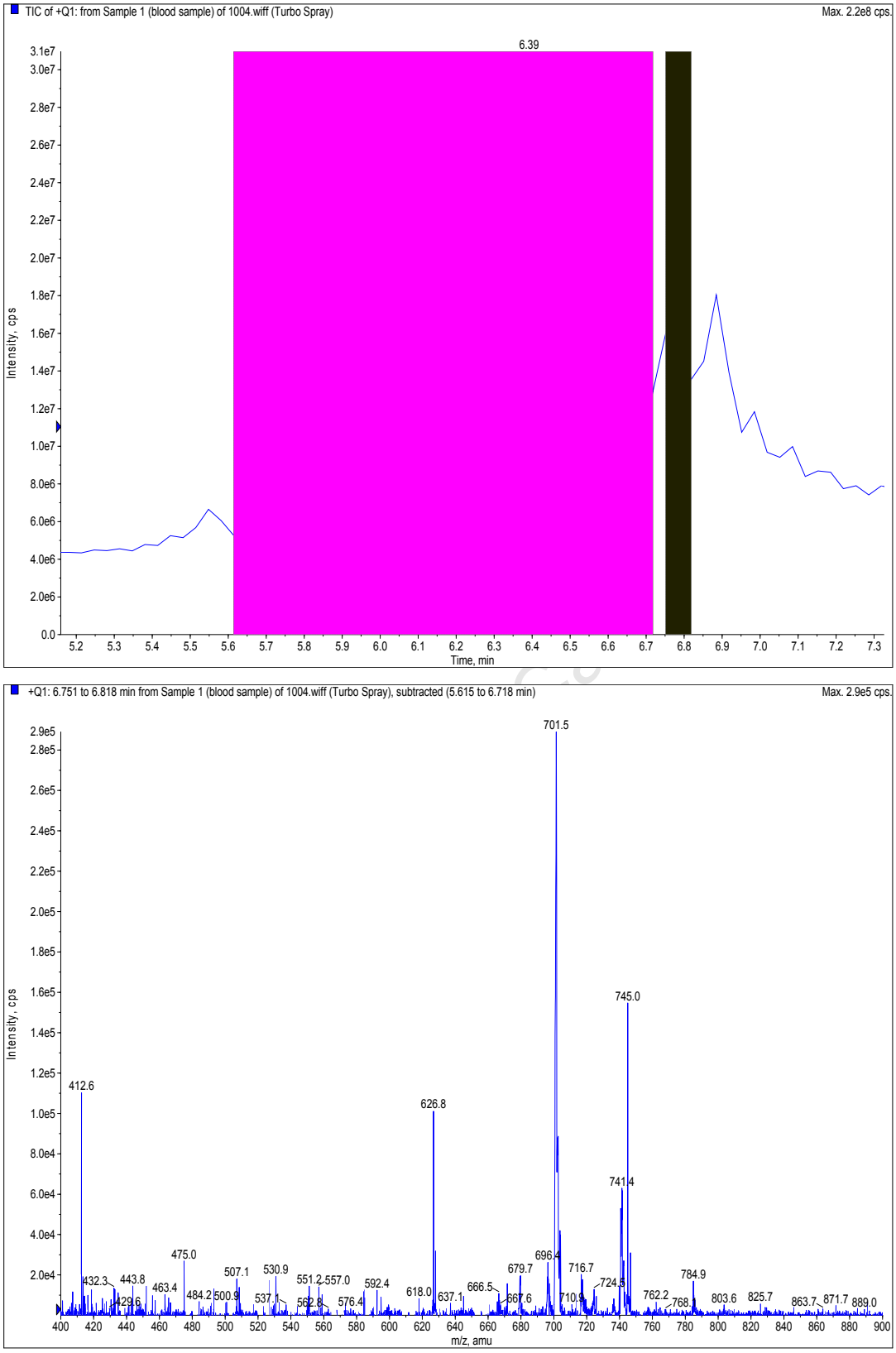

Figure 202 Chromatogram and mass spectrum of peak 2g

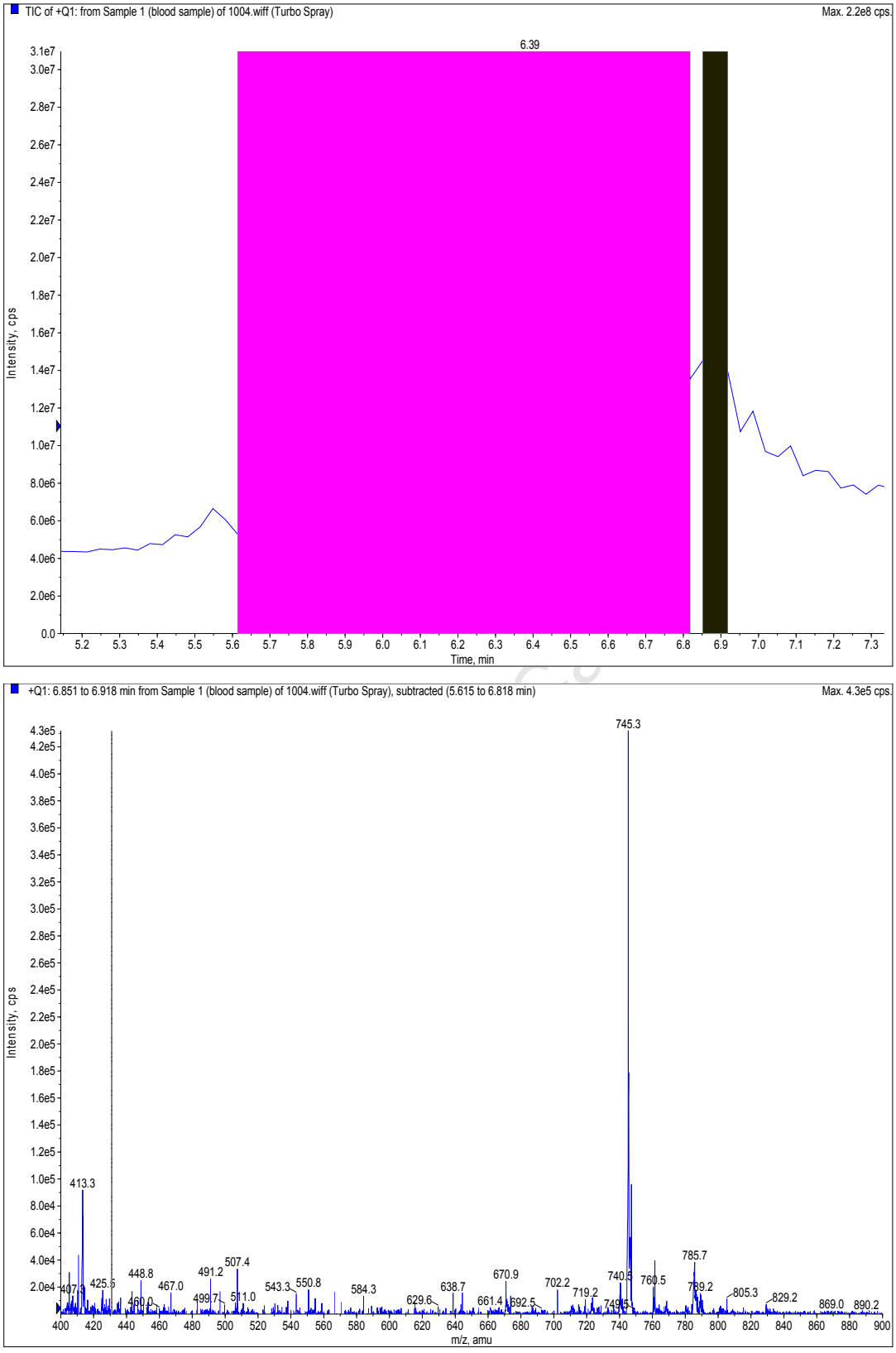

Figure 203 Chromatogram and mass spectrum of peak 2h

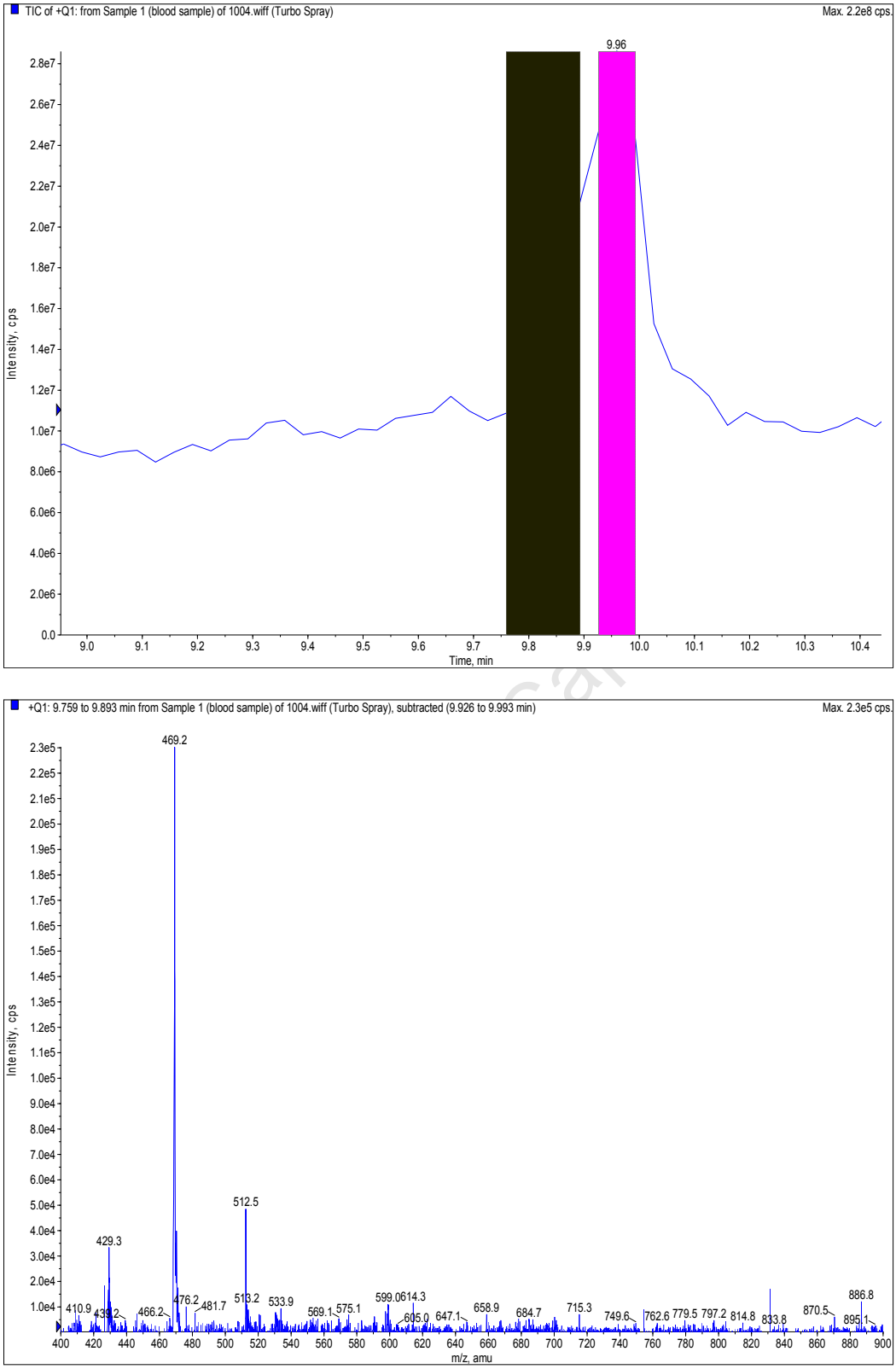

Figure 204 Chromatogram and mass spectrum of peak 3a

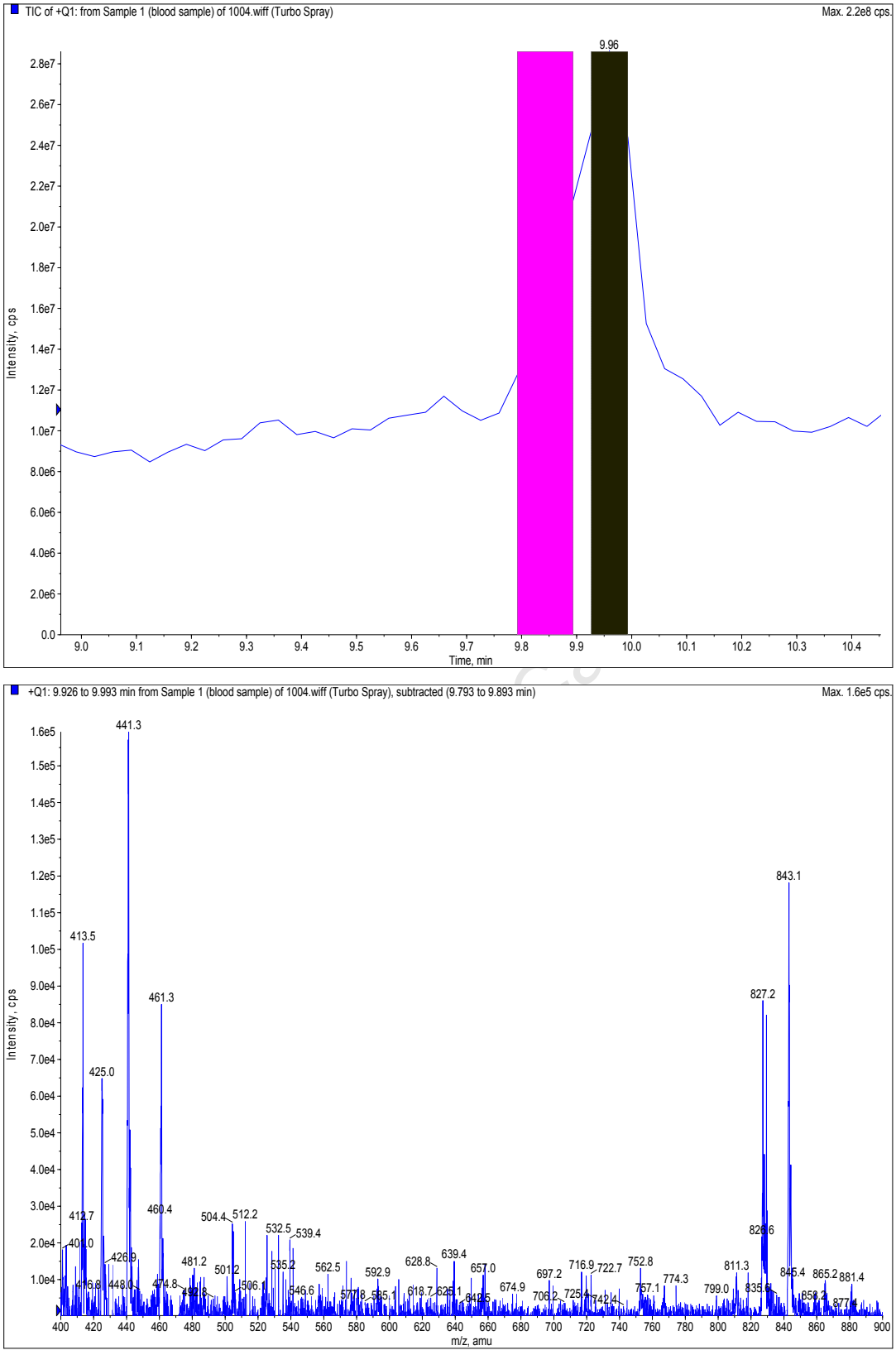

Figure 205 Chromatogram and mass spectrum of peak 3b

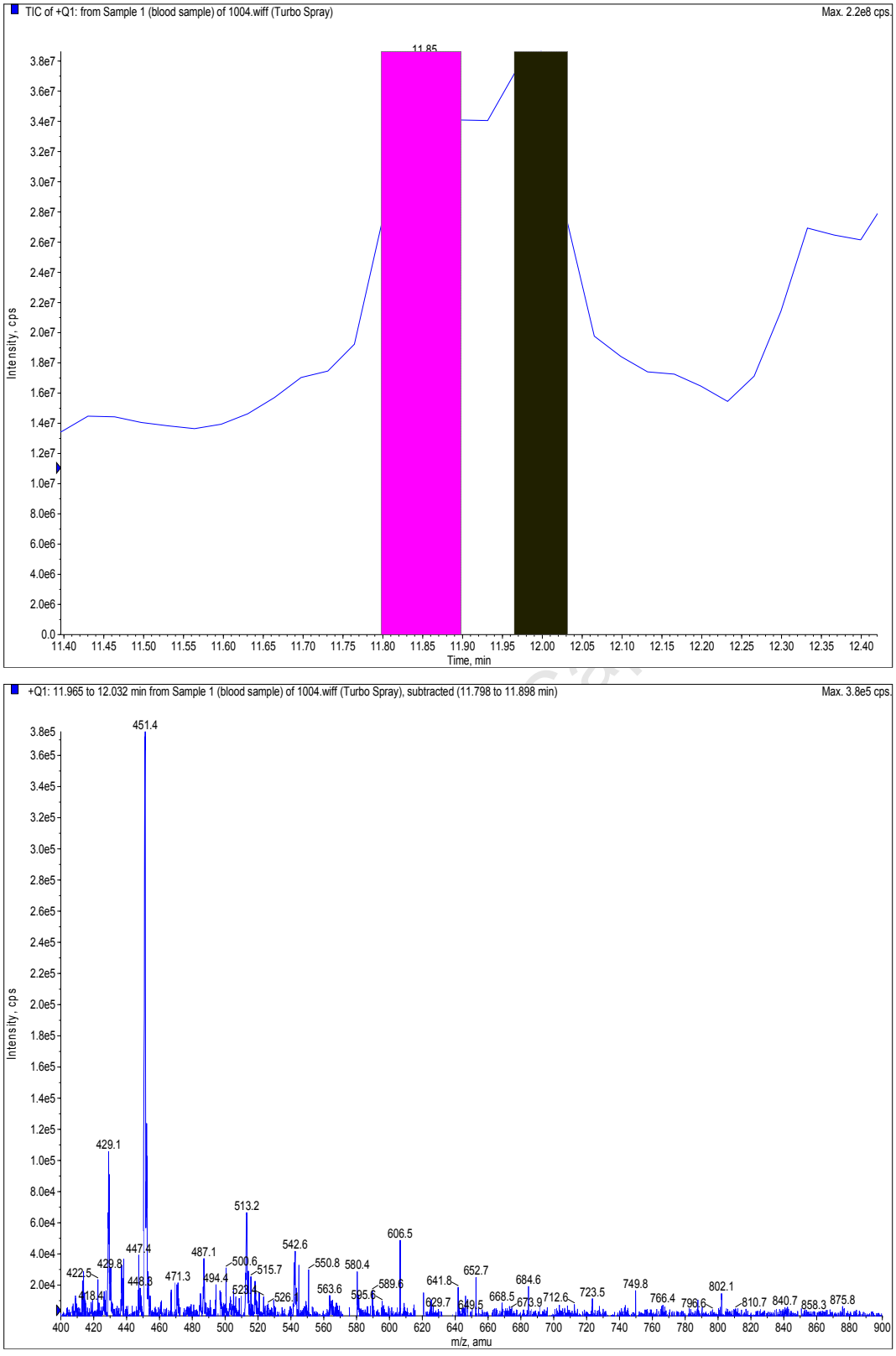

Figure 206 Chromatogram and mass spectrum of peak 4a

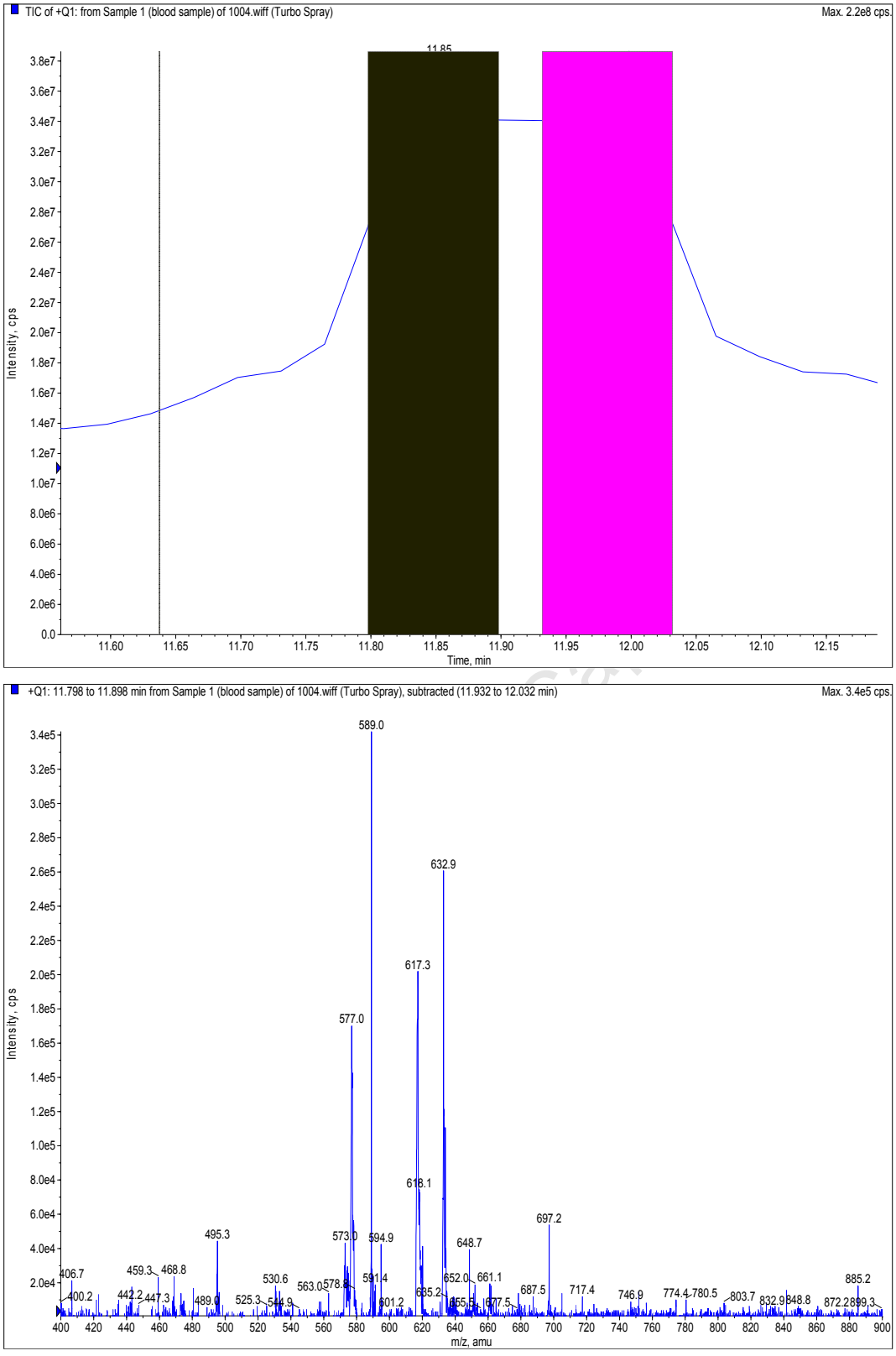

Figure 207 Chromatogram and mass spectrum of peak 4b

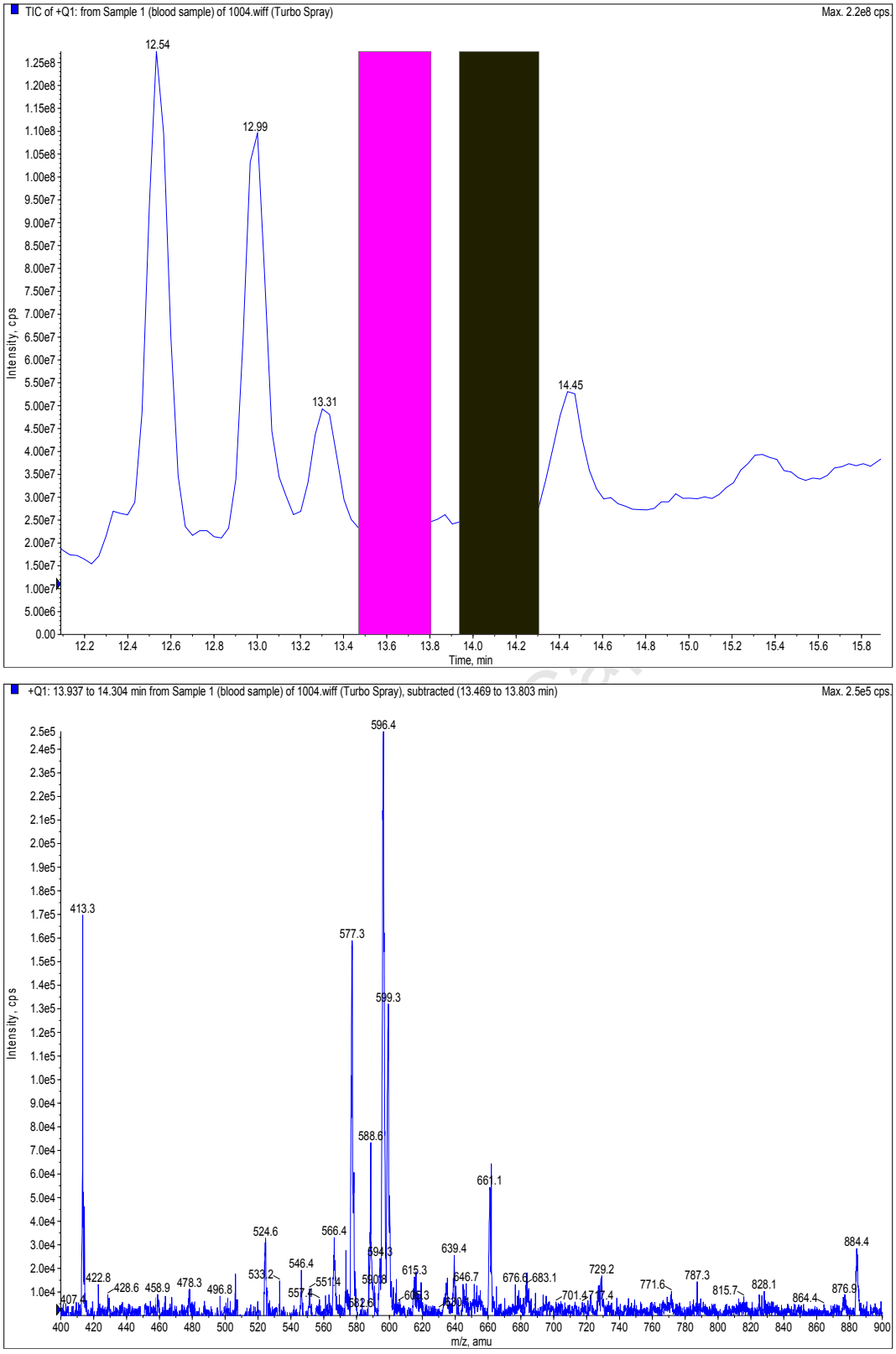

Figure 208 Chromatogram and mass spectrum of peak 5

LC-MS analysis: Urine sample
Chromatograms and mass spectra of peak groups 1 and 2

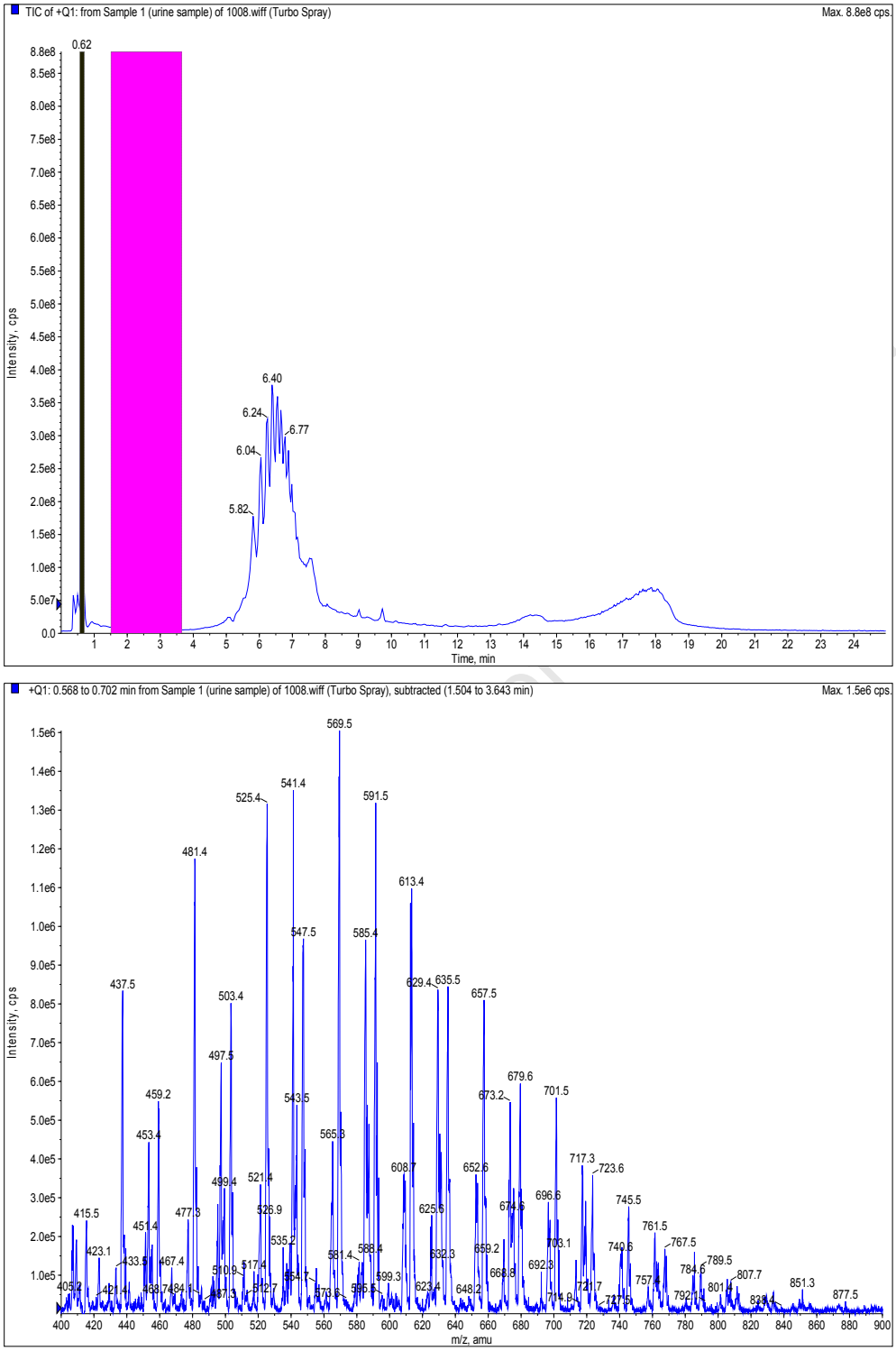

Figure 209 Chromatogram and mass spectrum of group 1

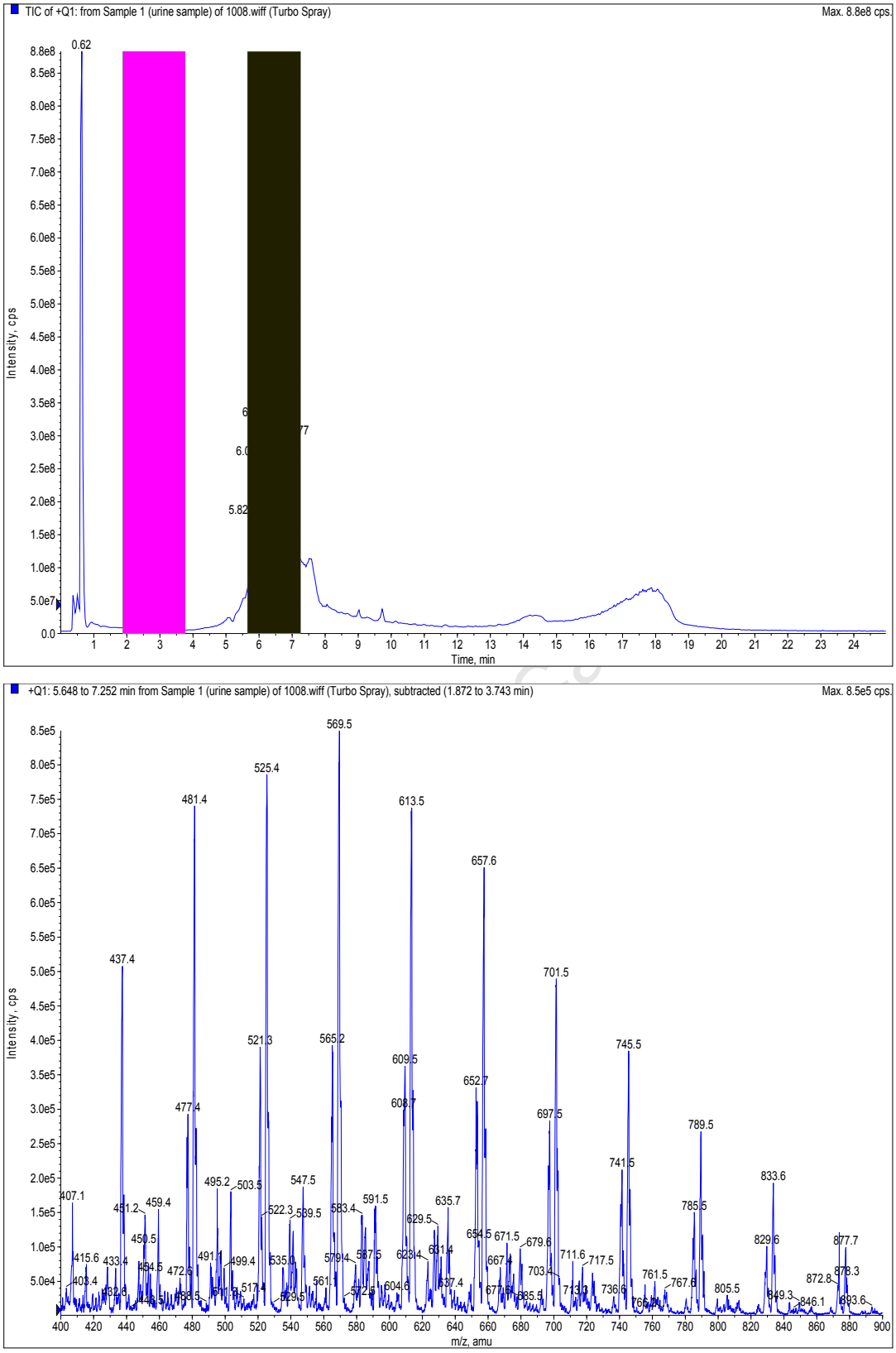

Figure 210 Chromatogram and mass spectrum of group 2

LC-MS analysis: Faeces sample
Chromatograms and mass spectra of peak groups 1 - 4

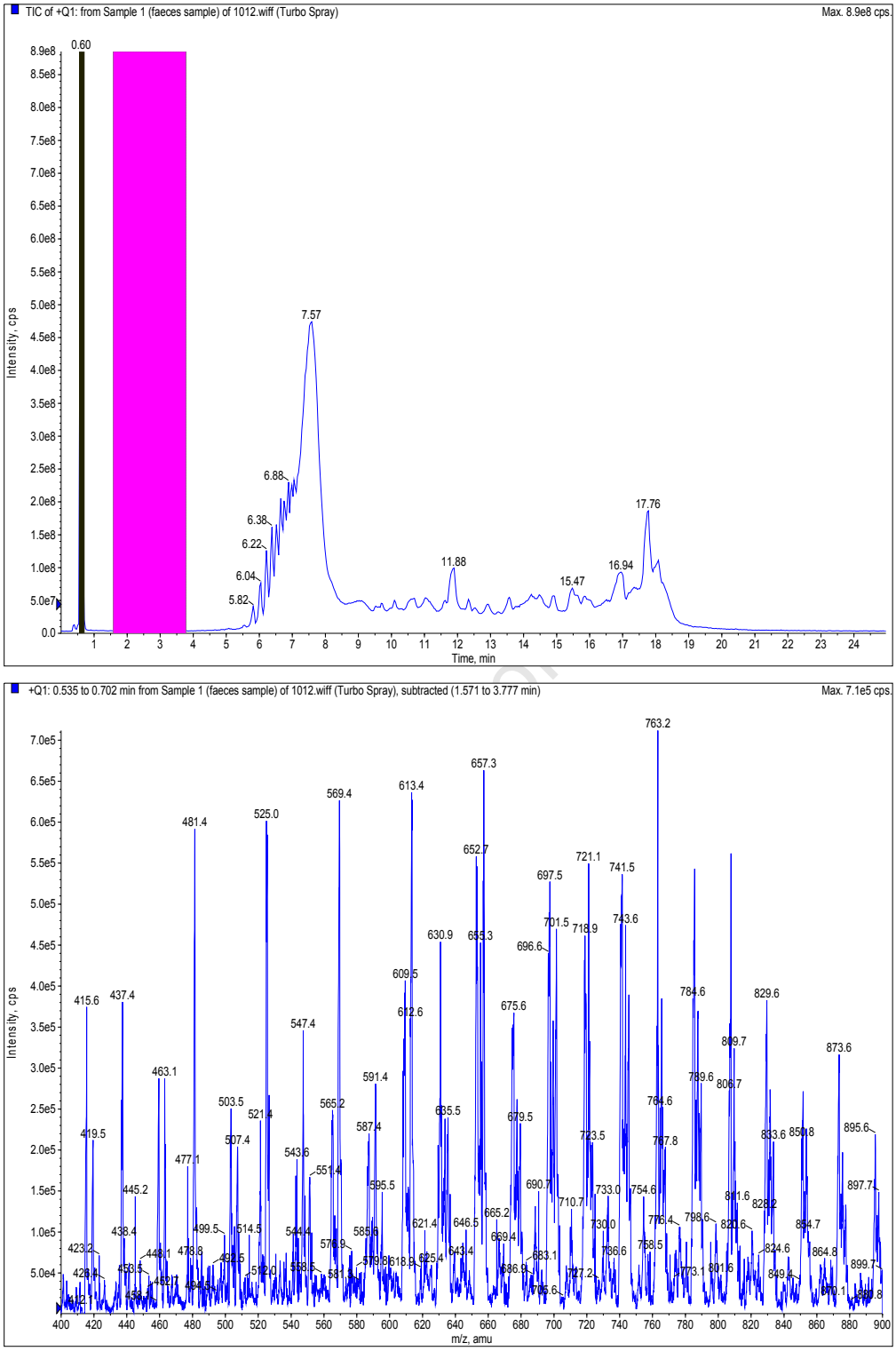

Figure 211 Chromatogram and mass spectrum of group 1

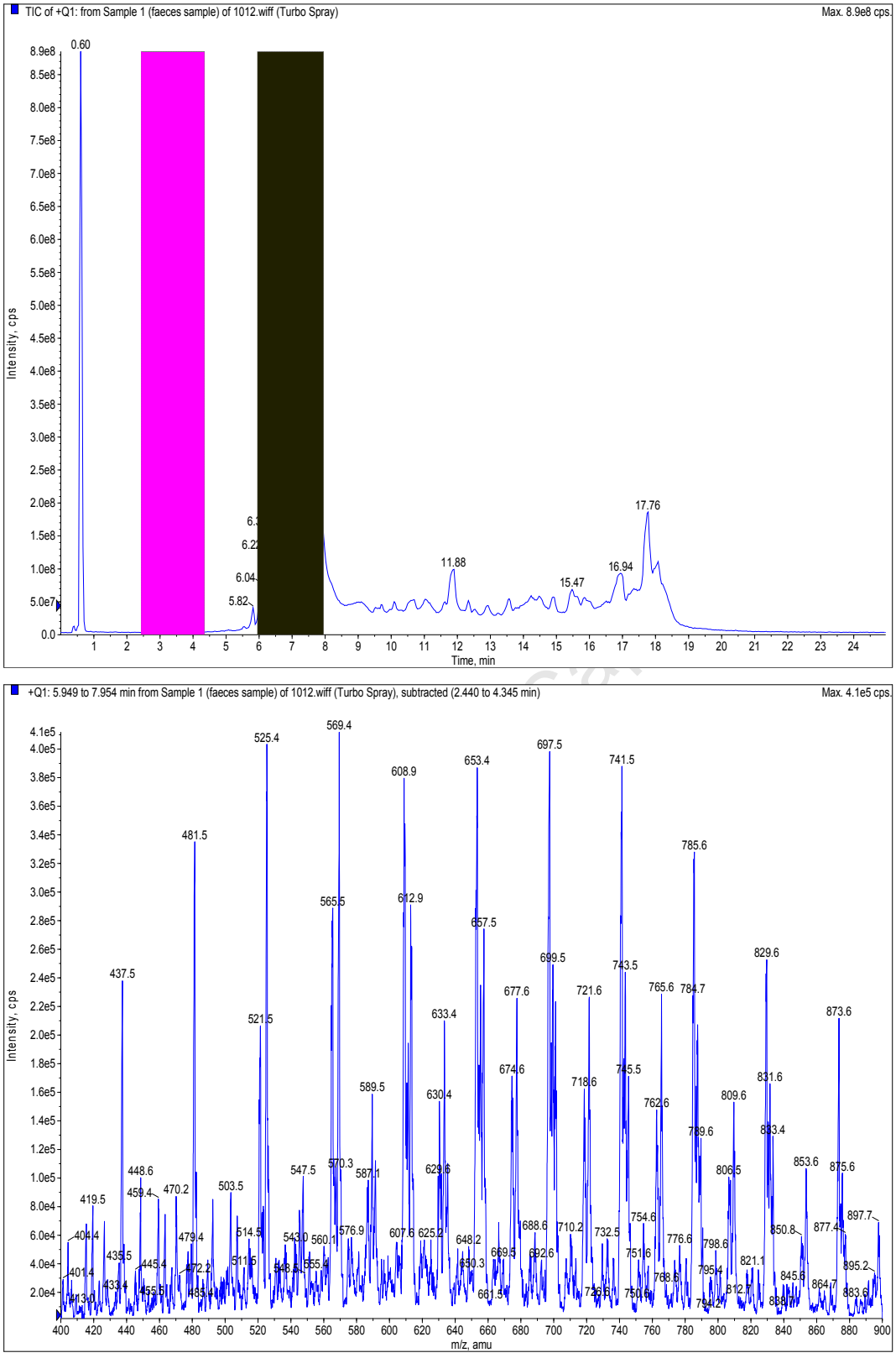

Figure 212 Chromatogram and mass spectrum of group 2

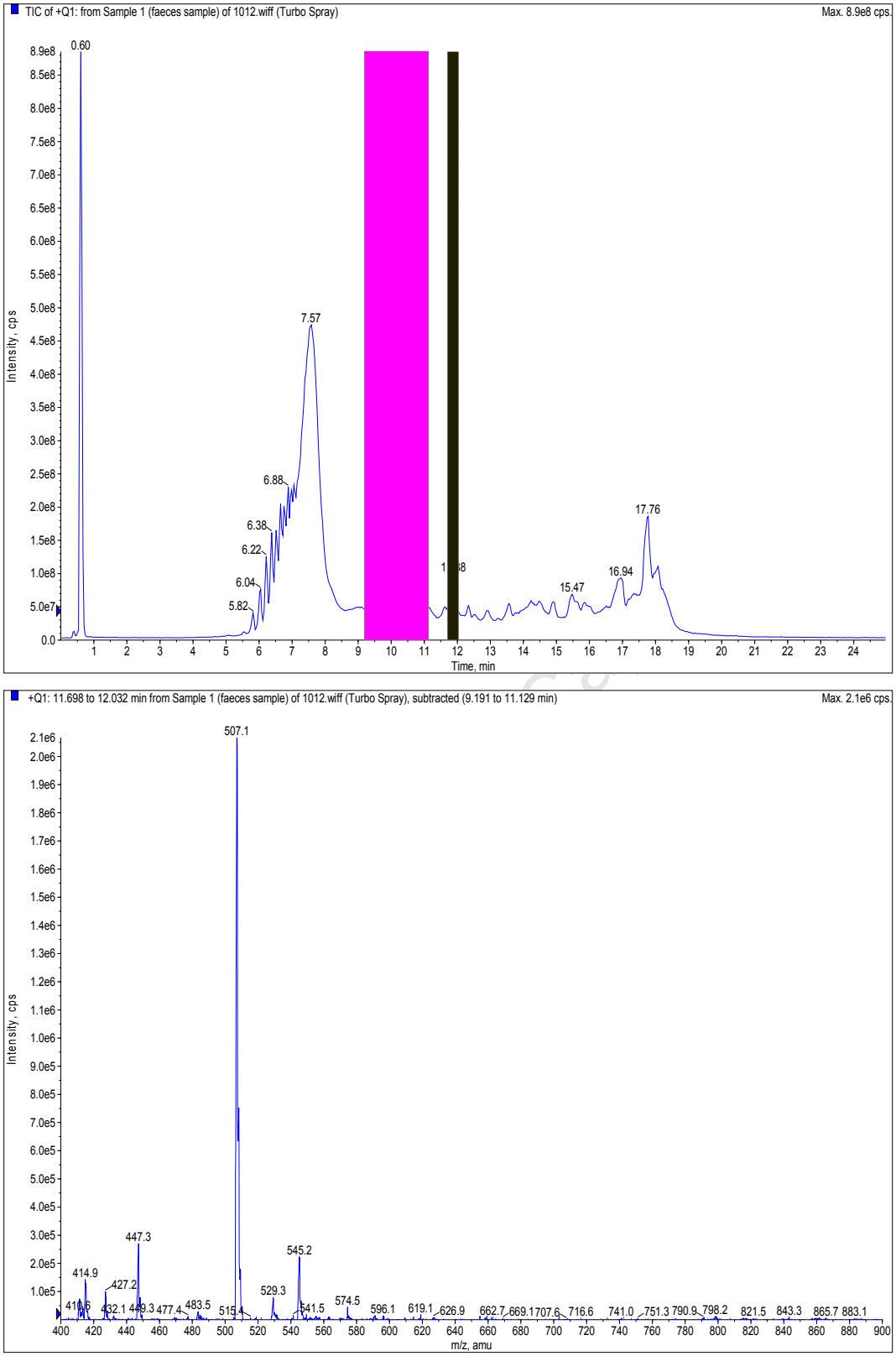

Figure 213 Chromatogram and mass spectrum of group 3

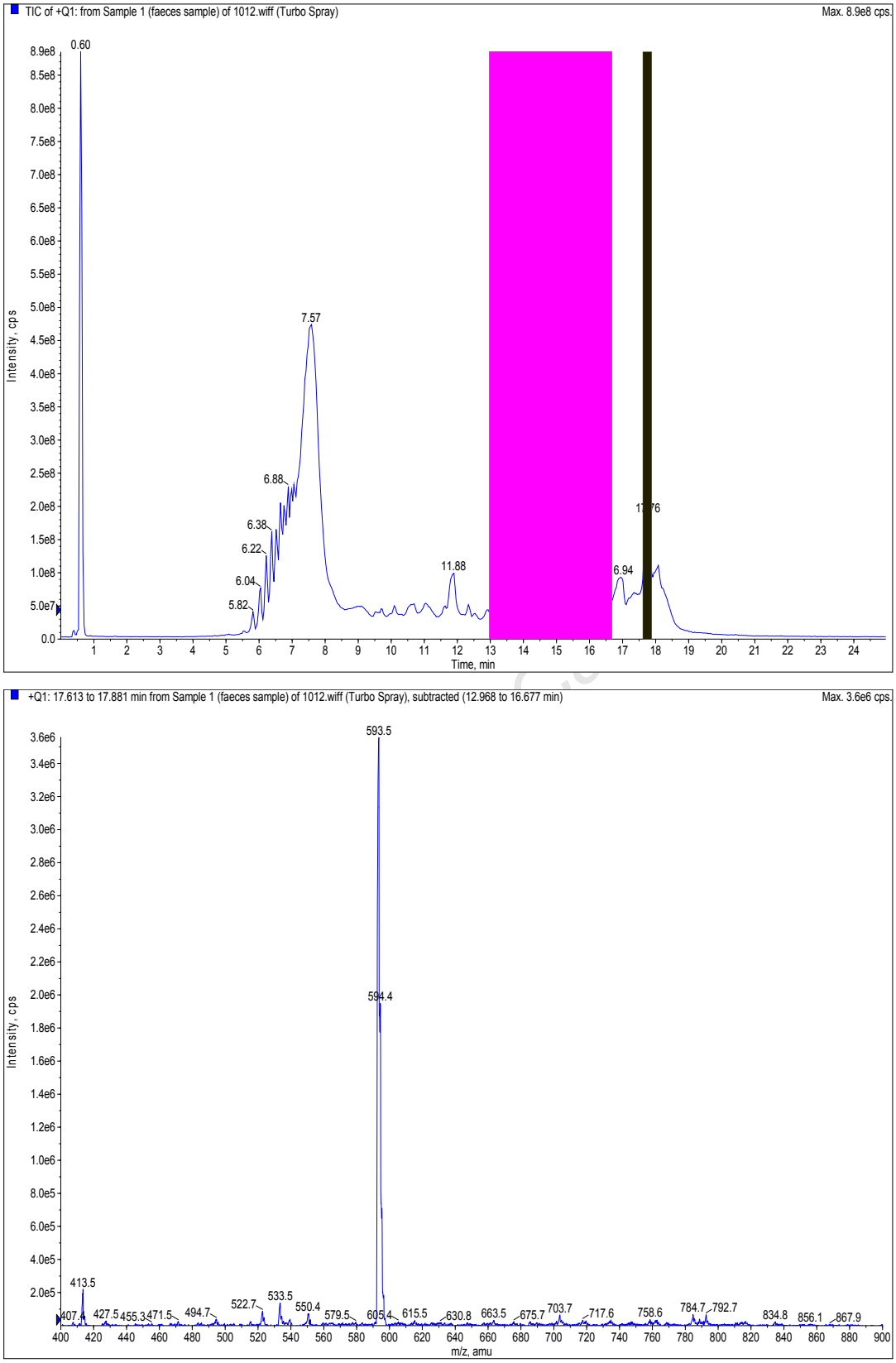

Figure 214 Chromatogram and mass spectrum of group 4

Precursor ion scan analysis: Blood sample
Chromatogram and mass spectrum of peak 1

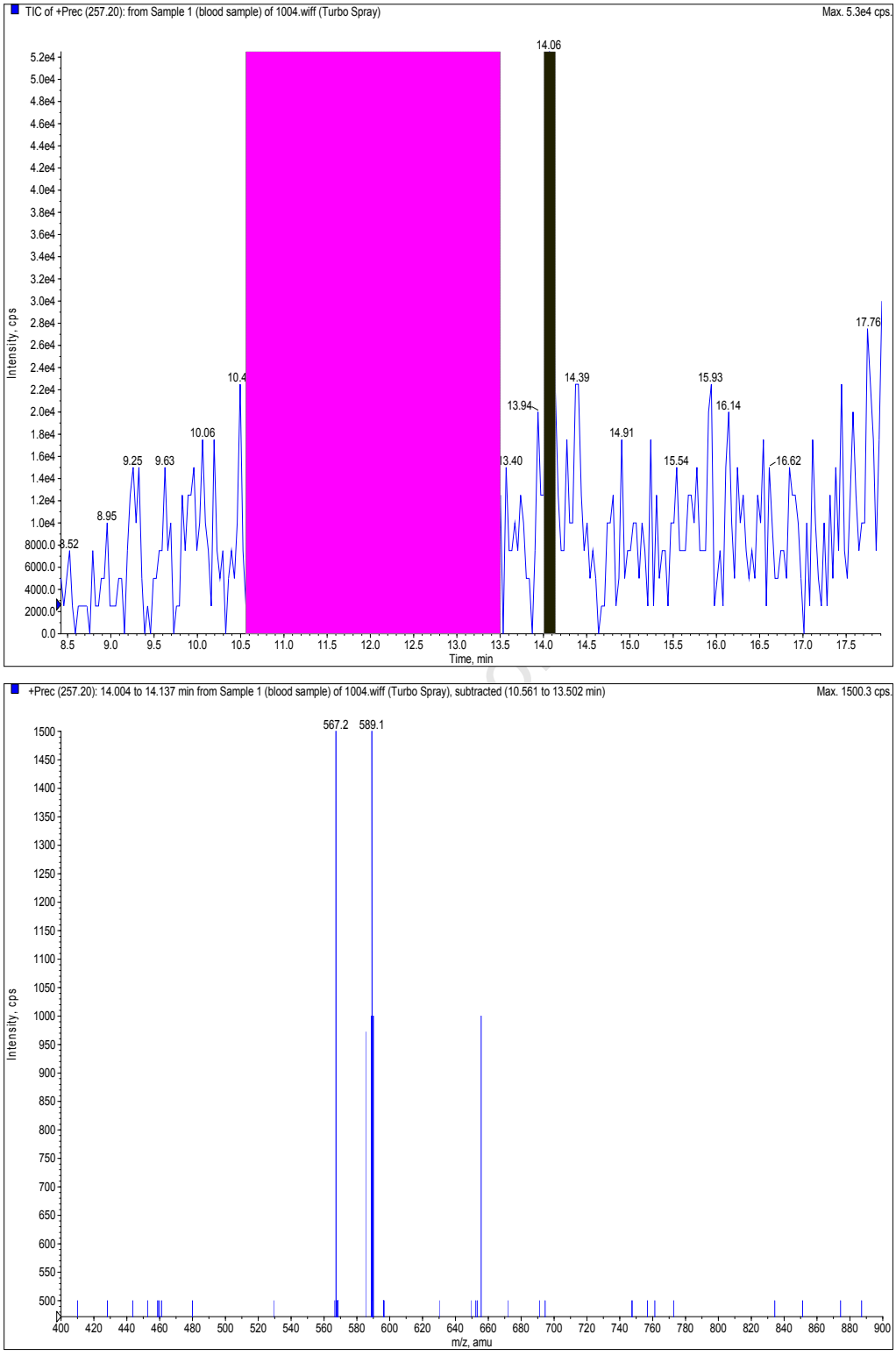

Figure 215 Chromatogram and precursor ion mass spectrum of peak 1

Precursor ion scan analysis: Urine sample
Chromatograms and mass spectra of peaks 1 and 2

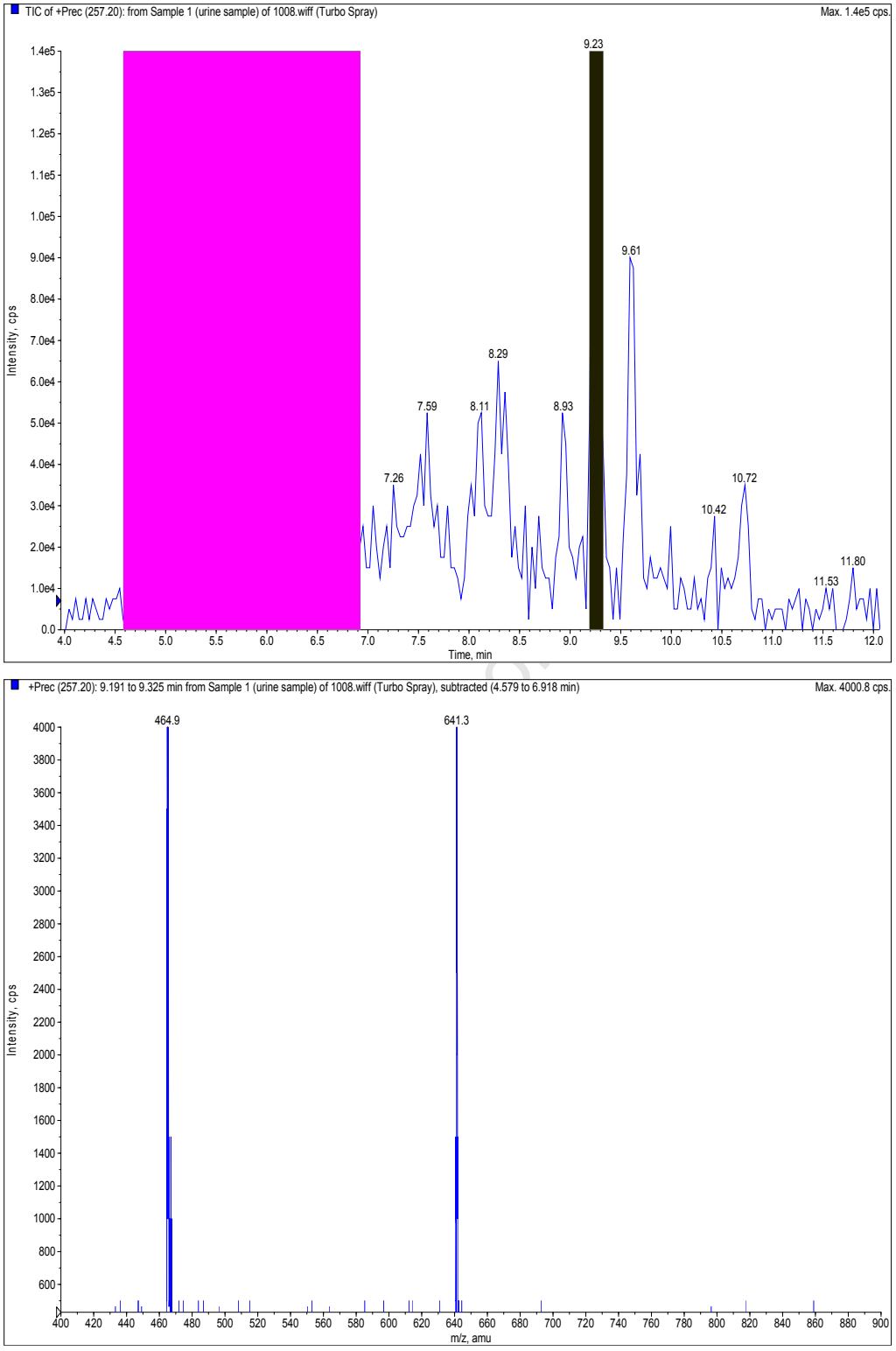

Figure 216 Chromatogram and precursor ion mass spectrum of peak 1

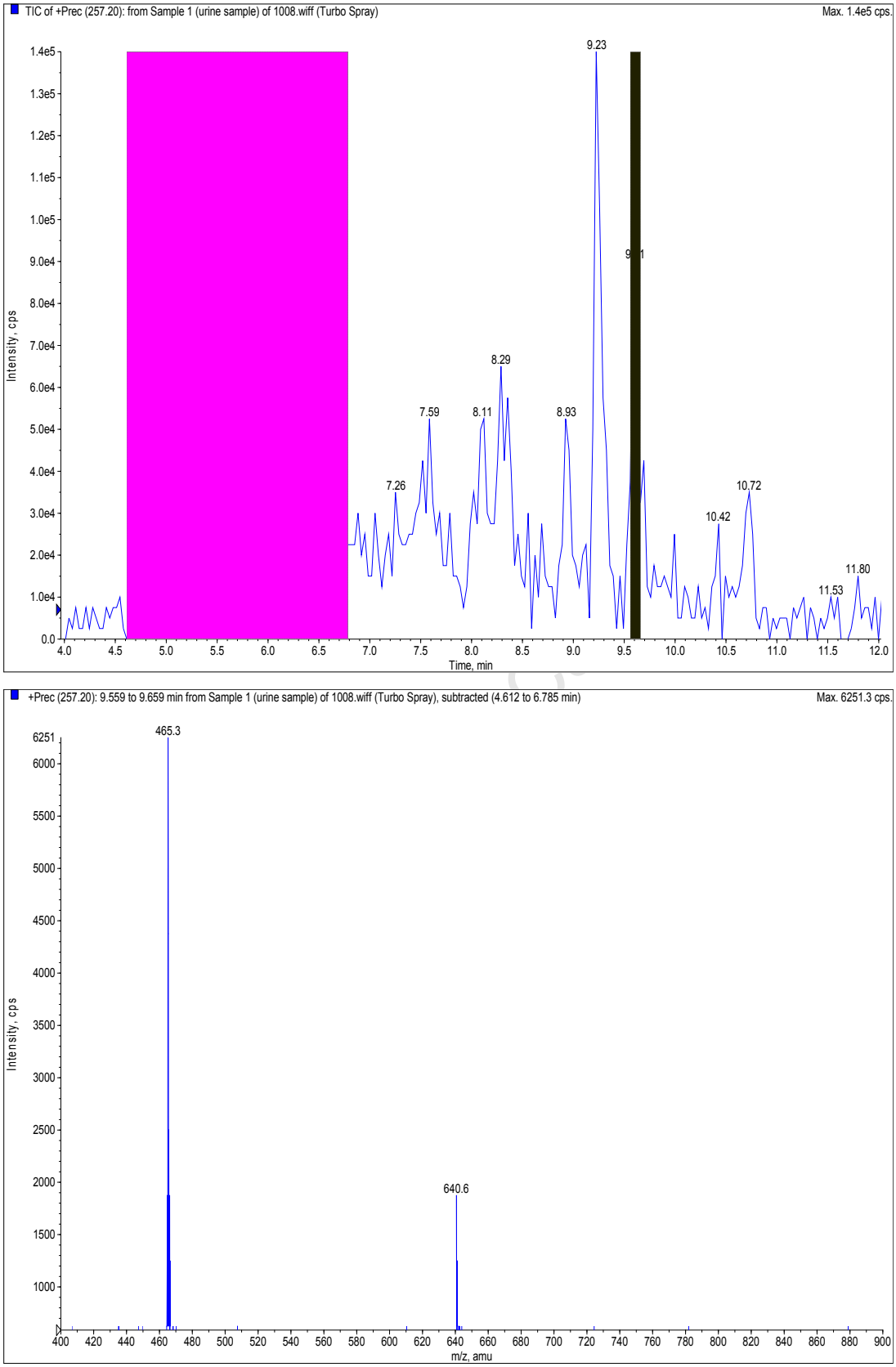

Figure 217 Chromatogram and precursor ion mass spectrum of peak 2

Precursor ion scan analysis: Faeces sample
Chromatograms and mass spectra of peaks 1 - 3

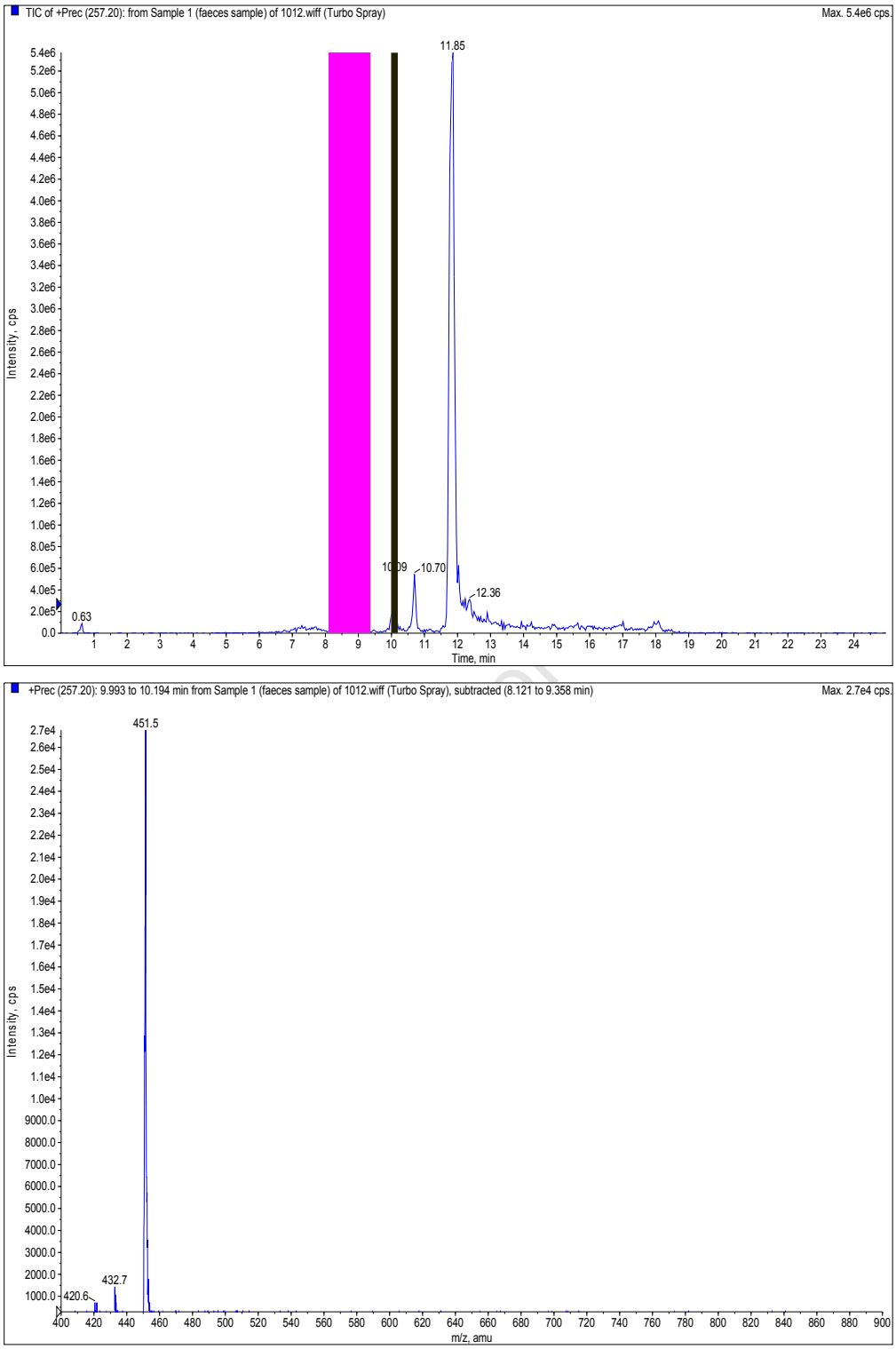

Figure 218 Chromatogram and precursor ion mass spectrum of peak 1

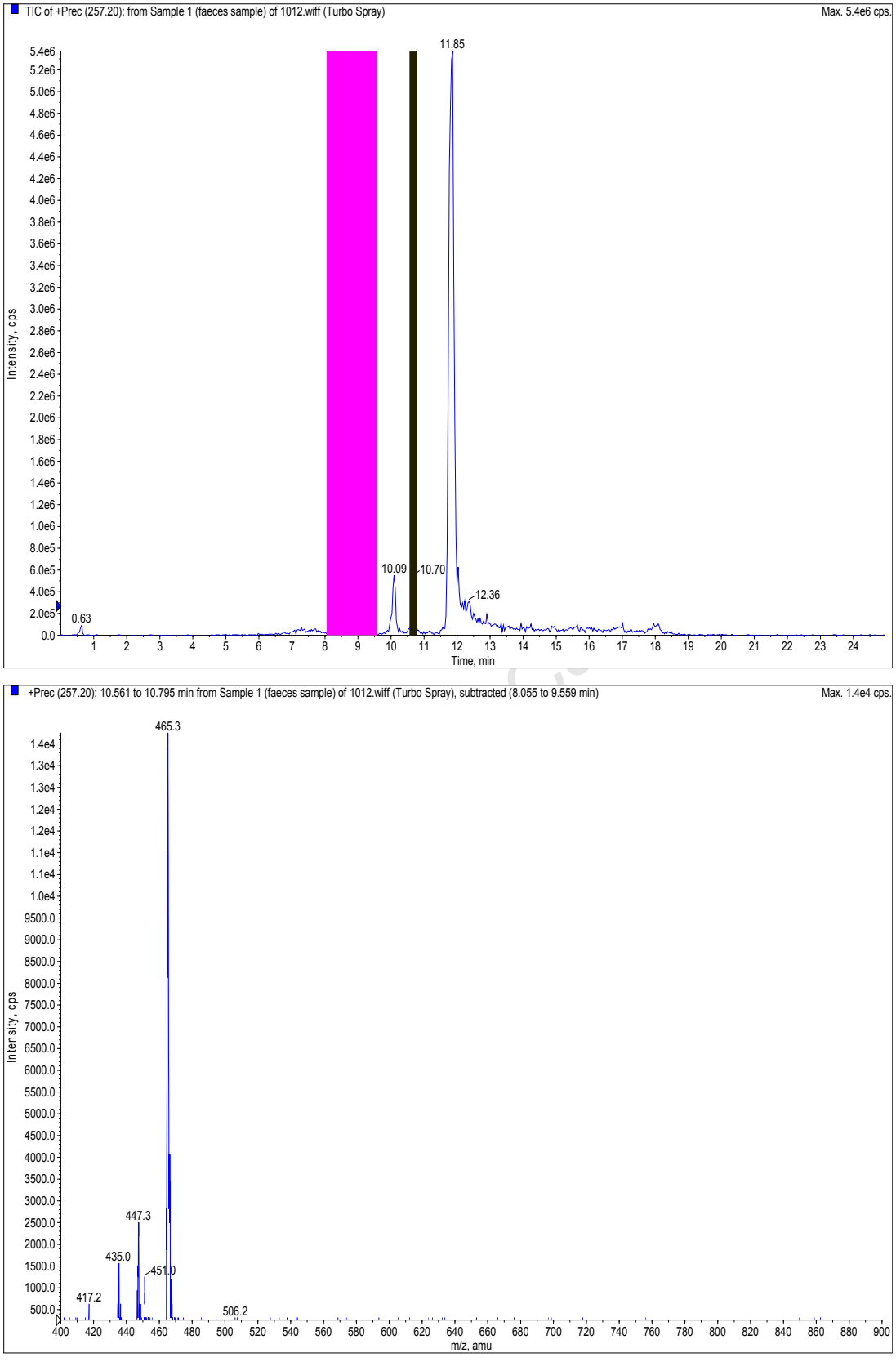

Figure 219 Chromatogram and precursor ion mass spectrum of peak 2

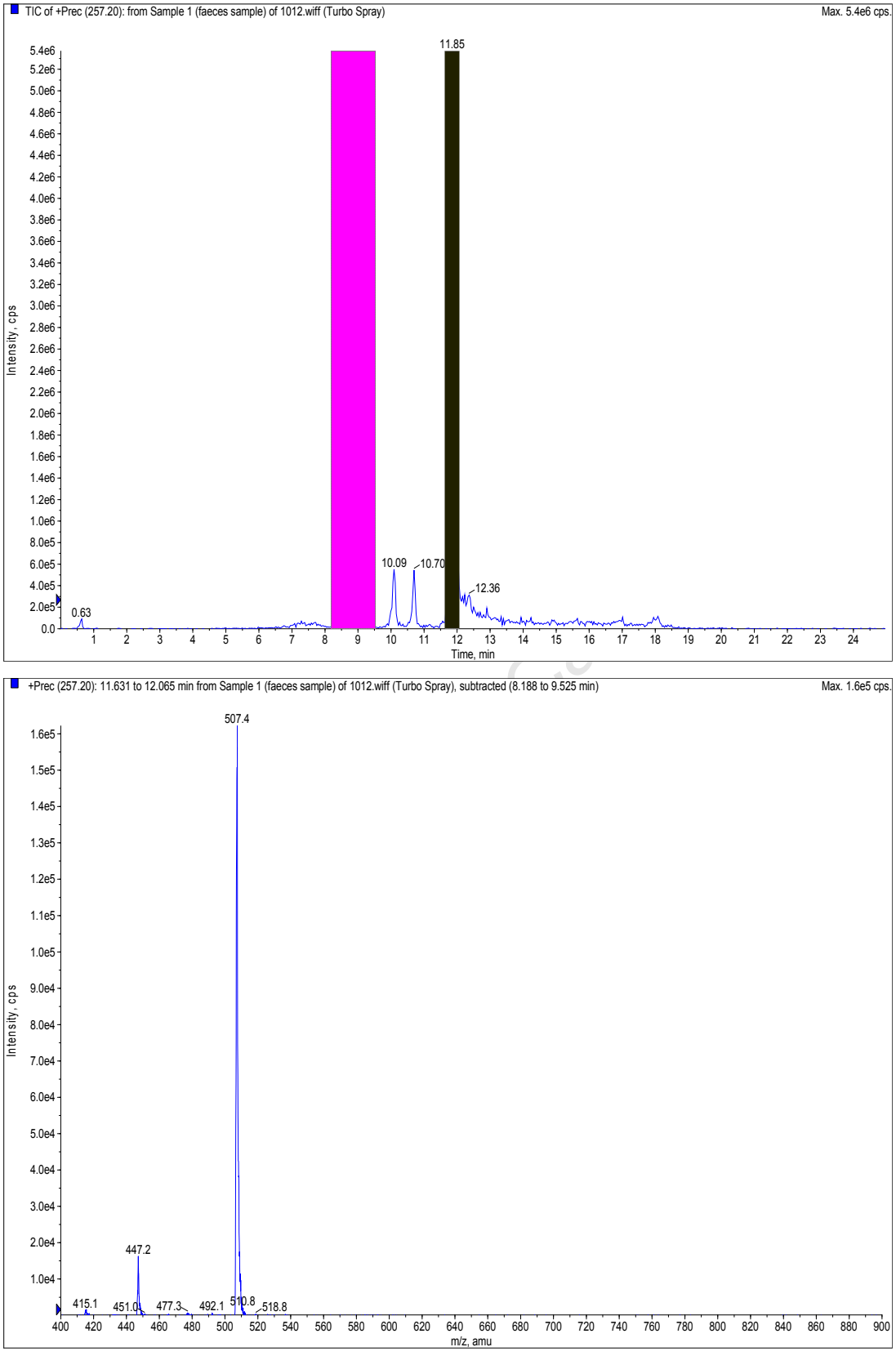

Figure 220 Chromatogram and precursor ion mass spectrum of peak 3

Neutral loss scan analysis: Blood sample
Chromatogram and mass spectrum of peaks 1

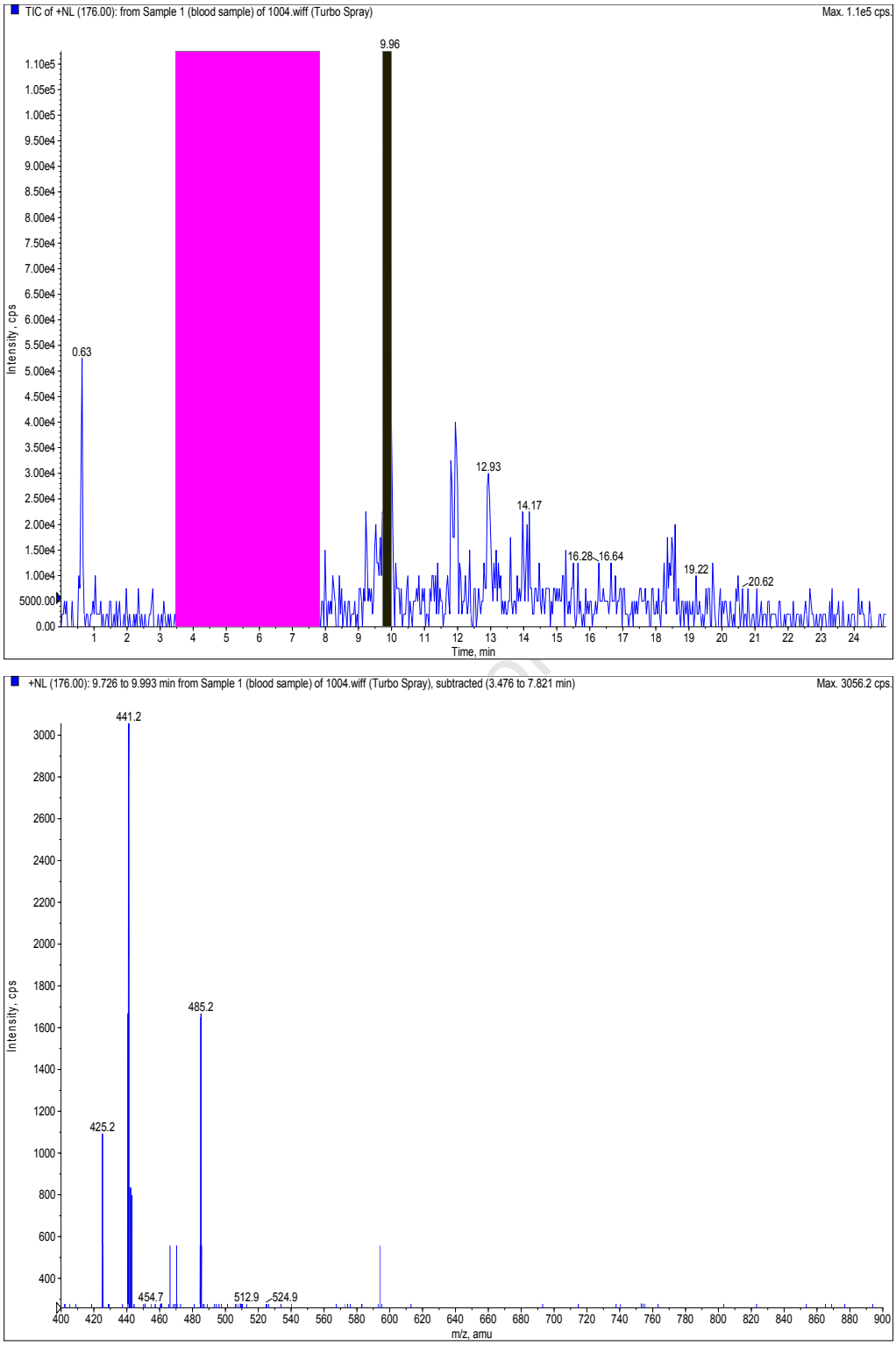

Figure 221 Chromatogram and neutral loss mass spectrum of peak 1

Neutral loss scan analysis: Urine sample
Chromatograms and mass spectra of peak groups 1 - 5

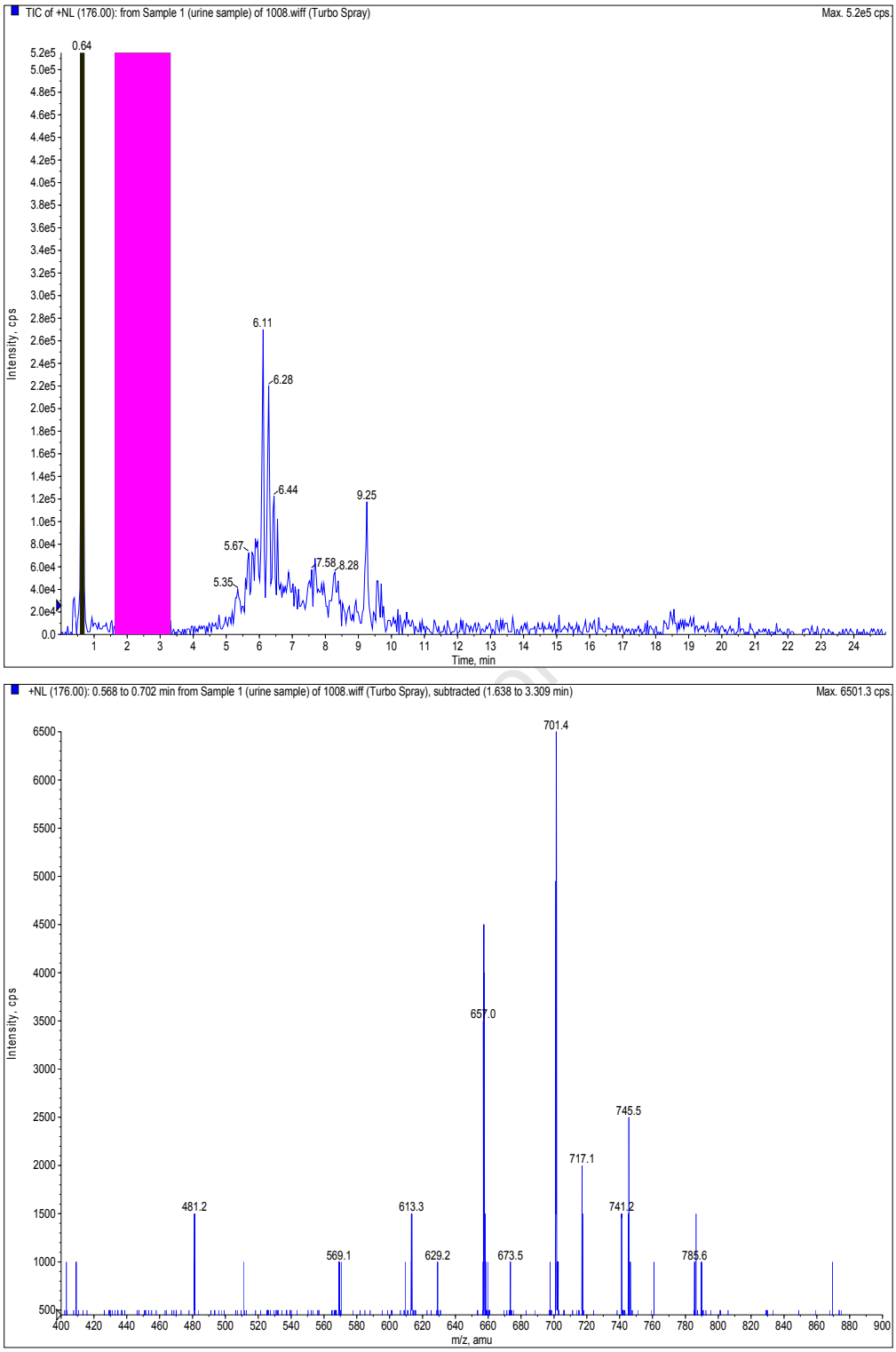

Figure 222 Chromatogram and neutral loss mass spectrum of peak 1

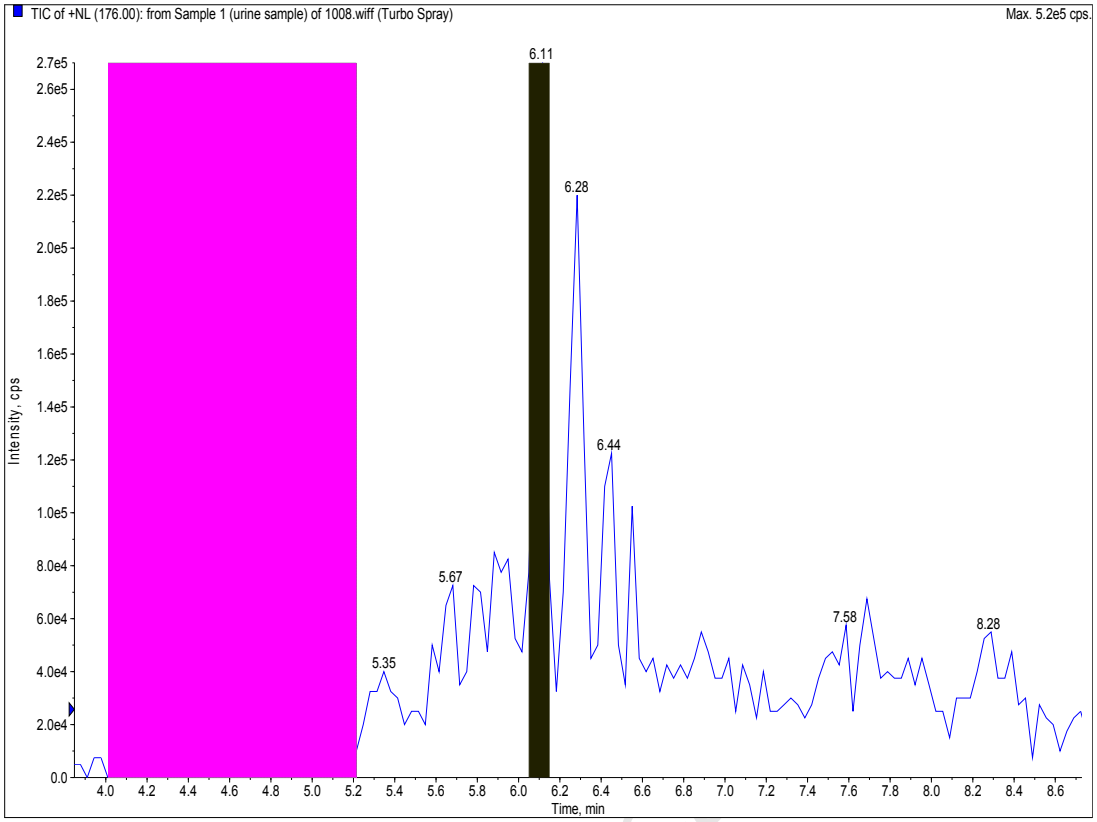

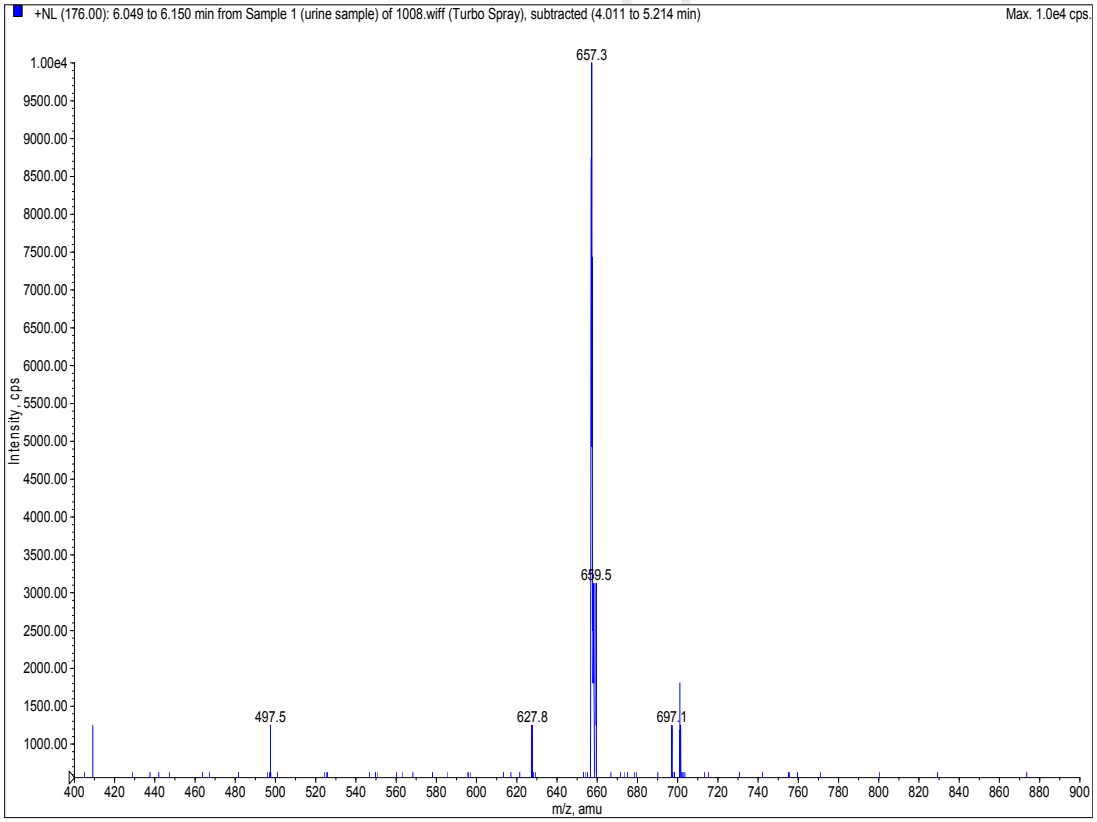

Figure 223 Chromatogram and neutral loss mass spectrum of peak 2

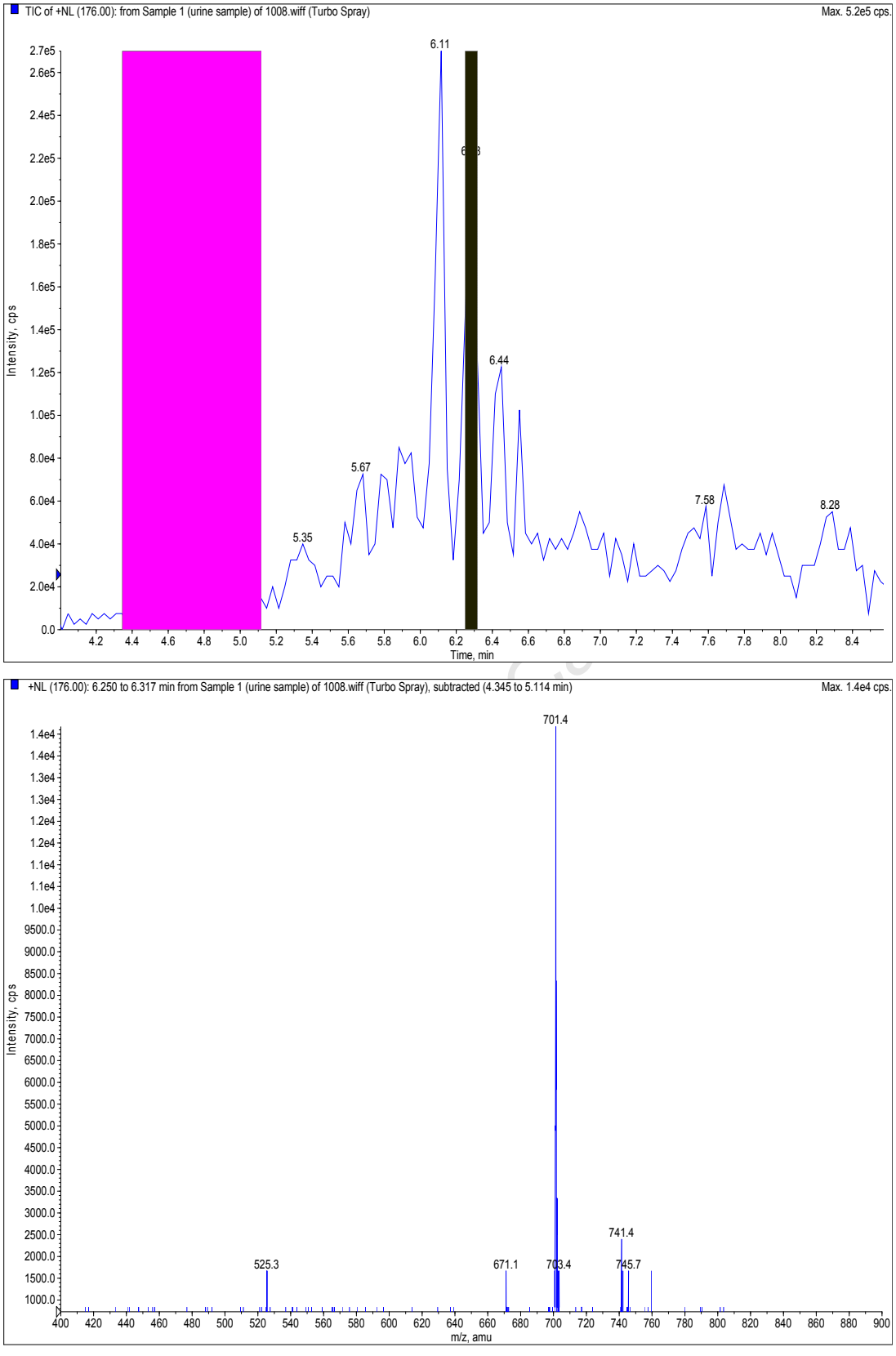

Figure 224 Chromatogram and neutral loss mass spectrum of peak 3

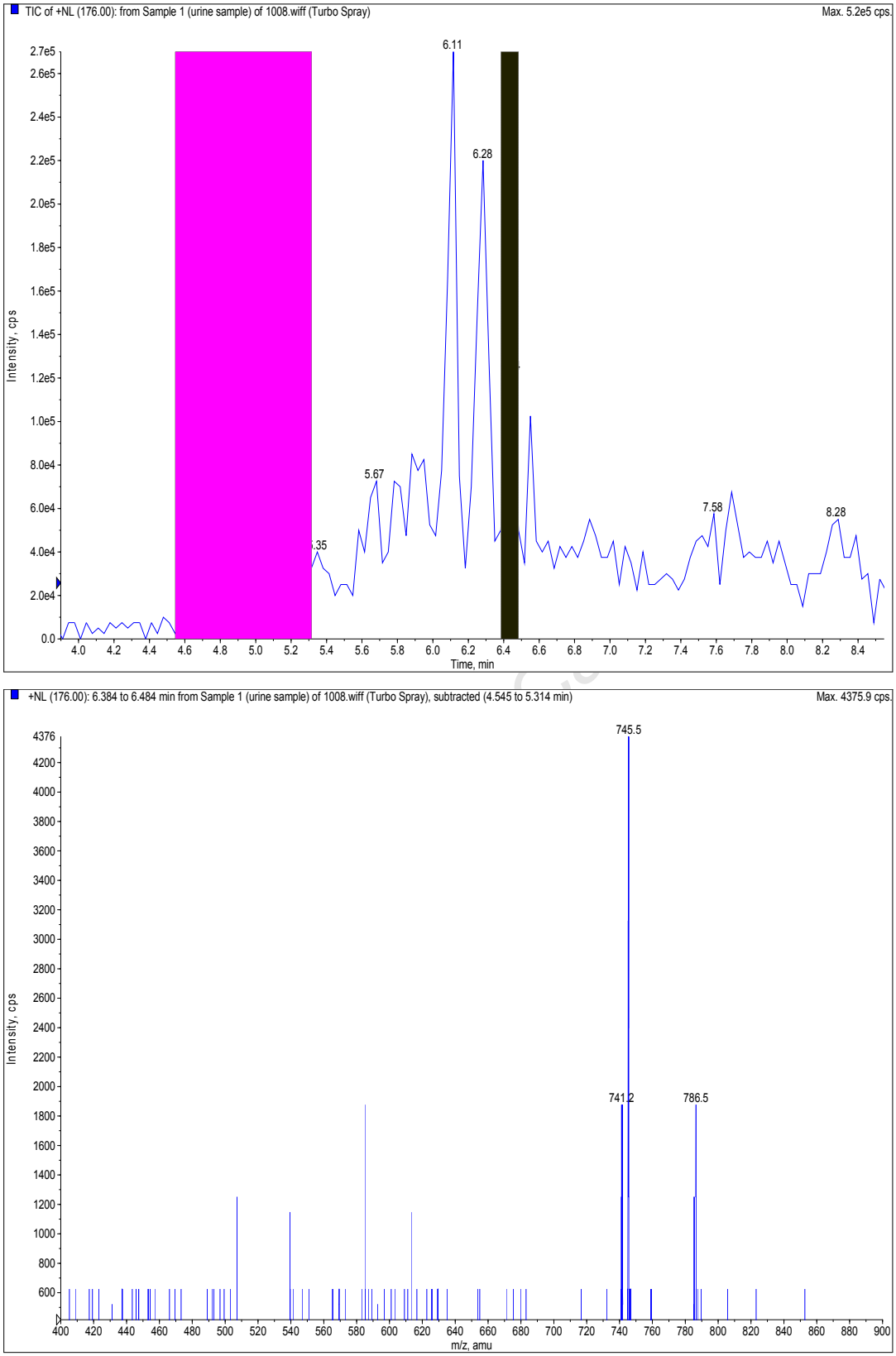

Figure 225 Chromatogram and neutral loss mass spectrum of peak 4

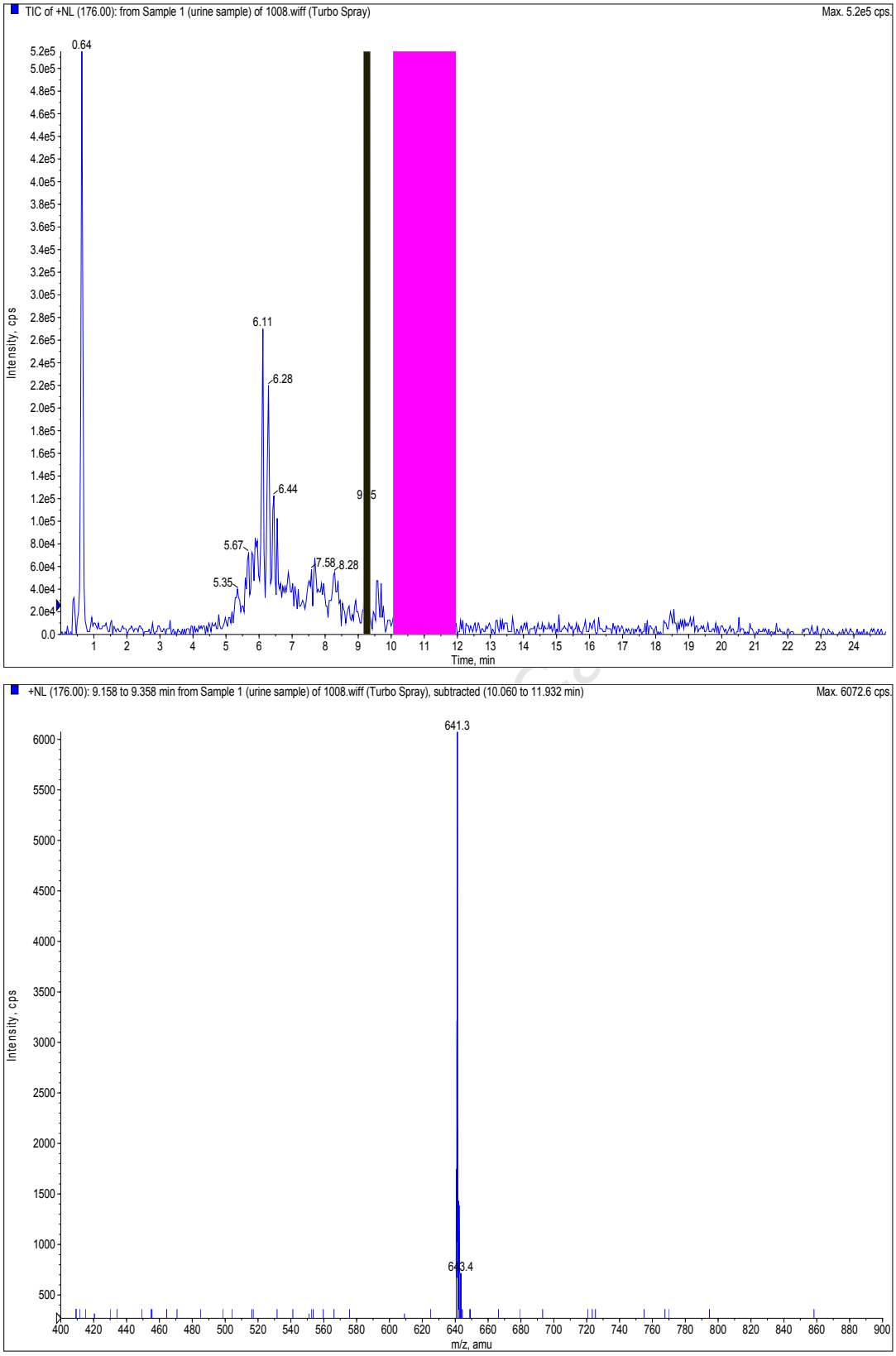

Figure 226 Chromatogram and neutral loss mass spectrum of peak 5

Neutral loss scan analysis: Faeces sample
Chromatograms and mass spectra of peak groups 1 – 3

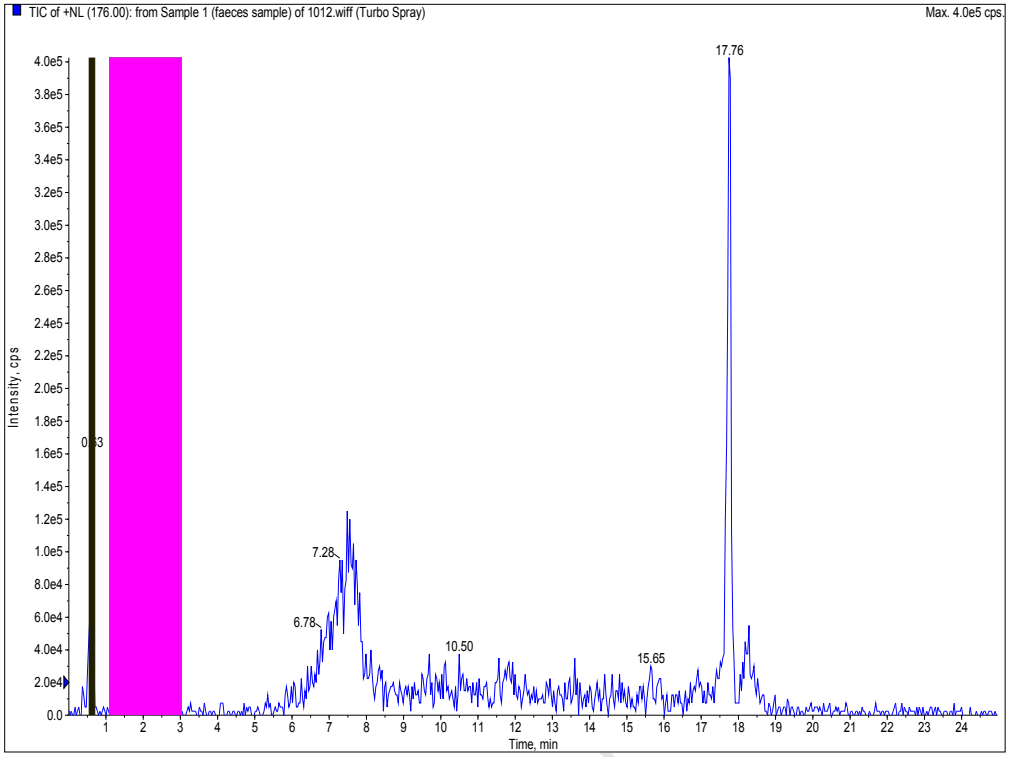

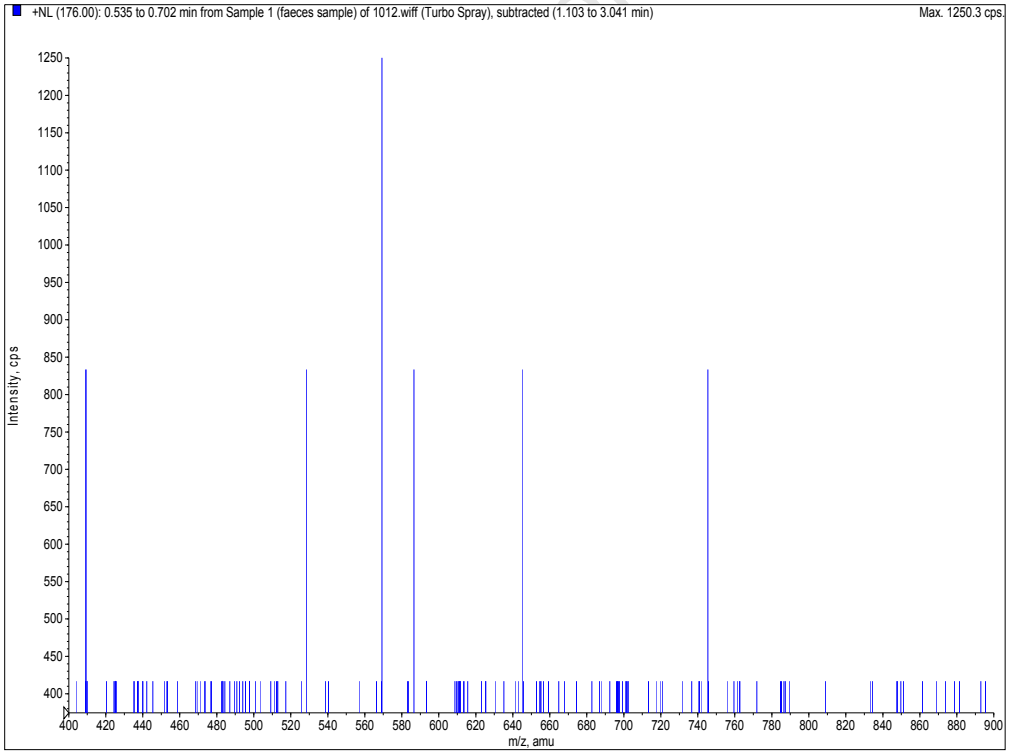

Figure 227 Chromatogram and neutral loss mass spectrum of peak 1

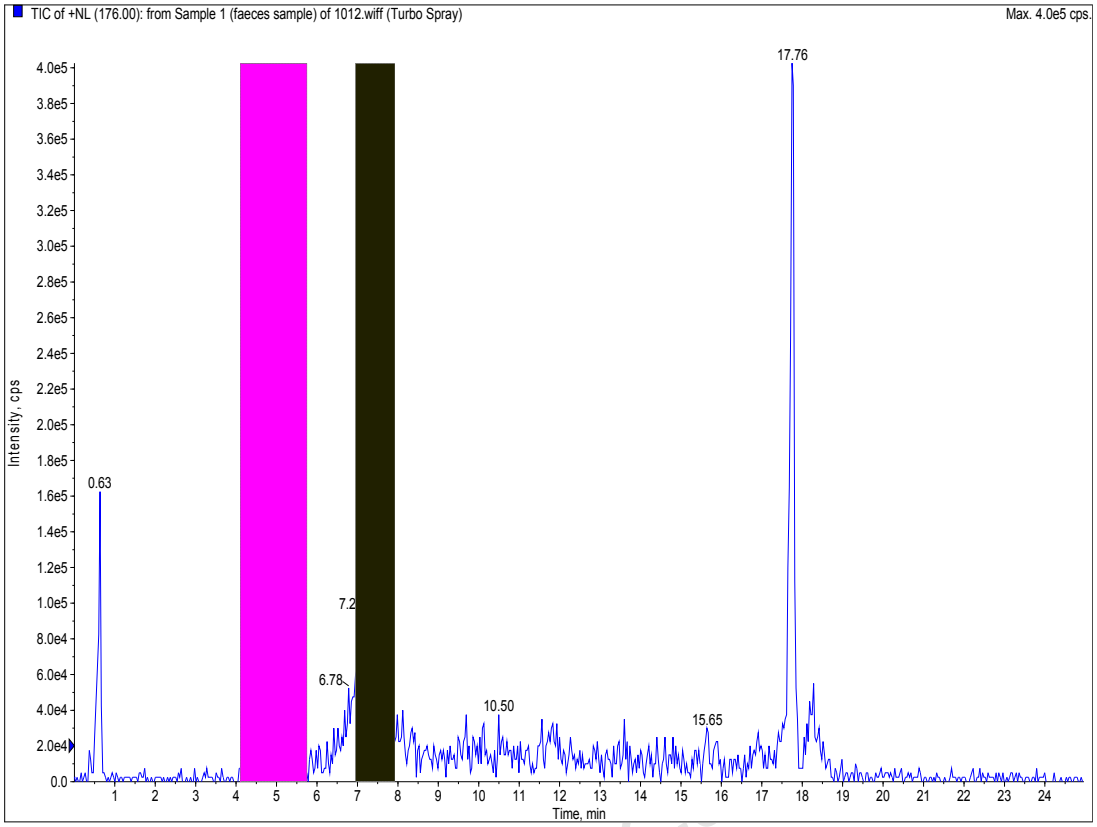

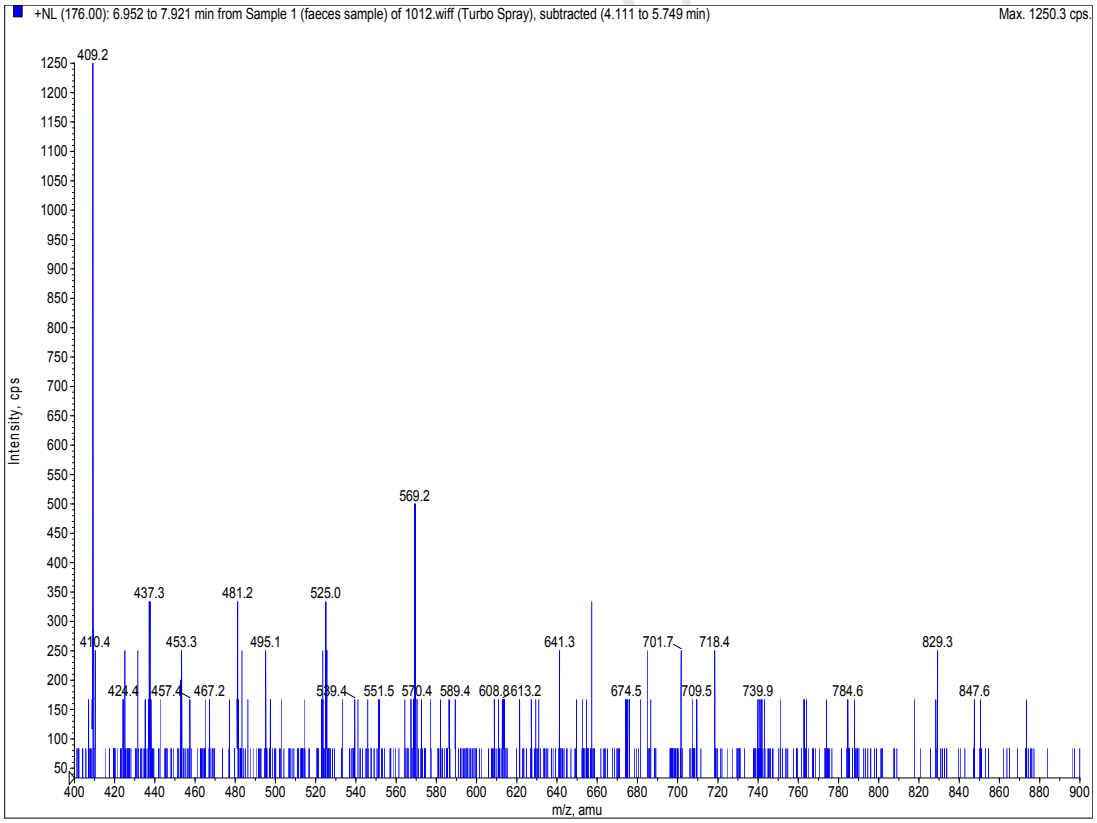

Figure 228 Chromatogram and neutral loss mass spectrum of peak 1

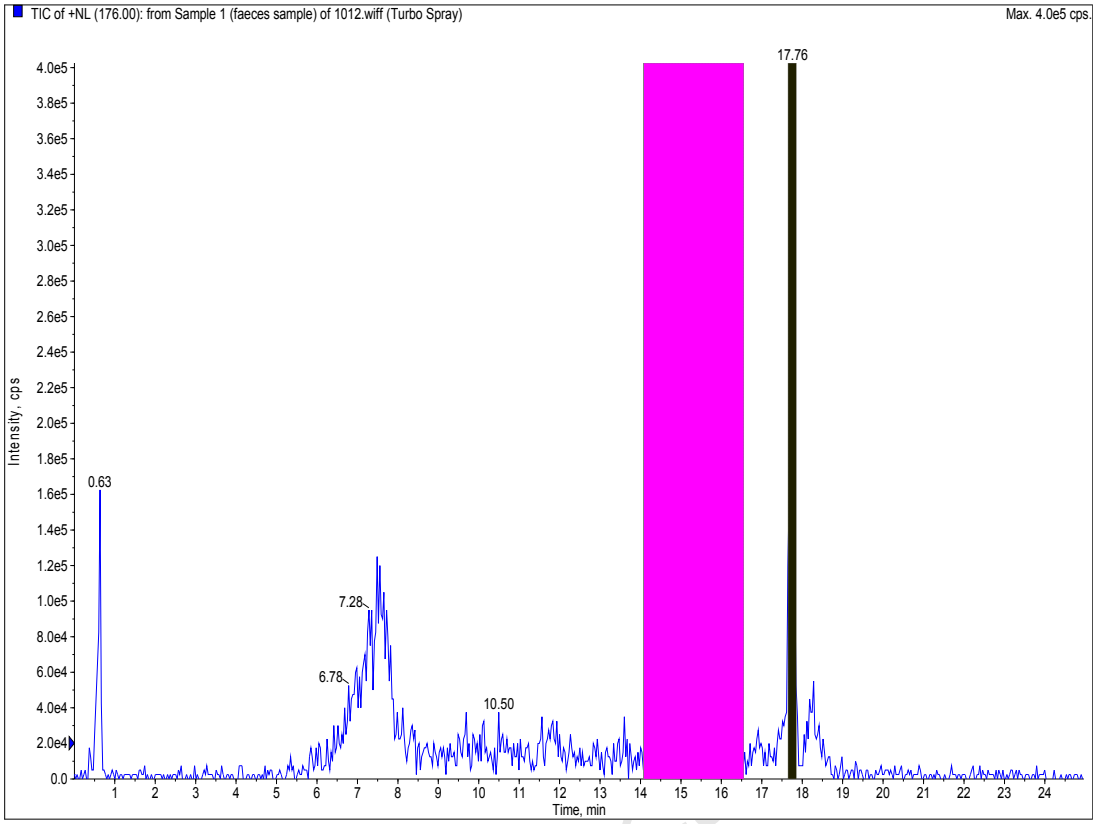

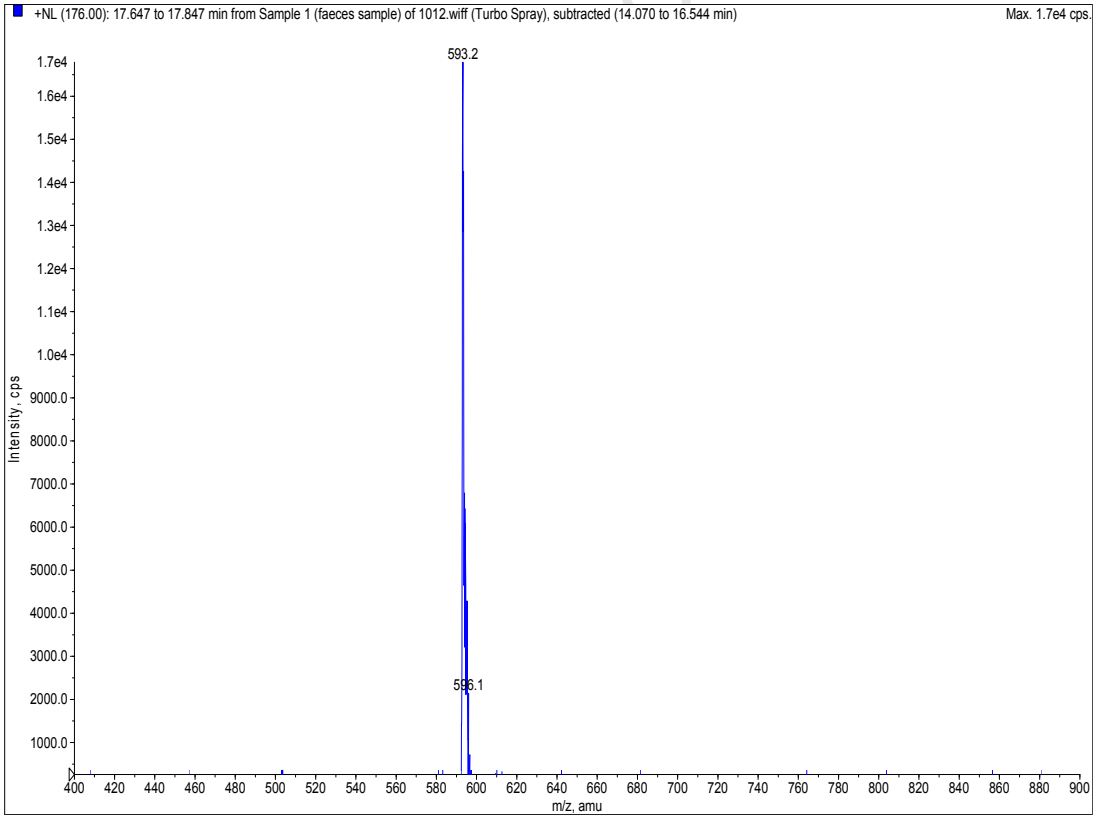

Figure 229 Chromatogram and neutral loss mass spectrum of peak 3